ISSN 2225-0719

2022

Volume 10 Issue 4
July / August

THE SECOND AFFILIATED HOSPITAL
CHONGQING MEDICAL UNIVERSITY

# Journal of Clinical and Translational Hepatology

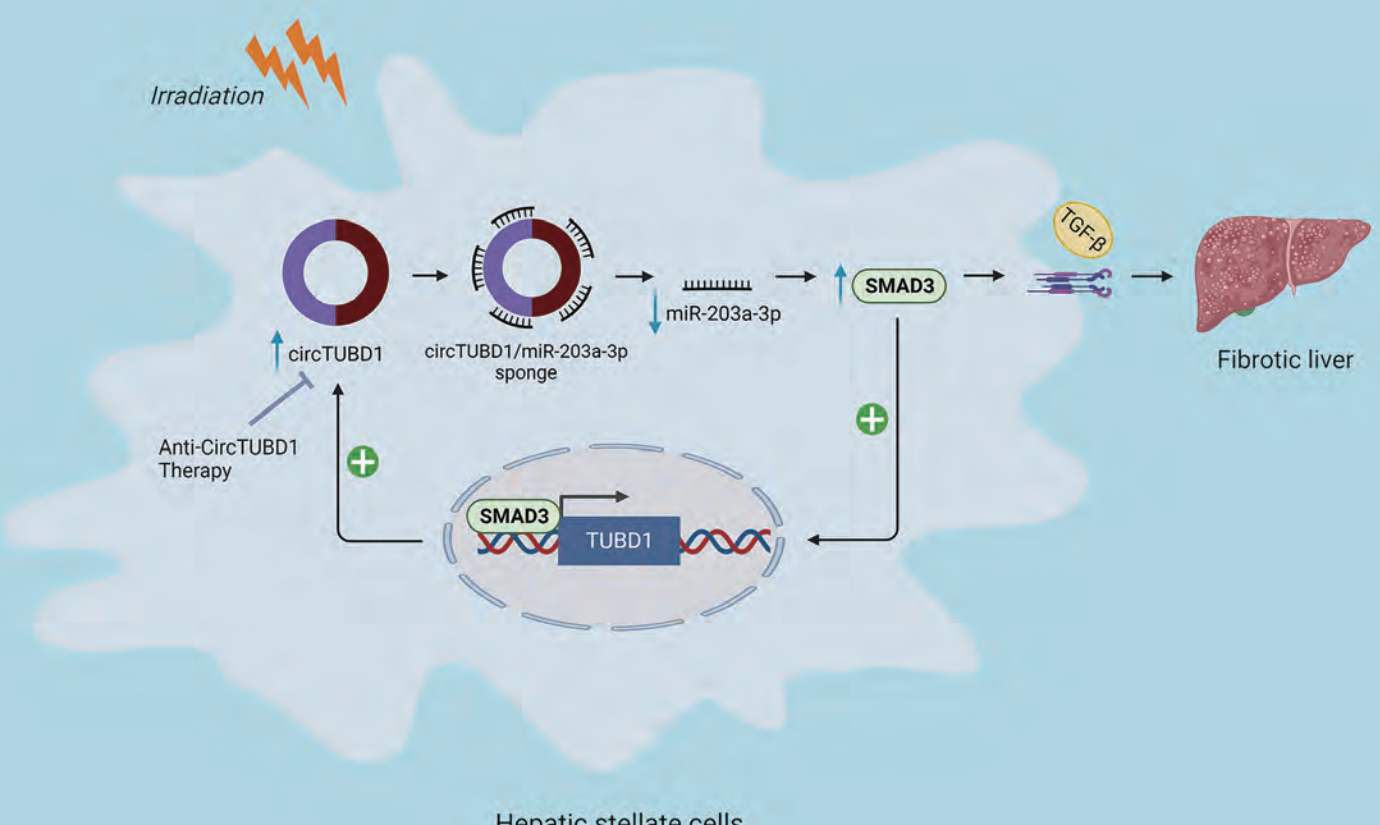


CircTUBD1: A Novel Circular RNA Molecule as a Therapeutic Target in Radiation-induced Liver Fibrosis

page 572

JCTH

OWNED BY THE SECOND AFFILIATED HOSPITAL OF CHONGQING MEDICAL UNIVERSITY
PUBLISHED BY XIA & HE PUBLISHING INC.
pISSN: 2225-0719; eISSN: 2310-8819
Frequency: Bimonthly
Launch date: September 28, 2013 (Volume 1, Issue 1)



## Contact Information

**Editorial Office**

**Managing Editors:** Dr. Huaidong Hu
Dr. Zhi Peng
Dr. Sandeep Kumar Karn
**Telephone:** +86-23-6370 1383
**Fax:** +86-23-6370 1383
**E-mail:** jcth@xiahepublishing.com
**Postal Address:** 74 Linjiang Road, Yuzhong District, 400010 Chongqing, CHINA

**Publisher**

Xia & He Publishing Inc.
**Website:** www.xiahepublishing.com
**E-mail:** service@xiahepublishing.com
**Postal Address:** 14090 Southwest Freeway, Suite 300, Sugar Land, Texas, 77478, USA

**Current Issue: Volume 10, Issue 4**
Publication date: August 28, 2022

## Aims and Scope

*Journal of Clinical and Translational Hepatology (JCTH, J Clin Transl Hepatol)* publishes high quality, peer-reviewed studies in the clinical and basic human health sciences of liver diseases. *JCTH* welcomes submissions of articles within its topical scope including: novel discoveries in clinical and basic hepatology; liver disease mechanisms; novel techniques in research and management of liver diseases; epidemiological/environmental factors of liver diseases; role of immune system function in liver diseases; acute and chronic hepatitis; cirrhosis; genetic and metabolic liver diseases and their complications; hepatobiliary diseases; liver cancer; drug metabolism; biliary disease; peritoneal tuberculosis. *JCTH* publishes various types of articles, including original article, review, short communication, systematic review, meta-analysis, case report, methodology article, letter to the editor, and editorial.

## Indexing & Abstracting

*JCTH* is now indexed in Science Citation Index Expanded (SCIE); PubMed; PubMed Central; Scopus; Baidu Scholar; CNKI Scholar; Dimensions; EBSCOhost; Google Scholar; Microsoft Academic; SafetyLit; ScienceOpen; Scilit; Semantic Scholar; Wanfang Data; Web of Science; WorldCat Discovery Services; Zetoc.

## Open Access



## Disclaimer



## Links

Journal Home: https://www.xiahepublishing.com/journal/jcth
Editorial Board: https://www.xiahepublishing.com/journal/jcth/editors
Archive: https://www.xiahepublishing.com/journal/jcth/archive
Instructions for Authors: https://www.xiahepublishing.com/journal/jcth/instruction
Online Submission System: https://www.editorialmanager.com/jcth/default.aspx

# JCTH

## Executive Associate Editors



## Associate Editors

# Associate Editors

# Editorial Board Members

JCTH

# Editorial Board Members

# JOURNAL OF CLINICAL AND TRANSLATIONAL HEPATOLOGY

## CONTENTS

2022 10(4):571–782

### Editorial



### Hot Topic Commentary



### Original Articles

## Review Articles

## Guideline



## Short Communication



## Case Report

*Journal of Clinical and Translational Hepatology* **2022** vol. 10(4) | 571–573
DOI: 10.14218/JCTH.2022.00132

Editorial

# CircTUBD1: A Novel Circular RNA Molecule as a Therapeutic Target in Radiation-induced Liver Fibrosis

Catherine Yujia Gu[1] and Terence Kin Wah Lee[1,2*]

[1]*Department of Applied Biology and Chemical Technology, The Hong Kong Polytechnic University, Hong Kong, China;* [2]*State Key Laboratory of Chemical Biology and Drug Discovery, The Hong Kong Polytechnic University, Hong Kong, China*

**Received:** 20 March 2022 | **Revised:** 19 April 2022 | **Accepted:** 27 April 2022 | **Published:** 11 May 2022

**Citation of this article:** Gu CY, Lee TKW. CircTUBD1: A Novel Circular RNA Molecule as a Therapeutic Target in Radiation-induced Liver Fibrosis. J Clin Transl Hepatol 2022;10(4):571–573. doi: 10.14218/JCTH.2022.00132.

Primary liver cancer is the sixth most commonly diagnosed cancer and the fourth leading cause of cancer mortality worldwide.[1] Liver transplantation and surgical resection are two curative therapeutic options for liver cancer patients at the early stages. However, most patients are diagnosed at advanced stages. For those patients, chemotherapy, targeted therapy, radiotherapy (RT), and combination therapy are employed to treat unresectable liver cancer.[2] Among the treatments, RT has emerged as an effective treatment for patients at an intermediate stage. However, the efficacy of RT is limited due to its radiotoxicity in liver tissues adjacent to tumors, resulting in radiation-induced liver disease (RILD).[3] RILD is an acute response within few weeks or a chronic response that occurs from months to years after RT. Hepatic stellate cells (HSCs),[4] the main fibrogenic cell type, are known to be radiosensitive and to release various profibrotic factors that promote liver fibrosis during RT, resulting in the development of radiation-induced liver fibrosis (RILF). RILF is becoming an increasingly serious problem as it could prevent irradiation dose escalation or terminate repeated irradiation treatment for liver cancer and is associated with a high mortality rate. Efficient treatment options for RILF are limited. Therefore, elucidation of the molecular mechanisms for the development of RILF is urgently needed in order to improve the survival of liver cancer patients treated with RT.

A recent study by Niu *et al*.,[5] titled "CircTUBD1 regulates radiation-induced liver fibrosis response via a circTUBD1/micro-203a-3p/Smad3 positive feedback loop," identified a circular RNA (circRNA) signaling pathway that is critically involved in the development of RILF. That study is based on a previous observation by the same group that circTUBD1 (has_circ_0044897) expression was significantly upregulated, with activation of a human hepatic stellate cell line (LX-2) following irradiation.[6] Based on that interesting lead, Niu *et al*.[5] devised this study to functionally characterize and elucidate the potential role of circTUBD1 in RILF using an *in vitro* 3-dimensional (3D) spheroid model of LX-2 cells as well as an *in vivo* RILF mouse model. Using a knockdown approach, these researchers found that suppression of circTUBD1 reduced the activity of LX-2 cells, as evidenced by a decrease in the expression of fibrosis-related markers at both mRNA and protein levels. Analysis in the CircInteractome database found that circTUBD1 shared response elements with micro-203a-3p. The binding of circTUBD1 and micro-203a-3p was further confirmed by dual-luciferase reporter assays, mutation analysis, and RNA pulldown assays. Functionally, the micro-203a-3p inhibitor not only aggravated radiation-induced activation of LX-2 cells but also partially rescued the suppressive effect of circTUBD1 knockdown in LX-2 cells, revealing the functional role of circTUBD1 as a sponge of micro-203a-3p to regulate RILF in LX-2 cells.

To further elucidate the downstream signaling of circTUBD1/micro-203a-3p, the investigators performed RNA sequencing to compare the genetic profiles between circTUBD1 and control LX-2 cells upon irradiation. The results suggested that the TGF-β signaling pathway was enriched and the expression and phosphorylation of SMAD3, a transcription factor related to the pathway, were repressed upon circTUBD1 knockdown. The observations echo the finding showing that the TGF-β/SMAD3 signaling pathway is a crucial mediator during the process of radiation-induced liver injury.[7] With the TargetScan database, multiple binding sites between micro-203a-3p and SMAD3-3′UTR were identified, and their interactions were further confirmed by dual-luciferase assays and functional characterization. The data show that circTUBD1 suppressed the micro-203a-3p/SMAD3 interaction, resulting in the upregulation of TGF-β signaling.

Additionally, the study provides mechanistic insight into how circTUBD1 expression is upregulated in HSCs following irradiation. Based on the GTAR and JASPAR databases, Niu *et al*.[5] revealed for the first time that SMAD3 potentially binds to multiple binding sites in the promoter region of TUBD1. Further confirmation analysis showed two effective SMAD3 binding sites in the promoter region of TUBD1. Chromatin immunoprecipitation (ChIP) quantitative real-time PCR analysis using a specific anti-SMAD3 antibody confirmed the physical interaction between SMAD3 and the TUBD1 promoter, and that the occupancy of SMAD3 was consistently decreased by knockdown of circTUBD1 in LX-2 cells. The potential positive SMAD3/circTUBD1 feedback loop was further confirmed by a knockdown experiment in which repression of SMAD3 significantly decreased TUBD1, pre-TUBD1, and circTUBD1 levels in LX-2 cells. These excit-

**Abbreviations:** 3D, 3-dimensional; circRNA, circular RNA; HSC, hepatic stellate cell; RILD, radiation-induced liver disease; RILF, radiation-induced liver fibrosis; RT, radiotherapy.

*__Correspondence to:__ Terence KW Lee, Room 805, Block Y, Department of Applied Biology and Chemical Technology, Lee Shau Kee Building, The Hong Kong Polytechnic University, Hong Kong, China. ORCID: https://orcid.org/0000-0003-0682-322X. Tel: +852-3400-8799, Fax: +852-2364-9932, E-mail: terence.kw.lee@polyu.edu.hk

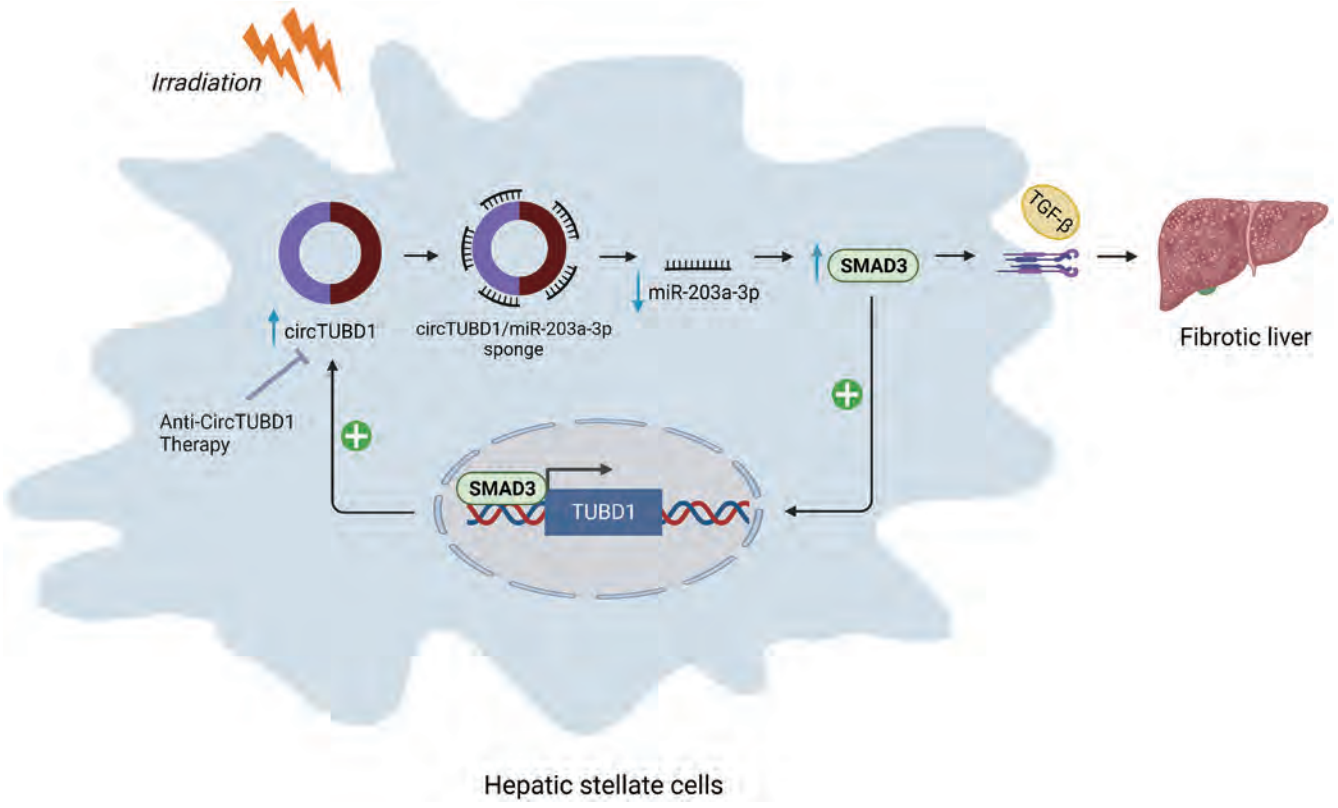


**Fig. 1. Schematic diagram of the role of circTUBD1 in the regulation of RILF via a circTUBD1/ micro-203a-3p /Smad3 positive feedback loop.**

ing findings indicated that SMAD3 was not only regulated by circTUBD1 but also in turn modulated the endogenous expression of circTUBD1 in LX-2 cells. Targeting the positive feedback loop is a potentially promising therapeutic strategy to alleviate liver fibrosis after irradiation.

To confirm the *in vitro* findings, Niu *et al.*[5] established a RILF mouse model in which the left liver was irradiated with 30 Gy with five fractions, 6 Gy per week, and examined the therapeutic effect of targeting the circTUBD1 signaling cascade by intravenous injection of adenoviral-based sh-circTUBD1 virus. With that RILF model, irradiation resulted in upregulation of the expression of fibrogenic markers including α-SMA, COL1A1, COL3A1, and CTGF. Knockdown of circTUBD1 partially offset the upregulated expression of these markers. Phenotypically, knockdown of circTUBD1 also alleviated the effect of irradiation on inflammatory infiltrates, excess collagen deposition around the vessel, and liver damage.

The study provides novel mechanistic insight into therapeutic strategies for RILF. First, it established a 3D spheroid model of LX-2 cells for the *in vitro* analysis of liver fibrosis upon irradiation, which provides a more physiological system compared to the 2-dimensional cell line approach. Second, it revealed the novel role of circTUBD1 in the regulation of RILF via a circTUBD1/micro-203a-3p/Smad3 positive feedback loop (Fig. 1). Most importantly, the study provides a novel therapeutic strategy to alleviate RILF by targeting the circTUBD1 signaling cascade. Although major progress has been made in circRNA research in recent years, targeting circRNA is still under investigation for potential clinical trials. A recent study showed that the CRISPR/Cas13 system showed promise in knocking down circRNAs with high specificity and efficiency.[8] Further investigation targeting circTUBD1 for RILF is highly warranted to translate the current results to the bedside. Additionally, because of recent advancements in biomedical technology, photoacoustic imaging can be employed to evaluate the therapeutic effect of suppressing circTUBD1 on RILF in mice.[9,10]

## Funding

This study was supported by the RGC General Research Fund (15102020 to T.K. Lee), Collaborative Research Fund (C7026-18G), Research Impact Fund (R5050-18F & R7022-20).

## Conflict of interest

TKL has been an editorial board member of *Journal of Clinical and Translational Hepatology* since 2021. CYG has no conflicts of interest related to this publication.

## Author contributions

Proposing the main opinions and writing the manuscript cooperatively (CYG, TKL), and editing the manuscript (TKL).

## References

[1] Siegel R, Naishadham D, Jemal A. Cancer statistics, 2013. CA Cancer J Clin 2013;63(1):11–30. doi:10.3322/caac.21166, PMID:23335087.
[2] Villanueva A, Hernandez-Gea V, Llovet JM. Medical therapies for hepatocellular carcinoma: a critical view of the evidence. Nat Rev Gastroenterol Hepatol 2013;10(1):34–42. doi:10.1038/nrgastro.2012.199, PMID:23147664.

[3] Straub JM, New J, Hamilton CD, Lominska C, Shnayder Y, Thomas SM. Radiation-induced fibrosis: mechanisms and implications for therapy. J Cancer Res Clin Oncol 2015;141(11):1985–1994. doi:10.1007/s00432-015-1974-6, PMID:25910988.
[4] Puche JE, Saiman Y, Friedman SL. Hepatic stellate cells and liver fibrosis. Compr Physiol 2013;3(4):1473–1492. doi:10.1002/cphy.c120035, PMID:24265236.
[5] Niu H, Zhang L, Wang B, Zhang GC, Liu J, Wu ZF, *et al*. CircTUBD1 Regulates Radiation-induced Liver Fibrosis Response via a circTUBD1/micro-203a-3p/Smad3 Positive Feedback Loop. J Clin Transl Hepatol 2022;10(4):680–691. doi:10.14218/JCTH.2021.00511.
[6] Chen Y, Yuan B, Wu Z, Dong Y, Zhang L, Zeng Z. Microarray profiling of circular RNAs and the potential regulatory role of hsa_circ_0071410 in the activated human hepatic stellate cell induced by irradiation. Gene 2017; 629:35–42. doi:10.1016/j.gene.2017.07.078, PMID:28774651.
[7] Hu Z, Qin F, Gao S, Zhen Y, Huang D, Dong L. Paeoniflorin exerts protective effect on radiation-induced hepatic fibrosis in rats via TGF-β1/Smads signaling pathway. Am J Transl Res 2018;10(3):1012–1021. PMID:29636890.
[8] He AT, Liu J, Li F, Yang BB. Targeting circular RNAs as a therapeutic approach: current strategies and challenges. Signal Transduct Target Ther 2021;6(1):185. doi:10.1038/s41392-021-00569-5, PMID:34016945.
[9] Lv J, Xu Y, Xu L, Nie L. Quantitative Functional Evaluation of Liver Fibrosis in Mice with Dynamic Contrast-enhanced Photoacoustic Imaging. Radiology 2021;300(1):89–97. doi:10.1148/radiol.2021204134, PMID:33904773.
[10] Yu Q, Huang S, Wu Z, Zheng J, Chen X, Nie L. Label-Free Visualization of Early Cancer Hepatic Micrometastasis and Intraoperative Image-Guided Surgery by Photoacoustic Imaging. J Nucl Med 2020;61(7):1079–1085. doi:10.2967/jnumed.119.233155, PMID:31806769.

*Journal of Clinical and Translational Hepatology* **2022** vol. 10(4) | 574–576
DOI: 10.14218/JCTH.2022.00278

Hot Topic Commentary

# SGLT-2 Inhibitor and GLP-1 Receptor Agonist Treatment for Patients with Nonalcoholic Fatty Liver Disease and Type 2 Diabetes Mellitus: Is Their Combination the Optimal Treatment Option?

Dimitrios Patoulias[1*] and Theodoros Michailidis[2]

[1]*Second Propedeutic Department of Internal Medicine, Aristotle University of Thessaloniki, General Hospital "Hippokration," Thessaloniki, Greece;* [2]*Second Department of Internal Medicine, Aristotle University of Thessaloniki, General Hospital "Hippokration," Thessaloniki, Greece*

**Received:** 5 June 2022 | **Revised:** 16 June 2022 | **Accepted:** 22 June 2022 | **Published:** 13 July 2022

**Citation of this article:** Patoulias D, Michailidis T. SGLT-2 Inhibitor and GLP-1 Receptor Agonist Treatment for Patients with Nonalcoholic Fatty Liver Disease and Type 2 Diabetes Mellitus: Is Their Combination the Optimal Treatment Option? J Clin Transl Hepatol 2022;10(4):574–576. doi: 10.14218/JCTH.2022.00278.

Nonalcoholic fatty liver disease (NAFLD) is a growing epidemic, representing the most common chronic liver disease worldwide.[1] NAFLD is highly associated with type 2 diabetes mellitus (T2DM) and obesity, conditions that increase morbidity and mortality.[2] A background of T2DM has also been shown to be predictive of cirrhosis and hepatocellular carcinoma occurrence in patients with T2DM, and cirrhotic patients with diabetes seem to have a higher risk of hepatic decompensation with manifestations of hepatic encephalopathy.[3] In addition, it should not be underestimated the significantly increased risk for cardiovascular disease (CVD) and chronic kidney disease (CKD) in subjects with NAFLD, regardless of T2DM presence.[4,5]

Newer antidiabetic drugs, like sodium-glucose co-transporter-2 (SGLT-2) inhibitors and glucagon-like peptide-1 receptor agonists (GLP-1RAs) have attracted scientific interest in the last decade, because of their multiple pleiotropic effects, with emphasis on cardio- and reno-protection with both drug classes.[6] Their potential role in the treatment of NAFLD has been widely discussed recently.[7]

A previous meta-analysis demonstrated that both drug classes provided a significant improvement in liver enzymes and steatosis in patients with NAFLD.[8] Two recent meta-analyses confirmed the beneficial effects of these drug classes on liver enzymes and liver fibrosis, along with significant improvements in the overall metabolic profile and glycemic control.[9,10] What is more, a recently published retrospective study documented that 5-year treatment with SGLT-2 inhibitors in patients with T2DM and NAFLD resulted in a significant improvement in liver steatosis and fibrosis, and that addition of a GLP-1RA was safe.[11] It has also been speculated that their diuretic effects might be of great value for cirrhotic patients with refractory ascites.[12] Some anecdotal data retrieved from small case series support this hypothesis.[13]

Regarding GLP-1RAs, a previous population-based retrospective cohort study found that treatment with this antidiabetic drug class resulted in a significant decrease in the risk of individual decompensation events, including ascites, spontaneous bacterial peritonitis, hepatorenal syndrome, esophageal variceal hemorrhage, and hepatic encephalopathy.[14] However, when SGLT-2 inhibitors and GLP-1RAs were directly compared, no significant difference in decompensation rates was observed.[14] Combining SGLT-2 inhibitors and GLP-1RA has been shown to be safe and highly efficacious in patients with T2DM, providing a greater reduction in glycated hemoglobin levels, body weight, and systolic blood pressure, compared with each drug class alone.[15] In addition, the cardiovascular benefit obtained by combining a SGLT-2 inhibitor and GLP-1RA seems to be greater than that obtained with a SGLT-2 inhibitor or GLP-1RA alone.[16]

Unfortunately, except for the observations made by Akuta and colleagues[11] in a small cohort of patients with NAFLD,[11] there is no evidence of a synergistic effect of a SGLT-2 inhibitor plus GLP-1RA on liver steatosis and/or fibrosis in patients with NAFLD. The greater reductions of glycated hemoglobin level and body weight shown in previous randomized controlled trials and meta-analyses, should be considered a major step in achieving increased benefits with treatment of liver steatosis by combining a SGLT-2 inhibitor and GLP-1RA.[15] In addition, greater reductions in subcutaneous fat and the visceral fat mass, should be expected with such a combination, along with a greater reduction in intrahepatic fat content, although that has to be confirmed in future trials.[17,18] Remarkably, only an observational study in a total of 24 patients with NAFLD and T2DM showed that addition of a SGLT-2 inhibitor to an incretin-based regimen with GLP-1RA or a DPP-4 inhibitor resulted in a significant decrease in alanine aminotransferase levels that led to nor-

**Abbreviations:** CKD, chronic kidney disease; CVD, cardiovascular disease; GLP-1RA, glucagon-like peptide-1 receptor agonists; NAFLD, nonalcoholic fatty liver disease; SGLT-2, sodium-glucose co-transporter-2; T2DM, type 2 diabetes mellitus.

[*]**Correspondence to:** Dimitrios Patoulias, Second Propedeutic Department of Internal Medicine, General Hospital "Hippokration," Konstantinoupoleos 49, 54642, Thessaloniki, Greece. ORCID: https://orcid.org/0000-0002-6899-684X. Tel: +30-6946900777, Fax: +30-2310225083, E-mail: dipatoulias@gmail.com

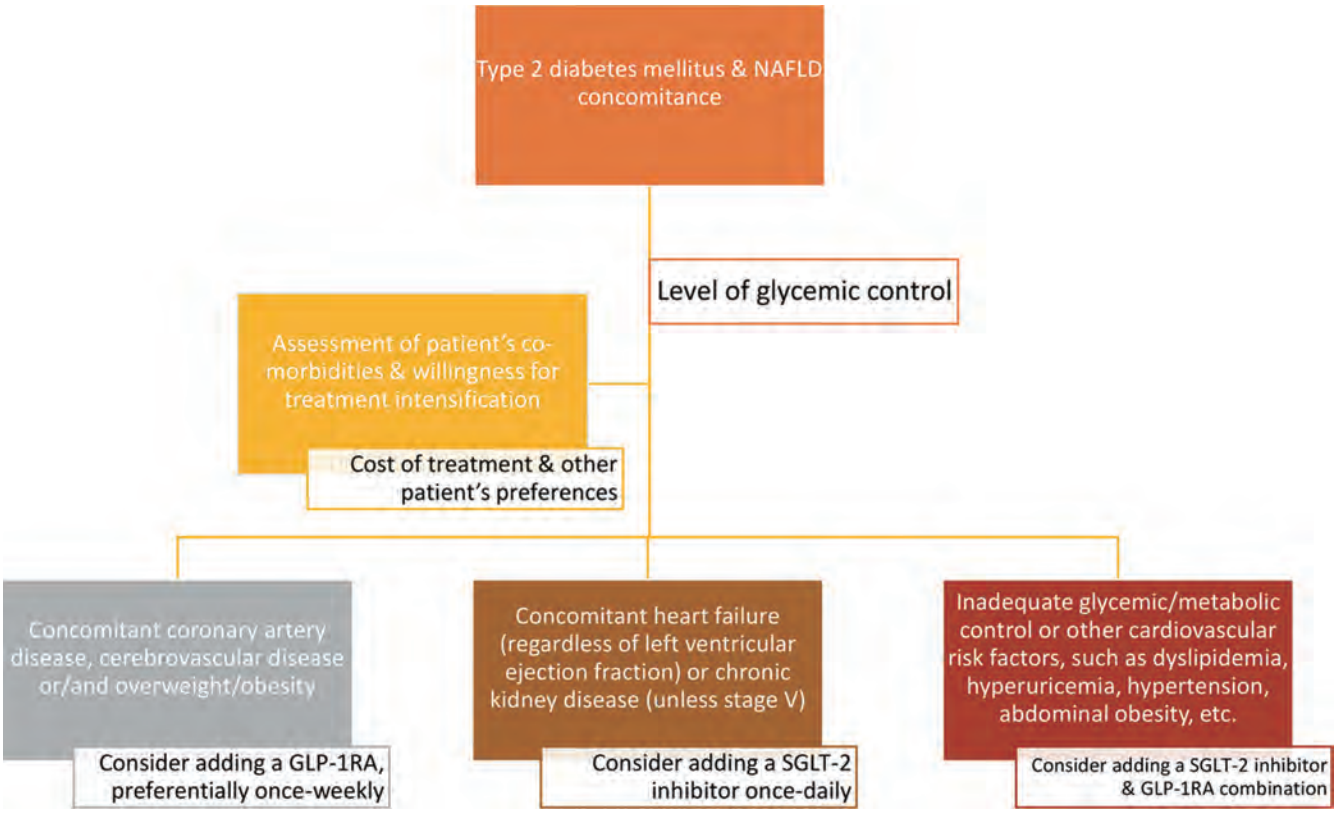


**Fig. 1. A simplified treatment approach for patients with NAFLD and type 2 diabetes mellitus.** NAFLD, nonalcoholic fatty liver disease.

malization and in a significant improvement in the FIB-4 index.[19]

Of course, it has to be admitted that the safety and efficacy of a great number of drug classes and investigational agents for the treatment of NAFLD with or without comorbidities testing are currently under investigation in clinical trials.[20] Peroxisome proliferator-activated receptor agonists, pyruvate carrier (MPC) inhibitors, farnesoid X receptor agonists, liver X receptor alpha inhibitors, fibroblast growth factor analogs/activators, dual GLP-1 and glucose-dependent insulinotropic peptide receptor analogs or agonists, thyroid hormone receptor (THR-β)-selective agonists, antioxidants, fibrosis-targeted treatment options, and their combinations, are being assessed for their potential incorporation into the armamentarium of NAFLD treatments.[20] Of note, some are also being tested in combination with either SGLT-2 inhibitors or GLP-1RAs.[20]

Therefore, it appears that such a combination would be of great value for patients with NAFLD and comorbidities, such as obesity, CVD, or even CKD (a simplified treatment approach is shown in Fig. 1). However, no studies have yet assessed the impact of such a combination on histological outcomes in patients with NAFLD and T2DM to confirm whether an SGLT-2 inhibitor/GLP-1RA combination might have beneficial synergistic effects on liver steatosis and fibrosis. Well-designed, prospective studies are required to answer this sound, scientific question. In addition, cost-effectiveness analyses are needed.

## Funding

None to declare.

## Conflict of interest

The authors have no conflict of interests related to this publication.

## Author contributions

DP and TM wrote the draft, DP critically revised the manuscript before submission.

## References

[1] Pappachan JM, Babu S, Krishnan B, Ravindran NC. Non-alcoholic Fatty Liver Disease: A Clinical Update. J Clin Transl Hepatol 2017;5(4):384–393. doi:10.14218/JCTH.2017.00013, PMID:29226105.
[2] Kumar R, Priyadarshi RN, Anand U. Non-alcoholic Fatty Liver Disease: Growing Burden, Adverse Outcomes and Associations. J Clin Transl Hepatol 2020;8(1):76–86. doi:10.14218/JCTH.2019.00051, PMID:32274348.
[3] Raff EJ, Kakati D, Bloomer JR, Shoreibah M, Rasheed K, Singal AK. Diabetes Mellitus Predicts Occurrence of Cirrhosis and Hepatocellular Cancer in Alcoholic Liver and Non-alcoholic Fatty Liver Diseases. J Clin Transl Hepatol 2015;3(1):9–16. doi:10.14218/JCTH.2015.00001, PMID:26356325.
[4] Mantovani A, Csermely A, Petracca G, Beatrice G, Corey KE, Simon TG, *et al*. Non-alcoholic fatty liver disease and risk of fatal and non-fatal cardiovascular events: an updated systematic review and meta-analysis. Lancet Gastroenterol Hepatol 2021;6(11):903–913. doi:10.1016/S2468-1253(21)00308-3, PMID:34555346.
[5] Mantovani A, Zaza G, Byrne CD, Lonardo A, Zoppini G, Bonora E, *et al*. Nonalcoholic fatty liver disease increases risk of incident chronic kidney disease: A systematic review and meta-analysis. Metabolism 2018;79:64–76. doi:10.1016/j.metabol.2017.11.003, PMID:29137912.
[6] Brown E, Heerspink HJL, Cuthbertson DJ, Wilding JPH. SGLT2 inhibitors and GLP-1 receptor agonists: established and emerging indications. Lancet 2021;398(10296):262–276. doi:10.1016/S0140-6736(21)00536-5, PMID:34216571.
[7] Snyder HS, Sakaan SA, March KL, Siddique O, Cholankeril R, Cummings

CD, *et al*. Non-alcoholic Fatty Liver Disease: A Review of Anti-diabetic Pharmacologic Therapies. J Clin Transl Hepatol 2018;6(2):168–174. doi:10.14218/JCTH.2017.00050, PMID:29951362.
[8] Kumar J, Memon RS, Shahid I, Rizwan T, Zaman M, Menezes RG, *et al*. Antidiabetic drugs and non-alcoholic fatty liver disease: A systematic review, meta-analysis and evidence map. Dig Liver Dis 2021;53(1):44–51. doi:10.1016/j.dld.2020.08.021, PMID:32912770.
[9] Ding C, Tang Y, Zhu W, Huang P, Lian P, Ran J, *et al*. Sodium-glucose cotransporter protein-2 inhibitors and glucagon-like peptide-1 receptor agonists versus thiazolidinediones for non-alcoholic fatty liver disease: A network meta-analysis. Acta Diabetol 2022;59(4):519–533. doi:10.1007/s00592-021-01830-7, PMID:34988690.
[10] Ng CH, Lin SY, Chin YH, Lee MH, Syn N, Goh XL, *et al*. Antidiabetic Medications for Type 2 Diabetics with Nonalcoholic Fatty Liver Disease: Evidence From a Network Meta-Analysis of Randomized Controlled Trials. Endocr Pract 2022;28(2):223–230. doi:10.1016/j.eprac.2021.09.013, PMID:34606980.
[11] Akuta N, Kawamura Y, Fujiyama S, Saito S, Muraishi N, Sezaki H, *et al*. Favorable impact of long-term SGLT2 inhibitor for NAFLD complicated by diabetes mellitus: A 5-year follow-up study. Hepatol Commun 2022. doi:10.1002/hep4.2005, PMID:35581956.
[12] Gao Y, Wei L, Zhang DD, Chen Y, Hou B. SGLT2 Inhibitors: A New Dawn for Recurrent/Refractory Cirrhotic Ascites. J Clin Transl Hepatol 2021;9(6):795–797. doi:10.14218/JCTH.2021.00418, PMID:34966642.
[13] Montalvo-Gordon I, Chi-Cervera LA, García-Tsao G. Sodium-Glucose Cotransporter 2 Inhibitors Ameliorate Ascites and Peripheral Edema in Patients With Cirrhosis and Diabetes. Hepatology 2020;72(5):1880–1882. doi:10.1002/hep.31270, PMID:32294260.
[14] Simon TG, Patorno E, Schneeweiss S. Glucagon-Like Peptide-1 Receptor Agonists and Hepatic Decompensation Events in Patients With Cirrhosis and Diabetes. Clin Gastroenterol Hepatol 2022;20(6):1382–1393.e19. doi:10.1016/j.cgh.2021.07.010, PMID:34256144.
[15] Mantsiou C, Karagiannis T, Kakotrichi P, Malandris K, Avgerinos I, Liakos A, *et al*. Glucagon-like peptide-1 receptor agonists and sodium-glucose co-transporter-2 inhibitors as combination therapy for type 2 diabetes: A systematic review and meta-analysis. Diabetes Obes Metab 2020;22(10):1857–1868. doi:10.1111/dom.14108, PMID:32476254.
[16] Patoulias D, Papadopoulos C, Karagiannis A, Doumas M. Which one should I choose, a glucagon-like peptide-1 receptor agonist or a sodium-glucose cotransporter 2 inhibitor? Or maybe both? Eur J Intern Med 2022;98:125–127.
[17] Zhu Y, Xu J, Zhang D, Mu X, Shi Y, Chen S, *et al*. Efficacy and Safety of GLP-1 Receptor Agonists in Patients With Type 2 Diabetes Mellitus and Non-Alcoholic Fatty Liver Disease: A Systematic Review and Meta-Analysis. Front Endocrinol (Lausanne) 2021;12:769069. doi:10.3389/fendo.2021.769069, PMID:34956080.
[18] Wei Q, Xu X, Guo L, Li J, Li L. Effect of SGLT2 Inhibitors on Type 2 Diabetes Mellitus With Non-Alcoholic Fatty Liver Disease: A Meta-Analysis of Randomized Controlled Trials. Front Endocrinol (Lausanne) 2021;12:635556. doi:10.3389/fendo.2021.635556, PMID:34220701.
[19] Ohki T, Isogawa A, Toda N, Tagawa K. Effectiveness of Ipragliflozin, a Sodium-Glucose Co-transporter 2 Inhibitor, as a Second-line Treatment for Non-Alcoholic Fatty Liver Disease Patients with Type 2 Diabetes Mellitus Who Do Not Respond to Incretin-Based Therapies Including Glucagon-like Peptide-1 Analogs and Dipeptidyl Peptidase-4 Inhibitors. Clin Drug Investig 2016;36(4):313–319. doi:10.1007/s40261-016-0383-1, PMID:26914659.
[20] Negi CK, Babica P, Bajard L, Bienertova-Vasku J, Tarantino G. Insights into the molecular targets and emerging pharmacotherapeutic interventions for nonalcoholic fatty liver disease. Metabolism 2022;126:154925. doi:10.1016/j.metabol.2021.154925, PMID:34740573.

*Journal of Clinical and Translational Hepatology* **2022** vol. 10(4) | 577–588
DOI: 10.14218/JCTH.2021.00289

Original Article

# Overexpression of Hepcidin Alleviates Steatohepatitis and Fibrosis in a Diet-induced Nonalcoholic Steatohepatitis

Hui Chen[1*], Wenshan Zhao[2,3], Xuzhen Yan[2,3], Tao Huang[2,3] and Aiting Yang[2,3,4*]

[1]*Digestive Department, Beijing Chaoyang Hospital, Capital Medical University, Beijing, China;* [2]*Experimental and Translational Research Center, Beijing Friendship Hospital, Capital Medical University, Beijing, China;* [3]*National Clinical Research Center of Digestive Diseases, Beijing, China;* [4]*Beijing Clinical Medicine Institute, Beijing, China*

**Received:** 17 July 2021 | **Revised:** 22 September 2021 | **Accepted:** 28 September 2021 | **Published:** 4 January 2022

## Abstract

***Background and Aims:*** Iron overload can contribute to the progression of nonalcoholic fatty liver disease (NAFLD) to nonalcoholic steatohepatitis (NASH). Hepcidin (Hamp), which is primarily synthesized in hepatocytes, is a key regulator of iron metabolism. However, the role of Hamp in NASH remains unclear. Therefore, we aimed to elucidate the role of Hamp in the pathophysiology of NASH. ***Methods:*** Male mice were fed a choline-deficient L-amino acid-defined (CDAA) diet for 16 weeks to establish the mouse NASH model. A choline-supplemented amino acid-defined (CSAA) diet was used as the control diet. Recombinant adeno-associated virus genome 2 serotype 8 vector expressing Hamp (rAAV2/8-Hamp) or its negative control (rAAV2/8-NC) was administered intravenously at week 8 of either the CDAA or CSAA diet. ***Results:*** rAAV2/8-Hamp treatment markedly decreased liver weight and improved hepatic steatosis in the CDAA-fed mice, accompanied by changes in lipogenesis-related genes and adiponectin expression. Compared with the control group, rAAV2/8-Hamp therapy attenuated liver damage, with mice exhibiting reduced histological NAFLD inflammation and fibrosis, as well as lower levels of liver enzymes. Moreover, α-smooth muscle actin-positive activated hepatic stellate cells (HSCs) and CD68-postive macrophages increased in number in the CDAA-fed mice, which was reversed by rAAV2/8-Hamp treatment. Consistent with the *in vivo* findings, overexpression of Hamp increased adiponectin expression in hepatocytes and Hamp treatment inhibited HSC activation. ***Conclusions:*** Overexpression of Hamp using rAAV2/8-Hamp robustly attenuated liver steatohepatitis, inflammation, and fibrosis in an animal model of NASH, suggesting a potential therapeutic role for Hamp.

**Citation of this article:** Chen H, Zhao W, Yan X, Huang T, Yang A. Overexpression of Hepcidin Alleviates Steatohepatitis and Fibrosis in a Diet-induced Nonalcoholic Steatohepatitis. J Clin Transl Hepatol 2022;10(4):577–588. doi: 10.14218/JCTH.2021.00289.

**Keywords:** Liver fibrosis; Hepatic stellate cell; Hepcidin; NASH; CDAA.

**Abbreviations:** ALT, alanine aminotransferase; AST, aspartate aminotransferase; CDAA, choline-deficient L-amino acid-defined; CSAA, choline-supplemented amino acid-defined; Hb, Hemoglobin; HSCs, hepatic stellate cells; NAFLD, nonalcoholic fatty liver disease; NASH, nonalcoholic steatohepatitis; rAAV, recombinant adeno-associated virus.

***Correspondence to:** Hui Chen, Digestive Department, Beijing Chaoyang Hospital, Capital Medical University, No. 5 Jingyuan Road, Shijingshan District, Beijing 100043, China. Tel: +86-10-51718484, Fax: +86-10-83165944, E-mail: chenhui_0516@126.com. Aiting Yang, Experimental and Translational Research Center, Beijing Friendship Hospital, Capital Medical University, No. 95 Yong'an Road, Xicheng District, Beijing 100050, China. ORCID: https://orcid.org/0000-0002-5671-696X. Tel: +86-10-63139311, Fax: +86-10-83165944, E-mail: yangaiting168@126.com

## Introduction

Nonalcoholic fatty liver disease (NAFLD) is one of the most prevalent liver diseases worldwide. Hepatic manifestation of metabolic syndrome associated with NAFLD is highly prevalent in obese and diabetic inidividuals.[1,2] Nonalcoholic steatohepatitis (NASH) is a subtype of NAFLD that can progress to cirrhosis, liver failure, hepatocellular carcinoma, and death. Despite the severe outcomes of NASH, there are no known efficacious treatments for NASH-related advanced fibrosis. Thus, there is an urgent need to develop new therapies.[3–5]

The pathogenesis of liver inflammation and fibrosis in patients with NAFLD is not completely understood. Other than insulin resistance, iron overload has been considered an indicator of inflammation and fibrosis. Accumulating evidence suggests that approximately one-third of USA and Chinese patients with biopsy-proven NAFLD develop hepatic iron stores.[6–8] Increased iron stores could be of pathogenic importance in NAFLD, since elevated iron levels can increase the risk of hepatocyte ballooning, inflammation, and fibrosis, all of which are characteristics of NASH. Iron reduction therapy could potentially reduce steatosis and insulin resistance, as well as serum transaminase activity in patients with NASH/NAFLD.[9–11] However, treatment of iron overload presents some challenges. A meta-analysis showed that iron depletion does not significantly improve indices of insulin resistance, liver enzyme levels, or liver histology compared to lifestyle changes alone in patients with NAFLD.[12]

Hepcidin (Hamp) is an acute-phase reactant produced primarily in the liver, that was first identified as an antimicrobial peptide and was subsequently shown to play a central role in regulating iron homeostasis. There is increasing evidence to suggest that its synthesis is regulated in response to inflammation, hypoxia, and iron homeostasis.[13,14] Taking this into account, the increased Hamp levels in NAFLD are most likely induced by elevated inflammatory cytokines; therefore, there has been great interest in evaluating Hamp as a potential non-invasive biomarker of NAFLD. Of note, serum Hamp levels have previously been reported to be

correlated with obesity but not liver disease.[15–17] Despite the fact that the mechanism through which Hamp induces NAFLD remains uncertain, excessive cytokines, such as interleukin (IL) 6, have a core function in Hamp production. More interestingly, Tsutsumi *et al*.[18] recently found that there was a significant inverse correlation between Hamp immunoreactivity and fibrosis in pediatric NAFLD patients, suggesting that these patients experienced a reduction in the Hamp-producing ability of the liver in response to iron levels, leading to subsequent fibrosis.

Our preliminary data also demonstrated that low levels of Hamp are associated with murine carbon tetrachloride ($CCl_4$)-induced liver fibrosis, leading to the hypothesis that Hamp might be effective in treating NASH-related fibrosis. Therefore, we sought to determine if Hamp contributes to the severity of steatosis, inflammation, and fibrosis in a mouse model of NASH induced by a choline-deficient l-amino acid-defined (CDAA) diet. We used a recombinant adeno-associated virus genome 2 serotype 8 (rAAV2/8) vector to efficiently transfect a Hamp overexpressing plasmid into liver cells to investigate the effects of Hamp on NASH-related inflammation and fibrosis in a mouse model.

## Methods

### *Experimental animals*

This study was approved by the Institutional Animal Care and Usage Committee of the Beijing Friendship Hospital, Capital Medical University. C57BL/6J mice were fed a CDAA diet (M10530i; Moldiets Co. Ltd., Chengdu, China) for 16 weeks to induce NASH. The control group received a CSAA diet (M10530Ci; Moldiets). Recombinant adeno-associated virus subtype 2/8 vector expressing Hamp (rAAV2/8-Hamp) or its negative control vector (rAAV2/8-NC) were amplified by Obio (Shanghai, China). Mice were treated with either the rAAV2/8-NC or rAAV2/8-Hamp via tail vein injection at a dose of $3\times10^{11}$ genome copies/mouse after 8 weeks of being fed either the CDAA or CSAA diet. The mice were housed on a 12 h light/dark cycle, with controlled temperature (23±2°C) at 40–60% humidity.

Food intake and body weight were monitored weekly. After a total of 16 weeks on the CDAA or CSAA diet, animals were euthanized and sacrificed. Serum was collected and frozen, and the livers and spleens were dissected, weighed, and snap-frozen for further analysis.

### *Hamp treatment*

The rat hepatic stellate cell (HSC) line-T6 was a gift from Dr. Scott Friedman (Mount Sinai Medical Center, New York, NY, USA). T6 cells were plated in Dulbecco's modified Eagle medium (DMEM) supplemented with 10% (v/v) fetal bovine serum (FBS). When cells reached 80–90% confluence, they were detached using trypsin and reseeded at $2\times10^5$ per well in a 6-well plate. T6 cells were cultured overnight in serum-free medium before experimentation. Cells were stimulated with Hamp (10 ng/mL or 100 ng/mL; Peptide Institute, Osaka, Japan) and cultured for 48 h. Control cells were left unstimulated.

### *Generation of Hamp-overexpressing hepatocyte cell line*

AML12 mouse hepatocytes (American Type Culture Collection, Manassas, VA, USA) were cultured in DMEM/F12 with 10% FBS supplemented with 1% Insulin-Transferrin-Selenium (ITS) (51500056; Invitrogen, Waltham, MA, USA), 40 ng/mL dexamethasone, and 1% penicillin streptomycin mixture. The plRES2-EGFP-NC and plRES2-EGFP-Hamp plasmids were transfected into AML12 cells using the EndoFectin™ Max transfection reagent (GeneCopoeia, Rockville, MD, USA) following the manufacturer's instructions. Briefly, AML12 cells ($5\times10^4$ per well) were seeded into a 12-well plate. After 24 h, the cells were transfected with either 2 or 4 μg of the plasmids using the EndoFectin™ Max transfection reagent.

### *Quantitative real-time (q)PCR analysis*

Total mRNA was extracted using the TRIzol reagent (Sigma-Aldrich, St. Louis, MO, USA) according to the manufacturer's protocol.[19] Reverse transcription was performed with 1 μg total RNA using the SuperScript™ VILO™ Master Mix (Invitrogen). The SYBR Green Real-time PCR Master Mix (Invitrogen) was used for qPCR. Primers used for qPCR are listed in Table 1. Glyceraldehyde-3-phosphate dehydrogenase (GAPDH) was used to normalize the PCR results, and the ΔΔCt method was used for quantification.

### *Western blot analysis*

Total cell lysates were homogenized in tissue lysis buffer (FNN0071; Invitrogen) supplemented with protease and phosphatase inhibitors (Roche, Basel, Switzerland).[20] Proteins were resolved by SDS-PAGE and transferred to nitrocellulose membranes (Amersham Biosciences, Buckinghamshire, UK). Membranes were then incubated with primary antibodies against alpha-smooth muscle actin (αSMA) (diluted 1:500; Abcam, Cambridge, UK), tissue inhibitor of metalloproteinase (TIMP)1 (diluted 1:500; Invitrogen), and β-actin (diluted 1:2,000; Peprotech, Rocky Hill, NJ, USA) overnight at 4°C. On the following day, the membranes were incubated with the appropriate secondary antibodies (Cell Signaling Technology, Danvers, MA, USA) and proteins were visualized using a chemiluminescent substrate (Invitrogen).

### *Histopathological analysis*

Liver samples were fixed with neutral-buffered formalin, embedded in paraffin, and cut into 4-μm thick sections that were stained with either hematoxylin and eosin (HE) or Sirius Red (SR), or prepared for immunohistochemistry (IHC) analysis of αSMA and CD68 expression.

Histological assessment and scoring were performed by a pathologist blinded to the study. Steatosis and lobular inflammation scoring on liver histology were performed using the clinical criteria outlined by Kleiner *et al*.[21] Activated HSCs and total macrophages were detected using an anti-αSMA antibody (diluted 1:200; Abcam) and an anti-CD68 antibody (diluted 1:500; Invitrogen), respectively. Morphometric quantification of SR staining (percentage of area) was performed at 200× in 10 random fields per mouse from five individual animals using ImageJ software. αSMA- and CD68-positive cells were quantified as the number of positively stained cells per high-power field (HPF).

For Oil-red O staining, optimal cutting temperature-embedded frozen tissue was sectioned at 7 μm and fixed in 10% neutral buffered formalin. After washing with distilled water, dried slides were subsequently incubated with 60% isopropanol and Oil-red O solution, then rinsed with 60% isopropanol solution and distilled water and mounted with glycerin. Morphometric quantification of Oil-red O staining (percentage of area) was performed at 200× in 10 random fields per

**Table 1. Primers used for qPCR**

| Gene | Primer sequences | Product size | Accession No |
|---|---|---|---|
| Hamp | F: 5′-CAATGTCTGCCCTGCTTTCT-3′ | 113 bp | NM_032541.2 |
| | R: 5′-TCTCCTGCTTCTCCTCCTTG-3′ | | |
| αSMA | F: 5′-GATGAAGCCCAGAGCAAGAG-3′ | 87 bp | XM_021152572.1 |
| | R: 5′-CTTTTCCATGTCGTCCCAGT-3′ | | |
| COL1A1 | F: 5′-GAGCGGAGAGTACTGGATCG-3′ | 158 bp | NM_007742.4 |
| | R: 5′-GCTTCTTTTCCTTGGGGTTC-3′ | | |
| CCR2 | F: 5′-GGCTCAGCCAGATGCAGTTAA-3′ | 76 bp | NM_011333.3 |
| | R: 5′-CCTACTCATTGGGATCATCTTGCT -3′ | | |
| TGFβ-1 | F: 5′-GAGGTCACCCGCGTGCTA-3′ | 70 bp | NM_011577.2 |
| | R: 5′-TGTGTGAGATGTCTTTGGTTTTCTC-3′ | | |
| Il10 | F: 5′-GCTCTTACTGACTGGCATGAG-3′ | 105 bp | NM_010548.2 |
| | R: 5′-CGCAGCTCTAGGAGCATGTG-3′ | | |
| TNFα | F: 5′-TCCCAGGTTCTCTTCAAGGGA-3′ | 51 bp | NM_001278601.1 |
| | R: 5′-GGTGAGGAGCACGTAGTCGG-3′ | | |
| TIMP-1 | F: 5′-CCAGAGCCGTCACTTTGCTT-3′ | 126 bp | NM_001294280.2 |
| | R: 5′-AGGAAAAGTAGACAGTGTTCAGGCTT -3′ | | |
| SREBP1c | F: 5′-TGGAGACATCGCAAACAAG-3′ | 274 bp | XM_030245748.1 |
| | R: 5′-GGTAGACAACAGCCGCATC-3′ | | |
| ChREBP | F: 5′-AGATGGAGAACCGACGTATCA-3′ | 104 bp | NM_001359237.1 |
| | R: 5′-ACTGAGCGTGCTGACAAGTC-3′ | | |
| Acc | F: 5′-GATGAACCATCTCCGTTGGC-3′ | 65 bp | XM_030245463.1 |
| | R: 5′-GACCCAATTATGAATCGGGAGTG-3′ | | |
| Scd1 | F: 5′-TGACCTGAAAGCCGAGAA-3′ | 342 bp | NM_009127.4 |
| | R: 5′-ATGTGCCAGCGGTACTCA-3′ | | |
| Adiponectin | F: 5′-TGTTCCTCTTAATCCTGCCCA-3′ | 104 bp | NM_009605.5 |
| | R: 5′-CCAACCTGCACAAGTTCCCTT-3′ | | |
| GAPDH | F: 5′-TCCACTCACGGCAAATTCAAC-3′ | 89 bp | XM_017321385.1 |
| | R: 5′-CGCTCCTGGAAGATGGTGATG-3′ | | |

αSMA, smooth muscle alpha-actin; COL1A1, collagen type I alpha 1 chain; CCR2, C-C motif chemokine receptor 2; TGFβ-1, transforming growth factor-beta 1; Il10, interleukin 10; TNF, tumor necrosis factor; TIMP-1, tissue inhibitor of metalloproteinase 1; SREBP1c, sterol-regulatory element binding protein-1c; ChREBP, carbohydrate response element binding protein; Acc, acetyl coenzyme A carboxylase; Scd1, steatoyl-coenzyme A desaturase 1; GAPDH, glyceraldehyde 3-phosphate dehydrogenase.

mouse from five individual animals using ImageJ software.

### *Serum biochemistry*

Serum samples were stored at −80°C until analyses could be performed. Serum aspartate aminotransferase (AST), alanine aminotransferase (ALT), and iron were measured using Olympus Beckman Coulter AU480 automatic biochemistry analysis system reagents (InTec Products, Shenzhen, China) provided by the manufacturer. Hemoglobin (Hb) levels were measured using the Mindray Bc 3000 Automatic Blood Cell Analyzer according to the manufacturer's recommendations.

### *Statistical analysis*

Data were expressed as mean±standard error of the mean (SEM) and were analyzed using GraphPad Prism software (v.5; GraphPad Software, La Jolla, CA, USA). A Student's *t*-test was used to compare values obtained from two groups. Data from multiple groups were compared using a one-way ANOVA followed by the Tukey's post-hoc test. Finally, *p*-values <0.05 were considered significant.

## Results

### *rAAV2/8-Hamp treatment increased Hamp expression in CDAA-induced NASH*

To investigate the anti-steatotic effects of Hamp, we fed mice a CDAA diet for 16 weeks, which is commonly used to induce steatosis in mouse models of NASH. The mice were administered a total dose of $3\times10^{11}$ genome copies per mouse of either rAAV2/8-Hamp or rAAV2/8-NC after 8 weeks of either

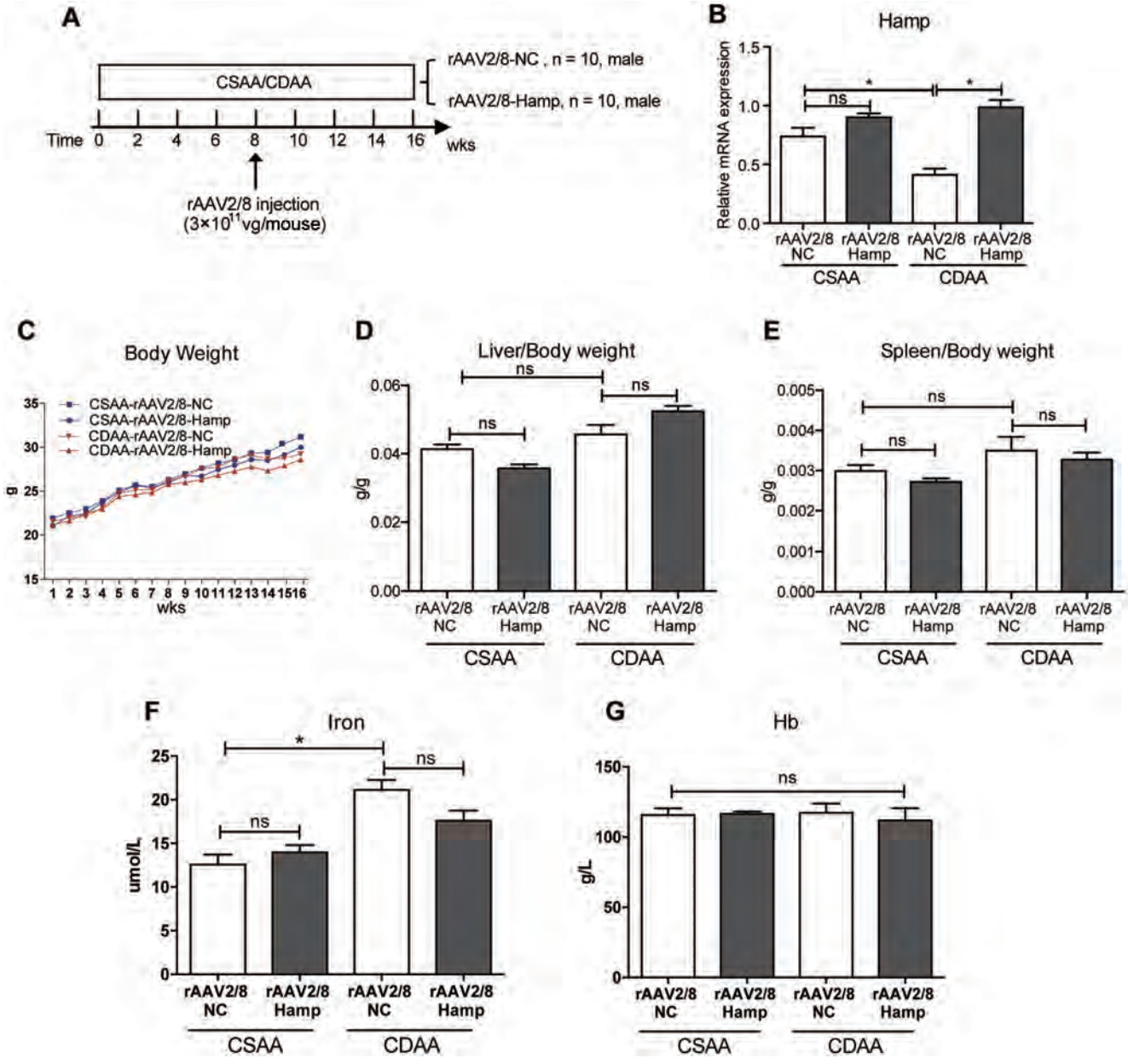


**Fig. 1. Hamp levels increased following rAAV2/8-Hamp treatment in mice fed CDAA or CSAA diets for 16 weeks.** (A) Male mice (8 weeks-old) were fed either the CSAA or CDAA diet for 16 weeks with rAAV2/8-NC or rAAV2/8-Hamp treatment at week 8 ($n$=10 per group). (B) Hamp gene expression, (C) growth curve, (D) relative liver mass, (E) relative spleen mass, (F) serum iron levels, and (G) Hb levels in mice fed either the CSAA or CDAA diet for 16 weeks. Data represent the mean±SEM of at least 10 animals per group. CDAA, choline-deficient L-amino acid-defined; CSAA, choline-supplemented amino acid-defined; rAAV, recombinant adeno-associated virus; NC, negative control; Hb, Hemoglobin.

the CDAA or control CSAA diet (Fig. 1A). We found that Hamp mRNA levels were significantly lower in the CDAA-fed mice compared to the CSAA-fed mice, as expected. We also found that Hamp was increased in all liver tissues from mice injected with rAAV2/8-Hamp compared to rAAV2/8-NC (Fig. 1B).

### *rAAV2/8-Hamp treatment reduced body weight gain without affecting iron status and Hb levels*

Both the CSAA and CDAA diets have been shown to cause a progressive and time-dependent increase in body weight. In our model, the CDAA-fed mice gained less body weight (~6% less) compared to the CSAA-fed mice after 16 weeks. It is worth noting that rAAV2/8-Hamp treatment decreased body weight gain in the control group (~5% lower) (Fig. 1C). Food intake (data not shown) following rAAV2/8-Hamp and rAAV2/8-NC treatment in both the CDAA- and CSAA-fed mice increased at similar rates and there were no differences in relative liver weight and spleen weight between the two groups (Fig. 1D–E).

Hamp is a master regulator of systemic iron homeostasis, and therefore tightly controls erythrocyte production. We measured serum iron and Hb levels among the four

groups of mice. Serum iron levels were significantly higher in the CDAA-fed mice compared to the CSAA-fed mice, but rAAV2/8-Hamp treatment did not significantly decrease serum iron levels compared to rAAV2/8-NC treatment in either the CDAA- or CSAA-fed mice (Fig. 1F). Hb levels were similar among the four groups (Fig. 1G). Our data suggest that overexpression of Hamp in liver tissue does not induce systemic iron overload or affect Hb levels.

### *rAAV2/8-Hamp treatment reversed steatosis in CDAA-fed mice*

We next determined whether increased Hamp expression following rAAV2/8-Hamp transduction reversed CDAA-induced hepatic steatosis. HE staining showed evidence of hepatic steatosis (primarily as micro- and macro-steatosis) in the CDAA-fed mice, and rAAV2/8-Hamp treatment remarkably decreased the hepatic lipid deposition in the CDAA-fed mice compared to the rAAV2/8-NC treatment (Fig. 2A). The semi-quantitative steatosis data were confirmed using lipid morphometry on Oil-red O stained liver sections; we observed an approximate three-fold decrease in the rAAV2/8-Hamp treatment group compared to the rAAV2/8-NC treatment group of the CDAA-fed mice (54.34±6.14% vs. 18.91±2.42%, respectively; $p<0.05$) (Fig. 2B). In addition, the steatosis score was lower in the rAAV2/8-Hamp treatment group compared to the rAAV2/8-NC treatment group (2.80±0.42 vs. 1.70±0.67, respectively; $p<0.05$) (Fig. 2C).

The CSAA-fed mice group showed significant glucose intolerance compared to that of the CDAA-fed mice group after a 16-week feeding. rAAV2/8-Hamp treatment significantly improved oral glucose tolerance at 60, 90, and 120 m after gavage with glucose in the CSAA group; however, there was no difference between rAAV2/8-Hamp and rAAV2/8-NC administration in the CDAA group. These results indicate that Hamp effectively attenuated CSAA-induced changes in metabolic parameters (Fig. 2D).

### *rAAV2/8-Hamp treatment modulates the expression of lipogenesis-related genes*

To further explore the underlying mechanisms of steatohepatitis, we determined the difference in lipid metabolism following rAAV2/8-Hamp treatment in both the CDAA- and CSAA-fed mice. Compared to the CSAA diet, the CDAA diet significantly down-regulated the expression of genes involved in *de novo* lipogenesis. These genes included carbohydrate response element binding protein (ChREBP), sterol regulatory binding protein 1c (SREBP1c), Stearoyl-CoA desaturase 1 (Scd1), acetyl-CoA carboxylase (Acc), and adiponectin. rAAV2/8-Hamp treatment down-regulated, although not significantly, the expression of these lipogenesis-related genes in the CSAA-fed mice. In contrast, rAAV2/8-Hamp treatment significantly up-regulated the expression of ChREBP and SREBP1c in the CDAA-fed mice but had no effect on the expression of Scd1 and Acc1 between the two groups (Fig. 3E–H). Interestingly, rAAV2/8-Hamp treatment increased adiponectin expression in the CDAA-fed mice compared to the rAAV2/8-NC treatment (Fig. 3I).

### *Hamp overexpression modulated adiponectin expression in AML12 cells*

To further evaluate the role of Hamp in hepatocyte adiponectin expression, we transfected mouse hepatocyte AML12 cells with either the pIRES2-Hamp or pIRES2-NC plasmid (Fig. 3A). Consistent with the *in vivo* study, we found that expression of adiponectin was dramatically elevated in the AML12 cells transfected with pIRES2-Hamp compared to pIRES2-NC (Fig. 3B–C).

### *rAAV2/8-Hamp treatment suppressed liver inflammation in CDAA-fed mice*

We next analyzed liver inflammation in the CDAA- and CSAA-fed mice treated with rAAV2/8-Hamp after 16 weeks. Immunostaining analysis of CD68, a well-established marker of activated macrophages, showed that CD68 expression was significantly increased in the CDAA-fed mice compared to the CSAA-fed mice. Treatment with rAAV2/8-Hamp significantly attenuated CDAA-induced macrophage infiltration and decreased the inflammation score (Fig. 4A–C).

Aspartate aminotransferase (AST) and alanine aminotransferase (ALT) activity significantly increased in the CDAA-fed mice compared to the CSAA-fed mice. Treatment with rAAV2/8-Hamp in the CDAA-fed mice significantly decreased the serum ALT and AST levels compared to the rAAV2/8-NC treatment (Fig. 4D–E).

In line with these findings, livers from the CDAA-fed mice had increased mRNA levels of chemokine (C-C motif) receptor 2 (CCR2) and tumor necrosis factor alpha (TNFα) compared to the CSAA-fed mice, whereas expression of these genes was suppressed in CDAA-fed mice treated with rAAV2/8-Hamp (Fig. 4F–G). The mRNA levels of Il10, a potent anti-inflammatory cytokine, were significantly higher in the livers of the CDAA-fed mice compared to the CSAA-fed mice, and expression of Il10 was slightly increased in the CDAA-fed mice treated with rAAV2/8-Hamp (Fig. 4H).

### *rAAV2/8-Hamp treatment ameliorated liver fibrosis in CDAA-fed mice*

Finally, we evaluated liver fibrosis in the CDAA- and CSAA-fed mice treated with rAAV2/8-Hamp after 16 weeks. Collagen deposition and HSC activation were significantly increased in the CDAA-fed mice compared to the CSAA-fed mice, and rAAV2/8-Hamp treatment reduced these fibrosis markers in the CDAA-fed mice, as assessed by SR staining and IHC detection of αSMA (Fig. 5A–C). Similarly, livers from CDAA-fed mice had increased mRNA levels of COL1A1, αSMA, and TIMP-1 compared to CSAA-fed mice, and rAAV2/8-Hamp treatment suppressed expression of these genes in the CDAA-fed mice (Fig. 5D–F).

### *Hamp supplementation showed anti-fibrotic effects in HSCs in vitro*

Considering the major pathophysiological role that HSCs have in fibrogenesis, we investigated the effect of Hamp in cultured HSC T6 cells. Specifically, we measured the expression of fibrogenetic genes (αSMA, TIMP-1, COL1A1, and transforming growth factor beta 1 [TGFβ-1]). Hamp (10 and 100 ng/mL) dose-dependently and significantly reduced the mRNA levels of fibrogenetic genes after 48 h of incubation compared to unstimulated HSCs (Fig. 6A–D). Reduction of αSMA and TIMP1 were also confirmed at the protein level, as determined by quantitative western blot analysis (Fig. 6E).

## Discussion

Iron-load is prevalent in a third of NAFLD patients and can

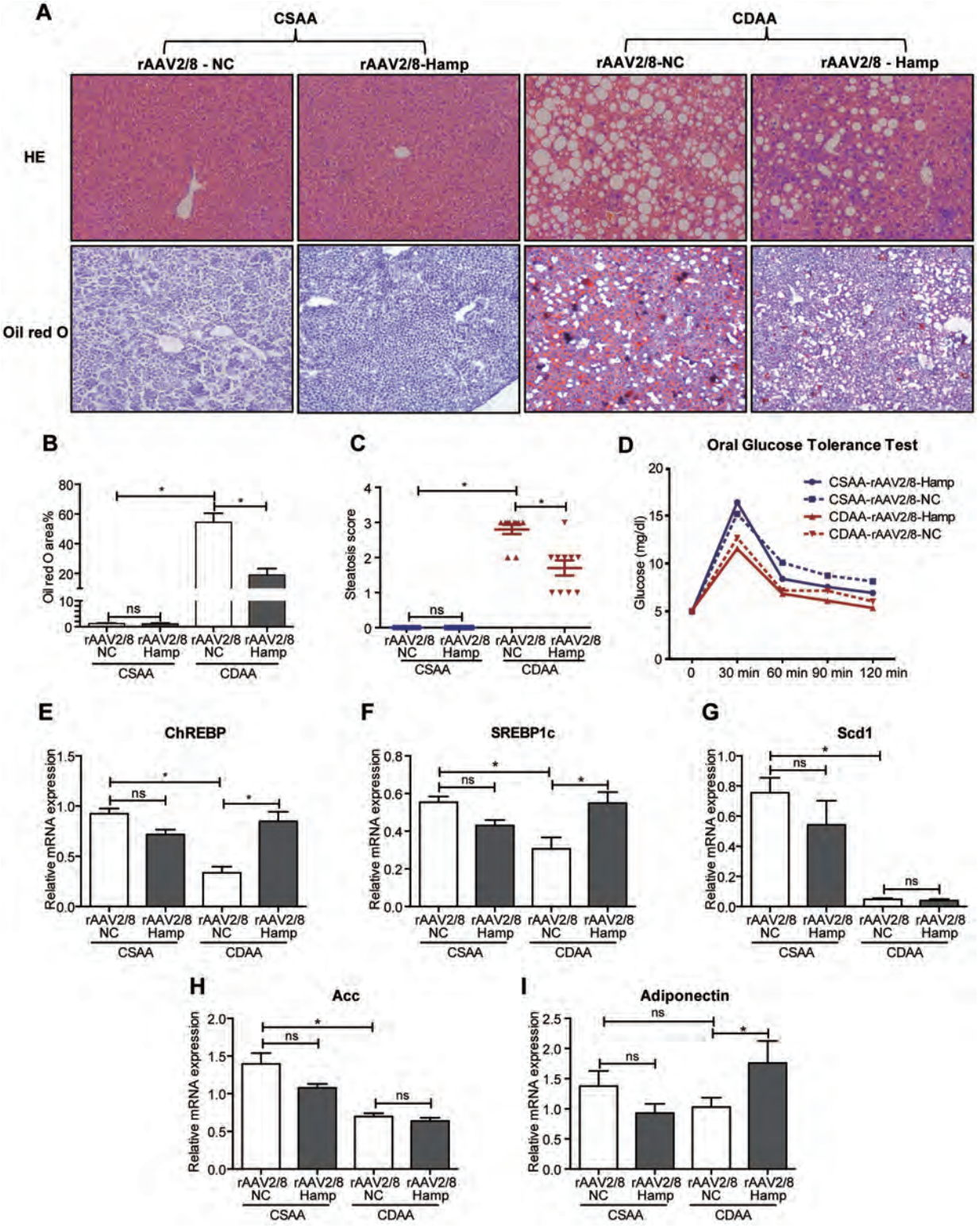


**Fig. 2. rAAV2/8-Hamp treatment showed anti-steatotic properties in CDAA-fed mice.** (A) Representative HE (original magnification 200×) and Oil-red O staining images (original magnification 100×) in liver sections of mice treated with rAAV2/8-Hamp or rAAV2/8-NC for up to 16 weeks. (B) Quantification of Oil-red O staining images of mice fed either the CDAA or CSAA diet. (C) Liver steatosis scores. (D) Oral glucose tolerance test. (E–I) Hepatic transcript levels of ChREBP, SREBP1c, Scd1, Acc, and adiponectin in mice fed either the CDAA or CSAA diet for 16 weeks. Data represent the mean±SEM of at least 10 animals per group. HE, hematoxylin-eosin; CDAA, choline-deficient L-amino acid-defined; CSAA, choline-supplemented amino acid-defined; rAAV, recombinant adeno-associated virus; ChREBP, carbohydrate response element binding protein; SREBP1c, sterol-regulatory element binding protein-1c; Scd1, steatoyl-coenzyme A desaturase 1; Acc, acetyl coenzyme A carboxylase.

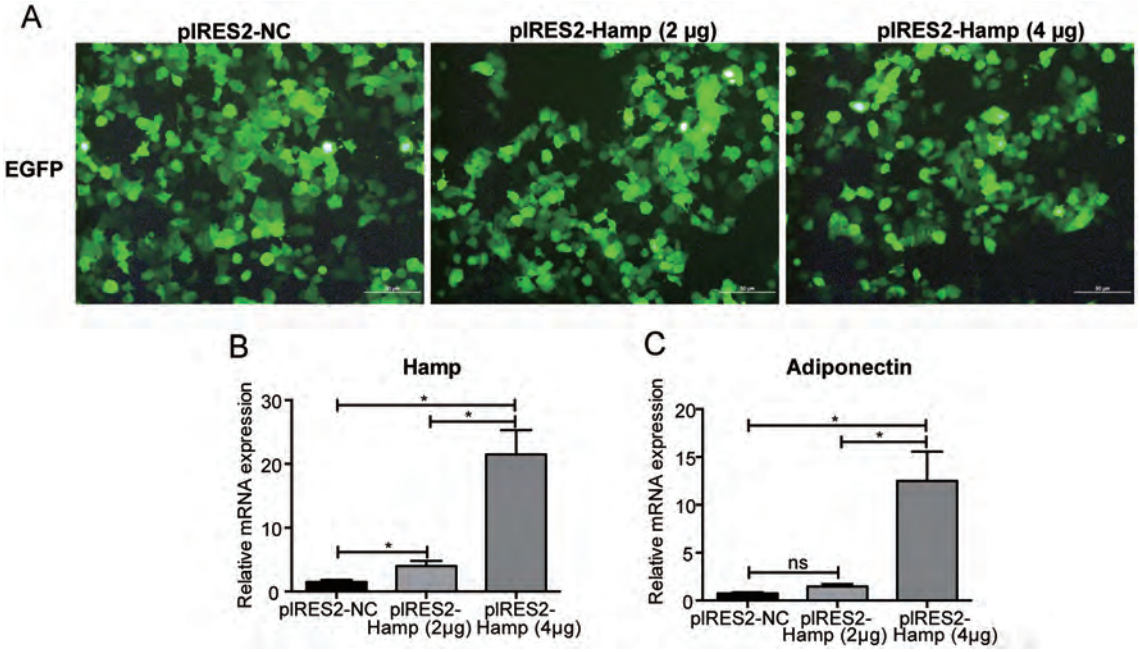


**Fig. 3. Hamp overexpression modulated adiponectin expression in AML12 cells.** AML12 hepatocytes were transduced with either the Hamp overexpression plasmid or the NC plasmid. (A) Transfection efficiency was visualized using fluorescence microscopy. (B, C) Transcript levels of Hamp and adiponectin. Data represent the mean±SEM. NC, negative control.

accelerate the progression of steatosis, fibrosis, cirrhosis, and hepatocellular carcinoma. As such, iron removal therapy has become a potential treatment strategy for NASH.[6,7] Given its role in regulating iron homeostasis, Hamp has gained attention as a promising therapeutic agent that can remove liver iron stores.[13,14] In the present study, our data showed that rAAV2/8-Hamp treatment significantly suppressed CDAA diet-induced steatosis, hepatic inflammation, and subsequent liver fibrosis in mice.

A choline-deficient diet can increase the onset of steatohepatitis features and fibrosis in mice, similar to patients with rapid NASH progression. Since our main focus is understanding how to best treat NASH-related fibrosis, we established the CDAA mouse model to best mirror pathology and pathogenesis of human NASH. In agreement with previous studies, the CDAA diet resulted in moderate hepatic lipoapoptosis, liver inflammation, and fibrosis, while the CSAA diet led to severe insulin resistance and absence of inflammation and fibrosis.[22–24] Mice on the CDAA developed macrovesicular steatosis in the liver, but the CDAA-fed mice developed a metabolic profile opposite to what is observed in human disease. We found that the CDAA diet significantly down-regulated the expression of genes involved in fatty acid synthesis, which might result from compensatory hepatic uptake of serum lipids or by impairment in very low-density lipoprotein secretion from the liver. NAFLD in patients has a complex and heterogeneous pathogenesis, thus it should be pointed out that animal models of NAFLD may not recapitulate all characteristics of human disease.

In our study, we first found that Hamp expression was significantly down-regulated and that iron stores were increased in the CDAA-fed mice, suggesting an important role for Hamp in the pathogenesis of NASH. Hamp is mostly produced by hepatocytes in response to iron loading in cells. As iron loads increase, Hamp expression also increases in hepatocytes, resulting in elevated serum Hamp level.[25] Patients with chronic liver diseases have evidence of liver dysfunction and anemia associated with inflammation but surprisingly also have lower serum Hamp levels compared to control subjects.[26] Similar findings have been reported in alcoholic chronic liver diseases,[27] chronic hepatitis C,[28,29] hepatitis B virus-related cirrhosis,[30–33] and in autoimmune liver diseases.[34] Hamp levels in NAFLD are difficult to interpret, since Hamp expression is likely to be regulated by complex mechanisms in response to diverse pathophysiological stimuli. In the later stages of NAFLD/NASH, serum Hamp levels are not suppressed, and the levels eventually decrease in NAFLD with advanced fibrosis, similar to other liver diseases.[18]

Although accumulating evidence shows that serum Hamp levels and iron metabolism are related to serum markers of steatosis, inflammation, fibrosis, and insulin resistance, no study has investigated if Hamp supplementation could be used as a therapeutic strategy for NASH. Here, we first investigated the possible effect of rAAV2/8-Hamp on CDAA diet-induced hepatic steatosis in mice. Our data demonstrated that treatment with rAAV2/8 significantly attenuated CDAA diet-induced hepatic steatosis without affecting iron and Hb levels. While the CDAA diet is a well-established nutritional NAFLD model, the metabolic profile of this diet does not completely reflect all properties of NAFLD. Specifically, other aspects of metabolic dysregulation are not necessarily accounted for because hepatic lipid accumulation in the model is mainly due to impaired secretion of very low-density lipoprotein. Our study showed that overexpression of Hamp corrected the abnormal expression of SREBP1c and ChREBP. This could partially explain the mechanism by which rAAV2/8-Hamp treatment can suppress CDAA diet-induced hepatic steatosis and regulate lipid metabolism. Furthermore, we noted that rAAV2/8-Hamp treatment normalized the loss in body weight in the CDAA diet-induced NASH model.

Increased inflammation is a hallmark of NASH. Thus, controlling liver inflammation may be a potential strategy to treat NASH. Macrophages are key cells that induce the release of inflammatory mediators, such as TNFα, CCR2, and

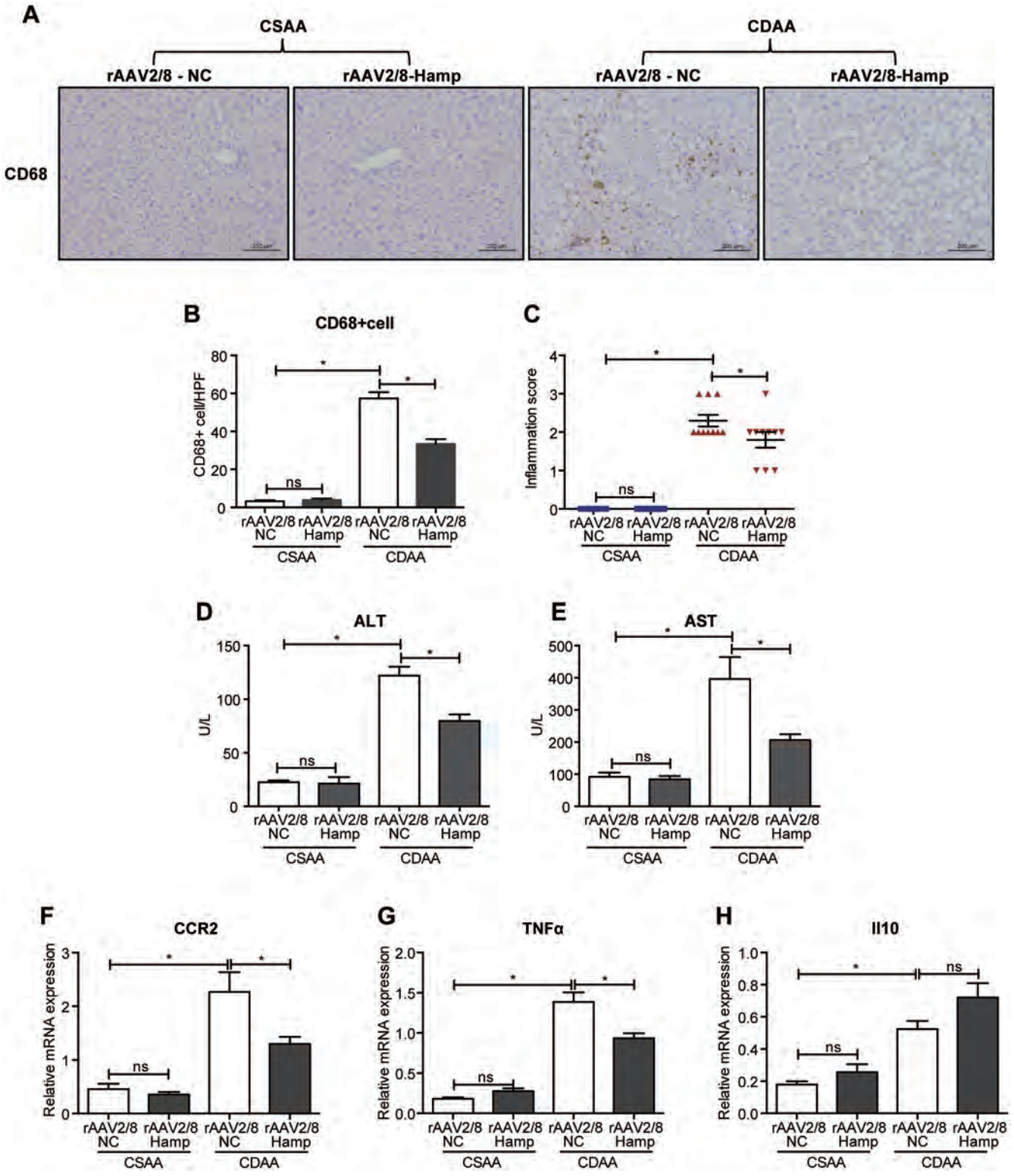


**Fig. 4. rAAV2/8-Hamp treatment suppressed hepatic inflammation in CDAA-fed mice.** (A) Representative CD68-positive macrophages (original magnification 200×) in liver sections of mice treated with rAAV2/8-Hamp or rAAV2/8-NC. (B) Quantification of images of mice fed either the CDAA or CSAA diet. rAAV2/8-Hamp treatment decreased (D) serum ALT and (E) AST levels in mice fed a CDAA diet compared with rAAV2/8-NC treatment. (F–H) Transcript levels of CCR2, TNFα and Il10. Data represent the mean±SEM of at least 10 animals per group. CDAA, choline-deficient L-amino acid-defined; CSAA, choline-supplemented amino acid-defined; rAAV, recombinant adeno-associated virus; ALT, alanine aminotransferase; AST, aspartate aminotransferase; NC, negative control; CCR2, C-C Motif chemokine receptor 2; TNF, tumor necrosis factor; Il10, interleukin 10.

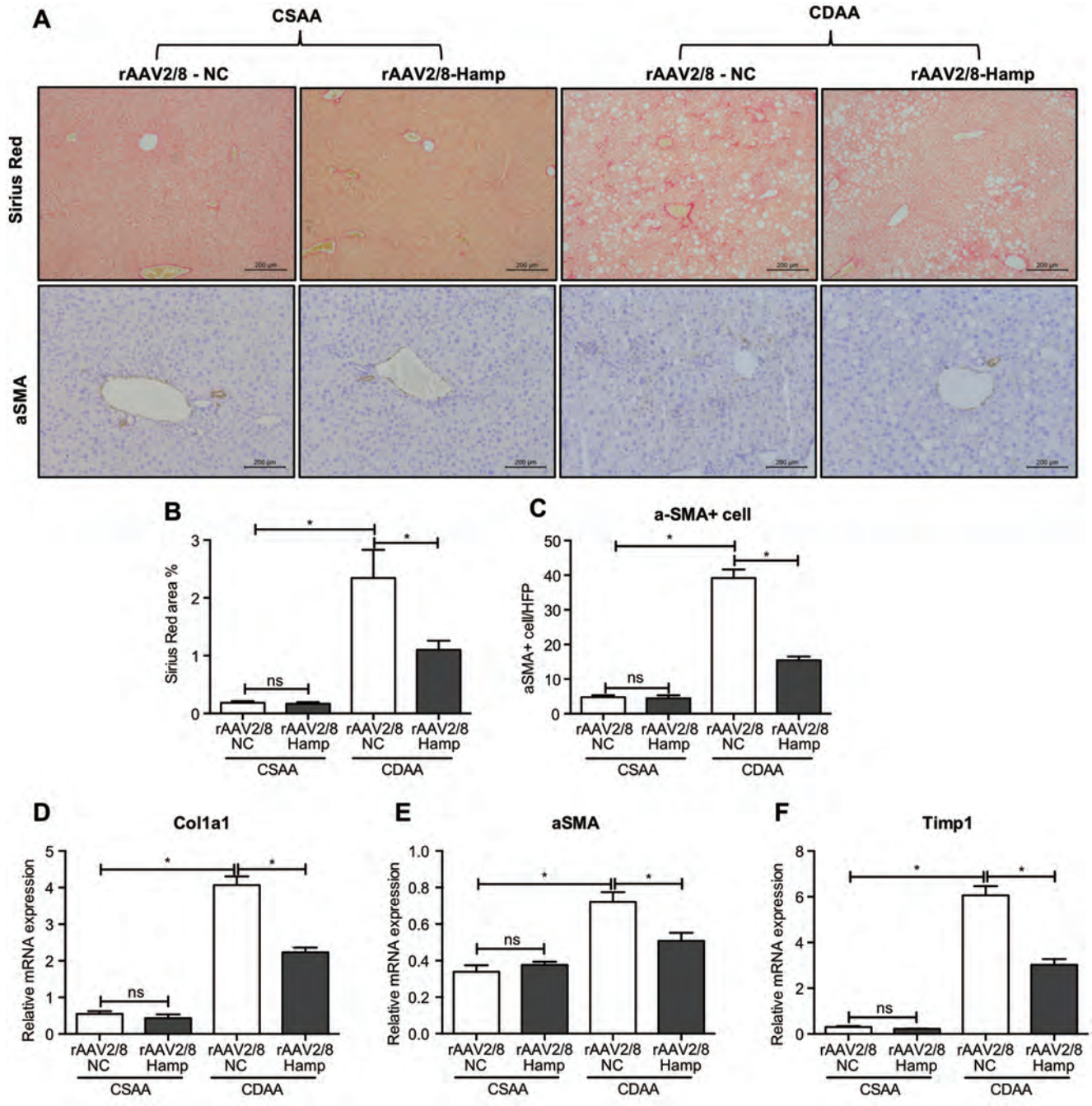


**Fig. 5. rAAV2/8-Hamp treatment suppressed hepatic fibrosis in mice fed a CDAA diet.** (A) Representative SR staining (top; original magnification 200×) and αSMA-positive HSCs (bottom; original magnification 200×) in liver sections of mice treated with rAAV2/8-Hamp or rAAV2/8-NC. (B–C) Quantification of images of mice fed either the CDAA or CSAA diet. (D–F) Transcript levels of COL1A1, αSMA, and TIMP-1. Data represent the mean±SEM of at least 10 animals per group. SR, sirius red; CDAA, choline-deficient L-amino acid-defined; CSAA, choline-supplemented amino acid-defined; rAAV, recombinant adeno-associated virus; αSMA, smooth muscle alpha-actin; HSCs, hepatic stellate cells; NC, negative control; COL1A1, collagen type I alpha 1 chain; TIMP-1, tissue inhibitor of metalloproteinase 1.

IL1β in NASH.[35–37] These inflammatory mediators further stimulate hepatocytes and HSCs to induce hepatocyte steatosis and fibrosis, respectively. As expected, overexpression of Hamp decreased the CDAA diet-induced levels of hepatic CD68-positive macrophages and altered the inflammatory response in our model, as indicated by a down-regulation in pro-inflammatory cytokines (TNFα and CCR2) and a slight up-regulation in the anti-inflammatory cytokine (IL10).

Hamp expression is controlled mainly at the transcriptional level by various stimuli, including inflammation, iron status, and hypoxia. The link between inflammation/infection and liver production of Hamp is attributed to IL6 produced at the sites of infection/inflammation. IL6 binds to the IL6-receptor and phosphorylates JAK-2/STAT3, which binds to and activates the Hamp promoter.[38] Importantly, Hamp can also influence the function of macrophages. Zla-

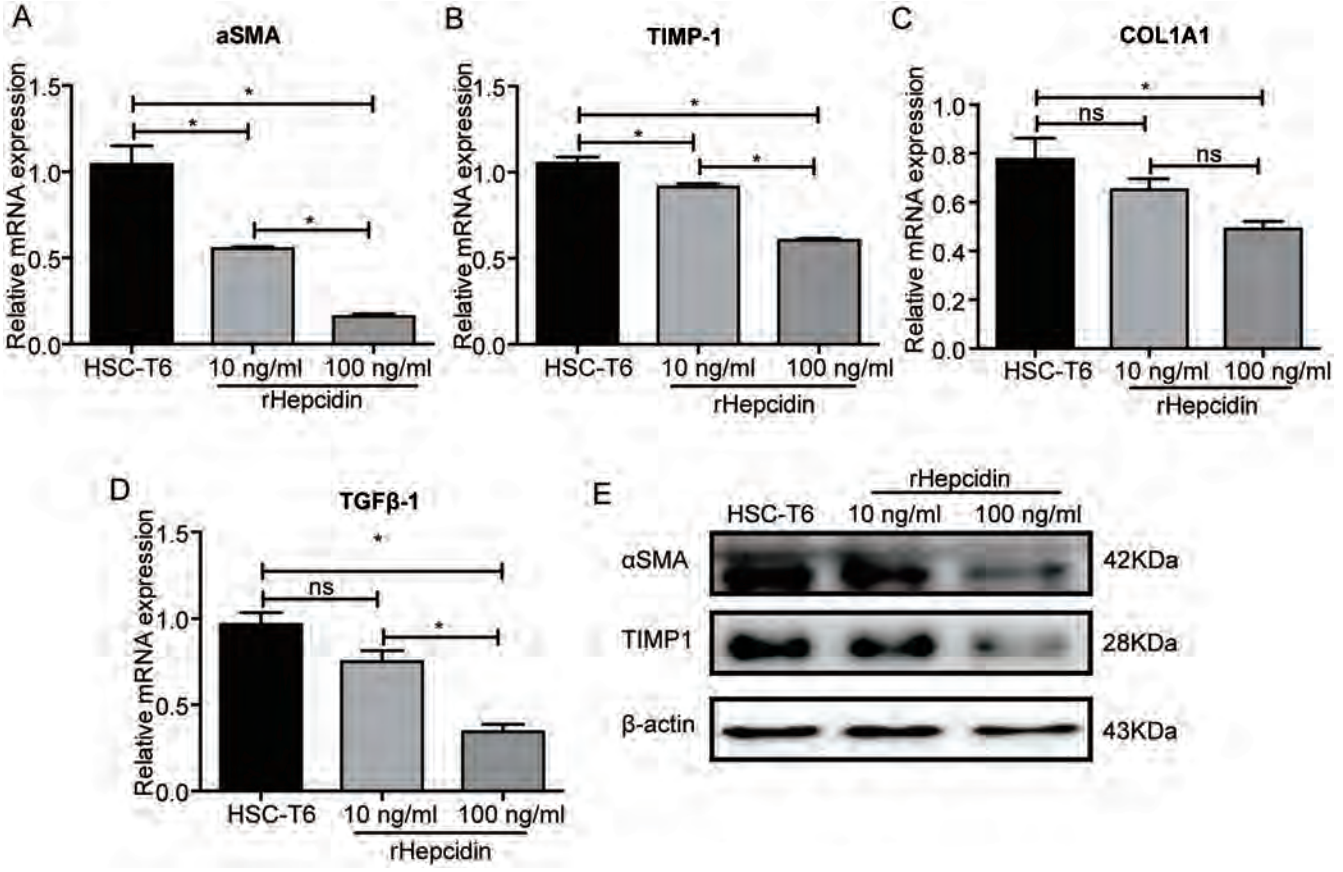


**Fig. 6. Effect of hepcidin on HSCs activation.** HSCs were stimulated with hepcidin (10 or 100 ng/mL) for 48 h. (A–D) Gene expression of (A) αSMA, (B) TIMP-1, (C) COL1A1, and TGFβ-1 (D) in HSCs. (E) Protein expression of αSMA and TIMP1 in HSCs. Data represent the mean±SEM. HSCs, hepatic stellate cells; αSMA, smooth muscle alpha-actin; TIMP-1, tissue inhibitor of metalloproteinase 1; COL1A1, collagen type I alpha 1 chain; TGFβ-1, transforming growth factor-beta 1.

tanova *et al*.[39] reported that Hamp-induction by IL6 and/or iron could reduce the secretion of IL4 and IL13 in macrophages, thereby inhibiting cardiac repair. In contrast, Hamp-deficiency in macrophages promoted the release of IL4 and IL13 by recombinant IL6. It has been suggested that Hamp is an upstream repressor of reparatory cytokines (IL4 and IL13) secreted by cardiac macrophages. A similar study showed that Hamp induces M1 macrophage polarization.[40] In contrast, another study showed that Hamp reduced M1 polarization of RAW264.7 macrophages. The authors explain that this discrepancy may be caused by factors such as differential simulation, iron concentration, and cell condition.[41] We found that overexpression of Hamp in liver cells decreased the number of CD68-positive macrophages in the liver**.** Moreover, mRNA expression of pro-inflammatory cytokines, such as CCR2 and TNFα, decreased significantly, suggesting a role for Hamp in liver inflammation and macrophage infiltration.

Our study suggests an important role of Hamp in HSC activation, which results in hepatic fibrosis following a CDAA diet. The CDAA diet decreased Hamp expression, which was accompanied by HSC activation, as demonstrated by an increase in αSMA-positive cells. Furthermore, expression of fibrotic genes (αSMA, TIMP-1, and COL1A1) was significantly reduced in the livers of the CDAA-fed mice following rAVV2/8-Hamp treatment. Consistent with our data, pharmacological administration of Hamp has been shown to improve fibrosis by blocking activation of HSCs both in the $CCl_4$ and bile duct ligation fibrosis models.[42,43] Conversely, when challenged with an iron-overload diet, Hamp knockout mice displayed significant liver fibrosis associated with iron accumulation and stellate cell activation.[44] In liver fibrosis, low Hamp levels cause high iron load and oxidative stress. Oxidative stress and lack of Hamp-induced suppression induces HSC activation, which results in scar tissue deposition and liver fibrosis.[34] Cell-based assays provide a mechanism whereby exogenous Hamp hinders TGFβ1-induced SMAD-3 phosphorylation in HSCs, inhibiting their activation. On the other hand, there have been contradictory reports as to the role of Hamp in NASH/NAFLD. Hamp knockout NAFLD mice develop liver damage. Although loss of Hamp is associated with a reduction in liver steatosis, liver fibrosis is present early and is more pronounced in the knockout mice compared to mice with normal Hamp expression.[45] Different animal models of NASH involve several factors, including various degrees of hepatocyte damage, insulin resistance, inflammation, and lipid metabolism, all of which can affect the regulation of Hamp. Therefore, regulation of Hamp and consequently iron homeostasis need to be further investigated.

It is noteworthy that the beneficial effects of Hamp overexpression on lipid metabolism and inflammation may be due to HSC activation and induced adiponectin expression. Adiponectin is the predominant adipokine made by adipose tissue and is involved in the regulation of hepatic lipid metabolism. In addition to its metabolic effects, growing evidence suggests that adiponectin possesses potent anti-fibrotic and anti-inflammatory properties.[46,47]

Altogether, we demonstrated for the first time that rAAV2/8-Hamp treatment ameliorated CDAA-induced inflammation and related liver fibrosis as well as improved lipid metabolic abnormalities, suggesting that rAAV2/8-mediated Hamp intervention may have beneficial effects on NASH. This increase in hepatic Hamp produced a marked induction of adiponectin both *in vivo* and *in vitro*. Furthermore, Hamp directly inhibited HSC fibrogenesis *in vitro*. To fully understand the protective and therapeutic function of Hamp, other dietary animal models, such as high fat- or western diet-induced NAFLD, should be explored.

## Funding

National Natural Science Foundation of China (No. 81900547).

## Conflict of interest

The authors have no conflict of interests related to this publication.

## Author contributions

Study conception and drafting of the manuscript (HC, AY), and performance of experiments or analysis of the resultant data (HC, WZ, XY, TH, AY). All authors read or revised the manuscript.

## Data sharing statement

All data are available upon request.

## References

[1] Wong RJ, Aguilar M, Cheung R, Perumpail RB, Harrison SA, Younossi ZM, *et al*. Nonalcoholic steatohepatitis is the second leading etiology of liver disease among adults awaiting liver transplantation in the United States. Gastroenterology 2015;148(3):547–555. doi:10.1053/j.gastro.2014.11.039.
[2] Schuppan D, Surabattula R, Wang XY. Determinants of fibrosis progression and regression in NASH. J Hepatol 2018;68(2):238–250. doi:10.1016/j.jhep.2017.11.012.
[3] Cusi K. A diabetologist's perspective of non-alcoholic steatohepatitis (NASH): Knowledge gaps and future directions. Liver Int 2020;40(Suppl 1):S82–S88. doi:10.1111/liv.14350.
[4] Schuppan D, Schattenberg JM. Non-alcoholic steatohepatitis: pathogenesis and novel therapeutic approaches. J Gastroenterol Hepatol 2013;28(Suppl 1):S68–S76. doi:10.1111/jgh.12212.
[5] Negro F. Natural history of NASH and HCC. Liver Int 2020;40(Suppl 1):S72–S76. doi:10.1111/liv.14362.
[6] Nelson JE, Klintworth H, Kowdley KV. Iron metabolism in Nonalcoholic Fatty Liver Disease. Curr Gastroenterol Rep 2012;14(1):8–16. doi:10.1007/s11894-011-0234-4.
[7] Sachinidis A, Doumas M, Imprialos K, Stavropoulos K, Katsimardou A, Athyros VG. Dysmetabolic Iron Overload in Metabolic Syndrome. Curr Pharm Des 2020;26(10):1019–1024. doi:10.2174/1381612826666200130090703.
[8] Xu J, Sun W, Yang L. Association between iron metabolism and cognitive impairment in older non-alcoholic fatty liver disease individuals: A cross-sectional study in patients from a Chinese center. Medicine (Baltimore) 2019;98(48):e18189. doi:10.1097/MD.0000000000018189.
[9] Abe N, Tsuchida T, Yasuda SI, Oka K. Dietary iron restriction leads to a reduction in hepatic fibrosis in a rat model of non-alcoholic steatohepatitis. Biol Open 2019;8(5):bio040519. doi:10.1242/bio.040519.
[10] Salaye L, Bychkova I, Sink S, Kovalic AJ, Bharadwaj MS, Lorenzo F, *et al*. A Low Iron Diet Protects from Steatohepatitis in a Mouse Model. Nutrients 2019;11(9):2172. doi:10.3390/nu11092172.
[11] Sumida Y, Kanemasa K, Fukumoto K, Yoshida N, Sakai K, Nakashima T, *et al*. Effect of iron reduction by phlebotomy in Japanese patients with non-alcoholic steatohepatitis: A pilot study. Hepatol Res 2006;36(4):315–321. doi:10.1016/j.hepres.2006.08.003.
[12] Murali AR, Gupta A, Brown K. Systematic review and meta-analysis to determine the impact of iron depletion in dysmetabolic iron overload syndrome and non-alcoholic fatty liver disease. Hepatol Res 2018;48(3):E30–E41. doi:10.1111/hepr.12921.
[13] Milic S, Mikolasevic I, Orlic L, Devcic E, Starcevic-Cizmarevic N, Stimac D, *et al*. The Role of Iron and Iron Overload in Chronic Liver Disease. Med Sci Monit 2016;22:2144–2151. doi:10.12659/msm.896494.
[14] Saneela S, Iqbal R, Raza A, Qamar MF. Hepcidin: A key regulator of iron. J Pak Med Assoc 2019;69(8):1170–1175.
[15] Bekri S, Gual P, Anty R, Luciani N, Dahman M, Ramesh B, *et al*. Increased adipose tissue expression of hepcidin in severe obesity is independent from diabetes and NASH. Gastroenterology 2006;131(3):788–796. doi:10.1053/j.gastro.2006.07.007.
[16] Auguet T, Aragonès G, Berlanga A, Martínez S, Sabench F, Binetti J, *et al*. Hepcidin in morbidly obese women with non-alcoholic fatty liver disease. PLoS One 2017;12(10):e0187065. doi:10.1371/journal.pone.0187065.
[17] Marmur J, Beshara S, Eggertsen G, Onelöv L, Albiin N, Danielsson O, *et al*. Hepcidin levels correlate to liver iron content, but not steatohepatitis, in non-alcoholic fatty liver disease. BMC Gastroenterol 2018;18(1):78. doi:10.1186/s12876-018-0804-0.
[18] Tsutsumi N, Nishimata S, Shimura M, Kashiwagi Y, Kawashima H. Hepcidin Levels and Pathological Characteristics in Children with Fatty Liver Disease. Pediatr Gastroenterol Hepatol Nutr 2021;24(3):295–305. doi:10.5223/pghn.2021.24.3.295.
[19] Yang AT, Hu DD, Wang P, Cong M, Liu TH, Zhang D, *et al*. TGF-β1 Induces the Dual Regulation of Hepatic Progenitor Cells with Both Anti- and Proliver Fibrosis. Stem Cells Int 2016;2016(2016):1492694. doi:10.1155/2016/1492694.
[20] Zhao W, Yang A, Chen W, Wang P, Liu T, Cong M, *et al*. Inhibition of lysyl oxidase-like 1 (LOXL1) expression arrests liver fibrosis progression in cirrhosis by reducing elastin crosslinking. Biochim Biophys Acta Mol Basis Dis 2018;1864(4 Pt A):1129–1137. doi:10.1016/j.bbadis.2018.01.019.
[21] Kleiner DE, Brunt EM, Van Natta M, Behling C, Contos MJ, Cummings OW, *et al*. Design and validation of a histological scoring system for nonalcoholic fatty liver disease. Hepatology 2005;41(6):1313–1321. doi:10.1002/hep.20701.
[22] Farrell G, Schattenberg JM, Leclercq I, Yeh MM, Goldin R, Teoh N, *et al*. Mouse Models of Nonalcoholic Steatohepatitis: Toward Optimization of Their Relevance to Human Nonalcoholic Steatohepatitis. Hepatology 2019;69(5):2241–2257. doi:10.1002/hep.30333.
[23] Gore E, Bigaeva E, Oldenburger A, Jansen YJM, Schuppan D, Boersema M, *et al*. Investigating fibrosis and inflammation in an ex vivo NASH murine model. Am J Physiol Gastrointest Liver Physiol 2020;318(2):G336–G351. doi:10.1152/ajpgi.00209.2019.
[24] Wei G, An P, Vaid KA, Nasser I, Huang P, Tan L, *et al*. Comparison of murine steatohepatitis models identifies a dietary intervention with robust fibrosis, ductular reaction, and rapid progression to cirrhosis and cancer. Am J Physiol Gastrointest Liver Physiol 2020;318(1):G174–G188. doi:10.1152/ajpgi.00041.2019.
[25] Nicolas G, Bennoun M, Devaux I, Beaumont C, Grandchamp B, Kahn A, *et al*. Lack of hepcidin gene expression and severe tissue iron overload in upstream stimulatory factor 2 (USF2) knockout mice. Proc Natl Acad Sci U S A 2001;98(15):8780–8785. doi:10.1073/pnas.151179498.
[26] Varghese J, Varghese James J, Karthikeyan M, Rasalkar K, Raghavan R, Sukumaran A, *et al*. Iron homeostasis is dysregulated, but the iron-hepcidin axis is functional, in chronic liver disease. J Trace Elem Med Biol 2020;58:126442. doi:10.1016/j.jtemb.2019.126442.
[27] Costa-Matos L, Batista P, Monteiro N, Simões M, Egas C, Pereira J, *et al*. Liver hepcidin mRNA expression is inappropriately low in alcoholic patients compared with healthy controls. Eur J Gastroenterol Hepatol 2012;24(10):1158–1165. doi:10.1097/MEG.0b013e328355cfd0.
[28] Ryan JD, Altamura S, Devitt E, Mullins S, Lawless MW, Muckenthaler MU, *et al*. Pegylated interferon-α induced hypoferremia is associated with the immediate response to treatment in hepatitis C. Hepatology 2012;56(2):492–500. doi:10.1002/hep.25666.
[29] Armitage AE, Stacey AR, Giannoulatou E, Marshall E, Sturges P, Chatha K, *et al*. Distinct patterns of hepcidin and iron regulation during HIV-1, HBV, and HCV infections. Proc Natl Acad Sci U S A 2014;111(33):12187–12192. doi:10.1073/pnas.1402351111.
[30] Lin D, Ding J, Liu JY, He YF, Dai Z, Chen CZ, *et al*. Decreased serum hepcidin concentration correlates with brain iron deposition in patients with HBV-related cirrhosis. PLoS One 2013;8(6):e65551. doi:10.1371/journal.pone.0065551.
[31] Vela D. Low hepcidin in liver fibrosis and cirrhosis; a tale of progressive disorder and a case for a new biochemical marker. Mol Med 2018;24(1):5. doi:10.1186/s10020-018-0008-7.
[32] Wang J, Dong A, Liu G, Anderson GJ, Hu TY, Shi J, *et al*. Correlation of serum hepcidin levels with disease progression in hepatitis B virus-related disease assessed by nanopore film based assay. Sci Rep 2016;6:34252. doi:10.1038/srep34252.
[33] Çam H, Yılmaz N. Serum hepcidin levels are related to serum markers for iron metabolism and fibrosis stage in patients with chronic hepatitis B: A cross-sectional study. Arab J Gastroenterol 2020;21(2):85–90. doi:10.1016/j.ajg.2020.04.013.
[34] Lyberopoulou A, Chachami G, Gatselis NK, Kyratzopoulou E, Saitis A, Gabeta S, *et al*. Low Serum Hepcidin in Patients with Autoimmune Liver Diseases. PLoS One 2015;10(8):e0135486. doi:10.1371/journal.pone.0135486.
[35] Sumida Y, Yoneda M. Current and future pharmacological therapies for NAFLD/NASH. J Gastroenterol 2018;53(3):362–376. doi:10.1007/s00535-017-1415-1.
[36] Miura K, Yang L, van Rooijen N, Ohnishi H, Seki E. Hepatic recruitment of macrophages promotes nonalcoholic steatohepatitis through CCR2. Am J Phys-

iol Gastrointest Liver Physiol 2012;302(11):G1310–G1321. doi:10.1152/ajpgi.00365.2011.
[37] Tacke F. Targeting hepatic macrophages to treat liver diseases. J Hepatol 2017;66(6):1300–1312. doi:10.1016/j.jhep.2017.02.026.
[38] Camaschella C, Nai A, Silvestri L. Iron metabolism and iron disorders revisited in the hepcidin era. Haematologica 2020;105(2):260–272. doi:10.3324/haematol.2019.232124.
[39] Zlatanova I, Pinto C, Bonnin P, Mathieu JRR, Bakker W, Vilar J, *et al*. Iron Regulator Hepcidin Impairs Macrophage-Dependent Cardiac Repair After Injury. Circulation 2019;139(12):1530–1547. doi:10.1161/CIRCULATIONAHA.118.034545.
[40] Liu E, Li Z, Zhang Y, Chen K. Hepcidin Induces M1 Macrophage Polarization in Monocytes or THP-1 Derived Macrophages. Iran J Immunol 2019;16(3):190–199. doi:10.22034/IJI.2019.80270.
[41] Gan ZS, Wang QQ, Li JH, Wang XL, Wang YZ, Du HH. Iron Reduces M1 Macrophage Polarization in RAW264.7 Macrophages Associated with Inhibition of STAT1. Mediators Inflamm 2017;2017:8570818. doi:10.1155/2017/8570818.
[42] Han CY, Koo JH, Kim SH, Gardenghi S, Rivella S, Strnad P, *et al*. Hepcidin inhibits Smad3 phosphorylation in hepatic stellate cells by impeding ferroportin-mediated regulation of Akt. Nat Commun 2016;7:13817. doi:10.1038/ncomms13817.
[43] Détivaud L, Nemeth E, Boudjema K, Turlin B, Troadec MB, Leroyer P, *et al*. Hepcidin levels in humans are correlated with hepatic iron stores, Hb levels, and hepatic function. Blood 2005;106(2):746–748. doi:10.1182/blood-2004-12-4855.
[44] Lunova M, Goehring C, Kuscuoglu D, Mueller K, Chen Y, Walther P, *et al*. Hepcidin knockout mice fed with iron-rich diet develop chronic liver injury and liver fibrosis due to lysosomal iron overload. J Hepatol 2014;61(3):633–641. doi:10.1016/j.jhep.2014.04.034.
[45] Lu S, Bennett RG, Kharbanda KK, Harrison-Findik DD. Lack of hepcidin expression attenuates steatosis and causes fibrosis in the liver. World J Hepatol 2016;8(4):211–225. doi:10.4254/wjh.v8.i4.211.
[46] Park PH, Sanz-Garcia C, Nagy LE. Adiponectin as an anti-fibrotic and anti-inflammatory adipokine in the liver. Curr Pathobiol Rep 2015;3(4):243–252. doi:10.1007/s40139-015-0094-y.
[47] Xu H, Zhao Q, Song N, Yan Z, Lin R, Wu S, *et al*. AdipoR1/AdipoR2 dual agonist recovers nonalcoholic steatohepatitis and related fibrosis via endoplasmic reticulum-mitochondria axis. Nat Commun 2020;11(1):5807. doi:10.1038/s41467-020-19668-y.

*Journal of Clinical and Translational Hepatology* **2022** vol. 10(4) | 589–594
DOI: 10.14218/JCTH.2021.00311

Original Article

# Validation of Non-invasive Fibrosis Scores for Predicting Advanced Fibrosis in Metabolic-associated Fatty Liver Disease

Xiaoning Chen[1], George Boon-Bee Goh[2,3], Jiaofeng Huang[1], Yinlian Wu[1], Mingfang Wang[1], Rahul Kumar[4], Su Lin[1*] and Yueyong Zhu[1*]

*[1]Department of Hepatology, Hepatology Research Institute, The First Affiliated Hospital of Fujian Medical University, Fuzhou, Fujian, China; [2]Department of Gastroenterology & Hepatology, Singapore General Hospital, Singapore; [3]Duke-NUS Medical School, Singapore; [4]Department of Gastroenterology and Hepatology, Duke-NUS Academic Medical Centre, Changi General Hospital, Singapore*

**Received:** 2 August 2021 | **Revised:** 27 September 2021 | **Accepted:** 16 November 2021 | **Published:** 12 January 2022

## Abstract

***Background and Aims:*** Metabolic-associated fatty liver disease (MAFLD) is a newly proposed terminology from 2020; yet, the applicability of conventional noninvasive fibrosis models is still unknown for it. We aimed to evaluate the performance of conventional noninvasive fibrosis scores in MAFLD. ***Methods:*** The NHANES 2017-2018 datasets were used to compare the performances of different noninvasive fibrosis scores in MAFLD, including the aspartate aminotransferase (AST) to platelet ratio index (APRI), body mass index (BMI)-AST/alanine aminotransferase (ALT) ratio and diabetes score (BARD), fibrosis-4 index (FIB-4), and NAFLD fibrosis score (NFS). Moreover, Asian patients with biopsy-proven MAFLD were enrolled to further validate the findings. ***Results:*** A total of 2,622 participants in the National Health and Nutrition Examination Survey (NHANES) cohort and 293 patients with MAFLD in the Asian cohort were included. Patients in the Asian cohort had a lower BMI and higher liver enzymes ($p<0.001$). The area under the receiver operating characteristic curve (AUROC) of NFS was the largest in the NHANES cohort and Asian cohorts (0.679 and 0.699, respectively). The AUROC of NFS was followed by APRI, FIB-4, and BARD in the NHANES cohort (0.616, 0.601, and 0.589, respectively). In the Asian cohort, the AUROC of APRI, FIB-4, and BARD for predicting advanced fibrosis were 0.625, 0.683, and 0.615, respectively. The performance of FIB-4 was better in the Asian cohort than that in the NHANES cohort. ***Conclusions:*** NFS is better for predicting advanced fibrosis in MAFLD. FIB-4 can be an alternative choice for MAFLD with high liver enzymes when NFS is unavailable. Novel efficient noninvasive fibrosis scoring systems are highly required for patients with MAFLD.

**Citation of this article:** Chen X, Goh GBB, Huang J, Wu Y, Wang M, Kumar R, *et al*. Validation of Non-invasive Fibrosis Scores for Predicting Advanced Fibrosis in Metabolic-associated Fatty Liver Disease. J Clin Transl Hepatol 2022;10(4):589–594. doi: 10.14218/JCTH.2021.00311.

**Keywords:** FIB-4; Metabolic-associated fatty liver disease; Liver fibrosis; NFS; Noninvasive fibrosis scores.

**Abbreviations:** ALT, alanine aminotransferase; APRI, AST to platelet ratio index; AST, aspartate aminotransferase; AUROC, area under the receiver operating characteristic curve; BARD, BMI-AST/ALT ratio and diabetes score; BMI, body mass index; CAP, controlled attenuation parameter; FIB-4, fibrosis-4 index; LSM, liver stiffness measurement; MAFLD, metabolic-associated fatty liver disease; NAFLD, nonalcoholic fatty liver disease; NFS, NAFLD fibrosis score; NHANES, National Health and Nutrition Examination Survey; NLR, negative likelihood ratio; NPV, negative predictive value; PLR, positive likelihood ratio; PPV, positive predictive value; ROC, receiver operating characteristic.

[*]**Correspondence to:** Yueyong Zhu and Su Lin, Department of Hepatology, Hepatology Research Institute, The First Affiliated Hospital, Fujian Medical University, Fuzhou, Fujian 350001, China. ORCID: https://orcid.org/0000-0002-0746-4911 (YZ) and https://orcid.org/0000-0001-7517-9859 (SL). Tel: +86-591-87981656 (YZ) and +86-591-87982526 (SL), Fax: +86-591-83356180 (YZ) and +86-591-87981600 (SL); E-mail: zhuyueyong@fjmu.edu.cn (YZ) and sumer5129@fjmu.edu.cn (SL)

## Introduction

With the growing epidemic of obesity and type 2 diabetes mellitus, nonalcoholic fatty liver disease (NAFLD) has become one of the most common chronic liver diseases worldwide.[1,2] It is reported that the global prevalence of NAFLD is approximately 25%, and the prevalence in the USA has risen from 20.0% to 31.9% in the past 3 decades.[3,4] There is a similar estimated prevalence of 29.62% in Asia.[5] NAFLD may progress through various fibrosis stages and has the potential to develop into cirrhosis and hepatocellular carcinoma. Liver fibrosis is closely related to a poor prognosis and is considered a strong prognostic predictor for NAFLD.[6–8] Therefore, identifying patients with advanced fibrosis for stratification and early intervention is critical for individualized management of NAFLD.

Liver stiffness measurement (LSM) and controlled attenuation parameter (CAP) using transient elastography are regarded as reliable methods for the diagnosis of liver fibrosis and steatosis in NAFLD.[9,10] Liver biopsy, the "gold standard" for diagnosing liver fibrosis, is impractical for wide usage in NAFLD due to its invasiveness, sampling variability, poor acceptability, and the high prevalence of NAFLD.[11,12] These limitations highlight the need for reliable noninvasive fibrosis scores. Currently, commonly used noninvasive fibrosis models include the aspartate aminotransferase (AST) to platelet ratio index (APRI),[13] body mass

index (BMI)-AST/alanine aminotransferase (ALT) ratio and diabetes score (BARD),[14] fibrosis 4 index (FIB-4),[15] and NAFLD fibrosis score (NFS).[16] The formulas for calculating these non-invasive scoring systems are shown in Supplementary Table 1. These models have been tested and perform well in predicting fibrosis in NAFLD.[17–19]

Metabolic-associated fatty liver disease (MAFLD) is a new concept, proposed in 2020 to revise the term NAFLD.[20] Unlike NAFLD, MAFLD does not need to exclude alcohol intake or any other liver diseases. MAFLD will be diagnosed if the patient has hepatic steatosis and any of the following three conditions: overweight/obesity, type 2 diabetes mellitus, or at least two metabolic abnormalities in nonobese individuals.[21] Considering the significant difference between MAFLD and NAFLD, the applicability of traditional noninvasive fibrosis scores requires re-evaluation. This study aimed to verify the performance of different noninvasive scores in predicting advanced fibrosis in MAFLD.

## Methods

### *Study population*

The study data were obtained from the latest National Health and Nutrition Examination Surveys (NHANES) 2017-2018, which is an unbiased survey dataset collected by the National Center for Health Statistics of the Centers for Disease Control and Prevention of the USA. The NHANES database has been frequently used for the study of fatty liver disease.[22–24] Currently, NHANES 2017-2018 is the only public database with FibroScan® liver fibrosis assessment, laboratory, and examination data. All NHANES datasets are anonymous and free to access online (https://www.cdc.gov/nchs/nhanes/index.htm).

Additionally, patients with biopsy-proven MAFLD were enrolled from the First Affiliated Hospital of Fujian Medical University in China and Singapore General Hospital in Singapore as an Asian validation cohort. As the hepatitis B virus infection rate is high in Asia, especially among Asian patients who undergo liver biopsy, MAFLD patients combined with hepatitis B were excluded in the Asian cohort. The study protocol was approved by the Ethics Committee of The First Affiliated Hospital of Fujian Medical University and Singapore General Hospital, conforming to the ethical guidelines of the Declaration of Helsinki. All patients provided written informed consent for the use of their data in research studies, such as this one.

### *Definition of MAFLD and fibrosis*

MAFLD was diagnosed based on the updated international expert consensus statement on MAFLD from 2020.[21] In the NHANES cohort, hepatic steatosis was measured by FibroScan®, with a criterion of CAP ≥248 dB/m.[25] Advanced fibrosis was defined as fibrosis grade ≥F3 (LSM ≥8.2 kPa).[26] Participants with a fasting time <3 h, <10 complete LSMs, or LSM interquartile range/median LSM ≥30% were considered as unsuccessful measurements and excluded.

All patients in the Asian cohort underwent percutaneous liver biopsy under ultrasonic guidance. When more than 5% of hepatocytes presented steatosis, fatty liver was diagnosed. Advanced fibrosis was defined as stage 3 or 4, according to the Metavir fibrosis stage.[27]

### *Statistical analysis*

The quantitative variables were expressed as mean ± standard deviation or median (interquartile range) and compared by Student's *t*-test or Mann-Whitney *U*-test. The qualitative variables were expressed as counts (percentages) and compared using the $\chi^2$ test. The receiver operating characteristic (ROC) curve was used to evaluate the performances of noninvasive models. The optimal cutoffs were chosen based on Youden's index. Statistical analyses were conducted using the SPSS software version 22.0 (IBM Corp., Armonk, NY, USA) and MedCalc software version 20.0 (MedCalc Software Ltd, Ostend, Belgium). A $p$-value <0.05 was considered statistically significant.

## Results

### *Baseline characteristics of participants*

The NHANES 2017-2018 dataset contained 9,254 participants. After excluding 3,776 cases with missing data and 405 cases with ineligible FibroScan® data, a total of 5,073 participants were eligible for final analysis (Fig. 1). Among them, a total of 2,622 (51.69%) participants met the criteria for MAFLD. Furthermore, a total of 293 patients with MAFLD were enrolled from The First Affiliated Hospital of Fujian Medical University in China and Singapore General Hospital in Singapore between 2005 to 2021 as an Asian cohort. A total of 356 (13.58%) participants of the NHANES cohort and 86 (29.35%) patients of the Asian cohort had advanced fibrosis (Fig. 1). Patients in the Asian cohort had a lower level of BMI, a higher prevalence of diabetes mellitus and high liver enzymes (all with a $p$-value <0.05; Table 1). Baseline characteristics of patients from China and Singapore in the Asian cohort are shown in Supplementary Table 2.

### *Performances of APRI, BARD, FIB-4, and NFS in predicting advanced fibrosis in the NHANES cohort*

The ROC curves were used to evaluate the performances of traditional noninvasive fibrosis scoring systems for predicting advanced fibrosis in the NHANES cohort (Fig. 2A). NFS had the largest AUROC (0.679; 95% CI: 0.648–0.709), followed by APRI (0.616; 95% CI: 0.583–0.650), FIB-4 (0.601; 95% CI: 0.569–0.63371), and BARD (0.589; 95% CI: 0.556–0.621). The optimal cutoff values of the four noninvasive models for predicting advanced fibrosis and the verification of previously reported cutoffs are shown in Table 2. The results showed the best cutoffs of NFS, APRI, FIB-4, and BARD for diagnosing advanced fibrosis in the NHANES cohort were 0.159, 0.3, 1.02, and 3, respectively. The thresholds for all models, except BARD, were lower than previously reported values.

With the newly established cutoffs, the accuracy of the four models ranged from 58.0% to 79.8% (Table 2). The positive likelihood ratio (PLR) and negative likelihood ratio (NLR) of the four models with the new thresholds ranged from 1.39–2.37 and 0.64–0.81, and diagnostic odds ratios did not exceed 3.5 (Table 2). These scoring systems all had high negative predictive values (NPVs) (>88%), but the positive predictive values (PPVs) were far from ideal (17.9–27.2%). By applying the previously reported cutoff value of NFS for predicting advanced fibrosis (0.676), the sensitivity, specificity, PLR, and NLR were 37.6%, 85.6%, 2.62, and 0.73, respectively. The performances of the other three scoring systems were also not sufficiently satisfactory (Table 2).

The pairwise comparison of the four noninvasive scores in the NHANES cohort is shown in Supplementary Table 3. The results suggested NFS had the best predictive performance and was statistically significantly better when compared to

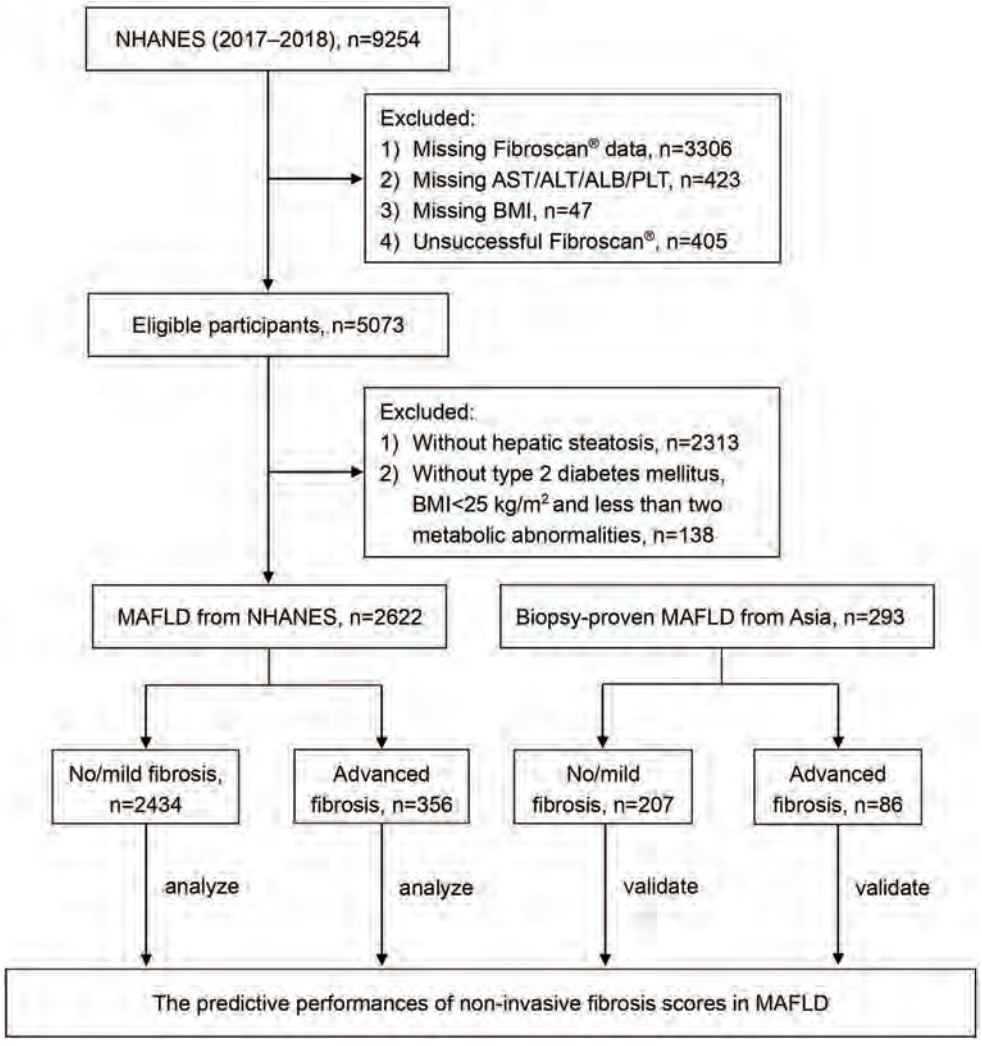


**Fig. 1. Flowchart for the analysis and validation of noninvasive fibrosis scores for predicting advanced fibrosis in MAFLD.** ALB, albumin; ALT, alanine aminotransferase; AST, aspartate aminotransferase; BMI, body mass index; MAFLD, metabolic associated fatty liver disease; NHANES, National Health and Nutrition Examination Surveys; PLT, platelet count.

the other three (NFS vs. APRI, $p=0.001$; NFS vs. BARD, $p<0.001$; NFS vs. FIB-4, $p<0.001$).

### *Performances of APRI, BARD, FIB-4, and NFS in predicting advanced fibrosis in the Asian cohort*

Figure 2B shows the ROC curves of the four noninvasive fibrosis scores when applied to the Asian cohort. The AUROC of NFS was still the largest (0.699; 95% CI: 0.639–0.747), followed by FIB-4, APRI, and BARD (0.683, 0.625, and 0.615, respectively; Table 3). The optimal cutoffs of APRI and FIB-4 in the Asian cohort were the same or very close to that in the NHANES cohort (0.3 vs. 0.3 and 1.02 vs. 1.21, respectively). However, the best cutoffs of NFS and BARD were lower than those in the NHANES cohort (−0.372 vs. 0.159 and 2 vs. 3, respectively). The accuracy of the four models ranged from 49.2.0% to 72.0%, which was not sufficiently good.

In the Asian cohort, NFS also had the largest AUROC, which was better than APRI and BARD with a statistically significant difference (NFS vs. APRI, $p=0.046$; NFS vs. BARD, $p=0.021$; Supplementary Table 4). The AUROC of FIB-4 was better in the Asian cohort than that in the NHANES cohort (0.683 vs. 0.601, $p=0.030$; Supplementary Table 5). The predictive capabilities of NFS and FIB-4 were not significantly different in the Asian cohort which had high liver enzymes (0.699 vs. 0.683, $p=0.519$).

## Discussion

The main finding of this study was that NFS is more reliable for predicting advanced fibrosis in patients with MAFLD. Overall, the performances of the four noninvasive scoring systems in MAFLD are not as good as previously reported for NAFLD.

Conventional noninvasive scoring systems calculated from readily available clinical and laboratory parameters are widely used for the assessment of advanced fibrosis in chronic liver disease.[28–30] The results of this study suggested that the NFS performed better than the other three non-invasive models in assessing advanced fibrosis for patients with MAFLD. This is probably because NFS includes many metabolism-related

**Table 1. Baseline characteristics of the patients with MAFLD**

| | NHANES cohort (*n*=2,622) | Asian cohort (*n*=293) | *P*-value |
|---|---|---|---|
| Age (years) | 50.70±18.36 | 49.47±13.49 | 0.264 |
| Male, *n* (%) | 1,388 (52.94) | 157 (53.58) | 0.833 |
| BMI (kg/m$^2$) | 32.47±6.83 | 29.64±6.89 | <0.001 |
| Diabetes mellitus, *n* (%) | 706 (26.93) | 161 (54.95) | <0.001 |
| Hypertension, *n* (%) | 1,304 (49.73) | 132 (45.05) | 0.190 |
| Platelet (×10$^9$/L) | 248.62±65.91 | 245.33±83.78 | 0.433 |
| Albumin (g/dL) | 4.10 (3.80, 4.30) | 4.16 (3.80, 4.40) | 0.001 |
| ALT (U/L) | 20.0 (15.0, 30.0) | 74.0 (40.0, 111.0) | <0.001 |
| AST (U/L) | 20.0 (16.0, 25.0) | 52.0 (33.5, 75.5) | <0.001 |
| TBIL (μmol/L) | 6.8 (5.1, 8.6) | 13.6 (10.0, 19.0) | <0.001 |
| GGT (U/L) | 24.0 (17.0, 37.0) | 82.0 (43.5, 137.5) | <0.001 |
| Triglyceride (mmol/L) | 1.45 (1.01, 2.12) | 1.67 (1.23, 2.42) | 0.247 |
| HDL-C (mmol/L) | 1.22 (1.03, 1.42) | 1.51 (1.12, 2.00) | 0.025 |
| Glycohemoglobin (%) | 6.03±1.21 | 7.68±1.65 | <0.001 |
| hs-CRP (mg/L) | 2.52 (1.20, 5.28) | 2.36 (0.82, 6.13) | 0.913 |
| HOMA-IR | 3.79 (2.43, 6.38) | 4.54 (2.78, 6.20) | 0.825 |

ALT, alanine aminotransferase; AST, aspartate aminotransferase; BMI, body mass index; hs-CRP, high-sensitivity C-reactive protein; GGT, γ-glutamyl transpeptidase; HDL-C, high-density lipoprotein cholesterol; HOMA-IR, homeostasis model assessment of insulin resistance; TBIL, total bilirubin.

parameters, such as BMI, impaired fasting glucose, and diabetes. However, it is also very complex and inconvenient in clinical practice. A novel, simpler, and more accurate noninvasive fibrosis scoring system is urgently required.

FIB-4 was initially exploited to assess fibrosis in patients with human immunodeficiency virus/hepatitis C virus.[15] Although FIB-4 did not perform well in the NHANES cohort, its performance was better in the Asian cohort. This may be a result of the increased liver enzymes and lower BMI among patients in the Asian cohort, because ALT and AST are crucial components of the calculation of FIB-4. Additionally, the generally lower BMI of Asians may not highlight the accuracy of NFS so well, as compared to the NHANES cohort. Whereas FIB-4 may be more accurate as BMI is not included. FIB-4 is easier to calculate than NFS because it includes only four clinical indicators. Therefore, FIB-4 can be an alternative choice for MAFLD with high liver enzymes when NFS is unavailable.

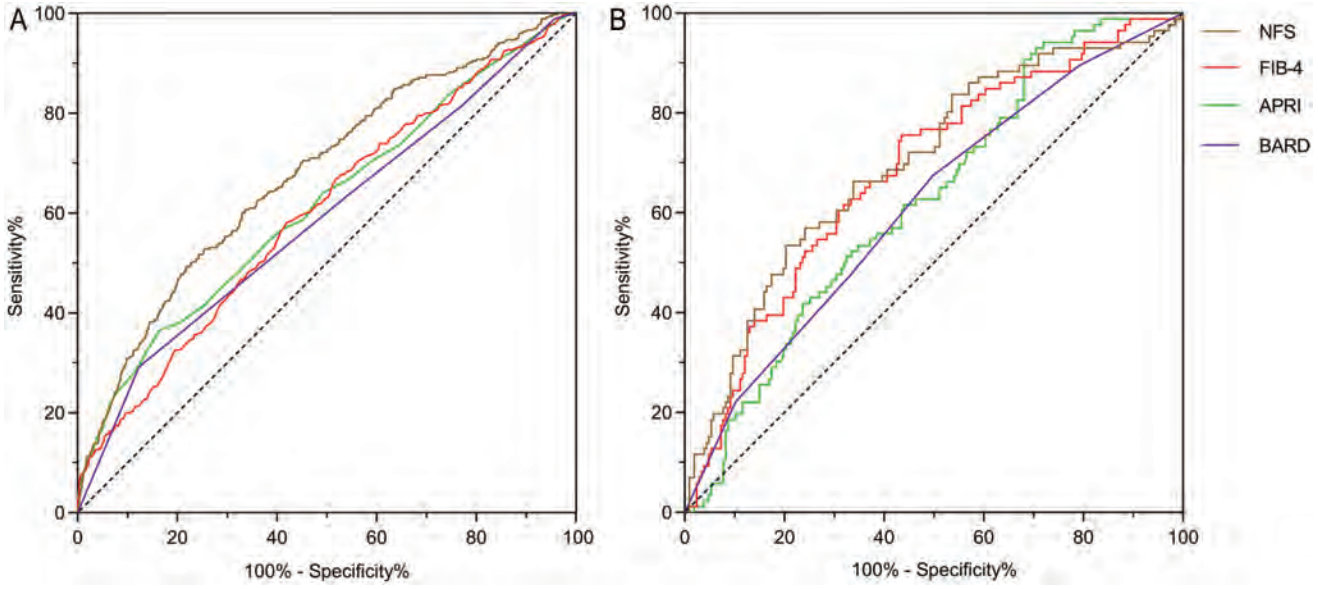


**Fig. 2. ROC curves of different scoring systems for advanced fibrosis in the two cohorts.** (A) ROC curves of different scoring systems for advanced fibrosis in the NHANES cohort. (B) ROC curves of different scoring systems for advanced fibrosis in the Asian cohort. ALT, alanine aminotransferase; APRI, AST to platelet ratio index; AST, aspartate aminotransferase; BARD, body mass index-AST/ALT ratio and diabetes score; FIB-4, fibrosis-4 index; NFS, NAFLD fibrosis score; ROC: Receiver operating characteristic.

**Table 2. Comparison of the performance among NFS, APRI, FIB-4, and BARD in the NHANES cohort**

| | Cutoffs | AUROC | Accuracy (%) | Sensitivity (%) | Specificity (%) | PPV (%) | NPV (%) | PLR | NLR | DOR | Youden's index |
|---|---|---|---|---|---|---|---|---|---|---|---|
| NFS | −1.455 | | 42.5 | 84.8 | 35.9 | 17.2 | 93.8 | 1.32 | 0.42 | 3.14 | 0.207 |
| | *0.159* | *0.679* | *72.4* | *51.7* | *75.7* | *25.1* | *90.9* | *2.13* | *0.64* | *3.33* | *0.274* |
| | 0.676 | | 79.1 | 37.6 | 85.6 | 29.1 | 89.7 | 2.62 | 0.73 | 3.59 | 0.233 |
| APRI | *0.3* | *0.616* | *77.6* | *36.5* | *84.0* | *26.4* | *89.4* | *2.29* | *0.76* | *3.01* | *0.205* |
| | 0.5 | | 85.2 | 14.3 | 96.3 | 37.8 | 87.7 | 3.86 | 0.89 | 4.34 | 0.106 |
| | 1.5 | | 86.6 | 2.3 | 99.9 | 80.0 | 86.7 | 25.46 | 0.98 | 25.98 | 0.022 |
| FIB-4 | *1.02* | *0.601* | *58.0* | *58.4* | *57.9* | *17.9* | *89.9* | *1.39* | *0.72* | *1.93* | *0.163* |
| | 1.30 | | 68.5 | 37.6 | 73.4 | 18.2 | 88.2 | 1.41 | 0.85 | 1.66 | 0.110 |
| | 1.45 | | 73.0 | 32.9 | 79.3 | 20.0 | 88.3 | 1.59 | 0.85 | 1.87 | 0.122 |
| | 2.67 | | 86.1 | 9.3 | 98.2 | 44.6 | 87.3 | 5.12 | 0.92 | 5.57 | 0.075 |
| | 3.25 | | 86.9 | 6.7 | 99.5 | 68.6 | 87.2 | 13.89 | 0.94 | 14.78 | 0.063 |
| BARD | 2 | | 48.0 | 63.8 | 45.5 | 15.5 | 88.9 | 1.17 | 0.80 | 1.46 | 0.093 |
| | *3* | *0.589* | *79.8* | *29.2* | *87.7* | *27.2* | *88.7* | *2.37* | *0.81* | *2.93* | 0.169 |

Best cutoff value is presented in italic font. AUROC, area under the receiver operating characteristic curve; DOR, diagnostic odds ratio; NLR, negative likelihood ratio; NPV, negative predictive value; PLR, positive likelihood ratio; PPV, positive predictive value.

The APRI score only includes the two parameters of AST and platelet count, and the BARD has no more than four variables. The APRI and BARD scores are simple to calculate and easy to acquire in clinical practice. APRI and BARD were originally developed to identify fibrosis in patients with hepatitis C and nondiabetic NAFLD.[13,14] However, their performance in predicting advanced fibrosis in patients with MAFLD is not satisfactory. The poor performance of BARD might be caused by the partial duplication of the BARD scoring variables and the MAFLD diagnostic variables.

It is worth mentioning that there are some differences between patients in the Asian cohort and patients in the NHANES cohort, like a higher prevalence of diabetes, a lower BMI, and high liver enzymes. The Asian cohort is composed of populations from China and Singapore but the NHANES cohort is mainly composed of Caucasians from the USA. Moreover, different from the population-based survey of the NHANES cohort, the increased liver enzyme was the main reason precipitating consultation in the biopsy-proven Asian cohort. These differences may explain why the cutoffs of NFS and BARD in the Asian cohort were lower than those in the NHANES cohort. This result also suggested that different races and regions may require different thresholds to distinguish advanced fibrosis in MAFLD.

This study is the first large-sample study using FibroScan® and liver biopsy to evaluate the utility of conventional noninvasive fibrosis scoring systems in MAFLD. However, it is necessary to acknowledge the limitations of this study. First, the diagnoses of hepatic steatosis and fibrosis in the NHANES cohort were based on FibroScan® rather than the "gold-standard", liver biopsy. This is because the study data were derived from the latest NHANES, which was a popu-

**Table 3. Comparison of the performance among NFS, APRI, FIB-4, and BARD in the Asian cohort**

| | Cutoffs | AUROC | Accuracy (%) | Sensitivity (%) | Specificity (%) | PPV (%) | NPV (%) | PLR | NLR | DOR | Youden's index |
|---|---|---|---|---|---|---|---|---|---|---|---|
| NFS | −1.455 | | 61.7 | 67.4 | 59.4 | 40.8 | 81.5 | 1.66 | 0.55 | 3.02 | 0.269 |
| | *−0.372* | *0.699* | *72.0* | *53.5* | *79.7* | *52.3* | *80.5* | *2.64* | *0.58* | *4.55* | *0.332* |
| | 0.676 | | 71.2 | 14.7 | 94.7 | 57.7 | 73.4 | 3.28 | 0.87 | 3.77 | 0.121 |
| FIB-4 | *1.21* | *0.683* | *62.1* | *75.6* | *56.5* | *41.9* | *84.8* | *1.74* | *0.43* | *4.05* | *0.321* |
| | 1.30 | | 61.4 | 67.4 | 58.9 | 40.6 | 81.3 | 1.64 | 0.55 | 2.98 | 0.264 |
| | 1.45 | | 65.9 | 60.5 | 68.1 | 44.1 | 80.6 | 1.90 | 0.58 | 3.28 | 0.297 |
| | 2.67 | | 70.6 | 26.7 | 88.9 | 50.0 | 74.5 | 2.41 | 0.82 | 2.94 | 0.151 |
| | 3.25 | | 70.3 | 18.6 | 91.8 | 48.5 | 73.1 | 2.27 | 0.89 | 2.55 | 0.116 |
| APRI | *0.3* | *0.625* | *49.2* | *90.7* | *31.9* | *35.6* | *89.2* | *1.33* | *0.29* | *4.59* | *0.226* |
| | 0.5 | | 52.9 | 65.1 | 47.8 | 34.1 | 76.7 | 1.25 | 0.73 | 1.71 | 0.130 |
| | 1.5 | | 69.6 | 17.4 | 91.3 | 45.5 | 72.7 | 2.01 | 0.90 | 2.23 | 0.097 |
| BARD | *2* | *0.615* | *55.2* | *67.4* | *50.2* | *36.0* | *78.8* | *1.36* | *0.65* | *2.09* | *0.177* |

Best cutoff value is presented in italic. AUROC, area under the receiver operating characteristic curve; DOR, diagnostic odds ratio; NLR, negative likelihood ratio; NPV, negative predictive value; PLR, positive likelihood ratio; PPV, positive predictive value.

lation-based survey and liver biopsy was not possible to be performed in the health examination cohort. Therefore, we validated the results in a biopsy-proven MAFLD population, which supported the findings based on the NHANES cohort. Second, the dataset used in this study is mainly composed of Caucasians in the USA and a small part of Asians, and it is unclear whether the results apply to other cohorts. The findings require further verification in more regions and races.

In conclusion, NFS is better for predicting advanced fibrosis in MAFLD. FIB-4 can be an alternative choice for MAFLD with high liver enzymes when NFS is unavailable. Novel efficient non-invasive fibrosis scoring systems are highly required for patients with MAFLD.

## Funding

This work was supported by the Fujian Province Health Education Joint Project (No. 2019-WJ-16) and the Fujian Province Health Technology Project (No. 2020CXA040).

## Conflict of interest

Goh GB and SL have been editorial board members of *Journal of Clinical and Translational Hepatology* since 2018 and 2021 respectively. The other authors have no conflict of interests related to this publication.

## Author contributions

Study concept and design (YZ, SL), acquisition of data (XC, GBG, MW), analysis and interpretation of data (XC, JH, YW), drafting of the manuscript (XC), critical revision of the manuscript (YZ, SL, GBG, RK), and study supervision (YZ, SL). All authors read and approved the final version of the manuscript.

## Data sharing statement

All data are available within the submitted article and its supplementary materials.

## References

[1] Paik JM, Golabi P, Younossi Y, Mishra A, Younossi ZM. Changes in the Global Burden of Chronic Liver Diseases From 2012 to 2017: The Growing Impact of NAFLD. Hepatology 2020;72(5):1605–1616. doi:10.1002/hep.31173, PMID:32043613.
[2] Younossi Z, Anstee QM, Marietti M, Hardy T, Henry L, Eslam M, *et al*. Global burden of NAFLD and NASH: trends, predictions, risk factors and prevention. Nat Rev Gastroenterol Hepatol 2018;15(1):11–20. doi:10.1038/nrgastro.2017.109, PMID:28930295.
[3] Cotter TG, Rinella M. Nonalcoholic Fatty Liver Disease 2020: The State of the Disease. Gastroenterology 2020;158(7):1851–1864. doi:10.1053/j.gastro.2020.01.052, PMID:32061595.
[4] Younossi ZM, Stepanova M, Younossi Y, Golabi P, Mishra A, Rafiq N, *et al*. Epidemiology of chronic liver diseases in the USA in the past three decades. Gut 2020;69(3):564–568. doi:10.1136/gutjnl-2019-318813, PMID:31366455.
[5] Li J, Zou B, Yeo YH, Feng Y, Xie X, Lee DH, *et al*. Prevalence, incidence, and outcome of non-alcoholic fatty liver disease in Asia, 1999-2019: a systematic review and meta-analysis. Lancet Gastroenterol Hepatol 2019;4(5):389–398. doi:10.1016/s2468-1253(19)30039-1, PMID:30902670.
[6] Hagström H, Nasr P, Ekstedt M, Hammar U, Stål P, Hultcrantz R, *et al*. Fibrosis stage but not NASH predicts mortality and time to development of severe liver disease in biopsy-proven NAFLD. J Hepatol 2017;67(6):1265–1273. doi:10.1016/j.jhep.2017.07.027, PMID:28803953.
[7] Taylor RS, Taylor RJ, Bayliss S, Hagström H, Nasr P, Schattenberg JM, *et al*. Association Between Fibrosis Stage and Outcomes of Patients With Nonalcoholic Fatty Liver Disease: A Systematic Review and Meta-Analysis. Gastroenterology 2020;158(6):1611–1625.e1612. doi:10.1053/j.gastro.2020.01.043, PMID:32027911.
[8] Angulo P, Kleiner DE, Dam-Larsen S, Adams LA, Bjornsson ES, Charatcharoenwitthaya P, *et al*. Liver Fibrosis, but No Other Histologic Features, Is Associated With Long-term Outcomes of Patients With Nonalcoholic Fatty Liver Disease. Gastroenterology 2015;149(2):389–397.e310. doi:10.1053/j.gastro.2015.04.043, PMID:25935633.
[9] Eddowes PJ, Sasso M, Allison M, Tsochatzis E, Anstee QM, Sheridan D, *et al*. Accuracy of FibroScan Controlled Attenuation Parameter and Liver Stiffness Measurement in Assessing Steatosis and Fibrosis in Patients With Nonalcoholic Fatty Liver Disease. Gastroenterology 2019;156(6):1717–1730. doi:10.1053/j.gastro.2019.01.042, PMID:30689971.
[10] Siddiqui MS, Vuppalanchi R, Van Natta ML, Hallinan E, Kowdley KV, Abdelmalek M, *et al*. Vibration-Controlled Transient Elastography to Assess Fibrosis and Steatosis in Patients With Nonalcoholic Fatty Liver Disease. Clin Gastroenterol Hepatol 2019;17(1):156–163.e152. doi:10.1016/j.cgh.2018.04.043, PMID:29705261.
[11] Ratziu V, Charlotte F, Heurtier A, Gombert S, Giral P, Bruckert E, *et al*. Sampling variability of liver biopsy in nonalcoholic fatty liver disease. Gastroenterology 2005;128(7):1898–1906. doi:10.1053/j.gastro.2005.03.084, PMID:15940625.
[12] Maheux A, Purcell Y, Harguem S, Vilgrain V, Ronot M. Targeted and non-targeted liver biopsies carry the same risk of complication. Eur Radiol 2019;29(11):5772–5783. doi:10.1007/s00330-019-06227-3, PMID:31076864.
[13] Wai CT, Greenson JK, Fontana RJ, Kalbfleisch JD, Marrero JA, Conjeevaram HS, *et al*. A simple noninvasive index can predict both significant fibrosis and cirrhosis in patients with chronic hepatitis C. Hepatology 2003;38(2):518–526. doi:10.1053/jhep.2003.50346, PMID:12883497.
[14] Harrison SA, Oliver D, Arnold HL, Gogia S, Neuschwander-Tetri BA. Development and validation of a simple NAFLD clinical scoring system for identifying patients without advanced disease. Gut 2008;57(10):1441–1447. doi:10.1136/gut.2007.146019, PMID:18390575.
[15] Sterling RK, Lissen E, Clumeck N, Sola R, Correa MC, Montaner J, *et al*. Development of a simple noninvasive index to predict significant fibrosis in patients with HIV/HCV coinfection. Hepatology 2006;43(6):1317–1325. doi:10.1002/hep.21178, PMID:16729309.
[16] Angulo P, Hui JM, Marchesini G, Bugianesi E, George J, Farrell GC, *et al*. The NAFLD fibrosis score: a noninvasive system that identifies liver fibrosis in patients with NAFLD. Hepatology 2007;45(4):846–854. doi:10.1002/hep.21496, PMID:17393509.
[17] Siddiqui MS, Yamada G, Vuppalanchi R, Van Natta M, Loomba R, Guy C, *et al*. Diagnostic Accuracy of Noninvasive Fibrosis Models to Detect Change in Fibrosis Stage. Clin Gastroenterol Hepatol 2019;17(9):1877–1885.e1875. doi:10.1016/j.cgh.2018.12.031, PMID:30616027.
[18] McPherson S, Stewart SF, Henderson E, Burt AD, Day CP. Simple non-invasive fibrosis scoring systems can reliably exclude advanced fibrosis in patients with non-alcoholic fatty liver disease. Gut 2010;59(9):1265–1269. doi:10.1136/gut.2010.216077, PMID:20801772.
[19] Xiao G, Zhu S, Xiao X, Yan L, Yang J, Wu G. Comparison of laboratory tests, ultrasound, or magnetic resonance elastography to detect fibrosis in patients with nonalcoholic fatty liver disease: A meta-analysis. Hepatology 2017;66(5):1486–1501. doi:10.1002/hep.29302, PMID:28586172.
[20] Eslam M, Sanyal AJ, George J. MAFLD: A Consensus-Driven Proposed Nomenclature for Metabolic Associated Fatty Liver Disease. Gastroenterology 2020;158(7):1999–2014.e1991. doi:10.1053/j.gastro.2019.11.312, PMID:32044314.
[21] Eslam M, Newsome PN, Sarin SK, Anstee QM, Targher G, Romero-Gomez M, *et al*. A new definition for metabolic dysfunction-associated fatty liver disease: An international expert consensus statement. J Hepatol 2020;73(1):202–209. doi:10.1016/j.jhep.2020.03.039, PMID:32278004.
[22] Lin S, Huang J, Wang M, Kumar R, Liu Y, Liu S, *et al*. Comparison of MAFLD and NAFLD diagnostic criteria in real world. Liver Int 2020;40(9):2082–2089. doi:10.1111/liv.14548, PMID:32478487.
[23] Ruhl CE, Everhart JE. Fatty liver indices in the multiethnic United States National Health and Nutrition Examination Survey. Aliment Pharmacol Ther 2015;41(1):65–76. doi:10.1111/apt.13012, PMID:25376360.
[24] Huang J, Ou W, Wang M, Singh M, Liu Y, Liu S, *et al*. MAFLD Criteria Guide the Subtyping of Patients with Fatty Liver Disease. Risk Manag Healthc Policy 2021;14:491–501. doi:10.2147/rmhp.S285880, PMID:33603515.
[25] Karlas T, Petroff D, Sasso M, Fan JG, Mi YQ, de Lédinghen V, *et al*. Individual patient data meta-analysis of controlled attenuation parameter (CAP) technology for assessing steatosis. J Hepatol 2017;66(5):1022–1030. doi:10.1016/j.jhep.2016.12.022, PMID:28039099.
[26] Cassinotto C, Boursier J, de Lédinghen V, Lebigot J, Lapuyade B, Cales P, *et al*. Liver stiffness in nonalcoholic fatty liver disease: A comparison of supersonic shear imaging, FibroScan, and ARFI with liver biopsy. Hepatology 2016;63(6):1817–1827. doi:10.1002/hep.28394, PMID:26659452.
[27] Bedossa P, Poynard T. An algorithm for the grading of activity in chronic hepatitis C. The METAVIR Cooperative Study Group. Hepatology 1996;24(2):289–293. doi:10.1002/hep.510240201, PMID:8690394.
[28] Wu YL, Kumar R, Wang MF, Singh M, Huang JF, Zhu YY, *et al*. Validation of conventional non-invasive fibrosis scoring systems in patients with metabolic associated fatty liver disease. World J Gastroenterol 2021;27(34):5753–5763. doi:10.3748/wjg.v27.i34.5753, PMID:34629799.
[29] Younes R, Caviglia GP, Govaere O, Rosso C, Armandi A, Sanavia T, *et al*. Long-term outcomes and predictive ability of non-invasive scoring systems in patients with non-alcoholic fatty liver disease. J Hepatol 2021;75(4):786–794. doi:10.1016/j.jhep.2021.05.008, PMID:34090928.
[30] Vilar-Gomez E, Chalasani N. Non-invasive assessment of non-alcoholic fatty liver disease: Clinical prediction rules and blood-based biomarkers. J Hepatol 2018;68(2):305–315. doi:10.1016/j.jhep.2017.11.013, PMID:29154965.

*Journal of Clinical and Translational Hepatology* **2022** vol. 10(4) | 595–599
DOI: 10.14218/JCTH.2021.00379

Original Article

# Sex-specific Cutoff Values of Visceral Fat Area for Lean vs. Overweight/Obese Nonalcoholic Fatty Liver Disease in Asians

Sunyoung Lee[1*], Kyoung Won Kim[2] and Jeongjin Lee[3]

*[1]Department of Radiology and Research Institute of Radiological Science, Severance Hospital, Yonsei University College of Medicine, Seoul, Republic of Korea; [2]Department of Radiology and Research Institute of Radiology, Asan Medical Center, University of Ulsan College of Medicine, Seoul, Republic of Korea; [3]School of Computer Science and Engineering, Soongsil University, Seoul, Republic of Korea*

**Received:** 28 August 2021 | **Revised:** 17 October 2021 | **Accepted:** 30 October 2021 | **Published:** 7 January 2022

## Abstract

***Background and Aims:*** Visceral obesity is a risk factor for nonalcoholic fatty liver disease (NAFLD). We investigated sex-specific optimal cutoff values for visceral fat area (VFA) associated with lean and overweight/obese NAFLD in an Asian population. ***Methods:*** This retrospective study included 678 potential living liver donors (mean age, 30.8±9.4 years; 434 men and 244 women) who had undergone abdominal computed tomography (CT) imaging and liver biopsy between November 2016 and October 2017. VFA was measured using single-slice abdominal CT. NAFLD was evaluated by liver biopsy (≥5% hepatic steatosis). Receiver operating characteristic curve analysis was used to determine cutoff values for VFA associated with lean (body mass index [BMI] <23 kg/m$^2$) and overweight/obese (BMI ≥23 kg/m$^2$) NAFLD. ***Results:*** Area under the curve (AUC) values with 95% confidence intervals (CI) for VFA were 0.82 (95% CI, 0.75–0.88) for lean and 0.74 (95% CI, 0.69–0.79) for overweight/obese men with NAFLD. The AUC values were 0.67 (95% CI, 0.58–0.75) for lean and 0.71 (95% CI, 0.62–0.80) for overweight/obese women with NAFLD. The cutoff values for VFA associated with lean NAFLD were 50.2 cm$^2$ in men and 40.5 cm$^2$ in women. The optimal cutoff values for VFA associated with overweight/obese NAFLD were 100.6 cm$^2$ in men and 68.0 cm$^2$ in women. ***Conclusions:*** Sex-specific cutoff values for VFA may be useful for identifying subjects at risk of lean and overweight/obese NAFLD.

**Citation of this article:** Lee S, Kim KW, Lee J. Sex-specific Cutoff Values of Visceral Fat Area for Lean vs. Overweight/Obese Nonalcoholic Fatty Liver Disease in Asians. J Clin Transl Hepatol 2022;10(4):595–599. doi: 10.14218/JCTH.2021.00379.

**Keywords:** Hepatic steatosis; Adipose tissue; Liver biopsy; Computed tomography..

**Abbreviations:** ALT, alanine aminotransferase; AST, aspartate aminotransferase; AUC, area under the curve; BMI, body mass index; CI, confidence interval; CT, computed tomography; HDL, high-density lipoprotein; HS, hepatic steatosis; MR, magnetic resonance; NAFLD, nonalcoholic fatty liver disease; ROC, receiver operating characteristic; SD, standard deviation; US, ultrasound; VFA, visceral fat area.

***Correspondence to:** Sunyoung Lee, Department of Radiology and Research Institute of Radiological Science, Severance Hospital, Yonsei University College of Medicine, 50-1 Yonsei-ro, Seodaemun-gu, Seoul 03722, Republic of Korea. Tel: +82-2-2228-7400, Fax: +82-2-2227-8337, E-mail: carnival0126@gmail.com

## Introduction

Nonalcoholic fatty liver disease (NAFLD) is a major etiology of chronic liver disease worldwide.[1] The diagnosis of NAFLD is confirmed by the presence of ≥5% hepatic steatosis (HS) either on imaging or histology in the absence of secondary causes for hepatic fat accumulation (e.g., excessive alcohol consumption, use of steatogenic medications, or hereditary disorders).[2] Although NAFLD is associated with obesity and has been reliably established as a hepatic manifestation of the metabolic syndrome, it can also occur in lean patients, i.e., those having body mass indices (BMIs) of <23 kg/m$^2$ in Asians or <25 kg/m$^2$ in non-Asians.[3,4] Recent studies have indicated that visceral obesity may have a more important role in development of the metabolic syndrome and NAFLD than generalized obesity.[5,6]

While the diagnosis of NAFLD can be determined by imaging, including ultrasonography, the controlled attenuation parameter of transient elastography, computed tomography (CT), and magnetic resonance (MR) spectroscopy or proton density fat fraction, histological analysis of liver biopsies is regarded as the gold standard.[7] For evaluation of visceral adiposity, CT imaging is considered the gold standard.[8] Although many studies have identified values for visceral adiposity associated with the metabolic syndrome,[9–14] few have focused on NAFLD.[15] Moreover, appropriate cutoff values for visceral fat area (VFA) stratified by sex and BMI for NAFLD have not been identified in studies using gold-standard methods. We aimed to identify sex-specific optimal cutoff values for VFA, measured by CT imaging, and associated with lean and overweight/obese NAFLD assessed by liver biopsy, in an Asian population.

## Methods

The study was approved by the institutional review board of our institution. The requirement for written informed consent was waived because the analysis was retrospective.

### *Study population*

Our institution's databases were retrospectively searched to identify living liver donor candidates who had undergone an abdominal CT imaging examination and ultrasound

**Table 1. Participant characteristics**

| | Total (*n*=678) | Male (*n*=434) | Female (*n*=244) | *p*-value |
|---|---|---|---|---|
| Age, y | 30.8±9.4 | 29.5±9.0 | 33.3±9.6 | <0.001 |
| Body mass index, kg/m$^2$ | 23.6±3.1 | 24.0±2.9 | 22.9±3.5 | <0.001 |
| AST, IU/L | 22.3±23.1 | 23.9±26.7 | 19.6±14.2 | 0.021 |
| ALT, IU/L | 21.9±29.5 | 25.3±34.6 | 16.0±15.5 | <0.001 |
| Total cholesterol, mg/dL | 177.1±35.3 | 177.7±35.2 | 175.8±35.4 | 0.498 |
| Triglyceride, mg/dL | 109.3 ±74.8 | 122.9±80.9 | 86.2±56.3 | <0.001 |
| HDL, mg/dL | 56.6±14.1 | 53.2±12.6 | 62.4±14.5 | <0.001 |
| Visceral fat area, cm$^2$ | 68.3±45.9 | 78.3±49.1 | 50.5±32.7 | <0.001 |

Data are mean±standard deviation. ALT, alanine aminotransferase; AST, aspartate aminotransferase; HDL, high-density lipoprotein.

(US)-guided percutaneous liver biopsy as part of a routine predonation evaluation between November 2016 and October 2017. The medical evaluation process consisted of three phases. Phase 1 comprised a clinical examination, review of the past medical history, and laboratory tests, including viral serology. Subjects who consumed more than 20 g of alcohol per day or used drugs regularly including herbal medications were considered inappropriate for liver donation. Donor candidates who had diabetes mellitus, hypertension, or any other significant medical diseases were excluded from right liver donation. Subjects with serologic evidence of hepatitis B or hepatitis C were excluded from liver donation. Phase 2 included liver CT to evaluate vascular anatomy, hepatic volume, and steatosis. Phase 3 consisted of MR cholangiography and indocyanine green retention tests.

### *CT image acquisition*

CT scans were performed with a 128-slice (Definition AS+ or Edge, Siemens, Erlangen, Germany) multidetector-row CT scanner. Unenhanced CT scans were obtained, followed by biphasic contrast-enhanced CT (hepatic arterial and portal venous phases) after administration of 150 mL of iopromide (Ultravist 370, Bayer Schering Pharma, Berlin, Germany) for anatomical mapping of the hepatic vasculature and CT volumetry. The scanning and reconstruction parameters were beam collimation of 128 slices by 0.6 mm, spiral pitch of 1, gantry rotation time of 0.5 s, tube voltage of 100 or 120 kVp, tube current of 120–200 mAs with automatic exposure control (Care Dose 4D, Siemens), and section thickness and interval of 5 mm.

### *Assessment of abdominal fat parameters*

A single axial CT image at the level of the inferior endplate of the L3 lumbar vertebra was processed for each patient. Abdominal CT image analysis was performed with a fully convolutional network-based automatic segmentation technique using a deep learning system.[16] Assessment of body composition was conducted using artificial intelligence software (AIDU, iAID Inc., Seoul, Republic of Korea).[16] CT images were automatically segmented to generate boundaries, with measurement of abdominal fat. The VFA (cm$^2$) was demarcated using fat-tissue thresholds (−190 to −30 Hounsfield units).

### *Liver biopsy*

As part of the living liver donor evaluation, US-guided percutaneous biopsy of the right hepatic lobe was performed using an 18-gauge needle (Stericut 18G coaxial, TSK Laboratory, Tochigi, Japan). Two or more biopsy specimens, each approximately 1.5 cm in length, were obtained and stained with hematoxylin and eosin. The degree of HS was assessed as the percentage of liver parenchyma replaced by steatotic droplets. NAFLD was defined as the presence of ≥5% HS.[2]

### *Data collection*

Demographic data (age and sex), anthropometric measurements (body weight and height), and laboratory parameters [serum AST, ALT, total cholesterol, triglycerides, high-density lipoprotein (HDL)] were collected. BMI (kg/m$^2$) status was determined using ethnicity-specific cutoff values of <23 kg/m$^2$ for lean, 23–24.9 kg/m$^2$ for overweight, and ≥25 kg/m$^2$ for obese.[17]

### *Statistical analysis*

Descriptive values are reported as mean±standard deviation (SD). Differences between male and female subjects were evaluated with two-sample *t*-tests. Subject characteristics of were analyzed according to lean vs. overweight/obese status and the presence or absence of NAFLD using one-way analysis of variance, followed by *post hoc* analysis using the Bonferroni method. Receiver operating characteristic (ROC) curve analysis was used to assess the accuracy of identifying the presence of NAFLD in lean and overweight/obese subjects. Accuracy was measured by area under the curve (AUC) with 95% confidence intervals (CIs). Sex-specific cutoff values for VFA were chosen to maximize the sum of the sensitivity and specificity of Youden's index. At optimal cutoff values, sensitivity and specificity with 95% CIs were determined. Statistical significance was set at a *p*-value of <0.05. Statistical analysis was performed with SPSS 23.0 (IBM Corp., Armonk, NY, USA) and MedCalc 16.2.1 (MedCalc Software, Ostend, Belgium).

## Results

A total of 678 subjects (30.8±9.4 years of age, 434 men, and 244 women) were included in the analysis. Their baseline characteristics are summarized in Table 1. The BMI, serum AST, ALT, and triglycerides, and VFA were higher in men and age and serum HDL were higher in women.

The study cohort was divided into subgroups by BMI and

**Table 2. Features of study subjects stratified by BMI and NAFLD status and subdivided by sex**

| | Lean without NAFLD | Lean NAFLD | Overweight/obese without NAFLD | Overweight/obese NAFLD | *p*-value |
|---|---|---|---|---|---|
| Male (*n*=434) | | | | | |
| n | 99 | 59 | 147 | 129 | |
| Age, y | 26.7±7.8 | 31.3±8.2[a] | 28.2±8.4 | 32.2±10.1[a,c] | <0.001 |
| Body mass index, kg/m$^2$ | 21.1±1.4 | 21.6±1.3 | 25.3±2.1[a,b] | 25.8±2.6[a,b] | <0.001 |
| AST, IU/L | 22.1±13.2 | 24.4±18.0 | 21.2±9.8 | 28.1±44.7 | 0.161 |
| ALT, IU/L | 17.9±12.8 | 28.2±23.2 | 22.0±14.2 | 33.4±57.6[a,c] | 0.004 |
| Total cholesterol, mg/dL | 168.4±29.9 | 187.2±37.7[a] | 175.2±35.4 | 183.5±35.8[a] | 0.001 |
| Triglyceride, mg/dL | 98.8±70.8 | 132.9±98.8 | 116.8±66.1 | 146.5±87.9[a,c] | <0.001 |
| HDL, mg/dL | 58.2±13.3 | 52.1±11.5[a] | 53.7±13.1[a] | 48.7±10.4[a,c] | <0.001 |
| Visceral fat area, cm$^2$ | 41.4±27.7 | 80.5±35.6[a] | 71.9±44.1[a] | 113.0±49.6[a,b,c] | <0.001 |
| Female (*n*=244) | | | | | |
| n | 114 | 21 | 69 | 40 | |
| Age, y | 33.6±8.4 | 34.9±8.7 | 31.1±9.8 | 35.4±12.3 | 0.109 |
| Body mass index, kg/m$^2$ | 20.5±1.6 | 20.7±1.4 | 25.6±2.5[a,b] | 26.5±3.1[a,b] | <0.001 |
| AST, IU/L | 19.6±16.0 | 17.7±3.1 | 19.8±15.4 | 20.5±9.7 | 0.909 |
| ALT, IU/L | 14.1±14.2 | 14.7±5.5 | 17.7±17.9 | 18.9±17.9 | 0.258 |
| Total cholesterol, mg/dL | 174.2±30.7 | 179.2±40.2 | 171.8±40.1 | 186.3±36.1 | 0.185 |
| Triglyceride, mg/dL | 77.7±58.7 | 75.9±47.3 | 87.2±48.8 | 115.3±56.8[a,b] | 0.004 |
| HDL, mg/dL | 65.8±14.0 | 66.1±17.0 | 60.2±14.4 | 54.2±10.9[a,b] | <0.001 |
| Visceral fat area, cm$^2$ | 32.1±19.0 | 47.1±27.2[a] | 61.1±28.5[a] | 86.8±35.9[a,b,c] | <0.001 |

Data are mean±standard deviation. ALT, alanine aminotransferase; AST, aspartate aminotransferase; BMI, body mass index; HDL, high-density lipoprotein; NAFLD, nonalcoholic fatty liver disease. [a]$p<0.05$ by *post hoc* analyses vs. lean without NAFLD. [b]$p<0.05$ by *post hoc* analyses vs. lean NAFLD. [c]$p<0.05$ by *post hoc* analysis vs. overweight/obese without NAFLD.

NAFLD as lean without NAFLD, lean with NAFLD, overweight/obese without NAFLD, and overweight/obese with NAFLD. The subgroup characteristics subdivided by sex are shown in Table 2. In men, subgroup differences in age, BMI, serum ALT, total cholesterol, triglyceride, and HDL levels, and VFA were significant ($p\leq0.004$). In women, subgroup differences in BMI, serum triglyceride, and HDL levels, and VFA were significant ($p\leq0.004$). In both lean and overweight/obese subjects, VFA tended to be higher in those with NAFLD than in those without NAFLD, and *post hoc* analysis showed that the VFA in lean subjects with NAFLD and overweight/obese without NAFLD of either sex were not significant (men, $p>0.999$ and women, $p=0.189$).

Table 3 and Figure 1 report the AUC values of VFA for identifying lean and overweight/obese NAFLD. NAFLD was found in 37.3% lean and 46.7% of overweight/obese men and 15.6% of lean and 36.7% of overweight/obese women. The AUCs were 0.82 (95% CI, 0.75–0.88) for lean and 0.74 (95% CI, 0.69–0.79) for overweight/obese men and 0.67 (95% CI, 0.58–0.75) for lean and 0.71 (95% CI, 0.62–0.80) for overweight/obese women. The optimal cutoff values for VFA for lean and overweight/obese NAFLD were 50.2 cm$^2$ and 100.6 cm$^2$, respectively, in men and 40.5 cm$^2$ and 68.0 cm$^2$, respectively, in women. In men, the sensitivity and specificity at the optimal VFA cutoffs were 81.4% (95% CI, 69.1–90.3%) and 71.7% (95% CI, 61.8–80.3%), respectively, for lean, and 61.2% (95% CI, 52.3–69.7%) and 76.2% (95% CI, 68.5–82.8%), respectively, for overweight/obese NAFLD. In women, the sensitivity and specificity at the optimal VFA cutoffs were 57.1% (95% CI, 34.0–78.2%) and 81.6% (95% CI, 73.2–88.2%), respectively, for lean NAFLD and 70.0% (95% CI, 53.5%–83.4%) and 69.6% (95% CI, 57.3–80.1%), respectively, for overweight/obese NAFLD.

**Table 3. Optimal cutoff values for VFA for identifying lean and overweight/obese NAFLD subdivided by sex**

| | Lean NAFLD | | Overweight/obese NAFLD | |
|---|---|---|---|---|
| | Male | Female | Male | Female |
| AUC (95% CI) | 0.82 (0.75–0.88) | 0.67 (0.58–0.75) | 0.74 (0.69–0.79) | 0.71 (0.62–0.80) |
| Optimal VFA cutoff value, cm$^2$ | 50.2 | 40.5 | 100.6 | 68.0 |
| Sensitivity (95% CI), % | 81.4 (69.1–90.3) | 57.1 (34.0–78.2) | 61.2 (52.3–69.7) | 70.0 (53.5–83.4) |
| Specificity (95% CI), % | 71.7 (61.8–80.3) | 81.6 (73.2–88.2) | 76.2 (68.5–82.8) | 69.6 (57.3–80.1) |

Optimal VFA cutoff values were defined by the maximal sum of sensitivity and specificity. AUC, area under the curve; CI, confidence interval; NAFLD, nonalcoholic fatty liver disease; VFA, visceral fat area.

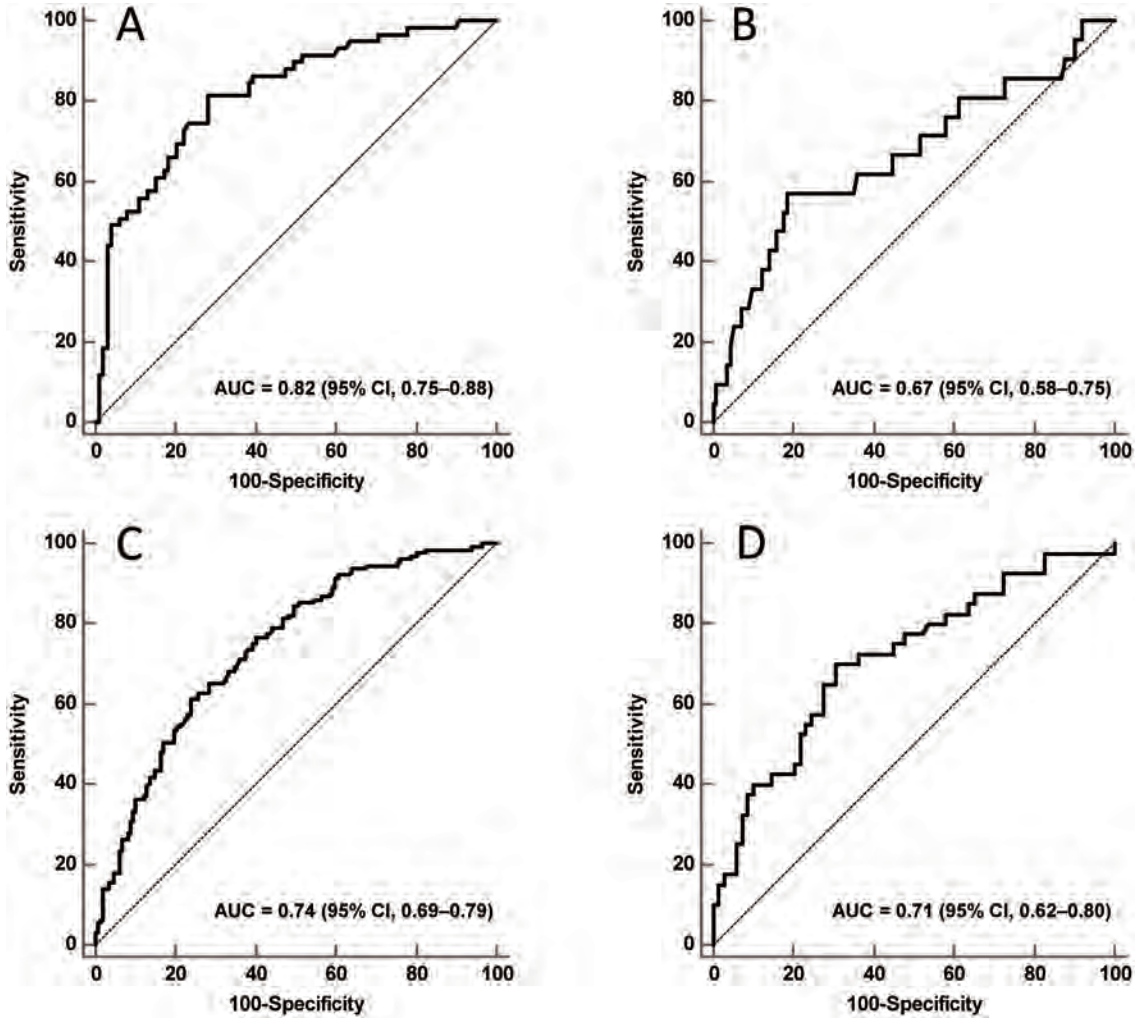


**Fig. 1. Receiver operating characteristic curves for visceral fat area to identify (A) lean nonalcoholic fatty liver disease (NAFLD) in men, (B) in lean women, (C) in overweight/obese men, and (D) overweight/obese in women.**

## Discussion

The VFA tended to be higher in subjects with NAFLD than in those without NAFLD in both lean and overweight/obese potential living liver donors who underwent abdominal CT imaging and liver biopsy. We also identified optimal VFA cutoff values for identifying the presence of NAFLD stratified by sex and BMI status.

Although obesity is generally related to NAFLD, a considerable number of patients with NAFLD are nonobese or even lean, and a substantial proportion of overweight or obese individuals do not develop NAFLD.[3] The development of NAFLD may be related to adipose tissue distribution, and visceral adipose tissue is widely accepted as a risk factor for NAFLD independent of generalized obesity.[18] Our study also demonstrated that the mean VFA was higher in subjects with NAFLD than in those without NAFLD in both lean and overweight/obese groups. Visceral fat has higher lipolytic activity, and directly releases free fatty acids into the liver via the portal circulation, which may substantially contribute to HS.[19] Increased visceral fat results in increased production of cytokines and adipokines, leading to disease progression in NAFLD.[3] In addition, our study showed that the VFA was not significantly different between lean subjects with NAFLD and overweight/obese subjects without NAFLD in either sex, indicating that visceral fat accumulation was as high in lean subjects with NAFLD as it was in overweight/obese individuals, which is consistent with a previous study in a Chinese population that used MR imaging to detect HS and measure visceral fat.[20]

Many studies have investigated the optimal cutoffs for visceral fat indices when screening for the metabolic syndrome,[9–14] but to the best of our knowledge, there has been only one study that established optimal VFA cutoffs for NAFLD.[15] In a study by Yoon *et al*.[15] in a Korean population, the optimal VFA cutoffs at the L4-L5 level for detecting NAFLD, measured by CT imaging, were 132 $cm^2$ in men and 119 $cm^2$ in women. In that study, the liver attenuation index derived from the difference between mean hepatic and splenic attenuation on unenhanced CT imaging was used in the diagnosis of NAFLD.[15] Unlike that study,[15] we generated sex-specific cutoff values for CT-measured VFA at the L3 level to separate metabolically normal Koreans from those with lean and overweight/obese NAFLD, as assessed by liver biopsy (i.e., the gold standard for an NAFLD diagnosis). We propose VFA cutoffs of 50.2 $cm^2$ in men and 40.5 $cm^2$ in women to identify those at risk of lean NAFLD, and 100.6 $cm^2$ in men and 68.0 $cm^2$ in women to identify those at risk

of overweight/obese NAFLD. The values may be useful for identifying patients in whom visceral obesity places them at increased risk for lean or overweight/obese NAFLD. In addition, they may be used as therapeutic target values for visceral fat reduction to resolve NAFLD.

The study has several limitations. First, it was a preliminary retrospective study conducted at a single center, and the number of enrolled subjects was not large. Prospective multicenter, studies with more participants are needed to confirm our results. Second, the study included potential living liver donors who had undergone liver biopsy as part of a predonation workup. The inclusion criteria were implemented to assess NAFLD and VFA using gold standard diagnostic methods, but that may have resulted in selection bias. Also, noninvasive evaluation of HS by transient elastography was not performed in this study. In addition, the enrolled subjects were relatively young adults capable of donating their livers. Therefore, it is unclear whether they are representative of the general population. Third, we included only Korean subjects, which may have limited the generalizability of our findings to other ethnicities. So, our findings need to be validated by trials in a broader population. Fourth, the prevalence of NAFLD in lean men (37.3%) was much higher than previously reported,[4,21,22] so it may have led to the better performance of AUC in lean men with NAFLD than in the other groups.

In conclusion, the cutoff values of CT-measured VFA for identifying NAFLD were influenced by sex and BMI. Sex-specific cutoff values for VFA may be useful for identifying lean and overweight/obese individuals at risk of NAFLD.

## Conflict of interest

The authors have no conflict of interests related to this publication.

## Author contributions

Contributed to the study concept and design, analysis and interpretation of data, drafting of the manuscript, material support, and study supervision (SL), acquisition of data (JL), critical revision of the manuscript for important intellectual content and administrative, technical support (KWK).

## Data sharing statement

The data used to support the findings of this study are available from the corresponding author upon request.

## References


[1] Younossi ZM, Koenig AB, Abdelatif D, Fazel Y, Henry L, Wymer M. Global epidemiology of nonalcoholic fatty liver disease-Meta-analytic assessment of prevalence, incidence, and outcomes. Hepatology 2016;64(1):73–84. doi:10.1002/hep.28431.

[2] Chalasani N, Younossi Z, Lavine JE, Charlton M, Cusi K, Rinella M, *et al*. The diagnosis and management of nonalcoholic fatty liver disease: Practice guidance from the American Association for the Study of Liver Diseases. Hepatology 2018;67(1):328–357. doi:10.1002/hep.29367.

[3] Kumar R, Mohan S. Non-alcoholic fatty liver disease in lean subjects: Characteristics and implications. J Clin Transl Hepatol 2017;5(3):216–223. doi:10.14218/JCTH.2016.00068.

[4] Ye Q, Zou B, Yeo YH, Li J, Huang DQ, Wu Y, *et al*. Global prevalence, incidence, and outcomes of non-obese or lean non-alcoholic fatty liver disease: a systematic review and meta-analysis. Lancet Gastroenterol Hepatol 2020;5(8):739–752. doi:10.1016/S2468-1253(20)30077-7.

[5] Feldman A, Eder SK, Felder TK, Kedenko L, Paulweber B, Stadlmayr A, *et al*. Clinical and metabolic characterization of lean caucasian subjects with non-alcoholic fatty liver. Am J Gastroenterol 2017;112(1):102–110. doi:10.1038/ajg.2016.318.

[6] Tobari M, Hashimoto E, Taniai M, Ikarashi Y, Kodama K, Kogiso T, *et al*. Characteristics of non-alcoholic steatohepatitis among lean patients in Japan: Not uncommon and not always benign. J Gastroenterol Hepatol 2019;34(8):1404–1410. doi:10.1111/jgh.14585.

[7] Stern C, Castera L. Non-invasive diagnosis of hepatic steatosis. Hepatol Int 2017;11(1):70–78. doi:10.1007/s12072-016-9772-z.

[8] Park BJ, Kim YJ, Kim DH, Kim W, Jung YJ, Yoon JH, *et al*. Visceral adipose tissue area is an independent risk factor for hepatic steatosis. J Gastroenterol Hepatol 2008;23(6):900–907. doi:10.1111/j.1440-1746.2007.05212.x.

[9] Oka R, Kobayashi J, Yagi K, Tanii H, Miyamoto S, Asano A, *et al*. Reassessment of the cutoff values of waist circumference and visceral fat area for identifying Japanese subjects at risk for the metabolic syndrome. Diabetes Res Clin Pract 2008;79(3):474–481. doi:10.1016/j.diabres.2007.10.016.

[10] Seo JA, Kim BG, Cho H, Kim HS, Park J, Baik SH, *et al*. The cutoff values of visceral fat area and waist circumference for identifying subjects at risk for metabolic syndrome in elderly Korean: Ansan Geriatric (AGE) cohort study. BMC Public Health 2009;9:443. doi:10.1186/1471-2458-9-443.

[11] Kim HI, Kim JT, Yu SH, Kwak SH, Jang HC, Park KS, *et al*. Gender differences in diagnostic values of visceral fat area and waist circumference for predicting metabolic syndrome in Koreans. J Korean Med Sci 2011;26(7):906–913. doi:10.3346/jkms.2011.26.7.906.

[12] Matsushita Y, Nakagawa T, Yamamoto S, Takahashi Y, Yokoyama T, Mizoue T, *et al*. Visceral fat area cutoff for the detection of multiple risk factors of metabolic syndrome in Japanese: the Hitachi Health Study. Obesity (Silver Spring) 2012;20(8):1744–1749. doi:10.1038/oby.2011.285.

[13] Doyle SL, Bennett AM, Donohoe CL, Mongan AM, Howard JM, Lithander FE, *et al*. Establishing computed tomography-defined visceral fat area thresholds for use in obesity-related cancer research. Nutr Res 2013;33(3):171–179. doi:10.1016/j.nutres.2012.12.007.

[14] Tsukiyama H, Nagai Y, Matsubara F, Shimizu H, Iwamoto T, Yamanouchi E, *et al*. Proposed cut-off values of the waist circumference for metabolic syndrome based on visceral fat volume in a Japanese population. J Diabetes Investig 2016;7(4):587–593. doi:10.1111/jdi.12454.

[15] Yoo HJ, Park MS, Lee CH, Yang SJ, Kim TN, Lim KI, *et al*. Cutoff points of abdominal obesity indices in screening for non-alcoholic fatty liver disease in Asians. Liver Int 2010;30(8):1189–1196. doi:10.1111/j.1478-3231.2010.02300.x.

[16] Park HJ, Shin Y, Park J, Kim H, Lee IS, Seo DW, *et al*. Development and validation of a deep learning system for segmentation of abdominal muscle and fat on computed tomography. Korean J Radiol 2020;21(1):88–100. doi:10.3348/kjr.2019.0470.

[17] Fan JG, Kim SU, Wong VW. New trends on obesity and NAFLD in Asia. J Hepatol 2017;67(4):862–873. doi:10.1016/j.jhep.2017.06.003.

[18] Li L, Liu DW, Yan HY, Wang ZY, Zhao SH, Wang B. Obesity is an independent risk factor for non-alcoholic fatty liver disease: evidence from a meta-analysis of 21 cohort studies. Obes Rev 2016;17(6):510–519. doi:10.1111/obr.12407.

[19] Finelli C, Tarantino G. Should visceral fat, strictly linked to hepatic steatosis, be depleted to improve survival? Hepatol Int 2013;7(2):413–428. doi:10.1007/s12072-012-9406-z.

[20] Chiyanika C, Wong VW, Wong GL, Chan HL, Hui SCN, Yeung DKW, *et al*. Implications of abdominal adipose tissue distribution on nonalcoholic fatty liver disease and metabolic syndrome: A Chinese general population study. Clin Transl Gastroenterol 2021;12(2):e00300. doi:10.14309/ctg.0000000000000300.

[21] Shi Y, Wang Q, Sun Y, Zhao X, Kong Y, Ou X, *et al*. The prevalence of lean/nonobese nonalcoholic fatty liver disease: A systematic review and meta-analysis. J Clin Gastroenterol 2020;54(4):378–387. doi:10.1097/MCG.0000000000001270.

[22] Lu FB, Zheng KI, Rios RS, Targher G, Byrne CD, Zheng MH. Global epidemiology of lean non-alcoholic fatty liver disease: A systematic review and meta-analysis. J Gastroenterol Hepatol 2020;35(12):2041–2050. doi:10.1111/jgh.15156.

*Journal of Clinical and Translational Hepatology* **2022** vol. 10(4) | 600–607
DOI: 10.14218/JCTH.2021.00348

Original Article

# A K-nearest Neighbor Model to Predict Early Recurrence of Hepatocellular Carcinoma After Resection

Chuanli Liu[1#], Hongli Yang[2#], Yuemin Feng[3#], Cuihong Liu[4], Fajuan Rui[1], Yuankui Cao[5], Xinyu Hu[2], Jiawen Xu[6], Junqing Fan[5], Qiang Zhu[3] and Jie Li[2,7,8*]

*[1]Department of Infectious Disease, Shandong Provincial Hospital Affiliated to Shandong Frist Medical University, Ji'nan, Shandong, China; [2]Department of Infectious Disease, Shandong Provincial Hospital, Cheeloo College of Medicine, Shandong University, Ji'nan, Shandong, China; [3]Department of Gastroenterology, Shandong Provincial Hospital Affiliated to Shandong Frist Medical University, Ji'nan, Shandong, China; [4]Department of Ultrasound Diagnosis and Treatment, Shandong Provincial Hospital Affiliated to Shandong Frist Medical University, Ji'nan, Shandong, China; [5]School of Computer Science, China University of Geosciences, Wuhan, Hubei, China; [6]Department of Pathology, Shandong Provincial Hospital Affiliated to Shandong Frist Medical University, Ji'nan, Shandong, China; [7]Department of Infectious Diseases, Nanjing Drum Tower Hospital, The Affiliated Hospital of Nanjing University Medical School, Nanjing, Jiangsu, China; [8]Institute of Viruses and Infectious Diseases, Nanjing University, Nanjing, Jiangsu, China*

**Received:** 19 August 2021 | **Revised:** 25 September 2021 | **Accepted:** 10 October 2021 | **Published:** 4 January 2022

## Abstract

***Background and Aims:*** Patients with hepatocellular carcinoma (HCC) surgically resected are at risk of recurrence; however, the risk factors of recurrence remain poorly understood. This study intended to establish a novel machine learning model based on clinical data for predicting early recurrence of HCC after resection. ***Methods:*** A total of 220 HCC patients who underwent resection were enrolled. Classification machine learning models were developed to predict HCC recurrence. The standard deviation, recall, and precision of the model were used to assess the model's accuracy and identify efficiency of the model. ***Results:*** Recurrent HCC developed in 89 (40.45%) patients at a median time of 14 months from primary resection. In principal component analysis, tumor size, tumor grade differentiation, portal vein tumor thrombus, alpha-fetoprotein, protein induced by vitamin K absence or antagonist-II (PIVKA-II), aspartate aminotransferase, platelet count, white blood cell count, and HBsAg were positive prognostic factors of HCC recurrence and were included in the preoperative model. After comparing different machine learning methods, including logistic regression, decision tree, naïve Bayes, deep neural networks, and k-nearest neighbor (K-NN), we choose the K-NN model as the optimal prediction model. The accuracy, recall, precision of the K-NN model were 70.6%, 51.9%, 70.1%, respectively. The standard deviation was 0.020. ***Conclusions:*** The K-NN classification algorithm model performed better than the other classification models. Estimation of the recurrence rate of early HCC can help to allocate treatment, eventually achieving safe oncological outcomes.

**Citation of this article:** Liu C, Yang H, Feng Y, Liu C, Rui F, Cao Y, *et al*. A K-nearest Neighbor Model to Predict Early Recurrence of Hepatocellular Carcinoma After Resection. J Clin Transl Hepatol 2022;10(4):600–607. doi: 10.14218/JCTH.2021.00348.

## Introduction

Primary liver cancer is the sixth most common cancer worldwide and the fourth leading cause of cancer-related death, accounting for ~90% of primary liver cancers.[1] Hepatocellular carcinoma (HCC) is the most frequent histologic type of liver cancer. The most effective first-line treatment is surgical resection for selected patients and is widely recommended by current guidelines.[2,3] However, patients with surgically resected HCC are still at risk of recurrence, with an annual rate of ≥ 10% and a recurrence rate of 70–80% after 5 years.[4] In addition, the reasons for postsurgical recurrence and how to prevent recurrence are unresolved. Therefore, identification of potentially curable patients at high risk for postoperative recurrence is critical to improve long-term survival after HCC resection.

HCC recurrence is the main postoperative complication, which is generally considered either early (less than 2 years) or late (more than 2 years).[5] However, early recurrence occurs in 30–50% of patients and accounts for more than 70% of tumor recurrences, and is the major cause of mortality. Previous studies have shown that early recurrence of HCC is usually related to aggressive tumor pathological features, such as large tumor size, multiple tumors,

**Keywords:** Hepatocellular carcinoma; Surgical resection; Recurrence; Machine learning; Prognostic model.

**Abbreviations:** Acc, accuracy; AFP, alpha-fetoprotein; ALP, alkaline phosphatase; AST, aspartate aminotransferase; DNN, deep neural networks; HCC, hepatocellular carcinoma; JIS, Japan Integrated Staging; K-NN, k-nearest neighbor; PIVKA-II, protein induced by vitamin K absence or antagonist-II; PLT, platelet count; Prc, precision; PT, prothrombin time; RFA, radio-ablation therapy; TACE, trans arterial chemoembolization; TNM, tumor-node-metastasis; TPR, recall rate; WBC, white blood cell.

[#]These authors contributed equally to this work.

[*]**Correspondence to:** Jie Li, Department of Infectious Diseases, Nanjing Drum Tower Hospital, The Affiliated Hospital of Nanjing University Medical School, Nanjing, Jiangsu 210000, China; ORCID: https://orcid.org/0000-0003-0973-8645. Tel: +86-15863787910, Email: lijier@sina.com

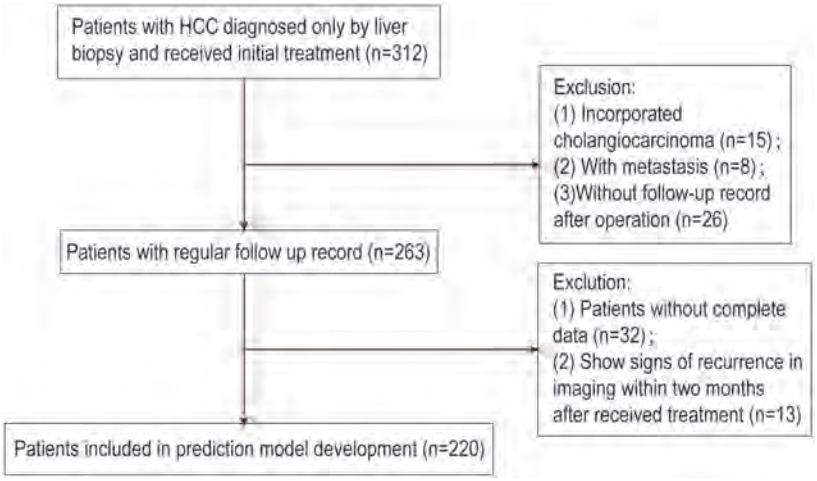


**Fig. 1. Study cohort selection.**

poor cell differentiation, and macroscopic or microscopic vascular invasion.[6] Other risk factors for HCC recurrence are cirrhosis, tumor size of > 5 cm, or portal vein invasion.[7]

The prognosis of HCC has traditionally been assessed by staging, such as the tumor-node-metastasis (TNM), Barcelona clinic liver cancer and Hong Kong liver cancer systems.[8–11] However, staging systems are not available to patients after surgical treatment and therefore do not predict postoperative recurrence. A few models including the Singapore liver cancer recurrence score and surgery-specific cancer of the liver Italian program (SS-CLIP),[12] have been developed specifically to detect tumor recurrence after surgical resection but none of them have been externally validated.[13]

Machine learning (ML) algorithms are techniques for data mining that use artificial intelligence to evaluate and analyze data, and can generate predictive models more efficiently and effectively than conventional methods by detecting hidden patterns within large data sets. Recent advances in ML models have helped to learn about features represented in data and to improve model performance in different HCC domains, including disease prediction, disease classification, and clinical practice.[14] Various types of model architectures have been used, such as logistic regression, k-nearest neighbor (K-NN), decision trees, naïve Bayes (NB), and deep neural networks (DNN).[15] Several examples of prognosis prediction methods using ML approaches based on pathological information to evaluate micro (mi)RNA expression in exosomes, circulating miRNA information, and to incorporate radiomics have been described,[16–19] but which tumor markers should be included in a surveillance program remains controversial. A more precise prognostic and recurrent prediction model is urgently needed.

In this study, we enrolled pathologically confirmed HCC patients to investigate the factors that are associated with tumor recurrence and to develop a prognostic model to improve the predictive accuracy for HCC recurrence using ML. We hope the model will provide clinicians with an appropriate surveillance tool for early detection of HCC recurrence and treatment.

## Methods

### *Patient population*

Of the 312 HCC patients diagnosed between September 2016 and June 2018 at Shandong Provincial Hospital, 220 patients recruited in this retrospective study. Patients (1) with HCC diagnosed by liver biopsy, (2) without other tumors on preoperative CT evaluation and, (3) receiving initial treatment were eligible for inclusion. Patients (1) with cholangiocarcinoma, or (2) metastasis, (3) without post-surgical follow-up; (4) younger than 18 years of age, and (5) with imaging evidence of recurrence within 2 months after treatment were excluded. All patients with HCC enrolled in this study were diagnosed by pathological evaluation. The study was approved by local Hospital Ethics Committee and patient informed consent was waived when data were collected. Figure 1 is a flow chart of patient selection. Patients were divided into two study groups by HCC recurrence and followed-up until recurrence of HCC, death, study conclusion on August 31, 2019. HCC recurrence of HCC was defined by clinical, radiological, and/or pathological diagnosis.

### *Dataset preparation*

We collected patient-related clinical, laboratory, and radiological information from medical records and at follow-up visits. (Tables 1 and 2). Thirty-seven patient characteristics were collected, including. age, etiology, treatment strategy, degree of tumor differentiation, tumor size, number of tumors, platelet count (PLT), alkaline phosphatase (ALP), total bilirubin, prothrombin time (PT), alpha-fetoprotein (AFP), aspartate aminotransferase (AST), white blood cell (WBC) count, protein induced by vitamin K absence or antagonist-II (PIVKA-II), HBsAg, and others.

### *Evaluation metrics*

We used logistic regression, K-NN, decision tree, NB, and DNN models to predict the recurrence of HCC from the patient information. The training cohort included 176 of the 220 patients; the testing cohort included the remaining 44. The training set contains a learned output that the model generalizes to new data. The algorithm flow is shown in Figure 2. The performance of the prediction results was evaluated by introducing four metrics, accuracy (Acc), precision (Prc), recall rate (TPR), and standard deviation (SD).

Acc was the ratio of the number of correctly classified samples and the total number of samples:

**Table 1. Patient characteristics**

| Characteristics | All patients (N=220) | Patients with recurrence (N=89) | Patients without recurrence (N=131) | *p*-value |
|---|---|---|---|---|
| Age | 56.65±10.39 | 55.89±10.63 | 57.16±10.23 | 0.37 |
| Sex | | | | |
| Male | 192 (87.27%) | 76 (85.39%) | 116 (88.55%) | 0.49 |
| Female | 28 (12.73%) | 13 (14.61%) | 15 (11.45%) | |
| Follow-up time | 7.64±8.04 | 9.71±7.97 | 14.0±6.36 | < 0.001 |
| Hypertension | 56 (25.45%) | 24 (26.97%) | 32 (24.42%) | 0.67 |
| Diabetes | 27 (12.27%) | 12 (13.48%) | 15 (11.45%) | 0.65 |
| Fatty liver | 9 (4.09%) | 2 (2.25%) | 7 (5.34%) | 0.25 |
| Cirrhosis | 186 (84.55%) | 70 (78.65) | 96 (73.28%) | 0.36 |
| Family history of liver cancer | 14 (6.37%) | 7 (7.86%) | 7 (5.34%) | 0.45 |
| Etiology | | | | |
| Alcohol | 8 (3.64%) | 3 (3.37%) | 5 (3.82%) | 0.83 |
| HBV | 131 (59.55%) | 54 (60.67%) | 77 (58.78%) | |
| HCV | 5 (2.28%) | 1 (1.12%) | 4 (3.05%) | |
| Alcohol and HBV | 64 (29.09%) | 25 (28.09%) | 39 (29.77%) | |
| Others | 12 (5.45%) | 6 (6.74%) | 6 (4.58%) | |
| Treatment strategy | | | | |
| Tumor resection | 131 (59.55%) | 47 (52.80%) | 84 (64.12%) | 0.09 |
| Resection and TACE | 89 (40.45%) | 42 (47.20%) | 47 (35.88%) | |
| Portal vein tumor thrombus | | | | |
| With | 41 (18.64%) | 26 (29.21%) | 15 (11.45%) | < 0.001 |
| Without | 179 (81.36%) | 63 (70.79%) | 116 (88.55%) | |
| Degree of tumor differentiation | | | | |
| Poorly differentiated | 39 (17.72%) | 22 (24.72%) | 17 (12.98%) | 0.08 |
| Moderately differentiated | 162 (73.64%) | 60 (67.42%) | 102 (77.86%) | |
| Well differentiated | 19 (8.64%) | 7 (7.86%) | 12 (9.16%) | |
| Tumor size | | | | |
| ≤5cm | 133 (60.45%) | 42 (47.19%) | 91 (69.47%) | < 0.001 |
| >5cm | 87 (39.55%) | 47 (52.81%) | 40 (30.53%) | |
| Number of tumors | | | | |
| Solitary | 186 (84.55%) | 73 (82.02%) | 113 (86.26%) | 0.50 |
| 2–3 | 34 (15.45%) | 16 (17.98%) | 18 (13.74%) | |

TACE, trans arterial chemoembolization.

$$Acc = \frac{TP + TN}{TP + TN + FP + FN}.$$

In the confusion matrix of classification results TP represents the positive samples that are predicted to be positive by the model, FP represents the negative samples that are predicted to be positive by the model, FN represents the positive samples that are predicted to be negative by the model, and TN represents the negative samples that are predicted to be negative by the model. Prc is the ratio of the number of correctly classified positive instances and the number of instances classified as positive:

$$Prc = \frac{TP}{TP + FP}.$$

TPR was the proportion of the number of positive cases correctly classified to the actual number of positive cases:

$$TPR = \frac{TP}{TP + FN}.$$

The SD is the extent of dispersion of the accuracy of random tests:

**Table 2. Patient laboratory findings**

| Variables | All patients (N=220) | Patients with recurrence (N=89) | Patients without recurrence (N=131) | *p*-value |
|---|---|---|---|---|
| White blood cell count, $\times 10^9$/L | 5.1 (2–82) | 5.2 (2.1–82) | 5.1 (2–15) | 0.62 |
| Red blood cell count, | 4.7 (1.7–5.8) | 4.7 (1.7–5.8) | 4.7 (3.1–5.6) | 0.44 |
| Hemoglobin, g/L | 14 (6–84) | 15 (10–84) | 14 (6–82) | 0.44 |
| Platelet count, $\times 10^9$/L | 175.30±82.63 | 184.79±81.72 | 168.86±82.93 | 0.16 |
| Alanine aminotransferase, U/L | 30.5 (10–581) | 37 (12–581) | 36 (10–209) | 0.64 |
| Aspartate aminotransferase, U/L | 38 (9–317) | 38.0 (9–317) | 38.0 (16.00–249.00) | 0.29 |
| Alkaline phosphatase, U/L | 76.5 (12–968) | 94 (23–968) | 61 (12–807) | 0.005 |
| γ-glutamyl transpeptadase, U/L | 104 (14–619) | 106 (14–427) | 103 (19–619) | 0.06 |
| Total bilirubin, m/L | 17 (7–74) | 16 (7–47) | 18 (7–74) | 0.06 |
| Direct bilirubin, um/L | 3 (1–97) | 3 (1–97) | 3 (1–64) | 0.77 |
| Indirect bilirubin, μm/L | 13 (5–61) | 13 (5–61) | 14 (5–56) | 0.06 |
| ALB, g/L | 41.59±5.18 | 41.55±4.41 | 41.85±5.65 | 0.38 |
| Glucose, mmol/L | 5.0 (2–14) | 5.0 (4–13) | 5.0 (2–14) | 0.41 |
| Cholesterol | 4.39±1.39 | 4.60±1.37 | 4.23±1.39 | 0.27 |
| Triglycerides, mmol/L | 0.88 (0.3–2.79) | 0.77 (0.3–1.8) | 0.9 (0.42–2.79) | 0.04 |
| High-density lipoprotein, mmol/L | 1.21 (0.37–4.06) | 1.25 (0.4–4.06) | 1.20 (0.37–3.19) | 0.95 |
| Low-density lipoprotein, mmol/L | 2.59±0.93 | 2.73±0.97 | 2.49±0.89 | 0.30 |
| PT, s | 13 (10–18) | 13 (10–17) | 13 (10–18) | 0.58 |
| PTA, % | 85.45±13.36 | 85.23±13.62 | 85.61±13.23 | 0.84 |
| Alpha-fetoprotein, ng/mL | 27.0 (1.1–998.0) | 59 (1.5–919.0) | 15.0 (1.1–998.0) | 0.001 |
| PIVKA-II, ng/mL | 604.81 (9.38–75,000) | 1,519.5 (16.00–75,000) | 355.29 (9.38–75,000) | 0.001 |
| Fibrosis-4 (FIB-4) | | | | |
| Low (<1.45) | 43 (19.55%) | 20 (22.47%) | 23 (17.56%) | 0.41 |
| Intermediate (1.45–3.25) | 110 (50.0%) | 46 (51.69%) | 64 (48.85%) | |
| High (>3.25) | 47 (21.35%) | 23 (25.84%) | 44 (33.59%) | |
| HBsAg, IU/mL | 5,790.5 (0.39–8,724.0) | 5,828.0 (0.41–8,002.0) | 5,122.0 (0.39–8,724) | 0.78 |

PIVKA-II, protein induced by vitamin K absence or antagonist-II.

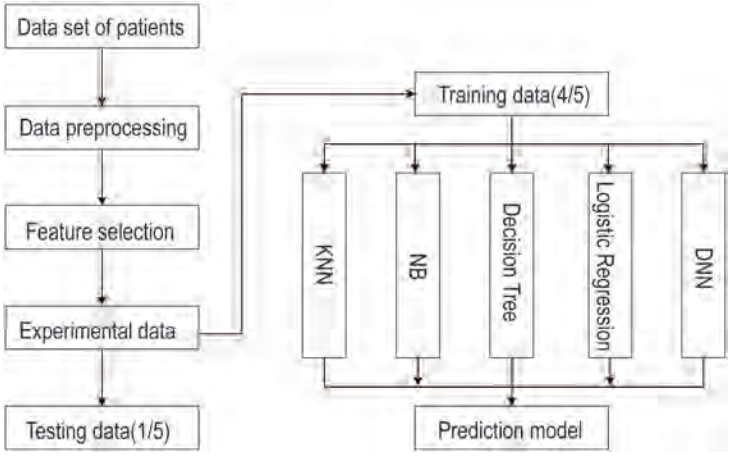


**Fig. 2. Algorithm flow.** K-NN, k-nearest neighbor; NB, naïve Bayes; DNN, deep neural networks.

$$\sigma = \sqrt{\frac{1}{N}\sum_{i=1}^{N} x_i - \mu},$$

where $x_1$, $x_2$, …, $xn$ are real numbers, μ is the arithmetic mean, and σ is the SD.

### *Statistical analysis*

Continuous variables were reported as means (SD) if they were normally distributed or a medians (IQR) if they were not. Categorical variables were reported as numbers and percentages (%). We assessed differences between severe and nonsevere patients with two-sample *t*-tests or the Wilcoxon rank-sum test depending on parametric or nonparametric data for continuous variables and Fisher's exact test for categorical variables. A two-sided α of less than 0.05 was considered statistically significant. The statistical analysis was performed with SPSS version 26.0 (IBM Corp., Armonk, NY, USA).

In the building of the predictive models, the Pearson correlation coefficient was used to find the independent predictors of severity of disease from 37 vectors. The predictive models were built based on five ML classification algorithms, i.e. logistic regression, K-NN, decision tree, NB and DNN model by using Python programming software version 3.6.5.

1. Pearson correlation coefficient and feature selection by univariate analysis were used. The Pearson coefficient between each patient characteristic and recurrence was calculated separately, and the characteristics with significant correlations were selected. The specific steps were as follows: To make the characteristics in the dataset $D = \{x_1, x_2, \ldots, x_m, y\}$ numerically comparable, the absolute values, maxima and minima of each were mapped to [0, 1];

$$x_i \leftarrow \frac{x_i - \min_{x_i}}{\max_{x_i} - \min_{x_i}}, y \leftarrow \frac{y - \min_y}{\max_y - \min_y}, D \leftarrow \{x_1, x_2, \cdots, x_m, y\}.$$

2. The correlation between each feature and the tag value $p(x_i, y)$

$$p(x_i, y) = \frac{\sum_{n=1}^{n}\left(x_i^k - \overline{x}_i\right)\left(y^k - \overline{y}\right)}{\sqrt{\sum_k^n\left(x_i^k - \overline{x}\right)^2 \sum_k^n\left(x_i^k - \overline{y}_i\right)^2}}$$

where $x_i^k$, $y^k$ represent the value of the k-th sample of the characteristic, and $\overline{x}_i$, $\overline{y}$ represent the sample mean value of the two characteristics, represents the total number of characteristics in the patient data.

3. To calculate the eigenvectors and eigenvalues of the covariance matrix the features with large influencing factors were selected as the optimal feature subset. The final data set was constructed based on the feature subset.

The K-NN algorithm was constructed as follows:

1. For data set , the distance from each sample $d_j = (x_j, y_i)$ to be classified x to all known samples, $L(d_i, d_j)$;

$$L\left(d_i, d_j\right) = \left(\sum_{l=1}^{m}\left|x_i^{(l)} - x_j^{(l)}\right|^2 + \left|y_i - y_j\right|^2\right)^{1/2}$$

was constructed.

2. Adjacent values of each sample were sorted in descending order according to the distance.
3. The k-nearest neighbors of each sample are obtained by determining the K value. According to the majority voting rule of the following formula, the sample x to be classified is classified into the category with the largest number of samples:

$$C_x = \text{argmax}_{j\in l}\Sigma_{y=}xkI(C_y = j)$$

Where j represents the tag values of different categories, and Y represents the k-nearest neighbors of sample x to be classified.

## Results

### *Patient characteristics*

The clinical characteristics of the patients are shown in Table 1. Most patients were men (192/220, 82.27%), and the mean age was 56.65 (SD = 10.39) years. Of the 220 HCC patients, 89 (40.5%) were recrudescent and 131(59.5%) were nonrecrudescent. The mean time from surgery to recurrence was 14 (SD = 6.36) months. Patients with recurrent HCC were more likely to have larger tumors (> 5 cm diameter, 52.81% vs. 30.53%, $P < 0.001$) and portal vein tumor thrombus (29.21% vs. 11.45%, $P < 0.001$). Some differences in the laboratory values of patients with recurrent and nonrecurrent HCC obtained on admission (Table 2) were significant.

### *Performance comparison*

In principal component analysis, we found nine key factors affecting the recurrence of HCC, including tumor size, tumor grade differentiation, portal vein tumor thrombus, PLT, AFP, PIVKA-II, AST, WBC, and HBsAg (Fig. 3). Tumor size, tumor differentiation grade, portal vein tumor thrombus, PLT, AFP, PIVKA-II, AST, WBC, HBsAg, and recurrence results of 176 patients in the training cohort were formed into a data set. The data sets were input into different ML algorithms (i.e. logistic regression, K-NN, decision tree, naïve Bayes, and DNN) to form the ML model. Then the data of 44 patients in the testing cohort were input into the five ML models for prediction. The prediction results from different models were evaluated by comparing the model performance metrics. The accuracies of the K-NN (70.6%), NB (60.9%), decision tree (57.5%), logistic regression (67.9%), and DNN (64.9%) models is reported in Figure 4. After comparing different ML methods, we choose the K-NN model as the optimal prediction model. In terms of accuracy and precision, K-NN algorithm was superior to other algorithms. It had 70.6% Acc and 70.1% Prc. The TPR was 51.9% and the SD was 0.02.

## Discussion

The ideal resection index is early solitary HCC, regardless of tumor size, and preserved liver function. Unfortunately, the rate of disease recurrence remains high, with early relapses considered to be "true relapses" and "relapses" afterward assumed to be mainly caused by *de novo* tumors. However, there is no reliable prediction tool for early HCC recurrence. In this study, we retrospectively evaluated 89 patients with early recurrence of HCC, which had different clinical characteristics and laboratory parameters compared with nonrecurrent patients. Using Pearson analysis, we discovered that early recurrence was mainly determined by aggressive characteristics of the primary (resected) tumor, including size, grade, differentiation, and higher serum AFP, PIVKA-II, PLT, AST, WBC, and HBsAg levels.

Currently, we can only use tumor markers such as AFP and PIVKA-II to determine HCC recurrence, because there is no useful postoperative recurrence marker. AFP is the most commonly used clinical biomarker of HCC, but its sensitivity and specificity are not ideal. AFP is a risk fac-

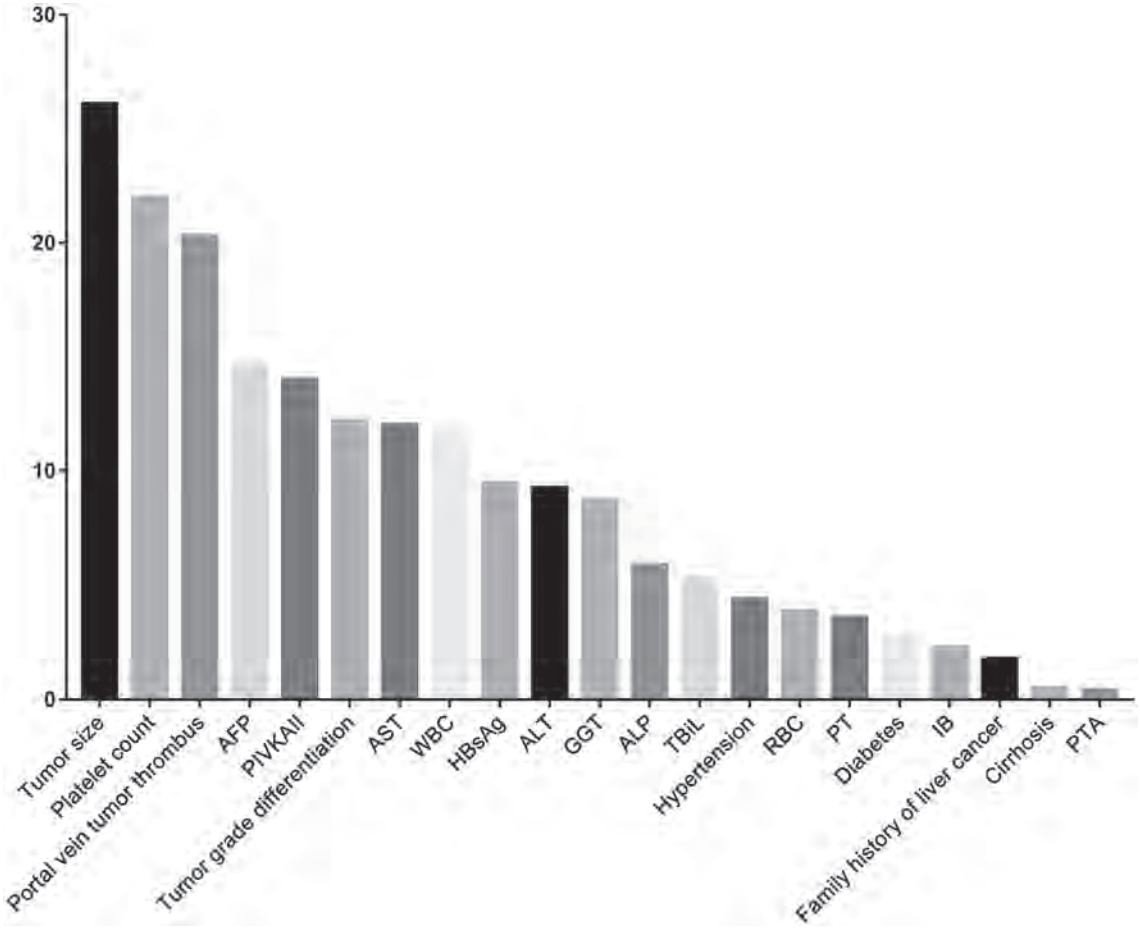


**Fig. 3. Variable importance plot for predicting tumor recurrence showing absolute values of Spearman correlation coefficients between markers and HCC recurrence.** AFP, alpha-fetoprotein; PIVKA-II, protein induced by vitamin K absence or antagonist-II; AST, aspartate amino transferase; WBC, white blood cells; HBsAg, hepatitis B surface antigen; ALT, alanine aminotransferase; GGT, gamma-glutamyl transpeptidase; ALP, alkaline phosphatase; TBiL, total bilirubin; RBC, red blood cell; PT, prothrombin time; IB, indirect bilirubin; PTA, prothrombin activity.

tor for the recurrence of HCC after radical treatment, and has been considered as a better prognostic predictor than cancer morphology alone.[20,21] PIVKA-II may play a role in the progression of HCC and is associated with HCC size, microvascular invasion, metastatic dissemination, and recurrence after tumor ablation. In fact, AFP levels are high in 40–60% of HCC patients and in 10–20% of early-stage tumors. It may also be elevated in many benign tumors.[22–24] Other studies have shown that the performance of PIVKA-II in HBV-related HCC varies across populations, with a sensitivity of 44–91% and specificity of 68–99% at a cutoff values between 40 and 150 mAU/mL.[25] The evidence supports the need for more sensitive and specific HCC markers, no method to predict the recurrence of surgically resected HCC is currently available.

Given the validated, good discriminatory performance of AFP and PIVKA-II prediction models, we studied a novel predictor of HCC recurrence based on the AFP model and including 36 additional serological, pathological, and radiological patient features. Nine features, tumor size, tumor grade differentiation, portal vein tumor thrombus, PLT, AFP, PIVKA-II, AST, WBC, and HBsAg were found influence the recurrence of HCC. The accuracy, recall, and precision of the model were 70.6%, 51.9%, 70.1%, respectively. The inclusion of more clinical markers might further improve the diagnostic accuracy.

In recent years, ML has developed rapidly, and has contributed to outstanding achievements in disease prediction and clinical practice. ML algorithms can be used to predict the outcome of a new observation, based on a training dataset containing previous observations where the outcome is known. It can detect complex nonlinear relationships between numerous variables that are useful in predictive applications.[26,27] Many research results show that prediction models based on ML significantly improve the accuracy of cancer diagnosis and prognosis prediction.[28–30] In this study, after data training and performance comparisons, we found a novel, sensitive, and stable K-NN model to predict the recurrence of HCC after surgery. We believe that it can help to identify individuals who are at high risk of early recurrence after tumor resection. K-NN algorithms are very effective nonparametric models that are widely used for classification, regression, and pattern recognition. It is highly appropriate to use the K-NN method to predict HCC recurrence of HCC, especially using a large chronic liver disease, tumor characteristics, and hepatic function dataset. The K-NN model was the optimal prediction model, with 70.6% accuracy. When developing the model to predict the risk of patient recurrence, we input nine key factors, tumor size, grade, and differentiation; portal vein tumor thrombus, PLT, AFP, PIVKA-II, AST, WBC, and HBsAg in the K-NN algorithm, which then was able to automatically estimate the HCC recurrence risk

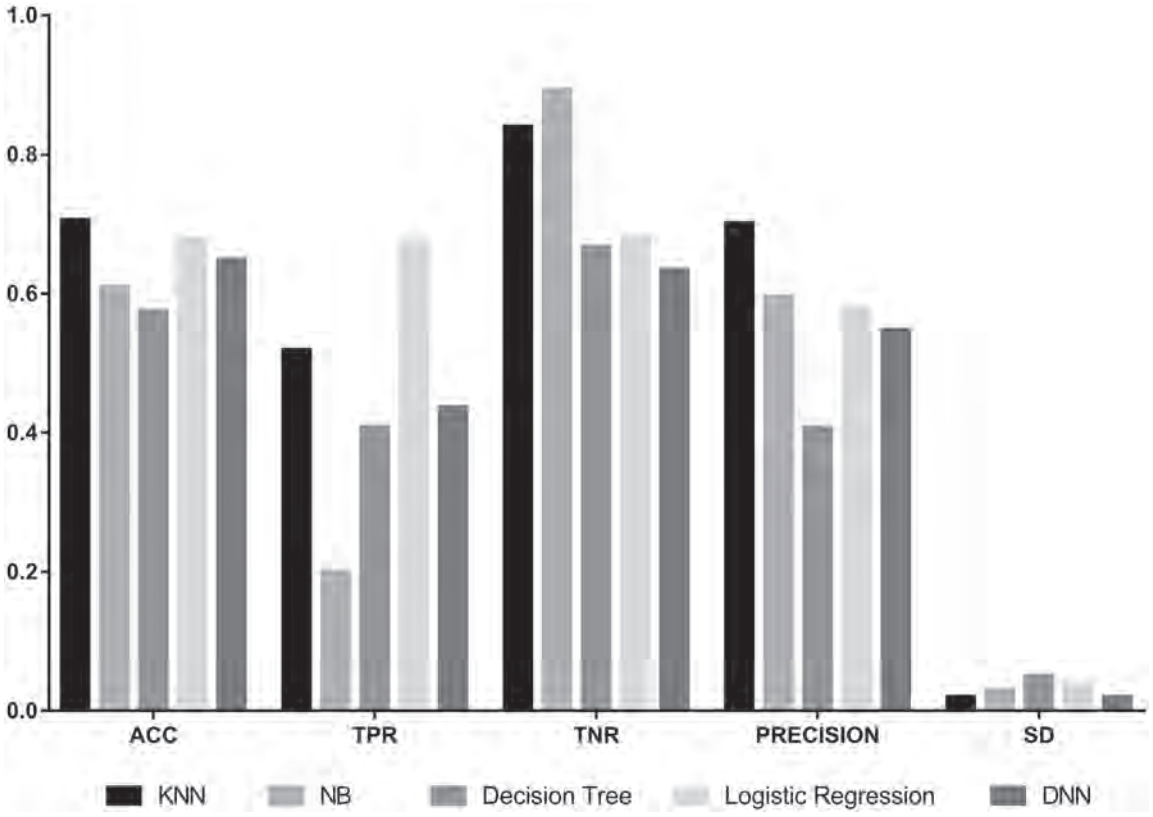


**Fig. 4. Accuracy, recall rate, true negative rate, precision, and standard deviation of different algorithms.** K-NN, k-nearest neighbor; NB, naïve Bayes; DNN, deep neural networks; ACC, accuracy; TPR, recall rate; TNR, true negative rate; SD, standard deviation.

of each patient.

This study has several limitations. It was limited by the small sample size and retrospective method. Some cases had incomplete documentation of laboratory testing, and most of the HCC patients included in our study had chronic hepatitis B infection. The limitations might have result in some bias in our general understanding of the disease. In addition, early and late recurrence were not distinguished in this study because of the relatively short follow-up. The two problems mentioned above can be resolved by additional study. The main limitations of ML algorithms are that they are best suited to predicting outcomes in the environment from which they are derived. Conversely, this limitation is also its strength, in that it is highly specific to the peculiarities of a particular center, enabling the best decision for each individual patient.

In conclusion, used ML to develop a K-NN model for predicting HCC recurrence that included a comprehensive evaluation of serological, pathological, and radiological features. The accuracy of this model was about 70.6%, which is much better than the models using only clinical or serological data. This K-NN model was sensitive and stable when used to predict the recurrence of HCC in patient after surgical resection.

## Funding

National Natural Science Fund (No.81970545; 82170609), Natural Science Foundation of Shandong Province (Major Project) (No. ZR2020KH006) and Ji'nan Science and Technology Development Project (No.2020190790).

## Conflict of interest

JL has been an editorial board member of *Journal of Clinical and Translational Hepatology* since 2021. The other authors have no conflict of interests related to this publication.

## Author contributions

Guarantor of article (JL), study concept and study supervision (JL), data collection and/or data interpretation (CL, HY, YF, YC), data analysis (JL), manuscript drafting (CL, HY, YF). All authors read and revised the manuscript.

## Data sharing statement

All data are available upon request.

## References

[1] Heimbach JK, Kulik LM, Finn RS, Sirlin CB, Abecassis MM, Roberts LR, *et al*. AASLD guidelines for the treatment of hepatocellular carcinoma. Hepatology 2018;67(1):358–380. doi:10.1002/hep.29086.
[2] EASL Clinical Practice Guidelines: Management of hepatocellular carcinoma. J Hepatol 2018;69(1):182–236. doi:10.1016/j.jhep.2018.03.019.
[3] Marrero JA, Kulik LM, Sirlin CB, Zhu AX, Finn RS, Abecassis MM, *et al*. Diagnosis, Staging, and Management of Hepatocellular Carcinoma: 2018 Practice Guidance by the American Association for the Study of Liver Diseases. Hepatology 2018;68(2):723–750. doi:10.1002/hep.29913.
[4] Bray F, Ferlay J, Soerjomataram I, Siegel RL, Torre LA, Jemal A. Global cancer statistics 2018: GLOBOCAN estimates of incidence and mortality worldwide for 36 cancers in 185 countries. CA Cancer J Clin 2018;68(6):394–

424. doi:10.3322/caac.21492.
[5] Zheng Q, Xu J, Gu X, Wu F, Deng J, Cai X, *et al*. Immune checkpoint targeting TIGIT in hepatocellular carcinoma. Am J Transl Res 2020;12(7):3212–3224.
[6] Yang Y, Ying G, Wu S, Wu F, Chen Z. In vitro inhibition effects of hepatitis B virus by dandelion and taraxasterol. Infect Agent Cancer 2020;15:44. doi:10.1186/s13027-020-00309-4.
[7] Zhou QH, Wu FT, Pang LT, Zhang TB, Chen Z. Role of γδT cells in liver diseases and its relationship with intestinal microbiota. World J Gastroenterol 2020;26(20):2559–2569. doi:10.3748/wjg.v26.i20.2559.
[8] Vauthey JN, Lauwers GY, Esnaola NF, Do KA, Belghiti J, Mirza N, *et al*. Simplified staging for hepatocellular carcinoma. J Clin Oncol 2002;20(6):1527–1536. doi:10.1200/jco.2002.20.6.1527.
[9] Llovet JM, Brú C, Bruix J. Prognosis of hepatocellular carcinoma: the BCLC staging classification. Semin Liver Dis 1999;19(3):329–338. doi:10.1055/s-2007-1007122.
[10] Kudo M, Chung H, Haji S, Osaki Y, Oka H, Seki T, *et al*. Validation of a new prognostic staging system for hepatocellular carcinoma: the JIS score compared with the CLIP score. Hepatology 2004;40(6):1396–1405. doi:10.1002/hep.20486.
[11] Okuda K, Ohtsuki T, Obata H, Tomimatsu M, Okazaki N, Hasegawa H, *et al*. Natural history of hepatocellular carcinoma and prognosis in relation to treatment. Study of 850 patients. Cancer 1985;56(4):918–928. doi:10.1002/1097-0142(19850815)56:4<918::aid-cncr2820560437>3.0.co;2-e.
[12] Chen P, Wang YY, Chen C, Guan J, Zhu HH, Chen Z. The immunological roles in acute-on-chronic liver failure: An update. Hepatobiliary Pancreat Dis Int 2019;18(5):403–411. doi:10.1016/j.hbpd.2019.07.003.
[13] Deng JW, Yang Q, Cai XP, Zhou JM, E WG, An YD, *et al*. Early use of dexamethasone increases Nr4a1 in Kupffer cells ameliorating acute liver failure in mice in a glucocorticoid receptor-dependent manner. J Zhejiang Univ Sci B 2020;21(9):727–739. doi:10.1631/jzus.B2000249.
[14] Ngiam KY, Khor IW. Big data and machine learning algorithms for healthcare delivery. Lancet Oncol 2019;20(5):e262–e273. doi:10.1016/s1470-2045(19)30149-4.
[15] Spann A, Yasodhara A, Kang J, Watt K, Wang B, Goldenberg A, *et al*. Applying Machine Learning in Liver Disease and Transplantation: A Comprehensive Review. Hepatology 2020;71(3):1093–1105. doi:10.1002/hep.31103.
[16] Itami-Matsumoto S, Hayakawa M, Uchida-Kobayashi S, Enomoto M, Tamori A, Mizuno K, *et al*. Circulating Exosomal miRNA Profiles Predict the Occurrence and Recurrence of Hepatocellular Carcinoma in Patients with Direct-Acting Antiviral-Induced Sustained Viral Response. Biomedicines 2019;7(4):87. doi:10.3390/biomedicines7040087.
[17] Yamamoto Y, Kondo S, Matsuzaki J, Esaki M, Okusaka T, Shimada K, *et al*. Highly Sensitive Circulating MicroRNA Panel for Accurate Detection of Hepatocellular Carcinoma in Patients With Liver Disease. Hepatol Commun 2020;4(2):284–297. doi:10.1002/hep4.1451.
[18] Corredor G, Wang X, Zhou Y, Lu C, Fu P, Syrigos K, *et al*. Spatial Architecture and Arrangement of Tumor-Infiltrating Lymphocytes for Predicting Likelihood of Recurrence in Early-Stage Non-Small Cell Lung Cancer. Clin Cancer Res 2019;25(5):1526–1534. doi:10.1158/1078-0432.ccr-18-2013.
[19] Ji GW, Zhu FP, Xu Q, Wang K, Wu MY, Tang WW, *et al*. Machine-learning analysis of contrast-enhanced CT radiomics predicts recurrence of hepatocellular carcinoma after resection: A multi-institutional study. Ebiomedicine 2019;50:156–165. doi:10.1016/j.ebiom.2019.10.057.
[20] Hakeem AR, Young RS, Marangoni G, Lodge JP, Prasad KR. Systematic review: the prognostic role of alpha-fetoprotein following liver transplantation for hepatocellular carcinoma. Aliment Pharmacol Ther 2012;35(9):987–999. doi:10.1111/j.1365-2036.2012.05060.x.
[21] Mazzaferro V, Droz Dit Busset M, Bhoori S. Alpha-fetoprotein in liver transplantation for hepatocellular carcinoma: The lower, the better. Hepatology 2018;68(2):775–777. doi:10.1002/hep.29835.
[22] Hakamada K, Kimura N, Miura T, Morohashi H, Ishido K, Nara M, *et al*. Des-gamma-carboxy prothrombin as an important prognostic indicator in patients with small hepatocellular carcinoma. World J Gastroenterol 2008;14(9):1370–1377. doi:10.3748/wjg.14.1370.
[23] Nanashima A, Morino S, Yamaguchi H, Tanaka K, Shibasaki S, Tsuji T, *et al*. Modified CLIP using PIVKA-II for evaluating prognosis after hepatectomy for hepatocellular carcinoma. Eur J Surg Oncol 2003;29(9):735–742. doi:10.1016/j.ejso.2003.08.007.
[24] Kim DY, Paik YH, Ahn SH, Youn YJ, Choi JW, Kim JK, *et al*. PIVKA-II is a useful tumor marker for recurrent hepatocellular carcinoma after surgical resection. Oncology 2007;72(Suppl 1):52–57. doi:10.1159/000111707.
[25] Loglio A, Iavarone M, Facchetti F, Di Paolo D, Perbellini R, Lunghi G, *et al*. The combination of PIVKA-II and AFP improves the detection accuracy for HCC in HBV caucasian cirrhotics on long-term oral therapy. Liver Int 2020;40(8):1987–1996. doi:10.1111/liv.14475.
[26] Giger ML. Machine Learning in Medical Imaging. J Am Coll Radiol 2018;15(3 Pt B):512–520. doi:10.1016/j.jacr.2017.12.028.
[27] Venkatesh R, Balasubramanian C, Kaliappan M. Development of Big Data Predictive Analytics Model for Disease Prediction using Machine learning Technique. J Med Syst 2019;43(8):272. doi:10.1007/s10916-019-1398-y.
[28] Montazeri M, Montazeri M, Montazeri M, Beigzadeh A. Machine learning models in breast cancer survival prediction. Technol Health Care 2016;24(1):31–42. doi:10.3233/thc-151071.
[29] Hasnain Z, Mason J, Gill K, Miranda G, Gill IS, Kuhn P, *et al*. Machine learning models for predicting post-cystectomy recurrence and survival in bladder cancer patients. PLoS One 2019;14(2):e0210976. doi:10.1371/journal.pone.0210976.
[30] Kim I, Choi HJ, Ryu JM, Lee SK, Yu JH, Kim SW, *et al*. A predictive model for high/low risk group according to oncotype DX recurrence score using machine learning. Eur J Surg Oncol 2019;45(2):134–140. doi:10.1016/j.ejso.2018.09.011.

*Journal of Clinical and Translational Hepatology* **2022** vol. 10(4) | 608–619
DOI: 10.14218/JCTH.2021.00301

Original Article

# Extracellular Polysaccharide from *Rhizopus nigricans* Inhibits Hepatocellular Carcinoma via miR-494-3p/TRIM36 Axis and Cyclin E Ubiquitination

Haixiong Yan, XiaoQian Ma, Ze Mi, Zhenhu He and Pengfei Rong*

*Department of Radiology, The Third Xiangya Hospital of Central South University, Changsha, Hunan, China*

**Received:** 21 July 2021 | **Revised:** 11 October 2021 | **Accepted:** 27 October 2021 | **Published:** 21 February 2022

## Abstract

***Background and Aims:*** This study was designed to uncover the mechanism for extracellular polysaccharide (EPS1-1)-mediated effects on hepatocellular carcinoma (HCC) development. ***Methods:*** HCC cells were treated with EPS1-1, miR-494-3p mimic, sh-TRIM36, and pcDNA3.1-TRIM36. The levels of miR-494-3p and TRIM36 were measured in normal hepatocytes, THLE-2, and HepG2 and HuH7HCC cell lines, along with the protein expression of cyclin D/E and p21. The proliferation, cell cycle, and apoptosis of HCC cells were assayed. The interactions between miR-494-3p and TRIM36, and between TRIM36 and cyclin E were assessed. Finally, the expression and localization of TRIM36 and cyclin E were monitored, and tumor apoptosis was detected, in tumor xenograft model. ***Results:*** EPS1-1 suppressed HCC cell proliferation and cyclin D/E expression and promoted apoptosis and p21 expression. miR-494-3p was upregulated and TRIM36 was downregulated in HCC cells. Transfection with miR-494-3p mimic or sh-TRIM36 facilitated HCC cell proliferation and the expression of cyclin D/E protein but they inhibited apoptosis and p21 expression in the presence of EPS1-1. Overexpression of TRIM36 further consolidated EPS1-1-mediated inhibition of HCC proliferation, cyclin D/E, and the promotion of apoptosis and p21 expression. Those effects were reversed by miR-494-3p overexpression. TRIM36 was a target gene of miR-494-3p, and TRIM36 induced cyclin E ubiquitination. EPS1-1 suppressed cyclin E expression, promoted TRIM36 expression and tumor apoptosis, all of which were abrogated by increasing the expression of miR-494-3p *in vivo*. ***Conclusions:*** EPS1-1 protected against HCC by limiting its proliferation and survival through the miR-494-3p/TRIM36 axis and by inducing cyclin E ubiquitination.

**Citation of this article:** Yan H, Ma XQ, Mi Z, He Z, Rong P. Extracellular Polysaccharide from *Rhizopus nigricans* Inhibits Hepatocellular Carcinoma via miR-494-3p/TRIM36 Axis and Cyclin E Ubiquitination. J Clin Transl Hepatol 2022;10(4):608–619. doi: 10.14218/JCTH.2021.00301.

## Introduction

Hepatocellular carcinoma (HCC) is the third leading cause of cancer-related death and remains one of the most aggressive malignancies worldwide.[1,2] Although liver resection is one of the most effective treatment options, the prognosis of HCC is extremely poor, with a 1-year survival of 40%.[3,4] Thus, identifying the underlying mechanisms contributing to the progression of HCC is crucial to facilitate the development of novel diagnostic biomarkers and effective therapeutic targets.

In recent years, considerable attention has been paid to the study of natural antitumor compounds with known biological activities and few or no side effects.[5,6] *Rhizopus nigrum*, a zygote filamentous fungus, has been extensively used by the pharmaceutical industry for production of organic acids and biotransformation.[7] An extracellular polysaccharide (EPS1-1) extracted from *R. nigricans* was found to exert antitumor activity and improve the immune response.[8–10] EPS1-1 was reported to not only suppresses colitis-related colorectal cancer[11] but also to have a role in ameliorating functional disorders of colorectal cancer in mice.[12] The involvement of EPS1-1 in biological processes including proliferation, metastasis, and apoptosis of colorectal cancer has been described.[13,14] Previous studies have indicated that EPS1-1 repressed the progression of HCC *in vitro* and *in vivo*,[15] but whether EPS1-1 can regulate biological processes and molecular mechanisms of HCC remains unclear.

Micro (mi)RNAs are small noncoding RNAs that post-transcriptionally regulate gene expression by degrading their target messenger (m)RNAs or by terminating translation. miRNAs are aberrantly expressed in a majority of human cancers, suggesting that they have essential roles in tumorigenesis and tumor development.[16] Moreover, miRNAs were reported to be involved in cellular processes including cell proliferation, apoptosis, and differentiation.[17] Up until now, a growing number of studies have elucidated the role of miRNA in the molecular pathogenesis of HCC. For example, abundant expression of miR-517a was associated

**Keywords:** Extracellular polysaccharide; EPS1-1; miR-494-3p; TRIM36; Ubiquitination; Hepatocellular carcinoma.

**Abbreviations:** CO-IP, co-immunoprecipitation; EPS1-1, extracellular polysaccharide; HCC, hepatocellular carcinoma; IHC, immunohistochemistry; miRNA, microRNA; MTT, methylthiazol tetrazolium; MUT, mutant type; NC, negative control; PI, propidium iodide; qRT-PCR, quantitative RT-PCR; SDS-PAGE, sodium dodecyl sulfate-polyacrylamide agarose gel electrophoresis; WT, wild type.

***Correspondence to:** Pengfei Rong, Department of Radiology, The Third Xiangya Hospital of Central South University, No. 138, Tongzipo Road, Yuelu District, Changsha, Hunan 410013, China. ORCID: https://orcid.org/0000-0001-5473-1982. Tel: +86-18684706350, Fax: +86-731-88618411, E-mail: rongpengfei66@163.com

with adverse outcomes in patients with HCC.[18] In contrast, miR-199a/b-3p and miR-219-5p were found to act as tumor suppressors in HCC.[19,20] Therefore, the identification of drug agents that substantially regulate oncogenic or tumor-suppressive miRNA expression may be a promising therapeutic strategy to treat or prevent human cancers. Previous studies have shown that miR-494-3p acts as an oncogene by stimulating the proliferation and invasion and suppressing apoptosis in glioma cells.[21] Also, increased miR-494-3p expression has been linked to HCC progression.[22] However, whether EPS1-1 can downregulate miRNAs, specifically miR-494-3p in HCC, remains unknown.

Our study investigated the potential involvement of EPS1-1 in the proliferation and apoptosis of HCC *in vitro* and its effect on tumor-bearing mice *in vivo*. Collectively, the findings demonstrate novel inhibitory effects of EPS1-1 on HCC development through modulation of the miR-494-3p/TRIM36 axis and ubiquitination of cyclin E.

## Methods

### *Clinical sample*

HCC and adjacent normal tissues were collected from 22 patients diagnosed at our hospital between October 2019 and December 2020. The tissues were preserved in liquid nitrogen for subsequent examination. All procedures involving humans were performed with the approval of the ethics committee of the Third Xiangya Hospital of Central South University and the informed consent of the patients or their relatives.

### *Cell culture*

THLE-2 normal human hepatocytes and HepG2 and HuH7 HCC cell lines were acquired from the Cell Bank of Chinese Academy of Sciences (Shanghai, China). Exopolysaccharide EPS1-1 was purified from the fermentation broth of *R. nigricans*. HepG2 and HuH7 cells were cultured in Dulbecco's Modified Eagle Medium (DMEM) supplemented with 10% fetal bovine serum (ThermoFisher Scientific, Waltham, MA, USA) at 37°C in a 5% $CO_2$ incubator. The cells at approximately 90% confluency were dissociated with 0.25% trypsin followed by addition of serum-containing medium to terminate digestion. The cells were then gently pipetted into single-cell suspension and passaged.

### *Transient transfection*

HepG2 and HuH7 cells were inoculated onto 96-well plates at a density of $1 \times 10^4$ cells/well. When the adherent cells reached 60% confluency, miR-494-3p inhibitor/mimic (100 nmol) plasmids containing silenced (sh-TRIM36, 2 μg) or overexpressed (oe-TRIM36, 2 μg) TRIM36, inhibitor/mimic negative control (NC) or sh-NC/oe-NC (Shanghai GenePharma Co., Ltd., Shanghai, China) was transfected into the cells with Lipofectamine 2000 (ThermoFisher Scientific) following the manufacturer's instructions. Subsequent experiments were carried out 48–72 h later.

### *Cell grouping*

Cells were allocated to be treated for 72 h with EPS1-1 25 μg/mL, 50 μg/mL, 100 μg/mL, or 200 μg/mL. After transfection, HCC cells were treated 200 μg/mL of EPS1-1 for 24 h and then divided into EPS1-1, EPS1-1 + mimic NC, EPS1-1 + miR-494-3p mimic, EPS1-1 + sh-NC, EPS1-1 + sh-TRIM36, EPS1-1 + oe-NC, EPS1-1 + oe-TRIM36 group, and EPS1-1 + oe-TRIM36 + miR-494-3p mimic groups. After transfection with pcDNA3.1 or pcDNA3.1-TRIM36, HCC cells were induced with 20 μM protease inhibitor MG132 for 4 h and divided into oe-NC + DMSO, oe-TRIM36 + DMSO, oe-NC + MG132, and oe-TRIM36 + MG132 groups.

### *Methylthiazol tetrazolium (MTT) assay*

Cells at a density of $5 \times 10^3$ cells/well were plated onto 96-well plates. At indicated time points (24, 48, or 72 h), 10 μl of MTT solution (5 mg/mL) was added to each well at 37°C for 4 h. Subsequently, 100 μL DMSO was added and the cells were incubated overnight at 37°C to terminate the reaction. The absorbance (optical density, OD) was recorded at a wavelength of 490 nm using a microplate reader (Sectramax 190, Molecular Devices Corp., Sunnyvale, CA, USA). The OD value represents cell viability. The results from three independent assays of each group were calculated and averaged. A proliferation curve was plotted for optimum visualization of the viability data.

### *Flow cytometry*

For the detection of cell apoptosis, single-cell suspensions of cells in each group were prepared and centrifuged at 2,000 rpm. After washing twice with phosphate buffered saline (PBS), the cells were resuspended in binding buffer. Then, 5 μL of Annexin-V-FITC and propidium iodide (PI) were added to 195 μL cell suspension containing $10^5$ cells and cultured for 10 min in the dark. Cell apoptosis was assayed by flow cytometry (BD FACS Canto II, 488N, San Jose, CA, USA).

For analysis of cell cycle events, cells from each group were seeded onto 6-well culture plates ($3 \times 10^5$ cells/well) for 24 h. Cells were then fixed with 4% paraformaldehyde (Shanghai Sangon Biological Engineering Co., Ltd., Shanghai, China) for 15 min before incubation with 50 μg/mL PI (Solarbio, Beijing, China) in the dark (37°C, 30 min). The fluorescence intensity of cells (excitation wavelength 488 nm) was assessed by flow cytometry (BD FACS Canto II, 488N, San Jose, CA, USA)

### *Quantitative RT-PCR (qRT-PCR)*

Total RNA was extracted using TRIzol reagent (Thermo Fisher Scientific, MA, USA) following the manufacturer's instructions. The extracted RNA was reverse transcribed into cDNA using a reverse transcription system (Promega, Madison, WI, USA). Gene expression was detected using a LightCycler 480 qRT-PCR instrument (Roche, IN, USA), and reactions were performed with a qRT-PCR kit (SYBR Green PCR kit, Takara Bio, Inc., Otsu, Japan). Thermal cycling conditions were: initial denaturation 5 min at 95°C, and 40 cycles of denaturation for 10 s at 95°C, annealing 10 s at 60°C, and elongation 20 s at 72°C. miR-494-3p and TRIM36 expression were normalized against U6 and GAPDH, respectively. Data were analyzed by the $2^{-\Delta\Delta Ct}$ method. The primer sequences are shown in Table 1.

### *Western blotting*

Cells were lysed in RIPA buffer containing Halt protease

**Table 1. Primer sequences for qRT-PCR assays**

| Primer | Sequence |
|---|---|
| miR-494-3p-F | CTCCAAAGGGCACATA |
| miR-494-3p-R | GCAGGGTCCGAGGTATTC |
| U6-F | GCTTGCTTCGGCAGCACATATAC |
| U6-R | TGCATGTCATCCTTGCTCAGGG |
| TRIM36-F | CTGCACTGAAACCAGCTCTTG |
| TRIM36-R | ACTAGCTCTGCTCACCCAAA |
| Cyclin E-F | CAACAAACACAGGGGGCAAC |
| Cyclin E-R | AGCTGTTTTTCGACCACCCA |
| GAPGH-F | GTCAGTGGTGGACCTGACCT |
| GAPDH-R | TGCTGTAGCCAAATTCGTTG |

F, forward; R, reverse.

inhibitor cocktail (Pierce, Rockford, IL, USA) and phosphatase inhibitors (Cayman Chemical, Ann Arbor, MI, USA), and the protein concentration was determined by the Bradford method. Sodium dodecyl sulfate-polyacrylamide agarose gel electrophoresis (SDS-PAGE) was run at 120 V for protein separation. Thereafter, the proteins were transferred from the gel to polyvinylidene fluoride (PVDF) membranes and blocked in TBS-Tween (TBS-T) supplemented with 0.05 g/mL bovine serum albumin for 1 h. The membranes were then incubated with primary antibodies against GAPDH (1:10,000, ab181602), TRIM36 (1:1,000, ab272672), and cyclin E (1:1,000, ab33911) (Abcam, Cambridge, MA, USA) overnight at 4°C. After washing with TBS-T, the membranes were incubated with goat anti-rabbit IgG (1:5,000, Beijing ComWin Biotech Co., Ltd., Beijing, China) for 2 h at room temperature, followed by washing three times in TBS-T. Protein bands were quantified by chemiluminescence imaging analysis system (GE Healthcare, Beijing, China) using an electrogenerated chemiluminescence (ECL) reagent.

### *Dual luciferase reporter assay*

Starbase database was used to predict the binding site between miR-494-3p and TRIM36, and TRIM36-3′UTR wild sequence and mutated TRIM36-3′UTR sequence were synthesized. These two sequences were cloned into dual luciferase reporter vector (pGL3-Basic) to construct the wild dual luciferase reporter (WT-TRIM36) and the mutant dual luciferase reporter (MUT-TRIM36) carrying the 3′UTR of TRIM36. HepG2 and HuH7 cells ($5 \times 10^5$/well) were seeded into 6-well plates and maintained in a humidified 5% $CO_2$ incubator for 24 h at 37°C. Thereafter, the cells were co-transfected with a pGL3-TRIM36-3′ UTR luciferase reporter vector and 5 μL of miR-494-3p mimic or its normal control (NC) for 6 h at 37°C using Lipofectamine 2000 following the manufacturer's recommendations.Dual luciferase reporter assay system was used to detect the activity.

### *Co-immunoprecipitation (CO-IP)*

Whole-cell lysates were centrifuged and incubated with 2 μg of anti-TRIM36 (sc-100881, Santa Cruz Biotechnology, Santa Cruz, CA, USA), anti-cyclin E (ab33911, Abcam, Cambridge, MA, USA) or normal IgG antibodies and protein G-Agarose beads (Roche Diagnostics Ltd, Shanghai, China) overnight at 4°C. The immunocomplexes were separated by SDS-PAGE and then blotted with the indicated antibodies.

### *Ubiquitination assay*

Oe-TRIM36 or oe-NC were transfected into HepG2 cells, after which the lysates were immunoprecipitated with IgG (ab172730) or anti-cyclin E (ab33911, Abcam, Cambridge, MA, USA) antibody at 4°C overnight. Bound proteins that eluted from the protein G-Agarose beads were separated by SDS-PAGE and then immunoblotted with an anti-Ub antibody (ab134953, Abcam, Cambridge, MA, USA).

### *Animals*

Pathogen-free (SPF) BALB/c male nude mice 4–5 weeks of age and weighing 14–18 g were obtained from Vital River Lab Animal Technology Co, Ltd (Beijing, China). The mice were bred under SPF conditions at the Third Xiangya Hospital of Central South University and kept at 26–28°C, 40–60% humidity, a 10 h light period, and water and food ad libitum for 1 week before use. All animal studies were performed following animal experimentation protocols approved by the Third Xiangya Hospital of Central South University, and care was taken to minimize pain to the animals.

### *Tumor xenograft experiments*

The experiments were done in compliance with the ethics committee of the Third Xiangya Hospital of Central South University. Twenty-four male BALB/C nude mice (Vital River, Beijing, China) weighing 14–18 g and 4–5 weeks of age were divided into control, EPS1-1, EPS1-1 + mimic NC, and EPS1-1 + miR-494-3p mimic groups of six mice each. HepG2 cells transfected with mimic NC or miR-494-3p mimic were maintained in DMEM (200 μg/mL) for 24 h. Stably transfected cells then were selected, identified, and cultured. The cells were dissociated with trypsin and gently pipetted to form single-cell suspensions. The cell density was adjusted to $10^5$ cells/mL. Mice were subcutaneously injected with 0.2 mL of the single-cell suspension and observed regularly to record the body weight and tumor length and width. The tumor size and volume were calculated weekly by detecting the luciferase activity of tumors using a real-time imaging system. After 28 days, the nude mice were sacrificed to obtain the tumors. The tumor weights and volumes were determined.

### *Immunohistochemistry (IHC)*

Sections were heated for 4 h in an oven at 65°C, after which the sections were dewaxed in xylene and ethanol. Thereafter, the sections were placed into a citrate antigen retrieval solution before being boiled in a pressure cooker, cooled to room temperature, and washed three times for 3 m in PBS before adding 3% peroxidase inhibitor for 10 min and washing again three times in PBS. A non-specific staining blocker was added for 15 min at room temperature. PBS-diluted primary antibodies against TRIM36 (1:100, sc-100881, Santa Cruz Biotechnology, Santa Cruz, CA, USA) and cyclin E (1:100, ab135380, Abcam, Cambridge, MA, USA) were added to the slides for incubation overnight at 4°C in a refrigerator. The next day, the sections were taken from the refrigerator and rewarmed for 1 h to room temperature to remove excess primary antibodies, followed by PBS wash-

ing (3 × 3 m). The sections were incubated with secondary antibody (1:1,000, ab6728, Abcam, Cambridge, MA, USA) for 30 min at room temperature before washing with PBS (3 × 3 m). A few drops of streptavidin-$H_2O_2$ were added to the sections and incubated for 15 min at room temperature, after which the sections were washed with PBS (3 × 3 m). The sections were then stained with hematoxylin for 2 min, washed with tap water for 10 min, differentiated in 2% hydrochloric acid alcohol for 15 s, and washed with tap water (10 min). Following dehydration in ethanol, permeabilization with xylene, and mounting, the sections were observed by light microscopy and photographed.

### *TUNEL assay*

Tumor sections were fixed 30 m in 0.5 mL 4% paraformaldehyde for 30 m. The paraformaldehyde was removed, the sections were washed once in 0.5 mL of PBS, and then permeabilized by 0.5 mL of Triton X-100 for 5 min. The permeabilization solution was discarded and the sections were washed twice in 0.5 mL PBS, each for 5 min. TUNEL reaction mixture (5 μL TdT plus 45 μL dUTP label) was added and incubated in the dark at room temperature for 1 h. The mixture was removed and the sections were washed three times in 0.5 mL PBS. After the PBS was discarded, DAPI was used for nuclear staining.

### *Immunofluorescence*

Tumor sections were baked in a 60°C incubator for 60–90 m and immersed in xylene for 10 m. Thereafter, the xylene was replaced and the sections were maintained in xylene for another 10 m. The sections were successively placed for 5 m in absolute, 95%, 85%, 75% ethanol, and distilled water followed by washing three times in PBS. Then, antigen retrieval was performed (0.01 M citrate buffer solution, pH 6.0; boiling in microwave oven and heating over low heat for 16 min), and the sections were washed three times for 5 m in PBS and blocked in 5% goat serum for 30 min at room temperature. Excess serum was removed and the sections were incubated at 4°C overnight with 50 μL of primary antibody against TRIM36 (1:100, ab272672) or cyclin E (1:100, ab33911) in a wet bot, with PBS as a negative control. After incubation, the sections were rewarmed to 37°C for 30–45 min and washed three times in PBS for 5 min. The sections were wiped dry, and multi-fluorescein-labeled homogenous secondary antibody (40–50 μL) was added for incubation 50 m at room temperature in the dark. After washing three times in PBS for 5 min, the sections were counterstained, and nuclei were stained for. 5 min with DAPI 5 μg/mL. The sections were rinsed four times for 5 min, and 30 μL of antifade reagent was added before coverslips were added. The tissue was observed by fluorescence microscopy (Leica, Germany).

### *Statistical analysis*

All experiments were conducted in triplicate except as otherwise noted, and the data were reported as means ± standard deviation. The statistical analysis as performed with SPSS 18.0 (IBM Corp., Armonk, NY, USA) and GraphPad Prism 6.0 (GraphPad Software Inc., San Diego, CA, USA). Between-group comparisons were performed by *t*-tests, and one-way analysis of variance was used for multiple-group comparisons followed by the Dunnett's multiple comparisons test. *P*-values <0.05 were considered statistically significant.

## Results

### *EPS1-1 suppresses HCC cell proliferation and promotes apoptosis*

The effects of EPS1-1 on HCC cells were investigated *in vitro* by assays of cell proliferation in cultures treated with concentrations from 25 to 200 μg/mL. EPS1-1 effectively reduced the proliferation of HepG2 and HuH7 HCC cells in time- and dose-dependent manners (Fig. 1A). Flow cytometry showed that EPS1-1 treatment resulted in a dose-dependent G0/G1 phase arrest in HepG2 and HuH7 cells (Fig. 1B), indicating that EPS1-1 inhibited the growth of HCC cells. The expression of the cell cycle regulatory proteins cyclin D/E and cyclin-dependent kinase inhibitor (CDKI) p21 was assessed by SDS-PAGE. EPS1-1 treatment significantly repressed cyclin D and cyclin E expression and enhanced p21 expression in a dose-dependent manner (Fig. 1C), corroborating the MTT and flow cytometry results that demonstrated the inhibition of HCC cell proliferation by EPS1-1. Annexin V-FITC/PI staining and flow cytometry found that compared with the control (0 μg/mL), cell apoptosis significantly increased after treatment with 100 μg/mL and 200 μg/mL EPS1-1 (Fig. 1D). The overall findings indicate that EPS1-1 inhibited the proliferation and stimulated the apoptosis of HCC cells *in vitro*.

### *EPS1-1 hinders HCC progression by inhibiting miR-494-3p*

miR-494-3p expression was greater in HepG2 and HuH7 HCC cells than it was in THLE-2 cells (Fig. 2A), and miR-494-3p expression was consistently found to be higher in cancer tissue collected from HCC patients compared with noncancerous, normal tissue collected from the patients (Fig. 2B). To evaluate the correlation of miR-494-3p expression with clinicopathological features, the patients were divided into groups with high or low miR-494-3p expression based on the mean value of miR-494-3p expression. As shown in Table 2, miR-494-3p was correlated with tumor size, tumor number and tumor, node, and metastasis (TNM) stage, but was not correlated with gender and age. To investigate the relationship of EPS1-1 treatment with miR-494-3p expression, miR-494-3p transcript levels were monitored in HCC cells after treatment with different doses of EPS1-1. miR-494-3p expression was significantly suppressed after EPS1-1 (100 μg/mL and 200 μg/mL) treatment compared with the control (0 μg/mL) (Fig. 2C). The data implied that EPS1-1 inhibited HCC cell proliferation and facilitated apoptosis by downregulating miR-494-3p expression. As 200 μg/mL EPS1-1 exhibited the most potent suppression of miR-494-3p in HCC cells compared with the control (Fig. 2C), that concentration was used in subsequent procedures.

The involvement of miR-494-3p in EPS1-1-modulated proliferation and apoptosis was confirmed in transfected HCC that overexpressed miR-494-3p. The transfection efficiency of the miR-494-3p mimic in HepG2 and HuH7 cells were assessed by qRT-PCR, which showed significantly enhanced miR-494-3p expression in HepG2 and HuH7 cells (Fig. 2D). The proliferation of HCC cells in the control, EPS1-1, EPS1-1 + mimic NC, and the EPS1-1 + miR-494-3p mimic groups showed that EPS1-1 treatment led to decreased HCC proliferation, but that the decrease was not sustained when miR-494-3p mimic was overexpressed in the EPS1-1 + miR-494-3p mimic group (Fig. 2E). Flow cytometry revealed that EPS1-1 treatment led to an increase in the percentage of cells in the G0/G1 phase compared with its control, but that was not observed in cells transfected with the miR-494-3p mimic (Fig. 2F**)**. To further study the effects on the cell cycle,

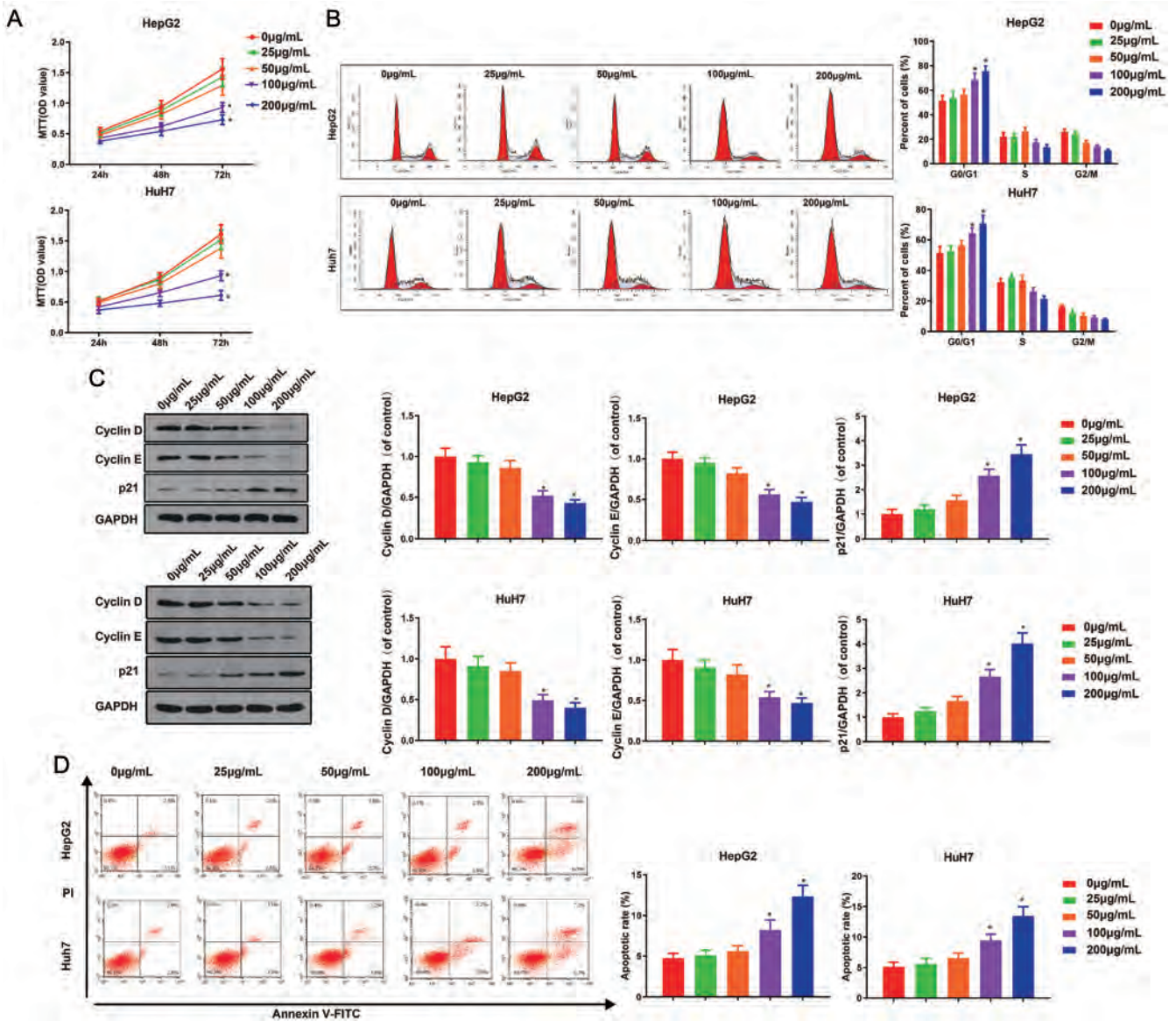


**Fig. 1. EPS1-1 inhibits HCC cell proliferation and facilitates apoptosis.** MTT assay of cell proliferation (A). Flow cytometry assay of the cell cycle (B). Western blot assay of the cell cycle regulatory proteins cyclin D, cyclin E, and p21 (C). Annexin V-FITC/PI staining assay of cell apoptosis (D). *$p<0.05$ vs. control. Data are means ± standard deviation; independent-sample *t*-test or one-way analysis of variance and Tukey's. Each assay was performed in triplicate. FCM, flow cytometry; HCC, hepatocellular carcinoma; PI, propidium iodide.

cyclin D and E, and p21 expression were assayed in western blots. Cyclin D and cyclin E expression were repressed and p21 expression was upregulated, and in spite of EPE1-1 treatment, the expression patterns were reversed when the miR-494-3p mimic was overexpressed (Fig. 2G). Annexin V-FITC/PI staining showed that EPS1-1 treatment increased apoptosis in HCC cells and that apoptosis decreased in the EPS1-1 + miR-494-3p mimic group (Fig. 2H) compared with control. Overall, the findings showed that EPS1-1 inhibited HCC cell proliferation and promoted apoptosis by suppressing miR-494-3p expression.

### *TRIM36 is a target gene of miR-494-3p*

To understand the mechanism of miR-494-3p-mediated HCC progression further, we screened for its targets, which led us to examine an E3 ubiquitin ligase TRIM36 expression in THLE-2 normal hepatocyte cells, and HCC cell lines. Reportedly, TRIM36 was downregulated in gastric cancer and prostate cancer, but little is known with regard to its function in the HCC. TRIM36 was weakly expressed at both transcript and protein levels in HepG2 and HuH7 cells in contrast to THLE-2 cells (Fig. 3A), and TRIM36 expression was downregulated in tissues collected from the HCC group patients compared with adjacent normal tissue (Fig. 3B). As shown in Figure 3C, StarBase, a database of known microRNA–mRNA interactions, indicated that miR-494-3p could bind to the 3′-UTR of TRIM36. The direct interaction between miR-494-3p and TRIM36 was confirmed with a dual luciferase reporter carrying the 3′-UTR of TRIM36, which showed that transfection of miR-494-3p mimic significantly

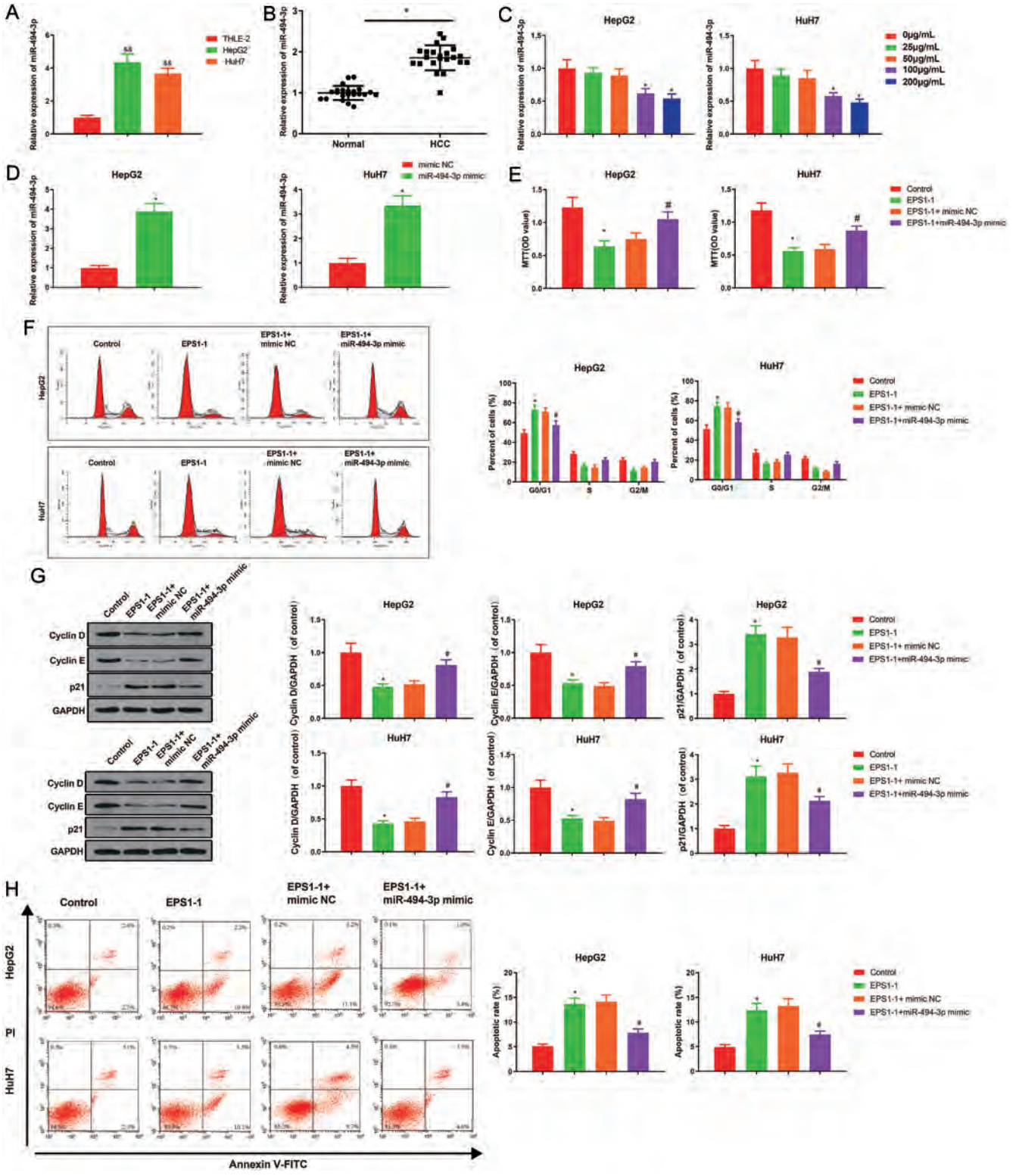


**Fig. 2. EPS1-1 inhibits HCC progression via inhibiting miR-494-3p.** miR-494-3p is strongly expressed in HepG2 and HuH7 HCC cells (A). miR-494-3p expression was increased in HCC tissues (B). EPS1-1 repressed miR-494-3p expression in HCC cells (C). qRT-PCR assay of the transfection efficiency of the miR-494-3p mimic (D). MTT assay of HCC cell proliferation (E). Flow cytometry assay of the HCC cell cycle in each study group were monitored by FCM (F). Western blot assays of the cell cycle regulatory proteins cyclin D, cyclin E, and p21 (G). Annexin V-FITC/PI staining assay of cell apoptosis (H). *$p<0.05$, **$p<0.01$ vs. control, mimic NC group or normal group. $^{\&\&}p<0.01$ vs. THLE-2, $^{\#}p<0.05$ vs. EPS1-1 + mimic NC. Data are means ± standard deviation; independent-sample *t*-test or one-way analysis of variance and Tukey's. Each assay was performed in triplicate. FCM, flow cytometry; HCC, hepatocellular carcinoma; PI, propidium iodide.

**Table 2. Correlation of miR-494-3p with the clinicopathological features of patients with hepatocellular carcinoma**

| Clinicopathological factor | Low miR-494-3p (*n* = 11) | High miR-494-3p (*n* = 11) | *p*-value |
|---|---|---|---|
| Sex | | | |
| Male, *n* | 5 | 7 | 0.6699 |
| Female, *n* | 6 | 4 | |
| Age, years | | | |
| ≤55 | 6 | 6 | 1 |
| >55 | 5 | 5 | |
| Tumor size, cm | | | |
| ≥5 | 1 | 9 | 0.0019** |
| <5 | 10 | 2 | |
| Tumor number | | | |
| Multiple | 2 | 8 | 0.0300* |
| Single | 9 | 3 | |
| TNM stage | | | |
| I-II | 8 | 2 | 0.0300* |
| III-IV | 3 | 9 | |

suppressed the luciferase activity of wild-type (WT)-TRIM36 ($p<0.01$) and that the luciferase activity of mutant (MUT)-TRIM36 was unaffected (Fig. 3D). In addition, qRT-PCR and western blotting confirmed that transfection of the miR-494-3p mimic significantly decreased TRIM36 expression and that inhibiting miR-494-3p led to elevated TRIM36 expression (Fig. 3E). The results indicate that TRIM36 was a direct downstream target of miR-494-3p.

### *EPS1-1 limits HCC cell development via the miR-494-3p/TRIM36 axis*

The role of TRIM36 in the inhibition of HCC by EPS1-1 was investigated by monitoring TRIM36 levels in HCC cells following EPS1-1 treatment at different concentrations. Both mRNA and protein expression of TRIM36 were significantly increased in cells treated with 100 μg/mL and 200 μg/mL EPS1-1 compared with the 0 μg/mL EPS1-1 control (Fig. 4A). To clarify the relative contributions of TRIM36 and miR-494-3p in EPS1-1-mediated effects on HCC, the cells were transfected with oe-TRIM36, sh-TRIM36, or miR-494-3p mimic+oe-TRIM36 before being treated with 200 μg/mL of EPS1-1. As expected, TRIM36 expression was reduced in the EPS1-1 + sh-TRIM36 group and elevated in the (EPS1-1 + oe-TRIM36) group compared with their non-silencing controls (Fig. 4C). Interestingly, when TRIM36 was cotransfected with miR-494-3p and then stimulated with EPS1-1, TRIM36 expression did not increase compared with the oe-TRIM36 group stimulated with EPS1-1 only (Fig. 4B, C), which supported a finding that TRIM36 was downstream of miR-494-3p in HCC. In addition, as shown in Figure 4D–G, HCC cell proliferation and cyclin D and cyclin E expression were significantly increased and p21 expression and apoptosis were significantly decreased when TRIM36 was silenced in spite of EPS1-1 stimulation. The results were reversed, with decreased proliferation and cyclin expression and increased apoptosis and p21 expression when TRIM36 was overexpressed, but the effects were minimized when miR-494-3p was upregulated despite TRIM36 overexpression (Fig. 4D–G). Collectively, the data demonstrate that EPS1-1 hindered HCC cell proliferation and stimulated cell apoptosis by regulating the miR-494-3p/TRIM36 signaling.

### *TRIM36 induces ubiquitination of cyclin E*

The results suggested that EPS1-1 and miR-494-3p regulate the expression of cyclin E protein in HCC, and the GeneCards database (https://www.genecards.org/) provided information regarding the unique E3 ubiquitin ligase activity of TRIM36. We therefore hypothesized that TRIM36 played a crucial role in cell proliferation, migration, and invasion by regulating the ubiquitination of cyclin E or cyclin D. The results showed that while TRIM36 was unable to ubiquitinate cyclin D, it did induce cyclin E ubiquitination. Overexpression of TRIM36 did not change cyclin E transcription (Fig. 5A), but significantly inhibited its protein expression (Fig. 5B), but that was blunted by treatment with the protease inhibitor MG132 (Fig. 5B), consistent with TRIM36 participation in the post-transcriptional regulation of cyclin E through ubiquitination. Co-immunoprecipitation procedures revealed that cyclin E was not pulled down by IgG treatment, but that anti-TRIM36 antibody managed to immune-precipitate cyclin E. Similarly, when cyclin E was immune-precipitated, TRIM36 expression effectively increased and coprecipitated (Fig. 5C). Analysis of ubiquitination further confirmed that TRIM36 induced ubiquitination of cyclin E (Fig. 5D). The data suggest that TRIM36 inhibited HCC development by binding and inducing the ubiquitination of cyclin E.

### *EPS1-1 inhibits tumor growth in vivo*

To examine the importance of miR-494-3p in the tumor-suppressive activity of EPS1-1 *in vivo*, subcutaneous xenografts in nude mice were evaluated. The experiments revealed that EPS1-1 treatment significantly reduced tumor volume and weight. The inhibitory functions of EPS1-1 were significantly reduced when the miR-494-3p mimic was added to the treatment (Fig. 6A, B). TUNEL assays showed that EPS1-1 treatment substantially promoted tumor cell apoptosis compared with the control. Apoptosis significantly decreased in the EPS1-1treated miR-494-3p mimic group

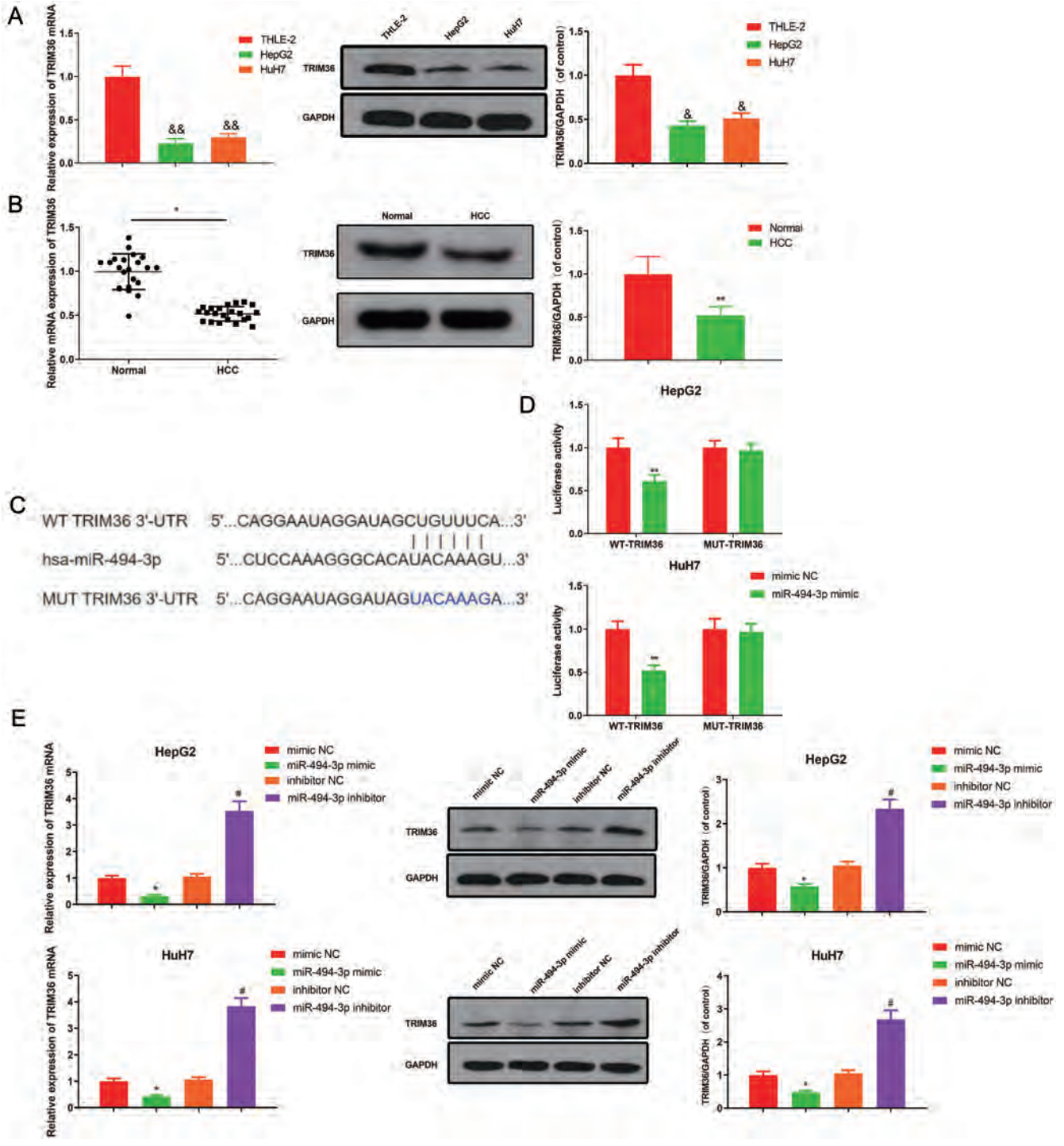


**Fig. 3. TRIM36 is a direct target gene of miR-494-3p.** qRT-PCR and western blot assays of TRIM36 expression in HCC cells and tissues (A, B). Possible miR-494-3p and TRIM36 binding sites predicated by StarBase (C). Dual luciferase reporter assay of the interaction between miR-494-3p and TRIM36 (D). qRT-PCR and western blot assays of TRIM36 expression in HCC cells in each study group (E). *$p<0.05$, **$p<0.01$ vs. mimic NC or normal cells. $^{\&}p<0.05$, $^{\&\&}p<0.01$ vs. THLE-2. $^{\#}p<0.05$ vs. inhibitor NC. Data are means ± standard deviation; independent-sample *t*-test. HCC, hepatocellular carcinoma.

compared to its control (Fig. 6C). The relationship between miR-494-3p, TRIM36, and the effects of EPS1-1 on the expression of TRIM36 and cyclin E were also evaluated *in vivo*. qRT-PCR and IHC staining confirmed that EPS1-1 treatment upregulated TRIM36 expression and downregulated cyclin E expression (Fig. 6D-E) and that miR-494-3p mimic treatment reduced TRIM36 expression and increased cyclin E expression (Fig. 6D–E). Immunofluorescence double staining found that TRIM36 co-localized with cyclin E in cell nuclei (Fig. 6F). Overall, these results show that EPS1-1 inhib-

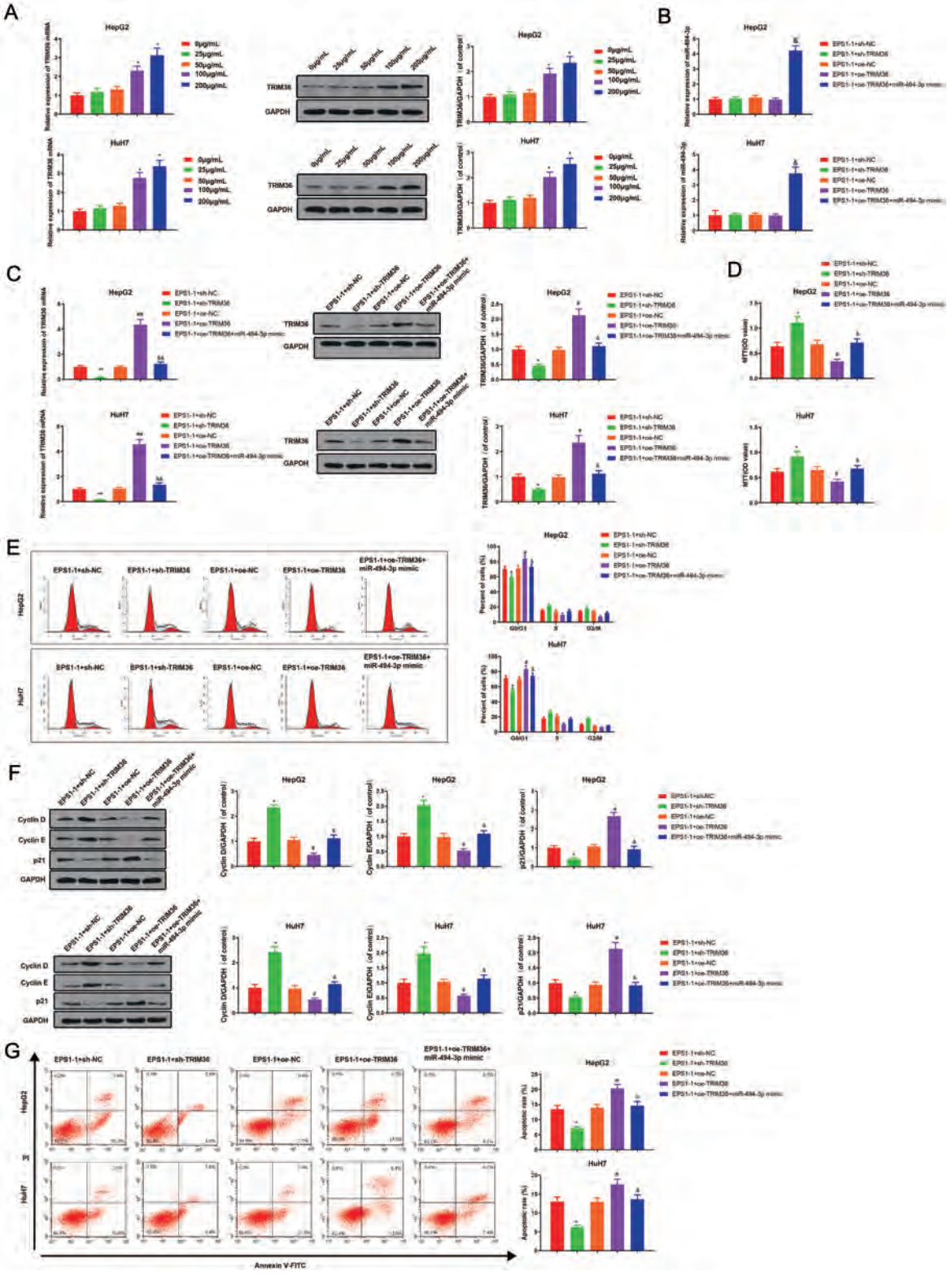


**Fig. 4. EPS1-1 affects HCC cell progression via miR-494-3p/TRIM36 axis.** qRT-PCR and western blot assays of TRIM36 expression in HCC cells treated with different concentrations of EPS1-1 (A). qRT-PCR assays of miR-494-3p expression (B). Expression of of TRIM36 mRNA and protein (C). Assays of HCC cell proliferation, cell cycle, cell cycle regulatory proteins, and cell apoptosis by MTT (D), FCM (E), Western blot (F), and Annexin V-FITC/PI staining (G), respectively. *$p<0.05$, **$p<0.01$ vs. control or EPS1-1 + sh-NC. $^{\#}P<0.05$; $^{\#\#}p<0.01$ vs. EPS1-1 + oe-NC; $^{\&}p<0.05$; $^{\&\&}p<0.01$ vs. EPS1-1 + oe-TRIM36. Data are means ± standard deviation; independent-sample *t*-test or one-way analysis of variance and Tukey's. Each assay was performed in triplicate. FCM, flow cytometry; HCC, hepatocellular carcinoma; PI, propidium iodide.

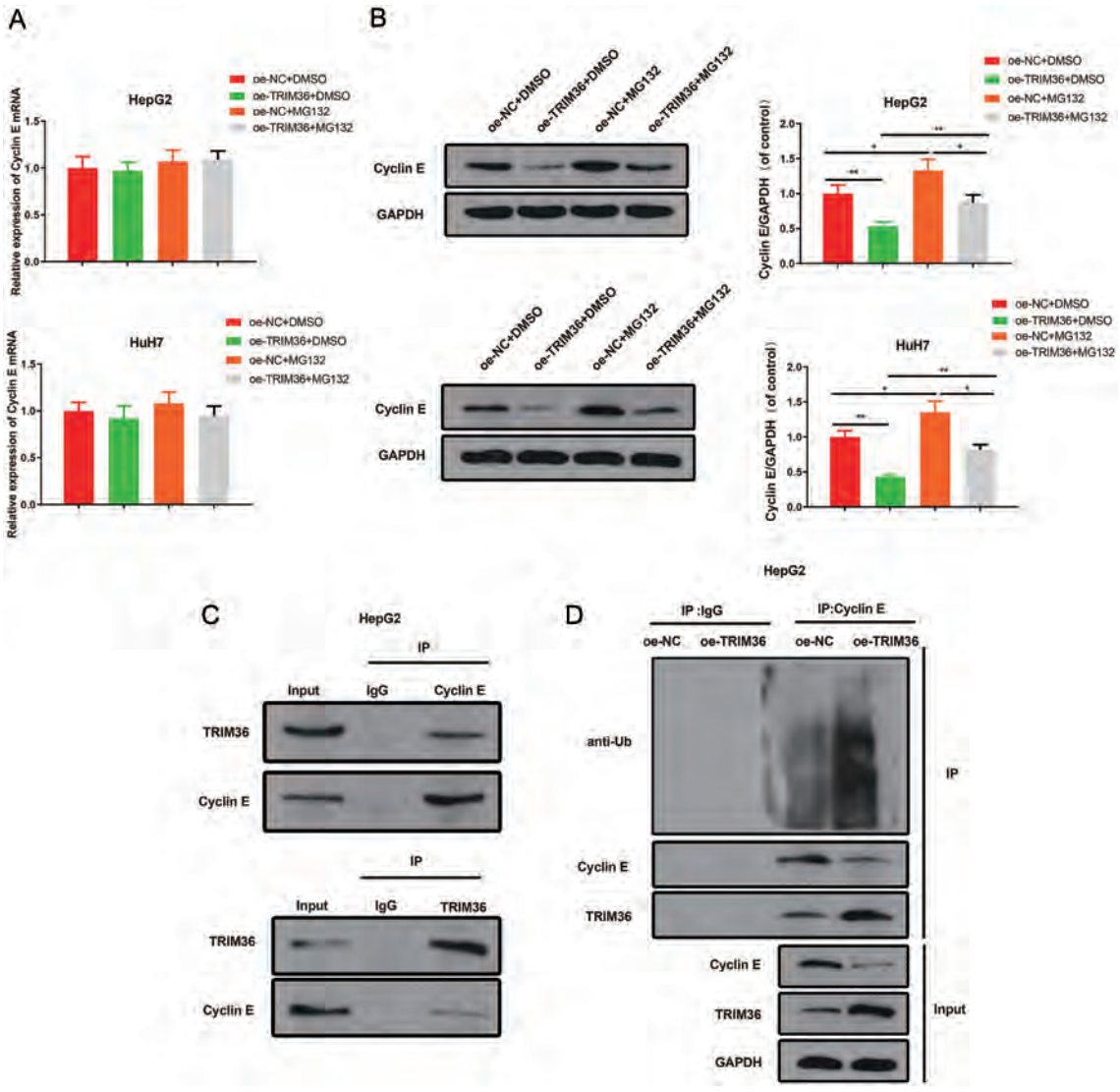


**Fig. 5. TRIM36 stimulates ubiquitination of cyclin E.** qRT-PCR and Western blot assays of cyclin E mRNA and protein expression (A, B). Co-immunoprecipitation (CO-IP) confirms the interaction between TRIM36 and cyclin E (C). TRIM36 elicits ubiquitination of cyclin E (D). *$p<0.05$, **$p<0.01$ vs. oe-NC+DMSO, oe-TRIM36+DMSO, or oe-NC+MG132. Data are means ± standard deviation; independent-samples *t*-test of one-way analysis of variance and Tukey's test. Each assay was performed in triplicate.

ited HCC development *in vivo* by modulating miR-494-3p/TRIM36 signaling and cyclin E ubiquitination.

## Discussion

In this study, we evaluated the effects of EPS1-1 on HCC *in vitro* and *in vivo*. We observed that EPS1-1 treatment inhibited HCC cell progression by downregulating the tumor promoter miR-494-3p to promote TRIM36 expression, which in turn induced ubiquitination of cyclin E. Previous studies have shown that EPS1-1 has antitumor activity *in vitro* and *in vivo*[9,23] and was reported to be a tumor suppressor in HCC,[15] but causative relationships have not been elucidated yet. This study investigated the *in vitro* and *in vivo* inhibition of HCC cell and tumor growth of HCC by EPS1-1 polysaccharide extracted from *R. nigrum*. EPS1-1, at concentrations of 25–200 μg/mL decreased HCC cell proliferation in a time- and dose-dependent manner. Cell cycle suppression is recognized as a potential target in cancer therapy,[24] and in this study, EPS1-1 treatment induced G0/G1 phase arrest in HCC cells. Cell cycle progression is dependent on CDK, arrested by CDK inhibitors, and activated by cyclin binding.[25] EPS1-1 reduced the expression of the cell cycle regulatory proteins cyclin D and cyclin E expression and it increased the expression of p21, a CDK inhibitor, (p21) in a dose-dependent manner, indicating potent inhibitory effects of EPS1-1 on HCC cell proliferation. Promotion of cell apoptosis is an important mechanism of action of anticancer drugs,[26] and EPS1-1 at 100 and 200 μg/mL significantly promoted the apoptosis of HCC cells. Our findings demonstrate the anti-proliferative and pro-apoptotic effects of EPS1-1 in HCC cells, which is not only in line with earlier studies but a further confirmation of the effects of EPS1-1 on cancer cell progression. Nonetheless, the working molecular mechanism of EPS1-1 has not been previously described.

In recent years, miRNAs have been shown to play sig-

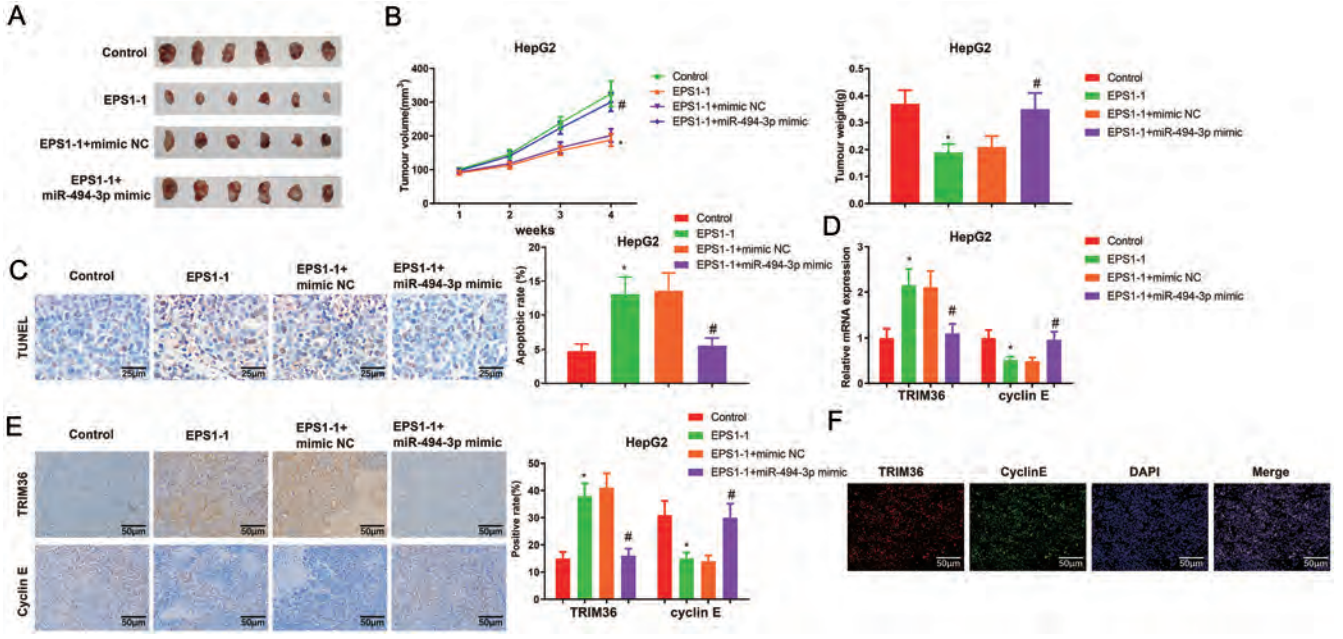


**Fig. 6. EPS1-1 suppresses tumor growth *in vivo*.** Photographs of subcutaneous xenograft tumor (A). Tumor volume and weight in each group (B). TUNEL staining assay of apoptosis (C). qRT-PCR and IHC assays of TRIM36 and cyclin E expression in tumor tissues of nude mice (D, E). Immunofluorescence assays show the location of TRIM36 and cyclin E (F). $n$ = 6, *$p$<0.05 vs. control; $^{\#}p$<0.05 vs. EPS1-1 + mimic NC. Data are means ± standard deviation; independent-samples $t$-test. IHC, immunohistochemistry.

nificant roles in modulating the progression of several types of cancers, including HCC.[27] Previous studies indicated that miR-494-3p is upregulated in HCC,[22,28] and suggested it is a tumor promoter in HCC. Herein, we demonstrated that miR-494-3p was a key player in EPS1-1-mediated inhibition of HCC. We also showed that miR-494-3p was overexpressed in HCC cells and significantly suppressed following EPS1-1 treatment (100 μg/mL and 200 μg/mL). Moreover, in the presence of EPS1-1, miR-494-3p overexpression significantly promoted proliferation and cyclin D/E expression in HCC cells while it decreased p21 expression, the percentage of cells in the G0/G1 phase, and apoptosis. Taken together, the data reveal that EPS1-1 suppressed HCC proliferation and boosted cell apoptosis via inhibiting miR-494-3p expression.

miRNAs directly bind to the 3′-UTR of target mRNAs and then downregulate expression of the corresponding gene.[29,30] TRIM36 a TRIM family member, was identified as a target of miR-320a.[31] Previously, TRIM36 downregulation was reported in gastric and prostate cancer cells and tissues, but its expression in HCC has not been reported.[32,33] We found that TRIM36 was weakly expressed in HCC and it had a binding site for miR-494-3p. Overexpression of miR-494-3p in HCC suppressed TRIM36 expression and inhibition of miR-494-3 enhanced TRIM36 expression. Increased TRIM36 expression has been shown to indicate a favorable prognosis, and TRIM36 is a tumor suppressor in prostate cancer by inhibiting cell proliferation and stimulating apoptosis.[32] This background prompted us to explore the role of TRIM36 in the inhibition of EPS1-1 in HCC. TRIM36 levels were upregulated by EPS1-1 treatment. Cell proliferation was enhanced, and cell apoptosis was decreased, by TRIM36 inhibition and EPS1-1 treatment. The presence of both EPS1-1 and TRIM36 overexpression effectively blunted the progression of HCC cells. Moreover, miR-494-3p overexpression partially counteracted the synergic effects of EPS1-1 and TRIM36 on suppressing HCC. The data support EPS1-1 suppression of HCC cell development via a miR-494-3p/TRIM36 axis. The TRIM protein family includes E3 ubiquitin ligases with activity related to a broad range of biological and pathological processes.[34] Our data demonstrated that TRIM36 has unique E3 ubiquitin ligase activity and TRIM36 overexpression induced the ubiquitination of cyclin E in HCC. Additionally, *in vivo* animal experiments revealed that administration of EPS1-1 repressed tumor growth in nude mice by regulating miR-494-3p/TRIM36 axis and ubiquitination of cyclin E. In addition to TRIM36, miR-494-3p has been reported to promote HCC metastasis by targeting PTEN,[22] and the regulatory activity was reported in non-small cell lung cancer and glioma in which miR-494-3p was sponged by the long noncoding RNA WT1-AS1.[21,35,36] In-depth studies are needed to elucidate the impact of the interactions between miR-494-3p and other known HCC targets, which would facilitate the development of miRNA-based treatment of HCC.

## Conclusion

In summary, our study describes a working molecular mechanism for EPS1-1 inhibition of proliferation and survival of HCC *in vitro* and *in vivo*. The inhibitory effects of EPS1-1 were achieved through downregulation of miR-494-3p expression and upregulation of TRIM36-mediated ubiquitination of cyclin E, ultimately regulating the progression of HCC. HCC treatments that include EPS1-1 may be useful and warrant further study.

## Funding

None to declare.

## Conflict of interest

The authors have no conflict of interests related to this pub-

lication.

## Author contributions

Study design (HY, PR), performance of experiments (HY, XM), analysis and interpretation of data (HY, ZM, ZH), manuscript writing (HY, XM), critical revision of the manuscript (PR, XM), technical or material support (PR).

## Ethical statement

All procedures involving humans were performed with the approval of the ethics committee of the Third Xiangya Hospital of Central South University and the informed consent of participants or their relatives.

## Data sharing statement

All data are accessible upon reasonable request to correspond author.

## References


[1] Jemal A, Bray F, Center MM, Ferlay J, Ward E, Forman D. Global cancer statistics. CA Cancer J Clin 2011;61(2):69–90. doi:10.3322/caac.20107, PMID:21296855.

[2] Lin YH, Wu MH, Huang YH, Yeh CT, Cheng ML, Chi HC, *et al*. Taurine up-regulated gene 1 functions as a master regulator to coordinate glycolysis and metastasis in hepatocellular carcinoma. Hepatology 2018;67(1):188–203. doi:10.1002/hep.29462, PMID:28802060.

[3] Uchino K, Tateishi R, Shiina S, Kanda M, Masuzaki R, Kondo Y, *et al*. Hepatocellular carcinoma with extrahepatic metastasis: clinical features and prognostic factors. Cancer 2011;117(19):4475–4483. doi:10.1002/cncr.25960, PMID:21437884.

[4] Uka K, Aikata H, Takaki S, Shirakawa H, Jeong SC, Yamashina K, *et al*. Clinical features and prognosis of patients with extrahepatic metastases from hepatocellular carcinoma. World J Gastroenterol 2007;13(3):414–420. doi:10.3748/wjg.v13.i3.414, PMID:17230611.

[5] Kokudo T, Hasegawa K, Shirata C, Tanimoto M, Ishizawa T, Kaneko J, *et al*. Assessment of Preoperative Liver Function for Surgical Decision Making in Patients with Hepatocellular Carcinoma. Liver Cancer 2019;8(6):447–456. doi:10.1159/000501368, PMID:31799202.

[6] Dong Z, Feng L, Hao Y, Chen M, Gao M, Chao Y, *et al*. Synthesis of Hollow Biomineralized CaCO3-Polydopamine Nanoparticles for Multimodal Imaging-Guided Cancer Photodynamic Therapy with Reduced Skin Photosensitivity. J Am Chem Soc 2018;140(6):2165–2178. doi:10.1021/jacs.7b11036, PMID:29376345.

[7] Pan TJ, Li LX, Zhang JW, Yang ZS, Shi DM, Yang YK, *et al*. Antimetastatic Effect of Fucoidan-Sargassum against Liver Cancer Cell Invadopodia Formation via Targeting Integrin αVβ3 and Mediating αVβ3/Src/E2F1 Signaling. J Cancer 2019;10(20):4777–4792. doi:10.7150/jca.26740, PMID:31598149.

[8] Hussain SS, Kumar AP, Ghosh R. Food-based natural products for cancer management: Is the whole greater than the sum of the parts? Semin Cancer Biol 2016;40-41:233–246. doi:10.1016/j.semcancer.2016.06.002, PMID:27397504.

[9] Yu W, Chen G, Zhang P, Chen K. Purification, partial characterization and antitumor effect of an exopolysaccharide from Rhizopus nigricans. Int J Biol Macromol 2016;82:299–307. doi:10.1016/j.ijbiomac.2015.10.005, PMID:26449531.

[10] Yu Z, Kong M, Zhang P, Sun Q, Chen K. Immune-enhancing activity of extracellular polysaccharides isolated from Rhizopus nigricans. Carbohydr Polym 2016;148:318–325. doi:10.1016/j.carbpol.2016.04.068, PMID:27185145.

[11] Bouattour M, Mehta N, He AR, Cohen EI, Nault JC. Systemic Treatment for Advanced Hepatocellular Carcinoma. Liver Cancer 2019;8(5):341–358. doi:10.1159/000496439, PMID:31768344.

[12] Feng B, Zhu Y, Sun C, Su Z, Tang L, Li C, *et al*. Basil polysaccharide inhibits hypoxia-induced hepatocellular carcinoma metastasis and progression through suppression of HIF-1α-mediated epithelial-mesenchymal transition. Int J Biol Macromol 2019;137:32–44. doi:10.1016/j.ijbiomac.2019.06.189, PMID:31252022.

[13] Song G, Lu Y, Yu Z, Xu L, Liu J, Chen K, *et al*. The inhibitory effect of polysaccharide from Rhizopus nigricans on colitis-associated colorectal cancer. Biomed Pharmacother 2019;112:108593. doi:10.1016/j.biopha.2019.01.054, PMID:30784912.

[14] Yu Z, Sun Q, Liu J, Zhang X, Song G, Wang G, *et al*. Polysaccharide from Rhizopus nigricans inhibits the invasion and metastasis of colorectal cancer. Biomed Pharmacother 2018;103:738–745. doi:10.1016/j.biopha.2018.04.093, PMID:29684852.

[15] Chu G, Miao Y, Huang K, Song H, Liu L. Role and Mechanism of Rhizopus Nigrum Polysaccharide EPS1-1 as Pharmaceutical for Therapy of Hepatocellular Carcinoma. Front Bioeng Biotechnol 2020;8:509. doi:10.3389/fbioe.2020.00509, PMID:32582655.

[16] Wilk G, Braun R. Integrative analysis reveals disrupted pathways regulated by microRNAs in cancer. Nucleic Acids Res 2018;46(3):1089–1101. doi:10.1093/nar/gkx1250, PMID:29294105.

[17] Li H, Zhao X, Shan H, Liang H. MicroRNAs in idiopathic pulmonary fibrosis: involvement in pathogenesis and potential use in diagnosis and therapeutics. Acta Pharm Sin B 2016;6(6):531–539. doi:10.1016/j.apsb.2016.06.010, PMID:27818919.

[18] Toffanin S, Hoshida Y, Lachenmayer A, Villanueva A, Cabellos L, Minguez B, *et al*. MicroRNA-based classification of hepatocellular carcinoma and oncogenic role of miR-517a. Gastroenterology 2011;140(5):1618–1628.e16. doi:10.1053/j.gastro.2011.02.009, PMID:21324318.

[19] Hou J, Lin L, Zhou W, Wang Z, Ding G, Dong Q, *et al*. Identification of miRNomes in human liver and hepatocellular carcinoma reveals miR-199a/b-3p as therapeutic target for hepatocellular carcinoma. Cancer Cell 2011;19(2):232–243. doi:10.1016/j.ccr.2011.01.001, PMID:21316602.

[20] Huang N, Lin J, Ruan J, Su N, Qing R, Liu F, *et al*. MiR-219-5p inhibits hepatocellular carcinoma cell proliferation by targeting glypican-3. FEBS Lett 2012;586(6):884–891. doi:10.1016/j.febslet.2012.02.017, PMID:22449976.

[21] Li XT, Wang HZ, Wu ZW, Yang TQ, Zhao ZH, Chen GL, *et al*. miR-494-3p Regulates Cellular Proliferation, Invasion, Migration, and Apoptosis by PTEN/AKT Signaling in Human Glioblastoma Cells. Cell Mol Neurobiol 2015;35(5):679–687. doi:10.1007/s10571-015-0163-0, PMID:25662849.

[22] Lin H, Huang ZP, Liu J, Qiu Y, Tao YP, Wang MC, *et al*. MiR-494-3p promotes PI3K/AKT pathway hyperactivation and human hepatocellular carcinoma progression by targeting PTEN. Sci Rep 2018;8(1):10461. doi:10.1038/s41598-018-28519-2, PMID:29992971.

[23] Cao J, Hou D, Lu J, Zhu L, Zhang P, Zhou N, *et al*. Anti-tumor activity of exopolysaccharide from Rhizopus nigricans Ehrenb on S180 tumor-bearing mice. Bioorg Med Chem Lett 2016;26(8):2098–2104. doi:10.1016/j.bmcl.2016.02.012, PMID:26951752.

[24] Siddiqui IA, Bharali DJ, Nihal M, Adhami VM, Khan N, Chamcheu JC, *et al*. Excellent anti-proliferative and pro-apoptotic effects of (-)-epigallocatechin-3-gallate encapsulated in chitosan nanoparticles on human melanoma cell growth both in vitro and in vivo. Nanomedicine 2014;10(8):1619–1626. doi:10.1016/j.nano.2014.05.007, PMID:24965756.

[25] Komata T, Kanzawa T, Takeuchi H, Germano IM, Schreiber M, Kondo Y, *et al*. Antitumour effect of cyclin-dependent kinase inhibitors (p16(INK4A), p18(INK4C), p19(INK4D), p21(WAF1/CIP1) and p27(KIP1)) on malignant glioma cells. Br J Cancer 2003;88(8):1277–1280. doi:10.1038/sj.bjc.6600862, PMID:12698196.

[26] Sverchinsky DV, Nikotina AD, Komarova EY, Mikhaylova ER, Aksenov ND, Lazarev VF, *et al*. Etoposide-Induced Apoptosis in Cancer Cells Can Be Reinforced by an Uncoupled Link between Hsp70 and Caspase-3. Int J Mol Sci 2018;19(9):2519. doi:10.3390/ijms19092519, PMID:30149619.

[27] Zhou J, Yu L, Gao X, Hu J, Wang J, Dai Z, *et al*. Plasma microRNA panel to diagnose hepatitis B virus-related hepatocellular carcinoma. J Clin Oncol 2011;29(36):4781–4788. doi:10.1200/JCO.2011.38.2697, PMID:22105822.

[28] Pollutri D, Patrizi C, Marinelli S, Giovannini C, Trombetta E, Giannone FA, *et al*. The epigenetically regulated miR-494 associates with stem-cell phenotype and induces sorafenib resistance in hepatocellular carcinoma. Cell Death Dis 2018;9(1):4. doi:10.1038/s41419-017-0076-6, PMID:29305580.

[29] Jaiswal A, Reddy SS, Maurya M, Maurya P, Barthwal MK. MicroRNA-99a mimics inhibit M1 macrophage phenotype and adipose tissue inflammation by targeting TNFα. Cell Mol Immunol 2019;16(5):495–507. doi:10.1038/s41423-018-0038-7, PMID:29849090.

[30] O'Neill LA, Sheedy FJ, McCoy CE. MicroRNAs: the fine-tuners of Toll-like receptor signalling. Nat Rev Immunol 2011;11(3):163–175. doi:10.1038/nri2957, PMID:21331081.

[31] Pandey A, Sahu AR, Wani SA, Saxena S, Kanchan S, Sah V, *et al*. Modulation of Host miRNAs Transcriptome in Lung and Spleen of Peste des Petits Ruminants Virus Infected Sheep and Goats. Front Microbiol 2017;8:1146. doi:10.3389/fmicb.2017.01146, PMID:28694795.

[32] Kimura N, Yamada Y, Takayama KI, Fujimura T, Takahashi S, Kume H, *et al*. Androgen-responsive tripartite motif 36 enhances tumor-suppressive effect by regulating apoptosis-related pathway in prostate cancer. Cancer Sci 2018;109(12):3840–3852. doi:10.1111/cas.13803, PMID:30238687.

[33] Man Z, Chen T, Zhu Z, Zhang H, Ao L, Xi L, *et al*. High expression of TRIM36 is associated with radiosensitivity in gastric cancer. Oncol Lett 2019;17(5):4401–4408. doi:10.3892/ol.2019.10122, PMID:30944633.

[34] Tan J, Shen J, Zhu H, Gong Y, Zhu H, Li J, *et al*. miR-378a-3p inhibits ischemia/reperfusion-induced apoptosis in H9C2 cardiomyocytes by targeting TRIM55 via the DUSP1-JNK1/2 signaling pathway. Aging (Albany NY) 2020;12(10):8939–8952. doi:10.18632/aging.103106, PMID:32463795.

[35] Wu C, Yang J, Li R, Lin X, Wu J, Wu J. LncRNA WT1-AS/miR-494-3p Regulates Cell Proliferation, Apoptosis, Migration and Invasion via PTEN/PI3K/AKT Signaling Pathway in Non-Small Cell Lung Cancer. Onco Targets Ther 2021;14:891–904. doi:10.2147/OTT.S278233, PMID:33603394.

[36] Qiu G, Tong W, Jiang C, Xie Q, Zou J, Luo C, *et al*. Long Noncoding RNA WT1-AS Inhibit Cell Malignancy via miR-494-3p in Glioma. Technol Cancer Res Treat 2020;19:1533033820919759. doi:10.1177/1533033820919759, PMID:32419643.

*Journal of Clinical and Translational Hepatology* **2022** vol. 10(4) | 620–626
DOI: 10.14218/JCTH.2021.00100

Original Article

# Hepatic Arterioportal Fistulas: A Retrospective Analysis of 97 Cases

Bendaxin Cao[1,2,3], Ke Tian[1], Hejun Zhou[2,3], Chenjie Li[2,3], Deliang Liu[2,3*] and Yuyong Tan[2,3*]

*[1]Department of Respiratory and Critical Care Medicine, Affiliated Nanhua Hospital, University of South China, Hengyang, Hunan, China; [2]Department of Gastroenterology, The Second Xiangya Hospital of Central South University, Changsha, Hunan, China; [3]Research Center of Digestive Disease, Central South University, Changsha, Hunan, China*

**Received:** 20 March 2021 | **Revised:** 3 June 2021 | **Accepted:** 16 November 2021 | **Published:** 10 January 2022

## Abstract

***Background and Aims:*** Hepatic arterioportal fistulas (HAPFs) are abnormal shunts or aberrant functional connections between the portal venous and the hepatic arterial systems. Detection of HAPFs has increased with the advances in diagnostic techniques. Presence of HAPFs over a prolonged period can aggravate liver cirrhosis and further deteriorate liver function. However, the underlying causes of HAPFs and the treatment outcomes are now well characterized. This study aimed to summarize the clinical characteristics of patients with HAPFs, and to compare the outcomes of different treatment modalities. ***Methods:*** Data of 97 patients with HAPFs who were admitted to the Second Xiangya Hospital between January 2010 and January 2020 were retrospectively reviewed. Demographic information, clinical manifestations, underlying causes, treatment options, and short-term outcomes were analyzed. ***Results:*** The main cause of HAPF in our cohort was hepatocellular carcinoma (78/97, 80.41%), followed by cirrhosis (10/97, 10.31%). The main clinical manifestations were abdominal distention and abdominal pain. Treatment methods included transcatheter arterial embolization ($n$=63, 64.9%), surgery ($n$=13, 13.4%), and liver transplantation ($n$=2, 2.1%); nineteen (19.6%) patients received conservative treatment. Among patients who underwent transcatheter arterial embolization, polyvinyl alcohol, lipiodol combined with gelatin sponge, and spring steel ring showed comparable efficacy. ***Conclusions:*** Hepatocellular carcinoma and cirrhosis are common causes of HAPFs. Transcatheter arterial embolization is a safe and effective method for the treatment of HAPFs, and polyvinyl alcohol, lipiodol combined with gelatin sponge, and spring steel ring showed comparable efficacy in our cohort.

**Citation of this article:** Cao B, Tian K, Zhou H, Li C, Liu D, Tan Y. Hepatic Arterioportal Fistulas: A Retrospective Analysis of 97 Cases. J Clin Transl Hepatol 2022;10(4):620–626. doi: 10.14218/JCTH.2021.00100.

**Keywords:** Hepatic arterioportal fistulas; Embolization; Hepatocellular carcinoma; Cirrhosis.

**Abbreviations:** CT, computed tomography; DSA, digital subtraction angiography; HAPFs, hepatic arterioportal fistulas; HCC, hepatocellular carcinoma; MRI, magnetic resonance imaging; PVA, polyvinyl alcohol.

***Correspondence to:** Yuyong Tan and Deliang Liu, Department of Gastroenterology, The Second Xiangya Hospital; Research Center of Digestive Disease, Central South University, No.139 Renmin Middle Road, Changsha, Hunan 410007, China. ORCID: https://orcid.org/0000-0002-0571-3136 (YT) and https://orcid.org/0000-0003-1541-2596 (DL). Tel: +86-15116280621, Fax: +86-731-85533525, E-mail: tanyuyong@csu.edu.cn (YT) and deliangliu@csu.edu.cn (DL)

## Introduction

Hepatic arterioportal fistulas (HAPFs) refer to abnormal shunts or aberrant functional connections between the portal vein and the hepatic artery.[1] HAPFs are rare entities; however, advances in diagnostic techniques have helped increase the detection rate of HAPFs. HAPFs can be congenital, although most of these lesions are acquired.[2] Common causes include hepatocellular carcinoma (HCC), cirrhosis, and iatrogenic (secondary to liver biopsy, transhepatic biliary drainage, transhepatic cholangiogram, and surgery).[3] Patients with HAPFs may be asymptomatic or can present with symptoms of portal hypertension (such as ascites, gastrointestinal bleeding, diarrhea, and congestive heart failure).[4,5] The symptoms are largely dependent on the size, location, shunt volume, and liver resistance of the fistula.[6,7] Moreover, HAPFs may impair the arterial blood perfusion in the liver, critically affecting the supply of oxygen and various nutrients to the liver, and eventually aggravating liver function.[8] Effective sealing of the fistula can reduce the portal pressure, increase blood perfusion, and hasten recovery.

The treatment modalities of HAPFs include surgery and minimally-invasive percutaneous interventions (usually transcatheter embolization). However, surgery is costly and is usually associated with major trauma and slow recovery. Conversely, transcatheter embolization offers the advantages of low morbidity, repeatability, and lower cost; therefore, it is regarded as the first-line treatment for HAPFs.[4,9–11] Various embolic agents have been used, such as lipiodol, gelatin sponge particles, spring steel coils, and polyvinyl alcohol (PVA) particles. The aim of embolization is to obliterate the fistula, improve clinical condition, and prolong survival time.[12] Embolization can be performed with a single material or a combination of materials; the type of embolic agent employed is primarily dependent on the size of the fistula. Each agent has its advantages and disadvantages, and can be chosen appropriately based on the individual circumstances. For example, lipiodol is useful in patients with poor or no blood shunt,[13–15] however, it can easily occlude small blood vessels and cause liver tissue ischemia. Therefore, it is not suitable in HCC cases with severe HAPFs.[16] PVA needs to be combined with a contrast agent and is effective in long-

term sealing, with fewer side effects. Spring steel coils are long-term embolization materials that are normally used for high-flow HAPFs; however, coils are typically used for simple shunts because in complex shunts, the coil may not reach small feeders that are difficult to access and distally located. Moreover, shunts with multiple feeders are prone to recanalization.[17,18] Gelatin sponge particles are a medium-term embolization material, which are typically resorbed within 2–4 weeks, leading to a high recanalization rate.[19]

Despite an increase in the reported cases of HAPFs, the clinical characteristics of these patients and the efficacy of the different embolization methods are not well characterized in the contemporary literature. In the present study, we sought to retrospectively summarize the characteristics of HAPFs treated in a single center and compare the efficacy of different embolization methods.

## Methods

This was a retrospective, single-center study conducted at a tertiary care hospital in China. The study was approved by the ethics committee of the Second Xiangya Hospital, Central South University. Written informed consent was obtained from all subjects. The study protocols conformed to the ethical principles enshrined in the latest version of the Declaration of Helsinki. Data pertaining to consecutive patients with HAPFs who were admitted to the Second Xiangya Hospital of Central South University between January 2010 and January 2020 were retrieved from the medical records. For all patients, the diagnosis of HAPF was based on imaging examination (digital subtraction angiography (DSA), Doppler ultrasound, computed tomography (CT), or magnetic resonance imaging (MRI)). On DSA, HAPFs manifest as filling of the contrast medium in the portal vein through the fistula in the arterial phase after injection of the contrast medium. CT or MRI signs of HAPFs include early visualization of the portal vein, early enhanced visualization of the portal vein, abnormal vascular mass, and wedge-shaped or triangular hepatic segment (Fig. 1). On Doppler ultrasound, HAPFs are characterized by bidirectional, low-impedance bidirectional blood flow in the portal vein (Fig. 2).

### *Treatment methods*

**Transcatheter arterial embolization:** After clearly displaying the location, size, and type of the fistula, the most appropriate embolization material and embolization method were selected to occlude the fistula. The embolic materials used were lipiodol (Guerbet Group, France, 1238 yuan per bottle), PVA (Cook Group, USA, 1450 yuan per bottle), gelatin sponge granule particle (made by our hospital, 98 yuan per piece), spring steel (Cook Group, USA, 1898 yuan per piece), or a combination of two or more materials of the above four materials. The size and number of embolic materials used depended on the size of fistula.

**Surgical treatment:** Some patients with liver cancer and hepatic artery fistula were treated by surgical resection of the lesion. Some patients with liver cancer were fitted with a chemotherapy pump when necessary.

**Liver transplantation:** Liver transplantation was performed in some patients with congenital HAPFs or liver cancer.

**Fig. 1. Representative computed tomography findings of HAPF showing early enhancement of the portal vein in the arterial phase.** HAPF, hepatic arterioportal fistula.

### *Assessment of treatment outcomes*

Short-term efficacy of transcatheter arterial embolization

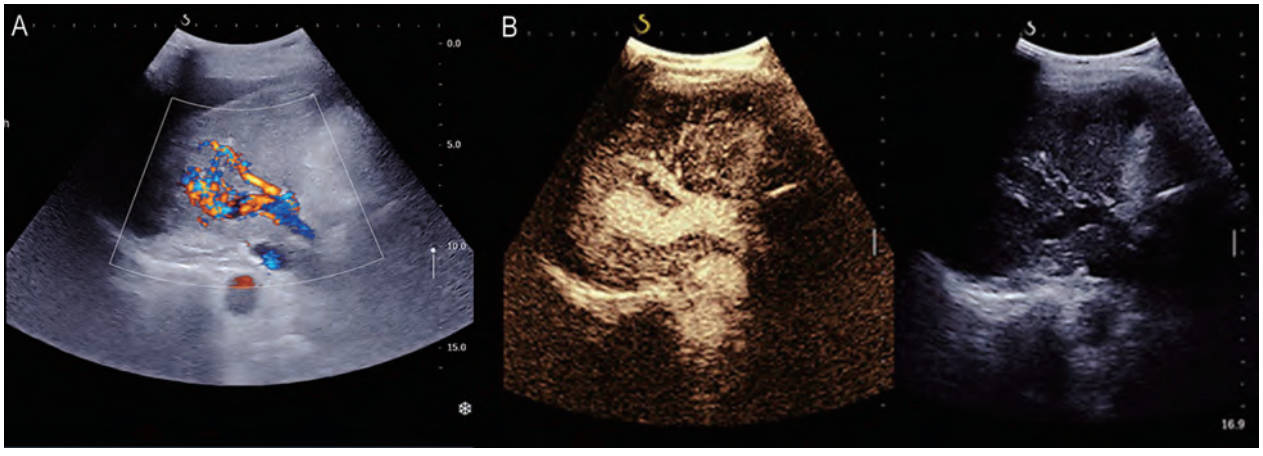


**Fig. 2. Ultrasound image showing HAPFs under Doppler (A) and Sonovue contrast (B).** HAPF, hepatic arterioportal fistula.

**Table 1. Clinical characteristics of the study population**

| Clinical feature | Value |
|---|---|
| Sex, % cases (*n*) | |
| Male | 85.57 (83) |
| Female | 15.43 (14) |
| Mean age in years | 52.06±13.81 |
| Etiology, % cases (*n*) | |
| HCC | 80.41 (78) |
| Cirrhosis* | 10.32 (10) |
| Congenital | 2.06 (2) |
| Portal spongiform transformation | 2.06 (2) |
| Portal hypertension | 2.06 (2) |
| Liver trauma | 1.03 (1) |
| Unclear | 2.06 (2) |
| HCC clinical classification, % cases (*n*) | 100 (78) |
| Massive | 41 (32) |
| Diffuse | 35.9 (28) |
| Nodular | 23.1 (18) |
| Clinical manifestations, % cases (*n*) | |
| Abdominal distension | 42.3 (41) |
| Abdominal pain | 40.2 (39) |
| Yellowish skin | 3.1 (3) |
| Anorexia | 2.1 (2) |
| Fatigue | 2.1 (2) |
| Chest pain | 2.1 (2) |
| Fever | 2.1 (2) |
| Hematemesis and melena | 1.0 (1) |
| Physical examination | 4.0 (4) |

*Nine out of the ten patients with liver cirrhosis had received medical intervention: three cases received liver biopsy, one received liver biopsy and laparoscopic cholecystectomy, two received endoscopic variceal ligation, on received endoscopic variceal ligation and transjugular intrahepatic portosystemic shunt (commonly known as TIPS), and two received cholecystectomy. There was no evidence of HAPFs before these medical interventions; therefore, it is difficult to clarify whether HAPFs were spontaneous or iatrogenic. HAPF, hepatic arterioportal fistula; HCC, hepatocellular carcinoma.

was assessed using the Child-Pugh score 3–7 days after the operation.[20] Long-term efficacy was defined as the closure of the fistula following application of the different embolization methods. Most of the HAPFs were induced by HCC; therefore, abdominal CT was used as the first-line surveillance method 1–2 months after the operation. Doppler ultrasound was also performed for patients who underwent lipiodol and/or coil treatment. Outcomes were graded as follows: (1) effective clinical closure: almost complete closure of the fistula; or (2) noneffective clinical closure: no change in the size of the fistula or aggravation of the fistula.

### *Statistical analysis*

SPSS 21.0 software (IBM Corp., Armonk, NY, USA) was used for statistical analysis. Continuous variables were presented as the mean±standard deviation, and the matched-sample *t* test was used for between-group comparisons. The efficacy of various plugging materials in causing obliteration of the fistula was compared using the chi-squared test. Two-tailed *p* values <0.05 were considered indicative of statistically significance.

## Results

A total of 97 HAPF patients were included in the analysis (mean age: 52.06±13.81years, range: 0–79); male: 83/95, 85.57%). Regarding etiology, in 80.41% (78/97) of the cases, HAPF was induced by HCC. Abdominal distension and pain were the most common clinical manifestations (Table 1), although it was sometimes difficult to determine whether the symptoms were attributable to HAPFs or the underlying diseases such as HCC and liver cirrhosis. Regarding treatment method, 63 cases (64.9%) underwent transcatheter arterial embolization, 13 cases (13.4%) underwent surgical resection, 2 cases (2.1%) received liver transplantation, and the remaining 19 cases (19.6%) received only conservative treatment (Fig. 3). All 13 patients who received surgical treatment had Barcelona Clinic Liver Cancer stage A HCC, and the tumor and the associated arteriovenous fistula were

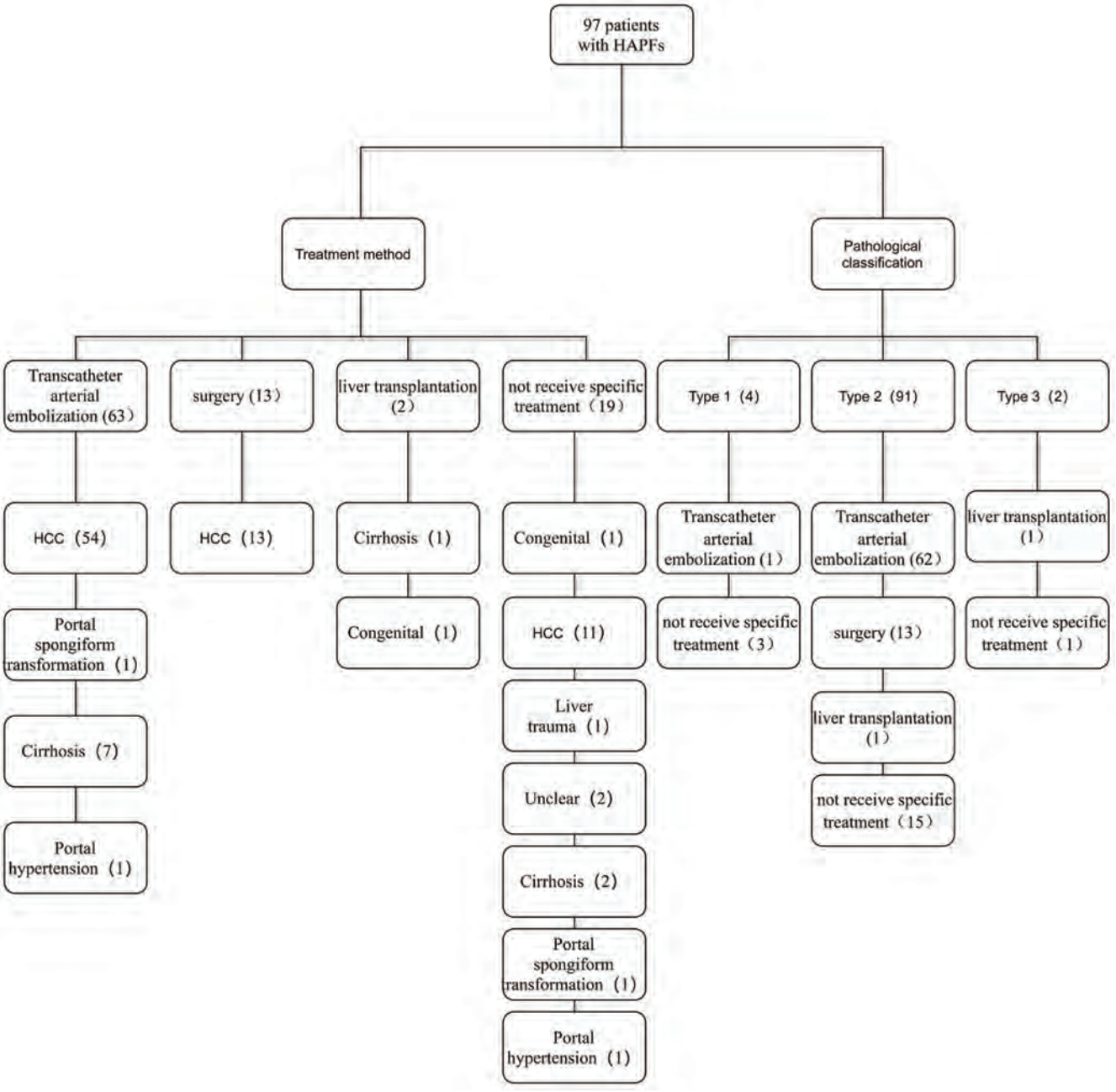


**Fig. 3. Flow chart for management of the 97 cases of HAPF in the present study.** HAPF, hepatic arterioportal fistula.

removed simultaneously. For the two patients who received liver transplantation, one patient had liver failure caused by chronic hepatitis B, and the other had congenital diffuse intrahepatic arteriovenous fistulas with biliary atresia. Among the 63 patients treated with transcatheter arterial embolization, 22 patients (22.7%) were treated with lipiodol embolization, 19 patients (19.5%) were treated with PVA embolization, 14 patients (14.4%) were treated with lipiodol+gelatin sponge granule particle embolization, and 8 patients (8.3%) were treated with spring steel embolization.

Among all the patients treated with transcatheter arterial embolization, discharge occurred at 3–5 days after the procedure and showed significant improvement in post-treatment liver function (assessed by Child-Pugh score) before discharge and at approximately 1 month after treatment ($p$=0.001; Table 2). Comparison of the outcomes revealed comparable efficacy PVA, lipiodol+gelatin sponge particles, and spring steel coils ($p$=0.447; Table 3). Liopiodol alone was not included in the comparison as it is not an embolic agent of choice for HAPF when used alone. Lipiodol is used in combination with other embolic agents or is used if HCC, per se, is cause of HAPF.

## Discussion

HAPF was first reported approximately 50 years ago.[21] It

**Table 2. Changes of liver function in patients after transcatheter arterial embolization.**

| Liver function status | Before therapy | 3–5 days after therapy | *p* value | Before therapy | 1 month after therapy* | *p* value |
|---|---|---|---|---|---|---|
| Child A | 47 | 58 | 0.001 | 42 | 55 | 0.001 |
| Child B | 16 | 5 | | 15 | 2 | |
| Child C | 0 | 0 | | 0 | 0 | |

*Six patients did not undergo liver function test at 1-month follow-up; therefore, only 57 cases are included.

is defined as an abnormal intrahepatic communication between the hepatic artery and the portal venous system. HAPF is an uncommon cause of presinusoidal portal hypertension and is believed to result from increased blood flow in the portal system. Accurate diagnosis of HAPFs is challenging, as the majority of patients are asymptomatic or have nonspecific symptoms. HAPFs are sometimes incidentally detected during imaging evaluations.[1,22–24] Symptomatic HAPFs often present with complications of portal hypertension, including ascites, gastrointestinal bleeding, or heart failure.[4,5] HAPFs are usually categorized into three classes, as follows: Type 1: small peripheral intrahepatic; Type 2: large central HAPF; and Type 3: diffuse congenital intrahepatic.[22] Type 1 is usually caused by percutaneous liver biopsy. Patients are usually asymptomatic, and the HAPF typically develops thrombosis within 1 month. Close follow-up using Doppler ultrasound is recommended for these lesions. Type 2 lesions can cause portal hypertension and hepatoportal sclerosis, progressing to portal fibrosis. These fistulas require intervention to prevent the irreversible hepatic parenchymal changes. Transcatheter arterial embolization is a feasible treatment method. Type 3 is congenital HAPFs, which are usually intrahepatic and diffuse, and they cause severe portal hypertension in infancy. In the present study, 81 of the 97 patients exhibited symptoms related to portal hypertension, such as abdominal distension (41/97), abdominal pain (39/97), and gastrointestinal bleeding (1/97), although the symptoms may have also been caused by primary diseases such as HCC and cirrhosis.

Four of the 97 cases in our study were possibly Type 1, 91 cases were Type 2, and the remaining 2 were Type 3. Generally, less than 10% of HAPFs cases are congenital, usually diffuse or multiple, and most are acquired HAPFs.[4,25] Idiopathic HAPFs have also been described.[9] Common acquired causes include malignant tumors, liver cirrhosis, severe blunt or penetrating trauma, iatrogenic injury, ruptured visceral aneurysm into the portal vein, portal vein thrombosis, and Budd-Chiari syndrome.[26–28] In our cohort, the most common cause of HAPF was HCC, followed by cirrhosis, and only two patients had congenital HAPF. During HCC progression, tumors tend to infiltrate the hepatic portal vein, resulting in direct communication between the hepatic artery and portal vein, forming HAPFs.[9] Congenital HAPFs should be considered in infants who have recurrent and severe upper gastrointestinal bleeding, failure to thrive, hepatic bruit, splenomegaly or ascites. It is a rare but treatable cause of portal hypertension.[29,30] In this study, there were two children with congenital HAPFs. One was a male newborn, and the abnormality was detected *in utero* during antenatal ultrasound examination. He had a congenital arteriovenous shunt, in addition to the absence of the inferior vena cava and changes in the descending aortic arch. No special treatment was administered. The other case was a 5-year-old girl who presented with hematemesis and underwent liver transplantation after diagnosis.

Low-flow fistulas with no obvious clinical symptoms of portal hypertension do not require active intervention,[5] and periodic follow-up is recommended. In symptomatic cases, the fistula should be actively treated. Sealing of the fistula is required for the recovery of liver function. Additionally, sealing of the fistula curbs the blood shunt between the hepatic artery and the portal vein, blocking the blood supply to the tumor and starving the tumor cells of nutrients, thereby protecting normal liver tissue and reducing distant metastasis caused by HAPFs.[6,31] Both transcatheter arterial embolization and surgery are methods that can reduce portal hypertension, increase functional portal vein blood, and improve liver function.[13,31] On liver function assessment of 63 patients treated with transcatheter arterial embolization, the Child-Pugh score of 11 patients shifted from Child B to Child A 3 to 5 days after treatment, and the score of another 11 patients shifted from Child B to Child A 1 month after treatment; this indicated that transcatheter arterial embolization can help improve the liver function.

The aim of treatment of HAPFs is to achieve fistula closure. The optimum catheter position should be as close as possible to the fistula site. Currently, there is no clear consensus with respect to the choice of embolic agent; the choice should be based on the embolization properties of the agent, the angio-architecture of the shunt and its underlying mechanism.[18] Lipiodol, gelatin sponge particles, absolute ethanol, spring steel coils, PVA particles, or a combination of the above materials have been reported for embolization of the HAPFs, with acceptable results in selected patients.[32–36] However, comparison between these materials is rare. In the study by Murata *et al*.,[32] transcatheter arterial chemoembolization of HCC-associated HAPFs with corresponding portal vein occlusion showed better therapeutic efficacy, tumor response and survival outcomes compared with shunt embolization with coils and/or gelatin sponge particles. Huang *et al*.,[37] treated 97 cases of HCC-associated HAPFs with ethanol ($n$=64) or gelfoam ($n$=33); they reported higher complete occlusion rate, lower recanalization rate and better survival in the ethanol group compared to that in the gelfoam group. In the present study, we treated 63 patients with four different materials, and we

**Table 3. Comparison of the outcomes of embolization of HAPFs with different embolization materials**

| Embolization method | Effective clinical closure | Noneffective clinical closure | Total | *p* value |
|---|---|---|---|---|
| Polyvinyl alcohol | 18 | 1 | 19 | 0.447 |
| Lipiodol+gelatin Sponge granules | 12 | 2 | 14 | |
| Spring steel | 8 | 0 | 8 | |
| Total | 51 | 12 | 63 | |

HAPF, hepatic arterioportal fistula.

retrospectively retrieved the medical data and compared their efficacies. We found no significant difference between PVA, lipiodol+gelatin sponge, and spring steel ring. We did not compare lipiodol with the other three materials because liopiodol alone is not an embolic agent of choice for HAPF, and it is used in combination with other embolic agent or used in treatment of HCC, if HCC, per se, is the cause of HAPF.

Some limitations of our study should be acknowledged. First, this was a single-center, retrospective study with a relatively small sample size. A prospective, large-scale study is required to obtain more definitive evidence. Second, this study was conducted at a tertiary hospital, where other embolization methods such as balloon occlusion or other new materials have not been used; therefore, our results may not be generalizable to patients treated in other settings. Third, most of the HAPFs in our cohort were Type 2, and the majority were induced by HCC, which may differ from those reported in Western countries.

In conclusion, most of the HAPFs are acquired, commonly due to HCC and cirrhosis, and usually present with nonspecific symptoms such as abdominal distention and pain. The choice of embolic material should be guided by the location, size, and shunt of the fistula. The therapeutic effect of PVA and spring steel rings is acceptable but prospective, large-scale studies are warranted to obtain more definitive evidence.

## Acknowledgments

We would like to thank the staff from the department of Radiology and department of Hepatobiliary Surgery for their help in diagnosis and treatment of some of the patients.

## Funding

None to declare.

## Conflict of interest

The authors have no conflict of interests related to this publication.

## Author contributions

Study concept and design (YT), acquisition of data (BC, DL), analysis and interpretation of data (BC, KT, HZ, CL), drafting of the manuscript (YT, BC), critical revision of the manuscript for important intellectual content (YT, BC, DL), administrative, technical, or material support, study supervision (YT, DL).

## Data sharing statement

The data used to support the findings of the study are available from the corresponding authors upon reasonable request.

## References

[1] Dessouky BAM, El Abd OL. Intrahepatic vascular shunts: strategy for early diagnosis, evaluation and management. Egypt J Radiol Nucl Med 2011; 42(1):19–34. doi:10.1016/j.ejrnm.2011.02.005.
[2] Lumsden AB, Allen RC, Sreeram S, Atta H, Salam A. Hepatic arterioportal fistula. Am Surg 1993;59(11):722–726. doi:10.1097/00000478-199311000-00018, PMID:8239193.
[3] Kumar A, Ahuja CK, Vyas S, Kalra N, Khandelwal N, Chawla Y, e al. Hepatic arteriovenous fistulae: role of interventional radiology. Dig Dis Sci 2012;57(10): 2703–2712. doi:10.1007/s10620-012-2331-0, PMID:22875308.
[4] Vauthey JN, Tomczak RJ, Helmberger T, Gertsch P, Forsmark C, Caridi J, *et al*. The arterioportal fistula syndrome: clinicopathologic features, diagnosis, and therapy. Gastroenterology 1997;113(4):1390–1401. doi:10.1053/gast.1997.v113.pm9322535, PMID:9322535.
[5] Capron JP, Gineston JL, Remond A, Lallement PY, Delamarre J, Revert R, *et al*. Inferior mesenteric arteriovenous fistula associated with portal hypertension and acute ischemic colitis. Successful occlusion by intraarterial embolization with steel coils. Gastroenterology 1984;86(2):351–355. PMID:6690362.
[6] Strodel WE, Eckhauser FE, Lemmer JH, Whitehouse WM Jr, Williams DM. Presentation and perioperative management of arterioportal fistulas. Arch Surg 1987;122(5):563–571. doi:10.1001/archsurg.1987.01400170069010, PMID:3555408.
[7] Eastridge BJ, Minei JP. Intrahepatic arterioportal fistula after hepatic gunshot wound: a case report and review of the literature. J Trauma 1997;43(3):523–526. doi:10.1097/00005373-199709000-00024, PMID:9314320.
[8] Hiraki T, Kanazawa S, Mimura H, Yasui K, Tanaka A, Dendo S, *et al*. Altered hepatic hemodynamics caused by temporary occlusion of the right hepatic vein: evaluation with Doppler US in 14 patients. Radiology 2001;220(2):357–364. doi:10.1148/radiology.220.2.r01au15357, PMID:11477237.
[9] Kumar N, de Goyet Jde V, Sharif K, McKiernan P, John P. Congenital, solitary, large, intrahepatic arterioportal fistula in a child: management and review of the literature. Pediatr Radiol 2003;33(1):20–23. doi:10.1007/s00247-002-0764-x, PMID:12497231.
[10] Routh WD, Keller FS, Cain WS, Royal SA. Transcatheter embolization of a high-flow congenital intrahepatic arterial-portal venous malformation in an infant. J Pediatr Surg 1992;27(4):511–514. doi:10.1016/0022-3468(92)90350-g, PMID:1522468.
[11] Katzen LB, Katzen BT, Katzen MJ. Treatment of carotid-cavernous fistulas with detachable balloon catheter occlusion. Adv Ophthalmic Plast Reconstr Surg 1987;7:157–165. PMID:3502734.
[12] Hirakawa M, Nishie A, Asayama Y, Ishigami K, Ushijima Y, Fujita N, *et al*. Clinical outcomes of symptomatic arterioportal fistulas after transcatheter arterial embolization. World J Radiol 2013;5(2):33–40. doi:10.4329/wjr.v5.i2.33, PMID:23494252.
[13] Wu H, Zhao W, Zhang J, Han J, Liu S. Clinical characteristics of hepatic Arterioportal shunts associated with hepatocellular carcinoma. BMC Gastroenterol 2018;18(1):174. doi:10.1186/s12876-018-0899-3, PMID:30419830.
[14] Li X, Feng GS, Zheng CS, Zhuo CK, Liu X. Influence of transarterial chemoembolization on angiogenesis and expression of vascular endothelial growth factor and basic fibroblast growth factor in rat with Walker-256 transplanted hepatoma: an experimental study. World J Gastroenterol 2003;9(11):2445–2449. doi:10.3748/wjg.v9.i11.2445, PMID:14606073.
[15] von Marschall Z, Cramer T, Höcker M, Finkenzeller G, Wiedenmann B, Rosewicz S. Dual mechanism of vascular endothelial growth factor upregulation by hypoxia in human hepatocellular carcinoma. Gut 2001;48(1):87–96. doi:10.1136/gut.48.1.87, PMID:11115828.
[16] Sergio A, Cristofori C, Cardin R, Pivetta G, Ragazzi R, Baldan A, *et al*. Transcatheter arterial chemoembolization (TACE) in hepatocellular carcinoma (HCC): the role of angiogenesis and invasiveness. Am J Gastroenterol 2008;103(4): 914–921. doi:10.1111/j.1572-0241.2007.01712.x, PMID:18177453.
[17] Furuse J, Iwasaki M, Yoshino M, Konishi M, Kawano N, Kinoshita T, *et al*. Hepatocellular carcinoma with portal vein tumor thrombus: embolization of arterioportal shunts. Radiology 1997;204(3):787–790. doi:10.1148/radiology.204.3.9280260, PMID:9280260.
[18] Chan WS, Poon WL, Cho DH, Chiu SS, Luk SH. Transcatheter embolisation of intrahepatic arteriovenous shunts in patients with hepatocellular carcinoma. Hong Kong Med J 2010;16(1):48–55. PMID:20124574.
[19] Zhou WZ, Shi HB, Liu S, Yang ZQ, Zhou CG, Xia JG, *et al*. Arterioportal shunts in patients with hepatocellular carcinoma treated using ethanol-soaked gelatin sponge: therapeutic effects and prognostic factors. J Vasc Interv Radiol 2015;26(2):223–230. doi:10.1016/j.jvir.2014.11.002, PMID:25645411.
[20] Wong CS, Lee WC, Jenq CC, Tian YC, Chang MY, Lin CY, *et al*. Scoring short-term mortality after liver transplantation. Liver Transpl 2010;16(2):138–146. doi:10.1002/lt.21969, PMID:20104481.
[21] Gryboski JD, Clemett A. Congenital hepatic artery aneurysm with superior mesenteric artery insufficiency: a steal syndrome. Pediatrics 1967;39(3): 344–347. PMID:6018965.
[22] Guzman EA, McCahill LE, Rogers FB. Arterioportal fistulas: introduction of a novel classification with therapeutic implications. J Gastrointest Surg 2006;10(4):543–550. doi:10.1016/j.gassur.2005.06.022, PMID:16627220.
[23] Remer EM, Motta-Ramirez GA, Henderson JM. Imaging findings in incidental intrahepatic portal venous shunts. AJR Am J Roentgenol 2007;188(2):W162–167. doi:10.2214/AJR.05.1115, PMID:17242223.
[24] Lee BB, Do YS, Yakes W, Kim DI, Mattassi R, Hyon WS. Management of arteriovenous malformations: a multidisciplinary approach. J Vasc Surg 2004;39(3):590–600. doi:10.1016/j.jvs.2003.10.048, PMID:14981454.
[25] Ibn Majdoub Hassani K, Mohsine R, Belkouchi A, Bensaid Y. Post-traumatic arteriovenous fistula of the hepatic pedicle. J Visc Surg 2010;147(5):e333–336. doi:10.1016/j.jviscsurg.2010.09.001, PMID:20932817.
[26] Heaton ND, Davenport M, Karani J, Mowat AP, Howard ER. Congenital hepatoportal arteriovenous fistula. Surgery 1995;117(2):170–174. doi:10.1016/s0039-6060(05)80081-9, PMID:7846621.
[27] Chavan A, Harms J, Pichlmayr R, Galanski M. Transcatheter coil occlusion of an intrahepatic arterioportal fistula in a transplanted liver. Bildgebung 1993;60(4):215–218. PMID:8118188.

[28] Akpek S, Ilgit ET, Cekirge S, Yücel C. High-flow arterioportal fistula: treatment with detachable balloon occlusion. Abdom Imaging 2001;26(3):277–280. doi:10.1007/s002610000174, PMID:11429952.
[29] Norton SP, Jacobson K, Moroz SP, Culham G, Ng V, Turner J, *et al*. The congenital intrahepatic arterioportal fistula syndrome: elucidation and proposed classification. J Pediatr Gastroenterol Nutr 2006;43(2):248–255. doi:10.1097/01.mpg.0000221890.13630.ad, PMID:16877994.
[30] Karnak I, Cil BE, Akay H, Haliloglu M, Ciftci AO, Senocak ME, *et al*. Congenital intrahepatic arterioportal fistula: an unusual cause of portal hypertension treated by coil embolization in an infant. Eur J Pediatr Surg 2009;19(4):251–253. doi:10.1055/s-2008-1038825, PMID:19065507.
[31] Yu JS, Kim KW, Jeong MG, Lee JT, Yoo HS. Nontumorous hepatic arterial-portal venous shunts: MR imaging findings. Radiology 2000;217(3):750–756. doi:10.1148/radiology.217.3.r00dc13750, PMID:11110939.
[32] Murata S, Tajima H, Nakazawa K, Onozawa S, Kumita S, Nomura K. Initial experience of transcatheter arterial chemoembolization during portal vein occlusion for unresectable hepatocellular carcinoma with marked arterioportal shunts. Eur Radiol 2009;19(8):2016–2023. doi:10.1007/s00330-009-1349-y, PMID:19238387.
[33] Miyayama S, Matsui O. Superselective Conventional Transarterial Chemoembolization for Hepatocellular Carcinoma: Rationale, Technique, and Outcome. J Vasc Interv Radiol 2016;27(9):1269–1278. doi:10.1016/j.jvir.2016.04.014, PMID:27345337.
[34] Uchida H, Ohishi H, Matsuo N, Nishimine K, Ohue S, Nishimura Y, *et al*. Transcatheter hepatic segmental arterial embolization using lipiodol mixed with an anticancer drug and Gelfoam particles for hepatocellular carcinoma. Cardiovasc Intervent Radiol 1990;13(3):140–145. doi:10.1007/BF02575465, PMID:2171772.
[35] Miyayama S, Matsui O, Yamashiro M, Ryu Y, Kaito K, Ozaki K, *et al*. Ultraselective transcatheter arterial chemoembolization with a 2-f tip microcatheter for small hepatocellular carcinomas: relationship between local tumor recurrence and visualization of the portal vein with iodized oil. J Vasc Interv Radiol 2007;18(3):365–376. doi:10.1016/j.jvir.2006.12.004, PMID:17377182.
[36] Shi HB, Yang ZQ, Liu S, Zhou WZ, Zhou CG, Zhao LB, *et al*. Transarterial embolization with cyanoacrylate for severe arterioportal shunt complicated by hepatocellular carcinoma. Cardiovasc Intervent Radiol 2013;36(2):412–421. doi:10.1007/s00270-012-0410-4, PMID:22580682.
[37] Huang MS, Lin Q, Jiang ZB, Zhu KS, Guan SH, Li ZR, *et al*. Comparison of long-term effects between intra-arterially delivered ethanol and Gelfoam for the treatment of severe arterioportal shunt in patients with hepatocellular carcinoma. World J Gastroenterol 2004;10(6):825–829. doi:10.3748/wjg.v10.i6.825, PMID:15040025.

*Journal of Clinical and Translational Hepatology* **2022** vol. 10(4) | 627–641
DOI: 10.14218/JCTH.2021.00216

Original Article

# Spindle and Kinetochore-associated Family Genes are Prognostic and Predictive Biomarkers in Hepatocellular Carcinoma

Chenhui Cai, Ying Zhang, Xu Hu, Sizhen Yang, Jiawen Ye, Zihan Wei and Tongwei Chu*

*Department of Orthopedics, Xinqiao Hospital, Third Military Medical University (Army Medical University), Chongqing, China*

**Received:** 9 June 2021 | **Revised:** 7 September 2021 | **Accepted:** 8 October 2021 | **Published:** 4 January 2022

## Abstract

***Background and Aims:*** Hepatocellular carcinoma (HCC) is one of the most frequent malignant tumors. Spindle and kinetochore-associated (SKA) family genes are essential for the maintenance of the metaphase plate and spindle checkpoint silencing during mitosis. Recent studies have indicated that dysregulation of SKA family genes induces tumorigenesis, tumor progression, and chemoresistance via modulation of cell cycle and DNA replication. However, the differential transcription of SKAs in the context of HCC and its prognostic significance has not been demonstrated. ***Methods:*** Bioinformatics analyses were performed using TCGA, ONCOMINE, HCCDB, Kaplan-Meier plotter, STRING, GEPIA databases. qRT-PCR, western blot, and functional assays were utilized for *in vitro* experiments. ***Results:*** We found remarkable upregulation of transcripts of SKA family genes in HCC samples compared with normal liver samples on bioinformatics analyses and *in vitro* validation. Interaction analysis and enrichment analysis showed that SKA family members were mainly related to microtubule motor activity, mitosis, and cell cycle. Immuno-infiltration analysis showed a correlation of all SKA family genes with various immune cell subsets, especially T helper 2 (Th2) cells. Transcriptional levels of SKA family members were positively associated with histologic grade, T stage, and α-fetoprotein in HCC patients. Receiver operating characteristic curve analysis demonstrated a strong predictive ability of SKA1/2/3 for HCC. Increased expression of these SKAs was associated with unfavorable overall survival, progression-free survival, and disease-specific survival. On Cox proportional hazards regression analyses, SKA1 upregulation and pathological staging were independent predictors of overall survival and disease-specific survival of HCC patients. Finally, clinical tissue microarray validation and *in vitro* functional assays revealed SKA1 acts an important regulatory role in tumor malignant behavior. ***Conclusions:*** SKA family members may potentially serve as diagnostic and prognostic markers in the context of HCC. The correlation between SKAs and immune cell infiltration provides a promising research direction for SKA-targeted immunotherapeutics for HCC.

**Citation of this article:** Cai C, Zhang Y, Hu X, Yang S, Ye J, Wei Z, *et al*. Spindle and Kinetochore-associated Family Genes are Prognostic and Predictive Biomarkers in Hepatocellular Carcinoma. J Clin Transl Hepatol 2022;10(4):627–641. doi: 10.14218/JCTH.2021.00216.

## Introduction

Hepatocellular carcinoma (HCC) accounts for 75–85% of primary liver cancers and is associated with high morbidity and mortality.[1] Due to the high propensity for recurrence and metastasis, the overall survival of patients with advanced HCC is extremely poor. Every year, more than 500,000 deaths are attributable to HCC worldwide.[2,3] Efforts have been made to understand the mechanism of the development, progression, and metastasis of HCC. Use of serum markers and advanced medical imaging techniques can facilitate early diagnosis of HCC.[4–6] Besides, molecular targeted therapy, chemotherapy, immunotherapy, and surgical resection are effective treatment methods for HCC.[7,8] However, the molecular characteristics of HCC are not well characterized. The lack of specific markers for tumor type or disease stage poses a significant challenge in the understanding and treatment of HCC.

Mitosis, the basic form of cell division, is a common biological process in eukaryotes. During mitosis, the spindle ensures the division of chromosomes into two equal groups of sister chromatids.[9] The spindle and kinetochore-associated (SKA) complex is composed of SKA1/2/3 proteins and maintains the attachment of intermediate spindle microtubules to the centromere, thus ensuring the completion of mitosis.[10,11] Dysfunction of the SKA complex leads to chromosomal congression failure and subsequent cell death.[12] Recent studies have shown that abnormal cell cycle and uncontrolled cell proliferation can be attributed to the overexpression of SKAs;

**Keywords:** Spindle and kinetochore-associated genes; Liver hepatocellular carcinoma; Prognostic value; Immune infiltration; Bioinformatics analysis.

**Abbreviations:** AFP, α-fetoprotein; AUC, area under the curve; CCK-8, Cell Counting Kit-8; DC, dendritic cell; DSS, disease-specific survival; ESCC, esophageal squamous cell carcinoma; FBS, fetal bovine serum; GEO, Gene Expression Omnibus; GEPIA, gene expression profiling interactive analysis; GO, gene ontology; HCC, hepatocellular carcinoma; HCCDB, Integrative Molecular Database of Hepatocellular Carcinoma; ICGC, International Cancer Genome Consortium; IHC, immunohistochemical; KEGG, Kyoto Encyclopedia of Genes and Genomes; LIHC, liver hepatocellular carcinoma; OS, overall survival; PFS, progression-free survival; PPI, protein-protein interaction; ROC, receiver operating characteristic; SKA, spindle and kinetochore-associated; ssGSEA, single sample gene set enrichment analysis; TCGA, The Cancer Genome Atlas; Th2, T helper 2; TILs, tumor-infiltrating lymphocytes; TPM, transcripts per million.

***Correspondence to:** Tongwei Chu, Department of Orthopedics, Xinqiao Hospital, Third Military Medical University (Army Medical University), No.83 Xinqiao Main Street, Shapingba District, Chongqing 400037, China. ORCID: https://orcid.org/0000-0003-0309-7082. Tel: +86-13708388336, E-mail: chtw@sina.com

moreover, studies have also suggested a potential role of SKAs in the genesis, progression, and chemotherapeutic resistance of various types of tumors.[13–18] In an *in vitro* study, G2/M blockade of pancreatic cancer was inhibited by upregulating the *SKA1* gene, which enhanced pancreatic cancer aggressiveness and malignancy.[15] SKA2 expression was found to be significantly upregulated in esophageal squamous cell carcinoma (ESCC) samples and inhibition of SKA2 mRNA level suppressed ESCC cell proliferation and migration.[19] SKA3 overexpression accelerated the cell cycle by activating the PI3K-Akt signaling, thereby promoting cervical cancer cell migration and proliferation.[14] However, the expression profile, molecular biological function, and prognostic significance of SKA in HCC have not been fully elucidated.

In our research, we carried out comprehensive bioinformatics analysis of the expression patterns of SKA family genes in HCC, investigated their association with immune infiltration, assessed their diagnostic and prognostic relevance in HCC. We observed markedly high expression of SKA family genes in HCC, which simultaneously showed good diagnostic significance for HCC. Interaction analysis (i.e. protein interaction and gene interaction) and enrichment analysis showed that SKA family members were mainly related to microtubule motor activity, mitosis, and cell cycle. Comprehensive immune infiltration analysis showed that all SKA family members were correlated with immune cell subsets, especially Th2 cells. We further demonstrated an inverse association between increased expression of SKA family members and the prognosis of HCC patients and identified SKA1 as an independent predictor of HCC patients. Further functional assays indicated that knockdown of SKA1 decreased the proliferation and invasion of HCC cells. Our research aimed to elucidate the specific functions and mechanisms of SKA family genes in the development of HCC from a new perspective; our findings may facilitate a better understanding of the pathogenetic mechanism of HCC and offer insights for the development of SKA-targeted tumor immunotherapy.

## Methods

### Data resource

We downloaded level three data of liver hepatocellular carcinoma (LIHC) patients from The Cancer Genome Atlas (TCGA) database (cancergenome.nih.gov/), which contains data of 374 samples of HCC and 50 samples of para-carcinoma tissue. The workflow type we chose was HTSeq-FPKM. Corresponding clinical information was also obtained from the TCGA data portal. For the sake of subsequent analysis, we converted the HTSeq-FPKM data into transcripts per million (TPM) reads.

### Gene expression profiling interactive analysis (GEPIA)

GEPIA is an online tool for analyses and visualization of RNA sequencing data of 9,700 tumors and 8,500 normal tissues.[20] In this study, transcriptional levels of SKA family genes in 20 distinct cancer samples and nonneoplastic control samples were acquired from GEPIA. Besides, we used a similar gene detection function in the “expression analysis module” to identify the most similar genes of SKA family genes.

### Integrative Molecular Database of Hepatocellular Carcinoma (HCCDB)

HCCDB is a specialized database that integrates multiple databases including Gene Expression Omnibus (GEO), International Cancer Genome Consortium (ICGC), etc. It contains expression spectrum analysis of more than 3,000 HCC samples (lifeome.net/database/hccdb/).[21] We applied this comprehensive database to identify the expression of SKA family genes in liver cancer.

### ONCOMINE

ONCOMINE database (oncomine.org) is an online data-mining tool that provides an integrated analysis of genome-wide expression in a wide variety of tumor samples and normal control samples.[22] We compared the transcription levels of SKA family members in different HCC samples and normal adjacent tissues. Statistical significance was considered at $p$-values <0.05. The fold change in our study was set to 2, and thresholds for statistical significance were set at 10%.

### STRING

STRING (string-db.org/) is a search tool that predicts a network of genes and proteins that may have an interacting association.[23] A protein-protein interaction (PPI) network analysis of SKAs and their most similar genes were conducted using the STRING and further processed using the visualization tool Cytoscape.

### GeneMANIA

GeneMANIA (genemania.org) is a visual database tool with highly accurate prediction algorithms providing information on physical interactions, coexpression, genetic interactions, and co-localization of query genes.[24] We used GeneMANIA to measure the predictive value of SKA family members.

### Functional enrichment analysis

To identify the gene ontology (GO) annotations and Kyoto Encyclopedia of Genes and Genomes (KEGG) pathways where SKAs and similar genes were enriched, functional enrichment analysis was carried out using the R package cluster profiler.[25] Enrichment analysis predicts the functional roles of SKA family genes and their similar genes based on three aspects, i.e., biological process, cellular component, and molecular function, while KEGG analysis defines the related pathways of SKA family genes and their similar genes.

### Immune infiltration analysis

The infiltration of 24 tumor-infiltrating immune cells in HCC samples was quantified by single sample gene set enrichment analysis (ssGSEA) methods using the GSVA R package. We scored the enrichment of every immunocyte based on gene signatures unique to 24 tumor-infiltrating lymphocytes (TILs), including B cells, T cells, macrophages, neutrophils, etc. Spearman correlation analysis was used to evaluate the correlation between SKAs and the tumor immune infiltration.

### Kaplan-Meier plotter

Kaplan-Meier plotter is an online tool for survival analysis of cancer patients, and it was used to assess the prognostic significance of the expression of SKA family gene mRNA in

HCC patients.[26,27] Survival outcomes included overall survival (OS), progression-free survival (PFS), and disease-specific survival (DSS). The optimal cutoff value was set through the KM plotter algorithm. *P*-values < 0.05 were considered significant.

### *Cell culture and transfection*

Normal human liver cell line (L-02 cells) and HCC cell lines (SMMC-7721, LM3, and Hep3) were used in our experimental study. They were purchased from the China Cell Bank (ATCC, Shanghai, China). All cell lines were grown in Dulbecco's Modified Eagle Medium (Gibco, Carlsbad, CA, USA) with 10% fetal bovine serum (FBS; Ausbian, Sydney, Australia) and 1% penicillin-streptomycin (Gibco, Carlsbad, CA, USA). Cells were maintained in an incubator at a constant temperature of 37°C with 5% $CO_2$. siRNA against SKA1 (5′-GCAUGUCAAGGAGCACCACAATTUUGUGGUGCUCCUUGACAUGCTT-3′) and short interfering noncoding oligonucleotides (5′-UUCUCCGAACGUGUCACGUTTACGUGACACGUUCGGAGAATT-3′)

were synthesized by Sangon Biotech (Sangon, Shanghai, China) and transfected into cells using Lipofectamine 2000 (Invitrogen, Carlsbad, CA, USA) following the product instructions. After 3 days of transfection, the cells were collected to determine the knockdown effects.

### *RNA extraction and quantitative real-time PCR*

Total RNA was isolated from cultured cells by Trizol reagent (Takara, Dalian, China). SYBR Premix Ex Taq II in a PCR detection system (Bio-Rad, Hercules, CA, USA) was used to assay the expression of target genes. cDNA was synthesized using PrimeScript RT reagent kits (Takara Dalian, China). The transcriptional levels were normalized to those of the internal control gene *GAPDH*. The sequences of all target genes are shown in Supplementary Table 5.

### *Western blotting*

The protein concentration of cells lysates were measured with a Bradford protein assay. Total proteins were isolated by 8% sodium dodecyl sulfate-polyacrylamide gel electrophoresis and transferred to polyvinylidene fluoride membranes. After being blocked with 5% bovine serum albumin at room temperature for 3 h, the membranes were incubated overnight at 4°C with anti-GAPDH (1:1,000; Proteintech, Chicago, IL, USA) and anti-SKA1 (1:1,000; Affinity, Cincinnati, OH, USA) primary antibodies. The membrane was then washed with phosphate buffered saline Tween and incubated with secondary antibodies (1:4,000) for 2 h The protein bands were visualized with an enhanced chemiluminescence detection kit (Biosharp, Hefei, China).

### *Cell proliferation and invasion assays*

Cell Counting Kit-8 (CCK-8) and colony formation assays were performed to assess cell proliferation. Cells maintained in 96-well plates were incubated with 10 μL CCK-8 solution (Dojindo, Kumamoto, Japan) at 37°C for 2.5 h. Cell viability was then determined by at 450 nm absorbance. To assay colony formation, about 2,500 HCC cells were seeded in six-well plates and cultured for 11 days. The colonies were then fixed in 4% paraformaldehyde and stained with crystal violet. Transwell assays were carried out to assess cell invasion. Cell migration was assayed in about $6\times10^3$ transfected HCC cells that were inoculated in serum-free medium on the Matrigel-coated upper surface of an 8 μm Transwell chamber (Corning, NY, USA). The culture medium in the lower chamber was supplemented with 350 μL of medium containing 10% FBS. The cells that had migrated through the membrane were stained with 0.5% crystal violet and counted by light microscopy.

### *HCC tissue microarray and immunohistochemical (IHC) staining*

Human HCC tissue microarrays (Cat No. IWLT-N-64LV41) containing 10 pairs of HCC and adjacent normal tissues were obtained from Wuhan Saiweier Biotechnology Co; Wuhan, China), and CDT1 expression was assayed by IHC staining using an anti-SKA1 antibody (1:250; Affinity, Cincinnati, OH, USA). And following the kit manufacturer's instructions. The H-score method was used to assess the expression of SKA1 protein. Positivity and H-scores (0–300) were reported as (1× % of cells with weak staining intensity) + (2× % of cells with moderate staining intensity) + (3× % of cells with strong staining intensity).

### *Statistical analysis*

The statistical analysis was performed with R version 3.6.3 (www.r-project.org). One-way analysis of variance was used to compare differences among the three groups, and between-group differences were compared using *t*-tests. Correlations of SKA expression and the clinical parameters of HCC patients were evaluated by the Wilcoxon signed-rank test. Univariate and multivariate Cox analysis was used to evaluate the prognostic significance of SKAs levels in terms of OS and DSS. Correlations of SKA family genes were assessed with Spearman's correlation coefficient. The performance of differentially expressed SKA family genes in distinguishing between HCC samples and normal liver samples was assessed by receiver operating characteristic (ROC) curve analysis using the pROC package (version 1.16.2).[28] An area under the ROC curve (AUC) >0.7 and from 0.5–0.7 indicated good and poor accuracy, respectively. The H-scores of HCC and adjacent healthy tissues were compared using paired *t*-tests. Statistical significance was defined as $p < 0.05$.

## Results

### *Transcription of SKAs in HCC patients*

There is accumulating evidence that SKAs are novel tumor biomarkers.[29,30] However, transcriptional analysis and prognostic significance of SKA genes in human HCC have not been well elucidated. Therefore, GEPIA was used to compare the transcription levels of SKA family genes between normal and tumor samples of 33 different cancers. The mRNA levels of SKA family genes were significantly increased compared with normal tissues in the analysis of HCC tissues ($p<0.001$, Supplementary Fig. 1).

We further compared the transcriptional levels of SKAs between HCC samples and normal control samples in the HCCDB database. The results of the ICGC GEO dataset (GSE22058, GSE22097, GSE54236, GSE64041, GSE25097, and ICGC-LIRI-JP) analysis all suggested abnormally high expression of SKA1/2/3 in HCC (Fig. 1). We also compared the differences of transcription levels of SKAs between HCC cancer samples and normal samples in the TCGA database.

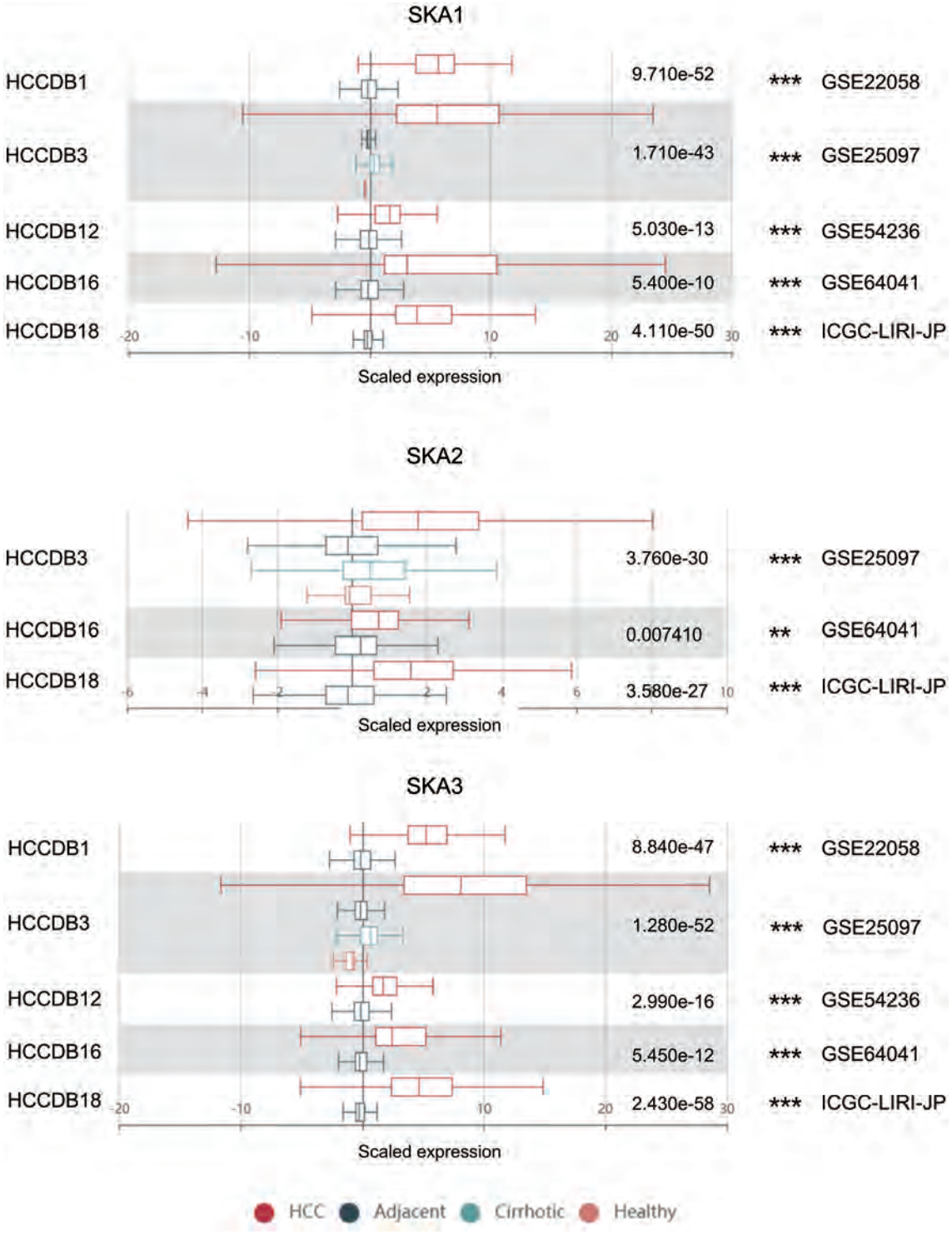


**Fig. 1. mRNA level of SKA family genes in different GEO and ICGC datasets (HCCDB).** *$p$<0.05, **$p$<0.01, ***$p$<0.001. GEO, Gene Expression Omnibus; HCCDB, Integrative Molecular Database of Hepatocellular Carcinoma; ICGC, International Cancer Genome Consortium; SKA, spindle and kinetochore-associated.

The mRNA levels of SKAs were markedly increased in HCC samples relative to normal liver samples, which was consistent with our previous result (Fig. 2A). The observation was also verified in paired HCC and normal tissues (Fig. 2B). We also compared the transcriptional levels of SKA family members between tumor tissues and normal control tissues in ONCOMINE databases. Specifically, the results from Chen datasets showed upregulation of SKA1 in HCC samples compared with that in normal samples, with fold changes of 1.212–2.534.[31–33] In Wurmbach datasets, HCC

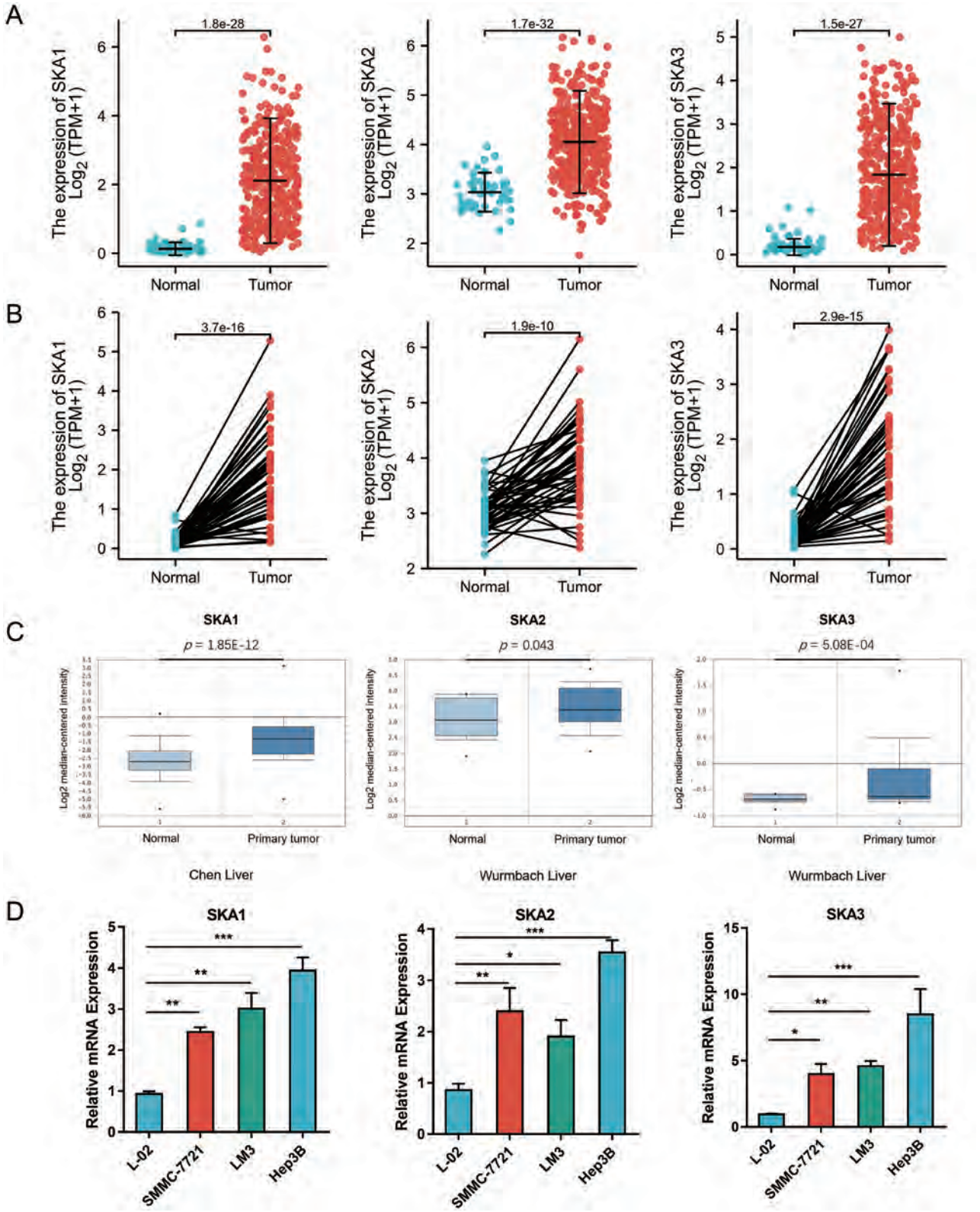


**Fig. 2. Transcriptional levels of SKAs in hepatocellular carcinoma samples and normal tissue samples.** (A) SKAs mRNA expression in normal and tumor tissues (TCGA). (B) SKA expression in paired tissues (TCGA). (C) SKA mRNA levels in normal and tumor tissues (ONCOMINE) (D) qRT-PCR results of SKA expression in normal human liver cell line and HCC cell lines. *$p$<0.05, **$p$<0.01, ***$p$<0.001. HCC, hepatocellular carcinoma; SKA, spindle and kinetochore-associated; TCGA, The Cancer Genome Atlas.

tissues showed a 1.266–1.331-fold increase in the mRNA expressions of SKA2 and SKA3 (Fig. 2C).[33] Finally, differences in the expression of SKAs were validated by qRT-PCR in normal human liver cell line and HCC cell lines (Fig. 2D).

### *Correlation and molecular interactions of SKAs in HCC*

Correlation between the expression levels of SKA family members in HCC was assessed using Spearman correlation analysis. Scatter plot results indicated a strong correlation between the transcriptional levels of SKA1/3 ($r$=0.890). Besides, there was a moderate correlation between SKA1 and SKA2 ($r$=0.590) and between SKA2 and SKA3 ($r$=0.640, Fig. 3A–C).

Through GEPIA, we identified genes whose expression patterns were similar to those of differentially expressed SKAs in HCC patients. The results of similar gene detection are presented in Supplementary Table 1. To elucidate the potential interactions among SKAs and their most similar genes, we further built a PPI network by STRING dataset analysis and Cytoscape visualization (Fig. 3D). The SKA family genes and their similar genes were associated with microtubule binding, microtubule motor activity, cytoskeletal protein binding, and the cell cycle. The gene-gene interaction network through GeneMANIA also revealed that SKAs and their associated genes (e.g., NUDT5, SPC24, DSN1, NDC80, CENPE, and BUB1) were primarily related to chromosome segregation, mitosis, nuclear division, and microtubule polymerization or depolymerization (Fig. 3E).

### *GO and KEGG enrichment analyses of SKA family members and their most similar genes*

To further investigate the potential mechanisms of SKAs in HCC, GO, and KEGG enrichment analyses were carried out to probe the functions and pathways of SKA family proteins and their most similar genes using the "ClusterProfiler" package in R software. The biological processes for these genes were predominantly enriched in mitotic nuclear division, nuclear division, organelle fission, and microtubule cytoskeleton organization. The molecular functions were mainly microtubule motor activity, motor activity, microtubule binding, and ATP-dependent microtubule motor activity. In terms of the cellular component category, the overexpressed SKA family members and their similar molecules were mainly associated with spindle, chromosome (centromeric region), mitotic spindle, and chromosomal region (Fig. 3F–H). The results of KEGG enrichment revealed several major KEGG pathways of SKAs and their similar genes, and included the p53 signaling pathway, cell cycle, and cell senescence (Fig. 3I). All the enriched pathways were tightly associated with the occurrence and progression of malignant tumors (Supplementary Table 2).[34,35]

### *Correlation between SKAs levels and immune infiltrates*

The complexity of immune cells in the tumor microenvironment influences the biological behavior of the tumor, prognosis, and outcomes of immunotherapy.[36,37] Therefore, we investigated the correlation between various immune cells infiltrating in the HCC microenvironment and SKA family members. All members of the SKA family showed a positive correlation with T helper 2 (Th2) cells [SKA1 ($r$=0.752, $p$<0.001), SKA2 ($r$=0.438, $p$<0.001), SKA3 ($r$=0.718, $p$<0.001)], T follicular helper cells (Tfhs) [SKA1 ($r$=0.235, $p$<0.001), SKA2 ($r$=0.126, $p$=0.015), SKA3 ($r$=0.218, $p$<0.001)], and T helper (Th) cells [SKA1 ($r$=0.203, $p$<0.001), SKA2 ($r$=0.178, $p$<0.001), SKA3 ($r$=0.261, $p$<0.001)], as well as a negative correlation with neutrophils [SKA1 ($r$=−0.308, $p$<0.001), SKA2 ($r$=0.224, $p$=0.015), SKA3 ($r$=0.343, $p$<0.001)] and dendritic cells (DCs) [SKA1 ($r$=−0.272, $p$<0.001), SKA2 ($r$=−0.326, $p$<0.001), SKA3 ($r$=−0.328, $p$<0.001)]. The correlation with Th2 was the most significant (Fig. 4A–C). We further compared the enrichment score of Th2 cells of HCC samples in SKA1-high and SKA1-low groups. Consistently, the results demonstrated that high SKA1 expression samples had a higher enrichment score of Th2 cells than those in low SKA1 expression samples (Fig. 4D–F). All the above analyses indicated the significant correlation between SKA family members and immune cell subsets, especially Th2 cells.

### *Relationship of mRNA levels of SKAs and clinicopathological features of HCC patients*

We further assessed the correlation between transcriptional levels of SKA genes and clinicopathologic features [such as histologic grade, T stage, and α-fetoprotein (AFP)] of HCC patients. The tissues obtained from HCC patients tended to express higher levels of SKAs mRNA as cancer stages advanced [SKA1, (G4 vs. G1, $p$<0.001), SKA2, (G3 vs. G2, $p$<0.001), SKA3, (G4 vs. G1, $p$<0.001)]. The highest mRNA levels of SKA family genes were predominantly found in grade 3 and grade 4 HCC (Fig. 5A–C). T stage has an important prognostic significance. Patients with high-T stage tumors tended to express higher mRNA levels of SKA1/2/3 according to the pathological T stage criterion ($p$<0.05) (Fig. 5D–F). AFP is a specific diagnostic biomarker for liver cancer. Therefore, we assessed the correlation between SKAs expression and AFP level. As expected, there were significant differences between the high-AFP group and the low-AFP group based on these SKAs expression ($p$<0.001, Fig. 5G–I). We further analyzed the association of SKAs expression with other clinical characteristics (e.g., age, sex, TNM stage, AFP, Child-Pugh grade, fibrosis Ishak score, vascular invasion, albumin, and prothrombin time) in HCC patients (Supplementary Table 3). High *SKA1* expression was significantly linked to T stage, AFP, and prothrombin time; high *SKA2* expression was significantly linked to age, T stage, AFP, and prothrombin time; high *SKA3* expression was significantly linked to T stage and AFP ($p$<0.05). The findings indicated the potential prognostic significance of the expression of SKA family members in patients with HCC.

### *Diagnostic and prognostic value of SKAs expression in HCC patients*

To identify the diagnostic role of mRNA expression of SKAs for HCC, the R statistics pROC package was used to construct ROC curves based on transcriptome sequencing and clinical data derived from the TCGA database. The diagnostic potential of mRNA expression of these SKAs for HCC was assessed based on AUC (Fig. 6A–C). The AUCs, optimal cutoff values sensitivity, specificity and Youden index for predicting HCC are shown in Supplementary Table 4. Statistical analysis of the differences in the AUCs of SKAs suggested that the AUC of SKA1 (0.982, 95% CI: 0.970–0.994) was the largest, followed by SKA3 (0.973, 95% CI: 0.957–0.989) and *SKA2* (0.887, 95% CI: 0.852–0.922). We also assessed the diagnostic value of SKA expression for multiple clinical features of HCC patients, such as the pathological stage and TNM stage (Supplementary Fig. 2). The results showed that SKA expression had a certain significance in the diagnosis of TNM staging and pathological staging, which implied that the transcriptional levels of SKAs had a relatively greater sensi-

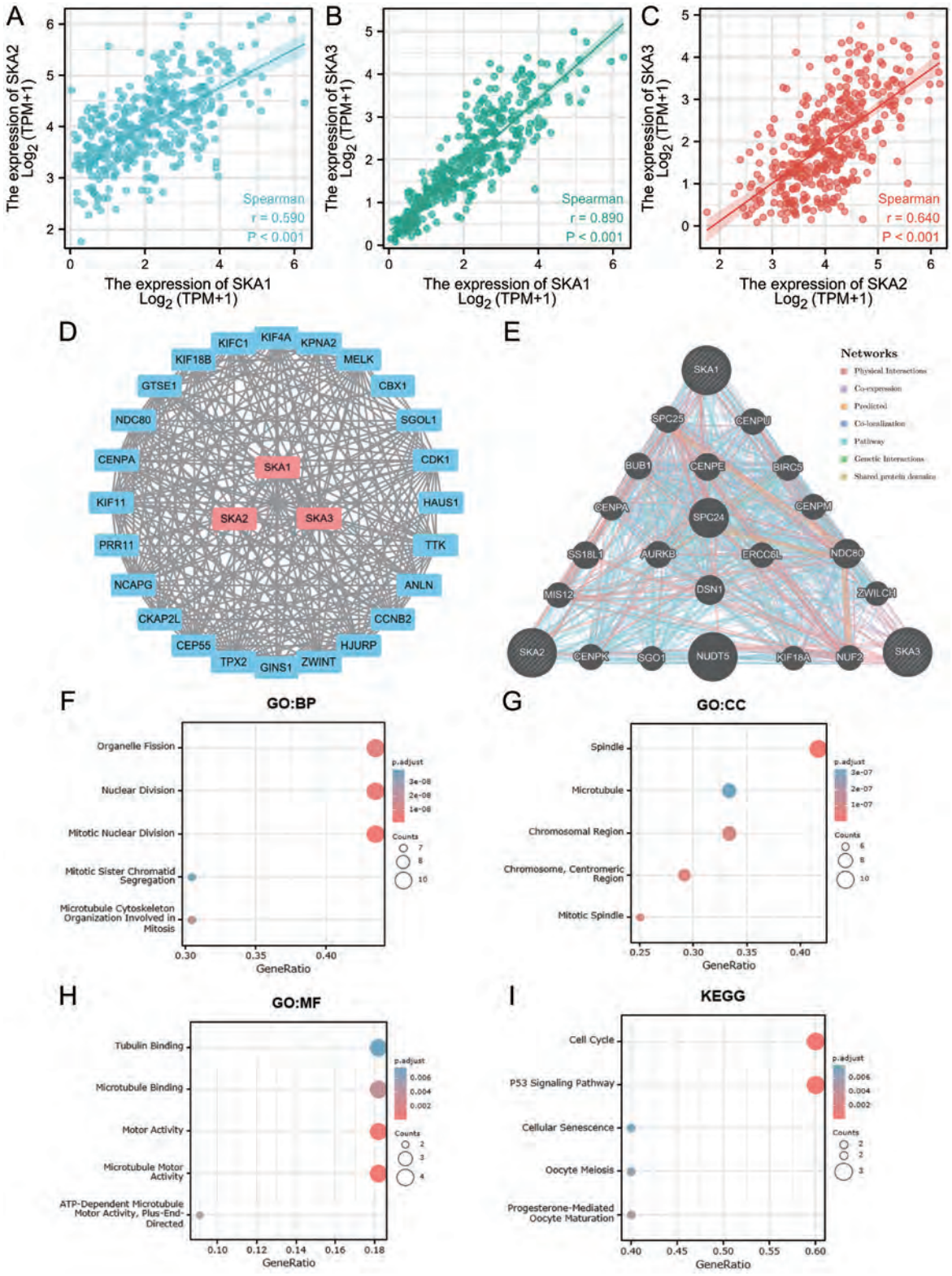


**Fig. 3. Expression correlations, interaction analyses and enrichment analysis of SKAs in HCC.** (A–C) Correlation scatter diagram of SKA family genes in HCC patients. (D) Interaction network of different expressed SKA family proteins on GeneMANIA datasets. (E) PPI network of different expressed SKAs and the 50 most similar genes based on STRING dataset analysis and Cytoscape visualization. (F–H) Bubble diagram results of GO enrichment analysis. (I) Bubble diagram results of KEGG enrichment analysis. GO, gene ontology; HCC, hepatocellular carcinoma; KEGG, and Kyoto Encyclopedia of Genes and Genomes; PPI, protein-protein interaction; SKA, spindle and kinetochore-associated.

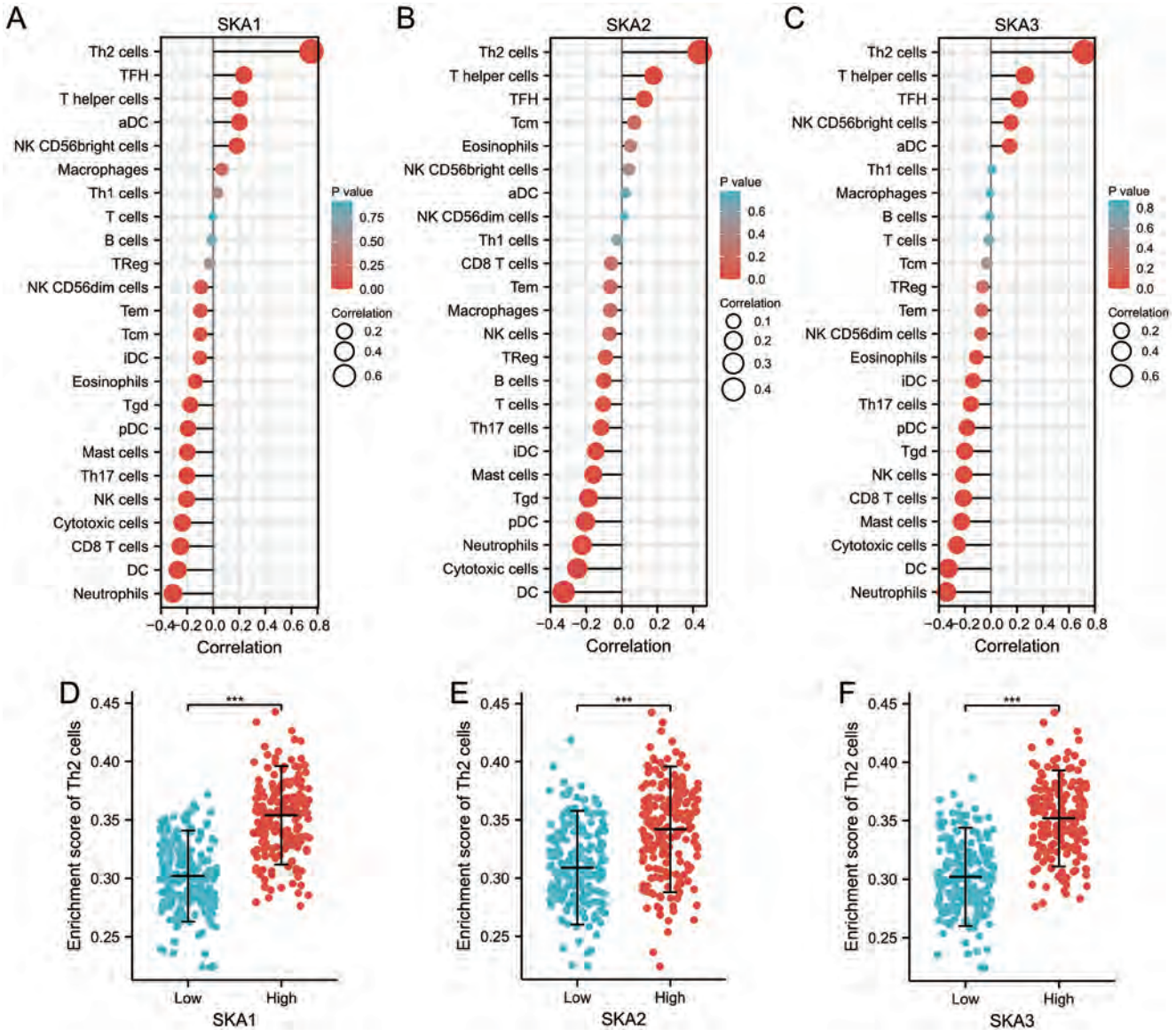


**Fig. 4. Association of SKAs with infiltration of tumor immune cells.** (A–C) Correlation between differentially expressed SKAs and infiltrating of 24 tumor immune cells (ssGSEA method). (D–F) Enrichment score of Th2 cells in HCC samples in SKA1-high and SKA1-low groups. Data are means ± SD. *$p<0.05$, **$p<0.01$, ***$p<0.001$. Th2, T helper 2; ssGSEA, single sample gene set enrichment analysis; HCC, hepatocellular carcinoma; SKA, spindle and kinetochore-associated.

tivity and specificity for the diagnosis of HCC. Furthermore, we analyzed the influence of the expressions of SKAs on the OS, PFS, and DSS to assess the prognostic significance of SKAs in HCC patients by Kaplan-Meier plotter analysis. The OS of patients with high expressions of SKA1/2/3 was remarkably lower than that of patients with low expression of the corresponding SKAs ($p<0.01$, Fig. 6D). In addition, increased mRNA expression of SKA1/2/3 were associated with poor PFS and DSS ($p<0.05$, Fig. 6E–F). The findings indicated the potential prognostic significance of SKA mRNA levels in HCC patients. We further assessed the prognostic value of SKA1/2/3 using univariate and multivariate Cox proportional hazards regression analysis (Table 1). RNA sequencing and clinical data of 374 HCC patients were Level 3 data of the LIHC project in the TCGA database. Univariate analysis showed an association of expression of SKA1/3 and pathologic stage with poor OS and DSS. The Child-Pugh grade was also associated with poor DSS. In multivariate analysis, high transcriptional levels of *SKA1* (HR=2.047, 95% CI: 1.211–3.459, $p=0.007$) and high pathologic stage (HR=1.920, 95% CI: 1.308–2.818, and $p<0.001$) were independent predictors of a significantly shorter OS of HCC patients. The expression of SKA1 mRNA, Child-Pugh grade, pathologic stage, and race were independent predictors of DSS. To sum up, we identified transcriptional levels of SKA1 as an independent predictor of OS and DSS of HCC patients.

### *SKA1 knockdown inhibited the in vitro tumorigenicity of HCC cells*

In the previous analysis, SKA1 was confirmed as an independent prognostic factor for HCC. To further validate the role of CDT1 in HCC, we performed IHC staining on HCC

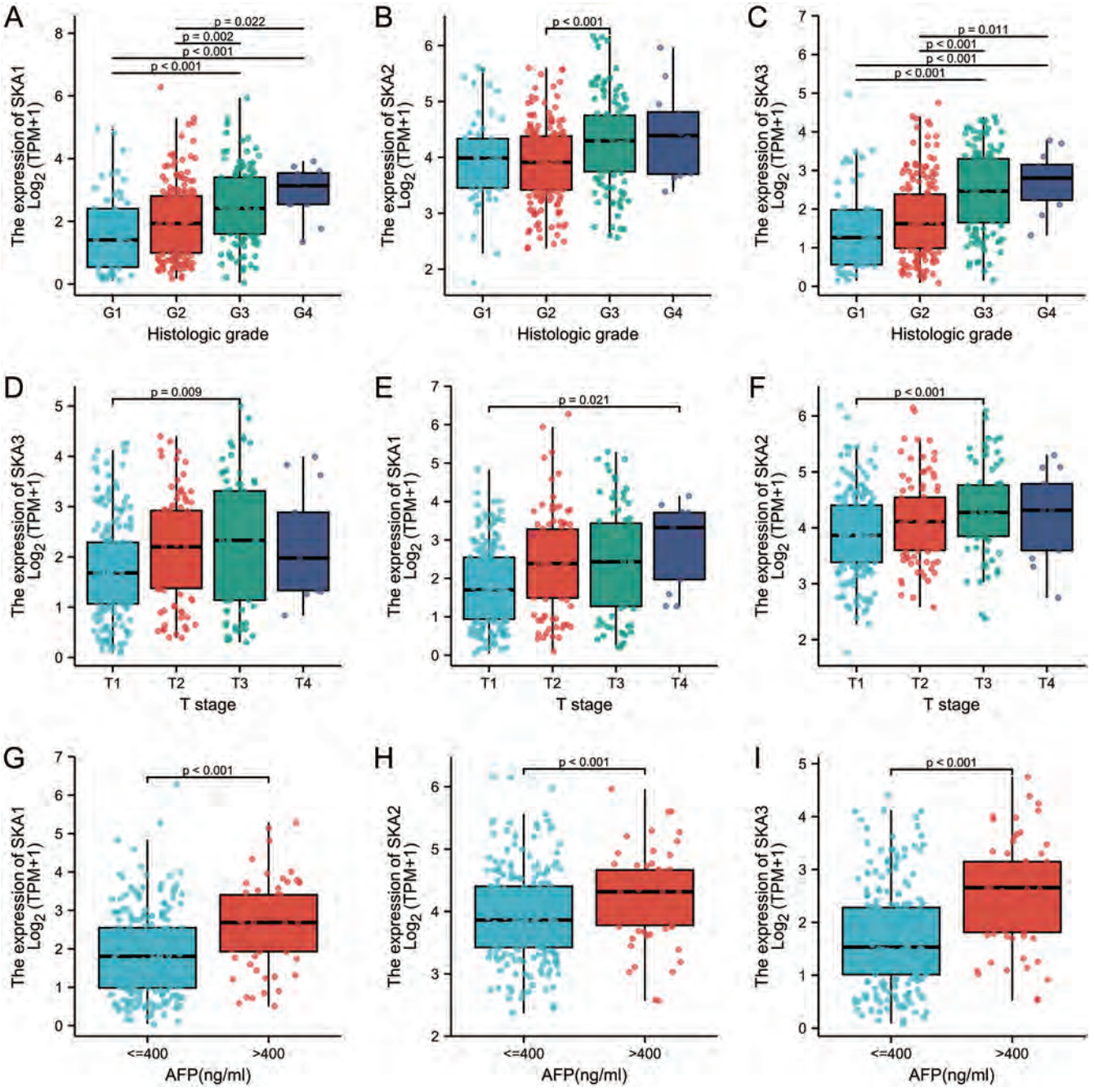


**Fig. 5. Association of mRNA levels of SKAs with clinicopathological parameters of patients with hepatocellular carcinoma.** (A–C) Relationship of SKA mRNA levels with histologic grade of HCC. (D–F) Correlation of SKA expression with T stage of HCC. (G–I) Relationship of SKA expression with AFP levels of HCC patients. **p*<0.05, ***p*<0.01, ****p*<0.001. AFP, α-fetoprotein; HCC, hepatocellular carcinoma; SKA, spindle and kinetochore-associated.

tissue microarrays. The results of the scatter plot analysis by paired *t*-tests revealed that SKA1 expression in HCC tissues was significantly higher than that in para-carcinoma tissues (Fig. 7A). The functional assays were also performed in LM3 and Hep3B cell lines. Western blot detection showed that SKA1 was markedly knocked down by SKA1 siRNA (Fig. 7B). CCK-8 and colony formation assays demonstrated that CDT1 knockdown significantly inhibited the proliferation and invasiveness of LM3 and Hep3B cells (Fig. 7C, E). CDT1 knockdown also significantly inhibited the invasiveness of HCC cells in Transwell assays (Fig. 7D). The results indicated that SKA1 knockdown suppressed the proliferation and invasiveness of HCC cells.

## Discussion

HCC is associated with high mortality and morbidity rates and accounts for approximately 75–85% of all primary liver cancers worldwide. The poor 5-year survival makes it the

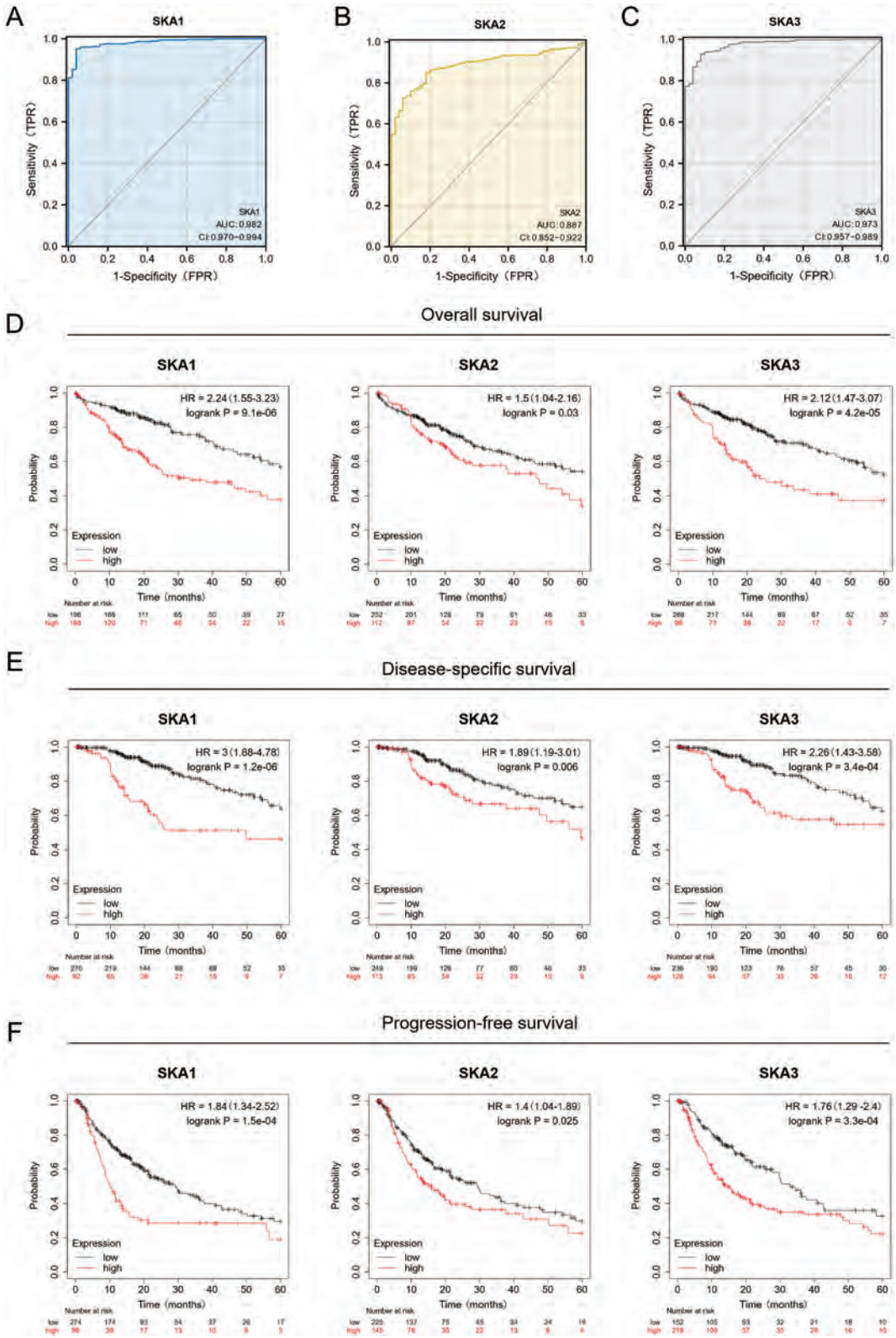


**Fig. 6. Diagnostic significance and prognostic value of differentially expressed SKA family genes in HCC patients.** (A–C) Diagnostic significance of different SKA mRNA levels in patients with HCC. (D) Correlation of differentially expressed SKAs and OS. (E) Correlation of differentially expressed SKAs and DSS. (F) Correlation of differentially expressed SKA and PFS. DSS, disease-specific survival; OS, overall survival; PFS, progression-free survival; HCC, hepatocellular carcinoma; SKA, spindle and kinetochore-associated.

**Table 1. Cox regression analyses of variables for OS and DSS in LIHC patients**

| Characteristics | OS | | | | DSS | | | |
|---|---|---|---|---|---|---|---|---|
| | Univariate analysis | | Multivariate analysis | | Univariate analysis | | Multivariate analysis | |
| | Hazard ratio (95% CI) | *p*-value | Hazard ratio (95% CI) | *p*-value | Hazard ratio (95% CI) | *p*-value | Hazard ratio (95% CI) | *p*-value |
| Age (>60 vs. <=60) | 1.205 (0.850–1.708) | 0.295 | | | 0.846 (0.543–1.317) | 0.458 | | |
| Gender (Male vs. Female) | 0.793 (0.557–1.130) | 0.200 | | | 0.813 (0.516–1.281) | 0.373 | | |
| Race (White vs. Asian and Black or African American) | 1.265 (0.881–1.816) | 0.203 | | | 1.547 (0.964–2.481) | 0.071 | 2.465 (1.113–5.458) | 0.026 |
| Pathologic stage (Stage II and Stage III and Stage IV vs. Stage I) | 2.090 (1.429–3.055) | <0.001 | 1.920 (1.308–2.818) | <0.001 | 2.909 (1.718–4.925) | <0.001 | 2.101 (1.043–4.233) | 0.038 |
| AFP (ng/ml) (>400 vs. <=400) | 1.075 (0.658–1.759) | 0.772 | | | 0.867 (0.450–1.668) | 0.668 | | |
| Fibrosis Ishak score (1/2 and ¾ and 5/6 vs. 0) | 0.772 (0.465–1.281) | 0.316 | | | 0.913 (0.474–1.757) | 0.784 | | |
| Vascular invasion (Yes vs. No) | 1.344 (0.887–2.035) | 0.163 | | | 1.277 (0.707–2.306) | 0.418 | | |
| Child-Pugh grade (B and C vs. A) | 1.643 (0.811–3.330) | 0.168 | | | 2.560 (1.123–5.834) | 0.025 | 3.090 (1.273–7.499) | 0.013 |
| SKA1 (High vs. Low) | 1.911 (1.341–2.724) | <0.001 | 2.047 (1.211–3.459) | 0.007 | 2.505 (1.566–4.008) | <0.001 | 2.872 (1.266–6.513) | 0.012 |
| SKA2 (High vs. Low) | 1.241 (0.878–1.752) | 0.221 | | | 1.489 (0.954–2.325) | 0.080 | 0.534 (0.240–1.189) | 0.124 |
| SKA3 (High vs. Low) | 1.545 (1.090–2.188) | 0.014 | 0.900 (0.542–1.494) | 0.683 | 1.778 (1.132–2.795) | 0.013 | 1.283 (0.536–3.071) | 0.576 |

LIHC, liver hepatocellular carcinoma; OS, overall survival; DSS, disease-specific survival.

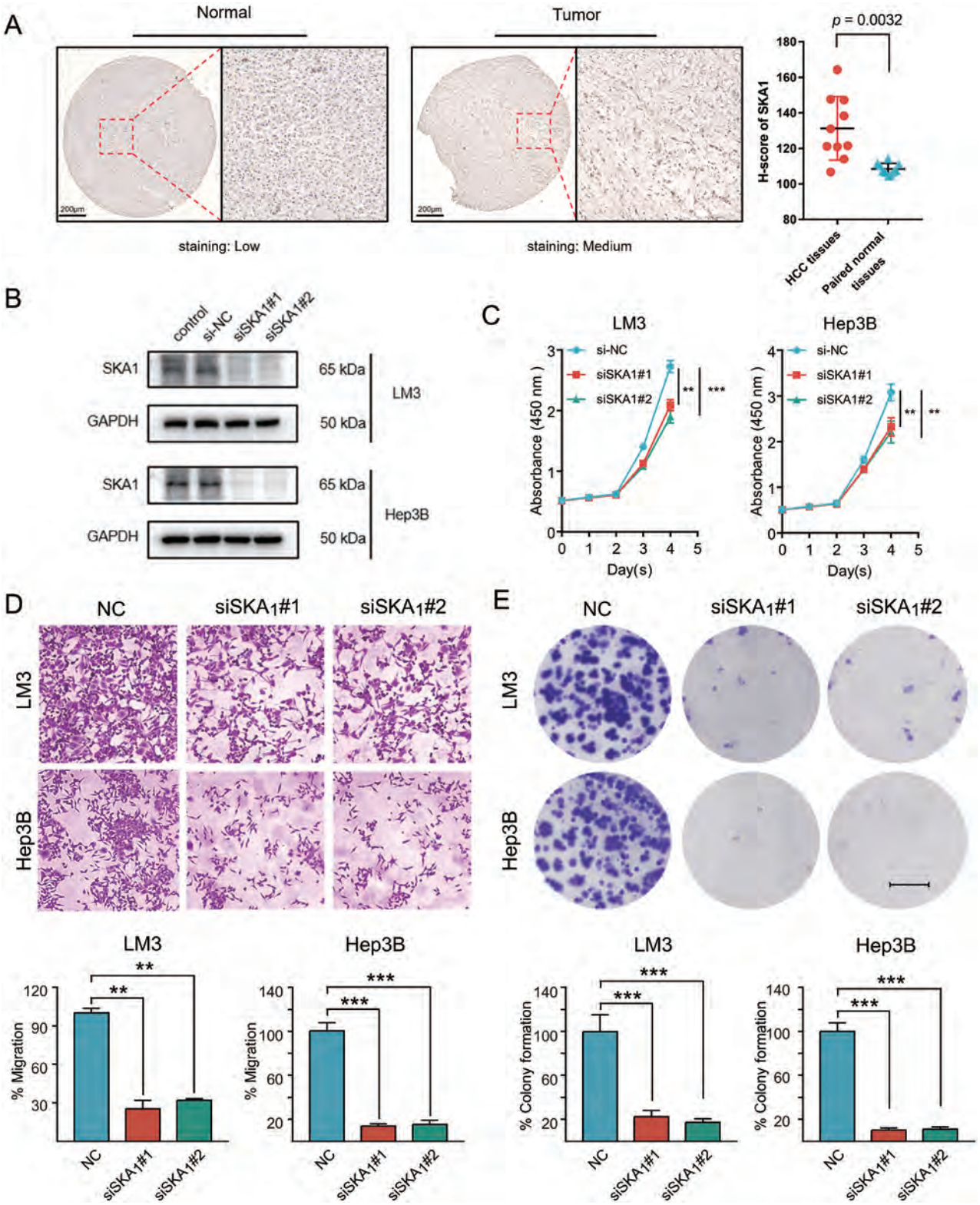


**Fig. 7. Knockdown of SKA1 suppressed the proliferation and invasion abilities of HCC cells.** (A) IHC staining results of SKA1 protein expression in HCC tissues and paired adjacent normal tissues and the corresponding scatter plot. (B) Western blot assay of SKA1 protein expression in SKA1-knockdown liver cancer cells. (C) The effect of CDT1 knockdown on cell viability was evaluated by CCK-8 assays. (D) Transwell assays reflected the effect of SKA1 knockdown on cell invasion in liver cancer cells. (E) Knockdown of SKA1inhibited clonogenic survival of HCC cells. Scale bars in (E) are 5 mm. Data are means ± SD of three independent experiments. *$p<0.05$, **$p<0.01$, ***$p<0.001$. CCK-8, Cell Counting Kit-8; HCC, hepatocellular carcinoma; IHC, immunohistochemical; SKA, spindle and kinetochore-associated.

second most common cause of death after lung cancer.[1] There are several risk factors for the occurrence and progression of HCC, including hepatitis B or C virus infection, aflatoxin exposure, contamination of drinking water, and excessive alcohol consumption.[38–40] Recent next-generation sequencing studies have demonstrated different evolutionary patterns of liver cancer and confirmed the high molecular heterogeneity in HCC;[1,41] the high incidence of metastasis and recurrence of liver cancer may be attributable to its high molecular heterogeneity. Although numerous studies have probed the molecular mechanisms that contribute to the occurrence, progression, and recurrence of HCC, there are limited therapeutic options to delay tumor progression and improve survival outcomes. Besides, the high metastasis and recurrence rates of HCC are a significant impediment to favorable treatment outcomes. The underlying mechanisms of the clinical characteristics of HCC are not well characterized. SKA family proteins, as essential mediators of mitosis and participate in the coordination of cell cycle and proliferation in eukaryotic cells. Several studies have demonstrated a close association between abnormal expression of SKAs and the occurrence or progression of tumors such as lung carcinoma,[29] invasive breast carcinoma,[17] prostatic intraepithelial neoplasia,[42] and other malignant tumors. However, the molecular mechanisms and functions of different SKA family members in HCC remain unclear. In this study, we used bioinformatics analysis to comprehensively and systematically describe the expression levels, diagnostic and prognostic significance, gene mutation patterns, transcriptional regulation, and immune cell infiltration levels of SKA family genes in HCC.

We found significantly higher expression levels of SKA1/2/3 in HCC tissues relative to nonneoplastic tissues. Significant upregulation of SKA1 has been demonstrated in a variety of tumors, such as non-small cell lung cancer,[43] prostate cancer,[42] and pancreatic ductal adenocarcinoma.[30] An *in vitro* study found that the transcriptional levels of SKA1 were significantly elevated in human non-small cell lung cancer tissues and positively correlated with the proliferation, invasion, and metastatic ability of lung cancer cell lines.[43] Li *et al*. reported that the overexpression of SKA1 induced centrosomal expansion of human prostatic epithelial cells by inducing centriole overduplication, which ultimately leads to spontaneous tumor formation in transgenic mouse models.[42] SKA1 has also been shown to be highly expressed in pancreatic ductal adenocarcinoma tissues compared with noncancer tissues. Survival analysis found that SKA1 expression was an independent prognostic factor for pancreatic cancer but was not related to relapse-free survival.[15] In our study, SKA1 expression was greater in HCC tissues than that in non-tumor tissue. We further explored the transcriptional levels of SKA1 in HCC and assessed their association with clinicopathological characteristics. The results showed a marked correlation of SKA1 expression with histologic grade, T stage, and AFP in HCC patients. Notably, ROC curve analysis showed that the expression of SKA1 had a good diagnostic value for liver cancer. Moreover, high SKA1 expression was linked with unfavorable outcomes in HCC patients. Through Cox proportional hazards regression analysis, we identified transcriptional expression of SKA1 as an independent predictor of poor OS and DSS of HCC patients. To further validate the role of SKA1 in HCC, we performed IHC staining of HCC tissue microarray and found that SKA1 expression in HCC tissues was markedly higher than that in para-carcinoma tissues. *In vitro* functional assays indicated that SKA1 knockdown significantly suppressed the proliferation and invasion abilities of HCC cells. To summarize, we identified SKA1 as an independent marker of survival outcomes in HCC and confirmed its important role in tumor cell malignant behavior.

Multiple studies have also focused on the oncogenic role of SKA2 in a variety of tumors. Wang *et al*. found significant upregulation of the transcriptional levels of SKA2 in breast cancer and that SKA2 knockdown inhibited the proliferation, invasion, and migration of breast cancer cells.[17] In another study, expression of SKA2 mRNA was higher in human ESCC tissues relative to nonneoplastic tissues, and SKA2 overexpression contributed to both proliferation and migration of ESCC cells via activation of Akt signaling *in vitro*.[19] A few studies have investigated the expression pattern, function, and mechanism of SKA2 in liver cancer. SKA2 expression was positively correlated with the expression of β-catenin in liver cancer cells *in vitro* and *in vivo*, and SKA2 knockdown inhibited tumor formation and growth in nude mice.[44] However, further studies are required to investigate the underlying molecular mechanisms, biological functions, and clinical applications of SKA2 in HCC. In the present study, HCC tissues showed higher expression of SKA2 compared with normal tissues, which was significantly linked with unfavorable histologic grade, T stage, and AFP levels. The results of ROC curve analysis suggested that SKA2 may be a potential diagnostic marker in HCC. Moreover, high SKA2 expression in HCC patients was correlated with unfavorable OS, PFS, and DSS. The results indicate the oncogenic role of SKA2 in HCC and its potential prognostic significance.

Similar to SKA1 and SKA2, the carcinogenic role of SKA3 has been demonstrated in multiple human malignancies, such as cervical cancer[14] and laryngeal squamous cell carcinoma.[45] An IHC study of 100 cervical cancer patients revealed overexpression of protein levels of SKA3 in advanced cervical cancer. High SKA3 expression was found to promote cervical cancer cell proliferation and invasion via the PI3K/Akt-dependent signaling.[14] In laryngeal squamous cell carcinoma, Li *et al*. initially revealed a role of SKA3 in regulating tumor proliferation through metabolic reprogramming and demonstrated that targeting SKA3 inhibited the chemotherapy and proliferation resistance of tumor cells by inhibiting glycolysis mediated by the PLK1-Akt axis.[45] The transcriptional levels of SKA3 were found to be significantly higher in pancreatic ductal adenocarcinoma tissues relative to para-carcinoma tissues and had a marked association with unfavorable prognosis and immune infiltration.[30] Consistent with the results of SKA1 and SKA2, our study revealed a higher transcriptional level of SKA3 in HCC samples compared with that in adjacent nonneoplastic tissues, and SKA3 expression showed a strong correlation with clinicopathological characteristics, such as histologic grade, T stage, and AFP levels. Early diagnosis of cancer is crucial for tracking the progression of the disease and early use of antitumor therapy. On ROC curve analysis, transcriptional levels of SKA3 were found to be highly sensitive and specific for the diagnosis of HCC. Predictably, HCC patients with high SKA3 expression showed markedly unfavorable OS, DFS, and DSS. The results revealed that SKA3 may be partially involved in the carcinogenic mechanism of HCC.

To further verify the possible oncogenic function of SKA family genes, we constructed a gene-gene interaction network of SKA family genes through GeneMANIA and a PPI network of SKAs and their most similar genes based on the STRING dataset. The two networks revealed that SKAs were primarily related to microtubule motor activity, cytoskeletal protein binding, and cell cycle, all of which were closely associated with abnormal proliferation of malignant tumors.

Subsequently, we explored the function of highly expressed SKAs and their similar genes through GO and KEGG enrichment analysis. As expected, the results showed that they were significantly related to cell cycle, cellular senescence, and the p53 signaling pathway. It is widely accepted that impaired regulation of the cell cycle leads to uncontrolled growth of normal cells and induces their transformation into tumor cells.[46,47] The p53 signaling pathway, which regulates the initiation of the cell cycle, is the most closely

related pathway found in human tumors.[48,49] Cellular senescence is a universal biological phenomenon, and recent studies have suggested that cellular senescence may contribute to the occurrence and development of tumors by inducing chronic inflammation.[50,51] Therefore, our results demonstrate the participation of SKA family genes in the carcinogenic mechanism of HCC and their potential value as new therapeutic targets.

As an important component of the tumor microenvironment, immune cell infiltration can have a significant impact on tumor progression as well as recurrence and is considered as a key determinant of responses to immunotherapy and clinical outcomes of cancer patients.[52,53] Recent studies have proven the SKA1 expression associated with an abundance of tumor-infiltrating immune cells in adrenocortical carcinoma was closely related with poor prognosis. It has also been reported that SKA1 and SKA3 have a vital role in the recruitment and regulation of immune-infiltrating cells in pancreas ductal adenocarcinoma, which eventually influence overall patient survival. Based on literature research and existing research basis, we analyzed the association of SKA and immune infiltration using the ssGSEA algorithm. We found that the transcriptional levels of SKA family genes were correlated with the infiltration of Th2 cells, Tfhs, and Th cells, neutrophils, and dendritic cells (DCs), especially Th2 cells. Helper T cells, both Th1 and Th2 cells, are important immune regulatory cells, and normally there is a dynamic equilibrium between Th1 and Th2 subtypes.[54] Increased secretion of Th2 cytokines in patients with malignant tumors induces Th1/Th2 drift, resulting in the imbalance of Th1/Th2.[55] Many tumors, including lung cancer, liver cancer, and gastric cancer, have a Th1/Th2 balance shift that is often dominated by Th2 cells in the body, which may be related to the immune escape of tumors.[56] Consistent with the above assumptions, we found a positive association of SKAs expression with Th2 cell infiltration in this study. We observed a significant positive correlation between mRNA levels of SKAs and markers of Th2 cells, thus revealing the underlying mechanism by which SKAs influence the immune microenvironment through altering the infiltration state of Th2 cells.

While our study revealed some important findings, there are some limitations. Most of the experimental results in this study are based on online bioinformatics data analysis, and further experiments are required to explore the underlying mechanisms. In addition, most of the analyses were based on transcriptome data. We did not explore the association between SKA family protein expression and the clinical outcomes of HCC patients. Finally, the specific mechanism by which SKA promotes the progression of HCC was not discussed in this review. Further study is required to address these issues.

## Conclusion

In summary, we performed differential expression profiling of SKA family genes in HCC. We analyzed the association of the expression of SKA family genes with tumor-infiltrating immune cells and found positive correlations with Th2 cells. We also evaluated the diagnostic and prognostic significance of SKA family members, identified SKA1 as an independent marker of survival outcomes in HCC, and confirmed its important role in tumor cell malignant behavior. Further experimental studies are required to confirm our findings.

## Acknowledgments

The authors thank the TCGA project and other groups for providing invaluable datasets for statistical analyses.

## Funding

This research was funded by the General project of Chongqing Natural Science Foundation of China (No. cstc2020jcyj-msxmX0688), National Key Research and Development Plan Project (2016YFC1101504), and the Clinical Research Project of the Second Affiliated Hospital of the Army Military Medical University (2018XLC2016).

## Conflict of interest

The authors have no conflict of interests related to this publication.

## Author contributions

Development of the idea, design of the research and drafting of the manuscript (CC), analysis of the data (YZ, XH, SY, JY, ZW), obtainment of copies of the studies, revision of the writing and project supervision (TC). All authors read and approved the submitted version.

## Data sharing statment

The datasets supporting the conclusions of this article are included within the article and the supplementary information files.

## References

[1] Sung H, Ferlay J, Siegel RL, Laversanne M, Soerjomataram I, Jemal A, *et al*. Global Cancer Statistics 2020: GLOBOCAN Estimates of Incidence and Mortality Worldwide for 36 Cancers in 185 Countries. CA Cancer J Clin 2021;71(3):209–249. doi:10.3322/caac.21660.
[2] Gao Q, Zhu H, Dong L, Shi W, Chen R, Song Z, *et al*. Integrated Proteogenomic Characterization of HBV-Related Hepatocellular Carcinoma. Cell 2019;179(5):1240. doi:10.1016/j.cell.2019.10.038.
[3] Zhang Q, He Y, Luo N, Patel SJ, Han Y, Gao R, *et al*. Landscape and Dynamics of Single Immune Cells in Hepatocellular Carcinoma. Cell 2019;179(4):829–845.e820. doi:10.1016/j.cell.2019.10.003.
[4] Mehta N, Dodge JL, Grab JD, Yao FY. National Experience on Down-Staging of Hepatocellular Carcinoma Before Liver Transplant: Influence of Tumor Burden, Alpha-Fetoprotein, and Wait Time. Hepatology 2020;71(3):943–954. doi:10.1002/hep.30879.
[5] Thein HH, Qiao Y, Zaheen A, Jembere N, Sapisochin G, Chan KKW, *et al*. Cost-effectiveness analysis of treatment with non-curative or palliative intent for hepatocellular carcinoma in the real-world setting. PloS one 2017;12(10):e0185198. doi:10.1371/journal.pone.0185198.
[6] Zhu AX, Kang YK, Yen CJ, Finn RS, Galle PR, Llovet JM, *et al*. Ramucirumab after sorafenib in patients with advanced hepatocellular carcinoma and increased α-fetoprotein concentrations (REACH-2): a randomised, double-blind, placebo-controlled, phase 3 trial. Lancet Oncol 2019;20(2):282–296. doi:10.1016/s1470-2045(18)30937-9.
[7] Kulik L, Heimbach JK, Zaiem F, Almasri J, Prokop LJ, Wang Z, *et al*. Therapies for patients with hepatocellular carcinoma awaiting liver transplantation: A systematic review and meta-analysis. Hepatology 2018;67(1):381–400. doi:10.1002/hep.29485.
[8] Llovet JM, Montal R, Sia D, Finn RS. Molecular therapies and precision medicine for hepatocellular carcinoma. Nat Rev Clin Oncol 2018;15(10):599–616. doi:10.1038/s41571-018-0073-4.
[9] Mitchison TJ, Salmon ED. Mitosis: a history of division. Nat Cell Biol 2001;3(1):E17–21. doi:10.1038/35050656.
[10] Gaitanos TN, Santamaria A, Jeyaprakash AA, Wang B, Conti E, Nigg EA. Stable kinetochore-microtubule interactions depend on the Ska complex and its new component Ska3/C13Orf3. EMBO J 2009;28(10):1442–1452. doi:10.1038/emboj.2009.96.
[11] Hanisch A, Silljé HH, Nigg EA. Timely anaphase onset requires a novel spindle and kinetochore complex comprising Ska1 and Ska2. EMBO J 2006;25(23):5504–5515. doi:10.1038/sj.emboj.7601426.
[12] Jeyaprakash AA, Santamaria A, Jayachandran U, Chan YW, Benda C, Nigg EA, *et al*. Structural and functional organization of the Ska complex, a key component of the kinetochore-microtubule interface. Mol Cell 2012;46(3):274–286. doi:10.1016/j.molcel.2012.03.005.
[13] Arai T, Okato A, Kojima S, Idichi T, Koshizuka K, Kurozumi A, *et al*. Regulation of spindle and kinetochore-associated protein 1 by antitumor miR-

10a-5p in renal cell carcinoma. Cancer Sci 2017;108(10):2088–2101. doi:10.1111/cas.13331.
[14] Hu R, Wang MQ, Niu WB, Wang YJ, Liu YY, Liu LY, *et al*. SKA3 promotes cell proliferation and migration in cervical cancer by activating the PI3K/Akt signaling pathway. Cancer Cell Int 2018;18:183. doi:10.1186/s12935-018-0670-4.
[15] Li T, Liu X, Xu B, Wu W, Zang Y, Li J, *et al*. SKA1 regulates actin cytoskeleton remodelling via activating Cdc42 and influences the migration of pancreatic ductal adenocarcinoma cells. Cell Prolif 2020;53(4):e12799. doi:10.1111/cpr.12799.
[16] Wang Y, Weng H, Zhang Y, Long Y, Li Y, Niu Y, *et al*. The PRR11-SKA2 Bidirectional Transcription Unit Is Negatively Regulated by p53 through NF-Y in Lung Cancer Cells. Int J Mol Sci 2017;18(3):534. doi:10.3390/ijms18030534.
[17] Wang Y, Zhang C, Mai L, Niu Y, Wang Y, Bu Y. PRR11 and SKA2 gene pair is overexpressed and regulated by p53 in breast cancer. BMB Rep 2019;52(2):157–162. doi:10.5483/BMBRep.2019.52.2.207.
[18] Zhang Q, Sivakumar S, Chen Y, Gao H, Yang L, Yuan Z, *et al*. Ska3 Phosphorylated by Cdk1 Binds Ndc80 and Recruits Ska to Kinetochores to Promote Mitotic Progression. Curr Biol 2017;27(10):1477–1484.e1474. doi:10.1016/j.cub.2017.03.060.
[19] Chen J, Yang HM, Zhou HC, Peng RR, Niu ZX, Kang CY. PRR11 and SKA2 promote the proliferation, migration and invasion of esophageal carcinoma cells. Oncol Lett 2020;20(1):639–646. doi:10.3892/ol.2020.11615.
[20] Tang Z, Li C, Kang B, Gao G, Li C, Zhang Z. GEPIA: a web server for cancer and normal gene expression profiling and interactive analyses. Oncol Lett 2017;45(W1):W98–W102. doi:10.1093/nar/gkx247.
[21] Lian Q, Wang S, Zhang G, Wang D, Luo G, Tang J, *et al*. HCCDB: A Database of Hepatocellular Carcinoma Expression Atlas. Genomics Proteomics Bioinformatics 2018;16(4):269–275. doi:10.1016/j.gpb.2018.07.003.
[22] Rhodes DR, Yu J, Shanker K, Deshpande N, Varambally R, Ghosh D, *et al*. ONCOMINE: a cancer microarray database and integrated data-mining platform. Neoplasia 2004;6(1):1–6. doi:10.1016/s1476-5586(04)80047-2.
[23] Szklarczyk D, Gable AL, Lyon D, Junge A, Wyder S, Huerta-Cepas J, *et al*. STRING v11: protein-protein association networks with increased coverage, supporting functional discovery in genome-wide experimental datasets. Nucleic Acids Res 2019;47(D1):D607–d613. doi:10.1093/nar/gky1131.
[24] Warde-Farley D, Donaldson SL, Comes O, Zuberi K, Badrawi R, Chao P, *et al*. The GeneMANIA prediction server: biological network integration for gene prioritization and predicting gene function. Nucleic Acids Res 2010;38(Web Server issue):W214–W220. doi:10.1093/nar/gkq537.
[25] Yu G, Wang LG, Han Y, He QY. clusterProfiler: an R package for comparing biological themes among gene clusters. OMICS 2012;16(5):284–287. doi:10.1089/omi.2011.0118.
[26] Győrffy B, Lanczky A, Eklund AC, Denkert C, Budczies J, Li Q, *et al*. An online survival analysis tool to rapidly assess the effect of 22,277 genes on breast cancer prognosis using microarray data of 1,809 patients. Breast Cancer Res Treat 2010;123(3):725–731. doi:10.1007/s10549-009-0674-9.
[27] Gyorffy B, Lánczky A, Szállási Z. Implementing an online tool for genome-wide validation of survival-associated biomarkers in ovarian-cancer using microarray data from 1287 patients. Endocr Relat Cancer 2012;19(2):197–208. doi:10.1530/erc-11-0329.
[28] Robin X, Turck N, Hainard A, Tiberti N, Lisacek F, Sanchez JC, *et al*. pROC: an open-source package for R and S+ to analyze and compare ROC curves. BMC Bioinformatics 2011;12:77. doi:10.1186/1471-2105-12-77.
[29] Chen C, Guo Q, Song Y, Xu G, Liu L. SKA1/2/3 serves as a biomarker for poor prognosis in human lung adenocarcinoma. Transl Lung Cancer Res 2020;9(2):218–231. doi:10.21037/tlcr.2020.01.20.
[30] Liu Y, Jin ZR, Huang X, Che YC, Liu Q. Identification of Spindle and Kinetochore-Associated Family Genes as Therapeutic Targets and Prognostic Biomarkers in Pancreas Ductal Adenocarcinoma Microenvironment. Front Oncol 2020;10:553536. doi:10.3389/fonc.2020.553536.
[31] Chen X, Cheung ST, So S, Fan ST, Barry C, Higgins J, *et al*. Gene expression patterns in human liver cancers. Mol Biol Cell 2002;13(6):1929–1939. doi:10.1091/mbc.02-02-0023.
[32] Roessler S, Jia HL, Budhu A, Forgues M, Ye QH, Lee JS, *et al*. A unique metastasis gene signature enables prediction of tumor relapse in early-stage hepatocellular carcinoma patients. Cancer Res 2010;70(24):10202–10212. doi:10.1158/0008-5472.Can-10-2607.
[33] Wurmbach E, Chen YB, Khitrov G, Zhang W, Roayaie S, Schwartz M, *et al*. Genome-wide molecular profiles of HCV-induced dysplasia and hepatocellular carcinoma. Hepatology 2007;45(4):938–947. doi:10.1002/hep.21622.
[34] Whibley C, Pharoah PD, Hollstein M. p53 polymorphisms: cancer implications. Nat Rev Cancer 2009;9(2):95–107. doi:10.1038/nrc2584.
[35] Phan TG, Croucher PI. The dormant cancer cell life cycle. Nat Rev Cancer 2020;20(7):398–411. doi:10.1038/s41568-020-0263-0.
[36] Wang S, Zhang Q, Yu C, Cao Y, Zuo Y, Yang L. Immune cell infiltration-based signature for prognosis and immunogenomic analysis in breast cancer. Brief Bioinform 2021;22(2):2020–2031. doi:10.1093/bib/bbaa026.
[37] Xiong Y, Wang K, Zhou H, Peng L, You W, Fu Z. Profiles of immune infiltration in colorectal cancer and their clinical significant: A gene expression-based study. Cancer Med 2018;7(9):4496–4508. doi:10.1002/cam4.1745.
[38] de Martel C, Maucort-Boulch D, Plummer M, Franceschi S. World-wide relative contribution of hepatitis B and C viruses in hepatocellular carcinoma. Hepatology 2015;62(4):1190–1200. doi:10.1002/hep.27969.
[39] El-Serag HB, Rudolph KL. Hepatocellular carcinoma: epidemiology and molecular carcinogenesis. Gastroenterology 2007;132(7):2557–2576. doi:10.1053/j.gastro.2007.04.061.
[40] Schaper M, Rodriguez-Frias F, Jardi R, Tabernero D, Homs M, Ruiz G, *et al*. Quantitative longitudinal evaluations of hepatitis delta virus RNA and hepatitis B virus DNA shows a dynamic, complex replicative profile in chronic hepatitis B and D. J Hepatol 2010;52(5):658–664. doi:10.1016/j.jhep.2009.10.036.
[41] Nault JC, Villanueva A. Intratumor molecular and phenotypic diversity in hepatocellular carcinoma. Clin Cancer Res 2015;21(8):1786–1788. doi:10.1158/1078-0432.Ccr-14-2602.
[42] Li J, Xuan JW, Khatamianfar V, Valiyeva F, Moussa M, Sadek A, *et al*. SKA1 overexpression promotes centriole over-duplication, centrosome amplification and prostate tumourigenesis. J Pathol 2014;234(2):178–189. doi:10.1002/path.4374.
[43] Shen L, Yang M, Lin Q, Zhang Z, Miao C, Zhu B. SKA1 regulates the metastasis and cisplatin resistance of non-small cell lung cancer. Oncol Rep 2016;35(5):2561–2568. doi:10.3892/or.2016.4670.
[44] Jiang J, Xu B, Zheng Y, Guo X, Chen F. Spindle and kinetochore-associated protein 2 facilitates the proliferation and invasion of hepatocellular carcinoma via the regulation of Wnt/β-catenin signaling. Exp Cell Res 2020;395(1):112181. doi:10.1016/j.yexcr.2020.112181.
[45] Gao W, Zhang Y, Luo H, Niu M, Zheng X, Hu W, *et al*. Targeting SKA3 suppresses the proliferation and chemoresistance of laryngeal squamous cell carcinoma via impairing PLK1-AKT axis-mediated glycolysis. Cell Death Dis 2020;11(10):919. doi:10.1038/s41419-020-03104-6.
[46] Kastan MB, Bartek J. Cell-cycle checkpoints and cancer. Nature 2004;432(7015):316–323. doi:10.1038/nature03097.
[47] Swanton C. Cell-cycle targeted therapies. Lancet Oncol 2004;5(1):27–36. doi:10.1016/s1470-2045(03)01321-4.
[48] Aubrey BJ, Kelly GL, Janic A, Herold MJ, Strasser A. How does p53 induce apoptosis and how does this relate to p53-mediated tumour suppression? Cell Death Differ 2018;25(1):104–113. doi:10.1038/cdd.2017.169.
[49] Mandinova A, Lee SW. The p53 pathway as a target in cancer therapeutics: obstacles and promise. Sci Transl Med 2011;3(64):64rv61. doi:10.1126/scitranslmed.3001366.
[50] Childs BG, Baker DJ, Kirkland JL, Campisi J, van Deursen JM. Senescence and apoptosis: dueling or complementary cell fates? EMBO Rep 2014;15(11):1139–1153. doi:10.15252/embr.201439245.
[51] Herranz N, Gil J. Mechanisms and functions of cellular senescence. J Clin Invest 2018;128(4):1238–1246. doi:10.1172/jci95148.
[52] Gajewski TF, Schreiber H, Fu YX. Innate and adaptive immune cells in the tumor microenvironment. Nat Immunol 2013;14(10):1014–1022. doi:10.1038/ni.2703.
[53] Li B, Severson E, Pignon JC, Zhao H, Li T, Novak J, *et al*. Comprehensive analyses of tumor immunity: implications for cancer immunotherapy. Genome Biol 2016;17(1):174. doi:10.1186/s13059-016-1028-7.
[54] Ding ZC, Blazar BR, Mellor AL, Munn DH, Zhou G. Chemotherapy rescues tumor-driven aberrant CD4+ T-cell differentiation and restores an activated polyfunctional helper phenotype. Blood 2010;115(12):2397–2406. doi:10.1182/blood-2009-11-253336.
[55] Ruterbusch M, Pruner KB, Shehata L, Pepper M. In Vivo CD4(+) T Cell Differentiation and Function: Revisiting the Th1/Th2 Paradigm. Annu Rev Immunol 2020;38:705–725. doi:10.1146/annurev-immunol-103019-085803.
[56] Matsuzaki J, Tsuji T, Imazeki I, Ikeda H, Nishimura T. Immunosteroid as a regulator for Th1/Th2 balance: its possible role in autoimmune diseases. Autoimmunity 2005;38(5):369–375. doi:10.1080/08916930500124122.

*Journal of Clinical and Translational Hepatology* **2022** vol. 10(4) | 642–650
DOI: 10.14218/JCTH.2021.00254

Original Article

# Diagnostic Accuracy of the Apparent Diffusion Coefficient for Microvascular Invasion in Hepatocellular Carcinoma: A Meta-analysis

Yuhui Deng[1,2#], Jisheng Li[3#], Hui Xu[1], Ahong Ren[1], Zhenchang Wang[1], Dawei Yang[1*] and Zhenghan Yang[1*]

*[1]Department of Radiology, Beijing Friendship Hospital, Capital Medical University, Beijing, China; [2]Medical Imaging Division, Heilongjiang Provincial Hospital, Harbin Institute of Technology, Harbin, Heilongjiang, China; [3]Department of Interventional Radiology, Yantai Penglai Traditional Chinese Medicine Hospital, Yantai, Shandong, China*

**Received:** 30 June 2021 | **Revised:** 13 October 2021 | **Accepted:** 27 October 2021 | **Published:** 4 January 2022

## Abstract

***Background and Aims:*** Microvascular invasion (MVI) is a major risk factor for the early recurrence of hepatocellular carcinoma (HCC) and it seriously worsens the prognosis. Accurate preoperative evaluation of the presence of MVI could greatly benefit the treatment management and prognosis prediction of HCC patients. The study aim was to evaluate the diagnostic performance of the apparent diffusion coefficient (ADC), a quantitative parameter for the preoperative diagnosis MVI in HCC patients. ***Methods:*** Original articles about diffusion-weighted imaging (DWI) and/or intravoxel incoherent motion (IVIM) conducted on a 3.0 or 1.5 Tesla magnetic resonance imaging (MRI) system indexed through January 17, 2021were collected from MEDLINE/PubMed, Web of Science, EMBASE, and the Cochrane Library. Methodological quality was evaluated using Quality Assessment of Diagnostic Accuracy Studies 2 (QUADAS-2). The pooled sensitivity, specificity, and summary area under the receiver operating characteristic curve (AUROC) were calculated, and meta-regression analysis was performed using a bivariate random effects model through a meta-analysis. ***Results:*** Nine original articles with a total of 988 HCCs were included. Most studies had low bias risk and minimal applicability concerns. The pooled sensitivity, specificity and AUROC of the ADC value were 73%, 70%, and 0.78, respectively. The time interval between the index test and the reference standard was identified as a possible source of heterogeneity by subgroup meta-regression analysis. ***Conclusions:*** Meta-analysis showed that the ADC value had moderate accuracy for predicting MVI in HCC. The time interval accounted for the heterogeneity.

**Citation of this article:** Deng Y, Li J, Xu H, Ren A, Wang Z, Yang D, *et al*. Diagnostic Accuracy of the Apparent Diffusion Coefficient for Microvascular Invasion in Hepatocellular Carcinoma: A Meta-analysis. J Clin Transl Hepatol 2022;10(4):642–650. doi: 10.14218/JCTH.2021.00254.

## Introduction

Hepatocellular carcinoma (HCC) is one of the most common primary liver malignancies and the third leading cause of tumor-related deaths worldwide.[1,2] Surgical resection and transplantation are currently considered the optimal treatments of HCC, and despite consistent improvement in recent decades, both early-stage and long-term prognosis remain poor because of high recurrence rates.[3] Studies of tumor characteristics, such as histological grade and tumor size,[4,5] have verified that microvascular invasion (MVI) is involved in early recurrence and poor long-term prognosis in HCC patients treated with resection or transplantation.[6,7] As preoperative evaluation of MVI is difficult, a noninvasive, highly accurate tool for evaluating the presence/absence of MVI in HCC patients would help to make treatment decisions.

Diffusion-weighted imaging (DWI) is a magnetic resonance imaging (MRI) technique that is widely accessible and its high sensitivity for detecting the restriction of water molecule movement, contributes to the imaging of liver lesions, including HCC.[8,9] The apparent diffusion coefficient (ADC) value, which reflects the combination of water molecular diffusion and capillary perfusion, has been investigated for lesion characterization, HCC histological grade assessment,[9,10–12] and preoperative assessment of MVI in HCC.[13–15] The varied results of available studies warrants a pooled analysis. This meta-analysis aimed to evaluate the diagnostic accuracy of the ADC value for predicting the presence of MVI in HCC.

## Methods

Preferred Reporting Items for Systematic Reviews and Me-

**Keywords:** Hepatocellular carcinoma; Meta-analysis; Diagnostic accuracy; Diffusion-weighted imaging; Microvascular invasion.

**Abbreviations:** ADC, apparent diffusion coefficient; AUROC, area under the receiver operating characteristic curve; DWI, diffusion-weighted imaging; HCC, hepatocellular carcinoma; IVIM, intravoxel incoherent motion; MRI, Magnetic resonance imaging; MVI, Microvascular invasion; QUADAS 2, Quality Assessment of Diagnostic Accuracy Studies 2.

[#]Contributed equally to this work.

[*]**Correspondence to:** Dawei Yang and Zhenghan Yang, Beijing Friendship Hospital, Capital Medical University, Yongan Road 95, West District, Beijing 100050, China. ORCID: https://orcid.org/0000-0002-1868-2746 (DY) and https://orcid.org/0000-0003-3986-1732 (ZY). Tel: +86-13488676354 (DY) and +86-13910831365 (ZY), Fax: +86-10-63138490, E-mail: yangdawei@ccmu.edu.cn (DY) and yangzhenghan@vip.163.com (ZY)

ta-Analyses (PRISMA)[16] was adopted as a guide for performing the meta-analysis.

### *Literature search*

The PICOS standard was used to guide the search.[17] We conducted a comprehensive search for studies on the diagnostic validity of all diffusion-related parameters for the preoperative evaluation of MVI in HCC in Web of Science, EMBASE, PubMed/MEDLINE, and the Cochrane Library until January 17, 2021. EndNote X9 software (Thomson Reuters, NY, USA) was used for efficient filtering. Details of the search strategy are shown in Supplement 1. Additionally, all references shown in the listed literature were manually checked.

### *Inclusion and exclusion criteria*

The inclusion criteria were as follows. (1) The diagnostic performance of MVI in HCC was evaluated using the ADC parameters of DWI or intravoxel incoherent motion (IVIM) in the original quantitative study. (2) The data provided by the study were sufficient to construct a diagnostic 2 × 2 table. (3) The article was published in English; and 4) at least 30 HCC patients were included. The exclusion criteria were as follows: (1) nonhuman research; and 2) literature published in formats including reviews, patents, guidelines, chapters, case reports, conference abstracts, letters, or editorials.

### *Data extraction and quality assessment*

Two observers with more than 6 years of experience in liver imaging performed the data extraction and quality assessment. For any disagreements in the above process, consensus was obtained with the help of a third radiologist with 16 years of liver imaging experience, as needed. The extracted data included basic data (true positives, false negatives, false negatives, and true negatives) and additional data (patient characteristics, imaging characteristics, and study characteristics) for meta-regression.[18] If multiple diagnostic performance data were provided in the original study, we chose the best outcome. All extracted data were entered into Microsoft Excel 2016 for further analysis. Quality assessment was performed with Quality Assessment of Diagnostic Accuracy Studies 2 (QUADAS-2).[19] The bias risk was rated as low, unclear, or high, and the clinical applicability concern was rated as low, unclear, or high, with converted scores of 1, 2, or 3, respectively.[20] In subsequent meta-regression analyses, the total scores of each study served as covariates to quantitatively represent the general risk of bias and applicability.

### *Pathological MVI in HCC*

MVI is defined as the presence of tumors in endothelial cells by microscopy, including the portal vein and hepatic vein.[21] In all included studies, MVI was divided into two groups (positive MVI or negative MVI).

### *Statistical analysis*

QUADAS evaluations of the included articles were performed with Review Manager 5.3 software (Cochrane Collaboration, Copenhagen, Denmark). Threshold effect assessment was conducted using Meta-Disc 1.4 software provided by Ramon y Cajal Hospital, Madrid, Spain.[22] The pooled sensitivity, specificity, positive likelihood ratio, negative likelihood ratio, and diagnostic odds ratio and their corresponding 95% confidence intervals (CIs) were determined by STATA 14 (StataCorp, College Station, Texas, USA) software using the MIDAS command.[23,24] Both the $I^2$ statistic ($I^2$>50%) and Cochran Q ($p$<0.05) were used to determine the possible occurrence of between-study heterogeneity.[25,26] Meta-regression was conducted to assess study heterogeneity.

## Results

### *Literature search*

After a comprehensive search, 435 records were retrieved. Initially, 148 records were removed by the automatic find-duplicate function embedded in Endnote X9 software, and 44 conference abstracts, 21 reviews, five meta-analyses, two case reports, two letters, and two editorials were excluded because their improper publication type. For a more accurate screening, we read the full texts of the remaining 211 records. After excluding seven non-English studies, those without sufficient data to extract, and 191 unrelated studies, nine studies eventually remained (Fig. 1).

### *Quality assessment and data extraction*

The detailed data of the included articles are shown in Table 1[13-15,27–32] and Supplement 2, including patient characteristics (country/region, year, average age, number of lesions, average size), research characteristics (research design, number of readers, recruitment methods, time interval between the index test and the reference standard, blindness to the index test during the reference test, blindness to the reference test during the index test), and imaging characteristics (MR manufacturer, MR field, MRI sequence, quantitative parameters, details of *b* values). The methodologic quality of all studies based on QUADAS-2 is shown in Figure 2. Generally, there was a low bias risk and minimal concern of clinical applicability in most studies. Five studies had an unclear bias risk because it was not certain whether consecutive patients were recruited. Unclear applicability concerns were present in four studies because of the relative simplicity of the patient inclusion and exclusion criteria. Only one study had an unclear bias risk because it was not clear whether the reference results were blinded during the index test. Five studies had an unclear bias risk because they did not report the status of blinding of the index test results during the reference test in the reference standard. Additionally, there were concerns of the applicability of two studies because of insufficient information on pathological MVI. Regarding flow and timing, one study that did not report the interval between the reference standard and MRI examinations, and three with time intervals greater than 1 month were regarded as having an unclear bias risk and a high bias risk, respectively.

### *Diagnosis of MVI in HCC*

Overall, the accuracy of the ADC value in predicting the presence of MVI was evaluated in nine studies including 988 HCCs. The details of pooled sensitivity, specificity, positive likelihood ratio, negative likelihood ratio, and diagnostic

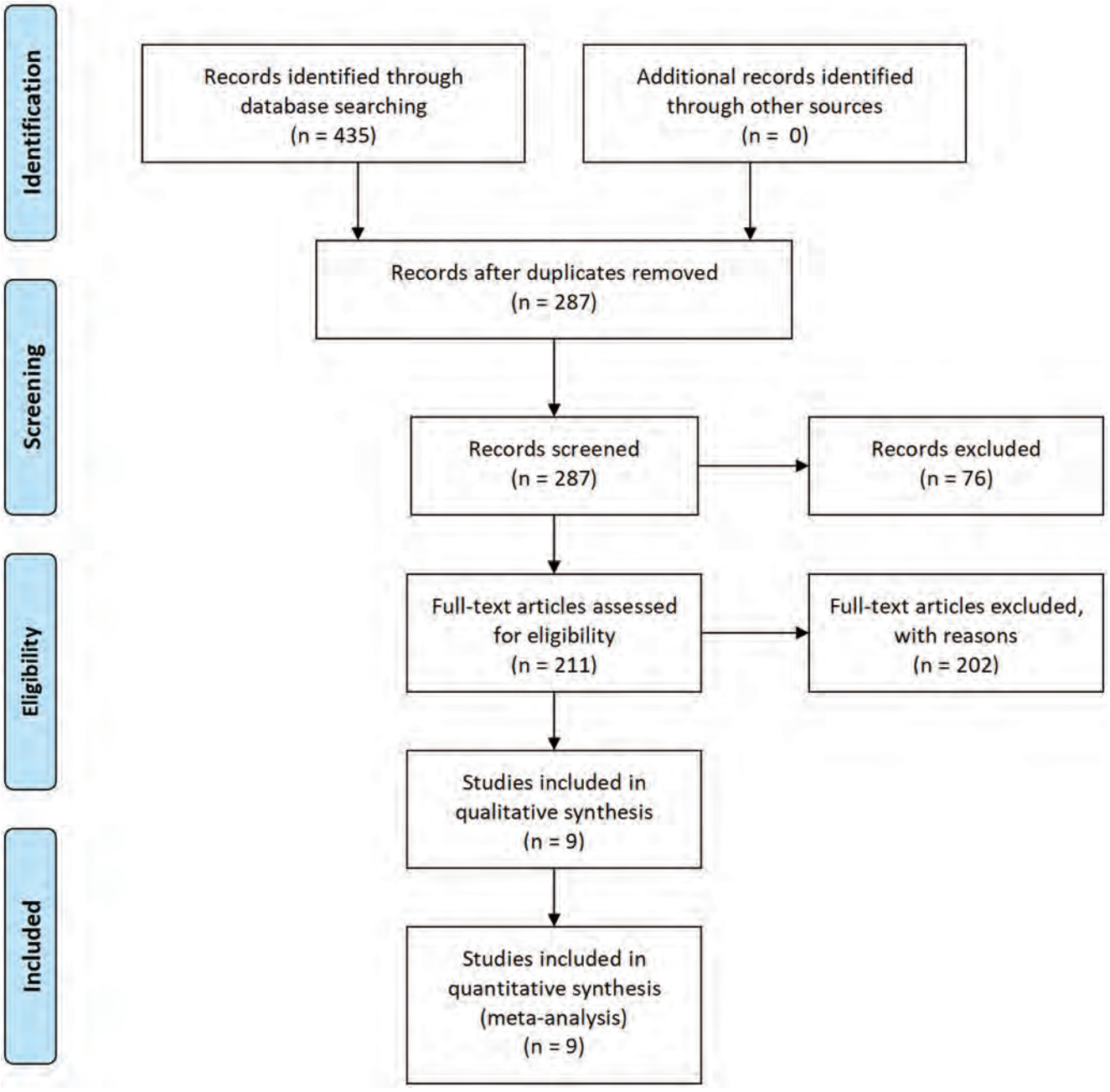


**Fig. 1. Flowchart of study selection.** ADC, apparent diffusion coefficient.

odds ratio were shown in Table 2. The area under the receiver operating characteristic curve (AUROC) of the ADC value was 0.78 for diagnosing MVI in HCC (Fig. 3). The forest plots showed that the between-study heterogeneities of ADC presented sensitivity ($p$=0.10, $I^2$=40.64%) and specificity ($p$ <0.01, $I^2$=70.59%, Fig. 4).

The Begg's funnel plot for ADC in predicting MVI (Z=2.40, $p$=0.016) are presented in Figure 5, which suggests slight asymmetry in the data. Therefore, in evaluating our funnel plots, we can report only that there may have been publication bias, which is difficult to quantify, and that no major publication bias was detected. There was no significant threshold effect ($p$=1.0) for ADC in diagnosing MVI in HCC.

### *Meta-regression*

Subgroup meta-regression analyses were performed with the following nine covariates: number of lesions (<90 or ≥90), average age (<54 or ≥54 years), average size (<30 or ≥30 mm), interval between the index test and the reference test (<30 or ≥30 days), blinding of the index test during the reference test (yes or unclear), blinding of the reference test during the index test (yes or unclear), concern of applicability score (<4 or ≥4), risk of bias score (≤6 or >6) and MR

**Table 1. Characteristics of the included studies**

| Patient characteristics | | | | Study characteristics | | | | | | | | Reference |
|---|---|---|---|---|---|---|---|---|---|---|---|---|
| Region | Age, years | Size, mm | Lesions, *n* | Study design | Consecutive | Readers, *n* | Blind 1 | Blind 2 | TI (days) | Risk score | Application score | |
| China | 51.97 | 63.1 | 135 | p | Yes | 2 | Yes | Yes | 14 | 4 | 3 | Wei *et al*.[27] |
| Japan | 66.7 | 20.72 | 73 | R | Yes | 2 | Yes | Unclear | 85 | 7 | 4 | Okamura *et al*.[15] |
| China | 52 | 19 | 94 | R | Unclear | 2 | Yes | Unclear | 14 | 6 | 3 | Rao *et al*.[28] |
| Korea | 56 | 34.06 | 67 | R | Unclear | 1 | Yes | Yes | 45 | 7 | 4 | Suh *et al*.[14] |
| China | 54.14 | 39.43 | 100 | unclear | Yes | Unclear | Unclear | Unclear | Unclear | 7 | 4 | Wang *et al*.[32] |
| China | 51.51 | 27.9 | 41 | p | Yes | 2 | Yes | Unclear | 30 | 5 | 3 | Li *et al*.[29] |
| China | 53.2 | 14.4 | 109 | R | Unclear | 2 | Yes | Yes | 16 | 5 | 4 | Xu *et al*.[13] |
| China | 59 | 57 | 318 | R | Unclear | 2 | Yes | Unclear | 7 | 6 | 5 | Zhao J *et al*.[30] |
| China | 50.6 | 56.7 | 51 | R | Unclear | 2 | Yes | Yes | 58 | 7 | 3 | Zhao W *et al*.[31] |

| Imaging characteristics | | | | | Reference |
|---|---|---|---|---|---|
| Sequence | Parameter | Field (T) | Manufacturer | *b*-value feature, s/mm$^2$ | |
| IVIM | ADC/D | 3 | GE | 0, 10, 20, 40, 80, 100, 150, 200, 400, 600, 800, 1,000, and 1,200 | Wei *et al*.[27] |
| DWI | ADC | 1.5/3.0 | Siemens/GE | 0, 1,000 | Okamura *et al*.[15] |
| DWI | ADC | 1.5 | Siemens | 0, 500 | Rao *et al*.[28] |
| DWI | ADC | 3 | Siemens | 50, 400, 800 | Suh *et al*.[14] |
| DWI | ADC | 3 | GE/Philips | 0, 100, 600 | Wang *et al*.[32] |
| IVIM | ADC/D | 3 | Philips | 0, 10, 20, 40, 80, 200, 400, 600, 1000 | Li *et al*.[29] |
| DWI | ADC | 1.5 | Siemens | 0, 500 | Xu *et al*.[13] |
| DWI | ADC | 1.5 | GE | 0, 800 | Zhao J *et al*.[30] |
| IVIM | ADC/D | 3 | GE | 0, 10, 20, 30, 40, 50, 60, 70, 80, 90, 100, 200, 300, 400, 500, 1,000 | Zhao W *et al*.[31] |

ADC, apparent diffusion coefficient; Application score, QUADAS score of clinical application concern; Blind 1, blinded to reference standard when assessing index test; Blind 2, blinded to index test when assessing reference test; *D*, tissue diffusivity; DWI, diffusion-weighted imaging; IVIM, intravoxel incoherent motion; P, prospective; R, retrospective; Risk score, QUADAS bias risk score; T, Tesla; TI, time interval between index test and reference standard.

parameter (DWI or IVIM). The results are shown in Table 3. The time interval ($p<0.01$ by the joint model) was a significant cause of heterogeneity. Studies with time intervals ≥ 30 days had significantly lower sensitivity and higher specificity than those with time intervals of <30 days (72% vs. 75% and 70% vs. 72%, respectively, $p<0.01$). In contrast, there were no sources of heterogeneity for mean age ($p=0.21$), mean size ($p=0.08$), number of lesions ($p=0.91$), blinding of the reference standard during the index test ($p=0.70$), blinding of the index test during the reference test ($p=0.49$), QUADAS risk of bias score ($p=0.35$), QUADAS applicability concern score ($p=0.11$) and MR sequence ($p=0.57$).

In addition, studies with a large number of lesions had the same specificity (70% vs. 70%, $p=0.12$) and a significantly higher sensitivity (74% vs. 72%, $p<0.01$) than those with a small number of lesions. Studies with a low risk of bias reported a significantly higher sensitivity than studies with a high risk of bias (75% vs. 71%, $p=0.02$). Studies with small sample sizes reported a significantly higher sensitivity and a significantly lower specificity (65% vs. 74%, $p=0.01$) than those with large sizes (79% vs. 69%, $p=0.04$). Studies with unclear blinding of the index test reported significantly higher sensitivity and specificity than studies with blinding of the index test (74% vs. 73%, $p<0.01$ and 73% vs. 66%, $p=0.02$, respectively). Studies using the DWI parameter reported a significantly higher sensitivity and a significantly lower specificity (67% vs. 75%, $p=0.01$) than those using the IVIM parameter (74% vs. 72%, $p=0.03$).

## Discussion

This meta-analysis included. nine original articles with 988 HCCs and assessed the diagnostic performance of the ADC value for predicting MVI, with a pooled sensitivity, specificity, and AUROC of 73%, 70% and 0.78, respectively. Our meta-analysis indicated that the ADC value had moderate

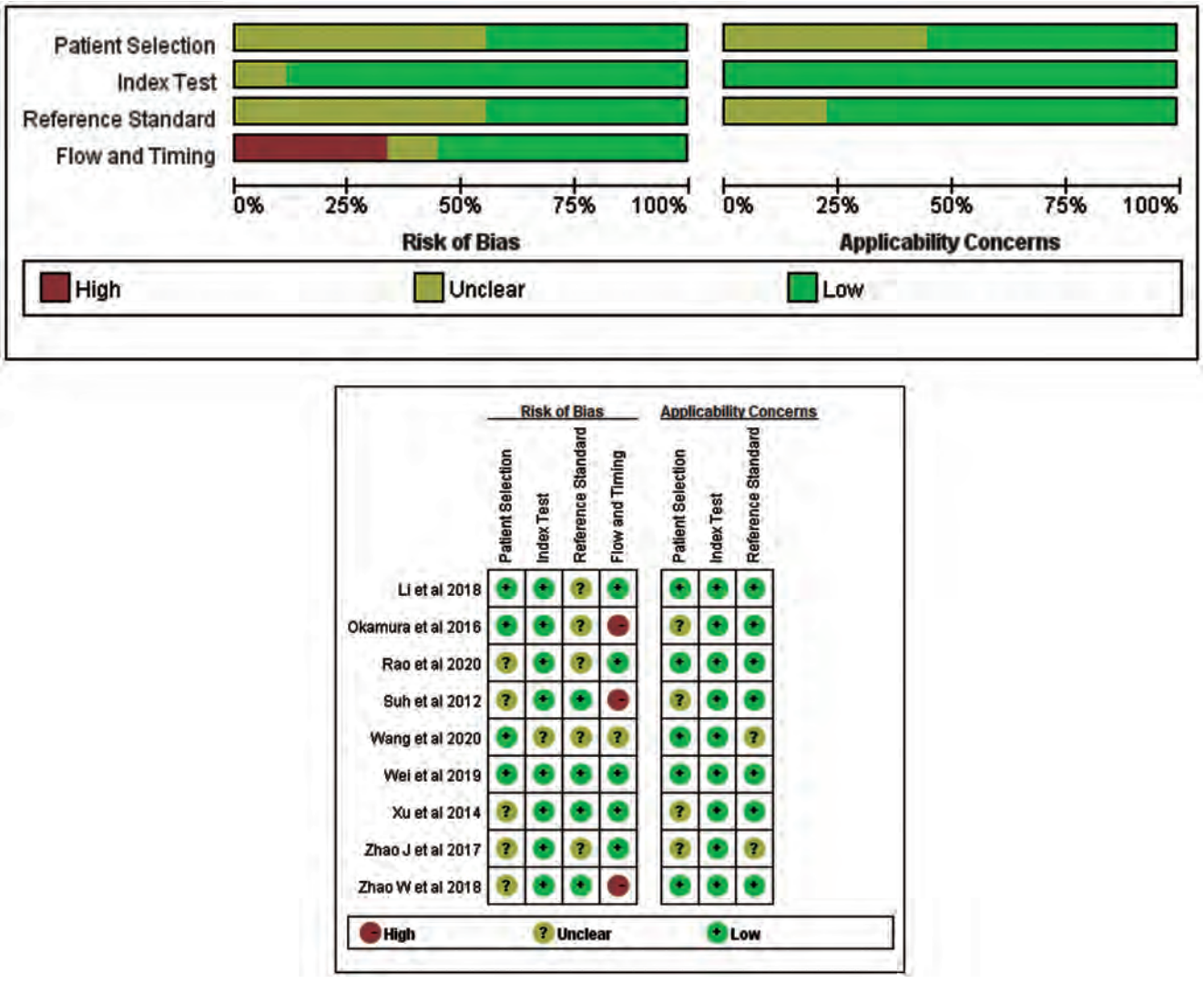


**Fig. 2. Stacked bar charts of Quality Assessment of Diagnostic Accuracy Studies 2 (QUADAS2) scores of methodologic study quality provide an overview of study quality in the whole meta-analysis.**

accuracy in predicting MVI in HCC, which was consistent with the findings of several high-impact original studies,[27–30] with a sensitivity and specificity of 71–76% and 65–66%, respectively. Several hypothetical reasons may contribute to the relation between the ADC value and the MVI status in HCC. First, MVI is more common in HCCs with higher histologic grades,[33] and the ADC value has been reported to accurately assess the histologic grade of HCC.[18] Therefore, it is possible that the ADC value could be used to predict MVI in HCC. Second, tumor embolism in MVI-positive hepatic vascular branches, such as the portal vein, hepatic vein and intracapsular vessel, can limit the diffusion of water molecules to some extent.[34] Additionally, the presence of MVI can further increase the infiltration of tumor cells, provide more nutrients needed for proliferation, increase the tumor-cell density, and further limit the diffusion of water molecules.[27] However, because of the intrinsic inability to separate the effects of capillary perfusion and molecular diffusion, the diagnostic performance of the ADC value is not as promising in predicting MVI in HCC.

Several studies have investigated the diagnostic accuracy of other diffusion parameters, including the mean apparent kurtosis coefficient and tissue diffusivity (*D*-value). Wang *et al*.[35] and Cao, *et al*.[36] found that higher mean kur-

**Table 2. Diagnostic accuracy of the apparent diffusion coefficient value for microvascular invasion of hepatocellular carcinoma**

| | Studies, *n* (patients, *n*) | AUROC | Sensitivity, % (95% CI) | Specificity, % (95% CI) | positive likelihood ratio, (95% CI) | Negative likelihood ratio, (95% CI) | Diagnostic odds ratio, (95% CI) |
|---|---|---|---|---|---|---|---|
| ADC | 9 (988) | 0.78 (0.74, 0.81) | 0.73 (0.68, 0.78) | 0.70 (0.62, 0.77) | 2.4 (2.0, 3.1) | 0.38 (0.32, 0.46) | 6 (5, 9) |

ADC, apparent diffusion coefficient; AUROC, area under the summary receiver operating characteristic curve; HCC, hepatocellular carcinoma; MVI, microvascular invasion.

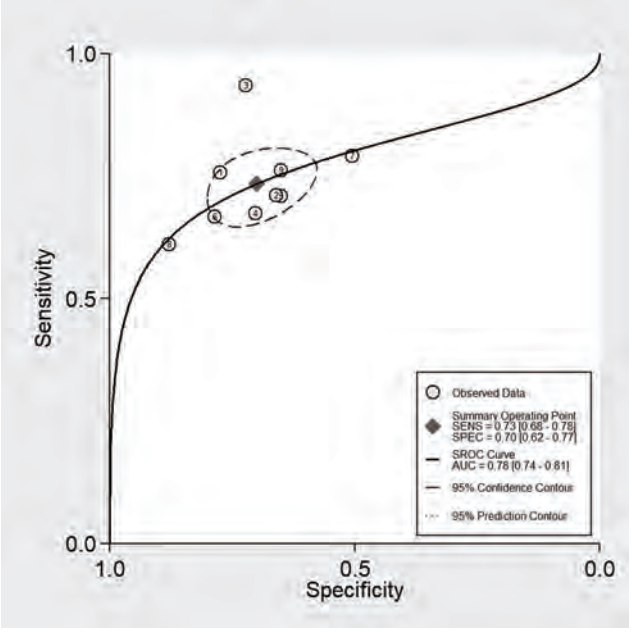


**Fig. 3. Summary receiver operating characteristic (SROC) plots of the apparent diffusion coefficient (ADC) value for microvascular invasion (MVI) of hepatocellular carcinomas.**

tosis values were potential predictors of MVI in HCC, with sensitivity, specificity and AUROC values of 70%, 77%, and 0.784 and 68.4%, 75%, and 0.77, respectively, which were comparable to the diagnostic performance of the ADC value calculated in this study. Diffusion kurtosis imaging (DKI), which reflects the heterogeneity and irregularity of tissue components, is an extension of diffusion tensor imaging for the detection of non-Gaussian water diffusion.[37] The higher mean kurtosis values may be caused by a more complex microenvironment with denser cellular structures and more irregular and heterogeneous lesions introduced by MVI, such as neoplastic cells, necrosis, and inflammation.[35] In theory, IVIM can distinguish true water molecule diffusion from microcapillary perfusion. Therefore, the true tissue molecular diffusivity (D) calculated by the IVIM technique is more effective than the ADC value in probing the small differences in water molecule diffusion induced by MVI.[38,39] To date, three published studies have examined the diffusion parameter of the *D*-value, and the results are inconsistent.[27,29,31] Wei *et al*.[27] found that the *D*-value was better than the ADC value for assessing MVI in HCC, with sensitivity, specificity and AUROC values of 78.2%, 75%, and 0.815, respectively. Zhao *et al*.[31] showed that the *D*-value had a moderate diagnostic performance for assessing MVI in HCC, with sensitivity, specificity and AUROC values of 66.7%, 88.9%, and 0.753, respectively. With limited studies and varied results, more studies are needed in the future to evaluate and confirm the diagnostic performance of the *D*-value and apparent kurtosis coefficient for MVI in HCC.

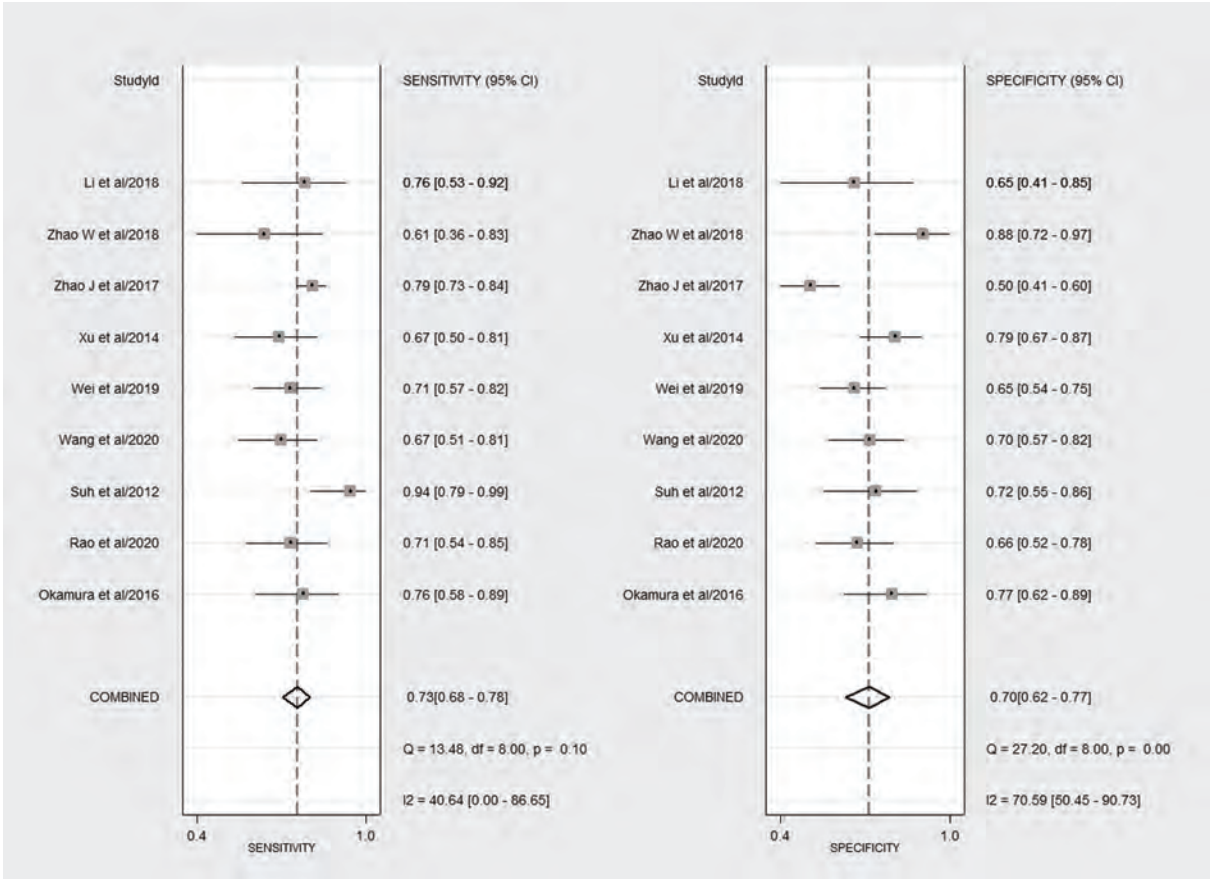


**Fig. 4. Forest plots of tests.** The accuracy estimates (sensitivity and specificity) of the apparent diffusion coefficient (ADC) value for microvascular invasion (MVI) of hepatocellular carcinomas.

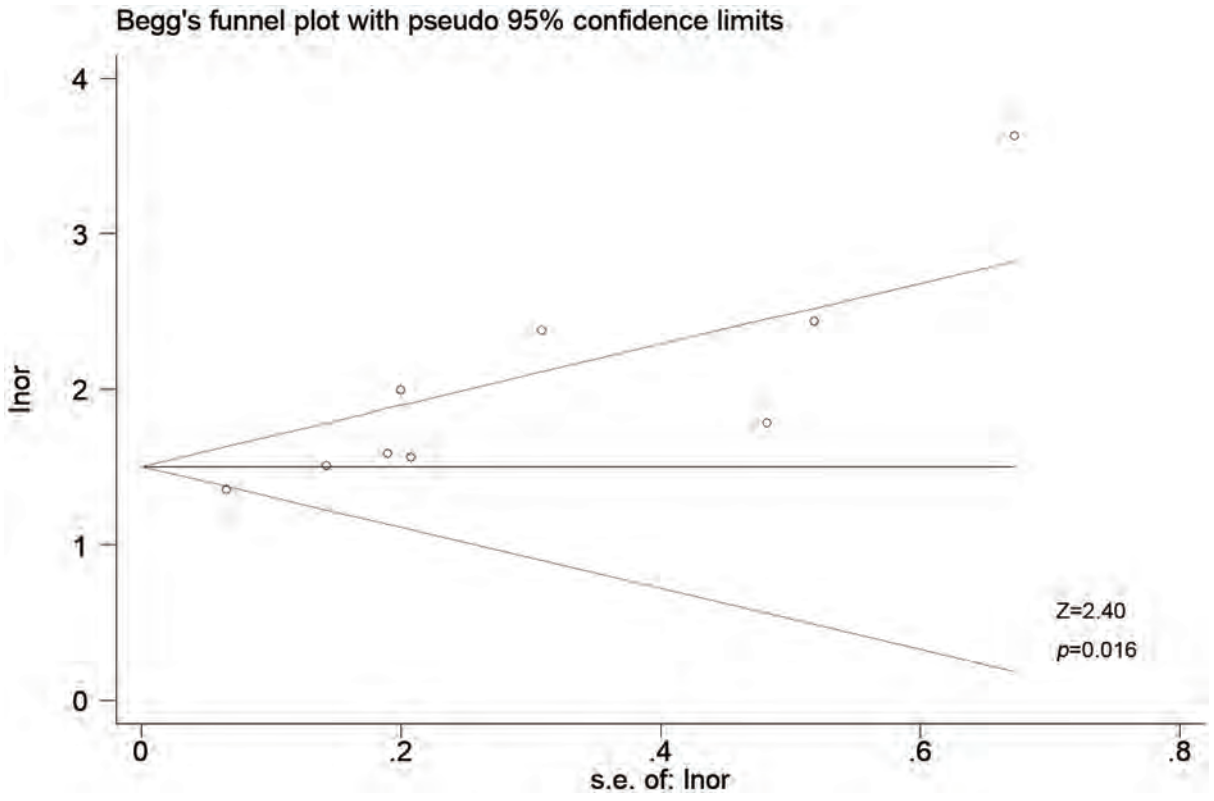


**Fig. 5. Begg's funnel plot for publication bias.** The apparent diffusion coefficient (ADC) value for microvascular invasion (MVI) of hepatocellular carcinomas.

**Table 3. Covariate meta-regression results of apparent diffusion coefficient value for microvascular invasion of hepatocellular carcinoma**

| Covariate | Sub-group | Studies, *n* | *p* | Summary sensitivity, % (95% CI) | *p1* | Summary specificity, 5 (95% CI) | *p2* |
|---|---|---|---|---|---|---|---|
| Age, years | <54 | 5 | 0.21 | 0.77 (0.72, 0.83) | 0.05 | 0.69 (0.59, 0.78) | 0.05 |
| | ≥54 | 4 | | 0.68 (0.61, 0.76) | | 0.72 (0.62, 0.82) | |
| Size, mm | <30 | 4 | 0.08 | 0.79 (0.73, 0.84) | 0.04 | 0.65 (0.55, 0.76) | 0.01 |
| | ≥30 | 5 | | 0.69 (0.62, 0.76) | | 0.74 (0.65, 0.82) | |
| Included lesions, *n* | <90 | 4 | 0.91 | 0.72 (0.64, 0.80) | 0.00 | 0.70 (0.59, 0.81) | 0.12 |
| | ≥90 | 5 | | 0.74 (0.68, 0.81) | | 0.70 (0.60, 0.80) | |
| Blind to reference | Yes | 8 | 0.70 | 0.74 (0.68, 0.79) | 0.18 | 0.71 (0.63, 0.78) | 0.72 |
| | Unclear | 1 | | 0.71 (0.57, 0.85) | | 0.65 (0.44, 0.86) | |
| Blind to index test, *n* | Yes | 4 | 0.49 | 0.73 (0.66, 0.80) | 0.00 | 0.66 (0.56, 0.77) | 0.02 |
| | Unclear | 5 | | 0.74 (0.67, 0.82) | | 0.73 (0.64, 0.82) | |
| Time interval, days | <30 | 4 | 0.00 | 0.75 (0.68, 0.82) | 0.03 | 0.72 (0.61, 0.83) | 0.24 |
| | ≥30 | 4 | | 0.72 (0.64, 0.80) | | 0.70 (0.58, 0.82) | |
| Risk score | ≤6 | 5 | 0.35 | 0.75 (0.69, 0.82) | 0.02 | 0.73 (0.63, 0.82) | 0.32 |
| | >6 | 4 | | 0.71 (0.63, 0.78) | | 0.67 (0.56, 0.78) | |
| Applicability concern score | <4 | 4 | 0.11 | 0.78 (0.69, 0.87) | 0.14 | 0.74 (0.65, 0.84) | 0.29 |
| | ≥4 | 5 | | 0.71 (0.63, 0.78) | | 0.67 (0.58, 0.76) | |
| Sequence | DWI | 6 | 0.57 | 0.74 (0.68, 0.80) | 0.03 | 0.67 (0.59, 0.75) | 0.01 |
| | IVIM | 3 | | 0.72 (0.62, 0.83) | | 0.75 (0.65, 0.86) | |

ADC, apparent diffusion coefficient; DWI, diffusion-weighted imaging; HCC, hepatocellular carcinoma; IVIM, intravoxel incoherent motion; MVI, microvascular invasion.

In addition to quantitative parameters, many qualitative parameters are available for evaluating MVI, such as non-smooth tumor margins, irregular rim-like enhancement in the arterial phase, peritumoral arterial phase hyperenhancement, and peritumoral hepatobiliary phase hypointensity on MRI. In a high-quality meta-analysis, Hong *et al*.[40] summarized multiple MRI features and concluded that rim arterial enhancement, arterial peritumoral enhancement, peritumoral hypointensity in the hepatobiliary phase (HBP), and non-smooth margins were significant predictors of MVI of HCC, with sensitivities and specificities of 36.4% and 87.9%, 49.7% and 81.5%, 44.2% and 91.1%, and 67.1% and 60.7%, respectively. A recent meta-analysis[41] of the evaluation of non-smooth tumor margins and peritumoral hypointensity in the HBP to preoperatively diagnose the presence of MVI in HCC obtained similar results with sensitivity, specificity and AUROC values of 73%, 61%, and 0.74 and 43%, 90%, and 0.76, respectively. Those parameters were similar to the ADC value in predicting MVI in HCC with moderate accuracy, but qualitative parameters are subjective. Even for experienced radiologists, there is a difference.[42] The ADC value can be quantitative or qualitative. As a quantitative parameter, compared with qualitative parameters, it is not limited by subjective differences of interpretation and has stronger practicability. In addition, the ADC value is one of the most commonly used clinical indicators and can be obtained without the use of contrast agents. Accordingly, we believe this work is necessary and useful, especially for those who are unable to undergo MRI enhancement for many reasons.

Compared with deep learning and radiomics, the diagnostic performance of the ADC value was inferior to that of the fusion-deep supervision net based on ADC, with sensitivity, specificity and AUROC values of 67.06% vs. 75.29%, 70.43% vs. 79.13%, and 71.24 vs. 79.69, respectively.[32] Additionally, the diagnostic performance of the ADC value was inferior to that of radiomics models based on MRI. Feng *et al*.[43] found that a radiomics model based on HBP images had a relatively high performance in predicting MVI in HCC, with sensitivity, specificity and AUROC values of 90%, 75%, and 0.83, respectively, in the validation cohort. A recent study[44] found that a radiomics model based on DWI combined with multiple phases of gadoxetate disodium-enhanced MRI had a higher performance in diagnosing MVI in HCC, with sensitivity, specificity and AUROC values of 96%, 86%, and 0.918 in the validation cohort. Therefore, the use of deep learning and radiomics can improve the diagnostic performance of MVI in liver cancer and is a direction for future research.

In this study, meta-regression analyses of nine covariates showed that only the time interval was a significant source of heterogeneity. Studies with time intervals <30 days exhibited significantly higher sensitivity and specificity than those with time intervals ≥30 days. The shorter the time interval between MRI examination and surgical resection, the more closely the imaging features reflect the tumor parenchyma, and the better the diagnostic effectiveness. Therefore, an appropriate time interval should be considered in future studies. Additionally, studies with tumor sizes of <30 mm exhibited significantly higher sensitivity and lower specificity than studies with tumors ≥30 mm. Generally, the larger the diameter of HCCs, the greater the possibility of the existence of MVI[45–47] and the easier it is to observe the imaging features; thus, the diagnostic efficiency of MVI is better. However, that result was not obtained in the study. A possible reason is that the larger the HCC is, the more prone it is to bleeding and necrosis, which affect the ADC measurement. Meta-regression was conducted for bias risk, and studies with low risk had higher sensitivity than studies with high risk (75% vs. 71%, $p$=0.02), which showed that improving the quality of test studies is essential. Meta-regression was also conducted for the blind to index test, and studies with unclear blinding had better sensitivity and specificity than those with blinding (74% vs. 73%, $p$ <0.01 and 73% vs. 66%, $p$=0.02). The measurement bias of the pathological results probably occurred because reviewers had some knowledge of the signal intensity. Meta-regression was also conducted for the number of included lesions, and studies with a large number of lesions had higher sensitivity than those with a small number of lesions (74% vs. 72%, $p$ <0.01), which indicated that increasing the number of samples is essential. Those covariates should be used to reduce heterogeneity as much as possible in further studies.

There were several limitations. First, most of the studies included in the meta-analysis were retrospective, which may cause patient and imaging technique selection biases. Second, we discussed the diagnostic accuracy of the D-value in predicting MVI in HCC in our discussion but did not include it in our meta-analysis because of the limited number of studies. Finally, only original articles in English were included in the meta-analysis. In conclusion, our meta-analysis found that the ADC value had moderate accuracy in noninvasively predicting pathological MVI in HCC. In future studies, artificial intelligence such as radiomics studies and deep learning based on a combination of multiple MRI sequences or more MRI features, including the D-value of IVIM, could be performed to investigate and verify potential improvements for predicting MVI in HCC.

## Acknowledgments

The authors would like to express our enormous appreciation and gratitude to all participants.

## Funding

The work was supported by the National Natural Science Foundation of China (Nos. 82071876, 61871276); Beijing Natural Science Foundation (No. 7184199); and Heilongjiang province Science Foundation for Youths (No. QC201807); Beijing Municipal Administration of Hospitals' Youth Programme (No.QML20200108).

## Conflict of interest

The authors have no conflict of interests related to this publication.

## Author contributions

Study concept and design (DY, ZY), acquisition of data (YD, JL), analysis and interpretation of data (DY, ZY, YD, JL), drafting of the manuscript (DY, YD), critical revision of the manuscript for important intellectual content (HX, AR, ZW), administrative, technical, and material support, study supervision (ZW).

## Data sharing statement

No additional data are available.

## References

[1] Golabi P, Fazel S, Otgonsuren M, Sayiner M, Locklear CT, Younossi ZM. Mor-

tality assessment of patients with hepatocellular carcinoma according to underlying disease and treatment modalities. Medicine (Baltimore) 2017; 96(9):e5904. doi:10.1097/md.0000000000005904, PMID:28248853.
[2] El-Serag HB. Epidemiology of viral hepatitis and hepatocellular carcinoma. Gastroenterology 2012;142(6):1264–1273.e1261. doi:10.1053/j.gastro.2011.12.061, PMID:22537432.
[3] Iguchi T, Shirabe K, Aishima S, Wang H, Fujita N, Ninomiya M, *et al*. New Pathologic Stratification of Microvascular Invasion in Hepatocellular Carcinoma: Predicting Prognosis After Living-donor Liver Transplantation. Transplantation 2015;99(6):1236–1242. doi:10.1097/tp.0000000000000489, PMID:25427164.
[4] Imamura H, Matsuyama Y, Tanaka E, Ohkubo T, Hasegawa K, Miyagawa S, *et al*. Risk factors contributing to early and late phase intrahepatic recurrence of hepatocellular carcinoma after hepatectomy. J Hepatol 2003;38(2):200–207. doi:10.1016/s0168-8278(02)00360-4, PMID:12547409.
[5] Cucchetti A, Piscaglia F, Caturelli E, Benvegnù L, Vivarelli M, Ercolani G, *et al*. Comparison of recurrence of hepatocellular carcinoma after resection in patients with cirrhosis to its occurrence in a surveilled cirrhotic population. Ann Surg Oncol 2009;16(2):413–422. doi:10.1245/s10434-008-0232-4, PMID:19034578.
[6] Sumie S, Kuromatsu R, Okuda K, Ando E, Takata A, Fukushima N, *et al*. Microvascular invasion in patients with hepatocellular carcinoma and its predictable clinicopathological factors. Ann Surg Oncol 2008;15(5):1375–1382. doi:10.1245/s10434-008-9846-9, PMID:18324443.
[7] Oishi K, Itamoto T, Amano H, Fukuda S, Ohdan H, Tashiro H, *et al*. Clinicopathologic features of poorly differentiated hepatocellular carcinoma. J Surg Oncol 2007;95(4):311–316. doi:10.1002/jso.20661, PMID:17326126.
[8] Koh DM, Collins DJ. Diffusion-weighted MRI in the body: applications and challenges in oncology. AJR Am J Roentgenol 2007;188(6):1622–1635. doi:10.2214/ajr.06.1403, PMID:17515386.
[9] Taouli B, Koh DM. Diffusion-weighted MR imaging of the liver. Radiology 2010;254(1):47–66. doi:10.1148/radiol.09090021, PMID:20032142.
[10] Lim KS. Diffusion-weighted MRI of hepatocellular carcinoma in cirrhosis. Clin Radiol 2014;69(1):1–10. doi:10.1016/j.crad.2013.07.022, PMID:24034549.
[11] Nishie A, Tajima T, Asayama Y, Ishigami K, Kakihara D, Nakayama T, *et al*. Diagnostic performance of apparent diffusion coefficient for predicting histological grade of hepatocellular carcinoma. Eur J Radiol 2011;80(2):e29–33. doi:10.1016/j.ejrad.2010.06.019, PMID:20619566.
[12] Mannelli L, Kim S, Hajdu CH, Babb JS, Taouli B. Serial diffusion-weighted MRI in patients with hepatocellular carcinoma: Prediction and assessment of response to transarterial chemoembolization. Preliminary experience. Eur J Radiol 2013;82(4):577–582. doi:10.1016/j.ejrad.2012.11.026, PMID:23246330.
[13] Xu P, Zeng M, Liu K, Shan Y, Xu C, Lin J. Microvascular invasion in small hepatocellular carcinoma: is it predictable with preoperative diffusion-weighted imaging? J Gastroenterol Hepatol 2014;29(2):330–336. doi:10.1111/jgh.12358, PMID:24033853.
[14] Suh YJ, Kim MJ, Choi JY, Park MS, Kim KW. Preoperative prediction of the microvascular invasion of hepatocellular carcinoma with diffusion-weighted imaging. Liver Transpl 2012;18(10):1171–1178. doi:10.1002/lt.23502, PMID:22767394.
[15] Okamura S, Sumie S, Tonan T, Nakano M, Satani M, Shimose S, *et al*. Diffusion-weighted magnetic resonance imaging predicts malignant potential in small hepatocellular carcinoma. Dig Liver Dis 2016;48(8):945–952. doi:10.1016/j.dld.2016.05.020, PMID:27338850.
[16] Frank RA, Bossuyt PM, McInnes MDF. Systematic Reviews and Meta-Analyses of Diagnostic Test Accuracy: The PRISMA-DTA Statement. Radiology 2018;289(2):313–314. doi:10.1148/radiol.2018180850, PMID:30015590.
[17] Moher D, Shamseer L, Clarke M, Ghersi D, Liberati A, Petticrew M, *et al*. Preferred reporting items for systematic review and meta-analysis protocols (PRISMA-P) 2015 statement. Syst Rev 2015;4(1):1. doi:10.1186/2046-4053-4-1, PMID:25554246.
[18] Yang D, She H, Wang X, Yang Z, Wang Z. Diagnostic accuracy of quantitative diffusion parameters in the pathological grading of hepatocellular carcinoma: A meta-analysis. J Magn Reson Imaging 2020;51(5):1581–1593. doi:10.1002/jmri.26963, PMID:31654537.
[19] Whiting PF, Rutjes AW, Westwood ME, Mallett S, Deeks JJ, Reitsma JB, *et al*. QUADAS-2: a revised tool for the quality assessment of diagnostic accuracy studies. Ann Intern Med 2011;155(8):529–536. doi:10.7326/0003-4819-155-8-201110180-00009, PMID:22007046.
[20] Yang D, Li D, Li J, Yang Z, Wang Z. Systematic review: The diagnostic efficacy of gadoxetic acid-enhanced MRI for liver fibrosis staging. Eur J Radiol 2020;125:108857. doi:10.1016/j.ejrad.2020.108857, PMID:32113153.
[21] Rodríguez-Perálvarez M, Luong TV, Andreana L, Meyer T, Dhillon AP, Burroughs AK. A systematic review of microvascular invasion in hepatocellular carcinoma: diagnostic and prognostic variability. Ann Surg Oncol 2013;20(1):325–339. doi:10.1245/s10434-012-2513-1, PMID:23149850.
[22] Zamora J, Abraira V, Muriel A, Khan K, Coomarasamy A. Meta-DiSc: a software for meta-analysis of test accuracy data. BMC Med Res Methodol 2006;6:31. doi:10.1186/1471-2288-6-31, PMID:16836745.
[23] Roberts DJ, Chaubey VP, Zygun DA, Lorenzetti D, Faris PD, Ball CG, *et al*. Diagnostic accuracy of computed tomographic angiography for blunt cerebrovascular injury detection in trauma patients: a systematic review and meta-analysis. Ann Surg 2013;257(4):621–632. doi:10.1097/SLA.0b013e318288c514, PMID:23470509.
[24] Vogelgesang F, Schlattmann P, Dewey M. The Evaluation of Bivariate Mixed Models in Meta-analyses of Diagnostic Accuracy Studies with SAS, Stata and R. Methods Inf Med 2018;57(3):111–119. doi:10.3414/me17-01-0021, PMID:29719917.
[25] Melsen WG, Bootsma MC, Rovers MM, Bonten MJ. The effects of clinical and statistical heterogeneity on the predictive values of results from meta-analyses. Clin Microbiol Infect 2014;20(2):123–129. doi:10.1111/1469-0691.12494, PMID:24320992.
[26] Leeflang MM, Deeks JJ, Takwoingi Y, Macaskill P. Cochrane diagnostic test accuracy reviews. Syst Rev 2013;2:82. doi:10.1186/2046-4053-2-82, PMID:24099098.
[27] Wei Y, Huang Z, Tang H, Deng L, Yuan Y, Li J, *et al*. IVIM improves preoperative assessment of microvascular invasion in HCC. Eur Radiol 2019;29(10):5403–5414. doi:10.1007/s00330-019-06088-w, PMID:30877465.
[28] Rao C, Wang X, Li M, Zhou G, Gu H. Value of T1 mapping on gadoxetic acid-enhanced MRI for microvascular invasion of hepatocellular carcinoma: a retrospective study. BMC Med Imaging 2020;20(1):43. doi:10.1186/s12880-020-00433-y, PMID:32345247.
[29] Li H, Zhang J, Zheng Z, Guo Y, Chen M, Xie C, *et al*. Preoperative histogram analysis of intravoxel incoherent motion (IVIM) for predicting microvascular invasion in patients with single hepatocellular carcinoma. Eur J Radiol 2018;105:65–71. doi:10.1016/j.ejrad.2018.05.032, PMID:30017300.
[30] Zhao J, Li X, Zhang K, Yin X, Meng X, Han L, *et al*. Prediction of microvascular invasion of hepatocellular carcinoma with preoperative diffusion-weighted imaging: A comparison of mean and minimum apparent diffusion coefficient values. Medicine (Baltimore) 2017;96(33):e7754. doi:10.1097/md.0000000000007754, PMID:28816952.
[31] Zhao W, Liu W, Liu H, Yi X, Hou J, Pei Y, *et al*. Preoperative prediction of microvascular invasion of hepatocellular carcinoma with IVIM diffusion-weighted MR imaging and Gd-EOB-DTPA-enhanced MR imaging. PLoS One 2018;13(5):e0197488. doi:10.1371/journal.pone.0197488, PMID:29771954.
[32] Wang G, Jian W, Cen X, Zhang L, Guo H, Liu Z, *et al*. Prediction of Microvascular Invasion of Hepatocellular Carcinoma Based on Preoperative Diffusion-Weighted MR Using Deep Learning. Acad Radiol 2021;28(Suppl 1):S118–S127. doi:10.1016/j.acra.2020.11.014, PMID:33303346.
[33] Pawlik TM, Delman KA, Vauthey JN, Nagorney DM, Ng IO, Ikai I, *et al*. Tumor size predicts vascular invasion and histologic grade: Implications for selection of surgical treatment for hepatocellular carcinoma. Liver Transpl 2005;11(9):1086–1092. doi:10.1002/lt.20472, PMID:16123959.
[34] Iima M, Le Bihan D. Clinical Intravoxel Incoherent Motion and Diffusion MR Imaging: Past, Present, and Future. Radiology 2016;278(1):13–32. doi:10.1148/radiol.2015150244, PMID:26690990.
[35] Wang WT, Yang L, Yang ZX, Hu XX, Ding Y, Yan X, *et al*. Assessment of Microvascular Invasion of Hepatocellular Carcinoma with Diffusion Kurtosis Imaging. Radiology 2018;286(2):571–580. doi:10.1148/radiol.2017170515, PMID:28937853.
[36] Cao L, Chen J, Duan T, Wang M, Jiang H, Wei Y, *et al*. Diffusion kurtosis imaging (DKI) of hepatocellular carcinoma: correlation with microvascular invasion and histologic grade. Quant Imaging Med Surg 2019;9(4):590–602. doi:10.21037/qims.2019.02.14, PMID:31143650.
[37] Rosenkrantz AB, Padhani AR, Chenevert TL, Koh DM, De Keyzer F, Taouli B, *et al*. Body diffusion kurtosis imaging: Basic principles, applications, and considerations for clinical practice. J Magn Reson Imaging 2015;42(5):1190–1202. doi:10.1002/jmri.24985, PMID:26119267.
[38] Guiu B, Cercueil JP. Liver diffusion-weighted MR imaging: the tower of Babel? Eur Radiol 2011;21(3):463–467. doi:10.1007/s00330-010-2017-y, PMID:21110195.
[39] Chandarana H, Taouli B. Diffusion and perfusion imaging of the liver. Eur J Radiol 2010;76(3):348–358. doi:10.1016/j.ejrad.2010.03.016, PMID:20399054.
[40] Hong SB, Choi SH, Kim SY, Shim JH, Lee SS, Byun JH, *et al*. MRI Features for Predicting Microvascular Invasion of Hepatocellular Carcinoma: A Systematic Review and Meta-Analysis. Liver Cancer 2021;10(2):94–106. doi:10.1159/000513704, PMID:33981625.
[41] Deng Y, Yang D, Xu H, Ren A, Yang Z. Diagnostic performance of imaging features in the HBP of gadoxetate disodium-enhanced MRI for microvascular invasion in hepatocellular carcinoma: a meta-analysis. Acta Radiol 2021:2841851211038806. doi:10.1177/02841851211038806, PMID:34459669.
[42] Min JH, Lee MW, Park HS, Lee DH, Park HJ, Lim S, *et al*. Interobserver Variability and Diagnostic Performance of Gadoxetic Acid-enhanced MRI for Predicting Microvascular Invasion in Hepatocellular Carcinoma. Radiology 2020;297(3):573–581. doi:10.1148/radiol.2020201940, PMID:32990512.
[43] Feng ST, Jia Y, Liao B, Huang B, Zhou Q, Li X, *et al*. Preoperative prediction of microvascular invasion in hepatocellular cancer: a radiomics model using Gd-EOB-DTPA-enhanced MRI. Eur Radiol 2019;29(9):4648–4659. doi:10.1007/s00330-018-5935-8, PMID:30689032.
[44] Chong HH, Yang L, Sheng RF, Yu YL, Wu DJ, Rao SX, *et al*. Multi-scale and multi-parametric radiomics of gadoxetate disodium-enhanced MRI predicts microvascular invasion and outcome in patients with solitary hepatocellular carcinoma ≤ 5 cm. Eur Radiol 2021;31(7):4824–4838. doi:10.1007/s00330-020-07601-2, PMID:33447861.
[45] Kim BK, Han KH, Park YN, Park MS, Kim KS, Choi JS, *et al*. Prediction of microvascular invasion before curative resection of hepatocellular carcinoma. J Surg Oncol 2008;97(3):246–252. doi:10.1002/jso.20953, PMID:18095300.
[46] Kaibori M, Ishizaki M, Matsui K, Kwon AH. Predictors of microvascular invasion before hepatectomy for hepatocellular carcinoma. J Surg Oncol 2010;102(5):462–468. doi:10.1002/jso.21631, PMID:20872949.
[47] Eguchi S, Takatsuki M, Hidaka M, Soyama A, Tomonaga T, Muraoka I, *et al*. Predictor for histological microvascular invasion of hepatocellular carcinoma: a lesson from 229 consecutive cases of curative liver resection. World J Surg 2010;34(5):1034–1038. doi:10.1007/s00268-010-0424-5, PMID:20127241.

*Journal of Clinical and Translational Hepatology* **2022** vol. 10(4) | 651–659
DOI: 10.14218/JCTH.2021.00347

Original Article

# 1,5-Anhydroglucitol Predicts Mortality in Patients with HBV-Related Acute-on-chronic Liver Failure

Lingjian Zhang[#], Yalei Zhao[#], Zhongyang Xie, Lanlan Xiao, Qingqing Hu, Qian Li, Shima Tang, Jie Wang and Lanjuan Li[*]

*State Key Laboratory for Diagnosis and Treatment of Infectious Diseases, National Clinical Research Center for Infectious Diseases, Collaborative Innovation Center for Diagnosis and Treatment of Infectious Diseases, The First Affiliated Hospital, College of Medicine, Zhejiang University, Hangzhou, Zhejiang, China*

**Received:** 19 August 2021 | **Revised:** 18 October 2021 | **Accepted:** 3 November 2021 | **Published:** 10 January 2022

## Abstract

***Background and Aims:*** 1,5-Anhydroglucitol (1,5AG) activity has been reported in chronic liver disease. Hepatitis B virus (HBV)-related acute-on-chronic liver failure (HBV-ACLF) patients have a high mortality. We aimed to discover the relationship between serum 1,5AG and the prognosis of HBV-ACLF. ***Methods:*** Serum 1,5AG levels were determined in 333 patients with HBV-ACLF, 300 without diabetes were allocated to derivation (n=206) and validation cohorts (n=94), and 33 were recruited to evaluate 1,5AG in those with diabetes. Forty patients with chronic hepatitis B, 40 with liver cirrhosis, and 40 healthy people were controls in the validation cohort. ***Results:*** In the derivation and validation cohorts, serum 1,5AG levels were significantly lower in nonsurvivors than in survivors. The AUC of 1,5AG for 28-day mortality was 0.811. In patients with diabetes, serum 1,5AG levels were also significantly lower in nonsurvivors than in survivors. In multivariate Cox regression analysis, serum 1,5AG levels were independently associated with 28-day mortality. A novel predictive model (ACTIG) based on 1,5AG, age, TB, cholesterol, and INR was derived to predict mortality. In ACTIG, the AUC for 28-day mortality was 0.914, which was superior to some prognostic score models. ACTIG was also comparable to those prognostic score models in predicting 6-month mortality. In mice with D-galactosamine/ lipopolysaccharide-induced liver failure, 1,5AG levels were significantly reduced in serum and significantly increased in urine and liver tissue. ***Conclusions:*** Serum 1,5AG levels are a promising predictor of short-term mortality in HBV-ACLF patients. The 1,5AG distribution changed in mice with D-galactosamine/ lipopolysaccharide-induced liver failure.

**Citation of this article:** Zhang L, Zhao Y, Xie Z, Xiao L, Hu Q, Li Q, *et al*. 1,5-Anhydroglucitol Predicts Mortality in Patients with HBV-Related Acute-on-chronic Liver Failure. J Clin Transl Hepatol 2022;10(4):651–659. doi: 10.14218/JCTH.2021.00347.

## Introduction

Acute-on-chronic liver failure (ACLF) is associated with high short-term mortality,[1,2] and hepatitis B virus (HBV) is a frequent etiology of ACLF in Asia.[3] The high mortality of HBV-ACLF had made it valuable to find novel markers to predict the prognosis.[4,5] 1,5-Anhydroglucitol (1,5AG) is obtained mainly from food, and nearly 99.9% is reabsorbed by glucose transporters in renal tubules to form a stable metabolic pool.[6] Because glucose competitively inhibits reabsorption,[7] 1,5AG is used as a biomarker to reflect glucose control and postprandial plasma glucose in diabetes.[8] 1,5AG activity has been reported in various diseases, including acute coronary syndrome, diabetes and end-stage renal disease.[9–11]

Yamagishi *et al*. found that 1,5AG levels were significantly reduced in cirrhotic patients compared with healthy people,[12] Koga *et al*. reported decreased serum 1,5AG levels in chronic liver disease and that low serum 1,5AG levels were linked to impaired liver function.[13] 1,5AG can be biosynthesized in the liver,[6,13,14] and previous research from our laboratory on plasma metabolites indicated that 1,5AG was a potential marker of liver regeneration in a rat model.[15] However, a relationship between HBV-ACLF and serum 1,5AG levels has not been reported. Here, we explored the correlation between serum 1,5AG levels and the prognosis of HBV-ACLF for the first time. We confirmed our results in a mouse model of D-galactosamine- and lipopolysaccharide (D-GaIn/LPS)-induced liver failure.

## Methods

### *Study population*

A group of 384 HBV-ACLF patients were recruited from May

**Keywords:** Acute-on-chronic liver failure; 1,5-anhydroglucitol; Prognosis.
**Abbreviations:** 1, 5AG, 1,5-anhydroglucitol; ACLF, acute-on-chronic liver failure; AFP, alpha-fetoprotein; ALP, alkaline phosphatase; ALT, alanine aminotransferase; AST, aspartate aminotransferase; AUC, area under the receiver operating curve; BUN, blood urea nitrogen; CHB, chronic hepatitis B; CLIF-C ACLF, Chronic Liver Failure Consortium Acute-on-Chronic Liver Failure score; COSSH-ACLF, Chinese Group on the Study of Severe Hepatitis B; D-GaIN, D-galactosamine; GGT, γ-glutamyl transpeptidase; HBV, hepatitis B virus; HC, healthy controls; HE, hepatic encephalopathy; HR, hazard ratio; INR, international normalised ratio; LC, liver cirrhosis; LPS, lipopolysaccharide; MELD, Model for End-stage Liver Disease score; TB, total bilirubin; TBA, total bile acid.

[#]Contributed equally to this work.
[*]**Correspondence to**: Lanjuan Li, Chief of Key Laboratory of Infectious Diseases, State Key Laboratory for Diagnosis and Treatment of Infectious Diseases, The First Affiliated Hospital, School of Medicine, Zhejiang University, Hangzhou, Zhejiang 310003, China. ORCID: https://orcid.org/0000-0001-6945-0593. Tel/Fax: +86-571-87236459, E-mail: ljli@zju.edu.cn

1, 2017, to December 31, 2020 at the First Affiliated Hospital, College of Medicine, Zhejiang University. Fifty-one were excluded, 300 without diabetes were separated into derivation ($n$=206) and validation cohorts ($n$=94), and a third cohort of 33 patients was recruited to evaluate 1,5AG in those with diabetes. Forty healthy controls (HC), 40 liver cirrhosis (LC) patients, and 40 chronic hepatitis B (CHB) patients were controls in the validation cohort. Exclusion characteristics were the presence of renal disease, hepatocellular carcinoma, extrahepatic malignancies, <18 years of age, pregnancy, other serious systemic diseases pre-existing liver disease (autoimmune liver disease, schistosomiasis disease, alcoholic liver disease, and so on). Fifty-one patients were excluded. Sixteen did not satisfy the Asian Pacific Association for the Study of the Liver ACLF criteria, five for lack of follow-up, six for hepatocellular carcinoma, three for extrahepatic malignancies, fourteen for pre-existing liver diseases, two for pre-existing renal diseases, and five for incomplete data.

HBV-ACLF was diagnosed by the Asian Pacific Association for the Study of the Liver criteria as previously described.[16] CHB was diagnosed by the 2009 American Association for the Study of Liver Diseases guidelines, and LC was diagnosed according to the 2012 North American consortium for the study of end-stage liver disease experience.[17–19] Prognostic score models, including the Model for End-Stage Liver Disease (MELD),[20] iMELD,[21] MELD-Na,[22] Chinese Group on the Study of Severe Hepatitis B (COSSH-ACLF),[23] and Chronic Liver Failure Consortium Acute-on-Chronic Liver Failure (CLIF-C ACLF)[24] were used to predict 28-day and 6-month mortality.

The study was approved by the Ethics Committee of the First Affiliated Hospital, College of Medicine, Zhejiang University and was conducted in compliance with the principles of the 1975 Declaration of Helsinki. Subjects gave informed consent to participate in the study. All animal experiments were performed under sodium pentobarbital anesthesia to minimize suffering and were approved by the Ethics Committee of the First Affiliated Hospital, Zhejiang University School of Medicine.

### *Animals*

Male C57BL/6J mice (20–25 g) were obtained from Beijing Vital River Laboratory Animal Technology Corporation. Liver injury was induced by injection of 400 mg/kg D-GaIN and 10 μg/kg LPS (Sigma, St Louis, MO, USA). Mice were sacrificed 6 h after injection, and liver tissue, urine and blood were collected for analysis. The survival of mice in the study groups was continuously monitored every 2 h for 24 h, and 24 mice (12 per group) were used.

### *Biochemical assays*

Serum, liver tissue, and urine were stored at −80ºC before use. 1,5AG was determined with ELISA kits (Abbexa, Cambridge, UK). ALT, AST, and serum glucose levels were determined with commercial kits (Jiancheng Bioengineering Institute, Nanjing, Jiangsu, China).

### *Statistical analysis*

Statistical analysis was performed with MEDCALC (Ostend, Belgium) and SPSS 18.0 (SPSS Inc., Chicago, IL, USA). Continuous variables were reported as means ± standard deviation \or medians with interquartile range. Differences were compared with Student's $t$-test, Mann-Whitney U tests, one-way analysis of variance or Kruskal-Wallis H tests, as appropriate. Categorical variables were reported as numbers and percentages (%), and differences were compared with chi-squared or Fisher's exact tests. Multivariate analysis of independent prognostic factors for HBV-ACLF was performed using Cox regression. Cumulative survival rates were compared by the Kaplan-Meier method and log-rank tests.

## Results

### *Patient baseline characteristics*

From 1 May 2017, to 31 December 2020, 384 patients with HBV-ACLF were enrolled. Based on the exclusion criteria, 51 were not included in the analysis, 83.5% of the derivation cohort. were men, and 34.0% died or underwent liver transplantation within 28 days. At 28 days the nonsurvivors were older ($p$=0.005), had higher white blood cell ($p$=0.008) and neutrophil ($p$=0.002) counts, higher total bilirubin (TB, $p$<0.001), hepatic encephalopathy (HE) grade ($p$<0.001), hypoglycemia ($p$=0.040), international normalized ratio (INR, $p$<0.001), ammonia ($p$=0.002), and blood urea nitrogen (BUN, $p$=0.005) than the survivors (Table 1). 1,5AG ($p$<0.001), triglycerides ($p$<0.001), cholesterol ($p$<0.001), alpha fetoprotein (AFP, $p$=0.001), and gamma glutamyl transpeptidase (GGT, $p$=0.007) were significantly higher in survivors than in nonsurvivors (Table 1). The incidence of organ failure including the liver ($p$=0.004), brain ($p$=0.006), and coagulation ($p$<0.001), was significantly higher in nonsurvivors (Table 1). The MELD, iMELD, MELD-Na, COSSH-ACLF and CLIF-C ACLF scores were also significantly higher in nonsurvivors (Table 1, all $p$<0.001). The clinical data of the validation cohort are shown in Supplementary Table 1.

### *Serum 1,5AG levels in HBV-ACLF*

As shown in Figure 1A, serum 1,5AG levels were lower in nonsurvivors than in survivors ($p$<0.001) in the derivation and validation cohorts. As the number of failed organs increased in the derivation cohorts, the serum 1,5AG levels significantly decreased ($p$<0.001, Fig. 1B). In the validation cohort, serum 1,5AG was significantly lower in HBV-ACLF nonsurvivors than in survivors and in the HC, CHB, and LC groups ($p$<0.05, Fig. 1C). 1,5AG levels were higher in the HC the than in the CHB and LC groups and the HBV-ACLF survivors and nonsurvivors ($p$<0.05, Fig. 1C). The characteristics of patients in the HC, CHB, and LC groups are shown in Supplementary Table 2. Patients in the LC group were older than those in the CHB, HC and HBV-ACLF groups. There were no significant sex differences of the four groups.

1,5AG levels in HBV-ACLF in 33 patients with diabetes are shown in Figure 1I. Serum 1,5AG levels were significantly lower in nonsurvivors ($p$<0.05) and lower in those with diabetes than without diabetes ($p$<0.01, Fig. 1H). In HBV-ACLF survivors, serum 1,5AG levels were also significantly lower in patients with diabetes ($p$<0.01, Supplementary Fig. 1A). In the nonsurvivor groups, there were no significant differences in serum 1,5AG levels between HBV-ACLF patients with and without diabetes ($p$=0.457, Supplementary Fig. 1B). The clinical characteristics of patients with diabetes are shown in Supplementary Table 3.

Correlations of serum 1,5AG levels and the laboratory values in the derivation cohort are shown in Supplementary Figure 3. Serum 1,5AG had a moderately positive correlation with serum uric acid ($r$=0.307) in patients without pre-existing hyperuricemia and a moderately negative

**Table 1. Baseline characteristics of the derivation cohort**

| Characteristic | HBV-ACLF (*n*=206) | | *p* |
|---|---|---|---|
| | Survivors (*n*=136) | Nonsurvivors (*n*=70) | |
| Age, years | 45.4±12.6 | 51.2±10.5 | 0.005 |
| Male sex | 109 (80.1) | 63 (90.0) | 0.071 |
| BMI (kg/m$^2$) | 24.0±3.6 | 23.5±3.6 | 0.358 |
| Liver cirrhosis | 72 (52.9) | 41 (58.6) | 0.442 |
| Complications | | | |
| Gastrointestinal hemorrhage | 5 (3.7) | 7 (10.0) | 0.128 |
| Ascites | 74 (54.4) | 38 (54.3) | 0.986 |
| Infection | 55 (40.4) | 33 (47.1) | 0.357 |
| HE | | | |
| I–II | 14 (10.3) | 19 (27.1) | <0.001 |
| III–IV | 4 (2.9) | 10 (14.3) | |
| Laboratory data | | | |
| ALT (U/L) | 160.5 (89.0, 376.5) | 255.0 (105.5, 405.0) | 0.258 |
| AST (U/L) | 128.5 (76.0, 214.0) | 147.0 (88.5, 230.8) | 0.263 |
| ALP (U/L) | 133.0 (108.0, 157.5) | 126.0 (107.8, 150.8) | 0.455 |
| Albumin (g/dL) | 31.2±4.0 | 31.7±4.5 | 0.478 |
| TB (μmol/L) | 327.9±109.8 | 412.4±126.5 | <0.001 |
| TBA (μmol/L) | 280.0±116.8 | 264.5±116.1 | 0.371 |
| GGT (U/L) | 79.0 (57.0, 116.5) | 62.0 (41.8, 106.0) | 0.007 |
| Creatinine (μmol/L) | 66.0 (55.0, 75.0) | 65.5 (55.0, 94.5) | 0.143 |
| BUN (mmol/L) | 4.0 (2.9, 5.4) | 4.7 (3.4, 6.8) | 0.005 |
| Triglycerides (mmol/L) | 1.3 (1.1, 1.8) | 1 (0.8, 1.3) | <0.001 |
| Uric acid (μmol/L) | 143.1±45.9 | 130.0±47.6 | 0.057 |
| Cholesterol (mmol/L) | 2.4±0.9 | 2.0±0.7 | <0.001 |
| White blood cell count ($10^9$/L) | 7.1±3.0 | 8.3±3.6 | 0.008 |
| Neutrophil count ($10^9$/L) | 4.9±2.7 | 6.3±3.3 | 0.002 |
| Hemoglobin (g/L) | 122.3±23.0 | 123.0±19.7 | 0.827 |
| Platelet count ($10^9$/L) | 112.5±57.4 | 101.6±51.2 | 0.183 |
| INR | 1.8 (1.6, 2.1) | 2.6 (2.1, 3.1) | <0.001 |
| Lg (DNA) | 5.2±1.6 | 5.9±1.9 | 0.010 |
| Ferritin (ng/mL) | 2,587.2 (1,525.5, 4,025.1) | 3,149.8 (1,866.8, 5,184.5) | 0.069 |
| AFP (ng/mL) | 154.5 (50.3, 353.8) | 49.1 (18.7, 186.7) | 0.001 |
| Sodium (mmol/L) | 137.7±3.4 | 137.8±4.6 | 0.852 |
| Serum ammonia (μmol/L) | 49.5±25.5 | 66.3±37.0 | 0.002 |
| Blood glucose (mmol/L) | 4.0 (3.4, 4.6) | 4.3 (3.4, 5.6) | 0.240 |
| Hypoglycemia (no.) | 8 (5.9) | 10 (14.5) | 0.040 |
| 1,5AG (μg /mL) | 36.7±12.5 | 23.3±8.7 | <0.001 |
| Organ failure | | | |
| Liver | 115 (84.6) | 69 (98.6) | 0.004 |
| Coagulation | 10 (7.4) | 41 (58.6) | <0.001 |
| Kidney | 0 (0.0) | 3 (4.3) | 0.069 |
| Brain | 4 (2.9) | 10 (14.3) | 0.006 |

*(continued)*

**Table 1.** - *(continued)*

| Characteristic | HBV-ACLF (*n*=206) | | *p* |
|---|---|---|---|
| | Survivors (*n*=136) | Nonsurvivors (*n*=70) | |
| Lung | 0 (0.0) | 1 (1.4) | 0.340 |
| Circulation | 0 (0.0) | 1 (1.4) | 0.340 |
| Severity score | | | |
| MELD | 21.2±3.7 | 27.4±6.4 | <0.001 |
| MELD-Na | 21.9±4.4 | 28.5±7.0 | <0.001 |
| iMELD | 38.4±6.3 | 46.4±8.6 | <0.001 |
| CLIF-C ACLF | 37.6±6.4 | 46.6±7.4 | <0.001 |
| COSSH-ACLF | 4.8±0.5 | 6.0±1.1 | <0.001 |
| HBV-ACLF (COSSH criteria) | | | |
| ACLF grade 1 | 126 (92.6) | 28 (40.0) | <0.001 |
| ACLF grade 2 | 9 (6.6) | 30 (42.9) | |
| ACLF grade 3 | 1 (0.7) | 12 (17.1) | |

Data are means ± standard deviation, numbers (%), or medians (interquartile range), as shown. 1,5AG, 1,5-anhydroglucitol; AFP, Alpha fetoprotein; ALP, Alkaline phosphatase; ALT, Alanine aminotransferase; AST, Aspartate aminotransferase; BUN, Blood urea nitrogen; CLIF-C ACLF, Chronic Liver Failure Consortium Acute-on-Chronic Liver Failure score; COSSH-ACLF, Chinese Group on the Study of Severe Hepatitis B; GGT, γ-glutamyl transpeptidase; HE, Hepatic encephalopathy; iMELD, Integrated MELD. INR, International normalized ratio; MELD-Na, MELD sodium; MELD, Model for End-stage Liver Disease score; TB, Total bilirubin; TBA, Total bile acid.

correlation with INR ($r$= −0.353, Supplementary Fig. 3A). Serum 1,5AG levels were not significantly correlated with AFP ($r$=0.078), BMI ($r$=0.095), blood glucose ($r$=−0.017), BUN ($r$=−0.122), TB ($r$=−0.106), or creatinine ($r$=−0.124, Supplementary Fig. 3A). Serum 1,5AG levels were also negatively correlated with COSSH-ACLF ($r$=−0.370), CLIF-C ACLF ($r$=−0.327), MELD ($r$=−0.323), iMELD ($r$=−0.318), and MELD-Na ($r$=−0.312) prognosis scores (Supplementary Fig. 3B). We confirmed the correlations in the validation cohort (Supplementary Fig. 4).

### *Predictive ability of serum 1,5AG levels for 28-day and 6-month mortality*

The predictive ability of serum 1,5AG levels for 28-day mortality was investigated in the derivation cohorts. The area under the receiver operating characteristic curve (AUC) of serum 1,5AG levels alone was 0.811 (Fig. 1D). Patients were stratified into low- and high-1,5AG groups using the optimal 1,5AG cutoff value of 29.5 μg/mL. The 28-day mortality was significantly higher in the low-1,5AG group ($p$<0.001, Fig. 1F). The sensitivity was 0.800 and specificity was 0.654. We confirmed the results in the validation cohort (Supplementary Fig. 2A and C). The predictive ability of serum 1,5AG in HBV-ACLF patients with diabetes was 0.763 (Supplementary Fig. 1C).

Six-month mortality was estimated in the derivation, validation, and HBV-ACLF with diabetes cohorts. Four patients lost to follow-up. The predictive ability of serum 1,5AG levels alone was 0.737 in the derivation cohort (Fig. 1E), 0.728 in the validation cohort (Supplementary Fig. 2B) and 0.688 in the HBV-ACLF with diabetes cohort (Supplementary Fig. 1D). Mortality was significantly higher in the low-1,5AG than in the high-1,5AG group in the derivation and validation cohorts ($p$<0.001; Figs 1G and 2D).

### *Independent prognostic predictors for short-term mortality*

In the derivation cohort, univariate Cox analysis found that HE grades, age, TB, creatinine, triglycerides, cholesterol, white blood cell count, neutrophil count, INR, Lg (DNA), ferritin, AFP, and serum 1,5AG levels (Table 2) were high-risk factors for the 28-day mortality of HBV-ACLF. Multivariate Cox regression indicated that serum 1,5AG level [(hazard ratio (HR) 0.918, $p$<0.001), TB level (HR 1.003, $p$=0.003), age (HR 1.026, $p$=0.022), INR (HR 3.724, $p$<0.001) and cholesterol level (HR 0.619, $p$=0.007)] were independent prognostic predictors of 28-day mortality of HBV-ACLF (Table 2).

A predictive model was developed from the multivariate Cox regression analysis with ACTIG=0.026×age+0.003×TB+1.315×INR−0.085×1,5AG−0.480×cholesterol. The AUC for 28-day mortality of the ACTIG model was 0.914, which was superior to those of MELD-Na (0.801, $p$<0.001), iMELD (0.774, $p$<0.001), MELD (0.812, $p$<0.001), COSSH-ACLF (0.861, $p$=0.028) and CLIF-C ACLF (0.825, $p$=0.002) for predicting 28-day mortality (Table 3, Fig. 2A). In predicting 6-month mortality (Table 3, Fig. 2B), ACTIG (0.865) was also comparable to that of MELD-Na (0.818, $p$=0.147), iMELD (0.805, $p$=0.069), MELD (0.825, $p$=0.206), COSSH-ACLF (0.857, $p$=0.751) and CLIF-C ACLF (0.820, $p$=0.136). Nonsurvivors had a significantly higher ACTIG score than survivors in the derivation and validation cohorts (Fig. 2C). We divided patients into high- and low-ACTIG groups by the cutoff value of 0.710. The 28-day and 6-month mortality of the high-ACTIG group was significantly higher than that of the low-ACTIG group ($p$<0.001, Fig. 2D and E). We confirmed the new model in the validation cohort (Supplementary Table 4, Fig. 2G and H) and HBV-ACLF patients with diabetes (Supplementary Fig. 1E and F).

### *1,5AG levels in D-GaIN/LPS-induced liver failure*

Previous studies reported that 1,5AG remains steady in blood, tissues and urine.[25,26] Therefore, the distribution balance of 1,5AG may be disrupted in ACLF patients. As HBV-ACLF does not have a standard animal model, we investigated 1,5AG levels in D-GaIN/LPS-induced liver failure. LPS/D-GaIN-treated mice began to die at 6 h, and the mortality rate was 75% (Fig. 3B). As shown in Figure 3B, serum ALT ($p$=0.014) and AST ($p$<0.001) levels were significantly increased in the D-

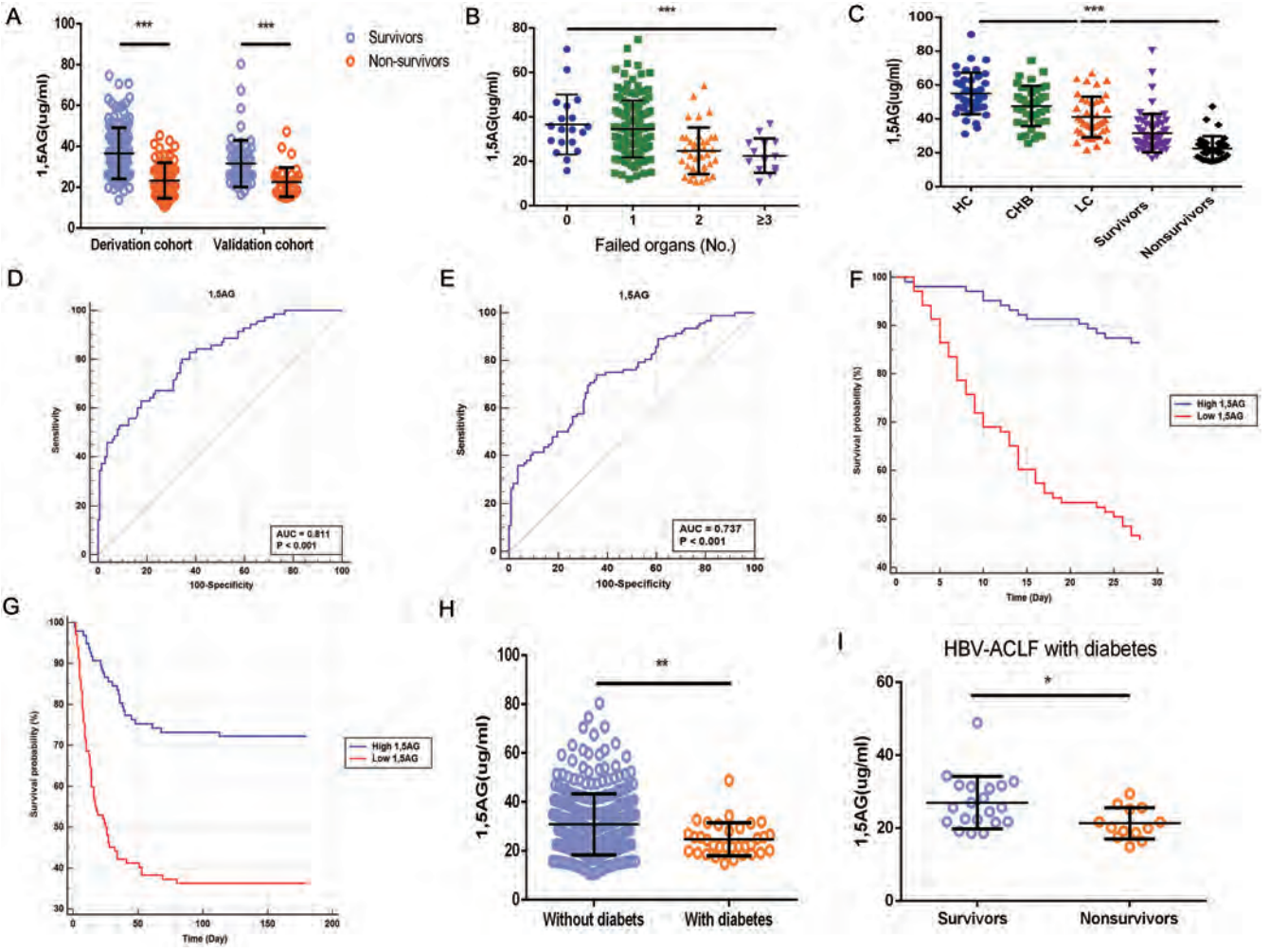


**Fig. 1. Serum 1,5-Anhydroglucitol (1,5AG) levels in patients with hepatitis B virus related acute-on-chronic liver failure (HBV-ACLF) and ability to predict 28 day and 6-month mortality.** Distribution of serum 1,5AG levels in the derivation and validation cohorts (a). Serum 1,5AG levels decreased with increasing failed organ numbers in the derivation cohort (b). Serum 1,5AG levels were significantly lower in HBV-ACLF nonsurvivors than in the survivors and the healthy controls (HC), chronic hepatitis B (CHB), and liver cirrhosis (LC) groups (c). Prediction of 28-day (d) and 6-month (e) mortality by serum 1,5AG levels in the derivation cohorts. Survival rates at 28 days (f) and 6 months (g) at high- and low serum 1,5AG levels in the derivation cohort. Serum 1,5AG levels in HBV-ACLF patients with and without diabetes (h). Serum 1,5AG level distribution in HBV-ACLF patients with diabetes (i). *$p<0.05$, **$p<0.01$ and ***$p<0.001$.

GaIN/LPS group at 6 h. Hematoxylin–eosin staining showed liver architecture disruption, vacuolization, disappearance of nuclei, ballooned hepatocytes, and severe tissue hemorrhage (Fig. 3A). Assays of 1,5AG concentration in serum, urine and liver tissue found that the 1,5AG levels were significantly reduced in serum ($p=0.001$, Fig. 3C) and significantly increased in urine ($p=0.005$, Fig. 3C) and liver tissue ($p.=0.009$, Fig. 3C) in the D-GaIN/LPS group. We also found lower glucose levels in the D-GaIN/LPS group ($p<0.001$, Fig. 3B).

## Discussion

Because of the high mortality of liver failure,[1] accurate biomarkers of prognosis are valuable. Here, we showed for the first time that serum 1,5AG levels were predictive of the 28-day and 6-month mortality of HBV-ACLF patients. We showed that serum 1,5AG levels were also significantly lower in HBV-ACLF nonsurvivors than in the survivors and the HC, CHB, and LC groups. In accord with previous studies,[12,13] we found lower serum 1,5AG levels in the LC and CHB groups than in the HC group. According to the optimal cutoff value, patients with lower serum 1,5AG levels had significantly higher 28 day and 6-month mortality. The results were validated in another cohort of HBV-ACLF patients, which strengthens the reliability of the predictive ability. It is well known that 1,5AG is related to diabetes. Thus, we also investigated 1,5AG levels in HBV-ACLF patients with diabetes. Serum 1,5AG levels were significantly lower in HBV-ACLF patients with diabetes. In patients with diabetes, we also found that serum 1,5AG levels were markedly lower in nonsurvivors than in survivors. Because of the small sample size, the association between serum 1,5AG levels and the prognosis of HBV-ACLF with diabetes needs to be confirmed in further studies.

Moreover, in multivariate Cox regression analysis of 28-day mortality, serum 1,5AG levels remained an independent prognostic factor when analyzed together with clinical parameters. We developed a new predictive model that was superior to MELD-Na, iMELD, MELD, COSSH-ACLF and CLIF-C ACLF in predicting 28-day mortality. It was also comparable to MELD-Na, iMELD, MELD, COSSH-ACLF and CLIF-C ACLF in predicting 6-month mortality. To our knowledge, there are only a few

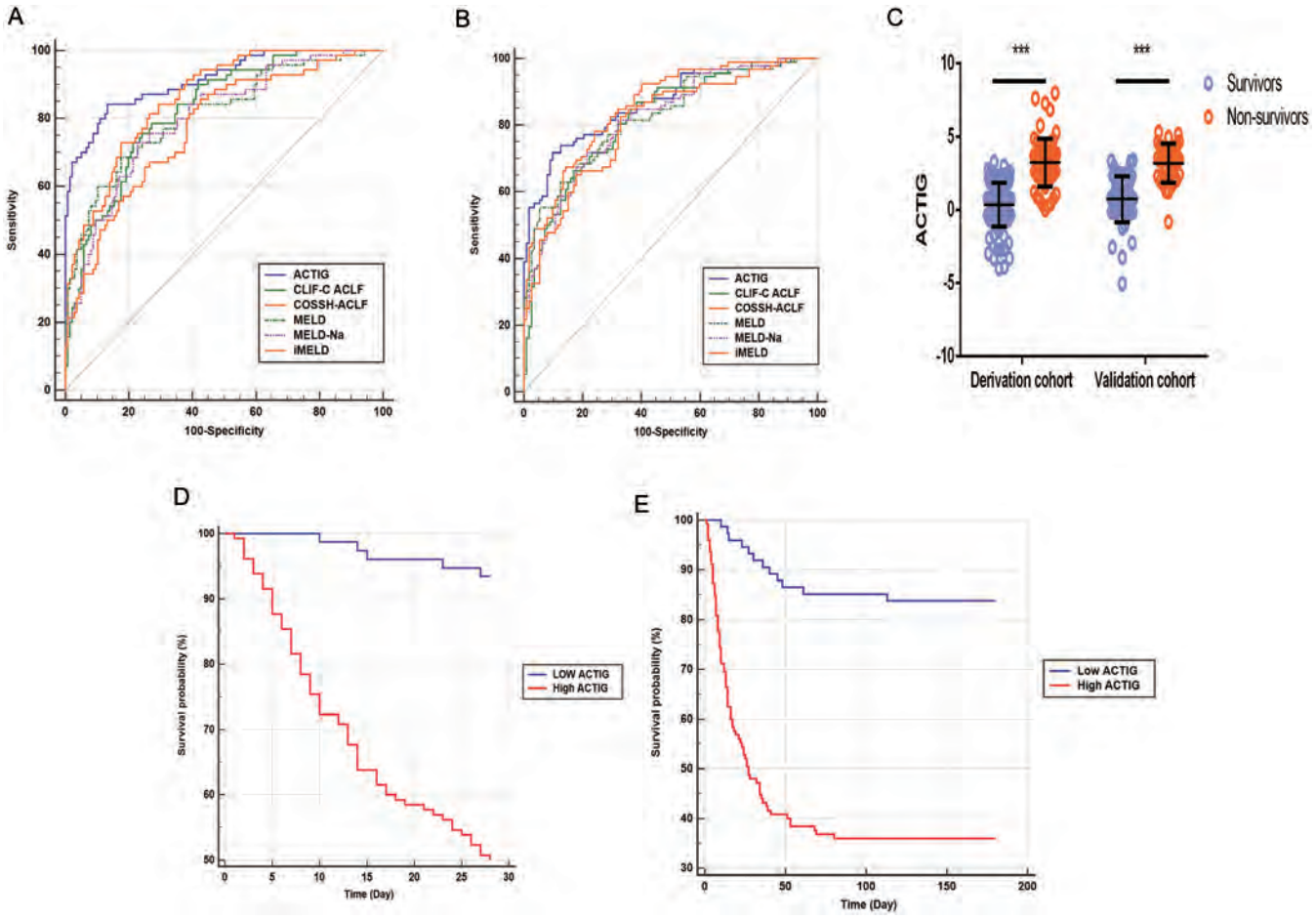


**Fig. 2. Prediction of 28 day and 6-month mortality of patients with HBV-ACLF, by ACTIG and other scores.** Prediction of 28 day (a), and 6-month (b), mortality in the derivation cohorts. ACTIG score distribution in both the derivation and validation cohorts (c). Survival rates at 28 days (d), and 6 months (e), in the low- and high-ACTIG score groups in the derivation cohort. ***$p$<0.001.

**Table 2. Independent risk factors for 28-day mortality**

| Variable | Univariate Cox regression model | | Multivariate Cox regression model | |
|---|---|---|---|---|
| | HR (CI 95 %) | *p* | HR (CI 95 %) | *p* |
| Age, years | 1.030 (1.011–1.050) | 0.002 | 1.026 (1.004–1.049) | 0.022 |
| HE | 2.248 (1.647–3.068) | <0.001 | | |
| TB (μmol/L) | 1.005 (1.003–1.007) | <0.001 | 1.003 (1.001–1.005) | 0.003 |
| Creatinine (μmol/L) | 1.012 (1.007–1.016) | <0.001 | | |
| Triglycerides (mmol/L) | 0.233 (0.117–0.465) | <0.001 | | |
| Cholesterol (mmol/L) | 0.526 (0.364–0.761) | 0.001 | 0.619 (0.437–0.876) | 0.007 |
| White blood cell count ($10^9$/L) | 1.101 (1.032–1.175) | 0.003 | | |
| Neutrophil count ($10^9$/L) | 1.129 (1.056–1.207) | <0.001 | | |
| INR | 2.901 (2.352–3.577) | <0.001 | 3.724 (2.583–5.368) | <0.001 |
| Lg (DNA) | 1.203 (1.048–1.382) | 0.009 | | |
| Ferritin | 1.000 (1.000–1.000) | 0.020 | | |
| AFP | 0.999 (0.997–1.000) | 0.016 | | |
| 1,5AG | 0.904 (0.878–0.930) | <0.001 | 0.918 (0.890–0.948) | <0.001 |

1,5AG, 1,5-anhydroglucitol; AFP, Alpha fetoprotein; HE, Hepatic encephalopathy; INR, International normalized ratio; TB, Total bilirubin; HR, Hazard ratio.

**Table 3. Comparison of the predictive value for patients with HBV-ACLF in derivation cohorts**

| Model | 28-day mortality | | | 6-month mortality | | |
|---|---|---|---|---|---|---|
| | AUC (95% CI) | *Z*-value | *p*-value | AUC (95% CI) | Z-value | *p*-value |
| *n*=206 | | | | *n*=204 | | |
| ACTIG | 0.914 (0.867–0.948) | | | 0.865 (0.810–0.908) | | |
| MELD | 0.812 (0.752–0.863) | 3.464 | <0.001 | 0.825 (0.766–0.875) | 1.266 | 0.206 |
| MELD-Na | 0.801 (0.740–0.853) | 3.753 | <0.001 | 0.818 (0.759–0.869) | 1.452 | 0.147 |
| iMELD | 0.774 (0.710–0.829) | 4.497 | <0.001 | 0.805 (0.744–0.857) | 1.816 | 0.069 |
| CLIF-C ACLFs | 0.825 (0.766–0.874) | 3.085 | 0.002 | 0.820 (0.760–0.870) | 1.490 | 0.136 |
| COSSH-ACLFs | 0.861 (0.806–0.905) | 2.204 | 0.028 | 0.857 (0.801–0.902) | 0.318 | 0.751 |

CLIF-C ACLF, Chronic Liver Failure Consortium Acute-on-Chronic Liver Failure score; COSSH-ACLF: Chinese Group on the Study of Severe Hepatitis B; MELD: Model for End-stage Liver Disease score; MELD-Na: MELD sodium; iMELD: Integrated MELD.

studies evaluating the association of 1,5AG level with liver diseases.[12,13] 1,5AG levels have not been studied thus far in ACLF patients. All the results demonstrated that the serum 1,5AG level is a promising biomarker for HBV-ACLF.

As an animal model, LPS/GaIN has been widely used to mimic clinical liver dysfunction.[27] We found that 1,5AG levels were significantly reduced in serum and significantly increased in urine and liver tissue in mice with D-GaIN/LPS-induced liver failure. That indicates that the distribution balance of 1,5AG was changed. Small amounts of 1,5AG are synthesized in the liver by the anhydrofructose pathway.[14] However, most 1,5AG originates from food, so impaired hepatic synthesis cannot explain the reduced serum 1,5AG levels.[13] It also cannot explain the increase in 1,5AG levels in the liver in our mouse model. It has been reported that 1,5AG remains balanced in blood, tissues and urine.[25] Koga *et al*.[13] found a correlation between 1,5AG levels and serum uric acid. [28] Uric acid is also reabsorbed in renal tubules. Therefore, they proposed that the low serum 1,5AG levels in patients with chronic liver disease may be associated with renal tubular dysfunction. According to a previously published study, patients with jaundice developed hypouricemia that

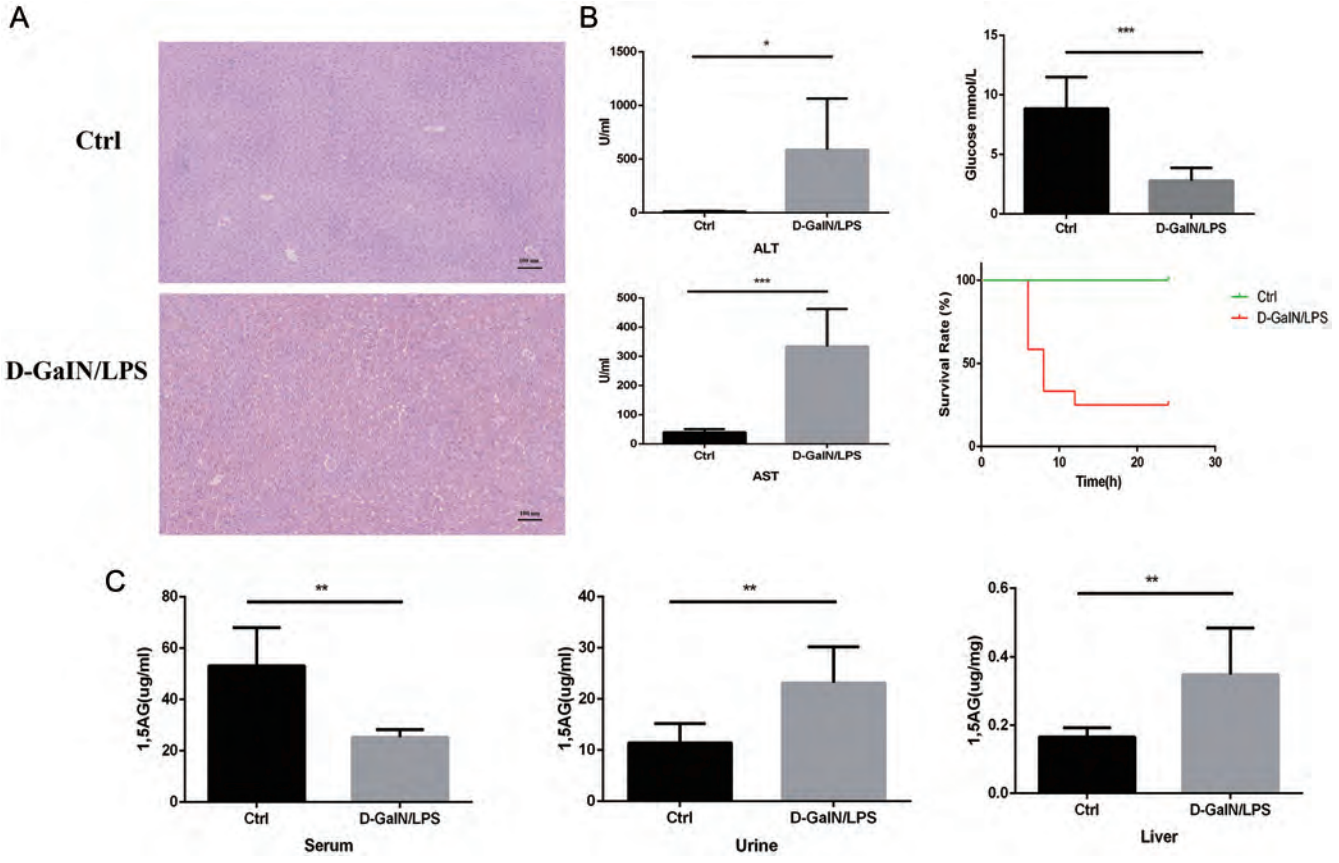


**Fig. 3. 1,5AG concentration in the D-galactosamine and lipopolysaccharide (D-GaIN/LPS)-induced liver failure model.** Hematoxylin–eosin-stained liver sections (100×). (a) Serum glucose, aspartate aminotransferase (AST) and alanine aminotransferase (ALT) levels in mice (*n*=6). (b) Survival rate of D-GaIN/LPS-induced liver failure (*n*=12). (b) 1,5AG concentration in serum (*n*=6), urine (*n*=6) and liver tissue (*n*=6). (c) **p*<0.05, ***p*<0.01 and ****p*<0.001.

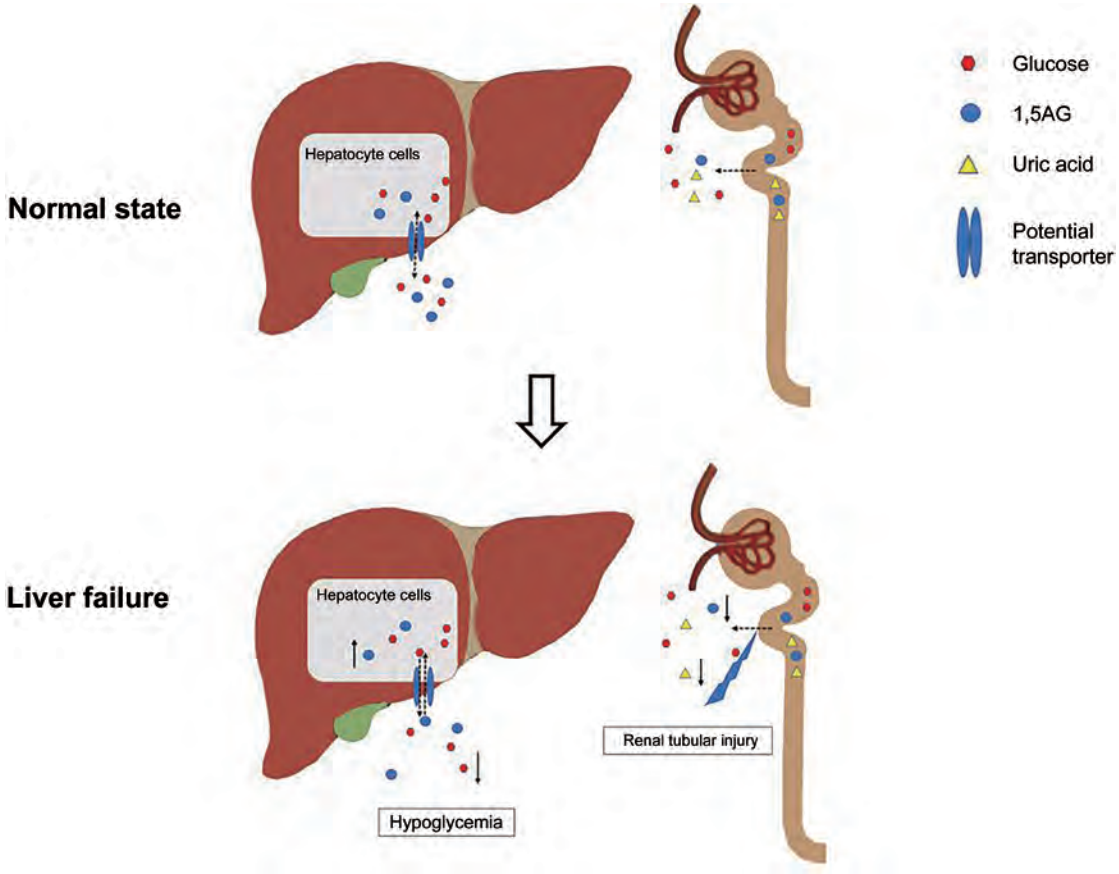


**Fig. 4. Potential low-level expression of 1,5-Anhydroglucitol (1,5AG) in liver failure.** 1,5AG, glucose and uric acid are reabsorbed in renal tubules. 1,5AG and glucose may share the same transporter and are competitive with each other in hepatocytes. Renal tubular injury decreases the reabsorption of 1,5AG and uric acid. The reduced blood glucose level causes 1,5AG to flow into hepatocytes.

was associated with renal tubular dysfunction.[29] However, they did not investigate urinary excretion of 1,5AG in chronic liver disease patients. Another study also found that serum 1,5AG and urinary excretion 1,5AG were closely correlated with urine N-acetyl-beta-glucosaminidase, which may indicate renal tubular damage.[30] Renal injury is a common complication of ACLF and is always related to poor outcomes.[31] We found a correlation between uric acid and serum 1,5AG levels in our HBV-ACLF patients. In our mouse model, 1,5AG levels were significantly increased in urine, but we did not find significant correlations between 1,5AG and creatinine and BUN. Creatinine is a marker of glomerular filtration function but not kidney tubular injury.[32] BUN cannot accurately reflect kidney function in patients with end-stage liver disease.[33] Based on those studies and our results, low serum 1,5AG levels in HBV-ACLF patients may be partly related to the decrease in reabsorption of 1,5AG caused by renal tubular injury, as illustrated by Figure 4. A future study may be required to detect specific biomarkers of renal tubular injury may be required to confirm the results.

However, the significantly increased 1,5AG levels in liver tissue still need to be explained. Serum 1,5AG levels were reported to dramatically increase during the oral glucose tolerance test.[34] An in vitro study found that after an acute glucose load, 1,5AG in the culture medium of hepatocytes increased slightly rather than declining. 1,5AG and glucose may share the same transporter and are competitive with each other in hepatocytes.[26] It is known that glucose metabolism is impaired during liver disease.[35] Our mouse model showed hypoglycemia, which may explain the increased 1,5AG levels in liver tissue. The HBV-ACLF nonsurvivor group also displayed a higher percentage of hypoglycemia. However, we did not find a significant relation between serum 1,5AG levels and blood glucose. The relationship between serum 1,5AG levels and blood glucose in ACLF should be investigated in the future.

Several study limitations may have influenced the results. First, the prognostic predictive ability of serum 1,5AG levels was only observed in a single center study with a retrospective cohort study. The result should be assessed in multicenter prospective studies. Second, our research only included ACLF patients with HBV infection, and the prognostic value of 1,5AG in liver failure caused by other etiologies needs further confirmation. Third, the D-GaIN/LPS-induced liver failure model cannot fully reflect the pathophysiological changes in ACLF patients, and we may need a better model to verify the results.

In summary, serum 1,5AG levels were a promising predictor of short-term mortality in patients with HBV-ACLF. 1,5AG distribution changed in a D-GaIN/LPS-induced liver failure model.

## Acknowledgments

We thank the Key research and development project of Department of Science and Technology of Zhejiang Province (2017C03051), Science Fund for Creative Research

Groups of the National Natural Science Foundation of China (No.81721091) and the National Natural Science Foundation of China (81900572) for supporting us.

## Funding

This study was supported by Key research and development project of Department of Science and Technology of Zhejiang Province (2017C03051), Science Fund for Creative Research Groups of the National Natural Science Foundation of China (No.81721091) and the National Natural Science Foundation of China (81900572).

## Conflict of interest

The authors have no conflict of interests related to this publication.

## Author contributions

Study concept and design (LL), acquisition of data and performing the experiments (LZ, YZ, ZX), analysis and interpretation of data (LZ, LX, QH), drafting the manuscript (LZ, QL, ST), review and editing (JW). All authors read and approved the final manuscript.

## Data sharing statement

No additional data are available.

## References

[1] Bernal W, Jalan R, Quaglia A, Simpson K, Wendon J, Burroughs A. Acute-on-chronic liver failure. Lancet 2015;386(10003):1576–1587. doi:10.1016/s0140-6736(15)00309-8, PMID:26423181.
[2] Xiao LL, Wu XX, Chen JJ, Yan D, Shi DY, Huang JR, *et al*. Progress in hepatitis B virus-related acute-on-chronic liver failure treatment in China: A large, multicenter, retrospective cohort study using a propensity score matching analysis. Hepatobiliary Pancreat Dis Int 2021;20(6):535–541. doi:10.1016/j.hbpd.2021.05.010, PMID:34303609.
[3] Hernaez R, Solà E, Moreau R, Ginès P. Acute-on-chronic liver failure: an update. Gut 2017;66(3):541–553. doi:10.1136/gutjnl-2016-312670, PMID:28053053.
[4] Jalan R, Gines P, Olson JC, Mookerjee RP, Moreau R, Garcia-Tsao G, *et al*. Acute-on chronic liver failure. J Hepatol 2012;57(6):1336–1348. doi:10.1016/j.jhep.2012.06.026, PMID:22750750.
[5] Yu J, Ye Y, Liu J, Xu Y, Lou B, Zhu J, *et al*. The role of hepatitis B core-related antigen in predicting hepatitis B virus recurrence after liver transplantation. Aliment Pharmacol Ther 2019;50(9):1025–1036. doi:10.1111/apt.15429, PMID:31339175.
[6] Yamanouchi T, Tachibana Y, Akanuma H, Minoda S, Shinohara T, Moromizato H, *et al*. Origin and disposal of 1,5-anhydroglucitol, a major polyol in the human body. Am J Physiol 1992;263(2 Pt 1):E268–273. doi:10.1152/ajpendo.1992.263.2.E268, PMID:1514606.
[7] Yamanouchi T, Shinohara T, Ogata N, Tachibana Y, Akaoka I, Miyashita H. Common reabsorption system of 1,5-anhydro-D-glucitol, fructose, and mannose in rat renal tubule. Biochim Biophys Acta 1996;1291(1):89–95. doi:10.1016/0304-4165(96)00050-5, PMID:8781530.
[8] Koga M. 1,5-Anhydroglucitol and glycated albumin in glycemia. Adv Clin Chem 2014;64:269–301. doi:10.1016/b978-0-12-800263-6.00007-0, PMID:24938022.
[9] Ouchi S, Shimada K, Miyazaki T, Takahashi S, Sugita Y, Shimizu M, *et al*. Low 1,5-anhydroglucitol levels are associated with long-term cardiac mortality in acute coronary syndrome patients with hemoglobin A1c levels less than 7.0. Cardiovasc Diabetol 2017;16(1):151. doi:10.1186/s12933-017-0636-1, PMID:29157245.
[10] Yamanouchi T, Ogata N, Tagaya T, Kawasaki T, Sekino N, Funato H, *et al*. Clinical usefulness of serum 1,5-anhydroglucitol in monitoring glycaemic control. Lancet 1996;347(9014):1514–1518. doi:10.1016/s0140-6736(96)90672-8, PMID:8684103.
[11] Rebholz CM, Grams ME, Chen Y, Gross AL, Sang Y, Coresh J, *et al*. Serum Levels of 1,5-Anhydroglucitol and Risk of Incident End-Stage Renal Disease. Am J Epidemiol 2017;186(8):952–960. doi:10.1093/aje/kwx167, PMID:28535187.
[12] Yamagishi S, Ohta M. Serum 1,5-anhydro-D-glucitol levels in liver cirrhosis. Acta Diabetol 1998;35(1):65–66. doi:10.1007/s005920050104, PMID:9625293.
[13] Koga M, Murai J, Saito H, Mukai M, Toya D, Tanaka N, *et al*. 1,5-Anhydroglucitol levels are low irrespective of plasma glucose levels in patients with chronic liver disease. Ann Clin Biochem 2011;48(Pt 2):121–125. doi:10.1258/acb.2010.010053, PMID:20736249.
[14] Yu S. The anhydrofructose pathway of glycogen catabolism. IUBMB Life 2008;60(12):798–809. doi:10.1002/iub.125, PMID:18785261.
[15] Zhao Y, Chen E, Huang K, Xie Z, Zhang S, Wu D, *et al*. Dynamic Alterations of Plasma Metabolites in the Progression of Liver Regeneration after Partial Hepatectomy. J Proteome Res 2020;19(1):174–185. doi:10.1021/acs.jproteome.9b00493, PMID:31802674.
[16] Wu D, Sun Z, Liu X, Rao Q, Chen W, Wang J, *et al*. HINT: a novel prognostic model for patients with hepatitis B virus-related acute-on-chronic liver failure. Aliment Pharmacol Ther 2018;48(7):750–760. doi:10.1111/apt.14927, PMID:30069888.
[17] Bajaj JS, O'Leary JG, Reddy KR, Wong F, Olson JC, Subramanian RM, *et al*. Second infections independently increase mortality in hospitalized patients with cirrhosis: the North American consortium for the study of end-stage liver disease (NACSELD) experience. Hepatology 2012;56(6):2328–2335. doi:10.1002/hep.25947, PMID:22806618.
[18] Sarin SK, Kumar M, Lau GK, Abbas Z, Chan HL, Chen CJ, *et al*. Asian-Pacific clinical practice guidelines on the management of hepatitis B: a 2015 update. Hepatol Int 2016;10(1):1–98. doi:10.1007/s12072-015-9675-4, PMID:26563120.
[19] Lok AS, McMahon BJ. Chronic hepatitis B: update 2009. Hepatology 2009;50(3):661–662. doi:10.1002/hep.23190, PMID:19714720.
[20] Wiesner R, Edwards E, Freeman R, Harper A, Kim R, Kamath P, *et al*. Model for end-stage liver disease (MELD) and allocation of donor livers. Gastroenterology 2003;124(1):91–96. doi:10.1053/gast.2003.50016, PMID:12512033.
[21] Luca A, Angermayr B, Bertolini G, Koenig F, Vizzini G, Ploner M, *et al*. An integrated MELD model including serum sodium and age improves the prediction of early mortality in patients with cirrhosis. Liver Transpl 2007;13(8):1174–1180. doi:10.1002/lt.21197, PMID:17663415.
[22] Biggins SW, Kim WR, Terrault NA, Saab S, Balan V, Schiano T, *et al*. Evidence-based incorporation of serum sodium concentration into MELD. Gastroenterology 2006;130(6):1652–1660. doi:10.1053/j.gastro.2006.02.010, PMID:16697729.
[23] Wu T, Li J, Shao L, Xin J, Jiang L, Zhou Q, *et al*. Development of diagnostic criteria and a prognostic score for hepatitis B virus-related acute-on-chronic liver failure. Gut 2018;67(12):2181–2191. doi:10.1136/gutjnl-2017-314641, PMID:28928275.
[24] Jalan R, Saliba F, Pavesi M, Amoros A, Moreau R, Ginès P, *et al*. Development and validation of a prognostic score to predict mortality in patients with acute-on-chronic liver failure. J Hepatol 2014;61(5):1038–1047. doi:10.1016/j.jhep.2014.06.012, PMID:24950482.
[25] Stickle D, Turk J. A kinetic mass balance model for 1,5-anhydroglucitol: applications to monitoring of glycemic control. Am J Physiol 1997;273(4):E821–830. doi:10.1152/ajpendo.1997.273.4.E821, PMID:9357814.
[26] Ying L, Ma X, Yin J, Wang Y, He X, Peng J, *et al*. The metabolism and transport of 1,5-anhydroglucitol in cells. Acta Diabetol 2018;55(3):279–286. doi:10.1007/s00592-017-1093-8, PMID:29318370.
[27] Bao S, Zhao Q, Zheng J, Li N, Huang C, Chen M, *et al*. Interleukin-23 mediates the pathogenesis of LPS/GalN-induced liver injury in mice. Int Immunopharmacol 2017;46:97–104. doi:10.1016/j.intimp.2017.03.001, PMID:28282579.
[28] Koga M, Murai J, Saito H, Mukai M, Kasayama S, Moriwaki Y, *et al*. Close relationship between serum concentrations of 1,5-anhydroglucitol and uric acid in non-diabetic male subjects implies common renal transport system. Clin Chim Acta 2009;410(1-2):70–73. doi:10.1016/j.cca.2009.09.024, PMID:19781540.
[29] Bairaktari E, Liamis G, Tsolas O, Elisaf M. Partially reversible renal tubular damage in patients with obstructive jaundice. Hepatology 2001;33(6):1365–1369. doi:10.1053/jhep.2001.25089, PMID:11391524.
[30] Yamanouchi T, Kawasaki T, Yoshimura T, Inoue T, Koshibu E, Ogata N, *et al*. Relationship between serum 1,5-anhydroglucitol and urinary excretion of N-acetylglucosaminidase and albumin determined at onset of NIDDM with 3-year follow-up. Diabetes Care 1998;21(4):619–624. doi:10.2337/diacare.21.4.619, PMID:9571353.
[31] Jiang QQ, Han MF, Ma K, Chen G, Wan XY, Kilonzo SB, *et al*. Acute kidney injury in acute-on-chronic liver failure is different from in decompensated cirrhosis. World J Gastroenterol 2018;24(21):2300–2310. doi:10.3748/wjg.v24.i21.2300, PMID:29881239.
[32] Ix JH, Shlipak MG. The Promise of Tubule Biomarkers in Kidney Disease: A Review. Am J Kidney Dis 2021;78(5):719–727. doi:10.1053/j.ajkd.2021.03.026, PMID:34051308.
[33] Edelstein CL. Biomarkers of acute kidney injury. Adv Chronic Kidney Dis 2008;15(3):222–234. doi:10.1053/j.ackd.2008.04.003, PMID:18565474.
[34] Goto M, Yamamoto-Honda R, Shimbo T, Goto A, Terauchi Y, Kanazawa Y, *et al*. Correlation between baseline serum 1,5-anhydroglucitol levels and 2-hour post-challenge glucose levels during oral glucose tolerance tests. Endocr J 2011;58(1):13–17. doi:10.1507/endocrj.k10e-224, PMID:21084770.
[35] Cotrozzi G, Casini Raggi V, Relli P, Buzzelli G. [Role of the liver in the regulation of glucose metabolism in diabetes and chronic liver disease]. Ann Ital Med Int 1997;12(2):84–91. PMID:9333317.

*Journal of Clinical and Translational Hepatology* **2022** vol. 10(4) | 660–668
DOI: 10.14218/JCTH.2021.00272

Original Article

# Complementary Presence of HBV Humoral and T-cell Response Provides Protective Immunity after Neonatal Immunization

Yunmei Huang[1], Yuting Yang[1], Tingting Wu[1], Zhiyu Li[1], Hongmei Xu[2], Ailong Huang[3] and Yao Zhao[1*]

[1]*National Clinical Research Center for Child Health and Disorders, China International Science and Technology Cooperation base of Child development and Critical Disorders, Ministry of Education Key Laboratory of Child Development and Disorders, Chongqing Key Laboratory of Child Infection and Immunity, Children's Hospital of Chongqing Medical University, Chongqing, China;* [2]*Department of Infection, Children's Hospital of Chongqing Medical University, Chongqing, China;* [3]*Institute for Viral Hepatitis, Ministry of Education Key Laboratory of Molecular Biology on Infectious Diseases, Chongqing Medical University, Chongqing, China*

**Received:** 8 July 2021 | **Revised:** 8 September 2021 | **Accepted:** 14 October 2021 | **Published:** 4 January 2022

## Abstract

***Background and Aims:*** Hepatitis B vaccination is the most cost effective way to prevent hepatitis B virus (HBV) infection. Hepatitis B vaccine (HepB) efficacy is usually assessed by anti-hepatitis B surface antigen (HBsAg) level, but there are few reports of humoral and cellular immune responses to HepB in children after neonatal vaccination. ***Methods:*** A group of 100 children with a history of primary hepatitis B immunization were included in this study to evaluate the efficacy of HepB. Blood samples were obtained from 80 children before, and 41 children after, a single HepB booster dose. Children with low anti-HBsAg (HBs) titers of <100 mIU/mL received a booster dose after giving their informed consent. Anti-HBsAg, T-cell response and percentage of B-cell subsets were assayed before and after the booster. ***Results:*** Of the 80 children, 81.36% had positive T cell and anti-HBsAg responses at baseline. After the booster dose, the anti-HBsAg titer ($p<0.0001$), positive HBsAg-specific T-cell response ($p=0.0036$), and spot-forming cells ($p=0.0003$) increased significantly. Compared with pre-existing anti-HBsAg titer <10 mIU/mL, the anti-HBsAg ($p=0.0005$) and HBsAg-specific T-cell responses ($p<0.0001$) increased significantly in preexisting anti-HBsAg titer between 10 and 100 mIU/mL group. Change of the HBV-specific humoral response was the reverse of the T-cell response with age. Peripheral blood lymphocytes, B cells, and subset frequency decreased. ***Conclusions:*** HBV immunization protection persisted at least 13 years after primary immunization because of the complementary presence of HBV-specific humoral antibodies and a T-cell immune response. One dose of a HepB booster induced protective anti-HBsAg and promoted an HBsAg-specific T-cell response. In HBV endemic regions, a HepB booster is recommended to children without anti-HBsAg because of effectiveness in HBV prevention.

**Citation of this article:** Huang Y, Yang Y, Wu T, Li Z, Xu H, Huang A, *et al*. Complementary Presence of HBV Humoral and T-cell Response Provides Protective Immunity after Neonatal Immunization. J Clin Transl Hepatol 2022;10(4):660–668. doi: 10.14218/JCTH.2021.00272.

## Introduction

Hepatitis B vaccination is the most cost effective way to prevent acute or chronic HBV infection and reduce complications of hepatitis B infection. The Chinese government has adopted routine hepatitis B vaccination, and importation of a yeast-derived hepatitis B vaccine (HepB) began in the late 1980s. Routine immunization began in 1992, and HepB was integrated into the Expanded Program of Immunization in 2002.[1] Following the implementation of routine HBV vaccination China has successfully changed from a highly endemic to a moderately endemic country. Serosurveys found that HBsAg seropositivity decreased by 52%, from 9.8% to 4.7% in the general population; by 97%, from 9.7% to 0.3% in children <5 years of age; and by 92.4%, from 10.5% to 0.8% in children <15 years of age from 1992 to 2014.[2–4] It is estimated that 80 million acute HBV infections and 20 million chronic HBV infections have been prevented since 1992.[5]

The need for a HepB booster in children after neonatal immunization is controversial. Many studies have not identified a need of booster immunization in healthy children. The protection afforded by primary HepB immunization can last 30 years; only 0.7% of vaccinees had HBV breakthrough infections in the 5–20 years after neonatal HBV vaccination.[6–8] Immune memory for HepB persists in children with waning or undetectable anti-HBsAg concentrations,[9] but the loss of HepB immune memory has been reported in 25–50% of vaccinees after 15 years of age,[10,11] and 10.1% had no immune response to a HepB booster after the initial vaccination.[12] A HepB booster has been recommended for at-risk youths who with a history

**Keywords:** Hepatitis B virus; Hepatitis B vaccine; Booster; Children.

**Abbreviations:** Anti-HBc, hepatitis B core antibody; Anti-HBsAg, hepatitis B surface antibody; CMIA, chemiluminescent microparticle immunoassay; ELISpot, enzyme-linked immunospot; HBsAg, hepatitis B surface antigen; HBV, hepatitis B virus; HepB, hepatitis B vaccine; IFN-γ, interferon gamma; PBMC, peripheral blood mononuclear cell; SFC, spot-forming cell.

[*]**Correspondence to:** Yao Zhao, National Clinical Research Center for Child Health and Disorders, Children's Hospital of Chongqing Medical University, Chongqing 400014, China. ORCID: https://orcid.org/0000-0003-4550-9436. Tel: +86-23-6363-3083, Fax: +86-23-6360-2136, E-mail: Zhaoy@cqmu.edu.cn

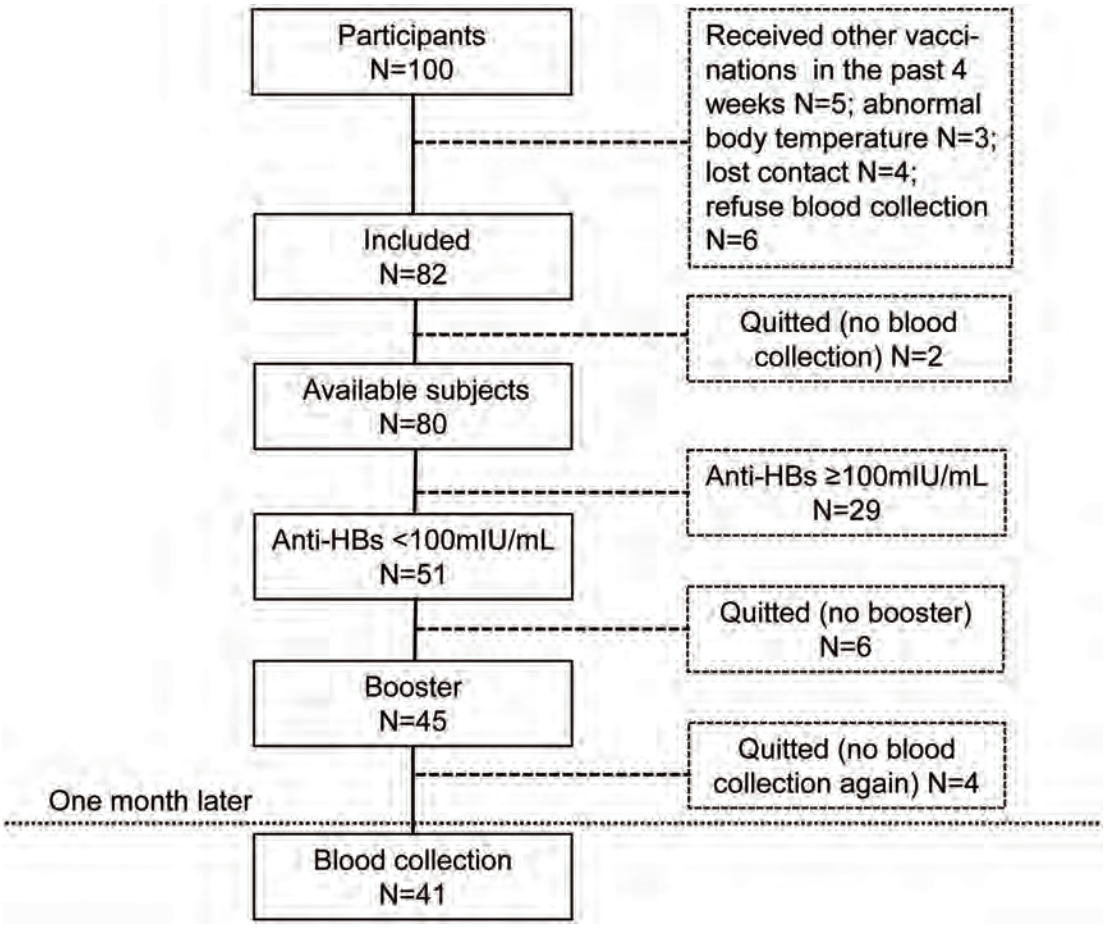


**Fig. 1. Flowchart of inclusion and withdrawal of study participants. Blood samples were obtained from 80 eligible children before a dose of HepB booster and 41 children post-booster.** N, number; Anti-HBsAg, antibodies to hepatitis B surface antigen.

of primary immunization. We previously reported that anti-HBsAg declined with age in children from 93.7% at 1 year of age to 42.3% at 9 years of age.[13,14] Whether a protective immune response is elicited in children without anti-HBsAg is no known, and the need for booster doses has not been resolved.

This study investigated the protective humoral and cellular immunity responses following primary immunization and a HepB booster for children who had lost protective antibodies. The efficacy of a HepB booster in children with low baseline anti-HBsAg levels between 10 and 100 mIU/mL was evaluated.

## Methods

### *Design and trial participants*

This prospective single-center cohort study was performed at Clinical Research Center of Children's Hospital of Chongqing Medical University, a general children hospital with patients from all over the country. The study was approved by the institutional ethics review committee of and registered at ClinicalTrials.gov (NCT03867643). All children and their legal guardians provided written informed consent. All procedures were conducted following the ethical principles of the Declaration of Helsinki.

Children born after January 1, 2005 in Chongqing, China who completed primary vaccination with a series of three doses of HepB containing 10 μg HBsAg each beginning at birth, and not receiving a booster dose were eligible for inclusion. Children with a history of allergy or adverse reaction to the vaccine, immunosuppressive treatment or immunodeficiency, any vaccination in the previous 4 weeks, with an acute disease or anti-infective therapy in the past 4 weeks, fever (axillary temperature ≥38°C) in the previous week, history of blood transfusion, history of infectious diseases (e.g., hepatitis, AIDS, syphilis, gonorrhea, etc.), family history of HBV in three generations of lineal relatives, or abnormalities on physical examination were excluded. Figure 1 is a flowchart of participant selection. A group of 100 children aged 1–13-year were included via the hospital's official website. Blood samples were obtained from 80 children before the HepB booster, which contained 20 μg HBsAg (Huabei Pharmaceutical Co., Hebei, China), and from 41 children 1 month after the booster.

### *HBV seromarkers*

Blood samples were collected for determination of HBV seromarkers by chemiluminescent microparticle immunoassay (CMIA) with the Architect system (Abbott Laboratories). HBsAg seropositivity was >0.05 IU/mL and anti-HBsAg titers ≥10 mIU/mL were considered seroprotective. Sample cutoff values of anti-hepatitis B e antigen ≥1.0 and anti-hepatitis B core antigen of ≥1.0 were considered positive.

**Table 1. Baseline characteristics of the 80 study participants**

| Variable | Anti-HBsAg <10 mIU/mL, *n*=21 (%) | 10≤ anti-HBsAg <100 mIU/mL, *n*=30 (%) | Anti-HBsAg ≥100 mIU/mL, *n*=29 (%) | *p*-value[a] |
|---|---|---|---|---|
| Sex | | | | |
| Boys | 15 (71.43) | 18 (60) | 11 (37.93) | 0.049* |
| Girls | 6 (28.57) | 12 (40) | 18 (62.07) | |
| Age, years | | | | |
| 1–3 | 2 (9.52) | 7 (23.33) | 6 (20.69) | 0.56 |
| 4–6 | 6 (28.57) | 9 (30) | 12 (41.38) | |
| 7–9 | 8 (38.10) | 6 (20) | 5 (17.24) | |
| 10–13 | 5 (23.81) | 8 (26.67) | 6 (20.69) | |
| Pregnancy | | | | |
| Normal | 17 (81) | 30 (100) | 27 (93.10) | 0.039* |
| Premature delivery | 4 (19) | 0 (0) | 2 (6.90) | |
| Birth weight | | | | |
| Normal | 17 (80.96) | 27 (90) | 26 (89.66) | 0.22 |
| Overweight | 2 (9.52) | 3 (10) | 3 (10.34) | |
| Underweight | 2 (9.52) | 0 (0) | 0 (0) | |
| History of allergies | 0 (0) | 0 (0) | 3(10.34) | |
| History of hepatitis infection | 0 (0) | 0 (0) | 0 (0) | |
| History of blood transfusion | 0 (0) | 0 (0) | 0 (0) | |
| History of surgery | 0 (0) | 0 (0) | 0 (0) | |
| History of radiotherapy and chemotherapy | 0 (0) | 0 (0) | 0 (0) | |
| History of HBV infection of parents or grandparents | 3 (14.29) | 8 (26.67) | 10 (34.48) | 0.28 |

[a]Pearson $\chi 2$ or Fisher exact test. *Statistically significant.

### *Detection of interferon (IFN)-γ-secreting HBsAg-specific T cells*

Peripheral blood mononuclear cells (PBMCs) were isolated by density gradient centrifugation, and HBsAg-specific cytokine-secreting T cells were identified with a human IFN-γ ELISpot PLUS assay (Mabtech, Stockholm, Sweden). IFN-γ precoated 96-well plates were preincubated with Roswell Park Memorial Institute (RPMI) 1640 medium (Gibco, Invitrogen, USA) for 30 minutes at room temperature before adding $5\times10^5$ PBMCs/well in 200 μL RPMI 1640. PBMCs were stimulated with 10 μg/ml of recombinant HBsAg (Bersee, Beijing, China). Wells containing PBMCs and RPMI 1640 with anti-CD3 mAb (Mabtech, Stockholm, Sweden) were positive controls and wells without any stimulant were negative controls. The culture plates were incubated for 48 h at 37°C in a 5% $CO_2$ atmosphere and were then read with an ELISpot reader (AID, Strassberg, Germany). A response two-fold greater than that of the negative control was considered positive.[15]

### *Assay of B lymphocyte subpopulations*

The B-cell phenotypes isolated from peripheral blood samples were evaluated by flow cytometry (FACSCanto II; BD Biosciences, SanJose, Calif). The mAbs were from BD Biosciences, and the B lymphocyte subpopulations included αCD19-ApC, αCD24-pE, αCD27-BV450, αCD38-perCp-Cy5.5, and αIgD-BV510. The data were analyzed by FACS Diva.

### *Statistical analysis*

The data were analyzed and compared by SPSS version 20.0 (IBM Corp. Armonk, NY, USA); graphs were drawn by Graphpad prism (version 8.0). Continuous variables were compared with the Student *t*-test. Comparisons of categorical variables were performed by $\chi^2$ or Fisher's exact tests. The Spearman rank correlation was used to evaluate the associations between ELISpot results and anti-HBsAg titers. *P*-values <0.05 were considered statistically significant.

## Results

### *Participant baseline characteristics*

The characteristics of the 80 available subjects are shown in Table 1 and the characteristics of the 51 participants with prebooster anti-HBsAg titers <100 mIU/mL are shown in Supplementary Table 1. All participants had received a three-dose primary neonatal HBV vaccination and were grouped by anti-HBsAg titer. Twenty-one had baseline titers of <10 mIU/mL, 30 had titers ≥10 and <100 mIU/mL, and 29 had titers ≥100 mIU/mL. Between-group comparisons of sex, age, weeks of pregnancy week, birth weight, and

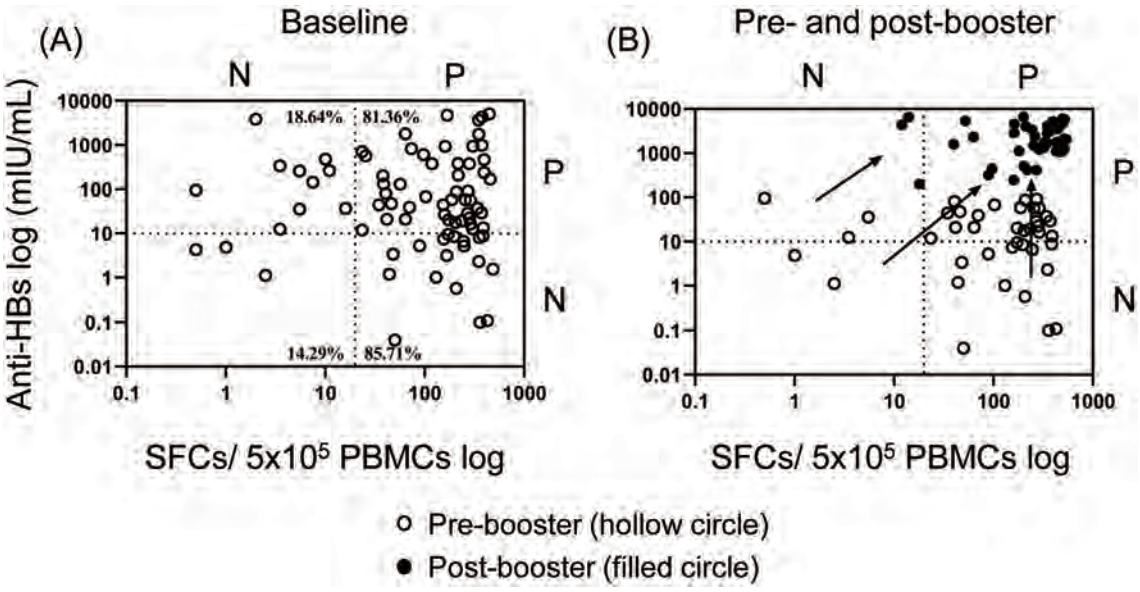


**Fig. 2. Distribution of positive and negative humoral and cellular immunity pre- and post-booster.** (A) Distribution of positive and negative anti-HBsAg and IFN-γ-secreting HBsAg-specific T cells at baseline ($n$=80). (B) Changes of anti-HBsAg titers and IFN-γ-secreting HBsAg-specific T cells prebooster (open circle) and post-booster (solid circle) ($n$=41). PBMCs, peripheral blood mononuclear cells; SFC, spot-forming cell; P, positive; N, negative; pre-, prebooster; post-, post-booster.

disease history among each group found that boys were at a lower titers than girls ($p$=0.049) and more preterm infants than normal term infants were anti-HBsAg negative at baseline ($p$=0.039).

### *HBsAg-specific T-cell responses are frequent in antibody-negative participants*

The ELISpot assay results of HBsAg-specific T-cell responses in children without anti-HBsAg and the distribution of positive and negative humoral and cellular immunity is shown in Figure 2. Of the antibody-negative participants, 85.71% had positive HBsAg-specific T-cell responses, 18.64% of the antibody-positive subjects had negative responses, and 96.25% of the children had positive HBsAg-specific T cell or anti-HBsAg responses. Of 41 children given a booster dose, all antibody-negative subjects became positive and their HBsAg-specific T-cell responses were enhanced.

### *Children with high prebooster anti-HBsAg titers had high post-booster humoral responses*

Pre- and post-booster anti-HBsAg titers are shown in Figure 3. The titers increased after booster administration to >100 mIU/mL in all children ($p$<0.0001) and to >1,000 mIU/mL in 56.25% those with prebooster titers of 0–10 mIU/mL and 100% of children with prebooster titers from 10–100 mIU/mL ($p$=0.0005). Children with high prebooster anti-HBsAg titers had higher humoral responses than those with low prebooster titers.

### *Post-booster IFN-γ-secreting HBsAg-specific T-cell response depended on the prebooster anti-HBsAg titer*

The pre- and post-booster HBsAg-specific T-cell responses are shown in Figure 4. The ELISpot results indicated significant increases of the percentage ($p$=0.0036) and the magnitude of response ($p$=0.0003) of spot-forming cells (SFCs) following booster administration. The magnitude of the response in IFN-γ-secreting HBsAg-specific T cells was not associated with the anti-HBsAg titer after neonatal immunization ($p$=0.1140). The post-booster T-cell response showed the same change trend as the humoral response, with a significant increase ($p$=0.0004) in the number of IFN-γ-secreting HBsAg-specific T cells. Compared with children with low anti-HBsAg prebooster titers (0–10 mIU/mL), those with pre-existing titers between 10 and 100 mIU/mL had significantly stronger HBsAg-specific T-cell responses to the booster vaccination. The intensity of T-cell immunoreactivity depended on the pre-existing anti-HBsAg titer.

### *Association between HepB humoral and T-cell response and age*

The association between humoral and T-cell response and age is shown in Figure 5, which shows the changes of anti-HBsAg titers and HBV-specific T-cell response in children of different ages. Post-booster anti-HBsAg titers increased significantly in all four age groups of the 41 children who were vaccinated. The anti-HBsAg titers were higher in 1- to 3-year-old than in 10- to 13-year-old children ($p$=0.031) and pre- and post-booster ELISpot assay results were significantly different in 10- to 13-year-old children ($p$=0.0172). As shown in Figure 5C, differences in prebooster anti-HBsAg titers were the opposite of T-cell values in each age group. The percentage of protective antibodies initially decreased with age and then increased in children 1–13 years of age. The T-cell response increased initially and then decreased. After the booster dose (Fig. 5D) the percentage of protective antibody titers decreased in each age group from 1 to 13 years of age, but the positive T-cell response increased in each age group. The overall positive anti-HBsAg and T-cell response rates in each age group were similar. The results show that the change of the HBV-specific humoral response was associated differences in the T-cell response in the four age groups.

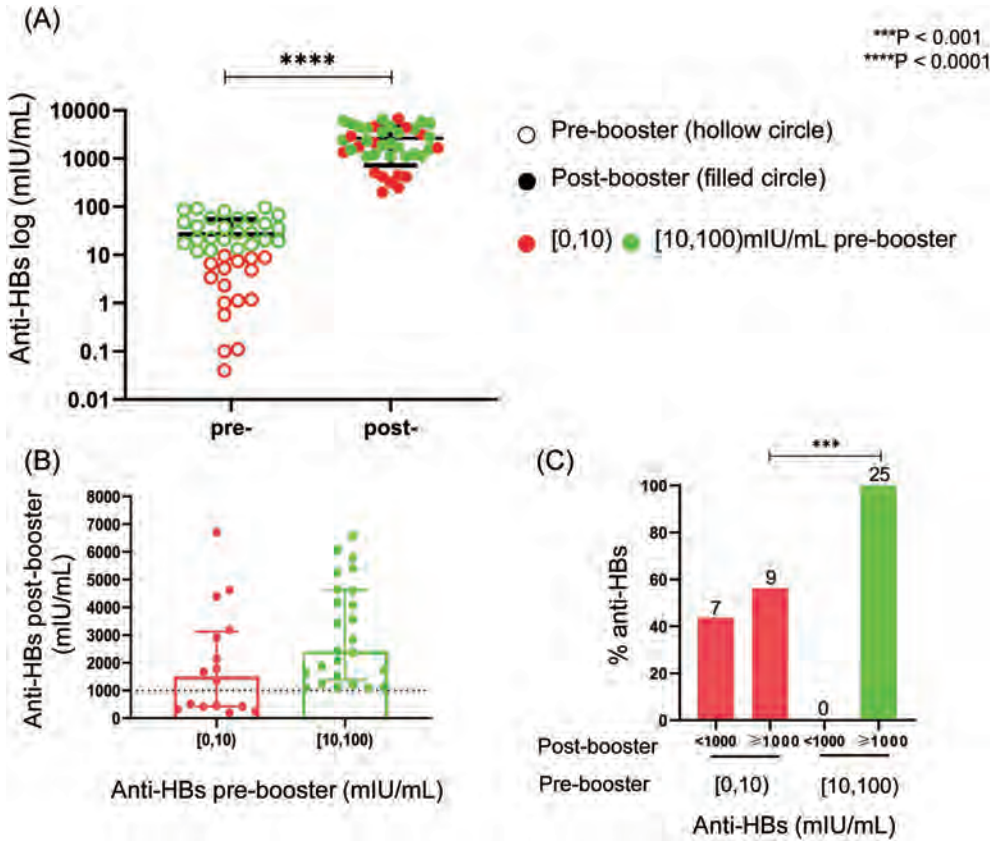


**Fig. 3. Humoral response to HepB booster vaccination in children (*n*=41).** Subjects were grouped by prebooster anti-HBsAg titer, 0–10 mIU/mL (red), 10–100 mIU/mL (green). (A) Prebooster (open circle) and post-booster (solid circle) Anti-HBsAg. (B) Post-booster Anti-HBsAg titer in children with different pre-existing anti-HBsAg. Boxes and whiskers are medians and interquartile range. (C) Percentage of children with post-booster anti-HBsAg of <1,000 mIU/mL and ≥1,000 mIU/mL in children with pre-existing anti-HBsAg of 0–10 mIU/mL and 10–100 mIU/mL. Pre-, pre-booster; Post-, post-booster.

### *Changes of immune B-cell subsets after booster administration*

The gating strategy for definition of the B-cell subsets is depicted in Figure 6A. Changes in the immune B-cell subsets before and after booster vaccination (Fig. 6) included a decrease in B-cell frequency in peripheral lymphocytes ($p$=0.0002), and antibody-secreting cells included plasmablasts. Changes in the numbers of $CD19^+$ B-cells were similar in participants with low and with high baseline anti-HBsAg titers. One month after booster vaccination, class-switched and unswitched memory B-cell frequencies decreased significantly. In children with low pre-existing anti-HBsAg titers (0–10 mIU/mL), there were a significant rise in naïve B cells ($p$=0.0387) and DN B cells ($p$=0.0134). In children with high baseline anti-HBsAg titers (10–100 mIU/mL), the percentages of both naïve B cells ($p$<0.0001) and DN B cells ($p$=0.0013) increased.

## Discussion

The Chinese Center for Disease Control and prevention (CDC) reported that three-dose HBV vaccination coverage before 1 year of age was 83–99.53% between 2001 and 2017.[16] Our previous serosurvey found that 46.03–72.29% of children from 1 to 14 years of age were seroprotected, and that 3.33–25.79% of all age groups had anti-HBsAg titers of <10 mIU/ml,[13] which was consistent with a CDC survey of HBV seroprevalence in various age groups in China.[4]

HepB is one of the safest available vaccines. It prevents HBV infection and reduces the occurrence of liver cancer.[17] All the children in this study had completed the three-dose primary vaccination series that begins with a dose at birth. We analyzed the immune response to a HepB booster dose after completing neonatal immunization to determine whether children without detectable anti-HBsAg (i.e., titers <10 mIU/mL) were still protected and whether or not children without anti-HBsAg need a HepB booster vaccination.

This is the first study to show that protective immunity from neonatal immunization exists in children because of the complementary presence of HBV-specific humoral and T-cell immune responses. A detectable T-cell response to HBsAg was found in 85.71% of children with anti-HBsAg titers of <10 mIU/mL. The presence of HBsAg-specific INF-γ in children up to 13 years of age suggests that protection may be long lasting. A study by Wang *et al* reported that most anti-HBsAg negative vaccinees had positive HBsAg-specific immune-cell responses.[18] Leuridan *et al* reported activation of immune cells in vaccinees based on cell proliferative response.[19] Long lasting cellular immunity has also been shown by detection of secretion of cytokines by Th1 and Th2 lymphocytes after stimulation by HBsAg.[7] The previous results confirm that T cell immunity persists regardless of anti-HBsAg, which is consistent with our results. HBsAg-specific T-cell responses initially increased and then a decrease with age, which was the reverse of changes in anti-HBsAg titers. In neonates, adaptive immune responses to pathogens are relatively weak and narrowly focused,

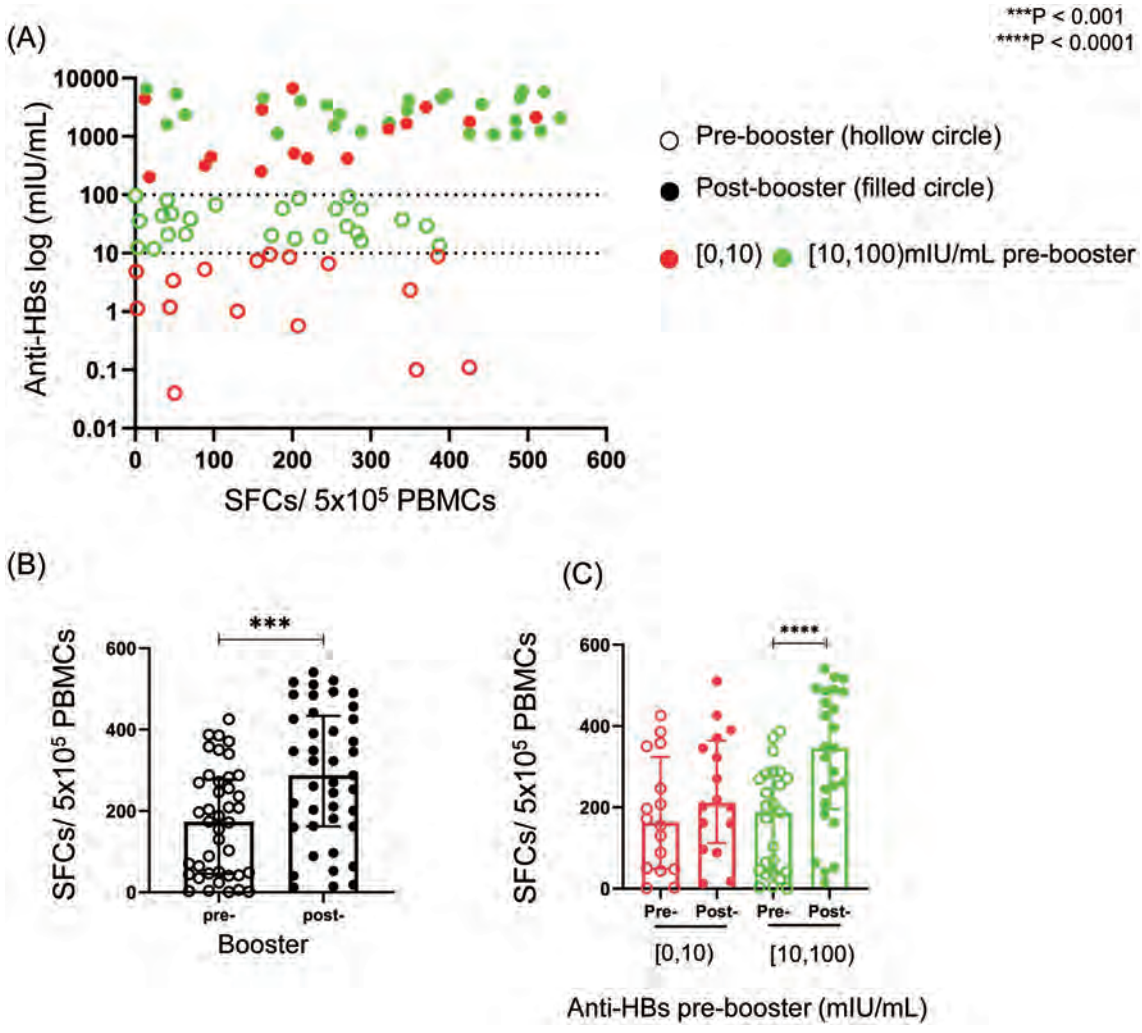


**Fig. 4. T-cell response to HepB booster vaccination (*n*=41).** Subjects were grouped by prebooster anti-HBsAg titer, 0–10 mIU/mL (red) or 10–100 mIU/mL (green). (A) Correlation of anti-HBsAg titer and IFN-γ–secreting HBsAg-specific T cells prebooster (open circle) and post-booster (solid circle). (B) IFN-γ–secreting HBsAg-specific T cells were significantly increased post- compared with prebooster ($p$=0.0004). (C) Post-booster HBsAg-specific T-cell responses were significantly stronger in children with higher pre-existing anti-HBsAg titers ($p$<0.0001). SFC, spot-forming cells; PBMCs, peripheral blood mononuclear cells; Pre-, pre-booster; Post-, post-booster.

causing T-cell hyporesponsiveness.[20] In younger children, HBV-specific T cells are lacking and fail to produce adequate amounts of IFN-γ, but the response gradually improves with age.[21] Before and after HepB booster, the direction of change in anti-HBsAg titer in this study was opposite that of the HBsAg-specific T-cell response in each age group. In vaccine development, determining the balance between humoral and cellular responses is the key challenge.[22] The complementary existence of anti-HBsAg and T-cell responses is important for the persistence of protection following vaccination. There is no need to worry about the decline in anti-HBsAg in populations. It is precisely because of the dynamic balance that screening for HBsAg-specific T-cell immunity is not recommended for the general population. Routine screening for anti-HBsAg in vaccinees is sufficient to evaluate the protection afforded by HepB.

One dose of HepB booster was effective in children without anti-HBsAg. All those given a HepB booster dose produced protective anti-HBsAg and an enhanced HBV-specific T-cell response 4 weeks after the vaccination. All children with anti-HBsAg <10mIU/ml produced anti-HBsAg with titers >100 mIU/mL, demonstrated an anamnestic response to the booster dose,[23] even when detectable anti-HBsAg were absent at the time of exposure. We found that humoral and T-cell responses to the HepB booster depended on the pre-existing anti-HBsAg titer. Only 56.25% of children with pre-booster anti-HBsAg <10mIU/ml had anti-HBsAg ≥1,000 mIU/mL 4 weeks post-vaccination. Those with prebooster anti-HBsAg <10mIU/ml were less likely to produce high titers of anti-HBsAg compared with children who had anti-HBsAg titers from 10 to 100 mIU/ml. Equally, the intensity of the T-cell booster response also depended on the prebooster anti-HBsAg titer. After the booster, the numbers of IFN-γ-secreting HBsAg-specific T cells in children with prebooster anti-HBsAg titers of 10–100 mIU/ml were significantly increased compared with children with anti-HBsAg titers <10mIU/ml. That has been previously reported.[24] Establishment of immune memory by routine vaccination against HBV at birth is key for the effectiveness of the HepB booster and for long-term immunity.

Although immune memory for HepB is persistent in children, a booster is recommended for children without an-

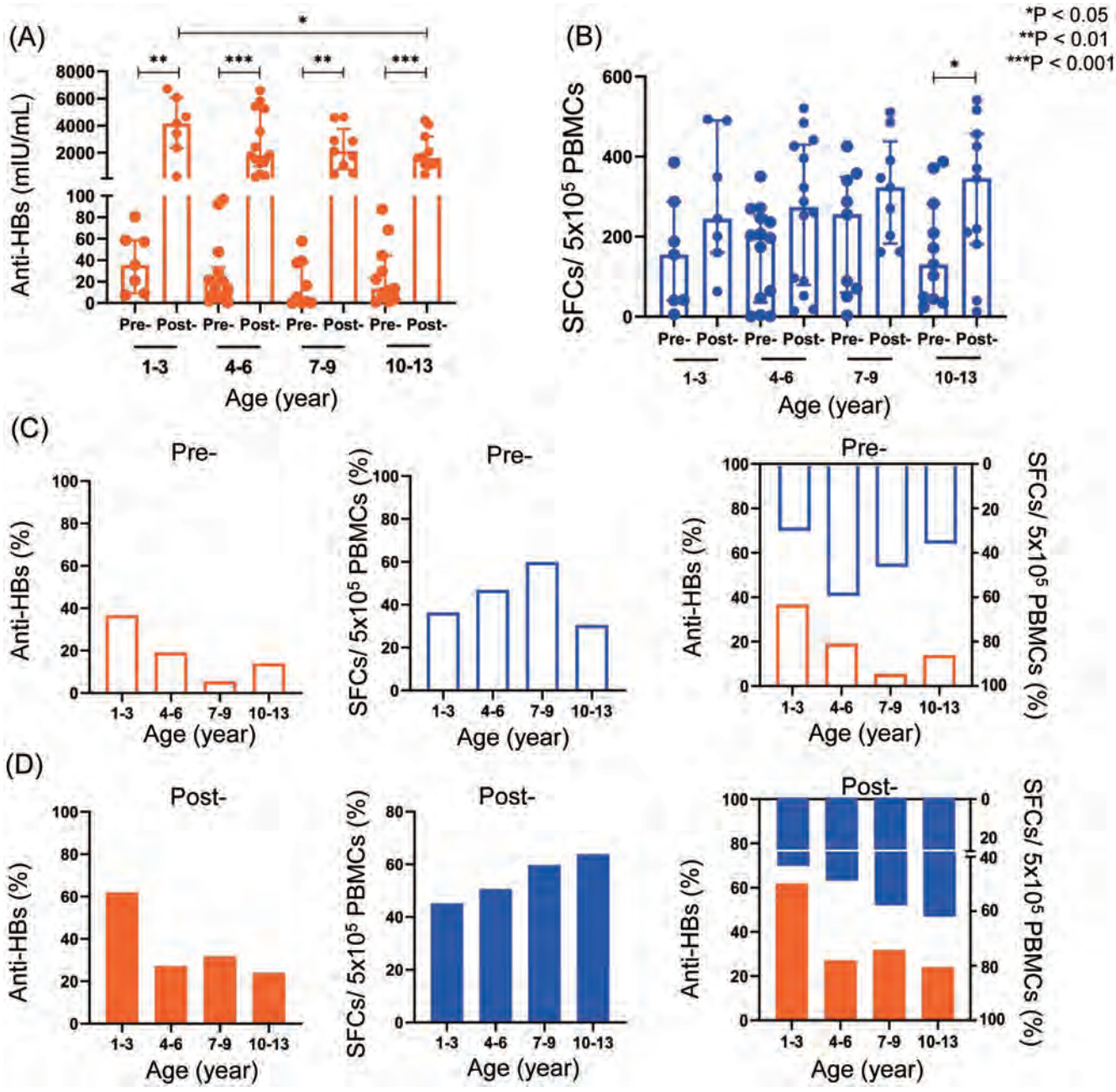


**Fig. 5. Age-related humoral (orange) and T-cell responses (blue) before and after booster vaccination.** Vaccinees ($n$=41) were stratified to groups 1–3, 4–6, 7–9, and 10–13 years of age. (A) Pre- and post-booster anti-HBsAg titers. (B) Pre- and post-booster IFN-γ-secreting HBsAg-specific T cells. (C, D) Age-related prebooster (open column) and post-booster (solid column) anti-HBsAg seropositivity and HBsAg-specific T-cell response. *Y*-axis: the median of each value divided by the maximum in children prebooster or post-booster. SFC, spot-forming cells; PBMCs, peripheral blood mononuclear cells; Pre-, pre-booster; Post-, post-booster.

ti-HBsAg in HBV endemic regions. The available evidence does not provide a compelling basis for recommending a booster dose of HepB.[6,25] Moreover, chronic HBV infection is on the decrease after primary immunization even in children without detectable (<10 mIU/mL) anti-HBsAg.[6,26] More attention should be paid to children over 10 years of age. According to our previous study, the prevalence of HBsAg and anti-HBc increased from 0.46% to 1.40% between 11 and 16 years of age compared with 5.69% to 7.8% between 1 and 10-years of age.[14] That suggests that the risk of exposure to HBV is increased in children who are older than 10 years of age. A HepB booster should be given at that age to reduce the risk of breakthrough infection. In this study, a significant number of vaccinees with low anti-HBsAg following neonatal vaccination had large increases of anti-HBsAg titer within 4 weeks of a single booster dose. HepB has been continuously improved since its launch in 1986. The safety of HepB has been confirmed and vaccination coverage in China has continuously improved.[1] Serosurveys show that the prevalence of HBV has significantly decreased,[2–4,27] and that the change is closely associated with hepatitis B vaccination. Some individuals with anti-

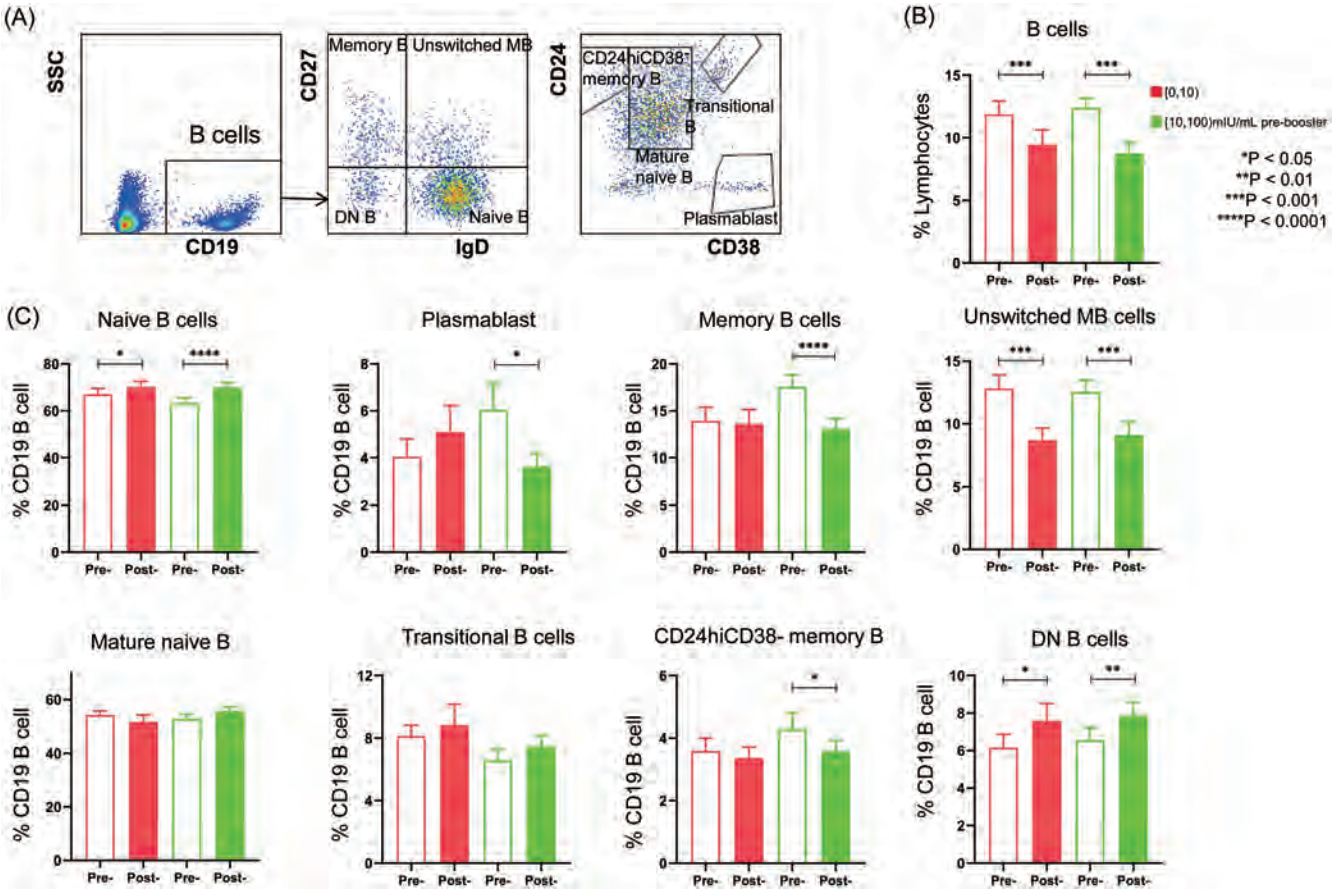


**Fig. 6. Peripheral immune B-cell subsets in participants ($n$=41) before (open column) and 1 month after hepatitis B booster vaccination (solid column).** Children were grouped by prebooster anti-HBsAg, 0–10 mIU/mL (red) and 10–100 mIU/mL (green). (A) Stepwise gating of B-cell for identification of memory B ($CD19^+$ $CD27^+$), CD24hi $CD38^-$ memory B ($CD19^+$ $CD24^{++}$ $CD38^-$), unswitched memory B ($CD19^+$ $CD27^+$ $IgD^+$), double negative B ($CD19^+$ $CD27^-$ $IgD^-$), mature naïve B ($CD24^{int}$ $CD38^{int}$); naïve B ($CD19^+$ CD27 $IgD^+$), transitional B ($CD19^+$ $CD24^{++}$ $CD38^{++}$) cell subsets and plasmablasts ($CD19^+$ $CD24^-$ $CD38^{++}$). (B) Among peripheral lymphocytes, B-cell frequency decreased in two groups ($p$ =0.0002). (C) In children with low pre-existing anti-HBsAg titers, naïve B cells ($p$=0.0387) and DN B cells ($p$=0.0134) increased and unswitched MB cells decreased ($p$=0.0005). In children with high anti-HBsAg titers naïve B cells ($p$ <0.0001) and DN B cells ($p$=0.0013) increased in subjects, and plasmablasts ($p$=0.0456), memory B cells ($p$=0.0001), unswitched MB cells ($p$=0.0002), and CD24hiCD38$^-$ memory B cells ($p$=0.0137) decreased. DN B, double negative B cell; MB, memory B cell; Pre-, prebooster; Post-, post-booster. *significant difference.

HBsAg <10mIU/ml and at high risk of HBV exposure will require only one HepB booster to achieve seroprotective anti-HBsAg titers.

In addition to a T-cell response, B cells respond to HepB by generating a protective anti-HBsAg titer. Our results found that total B cells, including some antibody-secreting cells, significantly decreased after booster vaccination. Decreases in plasmablasts, memory B cells, and unswitched memory B cells were observed in children with pre-existing anti-HBsAg titers of 10–100 mIU/ml. Immunization is known to be followed by rapid activation of circulating memory cells to terminally differentiate into low-affinity plasma cells or to form germinal centers, which mediate further proliferation and selection for antigen binding later.[28,29] In this study, there were declines in memory B cells, unswitched memory B cells and plasmablasts at 4 weeks post-booster. But the children did show a rise in anti-HBsAg in the peripheral blood, so they may have produced high affinity antibody-secreting cells at before blood collection.[30]

The main limitation of this study is the limited sample size. This study was a clinical trial and it was difficult to include a large numbers of children in each age group due to children's particularity. In addition, evaluation on the efficacy of one dose of HepB booster may be insufficient in this study. We were unable to assess the expression of other more activation markers or cytokines. Further study is warranted to evaluate more biomarkers in cellular response to HepB. More doses and long-term follow-up may also be required in the follow-up study.

In conclusion, this study had comprehensively analyzed humoral and cellular immune response to HepB booster in children after neonatal vaccination. Protection from primary HBV immunization persists at least 13 years after primary immunization on account of the complementary presence of HBV-specific humoral and T-cellular immune response. In addition, we demonstrated that one dose of HepB booster is efficient enough to produce protective anti-HBsAg and enhance HBsAg-specific T-cell responses. As an effective way, HepB booster immunization could be recommended to children without anti-HBsAg in the endemic areas to prevent HBV infection.

## Acknowledgments

We thank the staff of the Children's Hospital of Chongqing Medical University HBV vaccination study for their valuable contributions, especially Yue Lu, Zheng Xiang and Jiao Chen

for sample collection, Lina Zhou, Lu Huang and Linlin Niu for helpful discussion and all nurses for drawing blood. We also thank Biobank Center of Children's Hospital of Chongqing Medical University for sample storage. We especially thank all the children and their parents who participated, and thank them for their courage and kindness.

## Funding

This study was supported by the National Clinical Research Center for Child Health and Disorders General project (No. NCRCCHD-2019-GP-04), Central Government Guides Local Science and Technology Development projects-demonstration of Science and Technology Innovation projects, National Natural Science Foundation of China (No. 81371876), Outstanding Youth Foundation of Children's Hospital of Chongqing Medical University.

## Conflict of interest

The authors have no conflict of interests related to this publication.

## Author contributions

YZ, HX, AH and YH were responsible for the study concept and design, YH, YY, TW and ZL collected participant samples, YH, YY, TW and ZL performed study procedures, YH and YZ performed the statistical analysis and drafted the manuscript.

## Data sharing statement

The datasets in this study are available from the corresponding author upon reasonable request.

## References

[1] Centers for Disease Control and prevention (CDC). Progress in hepatitis B prevention through universal infant vaccination—China, 1997-2006. MMWR Morb Mortal Wkly Rep 2007;56:441–445. PMID:17495790.
[2] Xia GL, Liu CB, Cao HL, Bi SL, Zhan MY, Su CA, *et al*. Prevalence of hepatitis B and C virus infections in the general Chinese population. Results from a nationwide cross-sectional seroepidemiologic study of hepatitis A, B, C, D, and E virus infections in China, 1992. Int Hepatol Commun 1996;5:62–73. doi:10.1016/S0928-4346(96)82012-3.
[3] Liang X, Bi S, Yang W, Wang L, Cui G, Cui F, *et al*. Epidemiological serosurvey of hepatitis B in China—declining HBV prevalence due to hepatitis B vaccination. Vaccine 2009;27:6550–6557. doi:10.1016/j.vaccine.2009.08.048, PMID:19729084.
[4] Cui F, Shen L, Li L, Wang H, Wang F, Bi S, *et al*. prevention of Chronic Hepatitis B after 3 Decades of Escalating Vaccination policy, China. Emerg Infect Dis 2017;23:765–772. doi:10.3201/eid2305.161477, PMID:28418296.
[5] Yu W. Foreword. Hepatitis B and the impact of immunization in China and the WHO Western pacific Region. Vaccine 2013;31(Suppl 9):J2. doi:10.1016/j.vaccine.2012.07.070, PMID:24331016.
[6] Bruce MG, Bruden D, Hurlburt D, Zanis C, Thompson G, Rea L, *et al*. Antibody Levels and protection After Hepatitis B Vaccine: Results of a 30-Year Follow-up Study and Response to a Booster Dose. J Infect Dis 2016;214:16–22. doi:10.1093/infdis/jiv748, PMID:26802139.
[7] Simons BC, Spradling PR, Bruden DJ, Zanis C, Case S, Choromanski TL, *et al*. A Longitudinal Hepatitis B Vaccine Cohort Demonstrates Long-lasting Hepatitis B Virus (HBV) Cellular Immunity Despite Loss of Antibody Against HBV Surface Antigen. J Infect Dis 2016;214:273–280. doi:10.1093/infdis/jiw142, PMID:27056956.
[8] Poorolajal J, Mahmoodi M, Majdzadeh R, Nasseri-Moghaddam S, Haghdoost A, Fotouhi A. Long-term protection provided by hepatitis B vaccine and need for booster dose: a meta-analysis. Vaccine 2010;28:623–631. doi:10.1016/j.vaccine.2009.10.068, PMID:19887132.
[9] Salama II, Sami SM, Said ZN, Salama SI, Rabah TM, Abdel-Latif GA, *et al*. Early and long term anamnestic response to HBV booster dose among fully vaccinated Egyptian children during infancy. Vaccine 2018;36:2005–2011. doi:10.1016/j.vaccine.2018.02.103, PMID:29530634.
[10] Jan CF, Huang KC, Chien YC, Greydanus DE, Davies HD, Chiu TY, *et al*. Determination of immune memory to hepatitis B vaccination through early booster response in college students. Hepatology 2010;51:1547–1554. doi:10.1002/hep.23543, PMID:20209603.
[11] Hammitt LL, Hennessy TW, Fiore AE, Zanis C, Hummel KB, Dunaway E, *et al*. Hepatitis B immunity in children vaccinated with recombinant hepatitis B vaccine beginning at birth: a follow-up study at 15 years. Vaccine 2007;25:6958–6964. doi:10.1016/j.vaccine.2007.06.059, PMID:17714836.
[12] Lu CY, Ni YH, Chiang BL, Chen pJ, Chang MH, Chang LY, *et al*. Humoral and cellular immune responses to a hepatitis B vaccine booster 15-18 years after neonatal immunization. J Infect Dis 2008;197:1419–1426. doi:10.1086/587695, PMID:18444799.
[13] Yue X, Ge C, Zhuge S, He H, Yang H, Xu H, *et al*. Changes and analysis of anti-HBs titres after primary immunization in 1- to 16-year-old Chinese children: A hospital-based study. J Viral Hepat 2018;25:373–380. doi:10.1111/jvh.12818, PMID:29091317.
[14] Yang YT, Huang AL, Zhao Y. The prevalence of hepatitis B core antibody in vaccinated Chinese children: A hospital-based study. Vaccine 2019;37:458–463. doi:10.1016/j.vaccine.2018.11.067, PMID:30527659.
[15] Moodie Z, Price L, Gouttefangeas C, Mander A, Janetzki S, Löwer M, *et al*. Response definition criteria for ELISpOT assays revisited. Cancer Immunol Immunother 2010;59:1489–1501. doi:10.1007/s00262-010-0875-4, PMID:20549207.
[16] Cui F, Zhuang H. Achievement and prospect of Mother-to-child block of hepatitis B in Chinese newborns. Virologica Sinica 2019;9:321–326 (In Chinese).
[17] Nelson NP, Easterbrook PJ, McMahon BJ. Epidemiology of Hepatitis B Virus Infection and Impact of Vaccination on Disease. Clin Liver Dis 2016;20:607–628. doi:10.1016/j.cld.2016.06.006, PMID:27742003.
[18] Wang RX, Boland GJ, van Hattum J, de Gast GC. Long-term persistence of T cell memory to HBsAg after hepatitis B vaccination. World J Gastroenterol 2004;10:260–263. doi:10.3748/wjg.v10.i2.260, PMID:14716835.
[19] Leuridan E, Van Damme P. Hepatitis B and the need for a booster dose. Clin Infect Dis 2011;53:68–75. doi:10.1093/cid/cir270, PMID:21653306.
[20] Vyas AK, Jindal A, Hissar S, Ramakrishna G, Trehanpati N. Immune balance in Hepatitis B Infection: present and Future Therapies. Scand J Immunol 2017;86:4–14. doi:10.1111/sji.12553, PMID:28387980.
[21] Shrivastava S, Trehanpati N, Patra S, Kottilil S, Pande C, Trivedi SS, *et al*. Increased regulatory T cells and impaired functions of circulating CD8 T lymphocytes is associated with viral persistence in Hepatitis B virus-positive newborns. J Viral Hepat 2013;20:582–591. doi:10.1111/jvh.12078, PMID:23808997.
[22] Fouts TR, Bagley K, Prado IJ, Bobb KL, Schwartz JA, Xu R, *et al*. Balance of cellular and humoral immunity determines the level of protection by HIV vaccines in rhesus macaque models of HIV infection. Proc Natl Acad Sci U S A 2015;112:E992–999. doi:10.1073/pnas.1423669112, PMID:25681373.
[23] Wang ZZ, Gao YH, Lu W, Jin CD, Zeng Y, Yan L, *et al*. Long-term persistence in protection and response to a hepatitis B vaccine booster among adolescents immunized in infancy in the western region of China. Hum Vaccin Immunother 2017;13(4):909–915. doi:10.1080/21645515.2016.1250990, PMID:27874311.
[24] Posuwan N, Vorayingyong A, Jaroonvanichkul V, Wasitthankasem R, Wanlapakorn N, Vongpunsawad S, *et al*. Implementation of hepatitis B vaccine in high-risk young adults with waning immunity. PLoS One 2018;13:e0202637. doi:10.1371/journal.pone.0202637, PMID:30125298.
[25] FitzSimons D, Hendrickx G, Vorsters A, Van Damme P. Hepatitis B vaccination: a completed schedule enough to control HBV lifelong? Milan, Italy, 17-18 November 2011. Vaccine 2013;31:584–590. doi:10.1016/j.vaccine.2012.10.101, PMID:23142301.
[26] McMahon BJ, Bulkow LR, Singleton RJ, Williams J, Snowball M, Homan C, *et al*. Elimination of hepatocellular carcinoma and acute hepatitis B in children 25 years after a hepatitis B newborn and catch-up immunization program. Hepatology 2011;54:801–807. doi:10.1002/hep.24442, PMID:21618565.
[27] Wang S, Tao Y, Tao Y, Jiang J, Yan L, Wang C, *et al*. Epidemiological study of hepatitis B and hepatitis C infections in Northeastern China and the beneficial effect of the vaccination strategy for hepatitis B: a cross-sectional study. BMC Public Health 2018;18:1088. doi:10.1186/s12889-018-5984-6, PMID:30176842.
[28] Frölich D, Giesecke C, Mei HE, Reiter K, Daridon C, Lipsky pE, *et al*. Secondary immunization generates clonally related antigen-specific plasma cells and memory B cells. J Immunol 2010;185:3103–3110. doi:10.4049/jimmunol.1000911, PMID:20693426.
[29] McHeyzer-Williams LJ, Milpied PJ, Okitsu SL, McHeyzer-Williams MG. Class-switched memory B cells remodel BCRs within secondary germinal centers. Nat Immunol 2015;16:296–305. doi:10.1038/ni.3095, PMID:25642821.
[30] Galson JD, Trück J, Fowler A, Clutterbuck EA, Münz M, Cerundolo V, *et al*. Analysis of B Cell Repertoire Dynamics Following Hepatitis B Vaccination in Humans, and Enrichment of Vaccine-specific Antibody Sequences. EBioMedicine 2015;2:2070–2079. doi:10.1016/j.ebiom.2015.11.034, PMID:26844287.

*Journal of Clinical and Translational Hepatology* **2022** vol. 10(4) | 669–679
DOI: 10.14218/JCTH.2021.00127

Original Article

# Transplantation of Mesenchymal Stem Cells Attenuates Acute Liver Failure in Mice via an Interleukin-4-dependent Switch to the M2 Macrophage Anti-inflammatory Phenotype

Jinglin Wang[1,2,3#], Haoran Ding[1,2,3#], Jingchao Zhou[1,2,3#], Senzhe Xia[4], Xiaolei Shi[1,2,3*] and Haozhen Ren[1,2,3*]

*[1]Nanjing Drum Tower Hospital Clinical College of Traditional Chinese and Western Medicine, Nanjing University of Chinese Medicine, Nanjing, Jiangsu, China; [2]Department of Hepatobiliary Surgery, Affiliated Drum Tower Hospital of Nanjing University Medical School, Nanjing, Jiangsu, China; [3]Department of Hepatobiliary Surgery, Nanjing Drum Tower Hospital Clinical College of Nanjing Medical University, Jiangsu, China; [4]Department of Hepatobiliary Surgery, Nanjing Drum Tower Hospital Clinical College of Jiangsu University, Nanjing, Jiangsu, China*

**Received:** 1 April 2021 | **Revised:** 10 June 2021 | **Accepted:** 14 October 2021 | **Published:** 4 January 2022

## Abstract

***Background and Aims:*** Transplantation of mesenchymal stem cells (MSCs) derived from bone marrow (BM) is an alternative treatment of acute liver failure (ALF) mainly because of the resulting anti-inflammatory activity. It is not known how MSCs regulate local immune responses and liver regeneration. This study explored the effects of MSCs on hepatic macrophages and the Wnt signaling pathway in ALF. ***Methods:*** MSCs were isolated from BM aspirates of C57BL/6J mice, and transplanted in mice with ALF induced by D-galactosamine (D-Gal). The proliferation of hepatocytes was assayed by immunohistochemical (IHC) staining of Ki-67 and proliferating cell nuclear antigen (PCNA). The levels of key proteins in the Wnt signaling pathway were assayed by western blotting and cytokines were determined enzyme-linked immunosorbent assays (ELISAs). A macrophage polarization assay characterized the M1/M2 ratio. The potential role of interleukin-4 (IL-4) in the biological activity of MSCs was determined by silencing of IL-4. ***Results:*** Transplantation of allogeneic MSCs significantly attenuated D-Gal-induced hepatic inflammation and promoted liver regeneration. MSC transplantation significantly promoted a phenotypic switch from proinflamatory M1 macrophages to anti-inflammatory M2 macrophages, leading to significant Wnt-3a induction and activation of the Wnt signaling pathway in mice with D-Gal-induced ALF. Of the paracrine factors secreted by MSCs (G-CSF, IL-6, IL-1 beta, IL-4, and IL-17A), IL-4 was specifically induced following transplantation in the ALF model mice. The silencing of IL-4 significantly abrogated the phenotypic switch to M2 macrophages and the protective effects of MSCs in both the ALF model mice and a co-culture model in an IL-4 dependent manner. ***Conclusions:*** *In vivo* and *in vitro* studies showed that MSCs ameliorated ALF through an IL-4-dependent macrophage switch toward the M2 anti-inflammatory phenotype. The findings may have clinical implications in that overexpression of IL-4 may enhance the therapeutic effects of allogeneic MSC transplantation in the treatment of ALF.

**Citation of this article:** Wang J, Ding H, Zhou J, Xia S, Shi X, Ren H. Transplantation of Mesenchymal Stem Cells Attenuates Acute Liver Failure in Mice via an Interleukin-4-dependent Switch to the M2 Macrophage Anti-inflammatory Phenotype. J Clin Transl Hepatol 2022;10(4):669–679. doi: 10.14218/JCTH.2021.00127.

## Introduction

Acute liver failure (ALF) is an uncommon but life-threatening condition with high mortality.[1] Liver transplantation is an established salvage therapy for ALF, but the shortage of donors and the high cost of surgery are major considerations.[2,3] Therefore, there is an urgent need of alternative treatments for patients with ALF.

Mesenchymal stem cells (MSCs), also known as mesenchymal stromal cells, are adult stem cells present in adipose tissue, bone marrow (BM), skeletal muscle, umbilical cord blood, and synovium.[4] MSCs are good candidates for transplantation as they are easily obtained from a variety of tissues and expanded in culture. Unlike other types of stem cells (e. g. embryonic stem cells), MSCs avoid immune rejection and ethical issues related to stem cell transplantation.[5] In addition to self-renewal and differentiation along multiple lineages, MSCs modulate innate and adaptive immune responses through secretion of mediators like transforming growth factor beta (TGF-β), indoleamine 2,3-dioxygnase, cyclooxygenase 2 (COX2), prostaglandin E2 (PGE2), interleukin (IL)-4, and TNF-alpha stimulated gene (TSG)-6.[6] Accumulating evidence indicates that MSCs

**Keywords:** Acute liver failure; Mesenchymal stem cells; Interleukin 4; Macrophage; Wnt signaling pathway.

**Abbreviations:** ALF, acute liver failure; ALT, alanine transaminase; AST, aspartate aminotransferase; BM, bone marrow; COX2, cyclooxygenase 2; D-Gal, D-galactosamine; IL-4, interleukin-4; INOS, nitric oxide synthase; MCP-1, monocyte chemoattractant protein-1; MSCs, mesenchymal stem cells; $NH_3$, serum ammonia; PBS, phosphate buffered saline; PGE2, prostaglandin E2; PT, prothrombin time; TBS, tris buffered saline; TGF-β, transforming growth factor β; TSG-6, TNF-α-stimulating gene 6; TUNEL, TdT-mediated dUTP nick-end labeling.

[#]These authors contributed equally to this work.

[*]**Correspondence to:** Haozhen Ren and Xiaolei Shi, Nanjing Drum Tower Hospital Clinical College of Traditional Chinese and Western Medicine, Nanjing University of Chinese Medicine, No. 321, Zhongshan Road, Gulou District, Nanjing, Jiangsu 210008, China. Tel: +86-25-83106666, Fax: +86-25-83106666, E-mail: renhaozhen1984@163.com (HR) or sxl@nju.edu.cn (XS)

can exert immunosuppressive effects, such as anti-inflammatory activity, which is why MSC transplantation has been used to treat inflammatory diseases.[7] For example, allo- and autotransplantation of MSCs by portal vein injection to reduce D-galactosamine (D-Gal)-induced liver failure,[8,9] which is a widely used model of immune-induced hepatic failure.[10] From the perspective of clinical application, MSCs obtained by *in vitro* expansion have advantages compared with autologous transplantation. However, the mechanisms, including those underlying MSCs-mediated attenuation of D-Gal-induced liver failure, are complex and remain to be elucidated. In this study, we performed *in vivo* and *in vitro* investigations of the mechanisms underlying the therapeutic effects of MSCs on ALF induced by D-Gal in mice.

## Methods

### *Experimental animals*

C57BL/6J mice were purchased at 4–6 weeks of age from the Experimental Animal Center of Drum Tower Hospital, Nanjing University of Medical School (Nanjing, Jiangsu, China). The mice were maintained on a 12 h light/dark cycle in a room with suitable air pressure and temperature, and given axenic water and sterile standard pellet feed. The mice were used for preparation of MSCs and *in vivo* studies and were sacrificed by cervical dislocation on completion of the study procedures. The protocols involving experimental mice were reviewed and approved by the institutional animal care and use committee of Nanjing University (Nanjing, Jiangsu, China) and conducted following the National Institutes of Health (NIH) laboratory animal care and use guidelines.

### *Isolation and characterization of MSCs*

MSCs were isolated from fresh BM aspirates of C57BL/6J mice. Briefly, the soft tissues surrounding the femur, humerus, and tibia were cut to expose the BM cavity, followed by washing three times with phosphate buffered saline (PBS). The BM was collected and centrifuged at 1,200 rpm for 5 m. The cell pellet was resuspended in low-glucose Dulbecco's modified Eagle medium (DMEM, Gibco, Grand Island, NY, USA) with 10% fetal bovine serum (FBS), 100 U/mL penicillin, and 100 mg/mL streptomycin and cultured in a 37°C incubator with 5% $CO_2$. When the cells reached approximately 80% confluence, they were passaged. MSCs were used for transplantation at passages 3 to 6. The surface markers (e.g., CD29, CD44, CD45, CD90) were assayed by flow cytometry (FACScan; Becton Dickinson, San Diego, CA, USA).

### *Isolation and identification of hepatic macrophages*

Hepatic macrophages were isolated from the fresh liver tissues of C57BL/6J mice as previously described.[11] In brief, liver tissue was cut into small pieces and digested by incubating in 10 mL Roswell Park Memorial Institute 1640 (RPMI 1640, Gibco, Grand Island, NY, USA) medium containing 0.1% type IV collagenase at 37°C for 30 m. The resulting tissue homogenate was filtered through 70 μm stainless steel mesh to remove undigested tissue, and the cell suspension was centrifuged at 300×*g* (Eppendorf 5810R, Germany) at 4°C for 5 m. The cell pellet was resuspended in 10 mL RPMI 1640 and centrifuged at 300×*g* for 5 m at 4°C. The pellet cells were resuspended in 10 mL RPMI 1640 and centrifuged at 50×*g* for 3 m at 4°C. The cell pellet was resuspended in 10 mL RPMI 1640, and centrifuged at 50×*g* for 3 m at 4°C. The aqueous phase (clarified cell suspension) was transferred to a 10 mL tube, and centrifuged at 300×*g* for 5 min at 4°C. The pellet was resuspended and seeded in six-well plates at a density of $1–3\times10^7$ cells/well for culture in DMEM supplemented with 10% FBS and 100 U/mL penicillin/streptomycin in an 37°C incubator with 5% a $CO_2$ atmosphere for 2 h. Nonadherent cells (macrophages) were then harvested by gentle washing with PBS. The prepared hepatic macrophages were characterized by flow cytometry (FACScan; Becton Dickinson, San Diego, CA, USA) using a PE-Cyanine7-labeled anti-F4/80 monoclonal antibody (25-4801; eBioscience, USA) as previously described.

### *Co-culture of MSCs and macrophages*

For co-culture of MSCs and macrophages, hepatic macrophages were isolated from normal or ALF mouse livers and plated at $4\times10^5$ cells/well in the lower chamber of Transwell six-well plates with 0.4 μm pore membranes (Corning Inc., Corning, NY, USA). Macrophages were seeded in the upper chambers at $2\times10^5$ cells/well. Macrophages cultured alone and co-cultured with MSCs with short hairpin IL-4 knockdown were controls. After incubation for 24 h, hepatic macrophages were collected for flow cytometric analysis.

### *Mouse model of ALF and MSC transplantation*

C57BL/6J mice 4-6 weeks of age were used to establish a mouse model of ALF induced by intraperitoneal injection of D-Gal (0.6 g/kg). The C57BL/6J mice were randomly assigned to MSCs transplantation ($n$=20) or PBS transplantation ($n$=20). Twelve hours after induction of ALF, mice in the MSCs transplantation group were injected with $1\times10^6$ MSCs suspended in 0.5 mL PBS through the hepatic portal vein (MSCs group). Mice in the PBS-treatment group were injected with 0.5 mL PBS alone, and normal C57BL/6J mice without any transplantation were the control group.

To examine effects of MSC transplantation on survival and ALF, and to study the mechanisms, 10 mice were randomly selected from each of the MSC group and control groups. Blood and liver samples were collected at 24, 48, 72, 96, 120, 144, and 168 h after transplantation in the MSC and PBS groups. To investigate the hepatoprotection of Wnt-3a, 10 μg/kg recombinant Wnt-3a (R & D Systems, Minneapolis, MN, USA) in DMEM ($n$=10) and 0.1μM Wnt-C59 (SelleckChem, Houston, TX, USA) in with 0.5 mL 0.5% methylcellulose and 0.1% Tween-80 ($n$=10) were given by intravenous injection 24 h after injection of D-Gal.

### *Blood biochemistry*

Blood samples were collected from the vena cava and centrifuged at 3,000×*g* for 10 m. Serum levels of aspartate aminotransferase (AST), alanine aminotransferase (ALT), ammonia ($NH_3$), and prothrombin time (PT) were assayed with an autoanalyzer (Fuji, Tokyo, Japan).

### *Cytokine assays*

To evaluate the anti-inflammatory effect of MSCs transplantation, serum cytokines, including tumor necrosis factor alpha (TNF)-α, interferon (IFN)-γ, interleukin (IL)-1α, IL-1β, IL-4, IL-6, IL-10, and IL-17A, were determined by

enzyme-linked immunosorbent assay (ELISA) kits on day 3 after induction of ALF.

### *Real-time quantitative reverse-transcription polymerase chain reaction (qRT-PCR)*

Total RNA was extracted using TRIzol reagent (Invitrogen, Carlsbad, CA, USA). cDNA was synthesized using Superscript II reverse transcriptase sit (Invitrogen). qRT-PCR was performed to determine the relative mRNA expression of the genes of interest using Power SYBR Green PCR Master Mix (Takara, Tokyo, Japan). mRNA expression was calculated with the $2^{-\Delta\Delta CT}$ method and normalized to β-actin. The primer sequences are listed in Supplementary Table 1.

### *Labeling MSCs with DiR to track the transplanted MSCs*

MSCs were incubated with 50 μmol/L DiR buffer (Fanbo Biochemicals, Beijing, China) at 37°C for 20 m. The DiR-labeled MSCs were centrifuged at 453×*g* for 5 m and resuspended in PBS, following the manufacturer's protocol. *In vivo* imaging was performed with an *in vivo* imaging system using a charged-coupled device camera (IVIS Spectrum, Caliper Life Sciences, Runcorn, Cheshire, UK) on day 3 after MSC transplantation. Living Image version 4.3.1 (Caliper Life Sciences, Hopkinton, MA, USA) was used to analyze the image data.

### *Western blot assay*

Expression of non-phospho-β-catenin (active β-catenin), phospho-β-catenin, HGF, c-Myc, Cyclin D1, TCF1, and LEF1 was assayed by western blotting. Briefly, total protein, cytoplasmic protein, and nuclear protein were extracted from total liver tissue lysates and the cytoplasmic, and nuclear fractions following the kit manufacturer's instructions (Active Motif Company, Carlsbad, CA, USA). Protein concentration was determined with a bicinchoninic acid (BCA) assay (Sigma-Aldrich, St Louis, MO, USA). The protein extracts were separated by 12% sodium dodecyl sulfate-polyacrylamide gel electrophoresis (SDS-PAGE) and transferred to nitrocellulose membranes. The membrane were blocked with 5% (w/V) fat-free emulsion in Tris buffered saline (TBS) containing 0.05% Tween 20, and then incubated with primary antibodies overnight at 4°C. The membranes were the incubated with horseradish peroxidase-conjugated secondary antibodies (1:10,000 dil.). The antibody-bound bands were visualized and analyzed by electrochemiluminescence (ECL) and the signal intensity of each protein band was quantified with ImageJ (NIH, Bethesda, MD, USA). Primary antibodies used for western blot assays were listed in Supplementary Table 2.

### *Flow cytometry of M1/M2 macrophages*

M1 and M2 macrophages were characterized by flow cytometry to identify their specific surface markers. The classic CD11c M1 macrophage marker and the classic M2 macrophage markers were labeled with phycoerythrin (PE)-conjugated anti-mouse CD11c (Biolegend, San Diego, CA, USA) and fluorescein isothiocyanate (FITC) anti-mouse CD206 (Biolegend, San Diego, CA). Briefly, the cells were incubated with fluorescent labeled antibody for 30 m, washed with staining buffer at 4°C, fixed in PBS containing 2% paraformaldehyde, and assayed (FACScan; Becton Dickinson) following the manufacturer's instructions.

### *Histological and immunohistochemical assays*

Three 5 μm sections of each block of liver tissue were stained with hematoxylin and eosin (H-E) for histological evaluation. Apoptosis was assayed by TdT-mediated dUTP nick-end labeling (TUNEL) staining using a cell death detection kit (Roche, Frankfurt, Germany). The proliferation of hepatocytes was assayed by immunohistochemical (IHC) staining of Ki-67 and proliferating cell nuclear antigen (PCNA; AVIVA Systems Biology, Beijing, China). The expression of p-β-catenin, cyclin D1, and c-myc proteins was assayed by IHC staining. Semi-quantitative analysis was conducted with Image Pro Plus software (Media Cybernetics, Bethesda, MD, USA).

### *Immunofluorescence staining of M1 and M2 macrophage phenotype biomarkers*

M1/M2 macrophages were characterized by immunofluorescence staining of phenotype markers, including iNOS (an M1 marker), arginase-1 (Arg1, (an M2 marker), and F4/80 (a marker of murine macrophages). The primary antibodies were F4/80 (1:100, ab6640), arginase-1 (Arg1, 1:100, ab91279), and iNOS (1:500, ab178954 were all from Abcam and all were fluorescence labeled. Ten micrometer liver sections were blocked with a PBS blocking solution containing goat serum (Gibco) for 1 h at room temperature, and incubated with the primary antibody at 4°C overnight. The secondary antibody was added and incubated for 1h at room temperature. After washing for three times with PBS, the slides were incubated with diamidino-phenylindole (DAP for 10 m. The secondary antibodies were goat anti-rabbit IgG Alexa Fluor 488/594 (1:200, Invitrogen) and goat anti-rat IgG1 Alexa Fluor 488/594 (1:150, Invitrogen). Image Pro Plus 5.0 was used to count the number of stained macrophages and calculate the proportions of positive macrophages.

### *Macrophage depletion*

To determine the role of liver macrophages in MSC-promoted liver regeneration, 100 μL clodronate liposomes (Cl2MBP; Vrije Universiteit, Amsterdam, The Netherlands) was injected 48 h before treatment with D-Gal.

### *IL-4 shRNAs and transfection*

To silence IL-4 gene expression, three IL-4 specific shRNA target sequences were selected for IL-4 RNA interference short hairpin (sh)RNA1 (316–336) AAG CTG CAC CAT GAA TGA GTC; shRNA2 (181–201) AAC ACC ACA GAG AGT GAG CTC; and shRNA3 (47–67) AAT GTA CCA GGA GCC ATA TCC. The sequence of the IL-4 mismatch shRNA1 was AAG AGT AAG ATC CAC GTC. The negative control scrambled shRNA was from Ambion (Austin, TX). Lentiviral vector systems were used to deliver IL-4 shRNAs into MSCs to silence IL-4 gene expression following the manufacturer's instructions.

### *Ethical approval*

All animal procedures were performed with the approval

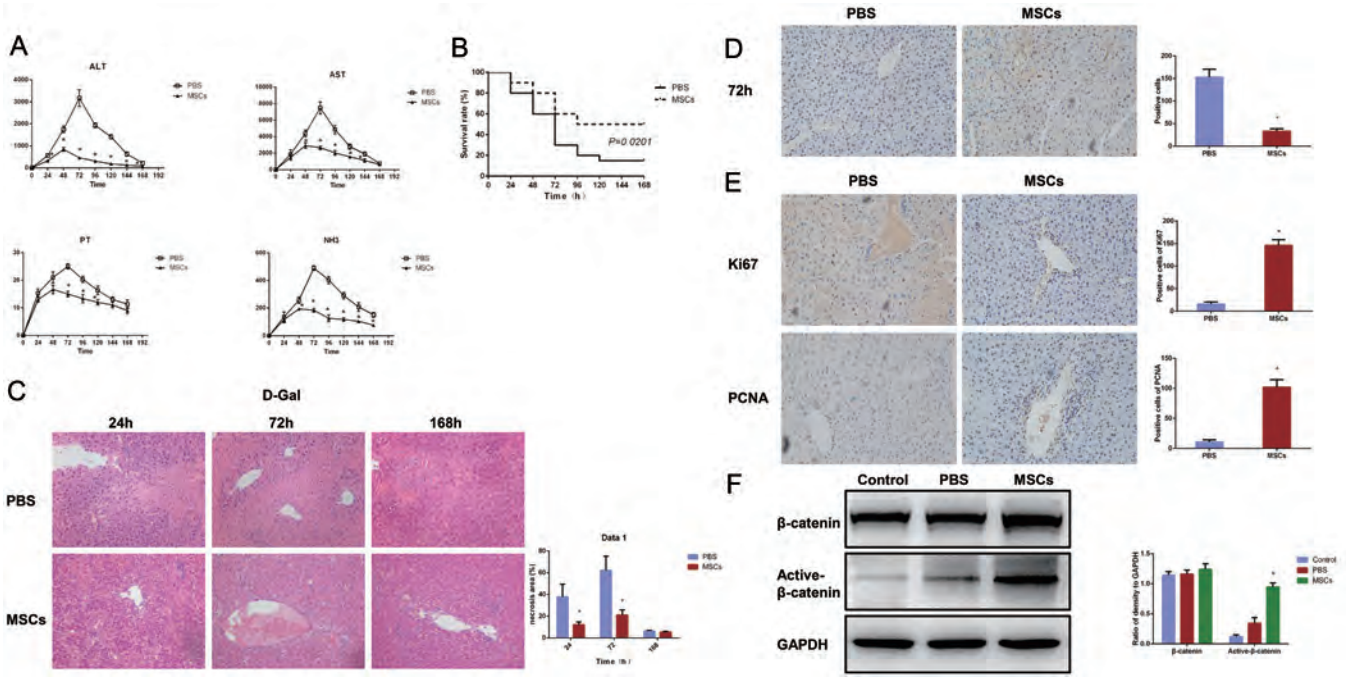


**Fig. 1. Mesenchymal stem cell transplantation attenuated D-Gal-induced ALF.** (A) Effects of mesenchymal stem cell (MSC) transplantation on serum levels of alanine transaminase (ALT), aspartate transaminase (AST), prothrombin (PT), and $NH_3$ at 24, 48, 72, 96, 120, 144, and 168 h after transplantation. Transplantation significantly decreased the levels of liver enzymes (ALT and AST), PT, and $NH_3$ after infusion; (B) Effects of MSC transplantation on survival included a significant reduction in mortality; (C) Hematoxylin and eosin staining of liver sections; (D) TUNEL staining assay of apoptosis; (E) Immunohistochemical staining of Ki67 and PCNA for assay of cell proliferation; (F) Western blots of β-catenin and active-β-catenin protein expression. *$p$<0.05 vs. phosphate buffered saline. Normal C57BL/6J mice without transplantation were controls.

of Ethics Committee for Animal Experimentation of the Affiliated Drum Tower Hospital of Nanjing University Medical School (No.20160601). All surgery was performed under isoflurane anesthesia, and all efforts were made to minimize animals suffering.

### *Statistical analysis*

The results were expressed as means±standard derivations (SDs) from at least three independent assays. The statistical analysis was performed by Prism, version 6.0 (GraphPad Software Inc., La Jolla, California, USA). Student's *t*-test was used to evaluate between-group differences, and *p*-values <0.05 were considered statistically significant.

## Results

### *Transplantation of MSCs attenuated D-Gal-induced ALF by promoting liver regeneration*

The protective effects of MSC transplantation are shown in Figure 1A. D-Gal administration significantly elevated serum ALT, AST, PT, and $NH_3$, all, of which were significantly decreased in the mice with MSC transplantation compared with those given PBS ($p$<0.05). MSC transplantation significantly improved the survival of mice exposed to D-Gal ($p$<0.05, Fig. 1B). H&E staining of liver sections showed that the area of necrosis in mice with MSC transplantation was significantly smaller than that in those given PBS only ($p$<0.05, Fig. 1C). TUNEL analysis revealed that there significantly fewer apoptotic hepatocytes in mice with MSC transplantation than in those given PBS only ($p$<0.05, Fig. 1D). The proliferation assays found that there were significantly more Ki-67- and PCNA-positive hepatocytes in the MSC transplantation group than in the PBS group ($p$<0.01, Fig. 1E).

Western blot assays found that the expression of hepatic active-β-catenin was significantly higher in the MSCs transplantation group than in the PBS group ($p$<0.05, Fig. 1F). The results show that MSC transplantation attenuated D-Gal-induced liver damage in this mouse model of ALF by promoting liver regeneration, with involvement of β-catenin.

### *MSC transplantation promoted liver regeneration with involvement of the hepatic Wnt/β-catenin signaling pathway*

Changes in the expression of proteins and mRNAs involved in the Wnt/β-catenin signaling pathway and association with liver regeneration were assayed. As shown in Figures 2 and 3, the expression of HGF, c-myc, and cyclin D1 mRNA and protein were significantly higher in the tissues from mice with MSC transplantation compared with those given PBS only (all $p$<0.05). The results provide additional evidence that MSC transplantation alleviated D-Gal-induced ALF by promoting liver regeneration involving the Wnt/ β-catenin signaling pathway. Wnt/β-catenin signaling modulates cytokine production. As shown in Figure 2C, cytokines levels differed significantly in mice with MSC transplantation and in those given PBS only ($p$<0.05). Consistent with the changes in cytokine levels, the expression of both Wnt3a mRNA and protein were significant higher in mice in the MSC transplantation in those in the PBS group (Fig. 2D, E),

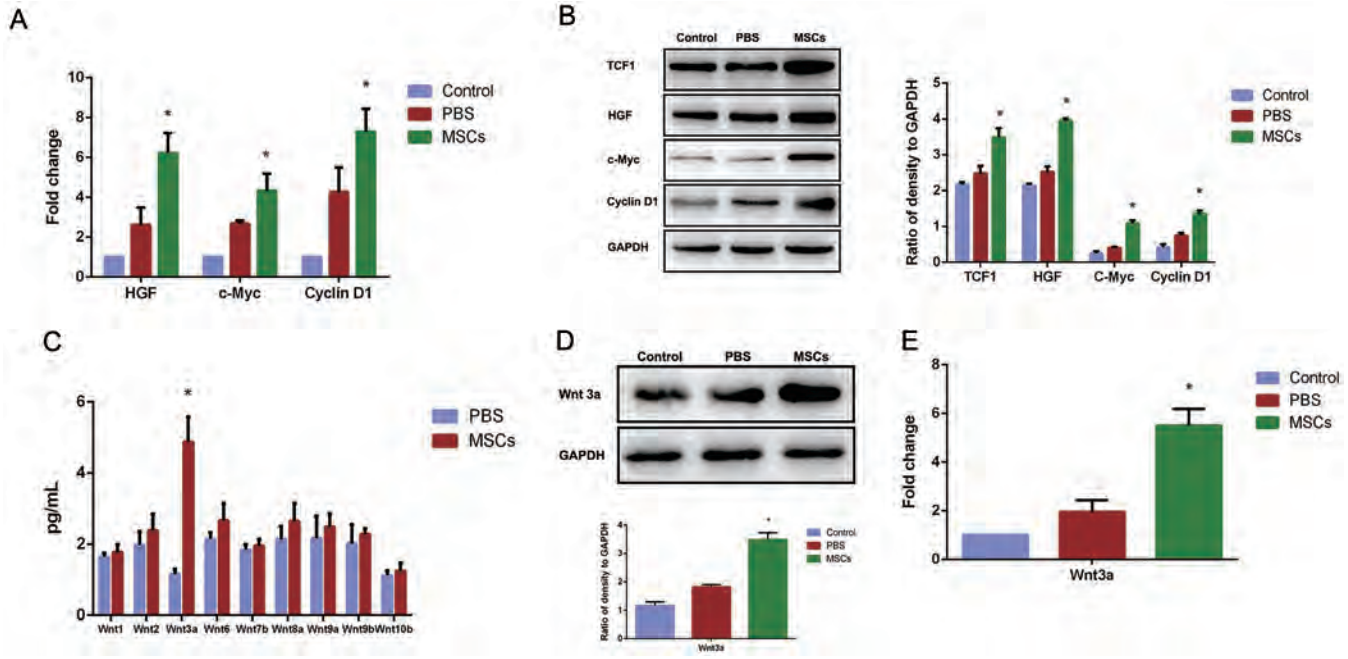


**Fig. 2. Mesenchymal stem cell (MSC) transplantation increased hepatic Wnt-3a mRNA and protein expression.** (A) mRNA expression of HGF, c-Myc, and Cyclin D1; (B) Western blot assays of TCF1, HGF, c-Myc, and cyclin D1 protein expression; (C) Liver cytokines associated with the Wnt signaling pathway measured by ELISA. (D) Western blots of Wnt-3a protein expression; (E) qRT-PCR assay of Wnt-3a mRNA expression. **p*<0.05 vs. phosphate buffered saline. Normal C57BL/6J mice without transplantation were controls.

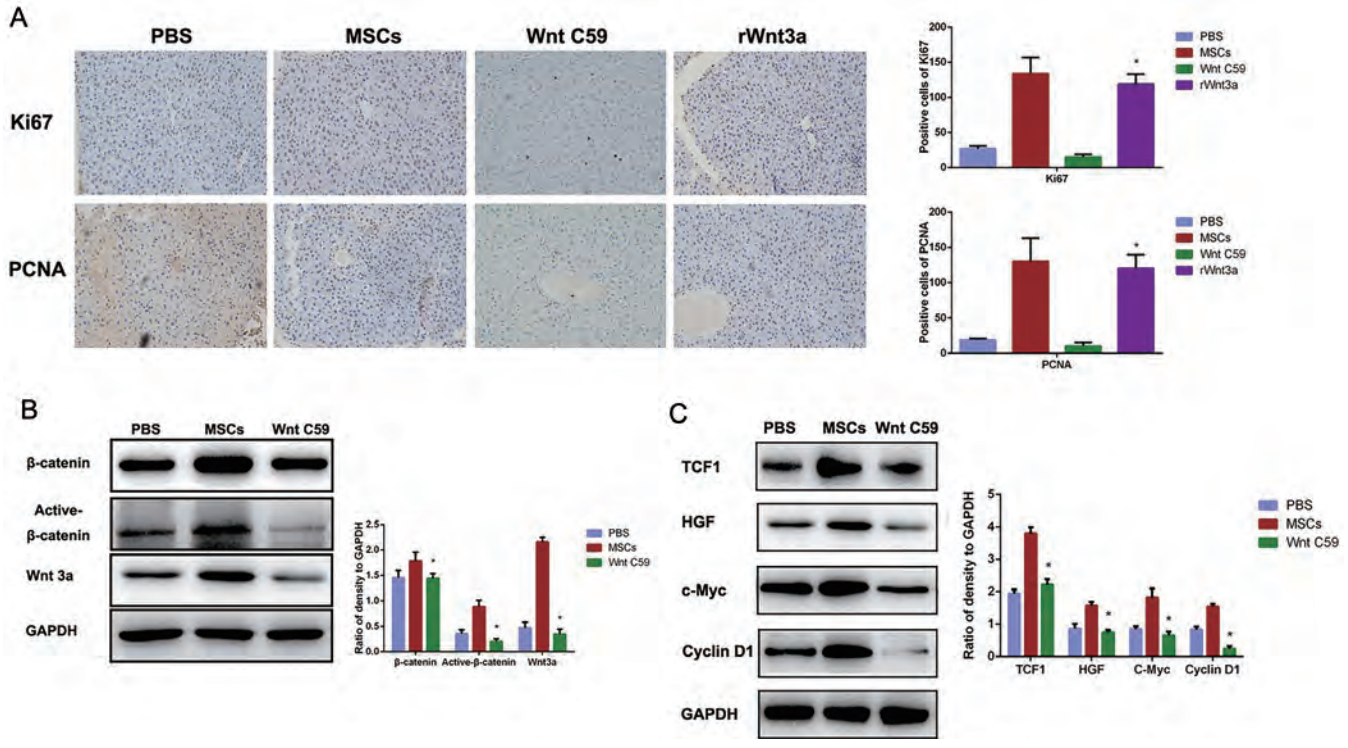


**Fig. 3. Effects of Wnt-3a and the Wnt signaling inhibitor on mesenchymal stem cell (MSC) transplantation-promoted liver regeneration.** (A) Immunohistochemical staining of Ki67 and PCNA (200×). Wnt-3a treatment significantly increased the number of Ki-67- and PCNA-positive hepatocytes. Wnt-C59 treatment significantly abrogated promotion of cell proliferation by MSCs. **p*<0.05 vs. Wnt-C59; (B) Western blots of β-catenin, active-β-catenin, and Wnt-3a expression. Wnt-C59 significantly decreased the expression of hepatic β-catenin, active-β-catenin, and Wnt-3a proteins. **p*<0.05 vs. MSCs transplantation; (C) Western blots of TCF1, HGF, c-Myc, and Cyclin D1 protein expression. Wnt-C59 significantly decreased the expression of TCF1, HGF, c-Myc, and Cyclin D1. Data are means±standard deviations. **p*<0.05 vs. MSC transplantation.

which is in line with the cytokine results.

The roles of Wnt-3a and the Wnt/β-catenin signaling pathway in MSC transplantation-induced liver regeneration, mice were injected with recombinant mouse Wnt-3a or Wnt-C59, Wnt/β-catenin signaling pathway inhibitor. As shown in Figure 3, Wnt-3a significantly increased the number of Ki-67- and PCNA-positive hepatocytes ($p<0.05$), Wnt-C59 significantly abrogated the proliferation promoting effects of MSC transplantation ($p<0.05$). Wnt-C59 also significantly decreased the expression of hepatic Wnt-3a, HGF, c-myc, and cyclin D1 proteins (Fig. 3B, C). The results indicated that the Wnt/β-catenin signaling pathway was involved in the promotion of liver regeneration in mice with D-Gal-induced ALF, and that upregulation of hepatic Wnt-3a ameliorated ALF.

### *MSC transplantation induced a macrophage switch toward anti-inflammatory M2 phenotype in D-Gal-induced ALF*

As shown in Figure 4A, the mRNA expression of F4/80, a cell surface marker of mouse macrophages as significantly increased in response to MSCs transplantation, but the mRNA expression of the markers of other immune cells in the liver remained unchanged. IHC staining (Fig. 4B) showed that there were significantly more F4/80-positive cells in MSC-transplanted mice than in those given PBS ($p<0.05$). Also, following transplantation, MSCs were found in the liver, but not detected in other organs, showing a great homing ability for the D-Gal-injured liver (Fig. 4C).

To determine the contributory roles of macrophages to the secretion of Wnt-3a after MSC transplantation, chloroethanol was used to promote inflammatory liver injury. After chloroethanol administration, no F4/80-positive cells were detected (Fig. 4D). Chlorohydrin treatment significantly increased serum levels of ALT/AST/PT/$NH_3$ and the extent of liver necrosis (Fig. 4E and F). Furthermore, chloroethanol significantly decreased the number of Ki-67- and PCNA-positive hepatocytes (Fig. 4G). The results suggested that a key protective role of liver macrophages was to increase Wnt-3a levels.

Changes in the expression of macrophage markers indicated that the transplantation of MSCs was associated with a switch from the M1 to the M2 phenotype. The mRNA expression of M1 markers, nitric oxide synthase (iNOS), TNF-α, and MCP-1, and M2 markers arginase 1 (Arg1), Mrc-2, and CD163 in mouse liver tissue is shown in Figure 5A. As shown in Figure 5B, Wnt-3a was localized to macrophages. Immunofluorescence staining that the number of iNOS-positive M1 macrophages was reduced and the number of Arg1-postive M2 macrophages was increased in MSC-transplanted mice compared the controls (Fig. 5C and D). The data indicated that MSC transplantation induced a switch in macrophage phenotypic from M1 to M2, leading to production of Wnt-3a.

### *MSC transplantation increased hepatic IL-4 expression in mice with D-Gal-induced ALF*

To investigate the mechanisms underlying the switch to proinflammatory M1 macrophages anti-inflammatory M2 macrophages we looked for changes in the expression of paracrine factors secreted by MSCs, including G-CSF, IL-6, IL-1 beta, IL-4, and IL-17A. IL-4 mRNA and protein expression were both significantly elevated in the MSC-transplanted mice compared with the PBS controls. The differences in IL-6, IL-1β, and IL-17A (Fig. 6) were not significant. The findings indicate that IL-4 induction was specific to MSCs.

### *Knockdown of IL-4 abrogated MSC transplantation-mediated phenotype switch toward M2 macrophages and protective effects in D-Gal-induced ALF*

To investigate the role of IL-4 in the switch from the M1 to the M2 macrophage phenotype, the IL-4 gene was silenced by shRNA-mediated interference. IL-4 expression was knocked down in mice treated with IL-4 shRNA compared with scrambled shRNA negative controls (Fig. 7A). IL-4 knockdown led to a significant increase in serum ALT/AST/PT/$NH_3$ (Fig. 7B) and the extent of liver necrosis (Fig. 7C). It did lead to a significant decrease in liver regeneration (Fig. 7D) and survival (Fig. 7E). Silencing IL-4 gene expression significantly affected the markers of M1 and M2 macrophages, resulting in increased hepatic iNOS mRNA expression (Fig. 7F), and decreased hepatic Arg1 mRNA expression (Fig. 7F). The results indicate that IL-4 was essential for the switch toward M2 macrophages and subsequent protective effects in D-Gal-induced ALF.

### *MSCs rely on IL4 to drive the phenotypic switch of mouse liver macrophages toward the M2 phenotype*

The dependence of the transplantation-mediated phenotypic switch on IL-4 was investigated an *in vitro* model of co-cultured MSCs and mouse liver macrophages (Fig. 8A, B). Flow cytometry confirmed that the number of CD11c-postive M1 macrophages was reduced and the number of CD206-postive M2 macrophages was increased in the D-Gal (+) shRNA-IL-4 MSC (+), scrambled shRNA MSC (−) group versus the D-Gal (+) shRNA-IL-4 MSC (−) scrambled shRNA MSCs (−) group ($p>0.05$, Fig. 8C). The number of CD11c-postive and CD206-postive macrophages was significantly reduced in the D-Gal (+) shRNA-IL-4 MSC (−), scrambled shRNA MSCs-scramble (+) group versus the D-Gal (+) shRNA-IL-4 MSC (−), scrambled shRNA MSCs (−) group ($p<0.05$, Fig. 8C). The data indicate that MSC-induced phenotype switch was IL-4-dependent. Interference of shRNA-transfected MSCs which prevented the switch to M2 macrophage due to the knockdown of IL-4. The findings indicate that IL-4 was essential for the observed switch to M2 macrophages following MSC transplantation in this D-Gal-induced ALF model.

## Discussion

Immune-mediated liver disease is often complicated by fulminant hepatitis or liver failure. MSC transplantation is an alternative treatment for ALF, but the therapeutic mechanisms need to be elucidated. The major novel findings of this study are: (1) MSC transplantation significantly ameliorated D-Gal-induced inflammation and stimulated liver regeneration (2) and induced a switch of hepatic macrophages from the M1 to the M2 phenotype. (3) Secretion of the paracrine factors IL-4 was specifically induced in following MSC transplantation compared with PBS control mice (4) Knockdown of IL-4 significantly abrogated the switch to anti-inflammatory M2 macrophages and attenuation of D-Gal-induced ALF. (5) Silencing of IL-4 in *in vitro* co-cultures of MSCs and hepatic macrophages showed that MSCs promoted the switch to M2 macrophages in an IL-4 dependent manner. The findings indicated that MSCs ameliorated ALF through IL-4-dependent macrophage switch toward M2 anti-inflammatory phenotype. These results are consistent with mediation of the protective effects of MSCs by increased levels of hepatic Wnt-3a, which in turn inhibited phosphorylation of β-catenin. The resulting increase of non-

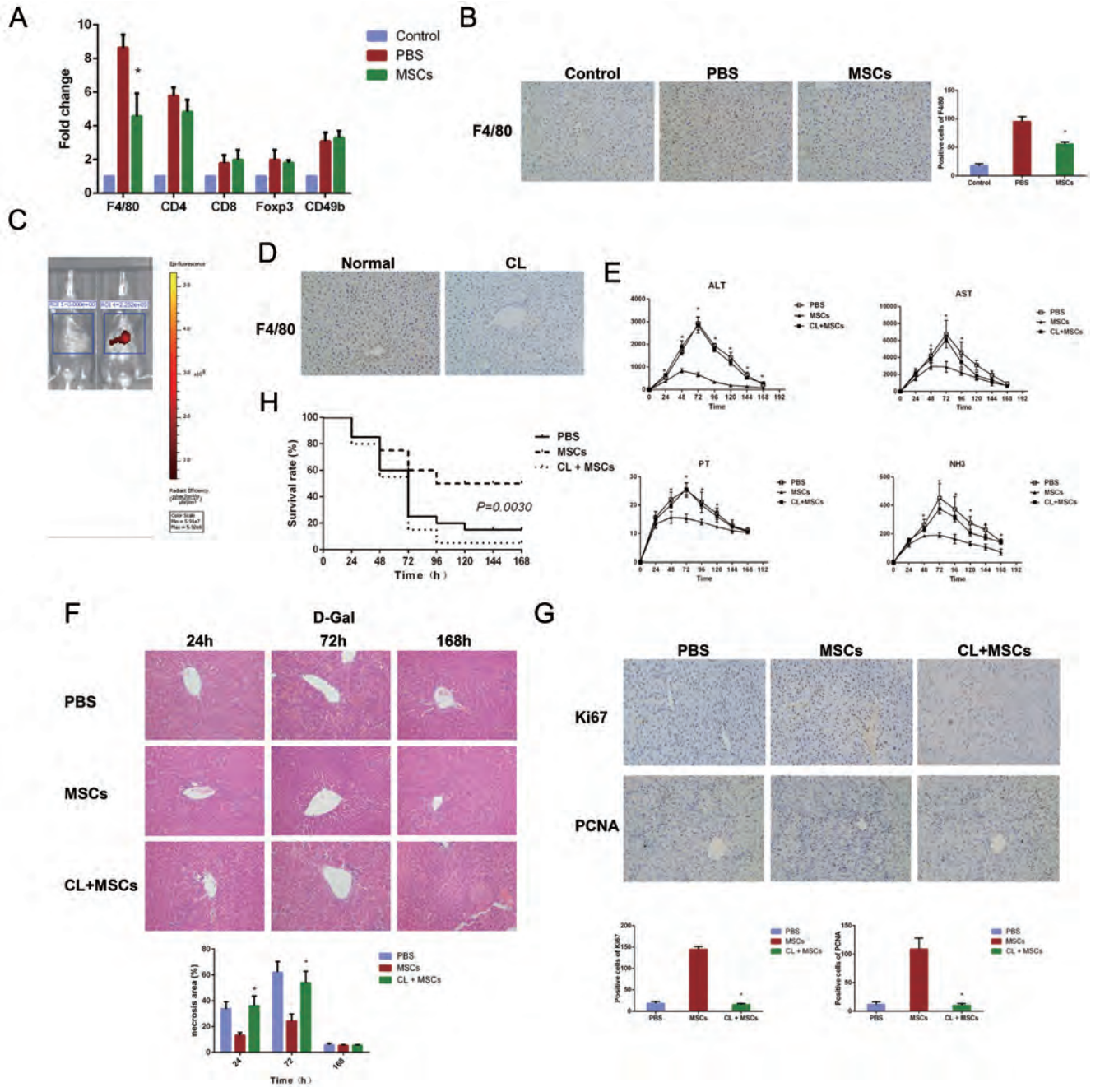


**Fig. 4. Role of hepatic macrophages in mesenchymal stem cell (MSC) transplantation-mediated effects on acute liver failure (ALF).** (A) F4/80, CD4, CD8, Foxp3, and CD49b mRNA expression. *$p$<0.05 vs. phosphate buffered saline (PBS). (B) F4/80 staining (200×). *$p$ < 0.05 vs. PBS transplantation group. (C) IVIS was used to identify distribution of DiR-labeled mesenchymal stem cells (MSCs). (D) F4/80 staining of liver sections after chloroethanol administration (200×); (E) Serum ALT, AST, PT, and $NH_3$ after MSC transplantation. *$p$<0.05 vs. MSC transplantation. (F) Hematoxylin and eosin staining of liver tissue (200×). *$p$<0.05 vs. MSC transplantation. (G) Ki67 and PCNA staining (200×). *$p$<0.05 vs. CL+MSCs. (H) Survival analysis. *$p$<0.05 vs. MSCs transplantation group. Normal C57BL/6J mice without transplantation were controls.

phospho-β-catenin (active β-catenin) led to upregulation of HGF, c-myc, and cyclin D1, which promoted liver regeneration. The macrophage phenotype switch can account for the increase of Wnt-3a that was associated with MSC transplantation. Allogeneic MSC transplantation has great therapeutic potential and may be used in clinical practice in the future.

It has been reported that transplantation of autologous MSCs can prevent liver injury caused by D-Gal in animal models.[8] The transplantation of autologous MSCs to treatment patients with severe ALF is not feasible because the severity of the condition makes it challenging to obtain autologous MSCs that meet quality and quantity standards. That is the reason we used allogeneic MSCs in this study. We transplanted BM-derived MSCs into recipient mice of the same species with different genes. The results showed that allogeneic MSCs transplantation achieved protective effects

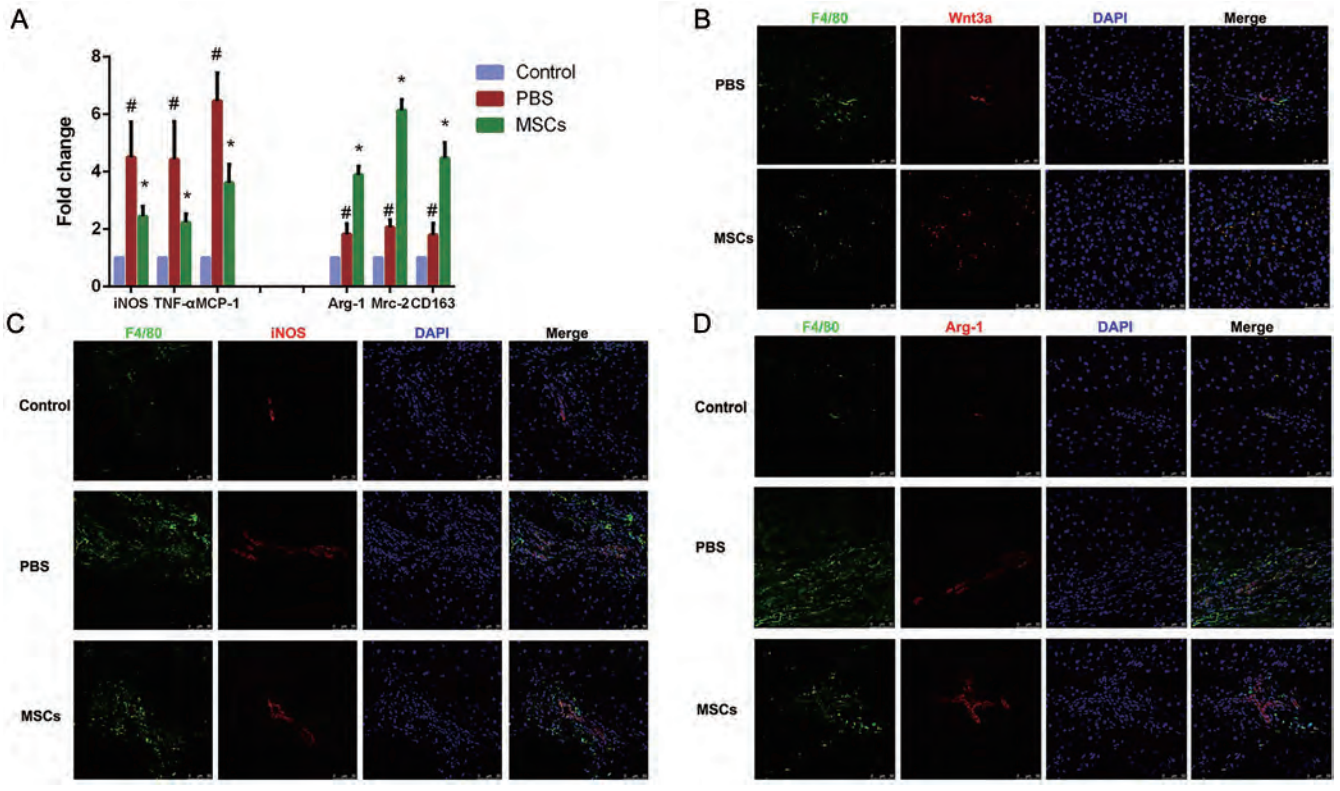


**Fig. 5. Mesenchymal stem cell (MSC) transplantation induced the phenotypic switching of liver macrophages to the M2 phenotype.** (A) The mRNA expression levels of nitric oxide synthase (iNOS), TNF-α, and MCP-1 markers of M1 phenotype and arginase 1 (Arg1), Mrc-2, and CD163 markers of M2 phenotype, in liver tissue. $^{\#}p<0.05$ vs. control. $^{*}p<0.05$ vs. phosphate buffered saline (PBS). Representative images of dihydroethdium (DHE) staining of (B) Wnt-3a, (C) iNOS, and (D) Arg-1 after mesenchymal stem cell transplantation or PBS. Green and red fluorescence indicate positive staining of target proteins. Normal C57BL/6J mice without transplantation were controls.

in mice with D-Gal-induced ALF.

We found that most transplanted MSCs homed to D-Gal-injured liver tissue. Twenty-four hours after intracavitary injection, MSCs were detected in the liver, but not in any other organs. Amiri F. *et al*.[12] found that MSCs migrated to the liver within 24 h after blood transfusion, and were able to reducing liver failure. However, several other studies have reported that MSCs were mainly found in the lungs, after administration, and not in the liver.[13] Lee KC *et al*.[14] also found that most MSCs were retained in the lungs, but reduced hepatocyte apoptosis. The inconsistency may be related to different injection methods. MSCs infused through the portal vein flow into the liver first, while MSCs given by tail vein infusion flow into the lungs first. Most of the injected MSCs remain in the liver or lungs in the form of emboli. Although no MSCs were detected in the liver after intravenous injection, hepatitis was still remarkably attenuated in animal models. In this study, BM-derived MSCs had a beneficial effect on ALF. MSCs transplanted into the liver reduced the inflammatory reaction and the liver injury

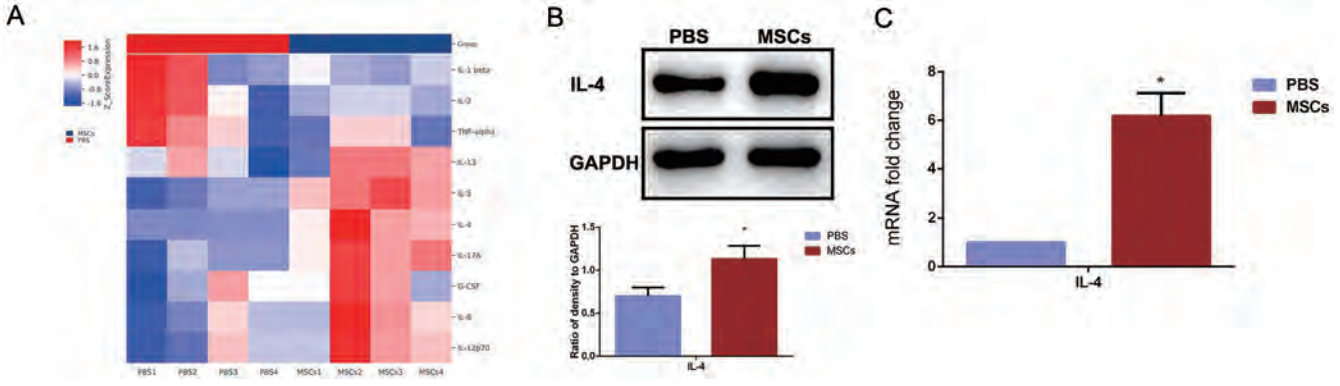


**Fig. 6. Mesenchymal stem cell (MSC) transplantation increased hepatic IL-4 expression in D-Gal-induced acute liver failure (ALF).** (A) G-CSF, IL-6, IL-1 beta, IL-4, and IL-17A paracrine factors secreted by MSCs determined by enzyme-linked immunosorbent assay. (B) Western blots of hepatic IL-4 protein after MSC transplantation or phosphate buffered saline; (C) qRT-PCR assay of IL-4 mRNA expression in the MSCs transplantation and control groups. $^{*}p<0.05$ vs. PBS.

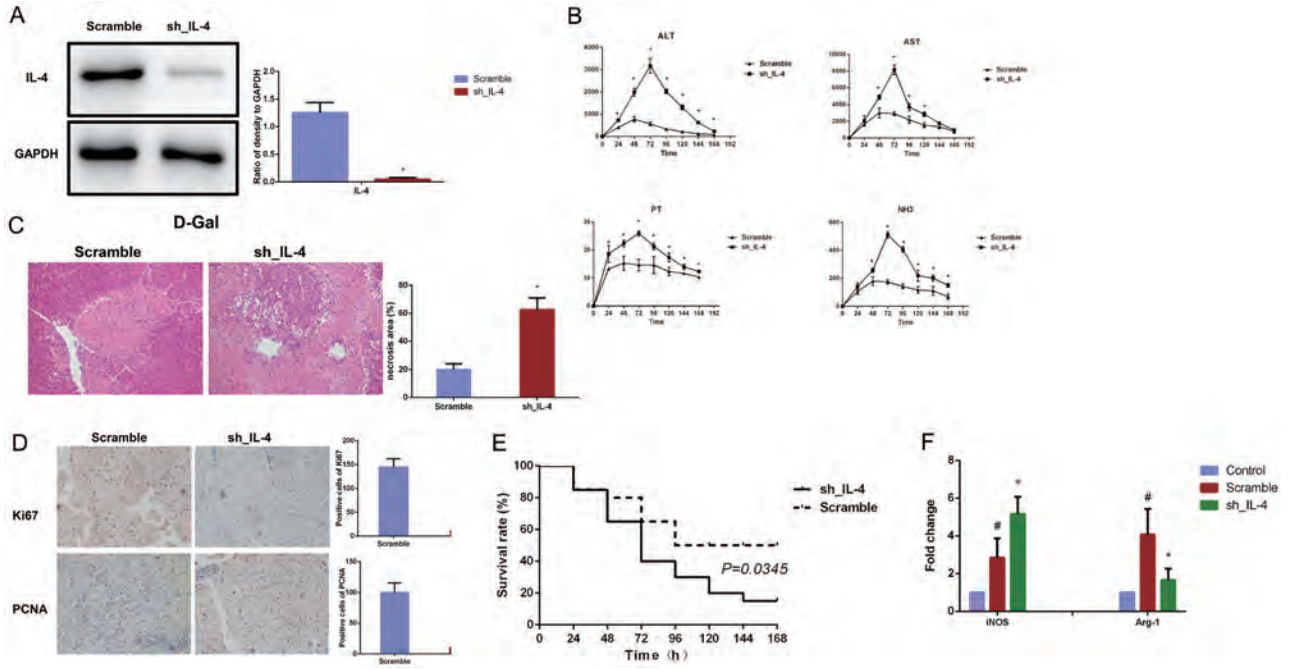


**Fig. 7. Silencing of IL-4 abrogated mesenchymal stem cell (MSC) transplantation promoted a switch to the macrophage M2 phenotype.** (A) Western blots of hepatic IL-4 protein in the MSCs transplantation and scrambled short hairpin RNA groups. (B) Serum alanine transaminase (ALT), aspartate transaminase (AST), prothrombin (PT), and $NH_3$ in the MSCs transplantation and scrambled short hairpin RNA groups. (C) Hematoxylin and eosin staining of liver tissue (200×). (D) Ki67 staining and PCNA staining (200×). (E) Survival analysis. (F) Expression of iNOS and Arg-1 mRNA. *$p<0.05$ vs. Scrambled short hairpin RNA negative control. $^{\#}p<0.05$ vs. scramble. Normal C57BL/6J mice without transplantation were controls.

by promoting a phenotypic switch to anti-inflammatory M2 macrophages, and the involvement of Wnt-3a, was supported by the finding that Wnt-c59, a Wnt-3a inhibitor, blocked the hepatoprotective effect of MSCs. The results indicate that Wnt-3a was involve in the liver protection of MSCs, especially in the regulation of macrophage polarization. In this study, it was found that the increase in Wnt-3a caused by MSCs promoted the recovery of liver injury by activating the Wnt signaling pathway, leading to upregulation of non-phospho-β-catenin expression.[15] It is well known that activation of the β-catenin pathway is indispensable for the repair of liver damage, and that β-catenin is a key protein in the regulation of the expression of cyclins A, D and E. Cyclins regulate the progression of cells from the G1 to the S phase of the cell cycle.[16,17] It has been found that within 24 h of D-Gal induced liver injury, the expression of nuclear and cytoplasmic β-catenin significantly increased in some hepatocytes. Elevated β-catenin could be the basis of liver lobule repair and promotion of liver regeneration. In this study, the increased expression of β-catenin was accompanied by increased expression of the HGF, c-myc and cyclin-D1. Consistent with previous studies, we found that the induction of β-catenin expression occurred before that of its target genes.[15]

Wnt-3a regulates the activation of various immune cells, such as macrophage phenotype transformation, and activation of regulatory T cell subsets and helper T cells. We found that the expression of Foxp3 was not changed, and that the number of CD4 T cells was significantly reduced. Therefore, the activation of Wnt-3a induced by MSC transplantation was closely related to macrophages. Moreover, Wnt-3a from macrophages rather than T cells has been shown to inhibit acute inflammation, which further supports our findings.[18] Ylostalo *et al*.[19] found that MSCs induced macrophage M2 polarization mainly through the COX2-dependent prostaglandin E2 pathway. In contrast to Ylostalo *et al*.,[19] we observed a significant increase in the expression of IL4 but not COX2 following MSC transplantation. In addition, the therapeutic effect of BM-derived MSCs was abrogated by IL-4 gene knockout, indicating that the IL4 gene was essential for the immunomodulatory activity of MSCs.

It merits attention that in our study, BM-derived MSC promoted a switch in macrophage phenotype from M1 to M2 by increasing Wnt-3a. The underlying mechanism involved production and secretion of IL-4 by BM-derived MSCs in the host inflammatory state, stimulated the reprogramming of the host liver macrophages, and increased the expression of Wnt-3a, which inhibited the liver inflammatory response and reduced liver injury.

In conclusion, the findings demonstrate that transplantation of allogeneic MSCs ameliorated ALF induced by D-Gal through an IL-4-dependent macrophage switch toward the M2 anti-inflammatory phenotype. Our findings may have clinical implications in that upregulation of IL-4 may enhance the therapeutic effects of allogeneic MSC transplantation in the treatment of ALF.

## Acknowledgments

The authors acknowledge the technical assistance provided by the staff of the Department of Hepatobiliary Surgery, The Affiliated Drum Tower Hospital of Nanjing University Medical School, Nanjing, China.

## Funding

This work was funded by the National Natural Science Foundation of China (81872359), Jiangsu Provincial key research and development (BE2020752), the Natural Sci-

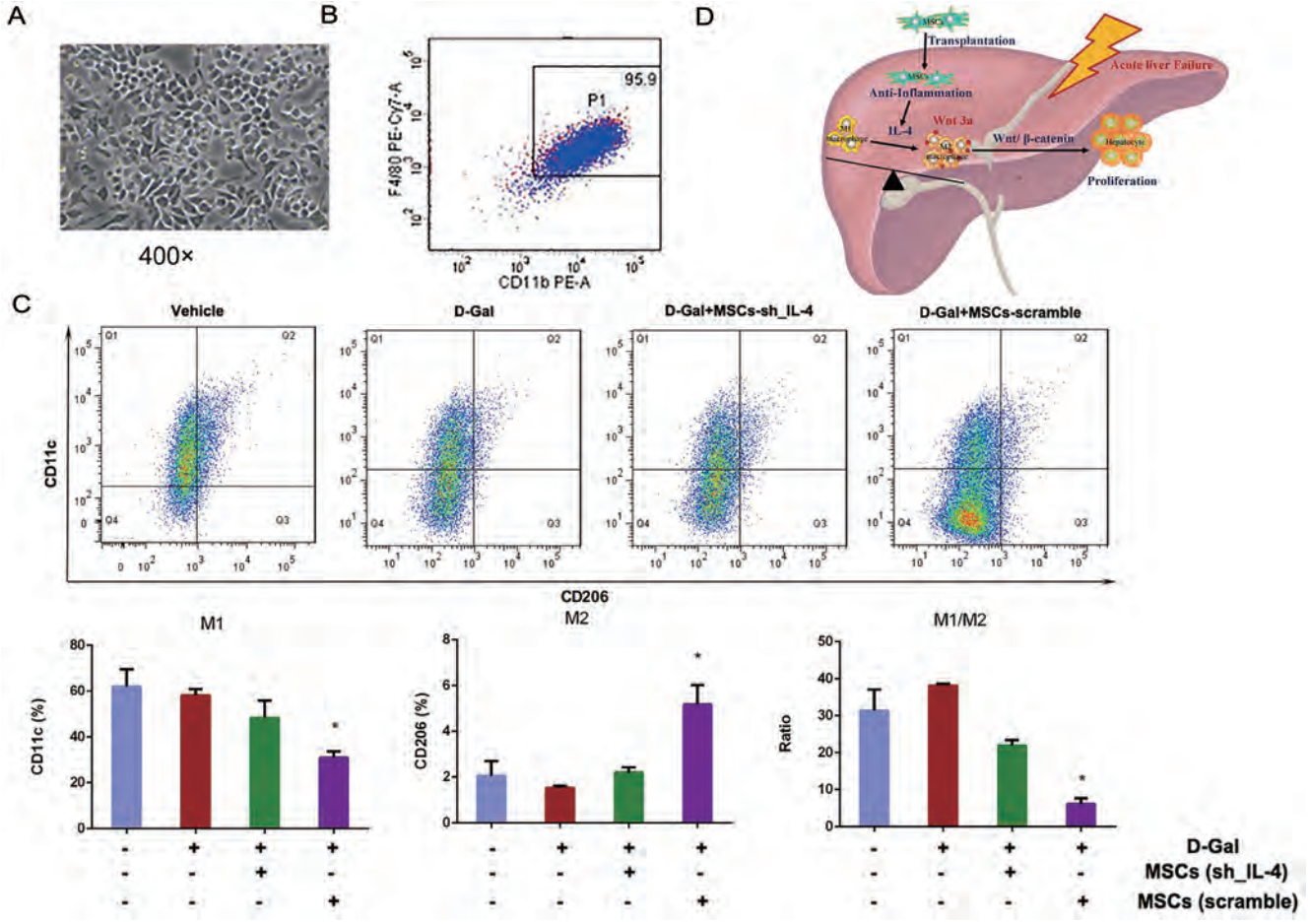


**Fig. 8. Hepatic macrophage switch toward the M2 phenotype was dependent on IL-4.** (A) Liver macrophages (400×). (B) Flow cytometry of liver macrophage purity. (C) Flow cytometry of the macrophage phenotype switch. (D) Graphical abstract. *$p$<0.05 vs. D-Gal(+) short hairpin RNA-IL-4 MSC(−), scrambled short-MSC(−) group.

ence Foundation of Jiangsu Province (BK20190114), the Nanjing Medical Science and Technique Development Foundation (QRX17129), Key Project supported by Medical Science and technology development Foundation, Nanjing Department of Health (JQX19002, YKK19070), the Nanjing Science and technology project (201911039), the Fundamental Research Funds for the Central Universities (0214-YG1312037), Project of Modern Hospital Management and Development Institute, Nanjing University and Aid project of Nanjing Drum Tower Hospital Health, Education & Research Foundation (NDYG2020047).

## Conflict of interest

The authors have no conflict of interests related to this publication.

## Author contributions

Conceived and designed the study (JW, HD, JZ, SX, XS, HR), collected the data (JW, HD, JZ, SX), assembled the data (JW, HD, JZ), performed data analysis and interpretation (JW, HD, JZ, XS, HR), wrote the manuscript (JW, HD, JZ, SX, XS, HR), provided financial support and study materials, and gave final approval of the manuscript (XS, HR). All authors read and approved the manuscript.

## Data sharing statement

The datasets generated during and/or analyzed during the current study are available from the corresponding author on reasonable request.

## References

[1] Alfaifi M, Eom YW, Newsome PN, Baik SK. Mesenchymal stromal cell therapy for liver diseases. J Hepatol 2018;68(6):1272–1285. doi:10.1016/j.jhep.2018.01.030.
[2] Michalopoulos GK, Bhushan B. Liver regeneration: biological and pathological mechanisms and implications. Nat Rev Gastroenterol Hepatol 2021;18(1):40–55. doi:10.1038/s41575-020-0342-4.
[3] Lee CW, Chen YF, Wu HH, Lee OK. Historical perspectives and advances in mesenchymal stem cell research for the treatment of liver diseases. Gastroenterology 2018;154(1):46–56. doi:10.1053/j.gastro.2017.09.049.
[4] Yin Z, Jiang K, Li R, Dong C, Wang L. Multipotent mesenchymal stromal cells play critical roles in hepatocellular carcinoma initiation, progression and therapy. Mol Cancer 2018;17(1):178. doi:10.1186/s12943-018-0926-6.
[5] Forbes SJ, Gupta S, Dhawan A. Cell therapy for liver disease: From liver transplantation to cell factory. J Hepatol 2015;62(1 Suppl):S157–S169. doi:10.1016/j.jhep.2015.02.040.
[6] Sala E, Genua M, Petti L, Anselmo A, Arena V, Cibella J, *et al*. Mesenchymal stem cells reduce colitis in mice via release of TSG6, independently of their

localization to the intestine. Gastroenterology 2015;149(1):163–176.e20. doi:10.1053/j.gastro.2015.03.013.
[7] Galipeau J, Sensébé L. Mesenchymal stromal cells: Clinical challenges and therapeutic opportunities. Cell Stem Cell 2018;22(6):824–833. doi:10.1016/j.stem.2018.05.004.
[8] Shi D, Zhang J, Zhou Q, Xin J, Jiang J, Jiang L, *et al*. Quantitative evaluation of human bone mesenchymal stem cells rescuing fulminant hepatic failure in pigs. Gut 2017;66(5):955–964. doi:10.1136/gutjnl-2015-311146.
[9] Sun L, Fan X, Zhang L, Shi G, Aili M, Lu X, *et al*. Bone mesenchymal stem cell transplantation via four routes for the treatment of acute liver failure in rats. Int J Mol Med 2014;34(4):987–996. doi:10.3892/ijmm.2014.1890.
[10] Chen Y, Kobayashi N, Suzuki S, Soto-Gutierrez A, Rivas-Carrillo JD, Tanaka K, *et al*. Transplantation of human hepatocytes cultured with deleted variant of hepatocyte growth factor prolongs the survival of mice with acute liver failure. Transplantation 2005;79(10):1378–1385. doi:10.1097/01.tp.0000160813.37515.97.
[11] Kegel V, Deharde D, Pfeiffer E, Zeilinger K, Seehofer D, Damm G. Protocol for isolation of primary human hepatocytes and corresponding major populations of non-parenchymal liver cells. J Vis Exp 2016(109):e53069. doi:10.3791/53069.
[12] Amiri F, Molaei S, Bahadori M, Nasiri F, Deyhim MR, Jalili MA, *et al*. Autophagy-modulated human bone marrow-derived mesenchymal stem cells accelerate liver restoration in mouse models of acute liver failure. Iran Biomed J 2016;20(3):135–144. doi:10.7508/ibj.2016.03.002.
[13] Higashimoto M, Sakai Y, Takamura M, Usui S, Nasti A, Yoshida K, *et al*. Adipose tissue derived stromal stem cell therapy in murine ConA-derived hepatitis is dependent on myeloid-lineage and CD4+ T-cell suppression. Eur J Immunol 2013;43(11):2956–2968. doi:10.1002/eji.201343531.
[14] Lee KC, Lin HC, Huang YH, Hung SC. Allo-transplantation of mesenchymal stem cells attenuates hepatic injury through IL1Ra dependent macrophage switch in a mouse model of liver disease. J Hepatol 2015;63(6):1405–1412. doi:10.1016/j.jhep.2015.07.035.
[15] Russell JO, Monga SP. Wnt/β-catenin signaling in liver development, homeostasis, and pathobiology. Annu Rev Pathol 2018;13:351–378. doi:10.1146/annurev-pathol-020117-044010.
[16] Schunk SJ, Floege J, Fliser D, Speer T. WNT-β-catenin signalling - a versatile player in kidney injury and repair. Nat Rev Nephrol 2021;17(3):172–184. doi:10.1038/s41581-020-00343-w.
[17] Perugorria MJ, Olaizola P, Labiano I, Esparza-Baquer A, Marzioni M, Marin JJG, *et al*. Wnt-β-catenin signalling in liver development, health and disease. Nat Rev Gastroenterol Hepatol 2019;16(2):121–136. doi:10.1038/s41575-018-0075-9.
[18] Zhao L, Jin Y, Donahue K, Tsui M, Fish M, Logan CY, *et al*. Tissue repair in the mouse liver following acute carbon tetrachloride depends on injury-induced Wnt/β-catenin signaling. Hepatology 2019;69(6):2623–2635. doi:10.1002/hep.30563.
[19] Ylöstalo JH, Bartosh TJ, Coble K, Prockop DJ. Human mesenchymal stem/stromal cells cultured as spheroids are self-activated to produce prostaglandin E2 that directs stimulated macrophages into an anti-inflammatory phenotype. Stem Cells 2012;30(10):2283–2296. doi:10.1002/stem.1191.

*Journal of Clinical and Translational Hepatology* **2022** vol. 10(4) | 680–691
DOI: 10.14218/JCTH.2021.00511

Original Article

# CircTUBD1 Regulates Radiation-induced Liver Fibrosis Response via a circTUBD1/micro-203a-3p/Smad3 Positive Feedback Loop

Hao Niu[1#], Li Zhang[1#], Biao Wang[1], Guang-Cong Zhang[2], Juan Liu[1], Zhi-Feng Wu[1], Shi-Suo Du[1,3] and Zhao-Chong Zeng[1,3*]

*[1]Department of Radiation Oncology, Zhongshan Hospital, Fudan University, Shanghai, China; [2]Department of Gastroenterology and Hepatology, Zhongshan Hospital, Fudan University, Shanghai, China; [3]Cancer Center, Zhongshan Hospital, Fudan University, Shanghai, China*

**Received:** 10 November 2021 | **Revised:** 19 January 2022 | **Accepted:** 20 January 2022 | **Published:** 28 February 2022

## Abstract

***Background and Aims:*** Radiation-induced liver fibrosis (RILF), delayed damage to the liver (post-irradiation) remains a major challenge for the radiotherapy of liver malignancies. This study investigated the potential function and mechanism of circTUBD1 in the development of RILF. ***Methods:*** By using a dual luciferase assay, RNA pull-down assays, RNA sequencing, chromatin immunoprecipitation (known as ChIP) assays, and a series of gain- or loss-of-function experiments, it was found that circTUBD1 regulated the activation and fibrosis response of LX-2 cells induced by irradiation via a circTUBD1/micro-203a-3p/Smad3 positive feedback loop in a 3D system. ***Results:*** Knockdown of circTUBD1 not only reduced the expression of α-SMA, as a marker of LX-2 cell activation, but also significantly decreased the levels of hepatic fibrosis molecules, collagen type I alpha 1 (COL1A1), collagen type III alpha 1 (COL3A1), and connective tissue growth factor (CTGF) in a three-dimensional (3D) culture system and RILF model *in vivo*. Notably, knockdown of circTUBD1 alleviated early liver fibrosis induced by irradiation in mice models. ***Conclusions:*** This study is the first to reveal the mechanism and role of circTUBD1 in RILF via a circTUBD1/micro-203a-3p/Smad3 feedback loop, which provides a novel therapeutic strategy for relieving the progression of RILF.

**Citation of this article:** Niu H, Zhang L, Wang B, Zhang GC, Liu J, Wu ZF, *et al*. CircTUBD1 Regulates Radiation-induced Liver Fibrosis Response via a circTUBD1/micro-203a-3p/Smad3 Positive Feedback Loop. J Clin Transl Hepatol 2022;10(4):680–691. doi: 10.14218/JCTH.2021.00511.

**Keywords:** circRNA; Radiation-induced liver fibrosis; Three-dimensional; Collagens; LX-2.

**Abbreviations:** 2D, two-dimensional; 3D, three-dimensional; COL1A1, collagen type I alpha 1; COL3A1, collagen type III alpha 1; CTGF, connective tissue growth factor; DAPI, diamidino-2-phenylindole; HSCs, hepatic stellate cells; RILF, radiation-induced liver fibrosis.

[#]Contributed equally to this work.

[*]**Correspondence to:** Zhao-Chong Zeng, Department of Radiation Oncology, Zhongshan Hospital, Fudan University, 180 Feng Lin Road, Shanghai 200032, China. ORCID: https://orcid.org/0000-0003-4330-3688. Tel: +86-21-64041990, Fax: +86-21-6404-8472, E-mail: zeng.zhaochong@zs-hospital.sh.cn

## Introduction

Radiotherapy is one of the most important nonsurgical treatments of liver malignancies[1] such as hepatocellular carcinoma and intrahepatic cholangiocarcinoma. However, the efficacy of radiotherapy for liver malignancy is severely limited by radiation-induced liver fibrosis (RILF),[2] which prevents re-irradiation or irradiation dose escalation for additional treatment of the cancer.[1–4] It cannot be ignored that patients with liver dysfunction have a decreased tolerance to radiation and are more likely to develop RILF after completion of radiotherapy.[2,5,6] Therefore, it is necessary to thoroughly clarify the central mechanisms underlying RILF and find suitable interventions to prevent or alleviate RILF occurrence and development.

However, research progress in RILF remains slow and no efficient therapies are available. One of the major obstacles is the lack of a stable fibrosis model induced by irradiation *in vitro*.[7] Hepatic stellate cells (HSCs) are the main fibrosis cell type of liver fibrosis.[8] However, human primary HSCs are difficult to culture because they have limited proliferation capacity. The two-dimensional (2D) culture model's rapid dedifferentiation limits observation of the long-term cell phenotypes of chronic liver diseases, such as hepatotoxicity or fibrosis. Thus, it is imperative to develop new *in vitro* systems for maintaining quiescent LX-2 cells during prolonged periods of culture. A 3D culture system has recently gained much attention as a reliable system *in vitro* for studying various molecular and screening therapeutic drugs.[7,9,10] Pingitore *et al*. established multilineage 3D spheroids as a model of liver steatosis and reported that LX-2 cells facilitate the compactness of 3D spheroids.[9] In addition, the 3D model system is more similar to *in vivo* conditions, which makes it a realistic system for *in vitro* translation studies.[10,11] These studies suggested that 3D cultures have potential as an *in vitro* model to explore mechanisms involved in chronic liver diseases.[7,9,11]

Increasing evidence shows that small RNA molecules have significant roles in the regulation of a variety of biological processes.[12] In addition, circRNAs characteristically have tissue-specific expression patterns[13] that indicate they have a potential role in the diagnosis and treatment of disease. It was reported that circ-10720 serves as a biomarker of hepatocellular carcinoma and is positively correlated with poor prognosis in hepatocellular carcinoma.[13] Hsa_circ_0070963 inhib-

its liver fibrosis by regulation of miR-223-3p and LEMD3.[14] The findings suggest that targeting circRNAs is a promising therapeutic strategy. However, the expression and function of circRNAs in RILF remain largely unexamined. Because conventional 2D cell culture is sensitive to irradiation, it restricts observation of the chronic phenotype of liver fibrosis induced by high-dose irradiation. To study RILF, we successfully established a 3D spheroid model of LX-2 cells, which greatly facilitated this research. To examine the mechanism of activation and fibrogenic response of LX-2 cells to irradiation, a circRNA microarray was used to screen differentially expressed circRNAs in irradiated and nonirradiated LX-2 cells in our previous study.[15] Among the significantly different circRNAs, circTUBD1 (hsa_circ_0044897) caught our attention because it was significantly upregulated, and its change was consistent with the activation of LX-2 cells. In this study, its role and regulation mechanism were further investigated in a 3D spheroid model of human HSCs LX-2 cells and in RILF mice models.

## Methods

### *3D spheroid culture*

LX-2 cells were purchased from the Shanghai Academy of Life Sciences (Shanghai, China) and cultured in Dulbecco's Modified Eagle Medium (HyClone Laboratories, Logan, UT, USA). LX-2 cells were seeded into ultra low-attachment 96-well plates (Corning, Corning, NY, USA) at 3,000 viable cells per well in 200 μL specific culture medium with 2% fetal bovine serum (FBS), 100 U/mL penicillin, and 100 μg/mL streptomycin. The spheroids were sufficiently compact at 3 days after seeding, and 50% of the medium was exchanged daily with fresh medium. Spheroids were transferred to spinner flasks and maintained on a constant temperature cell shaker with stirring at 50 rpm.

### *Cell irradiation with X-rays*

To minimize cell activation, the cells were cultured for 3–5 generations after irradiation. LX-2 cells were irradiated with a single dose of 8 Gy X-rays, a photon beam energy of 8 MV, and at a dose rate of 300 cGy/min using an ONCORTM linear accelerator (Siemens, Munich, Germany). The distance between the cell plates and the X-ray source was 100 cm. The cells were collected at the indicated times for subsequent experiments.

### *Cell viability assay*

To measure cell viability, a CellTiter-Glo Luminescent Cell Viability Assay kit (Promega, Madison, WI, USA) was used following the manufacturer's instructions to measure ATP content. Briefly, 50 μL reagent was added to each sample well. After disruption of spheroids by pipetting, the plate was incubated at room temperature for 20 min in the dark. Then, the plate was placed in a SpectraMax i3 (Molecular Devices, San Jose, CA, USA) counter and luminescence was measured with SoftMax Pro 6.3 software (Molecular Devices).

### *Immunofluorescence*

Briefly, 3D spheroidal cells were fixed with 8% paraformaldehyde for 12 h, embedded in OCT Cryomount, and then sectioned at 8 μm. The sections were permeabilized with 0.5% Triton X-100, blocked with 10% FBS, and then incubated with primary antibodies against α-SMA, COL1A1, COL3A1, CTGF (Cell Signaling Technology, Danvers, MA, USA) for 60 min at 37°C. All antibodies were diluted in 0.2% (w/v) bovine serum albumen in phosphate buffered saline. Sections were then probed with a Cy3-conjugated goat antimouse or antirabbit IgG secondary antibody for 30 min at 37°C. Nuclei were stained with antifade mounting medium containing diamidino-2-phenylindole (DAPI) (Beyotime Institute of Biotechnology, Shanghai, China). Images were obtained by fluorescence microscopy (model BZ 700; Keyence, Osaka, Japan).

### *RNA pull-down assay*

RNA pull-down assays were performed following the manufacturer's instructions. Briefly, for circTUBD1 to pull down endogenous miR-203a-3p, a biotin-coupled probe was designed to bind to the junction sites of circTUBD1, and a negative probe was used as a control. Biotin-circTUBD1 and its negative probe were incubated with 600 μg streptavidin magnetic beads (Life Technologies, Carlsbad, CA, USA) to form a biotin-coupled RNA complex. Total RNA was extracted from $2\times10^7$ LX-2 cells, and 200 μg total RNA was incubated with the biotin-coupled RNA complex. Bound RNAs were evaluated by qRT-PCR. The same method was used for biotin-miR-203a-3p mimics to pull down endogenous circTUBD1. The circTUBD1 probe, miR-203a-3p probe, and the corresponding negative control probes are listed in Supplementary Table 1.

### *RNA sequencing analysis*

LX-2 cells transfected with small interfering RNA targeting circTUBD1 and its negative control were treated with 8 Gy X-rays. After irradiation for 72 h, LX-2 cells were collected for RNA sequencing. Transcriptome sequencing and bioinformatics analysis was performed with an Illumina HiSeq2500 instrument at Shanghai Majorbio Biopharm Technology Co. Ltd. (Shanghai, China).

### *ChIP assay*

ChIP assays were performed following the manufacturer's protocol using the Magna Ch-IP G Assay kit (EMD Millipore, Temecula, CA, USA). Briefly, cells were cross-linked with 1% formaldehyde for 10 m at room temperature, and quenched with 0.25 mol/L glycine. The cell pellet was resuspended in lysis buffer and incubated on ice for 15 min. The pellet was resuspended in nuclear lysis buffer. Effective sonication was confirmed by bioanalyzer analysis. The chromatin fraction was incubated with an anti-SMAD3 mAb (1:100) overnight at 4°C. The protein/DNA cross links were reversed to obtain free DNA, and after cross links were reversed, the purified DNA was detected and amplified by PCR.

### *RILF model establishment and studies*

Male C57/B6J mice (6 weeks of age) were purchased from Shanghai Laboratory Animal Co. Ltd (SLAC, Shanghai, China) and maintained in pathogen-free conditions. Mice were randomly allocated to four groups of 12 each. The RILF model was constructed by irradiating the left liver with 30 Gy with five fractions, 6 Gy/per week. After 4 weeks of irradiation, adenovirus (Ad-cirTUBD1-NC, Ad-sh1-circTUBD1 and Ad-sh2-circTUBD1) were administrated through the tail vein at a titer of $5\times10^8$ pfu/mouse, once/week, three times. After 6 months of irradiation, the mice were killed by meth-

ods following the regulations of Animal Ethics Committee of Zhongshan Hospital, Fudan University. Liver tissue was collected for hematoxylin and eosin, Masson-trichrome, and Sirius red staining, immunohistochemistry (IHC), western blotting, and qRT-PCR assays.

### *Statistical analysis*

Statistical analysis was performed with GraphPad Prism 8 and SPSS v. 26.0.0.2. Results were compared by one-way analysis of variance, followed by Student's *t*-test for unpaired observations or Bonferroni's correction for multiple comparisons. A $p$-value of $<0.05$ was considered significant. Results were reported as means ± standard error of the means.

### *Supplementary Methods*

For details about other methods, please refer to Supplementary File 1.

## Results

### *Irradiation-induced human HSC activation and fibrosis response*

To detect the effect of irradiation on the viability of the LX-2 cell spheroids, ATP levels of spheroids irradiated with 8 Gy X-rays were measured. Spheroid viability increased within 3 days before irradiation and decreased after irradiation, but maintained higher levels until 4 days after irradiation compared with 2D culture (Fig. 1A, B). Compared with 12 h after irradiation, α-SMA began to increase significantly at 24 h and remained at a high level. Fibrotic indicators of HSCs, such as COL1A1, COL3A1, and CTGF, were not significantly increased within 24 h after irradiation, but began to increase at 48 h and reached the highest level at 72 h after radiation (Fig. 1C). Taken together, the results indicated that 72 h after irradiation was an appropriate time to evaluate fibrotic phenotypes of LX-2 cell spheroids.

### *Down-regulation of circTUBD1 inhibited irradiation-induced LX-2 cell activation and fibrosis response*

Knocking down circTUBD1 significantly reduced LX-2 cell viability, but LX-2 cells remained viable more than 6 days after irradiation (Fig. 2A, B). Compared with the nonirradiated group, irradiation significantly induced activation of LX-2 cells (e.g., increased α-SMA and expression of fibrosis-related molecules, including COL1A1, COL3A1, CTGF mRNA and protein. Down-regulation of circTUBD1 not only reduced LX-2 activity, but also significantly decreased the expression of fibrosis-related molecules (Fig. 2C, D). The relative expression of the proteins in Figure 2D is shown in Supplementary Figure 1A. We also performed immunofluorescence staining of the LX-2 spheroids, and the results were consistent with the results of qRT-PCR and western blotting (Fig. 2E). The relative quantitative fluorescence intensity in Figure 2E are shown in Supplementary Figure 1B.

### *MiR-203a-3p reversed the effect of circTUBD1 on the activation and profibrotic response of LX-2 cells*

The prediction results from Circinteractome database indicated that circTUBD1 shared response elements for miR-203a-3p (Fig. 3A). Dual luciferase reporter assays indicated that compared with the miR-203a-3p negative control, mimics of miR-203a-3p significantly reduced the luciferase activity of a reporter containing the wild-type circTUBD1 sequence. However, it had no effect on the mutant circTUBD1 sequence (Fig. 3B, C). The results confirmed that circTUBD1 directly bound to miR-203a-3p. RNA pull-down assays further confirmed that miR-203a-3p was substantially enriched by the bio-circTUBD1 probe. Likewise, circTUBD1 was pulled down by the wild-type bio-miR-646 probe (Fig. 3D, E). We also examined how circTUBD1 regulated the radiation-induced activation and fibrosis response of LX-2 cells through interactions with miR-203a-3p. The results indicated that the level of miR-203a-3p or circTUBD1 was not significantly changed in LX-2 cells transfected with knockdown of circTUBD1 or miR-203a-3p mimics, compared with the corresponding control (Fig. 3F, G). Compared with the negative control, miR-203a-3p inhibitor aggravated radiation-induced activation and fibrosis of LX-2 cells, including the increasing of α-SMA, COL1A1, COL3A1, CTGF (Fig. 3H, I). The relative expression of proteins in Figure 3I are shown in Supplementary Figure 2. The suppression caused by silencing circTUBD1 was partially reduced by miR-203a-3p inhibitor. These results further revealed that circTUBD1 sponged miR-203a-3p to regulate the radiation-induced activation and fibrosis response of LX-2 cells.

### *MiR-203a-3p mediated circTUBD1 through SMAD3 to regulate the radiation-induced activation and fibrosis of LX-2 cells*

The results of RNA sequencing suggested that the TGF-β signaling pathway ranked third among the top 15 enriched pathways and that the expression of SMAD3 was significantly downregulated after knockdown of circTUBD1 (Fig. 4A, B). To explore why knockdown of circTUBD1 resulted in the decrease of SMAD3, prediction database was used. The results of Targetscan indicated that there were multiple binding sites between miR-203a-3p and SMAD3-3′-untrasnlated region (UTR) (Fig. 4C). The dual luciferase assay findings revealed that miR-203a-3p mimics significantly reduced luciferase activity of the report vector containing wild-type of SMAD3 but had no significant effects on the mutant SMAD3 (Fig. 4D, E). These results showed that miR-203a-3p directly bound to SMAD3. To verify whether miR-203a-3p mediated the regulation of circTUBD1 through SMAD3, we transfected miR-203a-3p inhibitor into cells to knock down circTUBD1. The qRT-PCR and western blot results suggested that miR-203a-3p inhibitors partially reversed the inhibition effect of knocking down circTUBD1 on SMAD3, p-SMAD3, SMAD2, p-SMAD2, and TGF-β levels (Fig. 4F, G). The relative expression of the proteins in Figure 4G is shown in Supplementary Figure 3A. To examine whether SMAD3 was involved in radiation-induced activation and fibrosis response of LX-2 cells, we knocked down SMAD3. The results indicated that compared with the negative control, SMAD3 knockdown significantly inhibited radiation-induced activation and expression of fibrosis-related molecules in LX-2 cells, including the down-regulation of α-SMA, COL1A1, COL3A1, and CTGF. Knockdown of SMAD3 partially reversed the promotion effect of miR-203a-3p inhibitors on radiation-induced activation and fibrosis-related molecules of LX-2 cells (Fig. 4H–J). The relative expression of the proteins in Figure 4J is shown in Supplementary Figure 3B, C. The findings indicated that circTUBD was mediated by miR-203a-3p through SMAD3 to regulate the radiation-induced activation and fibrosis of LX-2 cells.

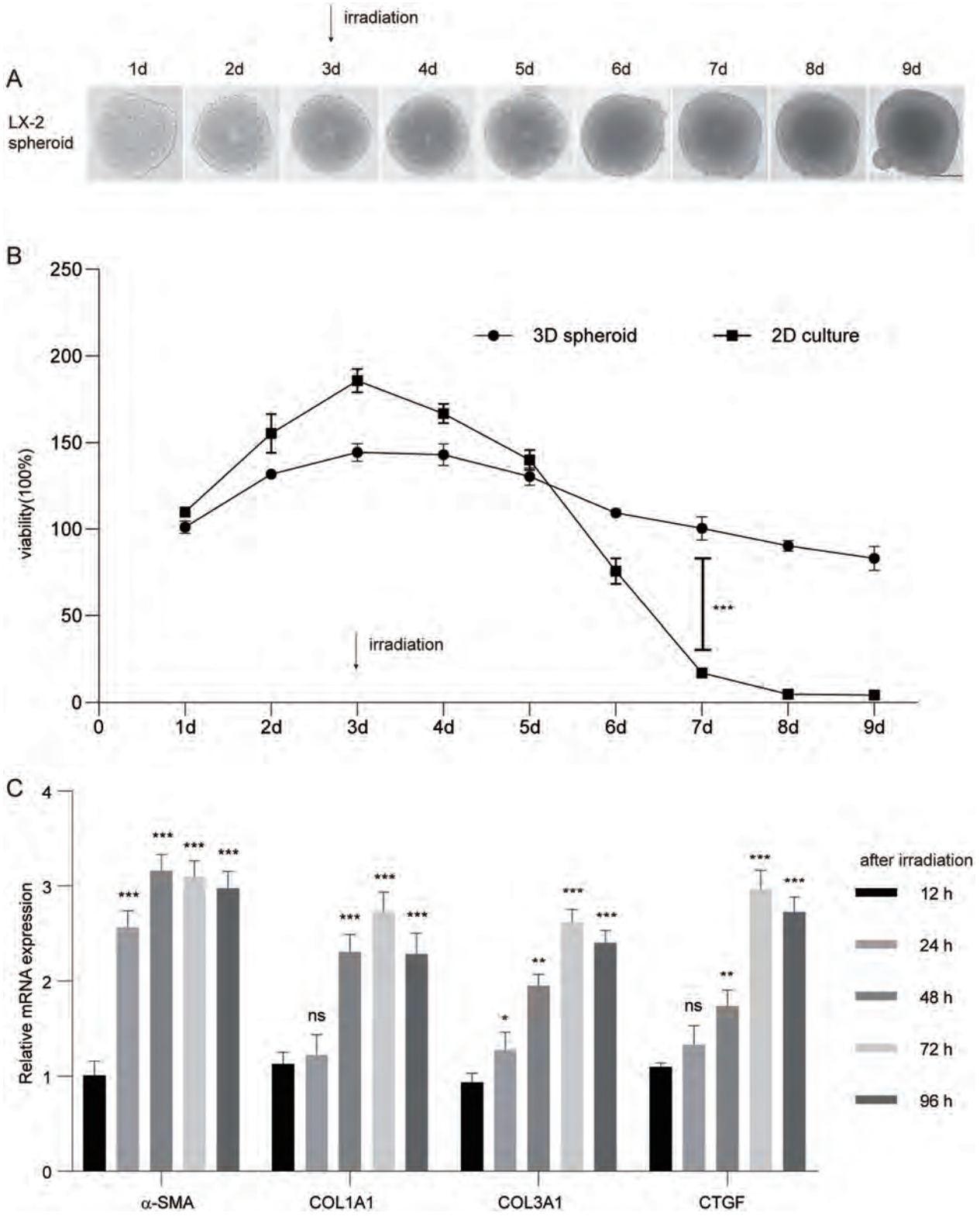


**Fig. 1. Irradiation induced the activation and fibrosis response of the human hepatic stellate line LX-2 cells.** (A) The representative morphology of LX-2 cells spheroids every day after irradiation (scale bar: 100 μm). (B) ATP level in LX-2 cells in 3D spheroid and 2D culture assayed by CellTiter-Glo Luminescent Cell Viability Assay Kits. (C) Expression of activation and fibrosis markers of LX-2 cells, including α-SMA, COL1A1, COL3A1, and CTGF assayed after irradiation by qRT-PCR. *$p$ <0.05, **$p$<0.01, ***$p$<0.001. Bars are means ± SEM of at least three independent assays. 2D, two-dimensional; 3D, three-dimensional; COL1A1, collagen type I alpha 1; COL3A1, collagen type III alpha 1; CTGF, connective tissue growth factor. *ns*, not significant.

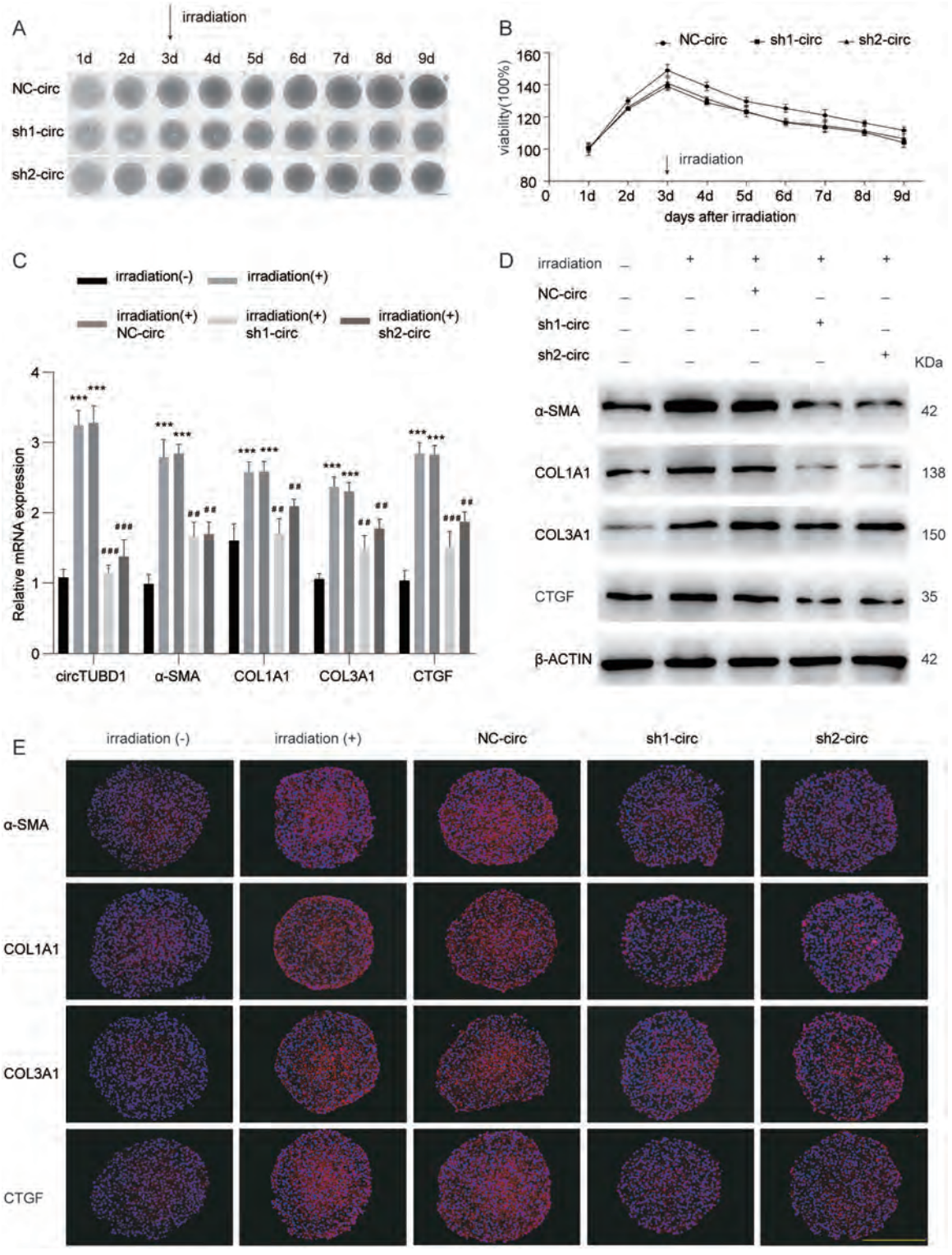


**Fig. 2. Down-regulation of circTUBD1 suppressed the irradiation-induced activation and fibrosis response of LX-2 cells.** (A, B) Representative images of 3D spheroids and the viability of transfected LX-2 cells with circTUBD1 knockdown every day after irradiation (scale bar: 100 μm). (C, D) qRT-PCR and western blot assays of circTUBD1, α-SMA, COL1A1, COL3A1, CTGF expression in transfected LX-2 cells with down-regulation of circTUBD1 and corresponding control 72 h after irradiation. (E) Representative images of immunofluorescence stained makers of activation and fibrosis molecules (CY3, red) in 3D spheroids of LX-2 cells with nucleic counterstained by DAPI (blue, scale bar: 200 μm). **p* vs. non-irradiation, $^{\#}p$ vs. NC-circ at 72 h after irradiation, ****p*<0.001. $^{\#\#}p$<0.01, $^{\#\#\#}p$<0.001. Bar are means ± SEM of at least three independent assays. NC-circ, negative control of circTUBD1; sh1-circ, short hairpin RNA 1 of circTUBD1; sh2-circ, short hairpin RNA 2 of circTUBD1. DAPI, 4′,6-diamidino-2-phenylindole; CY3, Cyanine3.

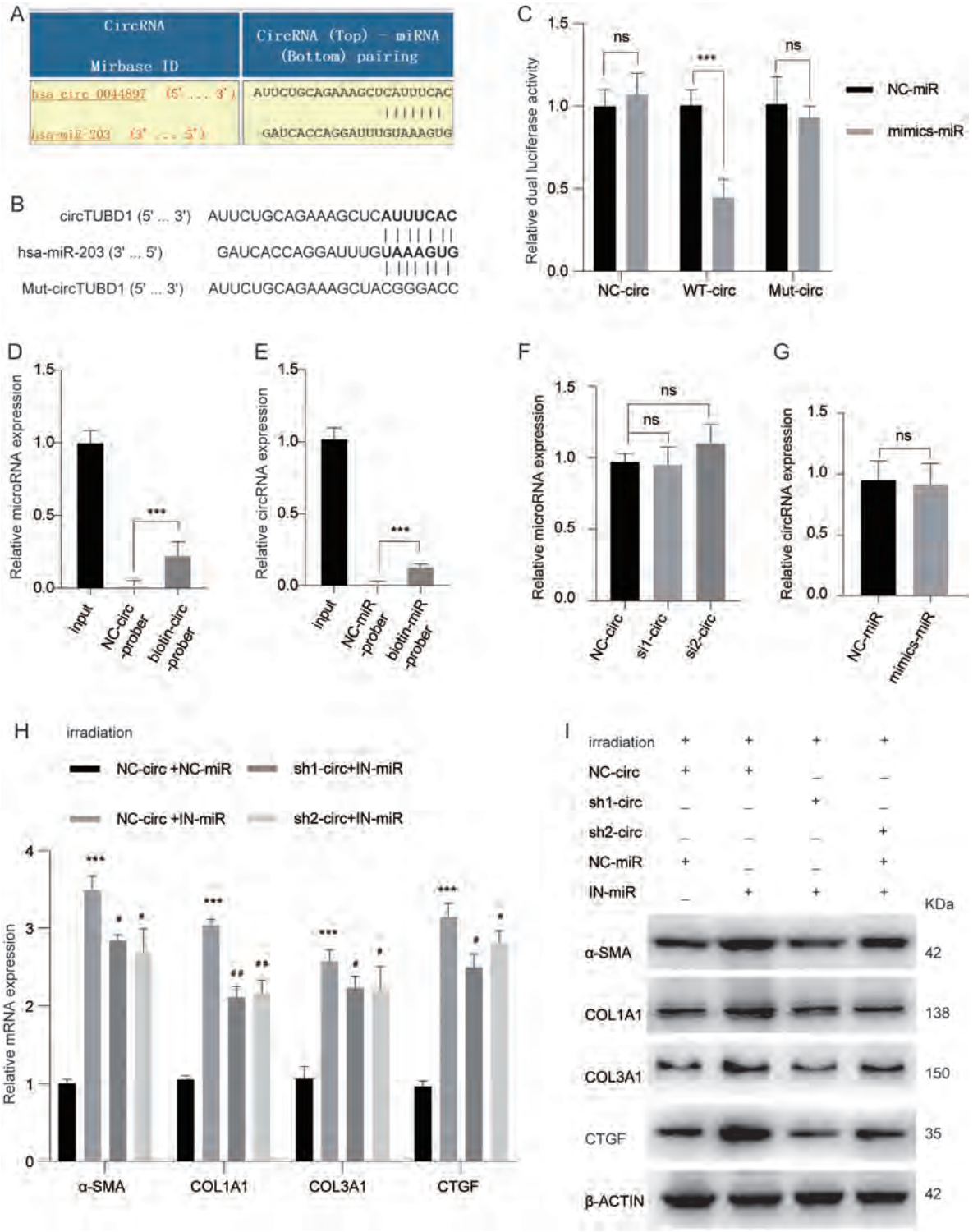


**Fig. 3. MiR-203a-3p reverses the effect of circTUBD1 on the activation and profibrotic response of LX-2 cells.** (A) Putative binding sites of circTUBD1 and microRNA response elements of miR-203a-3p predicted by Circinteractome. (B, C) Luciferase reporter assays in LX-2 cells co-transfected with wild-type, mutant circTUBD1, or negative control of luciferase vector and miR-203a-3p mimics, or negative control of miR-203a-3p mimics. (D, E) RNA pull-down assay followed by qRT-PCR of miR-203a-3p or circTUBD1 enriched with biotin-circTUBD1 probes or biotin-miR-203a-3p probes. (F, G) miR-203a-3p or circTUBD1 assayed by qRT-PCR in LX-2 cells transfected with knockdown of circTUBD1 or miR-203a-3p mimics. (H, I) α-SMA, COL1A1, COL3A1, CTGF in LX-2 expression assayed by qRT-PCR and western blot after co-transfection and knockdown of circTUBD1 with or without miR-203a-3p inhibitors or their negative controls. **p* vs. NC-circ and NC-miR, #*p* vs. NC-circ and IN-miR. *ns*: not significant, ****p*<0.001. #*p*<0.05, ##*p*<0.005. Bars are means ± SEM of at least three independent assays. NC-circ, negative control of circTUBD1; sh1-circ, sh1-TUBD1; sh2-circ, sh2-TUBD1; NC-miR, negative control of miR-203a-3p inhibitor; IN-miR, miR-203a-3p inhibitor; ns, not significant. WT, wild type; Mut, mutant.

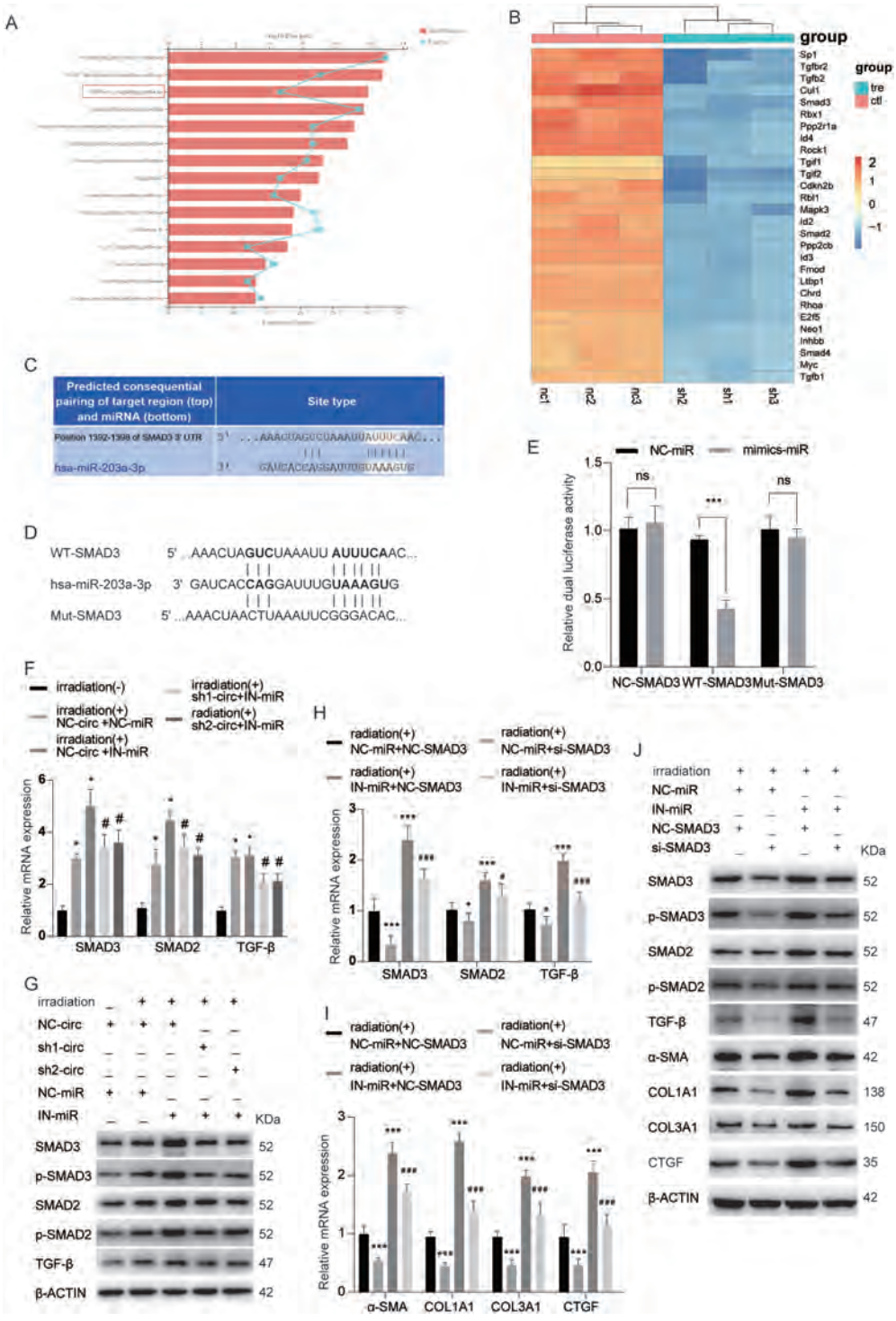


**Fig. 4. MiR-203a-3p mediates the regulation of circTUBD1 on SMAD3.** (A) TGF-β signaling pathway ranked third among the top 15 enriched pathways in the knockdown of circTUBD1 vs. control group by Kyoto Encyclopedia of Genes and Genomes pathway enrichment. (B) SMAD3 ranked fifth among the different genes contained in the TGF-β signaling pathway analyzed by cluster analysis and displayed in the heatmap. ($p$ <0.05 vs. NC-circTUBD1, red: high, blue: low). (C) Binding sites of the seed region of miR-203a-3p and SMAD3 3′-UTR predicted by Targetscan. (D, E) Luciferase reporter assay in LX-2 cells co-transfected with wild-type, mutant SMAD3, or negative control with miR-203a-3p mimics or negative control. (F, G) Expression of SAMD3, p-SAMD3, SAMD2, p-SAMD2 and TGF-β protein assayed after irradiation by qRT-PCR and western blot after co-transfection with knockdown of circTUBD1 and miR-203a-3p inhibitor or control in LX-2 cells. (H–J) qRT-PCR and western blot assays of the expression of fibrosis markers and molecules at 72 h after irradiation by in LX-2 cells transfected with knockdown of SMAD3 or negative control with miR-203a-3p inhibitors. *$p$ vs. NC-SMAD3 and NC-miR, $^{\#}p$ vs. IN-miR and NC-SMAD3 *ns*, not significant; *$p$<0.05; ***$p$<0.001; $^{\#}p$<0.05; $^{\#\#\#}p$<0.001. Bars are means ± SEM of at least three independent assays. NC-SMAD3, negative control of SMAD3; si-SMAD3, short interference RNA of SMAD3; NC-miR, negative control of miR-203a-3p inhibitor; IN-miR, miR-203a-3p inhibitor; ns, not significant.

### *CircTUBD1 was also be regulated by SMAD3 via a positive feed back*

The predicted results from GTAR and JASPAR database revealed that SMAD3, as a transcription factor, possessed multiple transcription factor binding sites (TFBSs) in the TUBD1 promoter region (Fig. 5A, B). The results of the dual luciferase assay revealed that there were two effective TFBSs on the TUBD1 promoter region that bound to SMAD3 (Fig. 5C, D). To further examine how SMAD3 regulated circTUBD1, specific primers were designed to detect expression of TUBD1 pre-mRNA and TUBD1, and circTUBD1 mRNA (Fig. 6E). To explore the transcriptional regulation of SMAD3 on TUBD1, we performed ChIP assays using a mAb against SMAD3. ChIP-PCR analysis confirmed the occupancy of SAMD3 on the promoter of TUBD1 (Fig. 5F, G). Moreover, knockdown of SMAD3 significantly decreased TUBD1, pre-TUBD1, and circTUBD1 expression in LX-2 cells (Fig. 5H–J). Taken together, the findings suggest that SMAD3 was not only regulated by cirTUBD1, but it also regulated endogenous expression of circTUBD1.

### *Knockdown of circTUBD1 alleviated the progression of irradiation-induced liver fibrogenesis in vivo model*

qRT-PCR and western blot assays found that irradiation induced up-regulation of α-SMA, COL1A1, COL3A1, and CTGF and knockdown of circTUBD1 partially alleviated the effect on the fibrosis makers (Fig. 6A, B). The relative expression of the proteins in Figure 6B are shown in Supplementary Figure 4. The RILF model was successfully constructed in C57BL/6 mice irradiated with 30 Gy X-ray in five fraction, manifested as the disruption of the regular lobular structure of liver, the extent of inflammatory cell infiltration (Fig. 6C), and excess collagen deposition around blood vessels 6 months after irradiation (Fig. 6 D, E). Notably, the results of immunohistochemistry confirmed that irradiation induced up-regulation of the above motioned fibrosis makers, and knockdown of circTUBD1 alleviated the fibrosis phenotype (Fig. 6F).

## Discussion

RILF delayed post-irradiation damage to the liver that is inevitable and can be lethal.[2,3,5] In this study, it was found that knockdown of circTUBD1 alleviated radiation-induced activation and fibrosis response in 3D culture systems *in vitro* and in a RILF mouse model, including inhibition of α-SMA expression, reduction in the expression of the fibrosis-promoting molecules COL1A1, COL3A1, and CTGF in LX-2 cells treated with irradiation. The study results revealed that circTUBD1 regulated the activation and fibrosis response of LX-2 cells induced by irradiation through a circTUBD1/micro-203a-3p/Smad3 positive feedback loop.

To date, more than 380 cell lines have been established as 3D models and are used in drug toxicology studies, cancer research, and metabolomics research. The 3D culture system helps us understand complex cell physiology and cell function in response to stimuli in a condition closer to the *in vivo* environment. A previous study found that cells in 3D culture system enhanced extracellular matrix deposition and expression of biomarkers.[11] Through optimization of culture conditions, we successfully established an LX-2 cell 3D spheroid culture system as an *in vitro* model for the study of the mechanism of RILF. Our results confirmed that viability of the LX-2 cells was maintained longer after irradiation in the 3D spheroid system. More important, we discovered that the increases in α-SMA, COL1A1, COL3A1, and CTGF induced by irradiation were significant higher in the 3D model than in 2D culture. It is possible that LX-2 cells were auto-activated in 2D culture. It was also found that irradiation induced significant increases in the expression of TGF-β and SMAD3 in activated LX-2 cells. The results are consistent with those of previous studies.[16,17] Taken together, our results and those of previous studies confirm that the 3D spheroid system is a useful *in vitro* model that has advantages over 2D culture for the study of chronic liver diseases.[11]

Many small RNAs have been identified as being involved in regulation of disease.[18] Different small RNAs are multidimensional and have significantly different biological activity. Dysregulation of small RNAs, like miRNAs and circRNAs, contributes to regulation of the progression of hepatic fibrosis by targeting mRNAs.[19] It has been reported that circRNA_000203 enhanced the expression of fibrosis-associated genes by derepressing targets of miR-26b-5p, Col1a2 and CTGF, in cardiac fibroblasts.[20] In this study, we showed that irradiation induced a significant increase of circTUBD1 in LX-2 cells. Knockdown of circTUBD1 inhibited HSC activation and profibrotic molecules, such as α-SMA, COL1A1, COL3A1, and CTGF. The results indicated that circTUBD1 was involved in radiation-induced LX-2 cell activation and profibrotic response. Study findings suggest that miR-203a-3p also inhibits HSC proliferation and attenuates liver fibrosis in mice via modulation of the p66Shc/β-catenin pathway induced by CCl4.[21] We found that miR-203a-3p inhibitor significantly promoted the radiation-induced activation and fibrosis of LX-2 cells. Our results, which were partially consistent with previous studies, confirmed that miR-203a-3p inhibited liver fibrosis. We also confirmed that knockdown of circTUBD1 could reverse the promotion effect of miR-203a-3p inhibitors on the radiation-induced activation and fibrosis of LX-2 cells. Our previous studies showed that LX-2 cells immediately secreted large amounts of proinflammatory cytokines, including interleukin (IL)-1β, IL6, and tumor necrosis factor alpha (TNF-α) 24 h after irradiation, which regulated by circTUBD1/miR-146a-5p/TLR4 pathway.[22] In this study, we found that HSCs began to synthesize a large amount of collagen at 48 h after radiation. Our previous work and the study results together suggest that radiation-induced activation of HSCs not only promote the secretion of inflammatory factors in the early stage but also promote the synthesis of fibrosis in the late stage through different signaling pathways.

The TGF-β/SMAD3 signaling pathway is an important mediator during regulation of responses to radiation-induced acute or chronic injury in the liver.[16,17] Experimental and clinical studies have found that the TGF-β/SMAD3 signaling pathway promotes a radiation dose-dependent increase in the inhibition of TGF-β/SMAD3 that reduces post-irradiation liver fibrosis in animals. Our LX-2 cell spheroid model also revealed an irradiation-induced activation of the TGF-β/SMAD3 signaling pathway. Anti-TGF-β therapy is a potential therapeutic strategy against RILF. Nevertheless, direct antagonization of TGF-β activity to reduce RILF will be a challenge because TGF-β is active in maintaining normal physiological activities in various cells of the liver. Therefore, the therapeutic approach of direct targeting of TGF-β to inhibit liver fibrosis would introduce unavoidable side effects. But we cannot completely negate the role of the TGF-β signaling pathway, as it may be a potential strategy to alleviate RILF by inhibiting downstream regulators like SMAD2 and SMAD3. Our previous study using circRNA microarrays revealed that circTUBD1 expression in LX-2 cells was specifically and significantly increased when induced by irradiation,[15] and Kyoto Encyclopedia of Genes and Genomes results suggested that the TGF-β signaling pathway ranked third among all pathways,

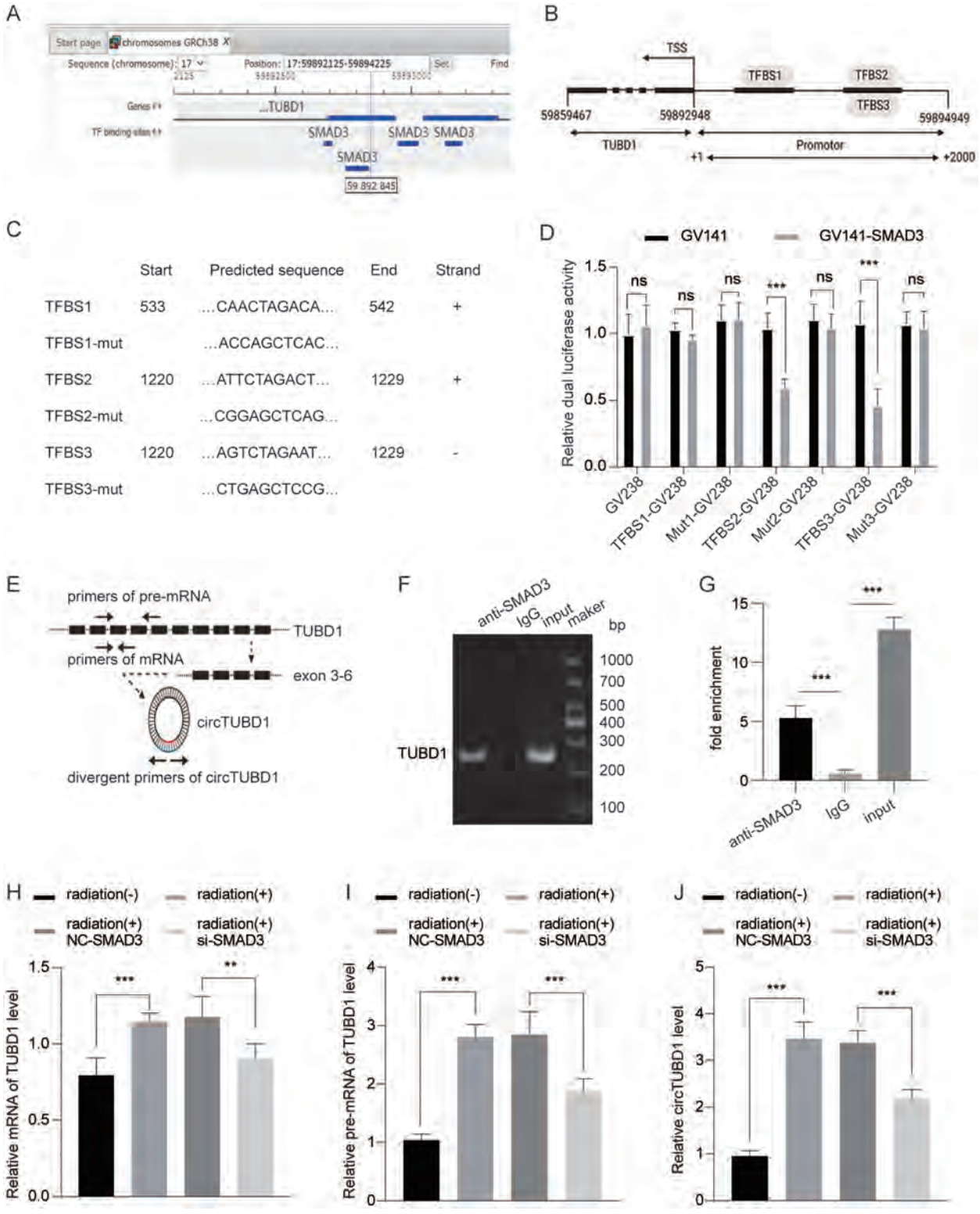


**Fig. 5. SMAD3 regulates circTUBD1 by targeting the pre-mRNA of TUBD1.** (A, B) TFBSs in the promoter region of TUBD1 for SMAD3 predicted by GTAR and JASPA data. (C, D) Luciferase reporter assay in LX-2 cells co-transfected with wild-type, mutant TFBS of TUBD1 in GV238 vector, or negative control with SMAD3 overexpression (GV141-SMAD3) or negative control. (E) Diagram of the specific primers designed to detect pre-mRNA of TUBD1, mRNA of TUBD1, and circTUBD1. (F, G) ChIP assay of the TUBD1 promoter using antibodies against SMAD3 in LX-2 cells and analyzed by PCR. (H, I) Expression of mRNA, pre-mRNA of TUBD1, and circTUBD1 in LX-2 cells by qRT-PCR. $^{**}p<0.01$, $^{***}p<0.001$. Bars are means ± SEM of at least three independent assays. NC-SMAD3, negative control of SMAD3; si-SMAD3, short interference RNA of SMAD3; NC-miR, negative control of miR-203a-3p inhibitor; IN-miR, miR-203a-3p inhibitor; ns, not significant.

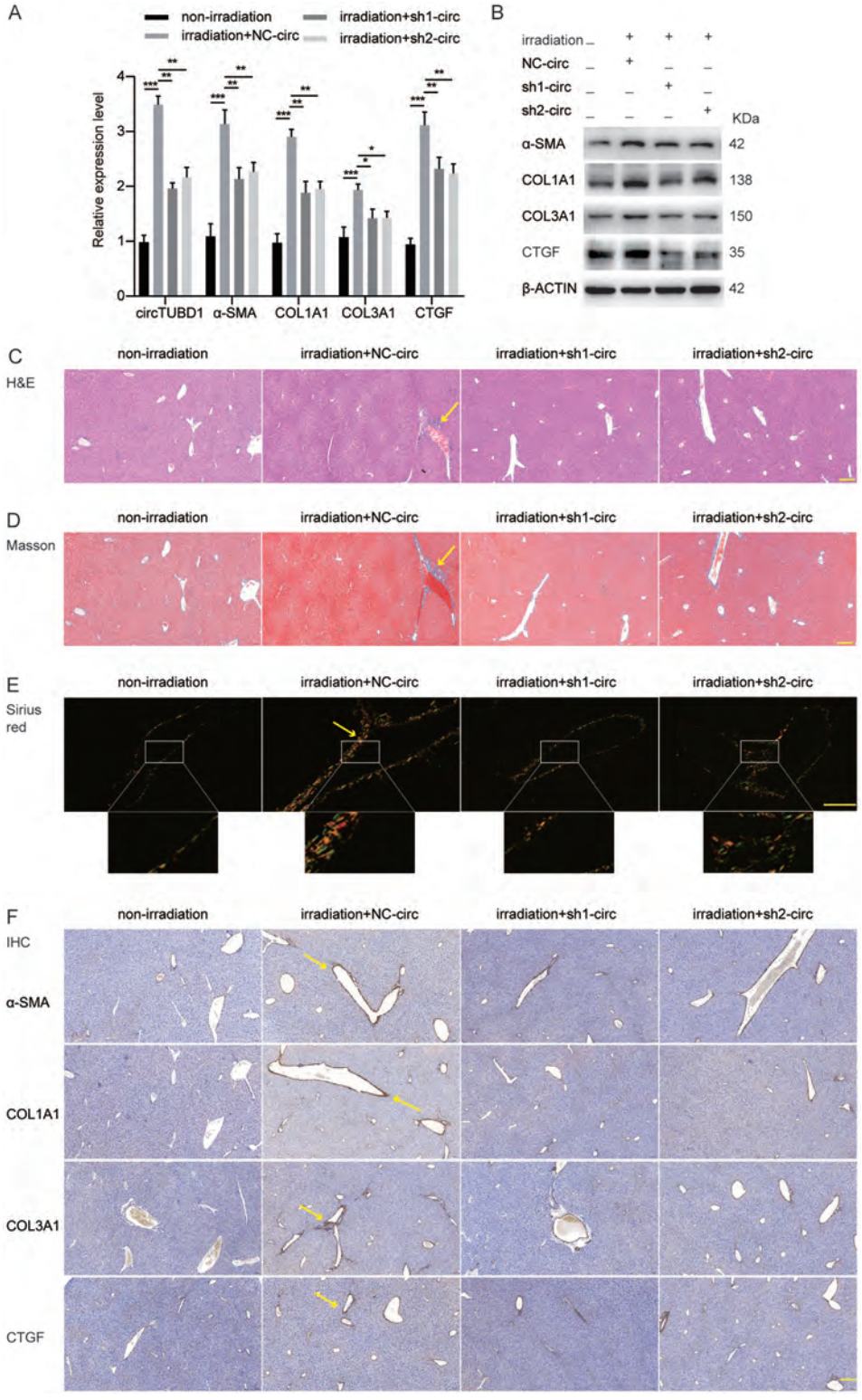


**Fig. 6. Knockdown of circTUBD1 alleviated irradiation-induced liver fibrogenesis *in vivo* model.** (A, B) qRT-PCR and Western blot assays of the relative expression of activation and fibrosis markers α-SMA, COL1A1, COL3A1, and CTGF in mice at 6 months after irradiation. (C) Hematoxylin and eosin stained tissue showed irradiation-induced disruption of the regular lobular structure of the liver and the infiltration of inflammatory cells (yellow arrow); scale bar: 500 μm. (D, E) Masson and Sirius red staining show excess collagen deposition around the vessel 6 months after irradiation (yellow arrow); scale bar: 500 μm). (F) Immunohistochemistry shows that knockdown of circTUBD1 reduced the fibrosis phenotype and fibrosis makers (α-SMA, COL1A1, COL3A1, and CTGF) induced by irradiation. *$p$ <0.05, **$p$<0.01, ***$p$<0.001. Bar represent means ± SEM of at least three independent assays. NC-circ, negative control of circTUBD1; sh1-circ, sh1-TUBD1; sh2-circ, sh2-TUBD1.

with significant differences after knockdown of circTUBD1. The result implied that altering circTUBD1 significantly affected the TGF-β pathway. We further confirmed that, as a sponge of miR-203a-3p, circTUBD1 was involved in regulation of the radiation-induced LX-2 cell profibrotic response through SMAD3. Although the general components of TGF-β/SMADs signaling is now understood, the core issue of how to control TGF-β/SMAD signaling in context remains unclear.[23,24] It has been reported that SMAD3 mediates the constitutive active loop between lncRNA PCAT7 and the TGF-β signaling pathway to promote cancer metastasis.[25] However, the central question of how the TGF-β/SMAD feedback model exerts its versatile and context-dependent functions in liver fibrosis is unclear. In this study, we found that the expression level of circTUBD1 changed after knockdown of SMAD3. Using different methods, we confirmed that SMAD3 was not only regulated by cirTUBD1, it also regulated the endogenous expression of circTUBD1 and forms a positive feedback. The feedback mode helps to adjust the signal strength more effectively.

In previous studies, RILF models were established by irradiation whole liver.[1,16] To exclude individual differences and better simulate focal radiation in clinical, we irradiated only the left liver of mice with X-rays. Compared with the right liver, the left liver manifested infiltration of a number of inflammatory cells infiltrate around blood vessels and vascular and interstitial congestion at early stages. The regular lobular structure was partially disrupted, and excess collagen was deposited in the interstitium, especially around the vessels. Notably, we observed that irradiation induced migration of HSCs to vascular spaces from the subendothelial space of Disse, which further confirmed that HSCs have an important role in irradiation-induced collagen deposition around the vessels. These results implied that knockdown of circTUBD1 inhibited the cascade reaction induced by the circTUBD1/micro-203a-3p/Smad3 positive feedback loop and reduced collagen secretion from HSCs, may be a potential strategy to alleviate the RILF.

## Conclusion

This study clarified the activities and mechanism of circTUBD1 in the process of RILF through a circTUBD1/miR-203a-3p/SMAD3 positive feedback loop by 3D model *in vitro* and RILF model in vivo. Knockdown of the specific circTUBD1 may be a potential strategy for effective prevention of RILF.

## Funding

This work was supported by National Natural Science Foundation of China (Grant Nos. 81773220 and 82003225). Shanghai Sailing Program (Grant No. 20YF1405500), the Youth Programme of Zhongshan Hospital, Fudan University (Grant No. 2020ZSQN24).

## Conflict of interest

The authors have no conflict of interests related to this publication.

## Author contributions

Study conception and design (ZCZ), data acquisition (HN, LZ), data analysis and interpretation (BW, GCZ), manuscript drafting (HN), manuscript revision for important intellectual content (JL, ZFW, SSD), and administrative, technical, material support, and study supervision (ZCZ).

## Ethical statement

The study was approved by the Zhongshan Hospital Research Ethics Committee.

## Data sharing statement

Research data will be shared upon reasonable request directed to the corresponding author.

## References

[1] Koay EJ, Owen D, Das P. Radiation-Induced Liver Disease and Modern Radiotherapy. Semin Radiat Oncol 2018;28(4):321–331. doi:10.1016/j.semradonc.2018.06.007, PMID:30309642.
[2] Straub JM, New J, Hamilton CD, Lominska C, Shnayder Y, Thomas SM. Radiation-induced fibrosis: mechanisms and implications for therapy. J Cancer Res Clin Oncol 2015;141(11):1985–1994. doi:10.1007/s00432-015-1974-6, PMID:25910988.
[3] Benson R, Madan R, Kilambi R, Chander S. Radiation induced liver disease: A clinical update. J Egypt Natl Canc Inst 2016;28(1):7–11. doi:10.1016/j.jnci.2015.08.001, PMID:26300327.
[4] Dawson LA, Normolle D, Balter JM, McGinn CJ, Lawrence TS, Ten Haken RK. Analysis of radiation-induced liver disease using the Lyman NTCP model. Int J Radiat Oncol Biol Phys 2002;53(4):810–821. doi:10.1016/s0360-3016(02)02846-8, PMID:12095546.
[5] Toesca DAS, Ibragimov B, Koong AJ, Xing L, Koong AC, Chang DT. Strategies for prediction and mitigation of radiation-induced liver toxicity. J Radiat Res 2018;59(suppl_1):i40–i49. doi:10.1093/jrr/rrx104, PMID:29432550.
[6] Chou CH, Chen PJ, Lee PH, Cheng AL, Hsu HC, Cheng JC. Radiation-induced hepatitis B virus reactivation in liver mediated by the bystander effect from irradiated endothelial cells. Clin Cancer Res 2007;13(3):851–857. doi:10.1158/1078-0432.Ccr-06-2459, PMID:17289877.
[7] van Grunsven LA. 3D in vitro models of liver fibrosis. Adv Drug Deliv Rev 2017;121:133–146. doi:10.1016/j.addr.2017.07.004, PMID:28697953.
[8] Puche JE, Saiman Y, Friedman SL. Hepatic stellate cells and liver fibrosis. Compr Physiol 2013;3(4):1473–1492. doi:10.1002/cphy.c120035, PMID:24265236.
[9] Pingitore P, Sasidharan K, Ekstrand M, Prill S, Lindén D, Romeo S. Human Multilineage 3D Spheroids as a Model of Liver Steatosis and Fibrosis. Int J Mol Sci 2019;20(7):1629. doi:10.3390/ijms20071629, PMID:30986904.
[10] Coll M, Perea L, Boon R, Leite SB, Vallverdú J, Mannaerts I, *et al*. Generation of Hepatic Stellate Cells from Human Pluripotent Stem Cells Enables In Vitro Modeling of Liver Fibrosis. Cell Stem Cell 2018;23(1):101–113.e107. doi:10.1016/j.stem.2018.05.027, PMID:30049452.
[11] Ravi M, Paramesh V, Kaviya SR, Anuradha E, Solomon FD. 3D cell culture systems: advantages and applications. J Cell Physiol 2015;230(1):16–26. doi:10.1002/jcp.24683, PMID:24912145.
[12] Zhang F, Zhang R, Zhang X, Wu Y, Li X, Zhang S, *et al*. Comprehensive analysis of circRNA expression pattern and circRNA-miRNA-mRNA network in the pathogenesis of atherosclerosis in rabbits. Aging 2018;10(9):2266–2283. doi:10.18632/aging.101541, PMID:30187887.
[13] Meng J, Chen S, Han JX, Qian B, Wang XR, Zhong WL, *et al*. Twist1 Regulates Vimentin through Cul2 Circular RNA to Promote EMT in Hepatocellular Carcinoma. Cancer Res 2018;78(15):4150–4162. doi:10.1158/0008-5472.Can-17-3009, PMID:29844124.
[14] Ji D, Chen GF, Wang JC, Ji SH, Wu XW, Lu XJ, *et al*. Hsa_circ_0070963 inhibits liver fibrosis via regulation of miR-223-3p and LEMD3. Aging 2020;12(2):1643–1655. doi:10.18632/aging.102705, PMID:32003753.
[15] Chen Y, Yuan B, Wu Z, Dong Y, Zhang L, Zeng Z. Microarray profiling of circular RNAs and the potential regulatory role of hsa_circ_0071410 in the activated human hepatic stellate cell induced by irradiation. Gene 2017;629:35–42. doi:10.1016/j.gene.2017.07.078, PMID:28774651.
[16] Kumar D, Yalamanchali S, New J, Parsel S, New N, Holcomb A, *et al*. Development and Characterization of an In Vitro Model for Radiation-Induced Fibrosis. Radiat Res 2018;189(3):326–336. doi:10.1667/rr14926.1, PMID:29351058.
[17] Hu Z, Qin F, Gao S, Zhen Y, Huang D, Dong L. Paeoniflorin exerts protective effect on radiation-induced hepatic fibrosis in rats via TGF-β1/Smads signaling pathway. Am J Transl Res 2018;10(3):1012–1021. PMID:29636890.
[18] Barcena-Varela M, Colyn L, Fernandez-Barrena MG. Epigenetic Mechanisms in Hepatic Stellate Cell Activation During Liver Fibrosis and Carcinogenesis. Int J Mol Sci 2019;20(10):2507. doi:10.3390/ijms20102507, PMID:31117267.
[19] Kristensen LS, Andersen MS, Stagsted LVW, Ebbesen KK, Hansen TB, Kjems J. The biogenesis, biology and characterization of circular RNAs. Nat Rev Genet 2019;20(11):675–691. doi:10.1038/s41576-019-0158-7, PMID:31395983.
[20] Tang CM, Zhang M, Huang L, Hu ZQ, Zhu JN, Xiao Z, *et al*. CircRNA_000203

enhances the expression of fibrosis-associated genes by derepressing targets of miR-26b-5p, Col1a2 and CTGF, in cardiac fibroblasts. Sci Rep 2017;7:40342. doi:10.1038/srep40342, PMID:28079129.
[21] Wang Z, Zhao Y, Zhao H, Zhou J, Feng D, Tang F, *et al*. Inhibition of p66Shc Oxidative Signaling via CA-Induced Upregulation of miR-203a-3p Alleviates Liver Fibrosis Progression. Mol Ther Nucleic Acids 2020;21:751–763. doi:10.1016/j.omtn.2020.07.013, PMID:32781430.
[22] Niu H, Zhang L, Chen YH, Yuan BY, Wu ZF, Cheng JC, *et al*. Circular RNA TUBD1 Acts as the miR-146a-5p Sponge to Affect the Viability and Pro-Inflammatory Cytokine Production of LX-2 Cells through the TLR4 Pathway. Radiat Res 2020;193(4):383–393. doi:10.1667/rr15550.1, PMID:32097101.
[23] Hu HH, Chen DQ, Wang YN, Feng YL, Cao G, Vaziri ND, *et al*. New insights into TGF-β/Smad signaling in tissue fibrosis. Chem Biol Interact 2018;292:76–83. doi:10.1016/j.cbi.2018.07.008, PMID:30017632.
[24] Xu F, Liu C, Zhou D, Zhang L. TGF-β/SMAD Pathway and Its Regulation in Hepatic Fibrosis. J Histochem Cytochem 2016;64(3):157–167. doi:10.1369/0022155415627681, PMID:26747705.
[25] Lang C, Dai Y, Wu Z, Yang Q, He S, Zhang X, *et al*. SMAD3/SP1 complex-mediated constitutive active loop between lncRNA PCAT7 and TGF-β signaling promotes prostate cancer bone metastasis. Mol Oncol 2020;14(4):808–828. doi:10.1002/1878-0261.12634, PMID:31925912.

*Journal of Clinical and Translational Hepatology* **2022** vol. 10(4) | 692–699
DOI: 10.14218/JCTH.2021.00353

Review Article

# Pluripotent Stem Cell-derived Strategies to Treat Acute Liver Failure: Current Status and Future Directions

Jingfeng Liu[1,2,3*], Zhiming Yuan[4] and Qingwen Wang[2,3*]

[1]*Institute of Biomedicine and Biotechnology, Shenzhen Institute of Advanced Technology, Chinese Academy of Science, Shenzhen, Guangdong, China;* [2]*Shenzhen Key Laboratory of Immunity and Inflammatory Diseases, Peking University Shenzhen Hospital, Shenzhen, Guangdong, China;* [3]*Department of Rheumatism and Immunology, Peking University Shenzhen Hospital, Shenzhen, Guangdong, China;* [4]*Department of Gastroenterology, Peking University Shenzhen Hospital, Shenzhen, Guangdong, China*

**Received:** 22 August 2021 | **Revised:** 17 January 2022 | **Accepted:** 12 February 2022 | **Published:** 9 March 2022

## Abstract

Liver disease has long been a heavy health and economic burden worldwide. Once the disease is out of control and progresses to end-stage or acute organ failure, orthotopic liver transplantation (OLT) is the only therapeutic alternative, and it requires appropriate donors and aggressive administration of immunosuppressive drugs. Therefore, hepatocyte transplantation (HT) and bioartificial livers (BALs) have been proposed as effective treatments for acute liver failure (ALF) in clinics. Although human primary hepatocytes (PHs) are an ideal cell source to support these methods, the large demand and superior viability of PH is needed, which restrains its wide usage. Thus, a finding alternative to meet the quantity and quality of hepatocytes is urgent. In this context, human pluripotent stem cells (PSC), which have unlimited proliferative and differential potential, derived hepatocytes are a promising renewable cell source. Recent studies of the differentiation of PSC into hepatocytes has provided evidence that supports their clinical application. In this review, we discuss the recent status and future directions of the potential use of PSC-derived hepatocytes in treating ALF. We also discuss opportunities and challenges of how to promote such strategies in the common applications in clinical treatments.

**Citation of this article:** Liu J, Yuan Z, Wang Q. Pluripotent Stem Cell-derived Strategies to Treat Acute Liver Failure: Current Status and Future Directions. J Clin Transl Hepatol 2022;10(4):692–699. doi: 10.14218/JCTH.2021.00353.

**Keywords:** Acute liver failure; Hepatocyte transplantation; Human pluripotent stem cells; Bioartificial liver system.

**Abbreviations:** ALF, Acute liver failure; BAL, Bioartificial liver; DE, Definitive endoderm; HB, Hepatoblast; hESC, Human embryonic stem cell; HLC, Hepatic like cell; HT, Hepatocytes Transplantation; iPSC, induced pluripotent stem cell; OLT, Orthotopic liver transplantation; PH, Primary hepatocytes; PSC, Pluripotent stem cell.

***Correspondence to**: Jingfeng Liu, Institute of Biomedicine and Biotechnology, Shenzhen Institute of Advanced Technology, Chinese Academy of Science, 1068 Xueyuan Avenue, Shenzhen University Town, Shenzhen, Guangdong, China. ORCID: https://orcid.org/0000-0002-8509-0572, Tel: +86-755-86392288, E-mail: oscar1356@smu.edu.cn; Qingwen Wang, Department of Rheumatism and Immunology, Peking University Shenzhen Hospital, 1120 Lianhua Rd, Futian District, Shenzhen, Guangdong 518035, China. Tel: +86-755-83923333, E-mail: wqw_sw@163.com

## Introduction

Liver diseases, including acute liver failure (ALF) are a public health challenge worldwide, because of death caused by liver dysfunction.[1–3] ALF is a severe condition with significant morbidity and mortality even for the patients without pre-existing liver disease. The causes of ALF vary geographically with viral infections of the liver, primarily hepatitis B, C, and E in developing countries and drug overdose-induced ALF, usually paracetamol (acetaminophen), in developed countries such as USA and parts of Europe.[4–8] Because of the severity of ALF, there are few ways to prevent or cure patients other than orthotopic liver transplantation (OLT), which is now the only treatment that is considered effective to avoid the life-threatening complications caused by ALF.[9–11] However, OLT is limited by the scarcity of available donor livers, complicated surgery procedures, and high financial burden.[12] Therefore, other than OLT and drug supplements for the maintenance of basic vital signs, there is a need for effective therapeutic treatments for ALF.

In recent years, hepatocytes transplantation (HT) and bioartificial liver (BAL) system have emerged as effective methods for the compensatory treatments of ALF related liver dysfunction.[13–16] These two methods potentially build up the fundamental niche for host liver regeneration and decelerate the disease progression, which creates a bridging time for OLT. As reported, effective HT involves reconstitution of as much as 2.5% functional liver tissue in treating acute-on-chronic liver failure (ACLF).[17] Consistent with that, primary hepatocytes (PHs) are considered the ideal cell source for such treatments. Unfortunately, it remains a bottleneck to meet the demand of large quantity and clinical quality of PH from limited viable organ donation. To solve these problems, studies have focused on developing strategies using human pluripotent stem cell (PSC)-derived hepatic-like cells (HLCs), including hepato-blasts and hepatocytes. The differentiation of PSCs into clinical-grade HLCs has been studied.[18–20] The aim of this review is to summarize the current opinions regarding the therapeutic effectiveness of PSC-derived HLC for ALF treatment and to discuss recent progresses in preclinical and clinical treatments and challenges, which need to be improved in using PSC-derived HLC (Fig. 1).

## Characteristics of ALF

ALF is characterized by severe injury of liver cells that has

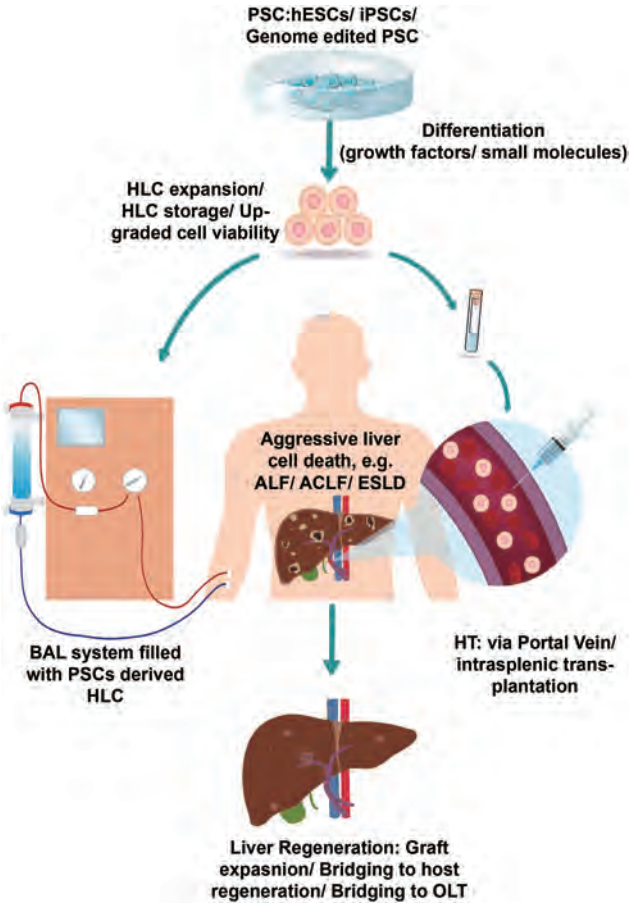


**Fig. 1. Producing pluripotent stem cell (PSC)-derived hepatic-like cells (HLCs) for use in bioartifical liver support and hepatocyte transplantation applications.** The advantage of using PSC derived of HLC is their unlimited proliferation potential, which addresses both the shortage of viable donor livers and primary hepatocytes. By differentiating PSC (hESCs or iPSCs) or genome edited PSC into HLC, we can obtain HLCs of the required quantity and quality for BAL and HT in severe liver disease (e.g., ALF, ACLF, and ESLD). After BAL or HT treatment, the ideal outcome is either graft expansion and the regeneration of the host liver or bridging to OLT. ALF, acute liver failure; ACLF, acute on chronic liver failure; BAL, bioartificial liver; ESLD, end-stage liver disease; hESC, human embryonic stem cell; HLC, hepatic-like cell; HT, hepatocyte transplantation; iPSC, induced pluripotent stem cell; OLT, orthotopic liver transplantation; PSC, pluripotent stem cell.

a rapid onset and leads to a frequent fatal outcome, with up to 30% mortality.[21] Paracetamol overdose and autoimmunity caused liver injuries are the most frequent causes in developed countries. HBV infection is the primary cause of ALF in developing countries.[2] Paracetamol toxicity, which induces mitochondrial oxidant stress-related cell death and sterile inflammatory responses in hepatocytes, accounts for more than 46% of the ALF cases in the USA.[22] At the early stage of paracetamol-induced liver injury, treatment with N-acetyl-cysteine or 4-methylpyrazole (fomepizole) can effectively control the progress.[23] However, at later stages, drugs are no longer effective to slow disease progression, which leaves OLT as the last option to save such patients. HBV infection has plagued China for a long time, and is involved in 84% of hepatocellular carcinoma and 77% of liver cirrhosis patients annually.[6] Control of HBV is fundamental to preventing ALF. Anti-HBV drugs focus on how to slow the replication of viral DNA, but completely eliminating HBV DNA is hard to achieve, and is the main reason of HBV relapse and progression.[24,25] Once the HBV replication is out of control, there's a large chance to cause ALF. The pathology and autopsy of ALF patients often shows widespread hepatic apoptosis and necrosis with few viable hepatocytes remaining, which leads to the failure of liver regeneration. To save ALF patients, the question to answer is how to buy time for patients to carry out liver regeneration.

Treatment of ALF must deal with systemic complications including the release of pro-inflammatory cytokines, multiple organ failure, and a hypotensive environment. Hepatic encephalopathy frequently appears because they hepatocyte death results in aberrant liver function and toxins that travel to the brain and affect the brain function. Although L-ornithine-L-aspartate and ornithine phenylacetate inhibit ammonia synthesis to relieve symptoms, OLT is current, y the last chance for ALF patients currently. Development of novel treatments of ALF patients is currently urgent.

## Current knowledge of the treatments for ALF

In addition to the basic symptomatic supporting treatments to stabilize the vital signs, cell therapy-based supplement for liver regeneration and bioartificial liver (BAL) support system have been developed as effective tools for ALF patients. Both of these methods require a large quantity of viable hepatocytes.

## BAL system

Before the emergence of BAL, abiotic artificial liver therapy, including plasmapheresis, hemoperfusion absorption, and venous hemodiafiltration, were used as clinical treatments with limited success.[26,27] The molecular adsorbent recirculating system and Prometheus system are widely used non-bioartificial liver systems with benefits for ALF patients.[28,29] However, as it relies on exogenous detoxification, is not able to provide an environment needed for hepatic regeneration as it is complicated to mimic all the functions of host hepatocytes. BAL systems include functional hepatocytes in a bioreactor that simulates the function of a normal human liver. To a large extent, it can not only remove the toxic substances but also provide functions such as synthesis and metabolism, which temporarily replace the function of the damaged liver in order to survive from the fatal onsets of ALF.[16,30] The indispensable factor within the BAL system are the functional hepatocytes. The quality of functional hepatocytes, the ease of obtaining them and safety are decisive in determining whether the BAL can play an important role in clinical treatment.

Prior to this, the main sources of functional hepatocytes were primary liver cells, porcine liver cells, human liver cancer cell lines like HepG2, HepaRG, and immortalized human liver cell lines like L-02. Human PH are the best for use in BALs, but organ sources are limited, and it is difficult to obtain a sufficient number of human PH for BALs. Porcine liver cells are used because of their functions, abundant source, and the easy accesses. For example, the AMC artificial liver system using porcine liver cells successfully helped 12 patients with ALF to gain time for OLT. One patient no longer needed because of the effectiveness of therapy.[31,32] The HepaAssist system, which uses porcine liver cells, is the only BAL system that has been a investigated in a multicenter randomized controlled clinical trial in the USA. Although it has achieved encouraging therapeutic effects in phase III clinical trials, it has not yet obtained Federal Drug Administration approval. It is underlying safety concerns including heterogeneous immune rejection and animal-derived virus infections have made it difficult to obtain regula-

**Table 1. Clinical use of hepatocyte transplantation to treat acute liver failure (ALF)**

| Time (year) | Number of recipients | Delivery route | Outcomes | Reference |
|---|---|---|---|---|
| Drug-induced ALF | | | | |
| 1999 | 2 | Portal vein | 2 Deaths: days 4 and 35 | 41 |
| 2000 | 3 | intrasplenic | 3 Deaths: 6 h, days 14, and 20 | 42 |
| 2006 | 6 | Intrasplenic and portal vein | 3 Deaths: days 1, 3, 18; 2 OLT: days 2 and 10; 1: Full recovery | 43 |
| Hepatitis virus-induced ALF | | | | |
| 2000 | 1 | Intrasplenic | 1 Full recovery | 45 |
| 2000 | 2 | Intrasplenic and portal vein | 2 Deaths: 18 h and day 52 | 42 |
| 2006 | 2 | Portal vein | 2 Deaths: days 2 and 7 | 43 |
| 2010 | 1 | Portal vein | 1 Death: day 11 | 44 |
| Acute-on-chronic liver failure | | | | |
| 2014 | 7 | Intrasplenic | 3: Full recovery; 3 Death: 2.5–12 months; 1: OLT | 17 |

tory approval.[33] The superiority of human liver cancer cell lines and immortalized human liver cell lines is that they can proliferate indefinitely *in vitro*. However, their functions are greatly compromised and there is a potential tumorigenic risk, which limits their application prospects. For example, the Vital Therapies artificial liver system, which uses C3A liver cancer cells, failed a phase III clinical trial because of poor therapeutic effects, even though the effectiveness in animal experiments was good.[34,35] Therefore, to obtain a large quantity and clinical-grade quality of functional hepatocytes is the major hindrance for BAL.

Nowadays, in the research of regenerative medicine, PSC has received much attention due to the potential to be differentiated into functional hepatocytes as the source of seed cells in the BAL system. Precise differentiation of human embryonic stem cell (hESCs) or induced pluripotent stem cell (iPSCs) into HLC has been achieved and improved tremendously. In addition, with the appearance of 3D culturing system, hepatic organoid formation brings out more mature HLC, which owns comprehensive functions.[36,37] Moreover, Lijian Hui of Shanghai also successfully transdifferentiated human fibroblasts into human hepatocytes (hiHep), and overexpressed SV40 Large T through gene editing, thus obtaining the ability to be expanded *in vitro*, providing a potential cell source for BAL.[38] This technology also successfully conducted a clinical trial of a bioartificial liver in 2016, and achieved good therapeutic effects, which greatly improved the confidence to promote hiHep into the clinic applications. In addition, bioreactors, as the key devices in BAL system, are able to provide a favorable proliferative and metabolic platform for a large-scale liver cell culture and storage.[39] For example, a fluidized-bed bioreactor with alginate-based spherical beads is able to scale up $10^{11}$ liver cells culture and retains their hepatic functions.[40] Yet the challenge is to extend such design to clinical applications.

## Hepatocyte transplantation (HT)

The concept of HT therapy was first described by scientists in the early 1970s. After more than 20 years of development, HT therapy was translated from animal experiments to clinical trials, and was shown to be effective in ALF, or acute-on-chronic liver failure (Table 1).[17,41–45] HT has several key therapeutic advantages. (1) It is less invasive OLT surgery and can be performed multiple times. (2). The patient's liver is preserved and retains its ability to regenerate itself. (3) With the development of gene editing and stem cell technology, HT can be coupled with targeted genome modifications, realizing individualized and precise treatment.[15,46] These advantages are not available in OLT or BAL support systems. So far, many liver diseases have undergone clinical trials of HT treatment, laying the foundation for clinical promotion and application.

How to gain time is a significant issue for ALF patients. For one thing, HT helps patients to regenerate their own livers, providing a proliferative niche for transplanted hepatocytes. While OLT is inevitable, HT plays a role as a transitional bridge connecting patients with an appropriate donor liver. In animal models of drug-induced ALF, HT significantly improves survival. In clinical trials, there have been more than 40 cases of ALF caused by drugs or viral infections treated by HT worldwide.[47,48] Although, they were not multicenter randomized controlled trials and the delivery method, volume of transplanted cells, and cell sources were not standardized, which makes them difficult to compare statistically, most patients responded well to treatment, with prolonged survival time, bridging to OLT, and even fully recovery (Table 1).[17,41] The limited clinical data fully confirms the therapeutic effect of HT, but it needs to be further standardized and unified.

## PSC-derived hepatocytes

With both BAL support or HT treatment, the key to success is the quality and quantity of functional liver cells. Human PSCs, including human embryonic stem cells (hESCs) and induced pluripotent stem cells (iPSCs), have unlimited proliferation ability and the pluripotency to differentiate into any somatic cell type. Therefore, the differentiation of PSCs into HLCs with similar gene expression profiles and functions as human hepatocytes can, to a large extent, solve the problem of limited sources of functional hepatocytes. Recent advances in stem cell research have found methods that have increased the ease of inducing *in vitro* differentiation into HLCs. However, often not more than $10^9$–$10^{10}$ the hepatocytes are available for treatment, which is a barrier

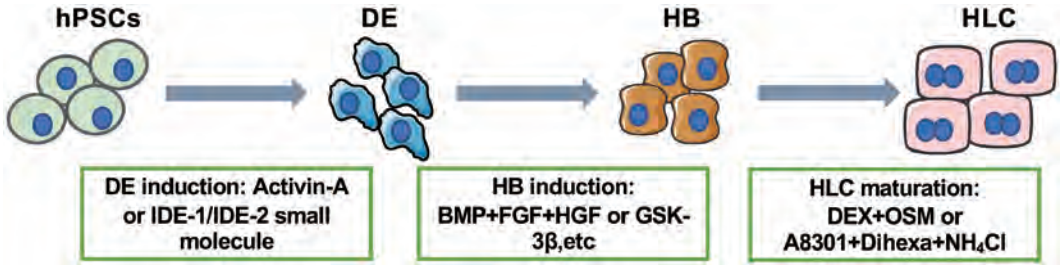


**Fig. 2. Introduction of the differentiation of human pluripotent stem cells (hPSCs) into mature hepatocyte-like cells (HLCs).** Adapting hPSCs with activin-A is a well-known protocol for definitive endoderm (DE) induction. IDE-1 and IDE-2 are small molecules that can replace activin-A, which is an easier and inexpensive way of induction. The combination of growth factors for hepatoblast (HB) induction is well studied. Hepatic-like cell (HLC) induction and maturation is the last step for a successful differentiation. This step can be induced by dexamethasone (DEX) and oncostatin M (OSM). Small molecules could be developed for use in clinical applications.

between PSC differentiation and clinical application. One of the obstacles is that the efficiency of differentiation is limited, which often accompanied by the risk of incomplete differentiation or incorrect cell fates, resulting in unpredictable safety issues. Additionally, the current hepatocyte culture system has not been well developed, which is hard to maintain the proliferation ability and the functions of cultured hepatocytes at the same time. Therefore, we need to reach a more comprehensive and in-depth understanding of the molecular mechanisms of direct differentiation of PSC into HLC, to establish an efficient and stable differentiation system. We need to find ways to culture and expand hepatocytes *in vitro* to obtain a large number of clinical-grade hepatocytes, which is of great significance for the treatment of ALF by BAL and HT. The paragraphs below review the current status and progress of PSCs used for the treatment of ALF.

## Differentiation of PSCs into HLCs

The study of precise differentiation of PSC into HLC *in vitro* is mainly through simulating the development of human liver, which is accomplished by adding growth factors and small molecules that regulate the related signal pathways. Methods described in the available studies can be used to induce the differentiation of PSC into definitive endoderm (DE), hepatoblasts (HB), and mature hepatic cells, i.e. HLCs. Although the specific induction schemes adopted by different research groups are not the same, the basic method is: (1) induction of DE cells by activin-A; (2) Transformation of DE to HB by treatment with FGF, BMP, and HGF; and (3) use of OSM and dexamethasone (DEX) to induce maturation of HB into HLC (Fig. 2).[49]

The induction of DE is the first step of differentiation and is a key step that determines the final differentiation efficiency. The most frequently used method is the induction of PSC to form DE cells by activin-A. The underlying mechanism is activation of the Nodal signaling pathway, which simulating the early steps of liver development *in vivo*.[50–52] Some studies have reported that inhibiting the PI3K signaling pathway was a prerequisite for the effective use of activin-A for DE induction. Adding PI3K signaling pathway inhibitors improves the efficiency of DE differentiation.[53] Adding a rho kinase (ROCK) inhibitor at that stage reduces cell apoptosis to a certain extent, which improves cell survival and differentiation efficiency. Compared with the complex signaling pathways regulated at the DE stage, the regulation of the differentiation of HB and HLC cells is relatively clear. *In vivo* studies of liver development, *in-vitro* coculture studies and the single-cell sequencing have shown that the transforming growth factor beta (TGF-β), Wnt and NOTCH signaling pathways are the pathways most involved in the induction of DE cells by growth factors such as BMP, FGF, and HGF. This step avoids the establishment of an incorrect cell fate (e.g., bile duct or pancreas cells) and improves the purification of HLC at the final stage.[54]

Differentiation induced by growth factors is recognized as an efficient method of obtaining functional HLCs, but growth factors are expensive and difficult to store, which limits their use for large-scale production of HLCs. In addition, most growth factors are protein products containing animal components that may cause adverse reactions associated with clinical use. In that context, a combination of small molecules can be used to replace the growth factors and obtain functional HLC with high efficiency. Properties of the small molecules include the ability to freely penetrate cell membranes, stable structures, no immunogenicity, low cost, and wide variety. The use of small-molecule compounds is expected to become a safer and more effective method of inducing clinical-grade HLCs. Recent reports by multiple research groups have described the use of small molecules to induce differentiation into HLCs. IDE1 and IDE2 are small molecules that can efficiently induce PSC to form DE, act much as activin-A by simulating the Nodal signaling pathway.[55] In the HB stage, glycogen synthase kinase (GSK)-3β is used to simulate the Wnt pathway to guide DE to a hepatic fate and not bile duct fate.[56,57] Recently, Asuma *et al*.[20] reported the use of small molecules to differentiate hESCs into HLC. A comparison of HLCs induced by small molecules and those derived from growth factors showed a considerable number of functions, such as albumen (ALB) secretion, CYP450 activity which metabolizes drugs and enzymes. In addition, Pan *et al*.[58] introduced an improved combination of small molecules for robust HLC induction. The use of small molecules activity has promising prospects, but further research is needed to develop more stable and efficient combinations of small molecules to increase effectiveness and safety for adapting to clinical use.

Functional HLCs can be obtained by direct differentiation of PSCs. There are also reports of transdifferentiating somatic cells to obtain functional HLCs. Hui, L *et al*.[38] reported that after human fibroblasts overexpressing the transcription factors FOXA3, HNF1α and HNF4α can be transdifferentiated into HLCs and perform a series of functions similar to those of PHs. Transdifferentiation provides another way to source of HLC, but it safety needs further verification, as such transcriptional factors are known to participate in the carcinogenesis of hepatocellular carcinoma.

## *In vitro* expansion of HLCs

Obtaining HLCs from PSCs has been validated by multiple

research groups, proving its reproducibility and efficiency. However, owing to the required volume of cells for transplantation for clinical applications, relying on the differentiated HLC is not enough. As a result, how to expand hepatocytes *in vitro* has attracted widespread attention in recent years. Hepatocytes are terminally differentiated cells, which makes them difficult to culturing *in vitro* and maintain their inherent functional properties. Hui Lijian *et al*.[59] reported that a combination of small molecules, adding Wnt3a to hepatocyte medium and removing Rspo1, Noggin, and forskolin increased the fold-expansion of human hepatocytes by 10,000 times. However, they found that the expanded hepatocytes had a bidirectional differentiation potential that placed them between HPCs and mature hepatocytes. It seems to be a complicated task to expand hepatocytes *in vitro*, and the research is focused on the expansion of hepatic progenitor cells like HBs that still have some degree of stemness.

Compared with mature hepatocytes, HBs has a stronger proliferation ability and the potential of rapid differentiation into both hepatocytes and bile duct cells.[60–63] Amplifying PSC-derived HBs is an ideal alternative source of hepatocytes. On the one hand, it is feasible to develop the proliferation potential of HB, and on the other hand, amplified HBs can be frozen to establish a cell bank, acting as seed cells that could be rapidly obtained for functional HLC differentiation. Recent reports have found that multiple small-molecule compounds are suitable for amplifying HB, such as the GSK-3β inhibitor CHIR99021, the TGF-β signaling pathway inhibitor A83-01, and the ROCK inhibitor Y27632. A recent study combined small molecules to simultaneously regulate the BMP/WNT/TGF-β/Hedgehog pathway, which not only maintains the stemness of HBs, but also retains their proliferative capacity. The HBs amplified by the combination had therapeutic effectiveness after transplantation into ALF-model mice.[64,65] Large-scale expansion of HBs, would be a major step in producing the HLCs in the quantity and with the quality required for clinical development and application.

## Clinical benefits of PSC-derived cell therapy

Much effort has been made worldwide to promote PSC-derived methods to cure chronic and acute illness. Induced PSC-derived retinal pigment epithelium cells have used clinically to cure patients with macular degeneration, with good outcomes 1 year after transplantation, which supports the use of PSC-derived cells in clinical applications.[66] The use of PSC-derived HLC for ALF, HT, and BAL applications would serve as a promising tool for clinical alternatives. The clinical indications and benefits of PSC-derived cell therapies for treating ALF or end-stage liver disease are summarized below.

### *Modulating the regeneration niche*

A positive outcome requires that HT promotes sufficient regeneration of the host liver. Besides increasing the homing and engraftment of transplanted hepatocytes, modulating the injury niche to include host immune responses such as the macrophage activation and cytokine release,[67,68] is also an important benefit of using PSC-derived HLCs. Unlike PH-derived HLCs, as hypoimmunogenic PSC-derived HLCs would modulate the host immune recruitment to restrain systemic inflammation. For example, phagocytosis mediated by macrophage activation might be limited by the CD47-SIRPα axis if PSC-derived HLCs overexpressing CD47 were transplanted.[69–72] Such clinical applications could be useful in a broader scope of liver disease and not limited to ALF.

### *Transplantation feasibility and safety*

Even if the shortage of donor livers could be solved, OLT is still a challenging procedure with risks including intraoperative bleeding, postsurgical cardiovascular dysfunction, and unavoidable death.[73,74] PSC-derived HT is a safer alternative with infusion that does not require major surgery and the possibility of multiple transplantation procedures.[75] Improvements in cell culture would make PSC-derived HLCs are a good alternative source of hepatocytes compared with PHs. The feasibility of PSC-derived HLCs is not limited by lack of a large quantity of HLCs, which can be cryopreserved to ensure a constantly available cell source for emergency treatment of ALF patients.[76,77]

## Individualized treatment

PSC-derived HLCs combined with Crispr/Cas9 genome editing and PSC differentiation would allow generating multiple PSC cell lines that met individual patient requirements or those of the primary illness.[78,79] For instance, the HBV-induced liver disease could theoretically be corrected by transplantation with HBV receptor (NTCP) knock-out or ectopic expression of NTCP variants in HLCs derived from edited PSCs.[80,81] Following transplantation in such patients, HBV could not enter hepatocytes as they lacked the receptor, which would avoiding the recurrence of HBV. Treatment might thus be adjusted depending on the pathophysiology of the primary illness that caused ALF.

## Challenges of current PSC based options

Clinical trials of HT and BAL support systems are ongoing, and strive to promote the two therapeutic methods with broad application prospects in clinical treatment. However, the novelty of the methods and the complexity of ALF, are challenging, and can be summarized as follows:

The lack of rigorous clinical trials makes it difficult to achieve a unified and standardized treatment. Most ALF patients indicated for HT and BAL are in a life-threatening stage of disease and require urgent treatment intervention. It is not possible for multiple centers to formulate detailed treatment procedures in time, which makes it difficult to reach a consensus. Standardized treatment indications, treatment procedures, countermeasures for complications, and the introduction of appropriate treatment guidelines are the prerequisites for the adoption of HT and BAL as clinical applications.

The key requirement of these two treatments is the quantity and quality of functional liver cells. No matter which method is used to obtain functional liver cells, an inevitable core problem is the immunogenicity of the cells. At present, adjuvant immunosuppressive agents or pretransplant radiotherapy are used in patients receiving HT, to suppress the patient's immune system and protect the transplanted cells. Once the immune system is suppressed, the patient is exposed to risks of tumorigenesis and infection. Recently, hypoimmunogenic PSC have been developed to overcome the issue of immune rejection. Through knocking out human lymphocyte antigen (HLA) Class I and II molecule accompanied by overexpression of the natural killer (NK) cell specific inhibition receptor (HLA-E) might help to evade host immune surveillance.[82,83] Human embryonic stem cells

overexpressing CTLA4-Ig and PD-L1 are immune-evasive and have shown therapeutic effectiveness in a humanized mouse model of acute liver injury.[84,85] Further research should be carried out to elucidate the underlying mechanism. Its safety should not be neglected as the risk of tumor formation increases without host immune recognition. The development of novel immune tolerance strategies is of great significance for HT therapy.

Improvement of transplanted-cell engraftment and homing needs to be studied. After the liver is damaged, hepatic stellate cells are activated, become fibroblasts, deposit collagen that makes it difficult for transplanted cells to enter damaged regions of the liver. Different routes of delivery have been validated, among which splenic transplantation and hepatic portal vein are typically used in clinical treatments. There are three ways of delivery via the portal vein, ultrasound guided intrahepatic portal vein puncture, transcutaneous splenic vein puncture, and intrahepatic portosystemic shunt via the hepatic venous system.[35] However, the procedures are associated with risks of portal vein hypertension, bleeding, or thrombosis.[86] Alternate routes include the hepatic artery, which has a higher blood flow velocity and lower thrombosis formation risk.[87] More clinical data should be collected to choose the appropriate routes of delivery. Coupling nanomaterials and HT is a novel opinion that would improve the viability, homing, and engraftment of transplanted hepatocytes.[88,89] Micro-encapsulated HLC patches or decellularized liver scaffolds would avoid intravenous or arterial injection.[90–92] Increasing the rate of homing of transplanted cells is a guarantee for the clinical therapeutic effectiveness of HT and needs further validation.

## Concluding remarks

In summary, HT and BAL support have bright prospects and application value in the treatment of ALF. PSC-derived HLCs have the potential for wide clinical application, but demonstration of effectiveness and lack of complications are still needed. The use of humanized immune system animal models can provide more accurate immune-response data for HT studies of reducing the immunogenicity of transplanted cells, establishing immune tolerance strategies, and safety. Last but not least, the combining various therapies for ALF treatment is a future trend.

## Funding

This research was supported by Shenzhen Key Laboratory of Inflammatory and Immunology Diseases (No. ZDSYS 20200811143756018), China Postdoctoral Science Foundation (No. 2021M693290), the Key Program for Basic Research of Shenzhen Science and Technology Innovation Commission (No. JCYJ20200109140203849) and Guangdong Basic and Applied Basic Research Foundation (No. 2021A1515111000).

## Conflict of interest

The authors have no conflict of interests related to this publication.

## Author contributions

Study concept and design (JL, QW), acquisition of data (JL, ZY), analysis and interpretation of data (JL, ZY), drafting of the manuscript (JL), critical revision (JL, ZY, QW), critical funding (JL, QW), administration (JL, QW), technical or material support (JL), and study supervision (JL, QW).

## Data sharing statement

All data are available upon reasonable request.

## References

[1] Zhao P, Wang C, Liu W, Chen G, Liu X, Wang X, *et al*. Causes and outcomes of acute liver failure in China. PLoS One 2013;8(11):e80991. doi:10.1371/journal.pone.0080991, PMID:24278360.
[2] Gu WY, Xu BY, Zheng X, Chen J, Wang XB, Huang Y, *et al*. Acute-on-Chronic Liver Failure in China: Rationale for Developing a Patient Registry and Baseline Characteristics. Am J Epidemiol 2018;187(9):1829–1839. doi:10.1093/aje/kwy083, PMID:29762630.
[3] Shen T, Liu Y, Shang J, Xie Q, Li J, Yan M, *et al*. Incidence and Etiology of Drug-Induced Liver Injury in Mainland China. Gastroenterology 2019;156(8):2230–2241.e11.doi:10.1053/j.gastro.2019.02.002,PMID:30742832.
[4] Xiao J, Wang F, Wong NK, He J, Zhang R, Sun R, *et al*. Global liver disease burdens and research trends: Analysis from a Chinese perspective. J Hepatol 2019;71(1):212–221. doi:10.1016/j.jhep.2019.03.004, PMID:30871980.
[5] Wang WJ, Xiao P, Xu HQ, Niu JQ, Gao YH. Growing burden of alcoholic liver disease in China: A review. World J Gastroenterol 2019;25(12):1445–1456. doi:10.3748/wjg.v25.i12.1445, PMID:30948908.
[6] Zhang Y, Zhang H, Elizabeth A, Liu XQ. Epidemiology of hepatitis B and associated liver diseases in china. Chin Med Sci J 2013;27(4):243–248. doi:10.1016/s1001-9294(13)60009-7, PMID:23294591.
[7] Wu T, Li J, Shao L, Xin J, Jiang L, Zhou Q, *et al*. Development of diagnostic criteria and a prognostic score for hepatitis B virus-related acute-on-chronic liver failure. Gut 2018;67(12):2181–2191. doi:10.1136/gutjnl-2017-314641, PMID:28928275.
[8] Zhao RH, Shi Y, Zhao H, Wu W, Sheng JF. Acute-on-chronic liver failure in chronic hepatitis B: an update. Expert Rev Gastroenterol Hepatol 2018;12(4):341–350. doi:10.1080/17474124.2018.1426459, PMID:29334786.
[9] Mazzoni A, Pardi C, Bortoli M, Uncini Manganelli C, Vanacore R, Urciuoli P, *et al*. High-volume plasmaexchange: an effective tool in acute liver failure treatment. Int J Artif Organs 2002;25(8):814–815. doi:10.1177/039139880202500810, PMID:12296467.
[10] Larsen FS, Schmidt LE, Bernsmeier C, Rasmussen A, Isoniemi H, Patel VC, *et al*. High-volume plasma exchange in patients with acute liver failure: An open randomised controlled trial. J Hepatol 2016;64(1):69–78. doi:10.1016/j.jhep.2015.08.018, PMID:26325537.
[11] Miró JM, Laguno M, Moreno A, Rimola A, Hospital Clinic Olt In Hiv Working Group. Management of end stage liver disease (ESLD): what is the current role of orthotopic liver transplantation (OLT)? J Hepatol 2006;44(1 Suppl):S140–S145. doi:10.1016/j.jhep.2005.11.028, PMID:16352366.
[12] Asrani SK, Devarbhavi H, Eaton J, Kamath PS. Burden of liver diseases in the world. J Hepatol 2019;70(1):151–171. doi:10.1016/j.jhep.2018.09.014, PMID:30266282.
[13] George J. Artificial liver support systems. J Assoc Physicians India 2004;52:719–722. PMID:15839451.
[14] Pareja E, Gomez-Lechon MJ, Cortes M, Bonora-Centelles A, Castell JV, Mir J. Human hepatocyte transplantation in patients with hepatic failure awaiting a graft. Eur Surg Res 2013;50(3-4):273–281. doi:10.1159/000351332, PMID:23796722.
[15] Anderson TN, Zarrinpar A. Hepatocyte transplantation: past efforts, current technology, and future expansion of therapeutic potential. J Surg Res 2018;226:48–55. doi:10.1016/j.jss.2018.01.031, PMID:29661288.
[16] García Martínez JJ, Bendjelid K. Artificial liver support systems: what is new over the last decade? Ann Intensive Care 2018;8(1):109. doi:10.1186/s13613-018-0453-z, PMID:30443736.
[17] Wang F, Zhou L, Ma X, Ma W, Wang C, Lu Y, *et al*. Monitoring of intrasplenic hepatocyte transplantation for acute-on-chronic liver failure: a prospective five-year follow-up study. Transplant Proc 2014;46(1):192–198. doi:10.1016/j.transproceed.2013.10.042, PMID:24507050.
[18] Koelfat KVK, van Mierlo KMC, Lodewick TM, Bloemen JG, van der Kroft G, Amygdalos I, Neumann UP, Dejong CHC, Jansen PLM, Olde Damink SWM, Schaap FG. Bile Salt and FGF19 Signaling in the Early Phase of Human Liver Regeneration. Hepatol Commun 2021;5(8):1400–1411. doi:10.1002/hep4.1728, PMID:34430784.
[19] Si-Tayeb K, Noto FK, Nagaoka M, Li J, Battle MA, Duris C, *et al*. Highly efficient generation of human hepatocyte-like cells from induced pluripotent stem cells. Hepatology 2010;51(1):297–305. doi:10.1002/hep.23354, PMID:19998274.
[20] Asumda FZ, Hatzistergos KE, Dykxhoorn DM, Jakubski S, Edwards J, Thomas E, *et al*. Differentiation of hepatocyte-like cells from human pluripotent stem cells using small molecules. Differentiation 2018;101:16–24. doi:10.1016/j.diff.2018.03.002, PMID:29626713.
[21] Stravitz RT, Lee WM. Acute liver failure. Lancet 2019;394(10201):869–881. doi:10.1016/s0140-6736(19)31894-x, PMID:31498101.
[22] Ramachandran A, Jaeschke H. Acetaminophen Hepatotoxicity. Semin Liver Dis 2019;39(2):221–234. doi:10.1055/s-0039-1679919, PMID:30849782.

[23] Akakpo JY, Ramachandran A, Kandel SE, Ni HM, Kumer SC, Rumack BH, *et al*. 4-Methylpyrazole protects against acetaminophen hepatotoxicity in mice and in primary human hepatocytes. Hum Exp Toxicol 2018;37(12):1310–1322. doi:10.1177/0960327118774902, PMID:29739258.
[24] Morikawa K, Shimazaki T, Takeda R, Izumi T, Umumura M, Sakamoto N. Hepatitis B: progress in understanding chronicity, the innate immune response, and cccDNA protection. Ann Transl Med 2016;4(18):337. doi:10.21037/atm.2016.08.54, PMID:27761441.
[25] Yang HC, Chen PJ. The potential and challenges of CRISPR-Cas in eradication of hepatitis B virus covalently closed circular DNA. Virus Res 2018;244:304–310. doi:10.1016/j.virusres.2017.06.010, PMID:28627393.
[26] Laleman W, Wilmer A, Evenepoel P, Verslype C, Fevery J, Nevens F. Review article: non-biological liver support in liver failure. Aliment Pharmacol Ther 2006;23(3):351–363. doi:10.1111/j.1365-2036.2006.02765.x, PMID:16422994.
[27] Li M, Sun J, Li J, Shi Z, Xu J, Lu B, *et al*. Clinical observation on the treatment of acute liver failure by combined non-biological artificial liver. Exp Ther Med 2016;12(6):3873–3876. doi:10.3892/etm.2016.3887, PMID:28105119.
[28] Karvellas CJ, Gibney N, Kutsogiannis D, Wendon J, Bain VG. Bench-to-bedside review: current evidence for extracorporeal albumin dialysis systems in liver failure. Crit Care 2007;11(3):215. doi:10.1186/cc5922, PMID:17567927.
[29] Saliba F, Samuel D. Artificial liver support: a real step forward. Minerva Med 2015;106(1):35–43. PMID:25367058.
[30] McKenzie TJ, Lillegard JB, Nyberg SL. Artificial and bioartificial liver support. Semin Liver Dis 2008;28(2):210–217. doi:10.1055/s-2008-1073120, PMID:18452120.
[31] Chamuleau RA. Artificial liver support in the third millennium. Artif Cells Blood Substit Immobil Biotechnol 2003;31(2):117–126. doi:10.1081/bio-120020168, PMID:12751830.
[32] van de Kerkhove MP, Di Florio E, Scuderi V, Mancini A, Belli A, Bracco A, *et al*. Bridging a patient with acute liver failure to liver transplantation by the AMC-bioartificial liver. Cell Transplant 2003;12(6):563–8. PMID:14579924.
[33] Demetriou AA, Brown RS Jr, Busuttil RW, Fair J, McGuire BM, Rosenthal P, *et al*. Prospective, randomized, multicenter, controlled trial of a bioartificial liver in treating acute liver failure. Ann Surg 2004;239(5):660–670. doi:10.1097/01.sla.0000124298.74199.e5, PMID:15082970.
[34] Nicolas CT, Hickey RD, Chen HS, Mao SA, Lopera Higuita M, Wang Y, *et al*. Concise Review: Liver Regenerative Medicine: From Hepatocyte Transplantation to Bioartificial Livers and Bioengineered Grafts. Stem Cells 2017;35(1):42–50. doi:10.1002/stem.2500, PMID:27641427.
[35] He YT, Qi YN, Zhang BQ, Li JB, Bao J. Bioartificial liver support systems for acute liver failure: A systematic review and meta-analysis of the clinical and preclinical literature. World J Gastroenterol 2019;25(27):3634–3648. doi:10.3748/wjg.v25.i27.3634, PMID:31367162.
[36] Kim JH, Jang YJ, An SY, Son J, Lee J, Lee G, *et al*. Enhanced Metabolizing Activity of Human ES Cell-Derived Hepatocytes Using a 3D Culture System with Repeated Exposures to Xenobiotics. Toxicol Sci 2015;147(1):190–206. doi:10.1093/toxsci/kfv121, PMID:26089346.
[37] Meier F, Freyer N, Brzeszczynska J, Knöspel F, Armstrong L, Lako M, *et al*. Hepatic differentiation of human iPSCs in different 3D models: A comparative study. Int J Mol Med 2017;40(6):1759–1771. doi:10.3892/ijmm.2017.3190, PMID:29039463.
[38] Huang P, Zhang L, Gao Y, He Z, Yao D, Wu Z, *et al*. Direct reprogramming of human fibroblasts to functional and expandable hepatocytes. Cell Stem Cell 2014;14(3):370–384. doi:10.1016/j.stem.2014.01.003, PMID:24582927.
[39] Yu CB, Pan XP, Li LJ. Progress in bioreactors of bioartificial livers. Hepatobiliary Pancreat Dis Int 2009;8(2):134–140. PMID:19357025.
[40] Selden C, Spearman CW, Kahn D, Miller M, Figaji A, Erro E, *et al*. Evaluation of encapsulated liver cell spheroids in a fluidised-bed bioartificial liver for treatment of ischaemic acute liver failure in pigs in a translational setting. PLoS One 2013;8(12):e82312. doi:10.1371/journal.pone.0082312, PMID:24367515.
[41] Strom SC, Chowdhury JR, Fox IJ. Hepatocyte transplantation for the treatment of human disease. Semin Liver Dis 1999;19(1):39–48. doi:10.1055/s-2007-1007096, PMID:10349682.
[42] Bilir BM, Guinette D, Karrer F, Kumpe DA, Krysl J, Stephens J, *et al*. Hepatocyte transplantation in acute liver failure. Liver Transpl 2000;6(1):32–40. doi:10.1002/lt.500060113, PMID:10648575.
[43] Fisher RA, Strom SC. Human hepatocyte transplantation: worldwide results. Transplantation 2006;82(4):441–449. doi:10.1097/01.tp.0000231689.44266.ac, PMID:16926585.
[44] Meyburg J, Hoerster F, Schmidt J, Poeschl J, Hoffmann GF, Schenk JP. Monitoring of intraportal liver cell application in children. Cell Transplant 2010;19(5):629–638. doi:10.3727/096368909x485058, PMID:20053320.
[45] Fisher RA, Bu D, Thompson M, Tisnado J, Prasad U, Sterling R, *et al*. Defining hepatocellular chimerism in a liver failure patient bridged with hepatocyte infusion. Transplantation 2000;69(2):303–307. doi:10.1097/00007890-200001270-00018, PMID:10670643.
[46] Iansante V, Mitry RR, Filippi C, Fitzpatrick E, Dhawan A. Human hepatocyte transplantation for liver disease: current status and future perspectives. Pediatr Res 2018;83(1-2):232–240. doi:10.1038/pr.2017.284, PMID:29149103.
[47] Hansel MC, Gramignoli R, Skvorak KJ, Dorko K, Marongiu F, Blake W, *et al*. The history and use of human hepatocytes for the treatment of liver diseases: the first 100 patients. Curr Protoc Toxicol 2014;62:14.12.1–14.1223. doi:10.1002/0471140856.tx1412s62, PMID:25378242.
[48] Flohr TR, Bonatti H Jr, Brayman KL, Pruett TL. The use of stem cells in liver disease. Curr Opin Organ Transplant 2009;14(1):64–71. doi:10.1097/MOT.0b013e328320fd7b, PMID:19337149.
[49] Mallanna SK, Duncan SA. Differentiation of hepatocytes from pluripotent stem cells. Curr Protoc Stem Cell Biol 2013;26:1G.4.1–1G.4.13. doi:10.1002/9780470151808.sc01g04s26, PMID:24510789.
[50] Loh KM, Ang LT, Zhang J, Kumar V, Ang J, Auyeong JQ, *et al*. Efficient endoderm induction from human pluripotent stem cells by logically directing signals controlling lineage bifurcations. Cell Stem Cell 2014;14(2):237–252. doi:10.1016/j.stem.2013.12.007, PMID:24412311.
[51] Tan JY, Sriram G, Rufaihah AJ, Neoh KG, Cao T. Efficient derivation of lateral plate and paraxial mesoderm subtypes from human embryonic stem cells through GSKi-mediated differentiation. Stem Cells Dev 2013;22(13):1893–1906. doi:10.1089/scd.2012.0590, PMID:23413973.
[52] Hannan NR, Segeritz CP, Touboul T, Vallier L. Production of hepatocyte-like cells from human pluripotent stem cells. Nat Protoc 2013;8(2):430–437. doi:10.1038/nprot.2012.153, PMID:23424751.
[53] Singh AM, Reynolds D, Cliff T, Ohtsuka S, Mattheyses AL, Sun Y, *et al*. Signaling network crosstalk in human pluripotent cells: a Smad2/3-regulated switch that controls the balance between self-renewal and differentiation. Cell Stem Cell 2012;10(3):312–326. doi:10.1016/j.stem.2012.01.014, PMID:22385658.
[54] Tafaleng EN, Chakraborty S, Han B, Hale P, Wu W, Soto-Gutierrez A, *et al*. Induced pluripotent stem cells model personalized variations in liver disease resulting from α1-antitrypsin deficiency. Hepatology 2015;62(1):147–157. doi:10.1002/hep.27753, PMID:25690322.
[55] Borowiak M, Maehr R, Chen S, Chen AE, Tang W, Fox JL, *et al*. Small molecules efficiently direct endodermal differentiation of mouse and human embryonic stem cells. Cell Stem Cell 2009;4(4):348–358. doi:10.1016/j.stem.2009.01.014, PMID:19341624.
[56] Touboul T, Chen S, To CC, Mora-Castilla S, Sabatini K, Tukey RH, *et al*. Stage-specific regulation of the WNT/β-catenin pathway enhances differentiation of hESCs into hepatocytes. J Hepatol 2016;64(6):1315–1326. doi:10.1016/j.jhep.2016.02.028, PMID:26921690.
[57] Du C, Feng Y, Qiu D, Xu Y, Pang M, Cai N, *et al*. Highly efficient and expedited hepatic differentiation from human pluripotent stem cells by pure small-molecule cocktails. Stem Cell Res Ther 2018;9(1):58. doi:10.1186/s13287-018-0794-4, PMID:29523187.
[58] Pan T, Tao J, Chen Y, Zhang J, Getachew A, Zhuang Y, *et al*. Robust expansion and functional maturation of human hepatoblasts by chemical strategy. Stem Cell Res Ther 2021;12(1):151. doi:10.1186/s13287-021-02233-9, PMID:33632328.
[59] Zhang K, Zhang L, Liu W, Ma X, Cen J, Sun Z, *et al*. In Vitro Expansion of Primary Human Hepatocytes with Efficient Liver Repopulation Capacity. Cell Stem Cell 2018;23(6):806–819.e4. doi:10.1016/j.stem.2018.10.018, PMID:30416071.
[60] Yanagida A, Ito K, Chikada H, Nakauchi H, Kamiya A. An in vitro expansion system for generation of human iPS cell-derived hepatic progenitor-like cells exhibiting a bipotent differentiation potential. PLoS One 2013;8(7):e67541. doi:10.1371/journal.pone.0067541, PMID:23935837.
[61] Lv L, Han Q, Chu Y, Zhang M, Sun L, Wei W, *et al*. Self-renewal of hepatoblasts under chemically defined conditions by iterative growth factor and chemical screening. Hepatology 2015;61(1):337–347. doi:10.1002/hep.27421, PMID:25203445.
[62] Zhang M, Sun P, Wang Y, Chen J, Lv L, Wei W, *et al*. Generation of Self-Renewing Hepatoblasts From Human Embryonic Stem Cells by Chemical Approaches. Stem Cells Transl Med 2015;4(11):1275–1282. doi:10.5966/sctm.2015-0051, PMID:26371343.
[63] Pan T, Chen Y, Zhuang Y, Yang F, Xu Y, Tao J, *et al*. Synergistic modulation of signaling pathways to expand and maintain the bipotency of human hepatoblasts. Stem Cell Res Ther 2019;10(1):364. doi:10.1186/s13287-019-1463-y, PMID:31791391.
[64] Huch M, Gehart H, van Boxtel R, Hamer K, Blokzijl F, Verstegen MM, *et al*. Long-term culture of genome-stable bipotent stem cells from adult human liver. Cell 2015;160(1-2):299–312. doi:10.1016/j.cell.2014.11.050, PMID:25533785.
[65] Kim Y, Kang K, Lee SB, Seo D, Yoon S, Kim SJ, *et al*. Small molecule-mediated reprogramming of human hepatocytes into bipotent progenitor cells. J Hepatol 2019;70(1):97–107. doi:10.1016/j.jhep.2018.09.007, PMID:30240598.
[66] Mandai M, Watanabe A, Kurimoto Y, Hirami Y, Morinaga C, Daimon T, *et al*. Autologous Induced Stem-Cell-Derived Retinal Cells for Macular Degeneration. N Engl J Med 2017;376(11):1038–1046. doi:10.1056/NEJMoa1608368, PMID:28296613.
[67] Possamai LA, Thursz MR, Wendon JA, Antoniades CG. Modulation of monocyte/macrophage function: a therapeutic strategy in the treatment of acute liver failure. J Hepatol 2014;61(2):439–445. doi:10.1016/j.jhep.2014.03.031, PMID:24703954.
[68] Triantafyllou E, Woollard KJ, McPhail MJW, Antoniades CG, Possamai LA. The Role of Monocytes and Macrophages in Acute and Acute-on-Chronic Liver Failure. Front Immunol 2018;9:2948. doi:10.3389/fimmu.2018.02948, PMID:30619308.
[69] Barclay AN, Van den Berg TK. The interaction between signal regulatory protein alpha (SIRPα) and CD47: structure, function, and therapeutic target. Annu Rev Immunol 2014;32:25–50. doi:10.1146/annurev-immunol-032713-120142, PMID:24215318.
[70] Hayat SMG, Bianconi V, Pirro M, Jaafari MR, Hatamipour M, Sahebkar A. CD47: role in the immune system and application to cancer therapy. Cell Oncol (Dordr) 2020;43(1):19–30. doi:10.1007/s13402-019-00469-5, PMID:31485984.
[71] Logtenberg MEW, Scheeren FA, Schumacher TN. The CD47-SIRPα Immune Checkpoint. Immunity 2020;52(5):742–752. doi:10.1016/j.immuni.2020.04.011, PMID:32433947.
[72] Leung CS, Li J, Xu F, Wong ASL, Lui KO. Ectopic expression of recipient CD47 inhibits mouse macrophage-mediated immune rejection against hu-

man stem cell transplants. FASEB J 2019;33(1):484–493. doi:10.1096/fj.201800449R, PMID:30004796.
[73] Eyvazian VA, Gordin JS, Yang EH, Aksoy O, Honda HM, Busuttil RW, *et al*. Incidence, Predictors, and Outcomes of New-Onset Left Ventricular Systolic Dysfunction After Orthotopic Liver Transplantation. J Card Fail 2019;25(3):166–172. doi:10.1016/j.cardfail.2018.10.013, PMID:30412734.
[74] Addeo P, Noblet V, Naegel B, Bachellier P. Large-for-Size Orthotopic Liver Transplantation: a Systematic Review of Definitions, Outcomes, and Solutions. J Gastrointest Surg 2020;24(5):1192–1200. doi:10.1007/s11605-019-04505-5, PMID:31919740.
[75] Tolosa L, Pareja E, Gómez-Lechón MJ. Clinical Application of Pluripotent Stem Cells: An Alternative Cell-Based Therapy for Treating Liver Diseases? Transplantation 2016;100(12):2548–2557. doi:10.1097/tp.0000000000001426, PMID:27495745.
[76] Messina A, Luce E, Hussein M, Dubart-Kupperschmitt A. Pluripotent-Stem-Cell-Derived Hepatic Cells: Hepatocytes and Organoids for Liver Therapy and Regeneration. Cells 2020;9(2):E420. doi:10.3390/cells9020420, PMID:32059501.
[77] Mun SJ, Ryu JS, Lee MO, Son YS, Oh SJ, Cho HS, *et al*. Generation of expandable human pluripotent stem cell-derived hepatocyte-like liver organoids. J Hepatol 2019;71(5):970–985. doi:10.1016/j.jhep.2019.06.030, PMID:31299272.
[78] Hockemeyer D, Jaenisch R. Induced Pluripotent Stem Cells Meet Genome Editing. Cell Stem Cell 2016;18(5):573–586. doi:10.1016/j.stem.2016.04.013, PMID:27152442.
[79] Hsu MN, Chang YH, Truong VA, Lai PL, Nguyen TKN, Hu YC. CRISPR technologies for stem cell engineering and regenerative medicine. Biotechnol Adv 2019;37(8):107447. doi:10.1016/j.biotechadv.2019.107447, PMID:31513841.
[80] Uchida T, Park SB, Inuzuka T, Zhang M, Allen JN, Chayama K, *et al*. Genetically edited hepatic cells expressing the NTCP-S267F variant are resistant to hepatitis B virus infection. Mol Ther Methods Clin Dev 2021;23:597–605. doi:10.1016/j.omtm.2021.11.002, PMID:34853804.
[81] Xu R, Hu P, Li Y, Tian A, Li J, Zhu C. Advances in HBV infection and replication systems in vitro. Virol J 2021;18(1):105. doi:10.1186/s12985-021-01580-6, PMID:34051803.
[82] Shani T, Hanna JH. Universally non-immunogenic iPSCs. Nat Biomed Eng 2019;3(5):337–338. doi:10.1038/s41551-019-0401-8, PMID:31036889.
[83] Xu H, Wang B, Ono M, Kagita A, Fujii K, Sasakawa N, *et al*. Targeted Disruption of HLA Genes via CRISPR-Cas9 Generates iPSCs with Enhanced Immune Compatibility. Cell Stem Cell 2019;24(4):566–578.e7. doi:10.1016/j.stem.2019.02.005, PMID:30853558.
[84] Liu J, Pan T, Chen Y, Liu Y, Yang F, Chen Q, *et al*. Repair of acute liver damage with immune evasive hESC derived hepato-blasts. Stem Cell Res 2020;49:102010. doi:10.1016/j.scr.2020.102010, PMID:33011360.
[85] Rong Z, Wang M, Hu Z, Stradner M, Zhu S, Kong H, *et al*. An effective approach to prevent immune rejection of human ESC-derived allografts. Cell Stem Cell 2014;14(1):121–130. doi:10.1016/j.stem.2013.11.014, PMID:24388175.
[86] Dissegna D, Sponza M, Falleti E, Fabris C, Vit A, Angeli P, *et al*. Morbidity and mortality after transjugular intrahepatic portosystemic shunt placement in patients with cirrhosis. Eur J Gastroenterol Hepatol 2019;31(5):626–632. doi:10.1097/meg.0000000000001342, PMID:30550458.
[87] Dwyer BJ, Macmillan MT, Brennan PN, Forbes SJ. Cell therapy for advanced liver diseases: Repair or rebuild. J Hepatol 2021;74(1):185–199. doi:10.1016/j.jhep.2020.09.014, PMID:32976865.
[88] Moniaux N, Faivre J. Will nano-fibers permit to turn liver cell transplantation into a curative tool against liver failure? J Hepatol 2010;52(2):150–152. doi:10.1016/j.jhep.2009.10.027, PMID:20006401.
[89] Jin Y, Wang H, Yi K, Lv S, Hu H, Li M, *et al*. Applications of Nanobiomaterials in the Therapy and Imaging of Acute Liver Failure. Nanomicro Lett 2020;13(1):25. doi:10.1007/s40820-020-00550-x, PMID:34138224.
[90] Dhawan A, Chaijitraruch N, Fitzpatrick E, Bansal S, Filippi C, Lehec SC, *et al*. Alginate microencapsulated human hepatocytes for the treatment of acute liver failure in children. J Hepatol 2020;72(5):877–884. doi:10.1016/j.jhep.2019.12.002, PMID:31843649.
[91] Pasqua M, Pereira U, de Lartigue C, Nicolas J, Vigneron P, Dermigny Q, *et al*. Preclinical characterization of alginate-poly-L-lysine encapsulated HepaRG for extracorporeal liver supply. Biotechnol Bioeng 2021;118(1):453–464. doi:10.1002/bit.27583, PMID:32997339.
[92] Zhang J, Chan HF, Wang H, Shao D, Tao Y, Li M. Stem cell therapy and tissue engineering strategies using cell aggregates and decellularized scaffolds for the rescue of liver failure. J Tissue Eng 2021;12:2041731420986711. doi:10.1177/2041731420986711, PMID:35003615.

*Journal of Clinical and Translational Hepatology* **2022** vol. 10(4) | 700–710
DOI: 10.14218/JCTH.2021.00374

Review Article

# Selecting an Appropriate Experimental Animal Model for Cholangiocarcinoma Research

Man Li[1], Xueli Zhou[1], Wei Wang[1], Baoan Ji[2], Yu Shao[1], Qianyu Du[1], Jinghao Yao[1] and Yan Yang[1*]

[1]*Department of Medical Oncology, The First Affiliated Hospital of Bengbu Medical College, Bengbu, Anhui, China;* [2]*Department of Cancer Biology, Mayo Clinic, Jacksonville, Florida, USA*

**Received:** 28 August 2021 | **Revised:** 5 December 2021 | **Accepted:** 3 January 2022 | **Published:** 11 February 2022

## Abstract

Cholangiocarcinoma (CCA) is a highly aggressive biliary tree malignancy with intrahepatic and extra-hepatic subtypes that differ in molecular pathogeneses, epidemiology, clinical manifestations, treatment, and prognosis. The overall prognosis and patient survival remains poor because of lack of early diagnosis and effective treatments. Preclinical *in vivo* studies have become increasingly paramount as they are helpful not only for the study of the fundamental molecular mechanisms of CCA but also for developing novel and effective therapeutic approaches of this fatal cancer. Recent advancements in cell and molecular biology have made it possible to mimic the pathogenicity of human CCA in chemical-mechanical, infection-induced inflammatory, implantation, and genetically engineered animal models. This review is intended to help investigators understand the particular strengths and weaknesses of the currently used *in vivo* animal models of human CCA and their related modeling techniques to aid in the selection of the one that is the best for their research needs.

**Citation of this article:** Li M, Zhou X, Wang W, Ji B, Shao Y, Du Q, *et al*. Selecting an Appropriate Experimental Animal Model for Cholangiocarcinoma Research. J Clin Transl Hepatol 2022;10(4):700–710. doi: 10.14218/JCTH.2021.00374.

## Introduction

Cholangiocarcinoma (CCA) comprises a heterogeneous group of biliary tree malignancies. The overall incidence and mortality of CCA have been increasing,[1] and the overall 5-year survival rate of all stages and subtypes is estimated as 7–20%.[2] CCA can be intrahepatic (iCCA), perihilar CCA, or distal dCCA. The latter two are described as extra-hepatic cholangiocarcinoma (eCCA), and account for up to 90% of CCA cases. Combined hepatocellular carcinoma (cHCC) includes both HCC and iCCA. The anatomical subtypes have different molecular and clinical characteristics.[3,4] The effectiveness of targeted therapy and immunotherapy has not been demonstrated in CCA,[5] and the poor prognosis of CCA stems from a lack of understanding of the molecular pathogenesis of its diverse subtypes and the lack of effective treatment.

Recent discovery of genetic alterations related to CCA by next-generation sequencing (NGS) is a great leap forward. For example, the tumor protein p53 gene (*TP53*), Kirsten rat sarcoma virus oncogene (*Kras*), recombinant human mothers against decapentaplegic homolog 4 (*SMAD4*) and BRCA-associated protein 1 gene have been identified in nearly 40% of CCA cases.[6] Moreover, distinct molecular mutation spectra are present in different anatomical subtypes, such as fibrous growth factor receptor (*FGFR*) gene fusion, mutations in isocitrate dehydrogenase 1 (*IDH1*) and the BRCA-associated protein 1 gene are more common in iCCA. *Kras* and E74 like ETS transcription factor 3 have increased mutation frequencies in eCCA, whereas alterations of epidermal growth factor receptor mutation, erb-b2 receptor tyrosine kinase 2 amplification, and phosphatase and tensin homolog (*PTEN*) deletion are more common in gallbladder cancer.[7–9]

Although NGS has broadened our knowledge of abnormal molecular alterations in CCA,[10] the functional consequences of these putative driver alterations have not yet been fully interpreted and translated into effective clinical management *in vivo*. Suitable animal models not only help in mechanistic exploration of CCA development and progression but also provide a good platform to explore new strategies for early clinical diagnosis and precise treatment of this disease. Herein, we review several current techniques and examples of CCA induction in animal models and provide insights into the advantages and limitations of these *in vivo* tools. Readers are also encouraged to refer to several previous review articles.[11–15] Compared with previous reviews we provide better coverage of the different aspects involved in carcinogenic mechanisms and the models used for the study of CCA. We also provide more educational background knowledge before the introduction of each specific model and its related techniques to facilitate understanding for introductory scholars. In addition, more detailed information in particular the subtypes of CCA (e.g., iCCA, eCCA, or a mixture with HCC) that can be tracked while describing each specific model is included in this review.

**Keywords:** Cholangiocarcinoma; Heterogeneity; Animal model; Genetically engineered model; Cancer cell of origin.

**Abbreviations:** Alb, albumin; CCA, cholangiocarcinoma; CHCC, combined hepatocellular carcinoma; DDC, 3,5-diethoxycarbonyl-1,4-dihydrocollidine; DEN, diethylnitrosamine; ECCA, extra-hepatic cholangiocarcinoma; FGFR, fibrous growth factor receptor; GEMs, genetically engineered models; HFD, high-fat diet; ICCA, intrahepatic cholangiocarcinoma; IDH, isocitrate dehydrogenase; Kras, Kirsten rat sarcoma virus oncogene; NGS, next-generation sequencing; NICD, Notch 1 intracellular domain; PDXs, patient-derived xenografts; PTEN, phosphatase and tensin homolog; SMAD4, recombinant human mothers against decapentaplegic homolog 4; TAA, thioacetamide; TAM, tamoxifen; TGF-β, transforming growth factor beta; TP53, tumor protein p53; YAP, Yes-associated protein.

[*]**Correspondence to:** Yan Yang, Department of Medical Oncology, The First Affiliated Hospital of Bengbu Medical College, Bengbu, Anhui 233004, China. ORCID: https://orcid.org/0000-0003-0887-2770. Tel: +86-552-3086178, Fax: +86-552-3074480, E-mail: qiannianhupo@163.com

**Table 1. Commonly used chemical-mechanical models**

| | | Dose | Route | Strain | Latency | Related to human CCA | Tumor type | Ref. |
|---|---|---|---|---|---|---|---|---|
| Chemicals | Furan | 15–60 mg/kg bwt | Gavage | Fischer 344 rats | 16 months | Developed intestinal epithelial metaplasia and bile duct fibrosis confined to the caudate and right hepatic lobes, eventually progressing to CCA | iCCA | 19 |
| | TAA | 300 mg/L | Water | Sprague-Dawley rats | 16–22 weeks | Developed multifocal bile duct hyperplasia with marked intestinal epithelial metaplasia, and then all of these rats developed invasive intestinal-type CCA with intense expression of CK19, similar to multistep progression of human CCA | iCCA | 23 |
| Chemical-mechanical | TAA-BDL | 0.05% | Water | Wistar rats | 30 weeks | Developed histologically invasive intestinal and mucin-producing CCA with positive expression of CK-7 and Claudin-4 | CCA | 30 |
| | DMN-BDL | 20 mg/kg | ip | Syrian hamsters | 40 weeks | Developed cholangiofibrosis, mucous cystadenoma, and CCA, accompanied by sequential bile duct obstruction and dilatation, formation of large cysts and necrosis and regeneration of the BECs, but without acute proliferative cholangitic lesions and epithelial hyperplasia of second order ducts | CCA | 31 |
| | DEN-LMBDL-DEN | 100 mg/kg ip and 25 mg/kg oral gavage | ip and oral gavage | BALB/C mice | 28 weeks | Developed liver injury, chronic cholestasis, fibrosis and cirrhosis, and CCA with physiopathological features of human CCA progression | CCA | 33 |

BDL, bile duct ligation; bwt, body weight; CCA, cholangiocarcinoma; DEN, diethylnitrosamine; DMN, dimethylnitrosamine; HCC, hepatocellular carcinoma; LMBDL, left and median bile duct ligation; iCCA, intrahepatic cholangiocarcinoma; ip, intraperitoneal injection; TAA, thioacetamide.

## Chemical-mechanical and infection-induced inflammatory models

### *Chemical-mechanical models*

Chemical carcinogens produce genotoxic effects by destroying DNA structural integrity, damaging cell membranes, and inducing inflammatory reactions, thus promoting the formation and development of CCA.[16] The commonly used carcinogens are furan, thioacetamide (TAA), diethylnitrosamine (DEN), and their combined models with bile duct ligation (Table 1).

### *Furan-induced models*

Furan is metabolized into reactive substances in the liver, and the long-term effects of these intermediates in reaction with hepatic macromolecular proteins may lead to a dose-dependent increase of liver tumors, including CCA.[17] Maronpot *et al*.[18] investigated the consequences of furan exposure in Fischer 344 rats, and found that continuous gavage with low concentrations of furan (2, 4, or 8 mg/kg body weight) for 2 years resulted in the formation of CCA in 86–100% of the rats. Short-term exposure to high concentrations of furan (30 mg/kg body weight) for 3 months eventually led to the evolution of biliary fibrosis to CCA in all the rats. Further mechanistic study has demonstrated that intrahepatic cholangiocarcinogenesis-related cellular changes, such as cholangiofibrosis and intestinal metaplasia, were induced after treatment with high concentrations of furan for 2 to 3 weeks.[19] Notably, long-term sustained furan exposure disrupted the microenvironment that stimulates hepatocyte differentiation and induces irreversible bile duct lesions at high concentrations[20] or non-neoplastic bile duct lesions at lower concentrations (<2 mg/kg body weight).[21]

### *TAA models*

TAA is metabolized in the liver to highly reactive sulfur dioxide, which covalently binds to cellular macromolecules to produce hepatotoxicity and induce the development of CCA. In 1984, Praet *et al*.[22] developed the first TAA-induced CCA model by feeding TAA-containing food to Lewis rats. Subsequently, in a study of Sprague-Dawley rats fed drinking water containing 300 mg/L TAA, 50% of the rats developed multifocal bile duct hyperplasia with marked intestinal epithelial metaplasia after only 9 weeks, and all the rats developed invasive iCCA within 16–22 weeks.[23] However, the model did not show systemic metastatic foci or cause death in rats at the end of the 6-month study. In contrast, severe proliferation of bile ducts and CCA with stromal desmo-

plasia, as seen in humans, were detected histologically in Wistar rats.[24] Recently, TAA-induced iCCA rat models were used to investigate the immunogenicity and efficacy of DNA cancer vaccines targeting cytotoxic T-lymphocyte antigen 4 blockade and programmed death-ligand 1.[25]

#### *Combined TAA-DEN models*

TAA was found to significantly potentiate the carcinogenic effects of DEN-mediated tumorigenesis in the context of precancerous lesions. The oncogenicity mainly resulted from DEN-indued DNA alkylation damage.[26,27] However, this combined TAA-DEN model has a low incidence of CCA accompanied by a high incidence of HCC, which limits the study of the iCCA subtype.

#### *Combined models of cholestasis and carcinogens*

Chronic biliary diseases such as primary sclerosing cholangitis, hepatobiliary stones, and choledochal cysts are associated with cholestasis, and the involvement of those diseases in the development of CCA is now recognized.[28] Surgical procedures, such as common bile duct ligation, mimic above pathological changes.[29] Various CCA models have been developed by combining the widely used chemical carcinogens DEN or dimethylnitrosamine with bile duct ligation,[30–33] and the models effectively characterize the multistep pathological evolution of human CCA from cystic hyperplasia to atypical hyperplasia and to CCA. However, bile duct ligation is relatively demanding for the operator and vulnerable to anesthetic and surgical risks.[33]

#### *Infection-induced inflammatory models*

Liver fluke infection induces chronic inflammation of the bile ducts and is an important risk factor for CCA formation. Oral administration of *Opisthorchis viverrini* metacercariae combined with dimethylnitrosamine or N-dimethylaminonitrosamine induces cholangiocarcinogenesis in hamsters *in vivo*.[34–37] Combined induction with infection and nitrosamines leads to liver injury, increased inflammation-mediated DNA fragmentation, mitochondrial apoptosis, and structural disruption, which in turn leads to tumor progression.[38] Studies addressing that type of etiology will improve our knowledge of the prevention of CCA disease. Thus, the development of CCA models following infection could be of importance, especially in the Far East, in which infections with liver flukes is a public health problem. However, the latency period of such models varies.

In summary, chemical-mechanical and infection-induced models effectively mimic the continuum of pathological changes in human liver tumor initiation and progression stages caused by environmental factors and provide useful preclinical platforms to study the etiology and chemoprevention of CCA. However, such models often lead to a simultaneous development liver cancer and other systemic tumors.[27] In addition, the associated genetic changes are unknown.

### Implantation models

#### *General considerations*

Implantation of established human or rodent cancer cells or tissues into a host animal can generate CCA in a relatively short period of time. Modeling is influenced by various factors, such as the biological characteristics and tumorgenicity of implanted tissue or cells, the volume of cells or tissue block, the implantation route, the site and procedure, and the genetic background and immune status of the host.

### Types of implantation

#### *Allograft models*

Allograft models involve the reimplantation of cells or tissues from animal into other inbred animal that have immune activity of the same strain and genetic background. Rizvi *et al*.[39] injected seven different C57BL/6 mouse CCA cell lines ($1\times10^6$ cells) into the lateral medial lobe of the liver of the same strain of mice. All mice formed tumors histologically and morphologically similar to human CCA after 4 weeks, with positive expression of the bile duct cell markers CK-7, CK-19, and SOX9, formation of hyperplastic connective tissue and malignant glands. The tumorgenicity of the implanted tissues or cells affected the modeling and the biological characteristics of CCA. For example, poorly invasive and tumorigenic BDEsp cells ($4\times10^6$ cells) and highly tumorigenic BDEneu cells ($4\times10^6$ cells) from the same immortalized rat BDE1 bile duct cell lines were inoculated into the bile ducts of the same strain of Fischer 344 rats. After 21–26 days the rats transplanted with BDEsp cells formed only nonmetastatic iCCA without biliary obstruction, whereas those transplanted with BDEneu cells exhibited biliary obstruction, extensive abdominal metastasis, and weight loss.[40] The above two models mimicked early versus late disease progression and metastasis of human iCCA, respectively.

Allografts can be used in immunocompetent hosts, facilitating the evaluation of the therapeutic response to antitumor drugs *in vivo* and have profound impacts on tumor immunology research and immunotherapeutic agent development. In a syngeneic transplantation model, cancer-associated fibroblasts in the tumor microenvironment have been identified as a potential antitumor target.[41] Moreover, the antitumor activity *in vivo* of imatinib mesylate,[42] sorafenib,[43] and vismodegib[44] was confirmed in several syngeneic orthotopic transplantation models. However, it is difficult to fully mimic the complex biological and molecular heterogeneity of human CCA.[45]

#### *Xenograft models*

Xenotransplantation involves the implantation of tumor cell lines or tissues into immunodeficient hosts of different species. Currently, the commonly used models include cell line-derived and patient-derived xenografts (PDXs). The first ectopic xenograft model was established by injecting cell line xenografts derived from intrahepatic metastatic human CCA tumor tissue subcutaneously into the flanks of nude mice. The histological characteristics were maintained after seven consecutive cell passages.[46]

**Orthotopic xenograft models:** Orthotopic transplantation involves the surgical implantation of CCA cells or tissue into the bile duct or liver. Micro-CT, MRI, ultrasound, and other methods can be used to evaluate tumor size and metastasis. Several orthotopic CCA xenograft models have been established for efficacy assessment of antitumor drugs[47] and mechanistic studies of either tumor progression[48] or stemness modulation[49] of iCCA. However, orthotopic CCA-PDX models are usually technically challenging to establish and require expensive and laborious longitudinal imaging to monitor tumor growth and therapeutic response. Recently, an orthotopic iCCA-PDX model has been

developed using ultrasound-guided intrahepatic injection and rapid and easy monitoring by minimally-invasive high-frequency ultrasound and bioluminescence imaging.[50] Such an iCCA model provides a favorable experimental tool to test the anticancer efficacy of chemotherapeutic agents in autochthonous environments.

**Ectopic xenograft models:** Ectopic transplantation generally involves subcutaneous injection of cells or tissue directly into the flanks of mice, which facilitates direct observation of tumor growth and size. In 2016, Cavalloni *et al*.[51] established the first iCCA-PDX model and a subsequent iCCA-PDX model endogenously expressing the *FGFR2-CCDC6* fusion protein.[52] In addition, various ectopic transplantation models have been used to identify the regulatory mechanisms of CCA biological behavior, such as abnormal upstream and downstream regulation of microRNAs[53,54] and long noncoding RNAs,[55,56] or activation of autophagy,[57,58] which provide potential therapeutic targets for antitumor drug development.

In general, xenograft models are the most important tool for preclinical drug screening and efficacy assessment because of their short latency, ease of operation, and ability to mimic many of the genetic and epigenetic abnormalities of human tumors. However, xenograft models do not reflect tumorigenesis,[45] immunodeficient hosts are not suitable for tumor immunology studies,[59] and phase III clinical trials of antitumor drugs screened based on the results of cell line-derived xenograft models often fail.[60] One reason is that the models do not fully encompass the heterogeneity of CAA. Highly transplantable iCCA and eCCA cell lines with disease heterogeneity have been established from a PDX model, which may be a promising platform for individualized anticancer drug screening.[61] Moreover, fresh human tumor tissue is not easily accessible. To overcome that, some studies have generated CCA models with metastasis biopsies[62] or secondary engraftment of cryopreserved tissues[63] obtained from CCA patients.

### *Genetically engineered models*

Genetically engineered models (GEMs) induce CCA by overexpression, deletion, or mutation of genes related to carcinogenesis through transgenes or gene transduction. GEMs can be used to explore the causes and molecular mechanisms of cholangiocarcinogenesis, progression, and metastasis at the level of specific genes, to identify biomarkers for prognosis, and to preclinically assess the therapeutic response to targeted drugs.[64,65] More importantly, GEM-based tumors are generated *de novo* in immunocompetent animals and are more representative of human tumorigenesis.

### *Conditional GEMs*

Recently, genomic complexity has been partially revealed by high-throughput sequencing, and the deletion of tumor suppressor genes such as *TP53*, *SMAD4*, and *PTEN*, or the activation of actionable oncogenes, like $Kras^{G12D}$ have been found in CCA.[7] More importantly, those genetic driver mutations can be functionally mimicked by a site-specific Cre recombinase (Cre)-loxP system in specific tissues or cells without affecting normal gene expression in other tissues or cells.[66] Cre activity can be induced by liver-specific albumin (Alb) promoter. Such recombinase activity is low at birth and gradually increases because of the gradual loss of a floxed target gene in the liver lineage, reaching its maximum activity at 4–6 weeks of age.[67] In contrast, a modified Cre-ERT recombinase system[68] can realize tissue- and time-specific manipulation of Cre recombinase activity by controlling the administration time of exogenous tamoxifen (TAM). Alb-Cre is expressed in both cholangiocytes and hepatocytes, and Alb-Cre driven GEM models often induce a mixture of iCCA and HCC. In addition to Alb, other promoters including Ah and SOX9, have also been used to mediate the activation of Cre recombinase. Here, we summarize the conditional gene expression and/or deletion models based on the commonly used Cre-loxP system in Table 2.

### *Liver-specific PTEN-SMAD4 knockout models*

Various alterations abrogate the antagonistic effect of *PTEN* on the PI3K/AKT/mTOR pathway, leading to biliary tract malignancies.[69] Although the frequency of *PTEN* variation in CCA was found to be only 0.6–11% through NGS,[7] human clinical specimens have shown that *PTEN* expression is lost or downregulated in CCA tissues compared with paracancerous tissues.[70] *SMAD4* is one of the most common tumor suppressor genes in CCA, and regulates cell growth through the transforming growth factor beta (TGF-β) signaling pathway.[71] Aberrant *SMAD4* expression has been found in various digestive malignancies.[72] In 2006, Xu *et al*.[73] crossed mice carrying *PTEN* conditional allele loss ($PTEN^{L}$) and/or *SMAD4* conditional allele loss ($SMAD4^{L}$) with mice carrying Alb-Cre recombinase. The findings showed that of the different genotypes, only $Alb\text{-}Cre^{+}$; $SMAD4^{L/L}$; $PTEN^{L/L}$ mice formed invasive CCA histologically similar to human iCCA at 4–7 months of age, and all died before 10 months of age. Mice with the $SMAD4^{L/L}$ alone genotype did not develop tumors. In contrast, homozygous deletion of *PTEN* alone resulted in HCC in 66.7% (8/12) of mice at 19 months of age.[74] Given the similar genetic backgrounds of mice and the gene-specific recombination system used by these two research teams, it is reasonable to assume that the model used by Xu *et al*.[73] might be a cHCC/iCCA model if the survival time of $Alb\text{-}Cre^{+}$; $SMAD4^{L/L}$; $PTEN^{L/L}$ mice is long enough. Xu *et al*.[73] confirmed that cholangiocarcinogenesis involved the activation of AKT, mTOR, ERK, and CyclinD1, as well as the inactivation of FOXO1. However, the model was established in the absence of chronic liver injury and inflammation, and there was no distant metastasis. Notably, the model was accompanied by the formation of salivary gland tumors, which may be tied to nonspecific expression of the Alb promotor.

### *Models combining liver-specific PTEN deletion with Kras activation*

*Kras* mutation has been found in 16.7% of iCCA cases.[75] In 2013, Marsh *et al*.[76] achieved *PTEN* deletion with *Kras* activation in both gallbladder epithelial cells and the intrahepatic bile duct system in adult mice with an Ah promoter-driven Cre-loxP system. It was found that *PTEN* deletion alone without *Kras* activation was sufficient to cause slow transformation of normal bile duct epithelium into low-grade malignancies, while dual mutations further shortened the latency of tumorigenesis and transformed tumors into more invasive phenotypes. Based on Cre activities mediated by Alb and TAM administration, or SOX9 promoter, mice with specific liver $Kras^{G12D}$ expression and *PTEN* homozygous deletion was induced intrahepatic cholangiocarcinogenesis.[77] Further investigation showed that in the presence of $LSL\text{-}Kras^{G12D}$, the type of *PTEN* gene deletion (homozygous or heterozygous) determined the fate of liver tumors with regard to formation from biliary or hepatocyte lineages because immunohistochemical staining revealed that $Alb\text{-}Cre^{+}$; $LSL\text{-}Kras^{G12D}$; $PTEN^{L/L}$ mice (AKPP) developed only iCCA; $Alb\text{-}Cre^{+}$; $LSL\text{-}Kras^{G12D}$; $PTEN^{L/+}$ mice (AKP) developed iCCA and HCC; while $Alb\text{-}Cre^{+}$; $LSL\text{-}Kras^{G12D}$; $PTEN^{+/+}$ mice (AK) developed only HCC. Notably, the spatiotemporal specificity of TAM-induced recom-

**Table 2. Conditional genetically engineered models mediated by Cre-loxP recombinase system**

| Genes targeted | Cre | Chemical induction | Latency | Tumor type | IHC | Comments (advantages/A; disadvantages/D) | Ref. |
|---|---|---|---|---|---|---|---|
| SMAD4$^{L/L}$; PTEN$^{L/L}$ | Alb-Cre | – | 4–7 months | iCCA | CK-19$^{+}$; Mucicarmine$^{+}$; Mucin 5AC$^{+}$; Hep Par1$^{-}$ | A: The formation of iCCA follows multistep progression of histopathological changes; 100% penetrance; progressed into invasive iCCA; histologically is similar to human iCCA; D: All mice died at about 10 months of age before potential HCC formation; No metastasis; Salivary gland tumor developed | 73 |
| LSL-Kras$^{V12/-}$; PTEN$^{L/L}$ | AhCre$^{ERT}$ | BNF/TAM | NA | GBC; iCCA | CK-19$^{+}$ | A: Short latency; widespread papillary neoplasia of BECs formed; D: Dual mutant mice did not survive long enough to develop the types of lesions seen in PTEN$^{L/L}$ mice; developed extensive noninvasive papillary neoplasms in the intrahepatic biliary system and invasive moderately differentiated adenocarcinomas of gall bladder with stromal desmoplasia without specific phenotype | 76 |
| LSL-Kras$^{G12D}$; PTEN$^{L/L}$ | Alb-Cre | – | 7 weeks of age | iCCA | α-SMA$^{+}$; Mucicarmine$^{+}$; CK-19$^{+}$; Pan-CK$^{+}$; Hep Par1$^{-}$ | A: All AKPP mice demonstrated abdominal distension accompanied by jaundice and weight loss, which recapitulates well those frequently observed in human iCCA; D: Short median survival | 77 |
| | Alb-Cre$^{ERT2}$ | Administered TAM at P10 | 2 months | iCCA | Mucin$^{+}$; CK-19$^{+}$; Pan-CK$^{+}$; Hep Par1$^{-}$ | A: Developed exclusive iCCA; iCCA originated from the cholangiocytes; D: The type of cell in which Cre-mediated recombination occurs varies with age | 77 |
| | SOX9-Cre$^{ERT2}$ | TAM | 12 weeks | iCCA, eCCA and pancreatic cancer | CK-19$^{+}$ | A: Short latency; developed pancreatic cancer, iCCA and eCCA using Cre-loxP under the control of SOX9 promotor, indicating that SOX9 had a potential role in hepatopancreatic ductal system and the intrapancreatic and intrahepatic ductal networks; provided a mouse model for study hepatopancreatic ductal carcinomas; D: Mixed liver cancer and pancreatic cancer, not exclusive iCCA; AKPP animals succumbed rapidly to ill-health, with a marked survival deficit | 78 |
| LSL-Kras$^{G12D}$; TP53$^{L/L}$ | Alb-Cre | – | 9 weeks | iCCA and HCC and cHCC-iCCA | Pan-CK$^{+}$; AFP$^{+}$ | A: Widespread local and distant metastasis; multistage progression; two of the most common gene mutations in human iCCA were involved; tumors arise from the malignant progression of precursor lesions in the bile ducts; D: A certain proportion of HCC is present, which may limit its application in iCCA research | 81 |
| | AAV8-TBG-Cre | DDC diet | 12–66 weeks | iCCA and HCC and cHCC-iCCA | Pan-CK$^{+}$, CK-19$^{+}$; Hnf 4α$^{-}$in iCCA; Hep Par1$^{+}$ in HCC | A: Full penetrance; tumor developed in the liver injury of ductular reaction, fibrosis, and inflammation similar to human liver cancer; D: Not exclusive iCCA | 83 |
| | SOX9-Cre$^{ERT2}$ | TAM; DDC diet | 30 weeks (average) postinjection | iCCA and HCC and cHCC-iCCA | Pan-CK$^{+}$; CK-19$^{+}$; Hnf 4α$^{-}$in iCCA | A: Full penetrance; tumor developed in the liver injury, fibrosis, and inflammation; adjacent liver to iCCA showed biliary intraepithelial neoplasia similar to precursor of human iCCA; D: Not exclusive iCCA | 83 |
| LSL-IDH2$^{R172K}$; LSL-Kras$^{G12D}$ | Alb-Cre | – | 33-58 weeks | iCCA | CK-19$^{+}$; Hep Par1$^{-}$ | A: Developed multifocal iCCA with peritoneal metastasis and splenic invasion; full penetrance; D: Long latency | 85 |

*(continued)*

**Table 2.** *(continued)*

| Genes targeted | Cre | Chemical induction | Latency | Tumor type | IHC | Comments (advantages/A; disadvantages/D) | Ref. |
|---|---|---|---|---|---|---|---|
| LSL-$Kras^{G12D}$; $TGFBR2^{L/L}$; $CDH1^{L/L}$ | $K19Cre^{ERT}$ | TAM; IL-33 | 20 days | eCCA | CK-$7^+$; CK-$19^+$; α-$SMA^+$ | A: Formed a model of biliary injury-related eCCA from EHBD; suggested PBGs as the cellular origin of eCCA; eCCA spread laterally along the biliary tree, and cancer cells were highly malignant and metastasized to the regional lymph nodes; periductal infiltrating growth and lymph node metastasis are characteristics of human eCCA; D: All $KTC-K19Cre^{ERT}$ mice died within 4 weeks after TAM administration | 89 |
| $TP53^{L/L}$ | – | CCL4 | 29 weeks | iCCA | CK-$19^+$ | A: The initiation and progression of iCCA in the setting of bile duct proliferation and associated fibrosis; developed lymph node metastasis; shares feature prominent in the human disease, including the presence of intrahepatic fibrosis, increased inflammation and a molecular profile; D: Long latency; penetrance is not high (54%) | 93 |
| | $Alb-Cre^{ERT}$ | TAM; TAA; | 26 weeks | CCA | NA | A: CCA arises following chronic inflammation caused by injury with TAA; developed multifocal invasive CCA; high penetrance (80%); D: Lack of detailed CCA subtype and phenotype identification results | 93 |

AFP, alpha-fetoprotein; AKPP mice, $Alb\text{-}Cre^+$; $LSL\text{-}Kras^{G12D}$; $PTEN^{L/L}$ mice; BECs, biliary epithelial cells; BNF/TAM, β-naphthoflavone and tamoxifen; CCL4, carbon tetrachloride; CDH1, a gene encoding E-cadherin molecule; cHCC-iCCA, combined hepatocellular carcinoma and intrahepatic cholangiocarcinoma; CK, cytokeratin; CK-19, cytokeratin 19; DDC, 3,5-diethoxycarbonyl-1,4-dihydrocollidin; EHBD, extra-hepatic bile duct; $K19Cre^{ERT}$, $Cre^{ERT}$ induced by TAM under the control of CK-19 promoter; NA, not available; Pan-CK, pan-cytokeratin; PBG, peribiliary gland; P10, postnatal day 10; SOX9: SRY-related high mobility group box transcription factor 9.

binase activity may be correlated with specific tumor type, as evidenced by the fact that TAM administration at 10 days of age induced Cre recombinase activity in hepatocytes and biliary cells, culminating in the intrahepatic cholangiocarcinogenesis, whereas administration on day 56 mediated genetic recombination only in hepatocytes, culminating in the formation of HCC and hepatocyte dysplasia, which also supports the conclusion that hepatocytes can serve as the cellular origin of iCCA. Based on the results obtained in the above models, Lin *et al*.[78] crossed mice expressing the $Kras^{G12D}$ allele and/or the *PTEN* allele with mice expressing Cre recombinase under the control of the *SOX9* gene and screened for $SOX9^+$; $Cre^{ERT2+}$; $LSL\text{-}Kras^{G12D}$; $PTEN^{L/L}$ ($S^+KPP$) mice. The model achieved *PTEN* deletion and *Kras* activation in the intrahepatic and extra-hepatic biliary epithelium and the pancreatic ductal epithelium, which eventually formed iCCA, eCCA, and pancreatic cancer, providing a platform for studying hepatopancreatic ductal carcinoma. Notably, $SOX9^+$ cells with deletion of the *PTEN* gene alone already have the potential to form HCC and iCCA using the same inducible Sox9-$Cre^{ERT}$-based approach,[79] indicating that loss of *PTEN* alone is sufficient to drive the transformation of $SOX9^+$ cells in the liver. In addition, a pancreatic and duodenal homeobox 1 promoter-driven Cre recombination system was used to mediate the knockout of *PTEN* or activation of $PIK3ca^{H1047R}$, a mutant of PI3K. Both were found to produce conditional GEMs of eCCA,[80] which faithfully recapitulates human eCCA and provides a novel platform for genome-wide mutagenesis screening.

### *Models combining $Kras^{G12D}$ activation with TP53 knockout*

The most common gene mutations in CCA are *Kras* and *TP53*.[6] In 2012, O'Dell *et al*.[81] established $Alb\text{-}Cre^+$; $Kras^{G12D}$; $TP53^{L/L}$ CCA models. Liver tumors formed as early as 9 weeks of age and were histopathologically confirmed to be 66% iCCA, 17% mixed HCC/iCCA, and 17% HCC. Most of the mice had symptoms of bloody ascites and tumor necrosis. In addition, 75% of the tumors invaded adjacent organs or developed distant metastases. It was also found that *TP53* gene deletion alone was not sufficient to cause liver lesions even over a sufficiently long time period. However, when combined with $Kras^{G12D}$ activation, both heterozygous and homozygous *TP53* mutations accelerated tumorigenesis and metastasis. Of note, a certain proportion of HCC was present in this model. To identify mechanisms driving precancerous lesions and subsequent progression toward invasive tumors that faithfully recapitulate human iCCA, a model that combined $Kras^{G12D}$ expression with a 3,5-diethoxycarbonyl-1,4-dihydrocollidine (DDC) diet had the potential to mimic multistep pathological changes of chronic cholangitis, ductular hyperplasia, cystic atypical hyperplasia, and eventually iCCA.[82] The model well represented the initiation and evolution of iCCA precursor lesions. When combined $Kras^{G12D}$ activation with *TP53* deletion in liver, the mice formed mixed HCC/iCCA. Notably, the cells of tumor origin differed with different promoters. For example, Cre-mediated $Kras^{G12D}$ activation and *TP53* deletion driven by the thyroid-binding globulin promoter in mice could result in mature hepatocyte-derived cHCC/iCCA, while the same genetic alterations driven by the SOX9 promoter eventually led to HCC/iCCA of biliary lineage origin.[83]

### *Models combining Kras activation and IDH2 mutation*

*IDH 1/2* mutations have been found in approximately 20% of iCCA cases.[84] $Alb\text{-}Cre^+$; $LSL\text{-}IDH2^{R172K}$; $LSL\text{-}Kras^{G12D}$ mice formed multifocal and palpable CK-$19^+$, Hep $Par1^-$

iCCA lesions at 33–58 weeks of age with peritoneal metastases and splenic invasion, whereas mice with *Kras*$^{G12D}$ activation alone formed single HCC nodules.[85] Mechanistically, mutant *IDH* inhibited the differentiation of hepatic progenitor cells in the liver after hepatocyte nuclear factor 4α inactivation, thus promoting iCCA formation. Because of the high mutation rate of *IDH* in tumors and the relatively mature clinical studies of *IDH* inhibitors,[86] the model is of great significance for the direct evaluation of therapeutic response to anti-iCCA agents. However, the model has a relatively long incubation period.

### *Models combining Kras activation with TGF-βR2 and CDH1 inactivation*

*FGFR2* gene fusions are seen in 13–45% of iCCA patients,[87,88] and frequent abnormal changes in TGF-β family receptors have been detected in eCCA by NGS.[6] Nakagawa *et al*.[89] first knocked Cre$^{ERT}$ into the endogenous K19 locus to obtain K19Cre$^{ERT}$ mice with TAM administration. Effective genetic recombination was confirmed with reporter mice. Then, *K19Cre*$^{ERT}$; *LSL-Kras*$^{G12D}$; *TGFβR2*$^{L/L}$ mice (KT-K19Cre$^{ERT}$) were generated by crossing *LSL-Kras*$^{G12D}$, *TGFβR2*$^{L/L}$ and *K19Cre*$^{ERT}$ mice and induced with TAM. All (15/15) *KT-K19Cre*$^{ERT}$ mice died of respiratory failure, which was probably caused by lung adenocarcinoma. *CDH1* gene deletion has been shown to promote liver tumor development in mice[90] and to lead to a series of pathological changes similar to those of primary sclerosing cholangitis in human. These mice showed an increased ductular reaction after 7 months of a high-fat diet (HFD).[91] HFDs cause nonalcoholic fatty liver disease,[92] and HFD-related models are a good tool for the study of the pathogenesis of iCCA in the context of chronic liver damage. HFDs also promote the initiation and deterioration of cHCC/iCCA in *CDH1*$^{L/L}$/*KRAS*$^{G12D}$ mice.[91] By crossing *KT-K19Cre*$^{ERT}$ and *CDH1*$^{L/L}$ mice with *Kras*$^{G12D}$ mice, Nakagawa *et al*.[89] established a *KTC-K19Cre*$^{ERT}$ mouse model characterized by *CDH1/TGFβR2* dual knockout and *Kras* activation, in which the pathological manifestations were histologically similar to human eCCA, with jaundice and lymph node metastases, but no bile duct tumors were observed with alterations in any of the aforementioned genes. However, the mice developed lung adenocarcinomas, leading to lung failure or death within 4 weeks, which is not suitable for long-term experimental studies.

### *Models combining TP53 deficiency with carcinogens*

A common limitation of transgenic CCA models is that the tumor initiation and formation do not involve chronic inflammation and liver injury, which limits the aggressive development of tumors. The exposure of transgenic mice to carcinogens can compensate for the lack of an inflammatory background in transgenic models. Intraperitoneal injection of transgenic mice with *TP53* deletions with $CCL_4$ three times a week for 4 months resulted in 54% of *TP53*$^{L/L}$ mice developing iCCA, and approximately 14% (1/7) mice developing lymph node metastasis at 29 weeks of age.[93] Using a similar approach, Guest *et al*.[94] fed hepatotoxic TAA to biliary epithelium-specific *TP53*-knockout transgenic mice in an attempt to induce a tumorigenic stress response. After 26 weeks, 80% of *TP53*$^{L/L}$ mice developed multifocal, invasive CCA in the liver.

### *Notch models*

Aberrant Notch activation can activate Notch 1 intracellular domain (NICD), which has been implicated in a variety of tumors.[95] The pathophysiological role of the Notch signaling pathway has been partially elucidated in CCA GEMs. For example, *Alb-Cre:: NICD* transgenic mice generated by crossing mice carrying a sequence encoding NICD overexpression with Cre mice activates the Notch signaling pathway, making mature hepatocytes transdifferentiate into biliary epithelial cells.[96] Implanting liver tissue from 9-month-old transgenic mice subcutaneously into SCID mice results in the formation of iCCA after 3 weeks.[97] Biliary tract malignancies are often accompanied by elevated levels of phosphorylated AKT.[69] Cellular fate-tracing results have shown that overexpression of *NICD* combined with *AKT* leads to the development of iCCA originating from hepatocytes.[98] Cirrhosis, chronic hepatitis B and C, and liver fluke infection are major risk factors for iCCA, which is often accompanied by chronic liver inflammation. In this context, iCCA has a high rate of *TP53* gene mutation.[99] In the basis of liver injury by TAA administration, *TP53*$^{L/L}$ transgenic mice develop iCCA originating from biliary epithelium.[100] This model mimics a common situation in human cholangiocarcinogenesis.

## Nonconditional GEMs

Nonconditional GEMs are usually established by local injection in the liver or bile duct and transposon- or duct-specific promoter-mediated constitutive activation of oncogenes. Transposons can carry relatively large exogenous gene fragments for efficient transposition in animals and are important tools in the field of transgenic animal modeling, of which a relatively commonly used one is the Sleeping Beauty transposon. Currently, several iCCA models have been constructed based on that system.

Phosphorylated AKT was found to be upregulated in eCCA.[101] Similar to AKT, Yes-associated protein (YAP) is a transcriptional activator associated with primary liver cancer development.[102] The method used to establish AKT/YAP models was to directly inject a transposase mixture containing *AKT/YAP* plasmids into the bile duct of wild-type C57BL/6 mice while ligating the bile draining duct so that the targeted oncogene remained in the left lobe of the liver. The mitogen IL-33, which has the ability to promote bile duct cell proliferation, inflammation, and liver fibrosis, was continuously injected intraperitoneally for 3 days after surgery, and its effect had been confirmed in previous studies.[103] Seventy-two percent of mice transduced with the *AKT/YAP* gene and treated with IL-33 developed tumors that had a morphology and phenotype similar to human CCA, accompanied by high expression of the cholangiocyte markers CK-7, CK-19, and SOX9. Only 20% of mice transduced with the *AKT/YAP* gene alone developed iCCA, indicating that IL-33 plays an important role in iCCA formation. However, knockout of focal adhesion kinase (*FAK*), a nonreceptor tyrosine kinase, in *AKT/YAP* mice delayed iCCA development and progression.[104] Wang *et al*.[105] used the same gene delivery technique to target liver with exogenous co-expression of *myr-AKT* and *Fbxw7F*, a dominant negative form of the tumor suppressor *Fbxw7*, and found the development of iCCA in *YAP* wild-type mice within a short time of approximately 54 day. In *YAP* homozygous deleted mice, the tumor latency was significantly prolonged. Using the same methods, histone lysine methyltransferase G9a, and NICD have been demonstrated to be involved in cholangiocarcinogenesis.[106,107] This model develops tumors quickly and can be used to study new therapeutic drugs for iCCA. However, it is technically demanding because it requires surgical ligation of the bile ducts and bile duct perfusion with drugs.

In addition to tail vein injection, electroporation can be used to introduce exogenous DNA into cells. However, different models of gene introduction have been found to have

different effects on the type of tumor that develops. For example, delivery of plasmids containing *Myc* and mutant *NRAS* proto-oncogene or *AKT1* via tail vein injection induces HCC, whereas transfection of the same plasmids by electroporation induces iCCA formation.[108] That indicates that the tumor microenvironment plays an important role in the development of CCA, and gene overexpression based on gene transduction modalities interact with the tumor microenvironment. Bovine protein 5 is a promoter that is actively expressed in both the stratified and pseudostratified epithelia of several organs, and is an important tool for constructing animal models of gene overexpression. A mouse model overexpressing wild-type erb-b2 receptor tyrosine kinase 2 under the control of the Bovine protein 5 promoter has been modeled, and all of these mice developed gallbladder adenocarcinoma at 4 months of age.[109] The model recapitulates the multistep evolution of gallbladder lesions.

Recently, clustered regularly interspaced short palindromic repeats (CRISPR)/CRISPR associated protein 9 (Cas9) system, a new somatic gene editing technology, has been developed to mediate highly specific and irreversible genomic screening. An advantage of the technique is that genome-wide screening identifies several novel genes associated with tumorigenesis. For example, Weber *et al*.[110] used the method to directly mediate multiple genetic mutations of up to 18 target gene sets in adult mouse liver somatic cells, and found that 100% of mice developed mixed HCC/iCCA after 20–30 weeks. CCA mouse models have also been established either via CRISPR/Cas9-mediated knockout of *Nf1*,[111] or through CRISPR/Cas9 system-based *KRAS*$^{G12D}$ activation and *TP53* deletion.[112] Notably, the latency period of iCCA in the latter was significantly shorter than that in the comparable conditional GEMs model.[112] Dasatinib sensitivity was tested in CRISPR/Cas9-mediated human iCCA cells with *IDH* mutation.[113]

Taken together, somatic gene integration models, especially those based on hydrodynamic injection and Sleeping Beauty transposon, are flexible, relatively easy to establish and have a short tumorigenic latency, therefore they are important tools to study gene and promoter functions. However, target gene transfection is mainly limited to the pericentral region and only lasts for a few hours to days.[114] Hydrodynamic delivery can also cause transient liver damage. In the meantime, because mutations are present in cancers in adult human cancers and affect only a small number of cells, CRISPR/Cas9-based models are more responsive to tumorigenesis in humans.

## Conclusions

There is no perfect animal model that meets all the needs of human CCA research. Choosing the right animal model for each experimental purpose is key. Multiple parameters such as tumor type, host immune activity, genetic alterations, and the tumor microenvironment, should be considered to weigh the advantages and disadvantages when selecting a model. For example, chemical-mechanical and infection-induced inflammatory models can simulate the entire process of tumor development by changing environmental factors, but an obvious shortcoming is the poor specificity of the tumors that develop, which may include tumors of multiple systems. Implantation models are easy to establish, but the tumors grow in immunodeficient animals, which makes it difficult to truly reflect the growth of human tumors. In contrast, GEMs can simulate the initiation of CCA at the genetic and molecular level, but available models using Alb-driven Cre-loxP system usually induce iCCA or a mixture of iCCA and HCC. Moreover, the latency period is long, the technology is demanding, and it is difficult to develop a system where the transgenic products fully and accurately reflect the growth of human tumors.

With the development of targeted therapy and immunotherapy, PDX models and GEMs are playing key roles in precision medicine. Humanized PDX models have benefits in immunotherapy drug screening in malignancies, such as nasopharyngeal carcinoma[115] and triple-negative breast cancer.[116] They also recapitulate the interactions of cancer, the tumor microenvironment, and the immune system in humans. Efforts should be made to develop humanized PDX models of all CCA subtypes to promote the development of individualized immunotherapy in the future. Simultaneously, there has been an active search for promoters that specifically target intrahepatic or extra-hepatic bile duct cells. Optimization of existing genetic recombination systems is a promising option. In addition, flexible CRISPR/Cas9 gene editing technique may be another favorable choice. Ongoing optimization of preclinical animal models through the integration of various technologies will contribute to rapid translation from bench to bedside.

## Funding

This work was supported by the Outstanding Young Talents Program in Higher Education Institutions of Anhui Province (No. gxfx2017066), the 512 Talent Cultivation Plan of Bengbu Medical College (No. by51202208), and the internal grants from both Distinguished Young Scholars Science Foundation (No. 2019byyfyjq02) and General New Technology Project (No. 2020144) of the First Affiliated Hospital of Bengbu Medical College. Baoan Ji is supported by the NCI-funded Mayo Clinic SPORE in Hepatobiliary Cancer (P50 CA210964).

## Conflict of interest

The authors have no conflict of interests related to this publication.

## Author contributions

Conceived the work, designed the outline of the review and supervised all aspects of the manuscript (YY); Participated in the literature search, scrutiny and interpretation, as well as in writing and editing the manuscript (ML, XZ, WW, YS, QD, JY); Contributed to review of the data and critical revision of the review (BJ). All authors read and approved the final manuscript.

## References

[1] Khan SA, Genus T, Morement H, Murphy A, Rous B, Tataru D. Global trends in mortality from intrahepatic and extrahepatic cholangiocarcinoma. J Hepatol 2019;71(6):1261–1262. doi:10.1016/j.jhep.2019.07.024, PMID:31558288.
[2] Banales JM, Marin JJG, Lamarca A, Rodrigues PM, Khan SA, Roberts LR, *et al*. Cholangiocarcinoma 2020: the next horizon in mechanisms and management. Nat Rev Gastroenterol Hepatol 2020;17(9):557–588. doi:10.1038/s41575-020-0310-z, PMID:32606456.
[3] Vicent S, Lieshout R, Saborowski A, Verstegen MMA, Raggi C, Recalcati S, *et al*. Experimental models to unravel the molecular pathogenesis, cell of origin and stem cell properties of cholangiocarcinoma. Liver Int 2019;39(Suppl 1):S79–S97. doi:10.1111/liv.14094, PMID:30851232.
[4] Rizvi S, Khan SA, Hallemeier CL, Kelley RK, Gores GJ. Cholangiocarcinoma - evolving concepts and therapeutic strategies. Nat Rev Clin Oncol 2018;15(2):95–111. doi:10.1038/nrclinonc.2017.157, PMID:28994423.
[5] Rizzo A, Ricci AD, Brandi G. Recent advances of immunotherapy for biliary tract cancer. Expert Rev Gastroenterol Hepatol 2021;15(5):527–536. doi:10.1080/17474124.2021.1853527, PMID:33215952.
[6] Nakamura H, Arai Y, Totoki Y, Shirota T, Elzawahry A, Kato M, *et al*. Genomic spectra of biliary tract cancer. Nat Genet 2015;47(9):1003–1010. doi:10.1038/ng.3375, PMID:26258846.

[7] Valle JW, Lamarca A, Goyal L, Barriuso J, Zhu AX. New Horizons for Precision Medicine in Biliary Tract Cancers. Cancer Discov 2017;7(9):943–962. doi:10.1158/2159-8290.Cd-17-0245, PMID:28818953.

[8] Wardell CP, Fujita M, Yamada T, Simbolo M, Fassan M, Karlic R, *et al*. Genomic characterization of biliary tract cancers identifies driver genes and predisposing mutations. J Hepatol 2018;68(5):959–969. doi:10.1016/j.jhep.2018.01.009, PMID:29360550.

[9] Montal R, Sia D, Montironi C, Leow WQ, Esteban-Fabró R, Pinyol R, *et al*. Molecular classification and therapeutic targets in extrahepatic cholangiocarcinoma. J Hepatol 2020;73(2):315–327. doi:10.1016/j.jhep.2020.03.008, PMID:32173382.

[10] Bekaii-Saab TS, Bridgewater J, Normanno N. Practical considerations in screening for genetic alterations in cholangiocarcinoma. Ann Oncol 2021;32(9):1111–1126. doi:10.1016/j.annonc.2021.04.012, PMID:33932504.

[11] Cadamuro M, Brivio S, Stecca T, Kaffe E, Mariotti V, Milani C, *et al*. Animal models of cholangiocarcinoma: What they teach us about the human disease. Clin Res Hepatol Gastroenterol 2018;42(5):403–415. doi:10.1016/j.clinre.2018.04.008, PMID:29753731.

[12] Loeuillard E, Fischbach SR, Gores GJ, Rizvi S. Animal models of cholangiocarcinoma. Biochim Biophys Acta Mol Basis Dis 2019;1865(5):982–992. doi:10.1016/j.bbadis.2018.03.026, PMID:29627364.

[13] Mohr R, Özdirik B, Knorr J, Wree A, Demir M, Tacke F, *et al*. In Vivo Models for Cholangiocarcinoma-What Can We Learn for Human Disease? Int J Mol Sci 2020;21(14):4993. doi:10.3390/ijms21144993, PMID:32679791.

[14] Massa A, Varamo C, Vita F, Tavolari S, Peraldo-Neia C, Brandi G, *et al*. Evolution of the Experimental Models of Cholangiocarcinoma. Cancers (Basel) 2020;12(8):2308. doi:10.3390/cancers12082308, PMID:32824407.

[15] Izumiya M, Kato S, Hippo Y. Recent Advances in Implantation-Based Genetic Modeling of Biliary Carcinogenesis in Mice. Cancers (Basel) 2021;13(10):2292. doi:10.3390/cancers13102292, PMID:34064809.

[16] Williams GM. Chemicals with carcinogenic activity in the rodent liver; mechanistic evaluation of human risk. Cancer Lett 1997;117(2):175–188. doi:10.1016/s0304-3835(97)00229-2, PMID:9377545.

[17] Burka LT, Washburn KD, Irwin RD. Disposition of [14C] furan in the male F344 rat. J Toxicol Environ Health 1991;34(2):245–257. doi:10.1080/15287399109531564, PMID:1920528.

[18] Maronpot RR, Giles HD, Dykes DJ, Irwin RD. Furan-induced hepatic cholangiocarcinomas in Fischer 344 rats. Toxicol Pathol 1991;19(4 Pt 2):561–570. doi:10.1177/019262339101900401, PMID:1668599.

[19] Elmore LW, Sirica AE. Phenotypic characterization of metaplastic intestinal glands and ductular hepatocytes in cholangiofibrotic lesions rapidly induced in the caudate liver lobe of rats treated with furan. Cancer Res 1991;51(20):5752–5759. PMID:1655260.

[20] Hickling KC, Hitchcock JM, Chipman JK, Hammond TG, Evans JG. Induction and progression of cholangiofibrosis in rat liver injured by oral administration of furan. Toxicol Pathol 2010;38(2):213–229. doi:10.1177/0192623309357945, PMID:20231548.

[21] Von Tungeln LS, Walker NJ, Olson GR, Mendoza MC, Felton RP, Thorn BT, *et al*. Low dose assessment of the carcinogenicity of furan in male F344/N Nctr rats in a 2-year gavage study. Food Chem Toxicol 2017;99:170–181. doi:10.1016/j.fct.2016.11.015, PMID:27871980.

[22] Praet MM, Roels HJ. Histogenesis of cholangiomas and cholangiocarcinomas in thioacetamide fed rats. Exp Pathol 1984;26(1):3–14. doi:10.1016/s0232-1513(84)80063-8, PMID:6207043.

[23] Yeh CN, Maitra A, Lee KF, Jan YY, Chen MF. Thioacetamide-induced intestinal-type cholangiocarcinoma in rat: an animal model recapitulating the multi-stage progression of human cholangiocarcinoma. Carcinogenesis 2004;25(4):631–636. doi:10.1093/carcin/bgh037, PMID:14656942.

[24] Al-Bader A, Mathew TC, Abul H, Al-Sayer H, Singal PK, Dashti HM. Cholangiocarcinoma and liver cirrhosis in relation to changes due to thioacetamide. Mol Cell Biochem 2000;208(1-2):1–10. doi:10.1023/a:1007082515548, PMID:10939622.

[25] Pan YR, Wu CE, Chen MH, Huang WK, Shih HJ, Lan KL, *et al*. Comprehensive Evaluation of Immune-Checkpoint DNA Cancer Vaccines in a Rat Cholangiocarcinoma Model. Vaccines (Basel) 2020;8(4):703. doi:10.3390/vaccines8040703, PMID:33255375.

[26] Fujii Y, Segawa R, Kimura M, Wang L, Ishii Y, Yamamoto R, *et al*. Inhibitory effect of α-lipoic acid on thioacetamide-induced tumor promotion through suppression of inflammatory cell responses in a two-stage hepatocarcinogenesis model in rats. Chem Biol Interact 2013;205(2):108–118. doi:10.1016/j.cbi.2013.06.017, PMID:23830814.

[27] Romualdo GR, Grassi TF, Goto RL, Tablas MB, Bidinotto LT, Fernandes AAH, *et al*. An integrative analysis of chemically-induced cirrhosis-associated hepatocarcinogenesis: Histological, biochemical and molecular features. Toxicol Lett 2017;281:84–94. doi:10.1016/j.toxlet.2017.09.015, PMID:28943392.

[28] Bridgewater J, Galle PR, Khan SA, Llovet JM, Park JW, Patel T, *et al*. Guidelines for the diagnosis and management of intrahepatic cholangiocarcinoma. J Hepatol 2014;60(6):1268–1289. doi:10.1016/j.jhep.2014.01.021, PMID:24681130.

[29] Dietrich CG, Geier A, Wasmuth HE, Matern S, Gartung C, de Waart DR, *et al*. Influence of biliary cirrhosis on the detoxification and elimination of a food derived carcinogen. Gut 2004;53(12):1850–1855. doi:10.1136/gut.2003.037507, PMID:15542527.

[30] Lozano E, Sanchez-Vicente L, Monte MJ, Herraez E, Briz O, Banales JM, *et al*. Cocarcinogenic effects of intrahepatic bile acid accumulation in cholangiocarcinoma development. Mol Cancer Res 2014;12(1):91–100. doi:10.1158/1541-7786.Mcr-13-0503, PMID:24255171.

[31] Thamavit W, Pairojkul C, Tiwawech D, Itoh M, Shirai T, Ito N. Promotion of cholangiocarcinogenesis in the hamster liver by bile duct ligation after dimethylnitrosamine initiation. Carcinogenesis 1993;14(11):2415–2417. doi:10.1093/carcin/14.11.2415, PMID:8242874.

[32] Liu T, Yang H, Fan W, Tu J, Li TWH, Wang J, *et al*. Mechanisms of MAFG Dysregulation in Cholestatic Liver Injury and Development of Liver Cancer. Gastroenterology 2018;155(2):557–571.e514. doi:10.1053/j.gastro.2018.04.032, PMID:29733835.

[33] Yang H, Li TW, Peng J, Tang X, Ko KS, Xia M, *et al*. A mouse model of cholestasis-associated cholangiocarcinoma and transcription factors involved in progression. Gastroenterology 2011;141(1):378–388.e4. doi:10.1053/j.gastro.2011.03.044, PMID:21440549.

[34] Thamavit W, Bhamarapravati N, Sahaphong S, Vajrasthira S, Angsubhakorn S. Effects of dimethylnitrosamine on induction of cholangiocarcinoma in Opisthorchis viverrini-infected Syrian golden hamsters. Cancer Res 1978;38(12):4634–4639. PMID:214229.

[35] Loilome W, Yongvanit P, Wongkham C, Tepsiri N, Sripa B, Sithithaworn P, *et al*. Altered gene expression in Opisthorchis viverrini-associated cholangiocarcinoma in hamster model. Mol Carcinog 2006;45(5):279–287. doi:10.1002/mc.20094, PMID:16550611.

[36] Upontain S, Sereerak P, Laha T, Sripa B, Tangkawatana P, Brindley PJ, *et al*. Granulin Expression in Hamsters during Opisthorchis viverrini Infection-Induced Cholangiocarcinogenesis. Asian Pac J Cancer Prev 2018;19(9):2437–2445. doi:10.22034/apjcp.2018.19.9.2437, PMID:30255697.

[37] Suksawat M, Techasen A, Namwat N, Yongvanit P, Khuntikeo N, Titapun A, *et al*. Upregulation of endothelial nitric oxide synthase (eNOS) and its upstream regulators in Opisthorchis viverrini associated cholangiocarcinoma and its clinical significance. Parasitol Int 2017;66(4):486–493. doi:10.1016/j.parint.2016.04.008, PMID:27143607.

[38] Laothong U, Pinlaor P, Boonsiri P, Pairojkul C, Priprem A, Johns NP, *et al*. Melatonin inhibits cholangiocarcinoma and reduces liver injury in Opisthorchis viverrini-infected and N-nitrosodimethylamine-treated hamsters. J Pineal Res 2013;55(3):257–266. doi:10.1111/jpi.12068, PMID:23772655.

[39] Rizvi S, Fischbach SR, Bronk SF, Hirsova P, Krishnan A, Dhanasekaran R, *et al*. YAP-associated chromosomal instability and cholangiocarcinoma in mice. Oncotarget 2018;9(5):5892–5905. doi:10.18632/oncotarget.23638, PMID:29464042.

[40] Sirica AE, Zhang Z, Lai GH, Asano T, Shen XN, Ward DJ, *et al*. A novel "patient-like" model of cholangiocarcinoma progression based on bile duct inoculation of tumorigenic rat cholangiocyte cell lines. Hepatology 2008;47(4):1178–1190. doi:10.1002/hep.22088, PMID:18081149.

[41] Mertens JC, Fingas CD, Christensen JD, Smoot RL, Bronk SF, Werneburg NW, *et al*. Therapeutic effects of deleting cancer-associated fibroblasts in cholangiocarcinoma. Cancer Res 2013;73(2):897–907. doi:10.1158/0008-5472.Can-12-2130, PMID:23221385.

[42] Fingas CD, Mertens JC, Razumilava N, Bronk SF, Sirica AE, Gores GJ. Targeting PDGFR-β in Cholangiocarcinoma. Liver Int 2012;32(3):400–409. doi:10.1111/j.1478-3231.2011.02687.x, PMID:22133064.

[43] Blechacz BR, Smoot RL, Bronk SF, Werneburg NW, Sirica AE, Gores GJ. Sorafenib inhibits signal transducer and activator of transcription-3 signaling in cholangiocarcinoma cells by activating the phosphatase shatterproof 2. Hepatology 2009;50(6):1861–1870. doi:10.1002/hep.23214, PMID:19821497.

[44] Razumilava N, Gradilone SA, Smoot RL, Mertens JC, Bronk SF, Sirica AE, *et al*. Non-canonical Hedgehog signaling contributes to chemotaxis in cholangiocarcinoma. J Hepatol 2014;60(3):599–605. doi:10.1016/j.jhep.2013.11.005, PMID:24239776.

[45] De Minicis S, Kisseleva T, Francis H, Baroni GS, Benedetti A, Brenner D, *et al*. Liver carcinogenesis: rodent models of hepatocarcinoma and cholangiocarcinoma. Dig Liver Dis 2013;45(6):450–459. doi:10.1016/j.dld.2012.10.008, PMID:23177172.

[46] Hudd C, Euhus DM, LaRegina MC, Herbold DR, Palmer DC, Johnson FE. Effect of cholecystokinin on human cholangiocarcinoma xenografted into nude mice. Cancer Res 1985;45(3):1372–1377. PMID:2982488.

[47] Bai X, Zhang H, Zhou Y, Nagaoka K, Meng J, Ji C, *et al*. Ten-Eleven Translocation 1 Promotes Malignant Progression of Cholangiocarcinoma With Wild-Type Isocitrate Dehydrogenase 1. Hepatology 2021;73(5):1747–1763. doi:10.1002/hep.31486, PMID:32740973.

[48] Zhu H, Han C, Lu D, Wu T. miR-17-92 cluster promotes cholangiocarcinoma growth: evidence for PTEN as downstream target and IL-6/Stat3 as upstream activator. Am J Pathol 2014;184(10):2828–2839. doi:10.1016/j.ajpath.2014.06.024, PMID:25239565.

[49] Lin Y, Cai Q, Chen Y, Shi T, Liu W, Mao L, *et al*. CAFs shape myeloid-derived suppressor cells to promote stemness of intrahepatic cholangiocarcinoma via 5-lipoxygenase. Hepatology 2022;75(1):28–42. doi:10.1002/hep.32099, PMID:34387870.

[50] McVeigh LE, Wijetunga I, Ingram N, Marston G, Prasad R, Markham AF, *et al*. Development of orthotopic tumour models using ultrasound-guided intrahepatic injection. Sci Rep 2019;9(1):9904. doi:10.1038/s41598-019-46410-6, PMID:31289364.

[51] Cavalloni G, Peraldo-Neia C, Sassi F, Chiorino G, Sarotto I, Aglietta M, *et al*. Establishment of a patient-derived intrahepatic cholangiocarcinoma xenograft model with KRAS mutation. BMC Cancer 2016;16:90. doi:10.1186/s12885-016-2136-1, PMID:26868125.

[52] Wang Y, Ding X, Wang S, Moser CD, Shaleh HM, Mohamed EA, *et al*. Antitumor effect of FGFR inhibitors on a novel cholangiocarcinoma patient derived xenograft mouse model endogenously expressing an FGFR2-CCDC6 fusion protein. Cancer Lett 2016;380(1):163–173. doi:10.1016/j.canlet.2016.05.017, PMID:27216979.

[53] Lixin S, Wei S, Haibin S, Qingfu L, Tiemin P. miR-885-5p inhibits proliferation and metastasis by targeting IGF2BP1 and GALNT3 in human intrahepatic cholangiocarcinoma. Mol Carcinog 2020;59(12):1371–1381. doi:10.1002/mc.23262, PMID:33052627.

[54] Gao J, Dai C, Yu X, Yin XB, Zhou F. Upregulated microRNA-194 impairs

stemness of cholangiocarcinoma cells through the Rho pathway via inhibition of ECT2. J Cell Biochem 2020;121(10):4239–4250. doi:10.1002/jcb.29648, PMID:31960990.
[55] Li F, Chen Q, Xue H, Zhang L, Wang K, Shen F. LncRNA MNX1-AS1 promotes progression of intrahepatic cholangiocarcinoma through the MNX1/Hippo axis. Cell Death Dis 2020;11(10):894. doi:10.1038/s41419-020-03029-0, PMID:33093444.
[56] Yu A, Zhao L, Kang Q, Li J, Chen K, Fu H. SOX2 knockdown slows cholangiocarcinoma progression through inhibition of transcriptional activation of lncRNA PVT1. Biochem J 2020;477(18):3527–3540. doi:10.1042/bcj20200219, PMID:32812642.
[57] Pan X, Wang G, Wang B. MicroRNA-1182 and let-7a exert synergistic inhibition on invasion, migration and autophagy of cholangiocarcinoma cells through down-regulation of NUAK1. Cancer Cell Int 2021;21(1):161. doi:10.1186/s12935-021-01797-z, PMID:33750398.
[58] He C, Xia J, Gao Y, Chen Z, Wan X. Chlorin A-mediated photodynamic therapy induced apoptosis in human cholangiocarcinoma cells via impaired autophagy flux. Am J Transl Res 2020;12(9):5080–5094. PMID:33042407.
[59] Blanquart C, Jaurand MC, Jean D. The Biology of Malignant Mesothelioma and the Relevance of Preclinical Models. Front Oncol 2020;10:388. doi:10.3389/fonc.2020.00388, PMID:32269966.
[60] Kung AL. Practices and pitfalls of mouse cancer models in drug discovery. Adv Cancer Res 2007;96:191–212. doi:10.1016/s0065-230x(06)96007-2, PMID:17161681.
[61] Vaeteewoottacharn K, Pairojkul C, Kariya R, Muisuk K, Imtawil K, Chamgramol Y, *et al*. Establishment of Highly Transplantable Cholangiocarcinoma Cell Lines from a Patient-Derived Xenograft Mouse Model. Cells 2019;8(5):496. doi:10.3390/cells8050496, PMID:31126020.
[62] Hernandez MC, Bergquist JR, Leiting JL, Ivanics T, Yang L, Smoot RL, *et al*. Patient-Derived Xenografts Can Be Reliably Generated from Patient Clinical Biopsy Specimens. J Gastrointest Surg 2019;23(4):818–824. doi:10.1007/s11605-019-04109-z, PMID:30756315.
[63] Hernandez MC, Yang L, Leiting JL, Sugihara T, Bergquist JR, Ivanics T, *et al*. Successful Secondary Engraftment of Pancreatic Ductal Adenocarcinoma and Cholangiocarcinoma Patient-Derived Xenografts After Previous Failed Primary Engraftment. Transl Oncol 2019;12(1):69–75. doi:10.1016/j.tranon.2018.09.008, PMID:30273859.
[64] Walrath JC, Hawes JJ, Van Dyke T, Reilly KM. Genetically engineered mouse models in cancer research. Adv Cancer Res 2010;106:113–164. doi:10.1016/s0065-230x(10)06004-5, PMID:20399958.
[65] Pirenne S, Lemaigre FP. Genetically engineered animal models of biliary tract cancers. Curr Opin Gastroenterol 2020;36(2):90–98. doi:10.1097/mog.0000000000000610, PMID:31850929.
[66] Kos CH. Cre/loxP system for generating tissue-specific knockout mouse models. Nutr Rev 2004;62(6 Pt 1):243–246. doi:10.1301/nr2004.jun243-246, PMID:15291397.
[67] Postic C, Magnuson MA. DNA excision in liver by an albumin-Cre transgene occurs progressively with age. Genesis 2000;26(2):149–150. doi:10.1002/(sici)1526-968x(200002)26:2<149::aid-gene16>3.0.co;2-v, PMID:10686614.
[68] Kim H, Kim M, Im SK, Fang S. Mouse Cre-LoxP system: general principles to determine tissue-specific roles of target genes. Lab Anim Res 2018;34(4):147–159. doi:10.5625/lar.2018.34.4.147, PMID:30671100.
[69] Corti F, Nichetti F, Raimondi A, Niger M, Prinzi N, Torchio M, *et al*. Targeting the PI3K/AKT/mTOR pathway in biliary tract cancers: A review of current evidences and future perspectives. Cancer Treat Rev 2019;72:45–55. doi:10.1016/j.ctrv.2018.11.001, PMID:30476750.
[70] Chung JY, Hong SM, Choi BY, Cho H, Yu E, Hewitt SM. The expression of phospho-AKT, phospho-mTOR, and PTEN in extrahepatic cholangiocarcinoma. Clin Cancer Res 2009;15(2):660–667. doi:10.1158/1078-0432.Ccr-08-1084, PMID:19147772.
[71] Kang YK, Kim WH, Jang JJ. Expression of G1-S modulators (p53, p16, p27, cyclin D1, Rb) and Smad4/Dpc4 in intrahepatic cholangiocarcinoma. Hum Pathol 2002;33(9):877–883. doi:10.1053/hupa.2002.127444, PMID:12378511.
[72] Miyaki M, Kuroki T. Role of Smad4 (DPC4) inactivation in human cancer. Biochem Biophys Res Commun 2003;306(4):799–804. doi:10.1016/s0006-291x(03)01066-0, PMID:12821112.
[73] Xu X, Kobayashi S, Qiao W, Li C, Xiao C, Radaeva S, *et al*. Induction of intrahepatic cholangiocellular carcinoma by liver-specific disruption of Smad4 and Pten in mice. J Clin Invest 2006;116(7):1843–1852. doi:10.1172/jci27282, PMID:16767220.
[74] Horie Y, Suzuki A, Kataoka E, Sasaki T, Hamada K, Sasaki J, *et al*. Hepatocyte-specific Pten deficiency results in steatohepatitis and hepatocellular carcinomas. J Clin Invest 2004;113(12):1774–1783. doi:10.1172/jci20513, PMID:15199412.
[75] Zou S, Li J, Zhou H, Frech C, Jiang X, Chu JS, *et al*. Mutational landscape of intrahepatic cholangiocarcinoma. Nat Commun 2014;5:5696. doi:10.1038/ncomms6696, PMID:25526346.
[76] Marsh V, Davies EJ, Williams GT, Clarke AR. PTEN loss and KRAS activation cooperate in murine biliary tract malignancies. J Pathol 2013;230(2):165–173. doi:10.1002/path.4189, PMID:23483557.
[77] Ikenoue T, Terakado Y, Nakagawa H, Hikiba Y, Fujii T, Matsubara D, *et al*. A novel mouse model of intrahepatic cholangiocarcinoma induced by liver-specific Kras activation and Pten deletion. Sci Rep 2016;6:23899. doi:10.1038/srep23899, PMID:27032374.
[78] Lin YK, Fang Z, Jiang TY, Wan ZH, Pan YF, Ma YH, *et al*. Combination of Kras activation and PTEN deletion contributes to murine hepatopancreatic ductal malignancy. Cancer Lett 2018;421:161–169. doi:10.1016/j.canlet.2018.02.017, PMID:29452147.
[79] Chen J, Debebe A, Zeng N, Kopp J, He L, Sander M, *et al*. Transformation of SOX9(+) cells by Pten deletion synergizes with steatotic liver injury to drive development of hepatocellular and cholangiocarcinoma. Sci Rep 2021;11(1):11823. doi:10.1038/s41598-021-90958-1, PMID:34083580.
[80] Falcomata C, Barthel S, Ulrich A, Diersch S, Veltkamp C, Rad L, *et al*. Genetic screens identify a context-specific PI3K/p27Kip1 node driving extrahepatic biliary cancer. Cancer Discov 2021;11(12):3158–3177. doi:10.1158/2159-8290.Cd-21-0209, PMID:34282029.
[81] O'Dell MR, Huang JL, Whitney-Miller CL, Deshpande V, Rothberg P, Grose V, *et al*. Kras(G12D) and p53 mutation cause primary intrahepatic cholangiocarcinoma. Cancer Res 2012;72(6):1557–1567. doi:10.1158/0008-5472.Can-11-3596, PMID:22266220.
[82] Di-Luoffo M, Pirenne S, Saandi T, Loriot A, Gérard C, Dauguet N, *et al*. A novel mouse model of cholangiocarcinoma uncovers a role for Tensin-4 in tumor progression. Hepatology 2021;74(3):1445–1460. doi:10.1002/hep.31834, PMID:33768568.
[83] Hill MA, Alexander WB, Guo B, Kato Y, Patra K, O'Dell MR, *et al*. Kras and Tp53 Mutations Cause Cholangiocyte- and Hepatocyte-Derived Cholangiocarcinoma. Cancer Res 2018;78(16):4445–4451. doi:10.1158/0008-5472.Can-17-1123, PMID:29871934.
[84] Fujiwara H, Tateishi K, Kato H, Nakatsuka T, Yamamoto K, Tanaka Y, *et al*. Isocitrate dehydrogenase 1 mutation sensitizes intrahepatic cholangiocarcinoma to the BET inhibitor JQ1. Cancer Sci 2018;109(11):3602–3610. doi:10.1111/cas.13784, PMID:30156013.
[85] Saha SK, Parachoniak CA, Ghanta KS, Fitamant J, Ross KN, Najem MS, *et al*. Mutant IDH inhibits HNF-4α to block hepatocyte differentiation and promote biliary cancer. Nature 2014;513(7516):110–114. doi:10.1038/nature13441, PMID:25043045.
[86] Rohle D, Popovici-Muller J, Palaskas N, Turcan S, Grommes C, Campos C, *et al*. An inhibitor of mutant IDH1 delays growth and promotes differentiation of glioma cells. Science 2013;340(6132):626–630. doi:10.1126/science.1236062, PMID:23558169.
[87] Sia D, Losic B, Moeini A, Cabellos L, Hao K, Revill K, *et al*. Massive parallel sequencing uncovers actionable FGFR2-PPHLN1 fusion and ARAF mutations in intrahepatic cholangiocarcinoma. Nat Commun 2015;6:6087. doi:10.1038/ncomms7087, PMID:25608663.
[88] Rizvi S, Yamada D, Hirsova P, Bronk SF, Werneburg NW, Krishnan A, *et al*. A Hippo and Fibroblast Growth Factor Receptor Autocrine Pathway in Cholangiocarcinoma. J Biol Chem 2016;291(15):8031–8047. doi:10.1074/jbc.M115.698472, PMID:26826125.
[89] Nakagawa H, Suzuki N, Hirata Y, Hikiba Y, Hayakawa Y, Kinoshita H, *et al*. Biliary epithelial injury-induced regenerative response by IL-33 promotes cholangiocarcinogenesis from peribiliary glands. Proc Natl Acad Sci U S A 2017;114(19):E3806–e3815. doi:10.1073/pnas.1619416114, PMID:28439013.
[90] Nakagawa H, Hikiba Y, Hirata Y, Font-Burgada J, Sakamoto K, Hayakawa Y, *et al*. Loss of liver E-cadherin induces sclerosing cholangitis and promotes carcinogenesis. Proc Natl Acad Sci U S A 2014;111(3):1090–1095. doi:10.1073/pnas.1322731111, PMID:24395807.
[91] Maeda S, Hikiba Y, Fujiwara H, Ikenoue T, Sue S, Sugimori M, *et al*. NAFLD exacerbates cholangitis and promotes cholangiocellular carcinoma in mice. Cancer Sci 2021;112(4):1471–1480. doi:10.1111/cas.14828, PMID:33506599.
[92] Kumar R, Priyadarshi RN, Anand U. Non-alcoholic Fatty Liver Disease: Growing Burden, Adverse Outcomes and Associations. J Clin Transl Hepatol 2020;8(1):76–86. doi:10.14218/jcth.2019.00051, PMID:32274348.
[93] Farazi PA, Zeisberg M, Glickman J, Zhang Y, Kalluri R, DePinho RA. Chronic bile duct injury associated with fibrotic matrix microenvironment provokes cholangiocarcinoma in p53-deficient mice. Cancer Res 2006;66(13):6622–6627. doi:10.1158/0008-5472.Can-05-4609, PMID:16818635.
[94] Guest RV, Boulter L, Dwyer BJ, Kendall TJ, Man TY, Minnis-Lyons SE, *et al*. Notch3 drives development and progression of cholangiocarcinoma. Proc Natl Acad Sci U S A 2016;113(43):12250–12255. doi:10.1073/pnas.1600067113, PMID:27791012.
[95] Bray SJ. Notch signalling: a simple pathway becomes complex. Nat Rev Mol Cell Biol 2006;7(9):678–689. doi:10.1038/nrm2009, PMID:16921404.
[96] Zong Y, Panikkar A, Xu J, Antoniou A, Raynaud P, Lemaigre F, *et al*. Notch signaling controls liver development by regulating biliary differentiation. Development 2009;136(10):1727–1739. doi:10.1242/dev.029140, PMID:19369401.
[97] Zender S, Nickeleit I, Wuestefeld T, Sörensen I, Dauch D, Bozko P, *et al*. A critical role for notch signaling in the formation of cholangiocellular carcinomas. Cancer Cell 2013;23(6):784–795. doi:10.1016/j.ccr.2013.04.019, PMID:23727022.
[98] Fan B, Malato Y, Calvisi DF, Naqvi S, Razumilava N, Ribback S, *et al*. Cholangiocarcinomas can originate from hepatocytes in mice. J Clin Invest 2012;122(8):2911–2915. doi:10.1172/jci63212, PMID:22797301.
[99] Ong CK, Subimerb C, Pairojkul C, Wongkham S, Cutcutache I, Yu W, *et al*. Exome sequencing of liver fluke-associated cholangiocarcinoma. Nat Genet 2012;44(6):690–693. doi:10.1038/ng.2273, PMID:22561520.
[100] Guest RV, Boulter L, Kendall TJ, Minnis-Lyons SE, Walker R, Wigmore SJ, *et al*. Cell lineage tracing reveals a biliary origin of intrahepatic cholangiocarcinoma. Cancer Res 2014;74(4):1005–1010. doi:10.1158/0008-5472.Can-13-1911, PMID:24310400.
[101] Kim BH, Kim K, Min HS, Chie EK, Jang JY, Kim SW, *et al*. Phosphorylated Akt Expression as a Favorable Prognostic Factor for Patients Undergoing Curative Resection and Adjuvant Chemoradiotherapy for Proximal Extrahepatic Bile Duct Cancer. Am J Clin Oncol 2017;40(2):158–162. doi:10.1097/coc.0000000000000121, PMID:25171299.
[102] Li H, Wolfe A, Septer S, Edwards G, Zhong X, Abdulkarim AB, *et al*. Deregulation of Hippo kinase signalling in human hepatic malignancies. Liver Int 2012;32(1):38–47. doi:10.1111/j.1478-3231.2011.02646.x, PMID:22098174.

98159.
[103] Marvie P, Lisbonne M, L'Helgoualc'h A, Rauch M, Turlin B, Preisser L, *et al*. Interleukin-33 overexpression is associated with liver fibrosis in mice and humans. J Cell Mol Med 2010;14(6b):1726–1739. doi:10.1111/j.1582-4934.2009.00801.x, PMID:19508382.
[104] Song X, Xu H, Wang P, Wang J, Affo S, Wang H, *et al*. Focal Adhesion Kinase (FAK) promotes cholangiocarcinoma development and progression via YAP activation. J Hepatol 2021;75(4):888–899. doi:10.1016/j.jhep.2021.05.018, PMID:34052254.
[105] Wang J, Wang H, Peters M, Ding N, Ribback S, Utpatel K, *et al*. Loss of Fbxw7 synergizes with activated Akt signaling to promote c-Myc dependent cholangiocarcinogenesis. J Hepatol 2019;71(4):742–752. doi:10.1016/j.jhep.2019.05.027, PMID:31195063.
[106] Ma W, Han C, Zhang J, Song K, Chen W, Kwon H, *et al*. The Histone Methyltransferase G9a Promotes Cholangiocarcinogenesis Through Regulation of the Hippo Pathway Kinase LATS2 and YAP Signaling Pathway. Hepatology 2020;72(4):1283–1297. doi:10.1002/hep.31141, PMID:31990985.
[107] Guo J, Fu W, Xiang M, Zhang Y, Zhou K, Xu CR, *et al*. Notch1 Drives the Formation and Proliferation of Intrahepatic Cholangiocarcinoma. Curr Med Sci 2019;39(6):929–937. doi:10.1007/s11596-019-2125-0, PMID:31845224.
[108] Seehawer M, Heinzmann F, D'Artista L, Harbig J, Roux PF, Hoenicke L, *et al*. Necroptosis microenvironment directs lineage commitment in liver cancer. Nature 2018;562(7725):69–75. doi:10.1038/s41586-018-0519-y, PMID:30209397.
[109] Kiguchi K, Carbajal S, Chan K, Beltrán L, Ruffino L, Shen J, *et al*. Constitutive expression of ErbB-2 in gallbladder epithelium results in development of adenocarcinoma. Cancer Res 2001;61(19):6971–6976. PMID:11585718.
[110] Weber J, Öllinger R, Friedrich M, Ehmer U, Barenboim M, Steiger K, *et al*. CRISPR/Cas9 somatic multiplex-mutagenesis for high-throughput functional cancer genomics in mice. Proc Natl Acad Sci U S A 2015;112(45):13982–13987. doi:10.1073/pnas.1512392112, PMID:26508638.
[111] Song CQ, Li Y, Mou H, Moore J, Park A, Pomyen Y, *et al*. Genome-Wide CRISPR Screen Identifies Regulators of Mitogen-Activated Protein Kinase as Suppressors of Liver Tumors in Mice. Gastroenterology 2017;152(5):1161–1173.e1161. doi:10.1053/j.gastro.2016.12.002, PMID:27956228.
[112] Mou H, Ozata DM, Smith JL, Sheel A, Kwan SY, Hough S, *et al*. CRISPR-SONIC: targeted somatic oncogene knock-in enables rapid in vivo cancer modeling. Genome Med 2019;11(1):21. doi:10.1186/s13073-019-0627-9, PMID:30987660.
[113] Saha SK, Gordan JD, Kleinstiver BP, Vu P, Najem MS, Yeo JC, *et al*. Isocitrate Dehydrogenase Mutations Confer Dasatinib Hypersensitivity and SRC Dependence in Intrahepatic Cholangiocarcinoma. Cancer Discov 2016;6(7):727–739. doi:10.1158/2159-8290.Cd-15-1442, PMID:27231123.
[114] Liu F, Song Y, Liu D. Hydrodynamics-based transfection in animals by systemic administration of plasmid DNA. Gene Ther 1999;6(7):1258–1266. doi:10.1038/sj.gt.3300947, PMID:10455434.
[115] Liu WN, Fong SY, Tan WWS, Tan SY, Liu M, Cheng JY, *et al*. Establishment and Characterization of Humanized Mouse NPC-PDX Model for Testing Immunotherapy. Cancers (Basel) 2020;12(4):1025. doi:10.3390/cancers12041025, PMID:32331230.
[116] Scherer SD, Riggio AI, Haroun F, DeRose YS, Ekiz HA, Fujita M, *et al*. An immune-humanized patient-derived xenograft model of estrogen-independent, hormone receptor positive metastatic breast cancer. Breast Cancer Res 2021;23(1):100. doi:10.1186/s13058-021-01476-x, PMID:34717714.

*Journal of Clinical and Translational Hepatology* **2022** vol. 10(4) | 711–717
DOI: 10.14218/JCTH.2022.00244

Review Article

# Severe Acute Hepatitis of Unknown Origin in Children: What Do We Know Today?

María Teresa Pérez-Gracia[1*], Antonio Tarín-Pelló[1] and Beatriz Suay-García[2]

[1]*Área de Microbiología. Departamento de Farmacia, Universidad Cardenal Herrera-CEU. CEU Universities, Alfara del Patriarca (Valencia), Spain;* [2]*ESI International Chair@CEU-UCH, Departamento de Matemáticas, Física y Ciencias Tecnológicas, Universidad Cardenal Herrera-CEU, CEU Universities, Alfara del Patriarca (Valencia), Spain*

**Received:** 21 May 2022 | **Revised:** 20 June 2022 | **Accepted:** 7 July 2022 | **Published:** 26 July 2022

## Abstract

In May 2022, the UK International Health Regulations National Focal Point notified World Health Organization of 176 cases of severe acute hepatitis of unknown etiology in children under 10 years of age. From that moment on, cases of severe acute hepatitis of unknown origin in children began to be reported in several countries. As of June 17, 2022, a total of 991 cases had been reported in 35 countries worldwide, 50 children needed a liver transplant and 28 patients died. According to information published by ECDC, 449 cases have been detected in 21 EU countries. The children were between 1 month and 16 years of age. Adenovirus was detected in 62.2% of the analyzed samples. So far, the cause of these cases is unknown and many hypotheses remain open, but hepatitis A–E viruses and COVID-19 vaccines have been ruled out. A possible hypothesis has been published to explain the cause of these cases of severe hepatitis, according to which it could be a consequence of adenovirus infection in the intestine in healthy children previously infected with SARS-CoV-2. No other clear epidemiological risk factors have been identified to date. Thus, at this time, the etiology of the current cases of hepatitis remains under active investigation.

**Citation of this article:** Pérez-Gracia MT, Tarín-Pelló A, Suay-García B. Severe Acute Hepatitis of Unknown Origin in Children: What Do We Know Today? J Clin Transl Hepatol 2022;10(4):711–717. doi: 10.14218/JCTH.2022.00244.

## Introduction

On April 5, 2022, the United Kingdom (UK) International Health Regulations (IHR) National Focal Point notified the World Health Organization (WHO) of 10 cases of severe acute hepatitis of unknown etiology in previously healthy children under 10 years of age in Scotland. The age of the children ranged from 11 months to 5 years. Nine cases had symptom onset during March 2022, and one had an earlier onset in January 2022. Symptoms included jaundice, diarrhea, vomiting, and abdominal pain. All 10 cases were detected while the patient was hospitalized. After initiating a nationwide investigation, by April 8, 2022, a total of 74 cases meeting the case definition had been identified in the UK.[1] As per the case definition, severe acute hepatitis was present with high levels of aminotransferases, i.e. alanine aminotransferase (ALT) and aspartate aminotransferase (AST) >500 IU/L). It is thus likely that there have been patients with milder cases of hepatitis that have not been reported. The clinical syndrome in the identified cases is acute hepatitis with very high transaminases, often with jaundice, and sometimes preceded by gastrointestinal symptoms. Some cases required transfer to specialized pediatric liver units and six children required liver transplantation. No child was reported to have died. On May 6, 2022, the UK published technical briefing, "*Investigation into acute hepatitis of unknown etiology in children in England*," that described 163 cases, 11 of which required liver transplantation and no deaths at that time.[2] From that moment on, cases of severe acute hepatitis of unknown origin in children began to be reported in several countries (Fig. 1).The latest report published by the UK Health Safety Agency indicates that there have been 260 cases, 12 of which required liver transplantation and no deaths.[3]

## Epidemiology

Worldwide, as of June 17, 2022, a total of 991 cases had been detected by the WHO, Centers for Disease Control (CDC), and the European Center for Disease Prevention and Control (ECDC) that were detected in 35 countries. Fifty children required liver transplantation and 28 died. Eleven deaths occurred in the United States (USA), seven in Indonesia, seven in Brazil, one in Mexico, one in Ireland, and one in Palestine (Fig. 2).[4–8]

According to information published by the ECDC,[9–11] 449 cases have been detected in 21 EU countries, the UK, Austria, Spain, Sweden, Portugal, Belgium, Denmark, France, Ireland, Italy, Germany, Latvia, Moldova, Netherlands, Norway, Serbia, Slovenia, Poland, Romania, Greece, and Cyprus. The remaining cases were detected in Argentina, Brazil, Canada, Costa Rica, Mexico, Panama, Puerto Rico, Indonesia, Israel, Japan, Palestine, Singapore, Malaysia,

**Keywords:** Hepatitis; Children; Unknown origin; SARS-CoV-2; Adenovirus.
**Abbreviations:** CDC, Centers for Disease Control; ECDC, the European Center for Disease Prevention and Control.
***Correspondence to:** María Teresa Pérez-Gracia, Área de Microbiología. Departamento de Farmacia, Universidad Cardenal Herrera-CEU. CEU Universities. C/ Ramón y Cajal s/n, 46115 Alfara del Patriarca (Valencia), Spain. ORCID: https://orcid.org/0000-0001-5083-9267. Tel/Fax: +34-961369000, E-mail: teresa@uchceu.es


**Fig. 1. Timeline of reported cases of hepatitis of unknown origin in children from April 5 to May 13.**

South Korea, and the USA (Table 1).

The cases reported in the European Union included children between 1 month and 16 years of age. The majority (76.6%) were under 5 years of age, 31.2% were admitted to the intensive care unit and 8.4% received a liver transplant. There was one death associated with this disease. Adenovirus was detected in 52.4% of the analyzed samples, and most of the positive samples were whole blood. SARS-CoV-2 PCR assays were positive in 10.6%, and antibodies against SARS-CoV-2 were detected in 63.5%. A total of 85.9% were not vaccinated against COVID-19.[9–11]

The clinical syndrome in all identified cases was acute hepatitis with markedly elevated liver enzymes. Many cases reported gastrointestinal symptoms including abdominal pain, diarrhea, and vomiting that preceded presentation with severe acute hepatitis, elevated liver enzyme levels (aspartate transaminase (AST) or alanine aminotransaminase (ALT) > 500 IU/L) and jaundice. Most cases did not have fever. Hepatitis is an inflammation of the liver that can be caused by viral infections, alcohol consumption, toxins, medications, and certain other medical conditions. So far, the cause of these cases is unknown, and many hypotheses remain open, but hepatitis A–E viruses have been ruled out. COVID-19 vaccines have also been ruled out, as most of the children are too young and had not been vaccinated. Other possible causes, including other types of coronaviruses, other infections, or environmental causes, are being actively investigated. At this stage the role of the viruses found in some of the cases in the hepatitis pathogenesis is still unclear. No other clear epidemiological risk factors have been identified to date, including recent international travel. Thus, at this time, the etiology of the current cases of hepatitis is still considered unknown and remains under active investigation. Laboratory testing for many infections,

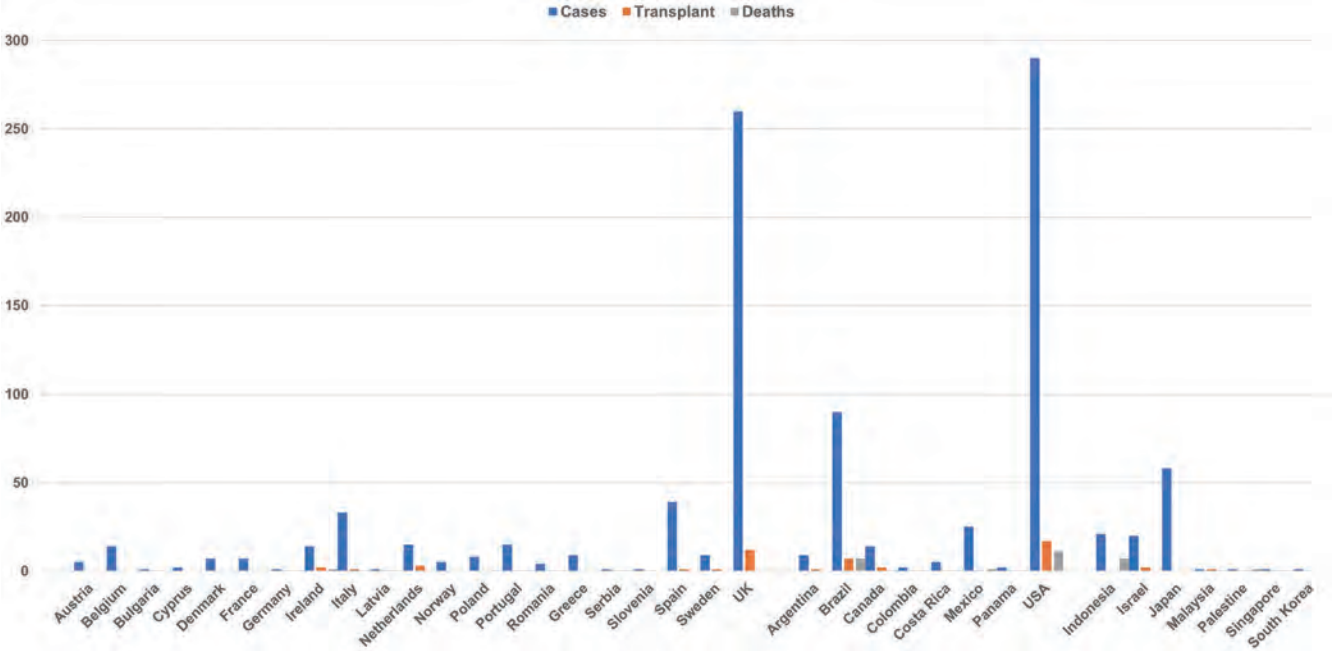


**Fig. 2. Worldwide distribution of cases, transplants, and deaths from severe acute hepatitis of unknown origin in children as of June 17, 2022.**

**Table 1. Summary of reported cases of severe acute hepatitis of unknown origin in children worldwide as of June 17, 2022**

| Country | Children, *n* | Reporting age criteria | Reporting protocol time frame | Age of pediatric patients | Transplants, *n* | Deaths, *n* | Age at death | Sex | Ethnicity |
|---|---|---|---|---|---|---|---|---|---|
| *Europe* | | | | | | | | | |
| Austria | 5 | | | <10 years | 0 | 0 | | | |
| Belgium | 14 | | | ≤10 years | 0 | 0 | | | |
| Bulgaria | 1 | | | | 0 | 0 | | | |
| Cyprus | 2 | | | | 0 | 0 | | | |
| Denmark | 7 | | | 6 <10 years and 1>10 years | 0 | 0 | | | |
| France | 7 | | | <10 years | 0 | 0 | | | |
| Germany | 1 | | | 5 years | 0 | 0 | | | |
| Ireland | 14 | | | 1–12 years | 2 | 1 | | | |
| Italy | 33 | | | <16 years | 1 | 0 | | | |
| Latvia | 1 | | | | 0 | 0 | | | |
| Netherlands | 15 | | | 11 months–8 years | 3 | 0 | | | |
| Norway | 5 | | | 1–5 years | 0 | 0 | | | |
| Poland | 8 | | | 7 years | 0 | 0 | | | |
| Portugal | 15 | | | | 0 | 0 | | | |
| Romania | 4 | | | 4 years | 0 | 0 | | | |
| Greece | 9 | Under 16 years | | | 0 | 0 | | | |
| Serbia | 1 | | | | 0 | 0 | | | |
| Slovenia | 1 | | | | 0 | 0 | | | |
| Spain | 39 | | | 18 months-16 years | 1 | 0 | | | |
| Sweden | 9 | | | | 1 | 0 | | | |
| United Kingdom | 260 | Up to 16 years | Since October 2021 | 2–5 years (median 3 years) | 12 | 0 | | 49% Female | 88.2% White |
| Total | 451 | | | | 20 | 1 | | | |
| *Americas* | | | | | | | | | |
| Argentina | 9 | | | 8 years rec transplant | 1 | 0 | | | |
| Brazil | 90 | | | 2 months-16 years (average 6 years) | 7 | 7 | | | |
| Canada | 14 | 1 month–16 years | Since October 1 2021 | | 2 | 0 | | | |
| Colombia | 2 | | | | 0 | 0 | | | |
| Costa Rica | 5 | | | | 0 | 0 | | | |

*(continued)*

**Table 1.** *(continued)*

| Country | Children, *n* | Reporting age criteria | Reporting protocol time frame | Age of pediatric patients | Transplants, *n* | Deaths, *n* | Age at death | Sex | Ethnicity |
|---|---|---|---|---|---|---|---|---|---|
| Mexico | 25 | | | < 8 years | 0 | 1 | 3 years | | |
| Panama | 2 | | | ≤2 years | 0 | 0 | | | |
| USA | 290 | Up to 10 years | | | 17 | 11 | All 10 years | | |
| Total | 437 | | | | 27 | 19 | | | |
| *Asia* | | | | | | | | | |
| Indonesia | 21 | | | | 0 | 7 | 2 | | |
| Israel | 20 | | | | 2 | 0 | | | |
| Japan | 58 | | | <17 years | 0 | 0 | | | |
| Malaysia | 1 | 1 month-18 years | | 4 years | 1 | 0 | | | |
| Palestine | 1 | | | 8 years | 0 | 1 | 8 years | | |
| Singapore | 1 | | | 10 months | 0 | 0 | | | |
| South Korea | 1 | | | | 0 | 0 | | | |
| Total | 103 | | | | 3 | 8 | | | |
| TOTAL | 991 | | | | 50 | 28 | | | |

chemicals, and toxins continues to be performed in the identified cases (Table 2).[12]

The UK has established a case definition and has developed a survey for the investigation of cases that meet the definition, which have been shared by the IHR with the rest of the countries.[12] The provisional confirmed case definition is a person presenting, after January 1, 2022 with an acute hepatitis which was not caused by hepatitis A–E viruses, or an expected presentation of metabolic, inherited or genetic, congenital or mechanical cause with serum transaminases >500 IU/L (AST or ALT), and ≤10 years of age. A possible case definition is a person presenting with acute hepatitis after January 1, 2022 with acute hepatitis not caused by hepatitis A–E viruses, or an expected presentation of metabolic, inherited, or genetic, congenital or mechanical cause with serum transaminases >500 IU/L (AST or ALT), who is 11–15 years of age. The Epi-linked case definition is a person presenting after January 1, 2022 with acute non-A–E hepatitis who is a close contact of a confirmed case. To prevent double-counting of cases, a person who is epi-linked but also meets the confirmed or possible case definition is recorded as a confirmed or possible case and the epi-link noted in their medical record.

As far as what we know today about liver biopsies and treatment of some of the children who have suffered from severe acute hepatitis, we have two studies conducted in Israel and in the UK.[13,14] In the study carried out in Israel, the authors reported five pediatric patients who recovered from COVID-19 and later presented with liver injury. Two types of clinical presentations were distinguishable. Two previously healthy infants 3 and 5 months of age presented with acute liver failure that rapidly progressed to liver transplantation. Their liver explants showed massive necrosis with cholangial proliferation and lymphocytic infiltrate. Three children, two were 8 years of age and one was 13 years of age, presented with hepatitis with cholestasis. Children had a liver biopsy significant for lymphocytic portal and parenchyma inflammation, along with bile duct proliferation. All three were started on steroid treatment. Their liver enzymes improved, and they were weaned successfully from treatment. For all five patients, extensive etiology workup for infectious and metabolic etiologies were negative.[13]

In the study conducted in King's College Hospital in the UK, the authors describe the course of eight children admitted to pediatric intensive care unit from February to May 2022.[14] The main reason for admission was neurologic deterioration (hepatic encephalopathy) with rising ammonia, lactate, and international normalized ratio. Patients were neuro-monitored with transcranial Dopplers (TCD) and reversed jugular venous saturation. Four patients had abnormal pulsatility index on TCD and six had low reversed jugular venous saturation, with the lowest being 25.9%, that required intervention. They were neuroprotected by early initiation of high-volume continuous kidney replacement therapy (CKRT) with a minimum CKRT dose of 60 mL/kg/h initiated within 24 h of admission, plasma exchange, use of hypertonic saline, noradrenaline to maintain cerebral perfusion pressure, temperature control and thiopentone infusion. All received *N*-acetylcysteine, and those positive for adenovirus received at least two doses of cidofovir. All eight children survived, with six requiring liver transplantation. One was re-transplanted and two survived without liver transplantation, one of who was delisted after 6 days on the super-urgent list as his clinical and biochemical condition improved.

Histopathology studies of the liver explant and in a few patient biopsies did not find evidence of adenovirus in hepatocytes, but all revealed hepatocyte necrosis and parenchymal collapse. The lack of adenovirus in hepatocytes, but severe liver injury leading to acute liver failure, may

**Table 2. Recommended laboratory tests in suspected cases of severe acute hepatitis in children**

| Sample type | Test | Pathogen |
|---|---|---|
| Blood* | PCR | Adenovirus, Enterovirus, CMV, EBV, HSV, Hepatitis A, Hepatitis C, Hepatitis E, HHV6 and HHV7 |
| Blood* | Serology | Hepatitis A, B, C, E, CMV, EBV, SARS-CoV-2 anti-S, SARS-CoV-2 anti-N (only if locally available) |
| Blood | Culture | Standard culture for bacteria/fungi (only if clinically indicated i.e. fever) |
| Throat swab* | PCR | Respiratory virus panel (including adenovirus/ enterovirus/influenza, SARS-CoV-2) |
| Stool* | PCR | Adenovirus, sapovirus, norovirus, enterovirus. Standard bacterial stool pathogen panel to include *Salmonella* spp. (or stool culture depending on local test availability) |
| Blood* (whole blood in EDTA and plasma separated specimens) | Toxicology | Local investigations according to history |
| Urine* | Toxicology | Local investigations according to history |

*Earliest possible sample.

have been related to an aberrant immune response from the host's liver immune system. Detailed characterization of immune infiltrates in the liver of children who progress to liver failure may identify a subgroup that responds to immunosuppression including steroids and avoids liver transplantation.[14]

## Investigations and main etiological hypotheses

The hypotheses being considered are that this hepatitis may be caused by: 1. An abnormal susceptibility or response of the host to adenovirus, which would cause the adenovirus to progress more frequently to hepatitis because of (a) lack of exposure during the COVID-19 pandemic; (b) prior infection with SARS-CoV-2 (including the Omicron variant) or other infection; (c) coinfection with SARS-CoV-2 or other virus; or (d) toxin, drug, or environmental exposure. (2) Increased frequency of normal adenovirus infections, which highlights a very rare or under-recognized complication. (3) A new adenovirus variant, with or without the contribution of a cofactor; (4) A post-infectious SARS-CoV-2 syndrome (including a restricted effect of Omicron); (5) Drug, toxin or environmental exposure; (6) A new pathogen acting alone or as a coinfection; (7) A new variant of SARS-CoV-2; or (8) SARS-CoV-2 envelope glycoprotein spike acting as a superantigen.

## Adenovirus

Adenovirus infection together with other cofactors that would enhance its effect remains the main causal hypothesis. Thus, of all cases reported from the UK that were tested for adenovirus (some identified as adenovirus 41F), 72% were positive. In recent weeks, according to UK respiratory infection surveillance data, the incidence of adenovirus infections has increased significantly compared with previous years, especially in children 1–4 years of age and children 5–9 years of age.[1]

Several hypotheses have been proposed to explain how adenoviruses might have changed their pathogenesis to cause hepatitis in healthy children: (1) Lack of exposure to pathogens during the COVID-19 pandemic may have generated an immune deficit in children and rendered them more susceptible to adenovirus infection generating a rarer and more severe condition. (2) Relaxation of restrictions has generated a massive wave of adenovirus infections, which would allow detection of a rarer outcome of infection. (3) A past infection or coinfection with another pathogen, or exposure to a toxin, drug, or environmental factor, has altered the response to adenovirus infection. (4) Infection with a new adenovirus that is capable of causing severe liver disease in children.

Adenoviruses are common pathogens that typically cause mild respiratory or gastrointestinal symptoms. Adenoviruses 40–41F are among the most frequent causes of viral gastroenteritis in children. In some cases, adenoviruses have been implicated in hepatitis in immunocompromised children and adults, and exceptionally in healthy individuals.[15–17] In addition, not all children have tested positive for adenovirus, and those who did test positive have often tested positive in only whole blood, and at very low concentrations, with the virus not being detected in liver and plasma samples. Adenoviruses are very common and may only be an incidental finding.

## SARS-CoV-2 acting as a superantigen

Recently, a hypothesis to explain the cause of these cases of severe hepatitis has been published, according to which it could be a consequence of adenovirus infection in the intestine in healthy children previously infected with SARS-CoV-2 and carriers of other viruses.[18,19] There is evidence that SARS-CoV-2 can persist in the gastrointestinal tract. In fact, the virus can be detected in the intestine for a much longer period in children than in adults.[2] Repeated release of viral protein in the intestinal epithelium would result in activation of the immune system. Specifically, part of the SARS-CoV-2 envelope, glycoprotein S, could act as a superantigen. Superantigens are a class of antigens that cause excessive and uncontrolled activation of the immune system. Specifically, they cause nonspecific (polyclonal) activation of T lymphocytes and massive release of cytokines (small proteins that regulate cell function). If a normal immune system response activates less than 0.001% of T lymphocytes, a superantigen activates up to 20%. Many bacterial toxins or viral molecules can act as superantigens that generate a massive nonspecific immune response that is not directed against a particular antigen or pathogen. Continuous and repeated activation because of adenovirus coinfection, could enhance a multisystem inflammatory syndrome (MIS-C) leading to acute hepatitis in children.

This syndrome appears in a small percentage of children for a few weeks to a few months after the child becomes ill, even if the illness is mild. It is usually quite severe, requiring hospitalization.[20] The liver is one of the most frequently affected organs. In fact, 43% of MIS-C cases result in hepatitis. The cause is thought to be impairment of the intestinal barrier, with the virus escaping into the bloodstream and causing inflammation.[21]

Another observation that tends to confirm this hypothesis is the presence in the spike protein of SARS-CoV-2 of a sequence not present in other coronaviruses and resembling another sequence in *Staphylococcus aureus* enterotoxin B that produces toxic shock syndrome.[22] It also acts as a superantigen, binding to major histocompatibility complex class II molecules on antigen-presenting cells and to the Vβ chains of the specific T-cell receptor (TCR).[23] The interaction results in the activation of a large proportion (up to 30%) of T cells and the massive release of proinflammatory cytokines[24] that trigger a rapid and potent inflammatory reaction. It has been shown in mice that an adenovirus infection generates hypersensitivity against enterotoxin B.[23] For those reasons, Brodin and Arditi suggest that children with acute hepatitis be investigated for SARS-CoV-2 persistence in stool, T-cell receptor skewing, and interferon gamma (IFN-γ) upregulation, because that would provide evidence of a SARS-CoV-2 superantigen mechanism in an adenovirus-41F-sensitized host.[18]

Along the same lines, Nishiura *et al.*[25] suggest that prior exposure to the Omicron variant (B.1.1.529) may be associated with an increased risk of severe hepatitis in children, indicating a critical need for cofactor studies. They analyzed the correlation between reported cases of Omicron variant and cases of acute hepatitis in children in 38 Organization for Economic Cooperation and Development countries and Romania between December 1, 2021, and April 27, 2022. Twelve of the 39 countries reported at least one case of hepatitis. The confirmed diagnoses of Omicron cases ranged from 4.4 to 11.9 million between the dates studied. In the remaining 27 countries, the cumulative number of cases of this variant ranged from 0.5 to 5.5 million. For example, a seroepidemiological study published in the US reported that approximately 75% of children were infected with Omicron variant by the end of February. It concluded that countries that reported more cases of this rare condition were those with a higher proportion of the population infected with Omicron.[25] According to all the studies that we have to date, episodes of severe acute hepatitis can be explained by a concatenation of two circumstances. (1) A SARS-CoV-2 infection with accumulation of virus in the intestine and outflow viral proteins into the bloodstream because increased intestinal permeability. (2) An adenovirus infection that sensitizes the immune system and causes an over reaction with subsequent liver inflammation. The hypothesis is complex, but whether children with acute hepatitis are carriers of SARS-CoV-2 in the stool, and whether evidence of superantigen-mediated immune activation is found, needs further investigation. If so, early application of immunomodulatory therapies could be considered to prevent liver damage and prevent transplantation. This therapy has been shown to be effective in some cases in Israel and in a case in a 3-year-old girl in the US.[26,27] On the other hand, if it is proven that the liver damage is directly caused by a virus, treatment with antivirals would be necessary.

For the moment all the hypotheses remain unproven. It is important to know the cause in order to identify cases as soon as possible and to find effective treatments. The lesson we draw from the available evidence is that, faced with such a complex situation, one must keep an open mind to all possible explanations. Unfortunately, the simplest one is not always the correct one.

## Funding

None to declare.

## Conflict of interest

MTPG has been an editorial board member of *Journal of Clinical and Translational Hepatology* since 2016. The other authors have no conflict of interests related to this publication.

## Author contributions

Study concept and design (MTPG); analysis and interpretation of data (MTPG, ATP, BSG), drafting of the manuscript (MTPG, ATP, BSG). All authors have made a significant contribution to this study and have approved the final manuscript.

## References

[1] UK Health Security Agency (Internet). Investigation into acute hepatitis of unknown aetiology in children in England. Technical briefing 1. 2022. Available from: https://assets.publishing.service.gov.uk/government/uploads/system/uploads/attachment_data/file/1071198/acute-hepatitis-technical-briefing-1_4_.pdf.
[2] United Kingdom Health Security Agency (Internet). Investigation into acute hepatitis of unknown aetiology in children in England. Technical briefing 2. 2022. Available from: https://assets.publishing.service.gov.uk/government/uploads/system/uploads/attachment_data/file/1073704/acute-hepatitis-technical-briefing-2.pdf.
[3] United Kingdom Health Security Agency (Internet). Research and analysis. Investigation into acute hepatitis of unknown aetiology in children in England: case update. 2022. Available from: https://www.gov.uk/government/publications/acute-hepatitis-technical-briefing/investigation-into-acute-hepatitis-of-unknown-aetiology-in-children-in-england-case-update#contents.
[4] World Health Organization (Internet). Disease Outbreak News; Acute hepatitis of unknown aetiology in children - Multi-country. 2022. Available from: https://www.who.int/emergencies/disease-outbreak-news/item/DON-389.
[5] CDC investigating 109 pediatric hepatitis cases; link to adenovirus unclear. *AAP News* 2022. Available from: https://publications.aap.org/aapnews/news/20212/CDC-investigating-109-pediatric-hepatitis-cases.
[6] Centers for Disease Control Health Advisory (Internet). Updated Recommendations for Adenovirus Testing and Reporting of Children with Acute Hepatitis of Unknown Etiology. 2022. Available from: HAN Archive - 00465 | Health Alert Network (HAN) (cdc.gov).
[7] Centers for Disease Control and Prevention (Internet). National Center for Immunization and respiratory diseases (NCIRD). Technical Report: Acute Hepatitis of Unknown Cause. 2022. Available from: https://www.cdc.gov/ncird/investigation/hepatitis-unknown-cause/technical-report.html.
[8] Baker JM, Buchfellner M, Britt W, Sanchez V, Potter JL, Ingram LA, *et al*. Acute Hepatitis and Adenovirus Infection Among Children - Alabama, October 2021-February 2022. MMWR Morb Mortal Wkly Rep 2022;71(18):638–640. doi:10.15585/mmwr.mm7118e1, PMID:35511732.
[9] European Centre for Disease Prevention and Control (ECDC) (Internet). Increase in severe acute hepatitis cases of unknown aetiology in children – 2022. Available from: https://www.ecdc.europa.eu/en/publications-data/increase-severe-acute-hepatitis-cases-unknown-aetiology-children.
[10] European Centre for Disease Prevention and Control (ECDC) (Internet). Increase in severe acute hepatitis cases of unknown aetiology in children –2022. Available from: https://www.ecdc.europa.eu/en/news-events/epidemiological-update-issued-19-may-2022-hepatitis-unknown-aetiology-children.
[11] European Centre for Disease Prevention and Control/WHO Regional Office for Europe (Internet). Hepatitis of Unknown Aetiology in Children, Joint Epidemiological overview. 2022. Available from: https://www.ecdc.europa.eu/en/hepatitis/joint-weekly-hepatitis-unknown-origin-children-surveillance-bulletin.
[12] Unite Kingdom Health Security Agency (Internet). Guidance. Increase in acute hepatitis cases of unknown aetiology in children. 2022. Available from: https://www.gov.uk/government/publications/hepatitis-increase-in-acute-cases-of-unknown-aetiology-in-children/increase-in-acute-hepatitis-cases-of-unknown-aetiology-in-children.
[13] Cooper S, Tobar A, Konen O, Orenshtein N, Kropach N, Landau Y, *et al*. Long COVID-19 Liver Manifestation in Children. J Pediatr Gastroenterol Nutr 2022. doi:10.1097/MPG.0000000000003521, PMID:35687535.
[14] Deep A, Grammatikopoulos T, Heaton N, Verma A, Dhawan A. Outbreak of hepatitis in children: clinical course of children with acute liver failure

admitted to the intensive care unit. Intensive Care Med 2022;48(7):958–962. doi:10.1007/s00134-022-06765-3, PMID:35687162.
[15] Khalifa A, Andreias L, Velpari S. Hepatitis in an immunocompetent adult linked to adenovirus. J Investig Med High Impact Case Rep 2022;10:23247096221079192. doi:10.1177/23247096221079192, PMID:35225036.
[16] Ozbay Hosnut F, Canan O, Ozcay F, Bilezikci B, Byington CL. Adenovirus infection as possible cause of acute liver failure in a healthy child: a case report. Turk J Gastroenterol 2008;19(4):281–283. PMID:19119490.
[17] Rocholl C, Gerber K, Daly J, Pavia AT, Byington CL. Adenoviral infections in children: the impact of rapid diagnosis. Pediatrics 2004;113(1 Pt 1):e51–56. doi:10.1542/peds.113.1.e51, PMID:14702495.
[18] Brodin P, Arditi M. Severe acute hepatitis in children: investigate SARS-CoV-2 superantigens. Lancet Gastroenterol Hepatol 2022;7(7):594–595. doi:10.1016/S2468-1253(22)00166-2, PMID:35576952.
[19] The Lancet Infectious Diseases. Explaining the unexplained hepatitis in children. Lancet Infect Dis 2022;22(6):743. doi:10.1016/S1473-3099(22)00296-1, PMID:35569492.
[20] Cantor A, Miller J, Zachariah P, DaSilva B, Margolis K, Martinez M. Acute hepatitis is a prominent presentation of the multisystem inflammatory syndrome in children: a singlecenter report. Hepatology 2020;72(5):1522–1527. doi:10.1002/hep.31526, PMID:32810894.
[21] Yonker LM, Gilboa T, Ogata AF, Senussi Y, Lazarovits R, Boribong BP, *et al*. Multisystem inflammatory syndrome in children is driven by zonulin-dependent loss of gut mucosal barrier. J Clin Invest 2021;131(14):e149633. doi:10.1172/JCI149633, PMID:34032635.
[22] Cheng MH, Zhang S, Porritt RA, Noval Rivas M, Paschold L, Willscher E, *et al*. Superantigenic character of an insert unique to SARS-CoV-2 spike supported by skewed TCR repertoire in patients with hyperinflammation. Proc Natl Acad Sci USA 2020;117(41):25254–25262. doi:10.1073/pnas.2010722117, PMID:32989130.
[23] Yarovinsky TO, Mohning MP, Bradford MA, Monick MM, Hunninghake GW. Increased sensitivity to staphylococcal enterotoxin B following adenoviral infection. Infect Immun 2005;73(6):3375–3384. doi:10.1128/IAI.73.6.3375-3384.2005, PMID:15908364.
[24] Brodin P. SARS-CoV-2 infections in children: understanding diverse outcomes. Immunity 2022;55(2):201–209. doi:10.1016/j.immuni.2022.01.014, PMID:35093190.
[25] Nishiura H, Jung S, Hayashi K. High population burden of Omicron variant (B.1.1.529) is associated with the emergence of severe hepatitis of unknown etiology in children. Int J Infect Dis 2022;122:30–32. doi:10.1016/j.ijid.2022.05.028, PMID:35577248.
[26] Efrati I. Israel examining 12 cases of kids' hepatitis after WHO warning. HAARETZ. 2022. Available from: https://www.haaretz.com/israel-news/israel-examining-12-cases-ofkids-hepatitis-after-who-warning-1.10752779.
[27] Osborn J, Szabo S, Peters AL. Pediatric Acute Liver Failure Due to Type 2 Autoimmune Hepatitis Associated With SARS-CoV-2 Infection: A Case Report. JPGN Rep 2022;3(2):e204. doi:10.1097/PG9.0000000000000204, PMID:35505826.

*Journal of Clinical and Translational Hepatology* **2022** vol. 10(4) | 718–725
DOI: 10.14218/JCTH.2022.00024

Review Article

# Infections in Alcoholic Hepatitis

Bhupinder Kaur[1], Russell Rosenblatt[2] and Vinay Sundaram[3*]

[1]*Internal Medicine Department, Cedars-Sinai Medical Center, Los Angeles, CA, USA;* [2]*Department of Gastroenterology and Hepatology, Weill Cornell Medicine, New York, NY, USA;* [3]*Department of Gastroenterology and Hepatology and Comprehensive Transplant Center, Cedars-Sinai Medical Center, Los Angeles, CA, USA*

**Received:** 13 January 2022 | **Revised:** 11 April 2022 | **Accepted:** 21 April 2022 | **Published:** 6 May 2022

## Abstract

Severe alcoholic hepatitis (sAH) is defined by a modified discriminant function ≥32 or model for end-stage liver disease (MELD) >20. Patients with sAH are in an immunocompromised state attributed to cirrhosis-related immunoparesis and corticosteroid use. Individuals with sAH often develop severe infections that adversely impact short-term prognosis. Currently, the corticosteroid prednisolone is the only treatment with proven efficacy in sAH; however, the combination of corticosteroid treatment and altered host defense in sAH has been thought to increase the risk of acquiring of bacterial, opportunistic fungal, and viral infections. Newer studies have shown that corticosteroids do not increase occurrence of infections in those with sAH; unfortunately, the lack of response to corticosteroids may instead predispose to infection development. Prompt and appropriate antibiotic treatment is therefore essential to improving patient outcomes. This review highlights common infections and risk factors in patients with sAH. Additionally, current diagnostic, therapeutic, and prophylactic strategies in these patients are discussed.

**Citation of this article:** Kaur B, Rosenblatt R, Sundaram V. Infections in Alcoholic Hepatitis. J Clin Transl Hepatol 2022; 10(4):718–725. doi: 10.14218/JCTH.2022.00024.

## Introduction

Alcoholic liver disease (ALD) involves a range of injury from simple steatosis to frank cirrhosis. Over the last decade there has been a rapid rise in the prevalence of ALD in the USA, particularly among patients younger than age 30.[1] These trends have intensified since the start of the coronavirus disease 2019 (COVID-19) pandemic with a notable increase in incidence of alcohol use disorder, ALD, and alcoholic hepatitis (AH).[2]

AH is considered the most severe form of alcohol-related liver disease. Clinical presentation typically includes recent or ongoing excessive alcohol intake, with a minimal threshold for women being 3 drinks (≥40 g per day) and for men 4 drinks (≥50–60 g per day).[3,4] The severity of AH is classically determined by a Maddrey (modified) discriminant function (mDF) of ≥32, based on a combination of prothrombin time and bilirubin levels.[5] More recently, the model for end-stage liver disease (MELD) has been utilized to identify severe AH, with a score >20 signifying severe AH.[6] In certain cases, patients may develop multiorgan failure (MOF) and the 3-month mortality rate can approach 40%.[7] The prevalence of severe AH has been reported to be as high as 20% in hospitalized patients.[8]

Certain patients with severe AH may require corticosteroid treatment with prednisolone, which is the only therapeutic option demonstrated to improve short-term survival for this condition. Currently, the use of steroids in AH is controversial, as studies have shown conflicting results.[9–11] In a meta-analysis of 11 randomized controlled trials (RCTs), which ultimately included 2,111 patients with sAH, it was demonstrated that corticosteroid treatment significantly reduced mortality at 28 days compared with placebo, with an overall 36% risk reduction.[9] However, the largest double-blinded placebo RCT regarding treatment of sAH, the STOPAH trial, did not demonstrate a statistically significant survival benefit at 28 days in patients receiving corticosteroids compared with placebo, while in a *post hoc* multivariable analysis, corticosteroids were associated with improved 28-day survival (odds ratio [OR] 0.609; $p$=0.015) but not at 90 days (OR 1.02) or 1-year (OR 1.01).[10] Despite these discrepancies, guidelines recommend that a MDF ≥32 or MELD score >20 indicate the need for treatment with corticosteroids.[11,12]

Patients with sAH, however, are at high risk of developing bacterial and fungal infections, due to immunoparesis related to disease pathogenesis and the immunosuppressive effects of corticosteroids.[13] A meta-analysis of 12 randomized trials found a cumulative incidence of infection of 20% in patients with AH during corticosteroid therapy.[14] Additionally, a cohort study found an infection incidence of 53% in 162 patients with biopsy-proven severe AH during a 90-day follow up.[15] The incidence of bacterial infection in the setting of severe AH is variable, ranging from 30% to 80% of cases,[16] leading to a significantly greater risk of mortality.[17]

The purpose of this review is to highlight common infections and risk factors in patients with sAH. Additionally, current prevention strategies in these patients will be summarized and discussed.

**Keywords:** Alcoholic hepatitis; Infections; Corticosteroids; STOPAH; Antibiotic treatment; Aspergillosis; Immunodeficiency; Alcoholic liver disease.

**Abbreviations:** ACLF, acute-on-chronic liver failure; AH, alcoholic hepatitis; ALD, alcoholic liver disease; IA, invasive aspergillosis; LPC, lipopolysaccharide; mDF, maddrey (modified) discriminant function; MELD, model for end-stage liver disease; NAC, N-acetylcysteine; RCT, randomized controlled trial; sAH, severe alcoholic hepatitis; SBP, spontaneous bacterial peritonitis; SIRS, systemic inflammatory response system; UTI, urinary tract infection.

***Correspondence to:** Vinay Sundaram, Department of Gastroenterology and Hepatology and Comprehensive Transplant Center, Cedars-Sinai Medical Center, 8635W. Third Street, Suite 1060W, Los Angeles, CA 90048, USA. ORCID: https://orcid.org/0000-0002-1450-7756. Tel: +1-310-423-6000, Fax: +1-310-423-6086, E-mail: vinay.sundaram@cshs.org

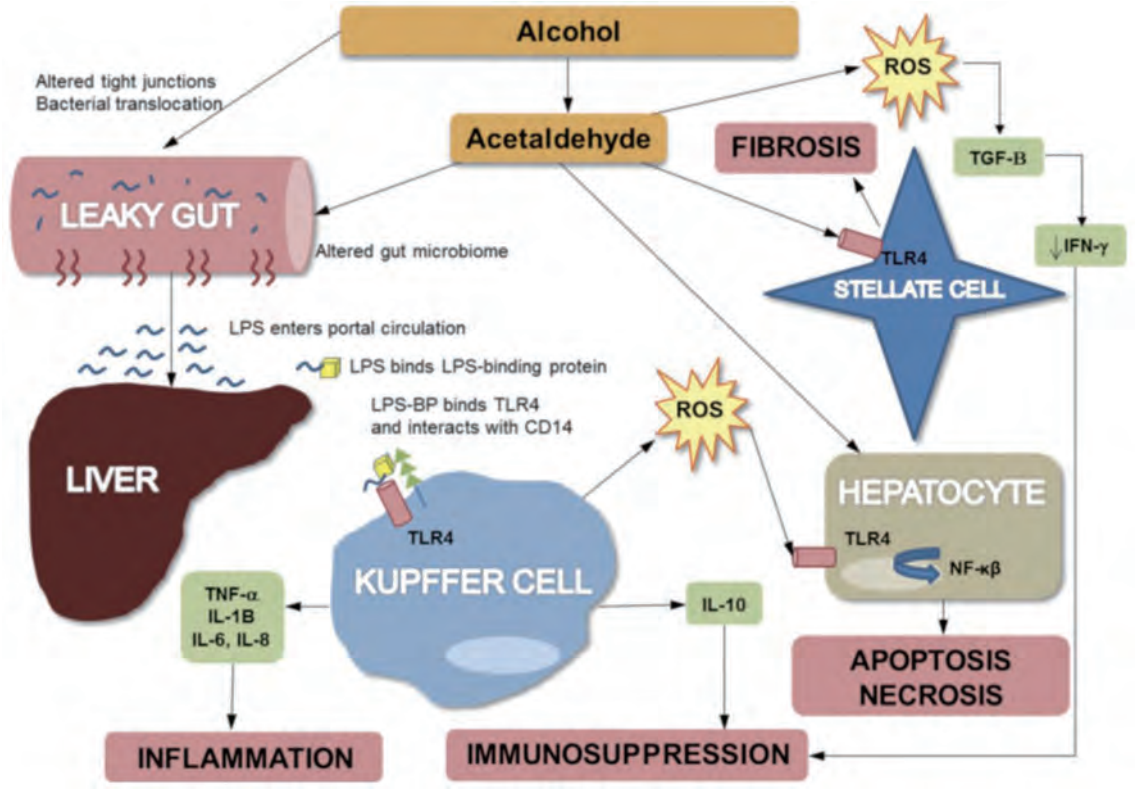


**Fig. 1. Alcohol and the innate immune response.** Alcohol and its metabolite acetaldehyde alter tight junctions among epithelial cells, leading to increased gut permeability, allowing increased levels of lipopolysaccharide (LPS) to enter the portal circulation. LPS binds toll-like receptor (TLR) 4 and activates a cascade of cytokines and chemokines that lead to a state of both inflammation and immunosuppression. BP, binding protein; IFN, interferon; IL, interleukin; NF, nuclear factor; ROS, reactive oxygen species; TGF, transforming growth factor. Permission has been obtained for reproduction by source: Clinics in Liver Disease, Article: Infection and Alcoholic Liver Disease.

## Risk factors for infection development

### *AH vs. cirrhosis-associated immune dysfunction*

AH is physiologically unique, when compared to cirrhosis, and often presents as a state of high-grade inflammation. Dysregulation of the immune system due to acute or recent alcohol use can lead to both an immunocompromised and proinflammatory state.[18] Alcohol and its metabolite acetaldehyde alter tight junctions among epithelial cells, leading to increased gut permeability, allowing increased level of pathogen-associated molecular pattern (PAMP) molecules, including lipopolysaccharide (LPS), to enter the portal circulation.[18,19] LPS binds to toll-like receptor (TLR) 4 on Kupffer cells in the liver to produce increased proinflammatory cytokines, including TNF-α, which activates the cell-death pathway triggering production of reactive oxygen species.[20] Additionally, this cascade of cytokines and chemokines can lead to a state of both inflammation and immunosuppression (Fig. 1).[18,20] One prospective study analyzed serum from 20 patients with acute AH, 16 patients with stable advanced alcohol-related cirrhosis, and 12 healthy controls. Compared to patients with advanced alcohol-related cirrhosis, those with acute AH had markedly greater suppression of T lymphocytes, due to overexpression of inhibitory receptors and reduced neutrophil antimicrobial activities. These alterations seem to be dependent on the higher chronic LPS exposure observed in severe AH.[21] Also, chronic and acute alcohol consumption are associated with a decrease in T cells, B cells, natural killer cells, monocytes, and an increase in proinflammatory cytokines.[13,19,22,23] Ultimately, findings suggest that excessive response of the immune system to PAMPs, including LPS, plays a role in the development of liver damage in AH, which is different from alcohol-related cirrhosis.[18–20,24]

In contrast, in compensated cirrhosis, damage-associated molecular patterns (DAMPS) from stressed/damaged tissue or necrotic hepatocytes activate circulating immune cells.[22] The progression of cirrhosis distorts hepatic architecture and impairs functional capacity. These events compromise the immune surveillance function of the liver and impairment of the bactericidal role of phagocytic cells. This low-grade systemic inflammation is a distinctive feature of compensated and stable decompensated cirrhosis.[19] The degree of systemic inflammation and immunodeficiency intensifies as the course of cirrhosis progresses.

Immunodeficiency is characteristically present in the setting of acute-on-chronic liver failure (ACLF) and often among patients with stable decompensated cirrhosis, contributing to episodes of acute decompensation triggered by bacterial infection.[19] Ultimately, this immunodeficiency increases the risk of infection at any stage of liver disease, with greater risk of infection correlating with higher ACLF grade.[25] In decompensated cirrhosis, gut barrier dysfunction arises from damage at all levels of intestinal barrier defense, which may contribute to the frequency and severity of complications.[26]

In summary, alcohol-induced derangement of the immune system via the LPS-TLR pathway triggers an extended inflammatory response, resulting in immune exhaustion and paralysis.[18,27] This process is offset by a dysregulated

compensatory anti-inflammatory pathway that predisposes patients with AH to infection.[18,27,28]

### *Corticosteroid-related immunosuppression*

Prednisolone, the primary treatment for sAH, may tip the balance between systemic inflammatory response system (SIRS) and compensatory anti-inflammatory response syndrome (CARS) toward CARS, which then results in immune paralysis, nosocomial infections, and multiple organ dysfunction.[13] Cirrhosis-associated immune dysfunction is characterized by increased expression of immune inhibitory markers and decreased phagocytic activity of neutrophils and monocytes, setting the stage for susceptibility to infections.[13,21] Prednisolone may also further exacerbate this diminished adaptive immune response, as it can suppresses cellular (Th1) immunity.[29] At the cellular level, prednisolone inhibits the access of leukocytes to inflammatory sites in several ways, including interfering with the function of leukocytes, endothelial cells, and fibroblasts, while also suppressing the production and effects of humoral factors involved in the inflammatory process.[30]

Several studies have demonstrated increased risk of infection among patients with AH treated with corticosteroids.[10,13,31,32] In the STOPAH trial, prednisolone nearly doubled the risk of infections reported as serious adverse events in patients with AH (13% vs. 7%, $p$=0.002).[10] In a post-hoc analysis that the STOPAH trial used to evaluate bacterial DNA levels to monitor for infection, it was noted that patients with sAH who were given prednisolone were at greater risk for developing serious infections compared to those who did not receive prednisolone.[31] Based on circulating DNA levels, 12% of patients with sAH were noted to have infection at baseline and 23% developed infection while on prednisolone treatment. The most common serious infections included respiratory tract infections and bacteremia.[31] Another observational study showed that corticosteroid use, along with younger age and higher MELD score, were independently associated with infection, specifically invasive fungal infections (IFIs).[32] However, separate studies have indicated that corticosteroids do not appear to increase the risk of infections in those with sAH, but rather the lack of response to corticosteroids may indicate greater risk of infection. A prospective study by Louvet *et al*.[33] analyzed a cohort of 246 patients and found that the infection risk was significantly greater in steroid non-responders compared to responders, at 42.5% vs. 11.1%, respectively ($p$<0.000001). Furthermore, that study showed that the development of infection may depend more upon the response to corticosteroid treatment (assessed by the Lille score) rather than the treatment of choice or duration.

### *Pharmacological interventions*

Trials have also investigated the efficacy of other medications for the treatment of sAH, including pentoxifylline, anti-tumor necrosis factor (TNF)-α agents (infliximab, etanercept), and granulocyte-colony stimulating factor (G-CSF) in severe AH. Pentoxifylline has been postulated to exert an anti-inflammatory effect through phosphodiesterase inhibition and increased cAMP levels, with the potential to reduce the risk of hepatorenal syndrome.[20] When analyzing infection risks, a study by Vergis *et al*.[31] demonstrated no association between pentoxifylline therapy and the incidence of serious infection ($p$=0.08), infection during treatment ($p$=0.20), or infection after treatment for sAH ($p$=0.27). In fact, adding pentoxifylline to corticosteroids may reduce the risk of infection compared with corticosteroid monotherapy.[34] Additionally, a network meta-analysis suggested that, in patients with severe AH, pentoxifylline and corticosteroids (alone and in combination with pentoxifylline or N-acetylcysteine [NAC]) can reduce short-term mortality.[35] Contrary to this, the STOPAH trial, along with several other studies, has provided data to support a survival benefit with prednisone but not pentoxifylline; subsequently, pentoxyfilline has not been recommended in the most current American Association for the Study of Liver Diseases (AASLD) guidelines.[9,12,36]

The role of anti-TNF-α, including infliximab and etanercept, in the setting of sAH has been evaluated. These agents inhibit the action of the major proinflammatory cytokine TNF-α, which mediates the immune-induced liver injury. Unfortunately, the anti-TNF-α strategies studied have been ineffective and increased the risk of bacterial infections and mortality, leading to early discontinuation of the trials evaluating these medications.[37,38]

G-CSF has been shown to favorably modify the intrahepatic immune environment and stimulate the regenerative potential of the liver. Under normal physiological conditions, G-CSF mobilizes CD34+ cells, increases hepatocyte-growth factor, and induces hepatic progenitor cell proliferation.[39] A randomized pilot study comparing pentoxifylline plus G-CSF with pentoxifylline alone for treatment of sAH demonstrated marked improvement in survival in the combination treatment group at 90 days (78.3% vs. 30.4%; $p$=0.001).[40] It is thought that neutrophil function enhanced via G-CSF use may improve the innate immune response to bacteria, diminish the risk of infection, and contribute to an improved outcome in patients with sAH.[41] However, a multicenter, randomized phase II trial showed that G-CSF did not improve patient survival and was unable to reduce the rate of complications including infections in patients with ACLF.[42]

Although some initial studies have shown encouraging results with G-CSF in patients with severe AH, more work needs to be done to characterize associated risks prior to initiating wide clinical use in the setting of AH.[43]

### *Bacterial pathogens*

The majority of infections among patients with sAH are bacterial, though it is uncertain which species are the most commonly acquired. One small study on AH showed that Gram-negative bacilli (GNB), predominantly *Escherichia coli*, represented 75% of all isolated bacteria.[44] Conversely, another small study analyzed the prevalence of bloodstream infections only in patients with AH. The investigators reported a significant prevalence of Gram-positive cocci (44%) and GNB presence of only 22%.[45] A cross-sectional analysis revealed that, among hospitalized patients with AH, prevalence of *Clostridium difficile* infection (CDI) was 1.6% or about 1.5-fold higher than that among hospitalized patients without AH.[46] Furthermore, CDI in these patients was associated with increased inpatient mortality.[46]

Regarding the site of infection, urinary tract and respiratory systems have been found to be more common in patients with AH.[47] A cohort study analyzed data from 121 patients with AH and showed pneumonia to be the most frequent infection (26%), followed by urinary tract infection (UTI) (23%) and skin and soft tissue infections (SSTIs) (8%), while spontaneous bacterial peritonitis (SBP) was found to be present in only 6% of infected patients.[48] A separate large, retrospective cohort study was conducted to evaluate patients with AH admitted between 2009 and 2014 to seven centers in Europe and the USA.[49] Among the

patients studied, 49% showed clinical or culture-based evidence of infection, primarily involving the lower respiratory tract or urinary tract. Gut commensal bacteria, particularly *E. coli* and *Enterobacter* species, were most commonly isolated in culture. Fungal infection was rarely seen.

Certain studies have shown that the most common infections sites differ before and after corticosteroid administration. For example, Louvet *et al*.[33] reported that prior to steroid treatment, SBP or bacteremia occurred more frequently (44%), followed by UTI (32%) and respiratory infections (13%). After or during corticosteroid treatment, there appeared to be a notable shift towards respiratory infections (40%), followed by SBP or bacteremia (28%) and UTI (18%). A separate meta-analysis from 2016 showed that, in patients with AH, corticosteroids-related infections included pneumonia (23%), UTI (10%), SBP (7%), and SSTI (2%).[14] In the STOPAH trial, respiratory infections accounted for 50% of all infections (both in treated and untreated groups) during follow-up. Lung infections were more common in patients who received prednisolone (7%) vs, those who did not receive prednisolone (3%).[10]

### *Fungal pathogens*

Fungal infection is associated with high mortality in critically-ill patients with cirrhosis.[50,51] However, there are limited studies looking specifically at invasive aspergillosis ( IA ) in the setting of AH. A meta-analysis demonstrated higher frequency of fungal infection occurrence among steroid-treated AH patients; in these patients, fungal infections were life-threatening, with a high mortality rate (approximately 33% compared to 12% in all steroid-treated infections).[14] In a cohort study of 94 patients with biopsy-proven sAH, IA incidence was 16%. The primary sites of infection included the lungs and central nervous system, while IA was disseminated in two cases. Of note, 13 cases of IA occurred in the context of corticosteroids, and 2 had received no specific treatment for AH.[52] These studies have shown that IA is a frequent complication of sAH and carries a very high risk of mortality. Along with liver disease, other risk factors of IA include neutropenia, hematologic malignancies, HIV, or organ transplantation.[53,54] Early and routine screening for IA may be beneficial.[52,55] Serum galactomannan (GM) has been demonstrated as a good screening test factor for IA in those with severe AH. The classical cutoff of ≥0.5 for serum GM has shown a high diagnostic performance, with sensitivity of 89%, specificity of 84%, positive predictive value of 67%, and negative predictive value of 95%.[52]

Invasive candidiasis incidence has been reported to be between 2% to 8% in patients with sAH.[52] A recent study, from 2021, demonstrated that human neutrophil responses to the fungal pathogen *C. albicans* are significantly diminished in patients with cirrhosis compared to healthy controls. This defect may be due to neutrophil exhaustion in the setting of persistently elevated circulating levels of inflammatory cytokines.[56] Patients with sAH present a more markedly reduced neutrophil antimicrobial activity, including phagocytosis and oxidative burst.[21] This underlying immune dysfunction in patients with AH may explain the lack of neutrophil functioning, thus increased prevalence of candidemia.

*Pneumocystis jirovecii* pneumonia (PJP) is another opportunistic fungal infection, which may occur in sAH.[57] Faria *et al*.,[58] analyzed seven ICU patients with biopsy-proven AH who developed bronchoalveolar lavage-confirmed PJP. Six of these patients received steroids for AH treatment prior to the diagnosis. All patients progressively developed acute respiratory distress requiring mechanical ventilation, ultimately leading to death despite receiving appropriate treatment. Additionally, two case reports have been published evaluating patients with human immunodeficiency virus (HIV) and steroid-treated AH who subsequently developed severe pneumopathy due to PJP.[59] Lastly, a report highlighted a case of PJP together with cytomegalovirus infection in an HIV-negative alcoholic patient.[60] Although small in sample size, these studies have shown that otherwise rare opportunistic infections, such as PJP, may occur in patients with AH, particularly in the setting of steroid use.

## Biomarkers of infection

Determining the presence of infection may be challenging in patients with AH, as cultures may be negative despite the presence of clinical indicators of active infection, such as leukocytosis.[15] One study showed that the SIRS criteria are met in approximately 50% of patients with sAH, even without documented infection.[15] Both C-reactive protein (CRP) and procalcitonin (PCT) have been investigated as potential biomarkers to determine the presence of underlying infection. Although CRP and PCT levels have been useful for detecting infection in cirrhosis, there have been inconsistencies in differentiating infection from SIRS without infection in AH. Among patients with AH, the findings of one study highlighted that a PCT cutoff of 0.45 ng/mL had positive and negative predictive values of 83% and 71% respectively for infection-associated SIRS, while CRP displayed no discriminative capability.[15] Another study found that serum PCT can be a useful marker for diagnosing sepsis in patients with AH and SIRS, and compares favorably with serum CRP levels.[61] On the other hand, in yet another study, PCT cutoff value failed to discriminate infected from non-infected patients with AH.[62] Therefore, although promising, biomarkers for underlying infection need further study, and in clinical settings should be carefully interpreted in combination with clinical assessment and correlation.

## Infection treatment and prevention

Management of sAH begins with thorough review of symptoms, physical exam findings, and infection workup, including chest radiography, urinalysis, cultures, ascitic fluid analysis, and viral serology (Table 1). If infection is detected, pathogen-directed therapy should be initiated (Fig. 2). Identification of an infection is critical prior to the initiation of steroids or immunosuppressant therapy to reduce risk of complications from these medications. If infection is unlikely, prevention strategies are focused on early treatment of sAH, based on discriminant function or MELD score. Additionally, the Lille score (which reassesses prognosis, identifies nonresponses, and guides therapy) may be used to determine whether corticosteroids should be discontinued.[12]

In patients with sAH, the development of infection may depend more on the response to corticosteroid treatment as assessed by the Lille score, rather than the treatment of choice or duration.[33] The response to corticosteroids based on the Lille score is significantly associated with improved survival.[63] The addition of intravenous of NAC to prednisolone may be used as a prevention strategy, as it has been reported to decrease the incidence of bacterial infections in patients with sAH. The adjunction of NAC to corticosteroid treatment has been shown to decrease the incidence of infections by 23%, when compared to corticosteroids alone.[64] Other supplementary infection prevention approaches include adequate patient nutrition. A RCT from 2016 showed that a daily caloric intake of fewer than 21.5 kcal/kg/day

**Table 1. sAH assessment and management**

| |
|---|
| History |
| Recent or ongoing excessive alcohol intake |
| Women=3 drinks (≥40 g per day) |
| Men=4 drinks (≥50-60 g per day) |
| Recent jaundice |
| Laboratory findings |
| mDF ≥32 (prothrombin time and bilirubin levels) |
| MELD >20 (bilirubin, creatinine, international normalized ratio) |
| Exam findings |
| Jaundice, icteric conjunctiva |
| Enlarged liver, ascites, caput medusa |
| Systemic hypotension, asterixis, confusion |
| Spider angiomata, palmar erythema |
| Gynecomastia, gonadal atrophy in men |
| Proximal muscle wasting, weight loss |
| Therapeutics |
| Prednisolone 40 mg/daily |
| Intravenous NAC+prednisolone 40 mg/day (may improve 30-day survival of patients with sAH) |
| Of note, pentoxifylline is no longer recommended in the treatment of AH |
| Duration/Response |
| Lillie model (albumin, creatinine, and prothrombin time) |
| Lille score <0.45: Responders to corticosteroids |
| Lille score ≥0.45: Non-responders |
| Cessation of corticosteroids after 7 days is recommended in non-responders |

MELD, Model for end-stage liver disease; AH, alcoholic hepatitis; mDF, maddrey (modified) discriminant function; NAC, N-acetylcysteine.

was associated with increased rates of infection and mortality at 6 months, when compared to higher intake (65.8% vs. 33.1%, $p<0.0001$).[65]

## Antimicrobials

Although patients with sAH are at increased risk of infection, evidence has not yet been reported to support a role for antibiotic prophylaxis. Currently, the use of prophylactic antibiotics in combination with corticosteroids is being investigated in the AntibioCor study.[66] An interim analysis of this study's data, presented as an abstract, revealed that infection rates in patients treated with amoxicillin/clavulanate plus corticosteroids were lower compared to those in the placebo group after 2 months of therapy (29.7% vs. 41.5%; hazard ratio [HR] 0.616, 95% confidence interval [CI] 0.417–0.909; $p=0.015$). Although a 30-day course of antibiotics with prednisolone did not improve 2-month survival in patients with sAH, they did reduce the likelihood of infections.[67] Careful restriction of prophylactic antibiotics to the high-risk populations could reduce the spread of multidrug-resistant bacteria.[47] Additionally, antifungal agents should be considered in patients with risk factors for fungal infections, including comorbid diabetes, acute kidney injury, longer hospital stays, and admission for bacterial infection.[51] Despite management of antibiotics, the presence of infection alone has not been shown to be a driver of short-term mortality. For example, one study observed that the use of antimicrobials early after admission delayed but did not reduce the occurrence of infections in patients with AH, without an effect on mortality.[49]

## Conclusions

Patients with AH are in an immunocompromised state, secondary to a combination of cirrhosis related immunoparesis and corticosteroids use, which may predispose them to higher risk of infection. To date, corticosteroids are the only treatment with proven efficacy in sAH. Nevertheless, corticosteroid impact on the occurrence of infection remains controversial. Some studies have shown that corticosteroid use may significantly reduce short-term mortality in patients with sAH.[9,10] Additionally, the combination of corticosteroid treatment and altered host defense in AH has been suggested as a cause of bacterial, opportunistic fungal, and viral infections.[68] Recent studies have shown that corticosteroids do not appear to increase occurrence of infections in those with sAH, though the lack of response to corticosteroids may increase infection risk.[33] However, screening for infections should be performed prior to corticosteroid initiation and during treatment, if clinically indicated. Physicians should be cognizant of recognizing potential infections in patients with ALD, in order to appropriately administer antibiotic therapy that will reduce the associated

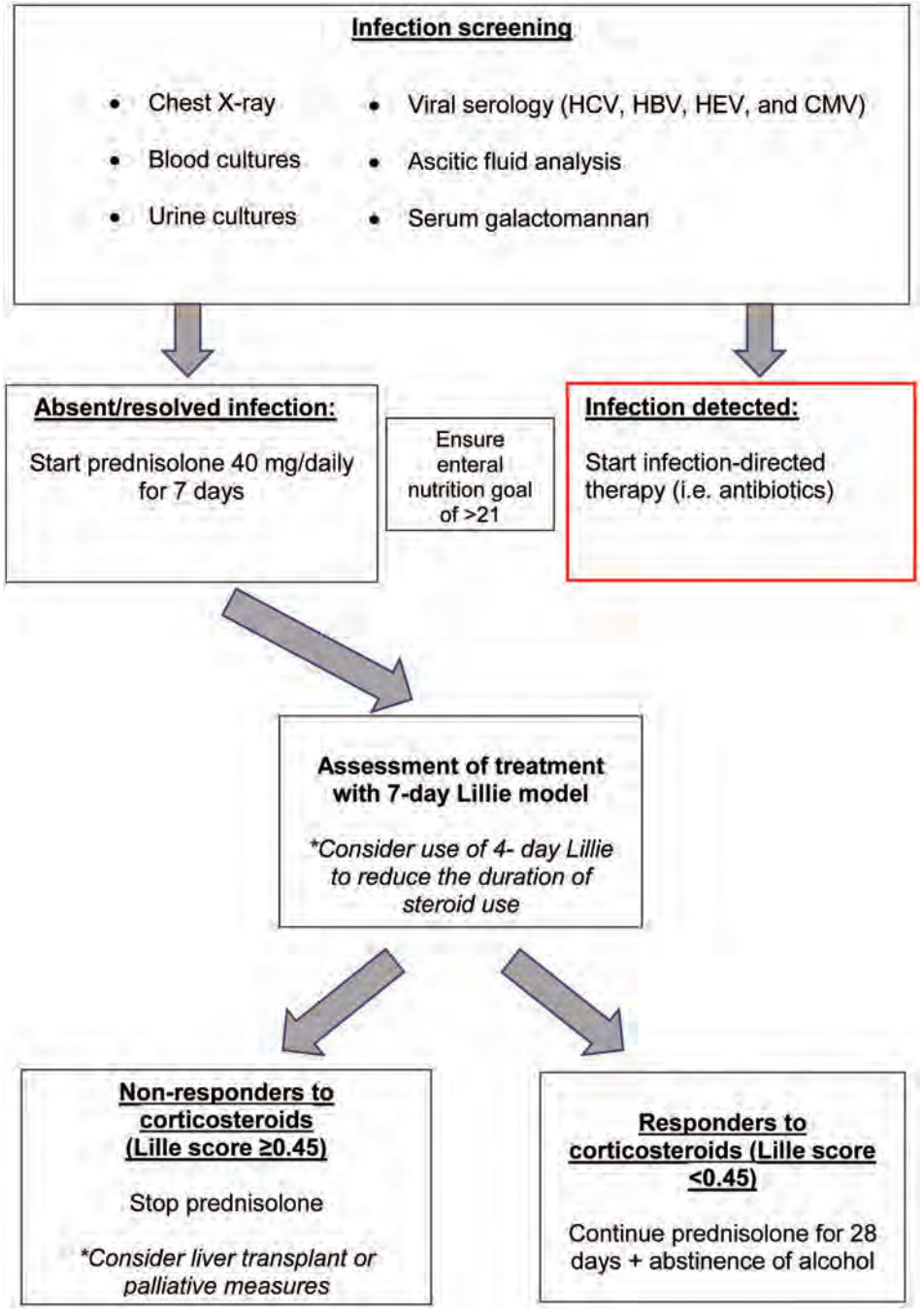


**Fig. 2. AH infection management.** CMV, cytomegalovirus; HBV, hepatitis B virus; HCV, hepatitis virus; HEV, hepatitis E virus.

mortality rate. The use of biomarkers such as CRP or PCT to aid in determination of infection development can be useful, though further studies are needed to justify their routine use. We recommend reassessment and potential antibiotic de-escalation at 48 h to reduce the spread of multidrug-resistant bacteria, fungi, or *Clostridium difficile*.

## Funding

None to declare.

## Conflict of interest

The authors have no conflict of interests related to this publication.

## Author contributions

Acquisition of data and drafting of the manuscript (BK, RS, VS), critical revision of the document for important intellec-

tual content (VS, RS). All authors approved the final version of the manuscript.

## References


[1] Tapper EB, Parikh ND. Mortality due to cirrhosis and liver cancer in the United States, 1999-2016: observational study. BMJ 2018;362:k2817. doi:10.1136/BMJ.K2817, PMID:30021785.

[2] Rutledge SM, Schiano TD, Florman S, Im GY. COVID-19 Aftershocks on Alcohol-Associated Liver Disease: An Early Cross-Sectional Report From the U.S. Epicenter. Hepatol Commun 2021;5(7):1151–1155. doi:10.1002/HEP4.1706, PMID:34533000.

[3] Singal AK, Bataller R, Ahn J, Kamath PS, Shah VH. ACG Clinical Guideline: Alcoholic Liver Disease. Am J Gastroenterol 2018;113(2):175–194. doi:10.1038/AJG.2017.469, PMID:29336434.

[4] Crabb DW, Bataller R, Chalasani NP, Kamath PS, Lucey M, Mathurin P, *et al*. Standard Definitions and Common Data Elements for Clinical Trials in Patients With Alcoholic Hepatitis: Recommendation From the NIAAA Alcoholic Hepatitis Consortia. Gastroenterology 2016;150(4):785–790. doi:10.1053/J.GASTRO.2016.02.042, PMID:26921783.

[5] Maddrey WC, Boitnott JK, Bedine MS, Weber FL Jr, Mezey E, White RI Jr. Corticosteroid therapy of alcoholic hepatitis. Gastroenterology 1978;75(2):193–199. PMID:352788.

[6] Dunn W, Jamil LH, Brown LS, Wiesner RH, Kim WR, Menon KV, *et al*. MELD accurately predicts mortality in patients with alcoholic hepatitis. Hepatology 2005;41(2):353–358. doi:10.1002/HEP.20503, PMID:15660383.

[7] Lucey MR, Mathurin P, Morgan TR. Alcoholic hepatitis. N Engl J Med 2009;360(26):2758–2769. doi:10.1056/NEJMRA0805786, PMID:19553649.

[8] O'Shea RS, Dasarathy S, McCullough AJ, Practice Guideline Committee of the American Association for the Study of Liver Diseases; Practice Parameters Committee of the American College of Gastroenterology. Alcoholic liver disease. Hepatology 2010;51(1):307–328. doi:10.1002/HEP.23258, PMID:20034030.

[9] Louvet A, Thursz MR, Kim DJ, Labreuche J, Atkinson SR, Sidhu SS, *et al*. Corticosteroids Reduce Risk of Death Within 28 Days for Patients With Severe Alcoholic Hepatitis, Compared With Pentoxifylline or Placebo-a Meta-analysis of Individual Data From Controlled Trials. Gastroenterology 2018;155(2):458–468.e8. doi:10.1053/J.GASTRO.2018.05.011, PMID:29738698.

[10] Thursz MR, Richardson P, Allison M, Austin A, Bowers M, Day CP, *et al*. Prednisolone or pentoxifylline for alcoholic hepatitis. N Engl J Med 2015;372(17):1619–1628. doi:10.1056/NEJMOA1412278, PMID:25901427.

[11] Arab JP, Díaz LA, Baeza N, Idalsoaga F, Fuentes-López E, Arnold J, *et al*. Identification of optimal therapeutic window for steroid use in severe alcohol-associated hepatitis: A worldwide study. J Hepatol 2021;75(5):1026–1033. doi:10.1016/J.JHEP.2021.06.019, PMID:34166722.

[12] Crabb DW, Im GY, Szabo G, Mellinger JL, Lucey MR. Diagnosis and Treatment of Alcohol-Associated Liver Diseases: 2019 Practice Guidance From the American Association for the Study of Liver Diseases. Hepatology 2020;71(1):306–333. doi:10.1002/HEP.30866, PMID:31314133.

[13] Singal AK, Shah VH, Kamath PS. Infection in Severe Alcoholic Hepatitis: Yet Another Piece in the Puzzle. Gastroenterology 2017;152(5):938–940. doi:10.1053/J.GASTRO.2017.02.030, PMID:28259797.

[14] Hmoud BS, Patel K, Bataller R, Singal AK. Corticosteroids and occurrence of and mortality from infections in severe alcoholic hepatitis: a meta-analysis of randomized trials. Liver Int 2016;36(5):721–728. doi:10.1111/LIV.12939, PMID:26279269.

[15] Michelena J, Altamirano J, Abraldes JG, Affò S, Morales-Ibanez O, Sancho-Bru P, *et al*. Systemic inflammatory response and serum lipopolysaccharide levels predict multiple organ failure and death in alcoholic hepatitis. Hepatology 2015;62(3):762–772. doi:10.1002/HEP.27779, PMID:25761863.

[16] Karakike E, Moreno C, Gustot T. Infections in severe alcoholic hepatitis. Ann Gastroenterol 2017;30(2):152–160. doi:10.20524/AOG.2016.0101, PMID:28243035.

[17] Garcia-Saenz-de-Sicilia M, Duvoor C, Altamirano J, Chavez-Araujo R, Prado V, de Lourdes Candolo-Martinelli A, *et al*. A Day-4 Lille Model Predicts Response to Corticosteroids and Mortality in Severe Alcoholic Hepatitis. Am J Gastroenterol 2017;112(2):306–315. doi:10.1038/AJG.2016.539, PMID:27922027.

[18] Chan C, Levitsky J. Infection and Alcoholic Liver Disease. Clin Liver Dis 2016;20(3):595–606. doi:10.1016/j.cld.2016.02.014, PMID:27373619.

[19] Albillos A, Martin-Mateos R, Van der Merwe S, Wiest R, Jalan R, Álvarez-Mon M. Cirrhosis-associated immune dysfunction. Nat Rev Gastroenterol Hepatol 2022;19(2):112–134. doi:10.1038/S41575-021-00520-7, PMID:34703031.

[20] Moreau R, Rautou PE. G-CSF therapy for severe alcoholic hepatitis: targeting liver regeneration or neutrophil function? Am J Gastroenterol 2014;109(9):1424–1426. doi:10.1038/AJG.2014.250, PMID:25196873.

[21] Markwick LJ, Riva A, Ryan JM, Cooksley H, Palma E, Tranah TH, *et al*. Blockade of PD1 and TIM3 restores innate and adaptive immunity in patients with acute alcoholic hepatitis. Gastroenterology 2015;148(3):590–602.e10. doi:10.1053/J.GASTRO.2014.11.041, PMID:25479137.

[22] Bonnel AR, Bunchorntavakul C, Reddy KR. Immune dysfunction and infections in patients with cirrhosis. Clin Gastroenterol Hepatol 2011;9(9):727–738. doi:10.1016/J.CGH.2011.02.031, PMID:21397731.

[23] Tilg H, Wilmer A, Vogel W, Herold M, Nölchen B, Judmaier G, *et al*. Serum levels of cytokines in chronic liver diseases. Gastroenterology 1992;103(1):264–274. doi:10.1016/0016-5085(92)91122-k, PMID:1612333.

[24] Albillos A, Lario M, Álvarez-Mon M. Cirrhosis-associated immune dysfunction: distinctive features and clinical relevance. J Hepatol 2014;61(6):1385–1396. doi:10.1016/J.JHEP.2014.08.010, PMID:25135860.

[25] Fernández J, Gustot T. Management of bacterial infections in cirrhosis. J Hepatol 2012;56(Suppl 1):S1–12. doi:10.1016/S0168-8278(12)60002-6, PMID:22300459.

[26] Albillos A, de Gottardi A, Rescigno M. The gut-liver axis in liver disease: Pathophysiological basis for therapy. J Hepatol 2020;72(3):558–577. doi:10.1016/J.JHEP.2019.10.003, PMID:31622696.

[27] Bataller R, Mandrekar P. Identifying molecular targets to improve immune function in alcoholic hepatitis. Gastroenterology 2015;148(3):498–501. doi:10.1053/J.GASTRO.2015.01.013, PMID:25613314.

[28] Chirapongsathorn S, Kamath PS, Shah V. Alcoholic hepatitis: Can we outwit the Grim Reaper? Hepatology 2015;62(3):671–673. doi:10.1002/HEP.27852, PMID:25891016.

[29] Franchimont D. Overview of the actions of glucocorticoids on the immune response: a good model to characterize new pathways of immunosuppression for new treatment strategies. Ann N Y Acad Sci 2004;1024:124–137. doi:10.1196/ANNALS.1321.009, PMID:15265777.

[30] Boumpas DT, Chrousos GP, Wilder RL, Cupps TR, Balow JE. Glucocorticoid therapy for immune-mediated diseases: basic and clinical correlates. Ann Intern Med 1993;119(12):1198–1208. doi:10.7326/0003-4819-119-12-199312150-00007, PMID:8239251.

[31] Vergis N, Atkinson SR, Knapp S, Maurice J, Allison M, Austin A, *et al*. In Patients With Severe Alcoholic Hepatitis, Prednisolone Increases Susceptibility to Infection and Infection-Related Mortality, and Is Associated With High Circulating Levels of Bacterial DNA. Gastroenterology 2017;152(5):1068–1077.e4. doi:10.1053/J.GASTRO.2016.12.019, PMID:28043903.

[32] Otero Sanchez L, Karakike E, Njimi H, Putignano A, Degré D, Hites M, *et al*. Clinical Course and Risk Factors for Infection in Severe Forms of Alcohol-Associated Liver Disease. Hepatology 2021;74(5):2714–2724. doi:10.1002/HEP.31984, PMID:34046927.

[33] Louvet A, Wartel F, Castel H, Dharancy S, Hollebecque A, Canva-Delcambre V, *et al*. Infection in patients with severe alcoholic hepatitis treated with steroids: early response to therapy is the key factor. Gastroenterology 2009;137(2):541–548. doi:10.1053/J.GASTRO.2009.04.062, PMID:19445945.

[34] Lee YS, Kim HJ, Kim JH, Yoo YJ, Kim TS, Kang SH, *et al*. Treatment of Severe Alcoholic Hepatitis With Corticosteroid, Pentoxifylline, or Dual Therapy: A Systematic Review and Meta-Analysis. J Clin Gastroenterol 2017;51(4):364–377. doi:10.1097/MCG.0000000000000674, PMID:27636406.

[35] Singh S, Murad MH, Chandar AK, Bongiorno CM, Singal AK, Atkinson SR, *et al*. Comparative Effectiveness of Pharmacological Interventions for Severe Alcoholic Hepatitis: A Systematic Review and Network Meta-analysis. Gastroenterology 2015;149(4):958–70.e12. doi:10.1053/J.GASTRO.2015.06.006, PMID:26091937.

[36] Thursz MR, Richardson P, Allison M, Austin A, Bowers M, Day CP, *et al*. Prednisolone or pentoxifylline for alcoholic hepatitis. N Engl J Med 2015;372(17):1619–1628. doi:10.1056/NEJMoa1412278, PMID:25901427.

[37] Naveau S, Chollet-Martin S, Dharancy S, Mathurin P, Jouet P, Piquet MA, *et al*. A double-blind randomized controlled trial of infliximab associated with prednisolone in acute alcoholic hepatitis. Hepatology 2004;39(5):1390–1397. doi:10.1002/HEP.20206, PMID:15122768.

[38] Boetticher NC, Peine CJ, Kwo P, Abrams GA, Patel T, Aqel B, *et al*. A randomized, double-blinded, placebo-controlled multicenter trial of etanercept in the treatment of alcoholic hepatitis. Gastroenterology 2008;135(6):1953–1960. doi:10.1053/J.GASTRO.2008.08.057, PMID:18848937.

[39] Spahr L, Lambert JF, Rubbia-Brandt L, Chalandon Y, Frossard JL, Giostra E, *et al*. Granulocyte-colony stimulating factor induces proliferation of hepatic progenitors in alcoholic steatohepatitis: a randomized trial. Hepatology 2008;48(1):221–229. doi:10.1002/HEP.22317, PMID:18537187.

[40] Singh V, Sharma AK, Narasimhan RL, Bhalla A, Sharma N, Sharma R. Granulocyte colony-stimulating factor in severe alcoholic hepatitis: a randomized pilot study. Am J Gastroenterol 2014;109(9):1417–1423. doi:10.1038/AJG.2014.154, PMID:24935272.

[41] Tato CM, Cua DJ. SnapShot: Cytokines IV. Cell 2008;132(6):1062.e1–1062.e2. doi:10.1016/J.CELL.2008.02.024, PMID:18358817.

[42] Engelmann C, Herber A, Franke A, Bruns T, Reuken P, Schiefke I, *et al*. Granulocyte-colony stimulating factor (G-CSF) to treat acute-on-chronic liver failure: A multicenter randomized trial (GRAFT study). J Hepatol 2021;75(6):1346–1354. doi:10.1016/j.jhep.2021.07.033, PMID:34364917.

[43] Kedarisetty CK, Kumar A, Sarin SK. Insights into the Role of Granulocyte Colony-Stimulating Factor in Severe Alcoholic Hepatitis. Semin Liver Dis 2021;41(1):67–78. doi:10.1055/s-0040-1719177, PMID:33764486.

[44] Verma S, Ajudia K, Mendler M, Redeker A. Prevalence of septic events, type 1 hepatorenal syndrome, and mortality in severe alcoholic hepatitis and utility of discriminant function and MELD score in predicting these adverse events. Dig Dis Sci 2006;51(9):1637–1643. doi:10.1007/S10620-006-9099-Z, PMID:16927139.

[45] Wernlund PG, Støy S, Lemming L, Vilstrup H, Sandahl TD. Blood culture-positive infections in patients with alcoholic hepatitis. Scand J Infect Dis 2014;46(12):902–905. doi:10.3109/00365548.2014.951682, PMID:25290580.

[46] Sundaram V, May FP, Manne V, Saab S. Effects of Clostridium difficile infection in patients with alcoholic hepatitis. Clin Gastroenterol Hepatol 2014;12(10):1745–52.e2. doi:10.1016/J.CGH.2014.02.041, PMID:24681081.

[47] Fernández J, Acevedo J, Castro M, Garcia O, de Lope CR, Roca D, *et al*. Prevalence and risk factors of infections by multiresistant bacteria in cirrhosis: a prospective study. Hepatology 2012;55(5):1551–1561. doi:10.1002/HEP.25532, PMID:22183941.

[48] Altamirano J, Miquel R, Katoonizadeh A, Abraldes JG, Duarte-Rojo A, Louvet A, *et al*. A histologic scoring system for prognosis of patients with alcoholic hepatitis. Gastroenterology 2014;146(5):1231–9.e1-6. doi:10.1053/J.GASTRO.2014.01.018, PMID:24440674.

[49] Parker R, Im G, Jones F, Hernández OP, Nahas J, Kumar A, *et al*. Clinical

and microbiological features of infection in alcoholic hepatitis: an international cohort study. J Gastroenterol 2017;52(11):1192–1200. doi:10.1007/S00535-017-1336-Z, PMID:28389732.
[50] Lahmer T, Messer M, Mayr U, Saugel B, Noe S, Schultheiss C, *et al*. Fungal "colonisation" is associated with increased mortality in medical intensive care unit patients with liver cirrhosis. Mycopathologia 2015;179(1-2):63–71. doi:10.1007/S11046-014-9825-6, PMID:25348847.
[51] Bajaj JS, Reddy RK, Tandon P, Wong F, Kamath PS, Biggins SW, *et al*. Prediction of Fungal Infection Development and Their Impact on Survival Using the NACSELD Cohort. Am J Gastroenterol 2018;113(4):556–563. doi:10.1038/AJG.2017.471, PMID:29257141.
[52] Gustot T, Maillart E, Bocci M, Surin R, Trépo E, Degré D, *et al*. Invasive aspergillosis in patients with severe alcoholic hepatitis. J Hepatol 2014;60(2):267–274. doi:10.1016/J.JHEP.2013.09.011, PMID:24055548.
[53] Falcone M, Massetti AP, Russo A, Vullo V, Venditti M. Invasive aspergillosis in patients with liver disease. Med Mycol 2011;49(4):406–413. doi:10.3109/13693786.2010.535030, PMID:21108575.
[54] Segal BH, Walsh TJ. Current approaches to diagnosis and treatment of invasive aspergillosis. Am J Respir Crit Care Med 2006;173(7):707–717. doi:10.1164/RCCM.200505-727SO, PMID:16387806.
[55] Lahmer T, Messer M, Schwerdtfeger C, Rasch S, Lee M, Saugel B, *et al*. Invasive mycosis in medical intensive care unit patients with severe alcoholic hepatitis. Mycopathologia 2014;177(3-4):193–197. doi:10.1007/S11046-014-9740-X, PMID:24710759.
[56] Knooihuizen SAI, Alexander NJ, Hopke A, Barros N, Viens A, Scherer A, *et al*. Loss of Coordinated Neutrophil Responses to the Human Fungal Pathogen, Candida albicans, in Patients With Cirrhosis. Hepatol Commun 2021;5(3):502–515. doi:10.1002/HEP4.1645, PMID:33681682.
[57] Edman JC, Kovacs JA, Masur H, Santi DV, Elwood HJ, Sogin ML. Ribosomal RNA sequence shows Pneumocystis carinii to be a member of the fungi. Nature 1988;334(6182):519–522. doi:10.1038/334519a0, PMID:2970013.
[58] Faria LC, Ichai P, Saliba F, Benhamida S, Antoun F, Castaing D, *et al*. Pneumocystis pneumonia: an opportunistic infection occurring in patients with severe alcoholic hepatitis. Eur J Gastroenterol Hepatol 2008;20(1):26–28. doi:10.1097/MEG.0B013E3282F16A10, PMID:18090986.
[59] Ichai P, Azoulay D, Feray C, Saliba F, Antoun F, Roche B, *et al*. Pneumopathies à pneumocystis carinii et à cytomégalovirus au décours d'hépatites alcooliques traitées par corticoïdes [Pneumocystis carinii and cytomegalovirus pneumonia after corticosteroid therapy in acute severe alcoholic hepatitis: 2 case reports]. Gastroenterol Clin Biol 2002;26(5):532–534. French. PMID:12122370.
[60] Ikawa H, Hayashi Y, Ohbayashi C, Tankawa H, Itoh H. Autopsy case of alcoholic hepatitis and cirrhosis treated with corticosteroids and affected by Pneumocystis carinii and cytomegalovirus pneumonia. Pathol Int 2001;51(8):629–632. doi:10.1046/J.1440-1827.2001.01249.X, PMID:11564218.
[61] Kumar K, Mohindra S, Raj M, Choudhuri G. Procalcitonin as a marker of sepsis in alcoholic hepatitis. Hepatol Int 2014;8(3):436–442. doi:10.1007/S12072-014-9540-X, PMID:26202645.
[62] Elefsiniotis IS, Skounakis M, Vezali E, Pantazis KD, Petrocheilou A, Pirounaki M, *et al*. Clinical significance of serum procalcitonin levels in patients with acute or chronic liver disease. Eur J Gastroenterol Hepatol 2006;18(5):525–530. doi:10.1097/00042737-200605000-00012, PMID:16607149.
[63] Louvet A, Naveau S, Abdelnour M, Ramond MJ, Diaz E, Fartoux L, *et al*. The Lille model: a new tool for therapeutic strategy in patients with severe alcoholic hepatitis treated with steroids. Hepatology 2007;45(6):1348–1354. doi:10.1002/HEP.21607, PMID:17518367.
[64] Nguyen-Khac E, Thevenot T, Piquet MA, Benferhat S, Goria O, Chatelain D, *et al*. Glucocorticoids plus N-acetylcysteine in severe alcoholic hepatitis. N Engl J Med 2011;365(19):1781–1789. doi:10.1056/NEJMOA1101214, PMID:22070475.
[65] Moreno C, Deltenre P, Senterre C, Louvet A, Gustot T, Bastens B, *et al*. Intensive Enteral Nutrition Is Ineffective for Patients With Severe Alcoholic Hepatitis Treated With Corticosteroids. Gastroenterology 2016;150(4):903–10.e8. doi:10.1053/J.GASTRO.2015.12.038, PMID:26764182.
[66] ClinicalTrials.gov. Efficacy of antibiotic therapy in severe alcoholic hepatitis treated with prednisolone (AntibioCor). Available from: https://clinicaltrials.gov/ct2/show/NCT02281929.
[67] Anthony RC. Adding amoxicillin/clavulanate to prednisolone yields no survival benefit in severe alcoholic hepatitis. Available from: https://specialty.mims.com/topic/adding-amoxicillin-clavulanate-to-prednisolone-yields-no-survival-benefit-in-severe-alcoholic-hepatitis.
[68] Gustot T, Fernandez J, Szabo G, Albillos A, Louvet A, Jalan R, *et al*. Sepsis in alcohol-related liver disease. J Hepatol 2017;67(5):1031–1050. doi:10.1016/J.JHEP.2017.06.013, PMID:28647569.

*Journal of Clinical and Translational Hepatology* **2022** vol. 10(4) | 726–729
DOI: 10.14218/JCTH.2020.00080

Review Article

# Hepatic Histoplasmosis: An Update

Maimuna Sayeed[1], Md Benzamin[1*], Luthfun Nahar[1], Masud Rana[2] and Aisharza Sultana Aishy[3]

*[1]Department of Paediatric Gastroenterology & Nutrition, Bangabandhu Shiekh Mujib Medical University (BSMMU), Dhaka, Bangladesh; [2]Hazi Asmot Ali Medical Centre, Bhairab, Kishoregonj, Dhaka, Bangladesh; [3]Jalalabad Ragib-Rabeya Medical College, Sylhet, Bangladesh*

**Received:** 24 August 2020 | **Revised:** 8 November 2020 | **Accepted:** 1 July 2021 | **Published:** 22 September 2021

## Abstract

*Histoplasma capsulatum* is the most common cause of endemic mycosis in developing countries. It is a self-limited and asymptomatic disease in immunocompetent individuals but remains a frequent cause of opportunistic infection in patients with compromised immune status. Liver involvement as a part of disseminated histoplasmosis is well known. However, liver infection as a primary manifestation of histoplasmosis without evidence of primary lung involvement is rare. In conclusion, clinicians should be aware of isolated histoplasmosis affecting the hepatobiliary system, and careful evaluation is warranted to confirm the diagnosis. Given the appropriate clinical context, histoplasmosis should be considered in both immunocompetent and immunocompromised patients, regardless of pulmonary symptoms, in non endemic as well as endemic areas.

**Citation of this article:** Sayeed M, Benzamin M, Nahar L, Rana M, Aishy AS. Hepatic histoplasmosis: An update. J Clin Transl Hepatol 2022;10(4):726–729. doi: 10.14218/JCTH.2020.00080.

## Introduction

Histoplasmosis is a systemic fungal disease that is caused by the dimorphic fungus *Histoplasma capsulatum*, which usually infects an individual by way of the respiratory tract. Cases comprise two distinct groups of conditions—the subcutaneous and systemic mycoses. The fungal infection has recently emerged as an important opportunistic infection among immunocompromised patients living in endemic areas for this fungus, and are prone to develop more severe disease.[1]

## Epidemiology

Histoplasmosis is distributed worldwide but endemic in the Americas, Africa, and Asia. The actual incidence of histoplasmosis is not known, as the majority of the studies done on this subject have been limited to regions affected by outbreaks of the disease. Globally, about half a million people get infected with *Histoplasma* infection every year. However, approximately 100,000 people develop disseminated histoplasmosis,[2] which is associated with high mortality rates (ranging between 30–50% if treated and 100% if not).[3–5] In North America, the area of highest endemicity is in the Mississippi and Ohio River Valleys of the USA. In these areas, the incidence of histoplasmosis reaches up to an estimated 6.1 cases per 100,000.[6,7] Through a 2011–2014 surveillance of cases in the USA, state-specific annual incidence rates were found to range from 0 to 4.3/100,000 population.[8]

A recent systematic literature review of both case volume and type of histoplasmosis in Southeast Asia, excluding the Indian sub-continent, found a total of 407 cases.[9] Most cases (255 (63%)) were disseminated histoplasmosis.[9] The highest burden of histoplasmosis was noted in Myanmar, Bali, and Surabaya in Indonesia, Ho ChiMinh City in Vietnam, southern Thailand, and north Luzon in the Philippines. In the East African region, a study from Northern Tanzania retrospectively identified 9 (0.9%) cases of probable histoplasmosis among 970 febrile in-patients.[10]

In Bangladesh, all variants of fungal infections are tracked and some studies have documented their frequency. In a study of 3,435 patients attending a dermatology clinic, 601 (17.5%) were diagnosed with superficial fungus infections.[11] Deep mycoses are also an important evolving problem, as evidenced by reports of 16 cases of histoplasmosis with varying clinical manifestations.[12,13] Isolated hepatic histoplasmosis is an uncommon condition; liver involvement is commonly associated with disseminated histoplasmosis. *H. capsulatum* has been recovered from soil of the Gangetic plains.[14] When soil is disturbed by construction or excavation, the spores become airborne and are then inhaled.[15] Considering the likeness of geo-climatic conditions, it is possible that many more cases of histoplasmosis occur in Bangladesh than are currently documented.

## Pathogenesis

Upon inhalation of airborne spores, once they reach the alveoli, they convert to a yeast form, which is the tissue-invasive form. The current multiplying yeasts are then phagocytosed by alveolar macrophages, that are initially incapable of killing the fungus. The ingested yeasts multiply inside the macrophages and during the pre-immune phase of the illness, and they are then spread throughout the body via the lymphatics to organs rich in reticuloendothelial cells.[16]

**Keywords:** *Histoplasma capsulatum*; Histoplasmosis; Hepatic manifestation; Mycosis.

**Abbreviations:** AIDS, acquired immune deficiency syndrome; GGT, γ-glutamyl transferase.

[*]**Correspondence to:** Md Benzamin, Department of Paediatric Gastroenterology & Nutrition, Bangabandhu Shiekh Mujib Medical University (BSMMU), Dhaka, Bangladesh. ORCID: https://orcid.org/0000-0002-8239-6541. Tel: +88-1719183948, E-mail: drmd.benzamin@yahoo.com

Hematogenous dissemination usually occurs before cellular immunity develops, during the first 2 weeks.[17] In an immunocompetent host, once sufficient cell-mediated immunity develops, the infection is eliminated by cytokines (e.g., interferon-γ and interleukin-12) which aid macrophages in either killing the organism or halting their progression by forming a calcified granuloma.[18] In immunosuppressed patients, especially those with defective cell-mediated immunity, these defense mechanisms are impaired, causing reactivation of old foci or a progressive dissemination involving the extra-pulmonary tissues.[19] The typical incubation period is 7–21 days.[15]

## Predisposing factors

A variety of conditions can predispose to disseminated histoplasmosis, such as immunocompromised condition (i.e. acquired immune deficiency syndrome (AIDS)), taking of immunosuppressive medications (i.e. glucocorticoids, anti-rejection therapies in solid organ transplantation, or TNF-α inhibitor therapies), primary immunodeficiency, and extremes of age.[20–22]

## Clinical features

Histoplasmosis can present in various forms, including:

- Asymptomatic primary infection
- Acute pulmonary histoplasmosis
- Sequelae: mediastinal granuloma, rheumatologic syndromes, pericarditis
- Chronic pulmonary histoplasmosis
- Disseminated histoplasmosis
- Other: mediastinal fibrosis, broncholithiasis, central nervous system histoplasmosis, gastrointestinal histoplasmosis, hepatic histoplasmosis.[19,23]

The most common symptoms of the disseminated forms are fever (89.1%), respiratory symptoms (38.1%), weight loss (37.4%), and various common signs, including splenomegaly (72%), hepatomegaly (68.1%) and lymphadenopathy (41.2%).[24] Initial infection occurs in the lung alveoli, and then is transformed by the reticuloendothelial system and spread to various organs, resulting in progressive disseminated histoplasmosis.[23]

## Hepatic histoplasmosis

Hepatic histoplasmosis can occur both in children and adults, in immunocompetent and immunocompromised patients, and in endemic and nonendemic areas.[24] Hepatic involvement is frequent in disseminated histoplasmosis. The liver is reportedly involved in about 90% of patients with disseminated histoplasmosis.[25] However, liver histoplasmosis as a primary sign of histoplasmosis without lung involvement is uncommon. Patients with primary liver involvement usually present with nonspecific symptoms, such as fever, fatigue, nausea, vomiting, weight loss, and elevation of liver enzymes. They may present with stigmata of chronic liver disease, portal hypertension, ascites, and/or varices. These features may be due to chronic parenchymal liver disease resulting from histoplasma-induced liver injury. The full spectrum of hepatic manifestations of this disease is unknown but spans the range in the literature from mildly abnormal liver enzymes to severe icteric cholestasis with fever and pain.[24–26]

*H.capsulatum* is an uncommon cause of granulomatous liver disease. There are few case reports on hepatic histoplasmosis with atypical presentations. Sartin *et al*.[27] from the Mayo Clinic (Rochester, MN, USA) found histoplasmosis comprised 4.5% (4 of 88) of cases of idiopathic granulomatous disease. Cholestasis due to *H. capsulatum* in the setting of primary liver manifestation has been rarely detected. Only a few case reports of liver biopsy-proven histoplasmosis have reported associated cholestasis.[25,28–30]

The typical clinical presentations are fever and jaundice in the setting of immunosuppression. Right upper quadrant pain might be confused with biliary colic in cases of cholestatic hepatitis secondary to disseminated histoplasmosis.[24] Clinically, these patients are usually symptomatic with elevated liver enzymes and pyrexia of unknown origin.[31] There is one case report in the publicly available literature that describes a patient with acute cholestatic granulomatous hepatitis with disseminated histoplasmosis.[24] Obstruction by peri-portal lymph nodes results in obstructive jaundice.[20] Two case reports by Park *et al*.[24] and Kothadia *et al*.[30] describe patients who underwent laparoscopic cholecystectomy for uncertain etiology shortly before being diagnosed with disseminated histoplasmosis. Nahar *et al*.[28] reported a patient with disseminated histoplasmosis that presented as chronic liver disease with portal hypertension.

## Diagnosis

Disseminated histoplasmosis can be diagnosed using various methods, like antigen detection, cultures, serology, or direct microscopy. Recovery of the organism from a biologic extra-pulmonary specimen is the gold standard.[16]

Laboratory values are highly variable for this disease. Transaminase levels are usually above the upper limit of normal, and the elevated alkaline phosphatase level is often as high as >2,100 U/L. In addition, high total bilirubin is usually associated with a concomitant rise in direct bilirubin, and γ-glutamyl transpeptidase (GGT) is significantly elevated as demonstrated by the case reported by Gill *et al*.[31] A liver biopsy is often obtained in conjunction with serum and urine antigen studies to establish the diagnosis.

The tissue response in histoplasmosis causes granulomas that are visible by histopathologic examinations. Grocott-Gomorimethenamine-silver nitrate and periodic acid-Schiff stains are useful for visualizing *Histoplasma* organisms in tissues. The early lesions in the tissue specimen contain a large number of macrophages and lymphocytes, with occasional epithelioid cells and multinucleated giant cells. Histological examination shows varying degrees of central caseation and occasionally calcification. Areas of caseous necrosis with a surrounding fibrous capsule which prevents the spread of the organism are characteristic. *H. capsulatum* may also be seen in tissues inside macrophages (Fig. 1).[29] If features of portal hypertension are present, then esophagogastrodudenoscopy should be performed to identify and evaluate varices (Fig. 2).[28]

## Treatment

Prompt diagnosis and initiation of antifungal therapy are crucial in immunocompromised, who otherwise have a fatality rate of 100% if left untreated,[8] The agents most commonly used for the treatment of histoplasmosis are amphotericin B and itraconazole. For moderately severe to severe disease, liposomal amphotericin B (3mg/kg/day) is suggested for 1–2 weeks, followed by oral itraconazole (200mg thrice daily for 3 days and then 200mg twice daily for a total of at least 12 months). Liposomal formulation is preferred to deoxycholate, due to its superior side effect profile, better response rate, and survival benefit. Patients with mild-to-moderate disease can be treated with itraconazole.[30]

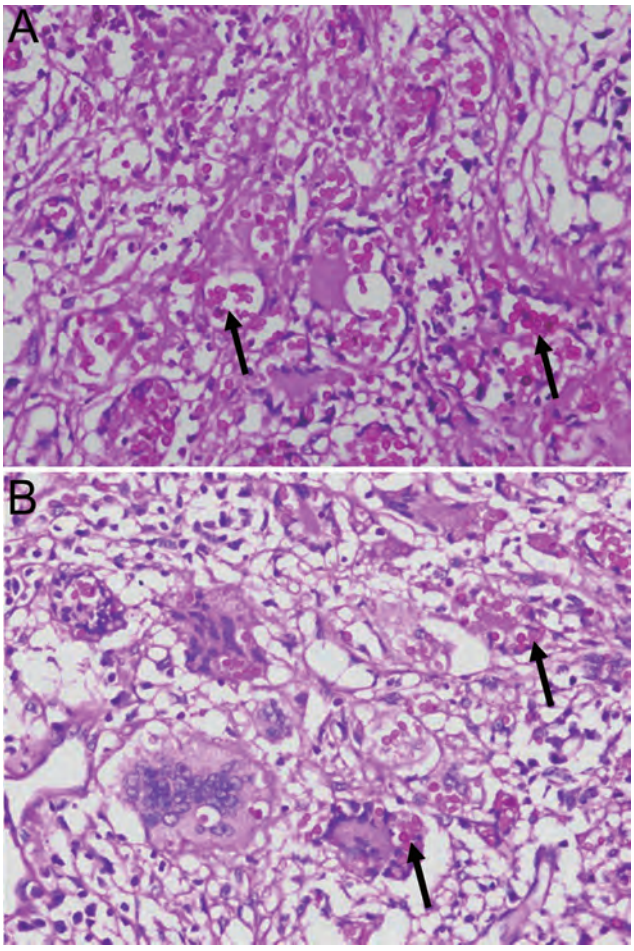


**Fig. 1. Histopathological examination.** (A, B) Representative staining samples. Arrows indicate *H. capsulatum*.

## Monitoring

Antigen levels in urine can be used to monitor the response to treatment. Antigen levels usually decline by the end of 12 weeks, and more rapidly in serum than in urine. Most of the decline in antigen level was seen in the first 2 weeks of therapy.[32] An increase in antigen concentration indicates relapse or treatment failure, and further evaluation of the adequacy of treatment is needed.[22]

## Conclusions

The liver is involved in about 90% of patients with disseminated histoplasmosis. Hepatic histoplasmosis can present as granulomatous hepatitis, as stigmata of chronic liver disease, portal hypertension, comprising ascites or varices, or with elevated liver enzymes. The most common hepatic finding seen on liver biopsy is portal lymphohistiocytic inflammation. Discrete hepatic granulomas are found in less than 20% cases of involved livers. There are limited case reports of disseminated histoplasmosis presenting as primary hepatic histoplasmosis. A high clinical suspicion is warranted in patients who present with stigmata of chronic liver disease and portal hypertension with no evidence of cirrhosis, especially if the person lives in or has visited an endemic area.[28]

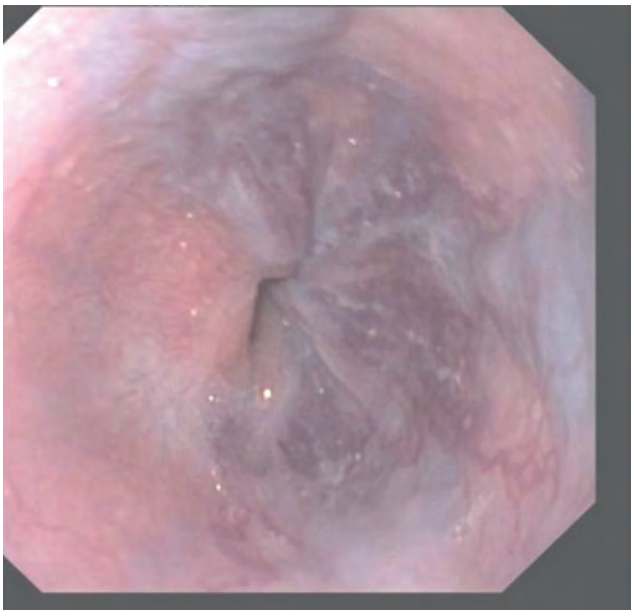

**Fig. 2. Large esophageal varices in a child with disseminated histoplasmosis.**

## Funding

None to declare.

## Conflict of interest

The authors have no conflict of interests related to this publication.

## Author contributions

Literature review (MS, MB, LN, MR, ASA), manuscript writing (MS, MB), histopathology and endoscopy picture collection, and manuscript editing (LN, MR, ASA).

## References

[1] Cano MV, Hajjeh RA. The epidemiology of histoplasmosis: a review. Semin Respir Infect 2001;16(2):109–118. doi:10.1053/srin.2001.24241.
[2] Denning DW. Minimizing fungal disease deaths will allow the UNAIDS target of reducing annual AIDS deaths below 500 000 by 2020 to be realized. Philos Trans R Soc Lond B Biol Sci 2016;371(1709):20150468. doi:10.1098/rstb.2015.0468.
[3] Adenis A, Nacher M, Hanf M, Vantilcke V, Boukhari R, Blachet D, *et al*. HIV-associated histoplasmosis early mortality and incidence trends: from neglect to priority. PLoS Negl Trop Dis 2014;8(8):e3100. doi:10.1371/journal.pntd.0003100.
[4] Brown GD, Denning DW, Gow NA, Levitz SM, Netea MG, White TC. Hidden killers: human fungal infections. Sci Transl Med 2012;4(165):165rv13. doi:10.1126/scitranslmed.3004404.
[5] Almeida MA, Almeida-Silva F, Guimarães AJ, Almeida-Paes R, Zancopé-Oliveira RM. The occurrence of histoplasmosis in Brazil: A systematic review. Int J Infect Dis 2019;86:147–156. doi:10.1016/j.ijid.2019.07.009.
[6] Manos NE, Ferebee SH, Kerschbaum WF. Geographic variation in the prevalence of histoplasmin sensitivity. Dis Chest 1956;29(6):649–668. doi:10.1378/chest.29.6.649.
[7] Baddley JW, Winthrop KL, Patkar NM, Delzell E, Beukelman T, Xie F, *et al*. Geographic distribution of endemic fungal infections among older persons, United States. Emerg Infect Dis 2011;17(9):1664–1669. doi:10.3201/eid1709.101987.
[8] Armstrong PA, Jackson BR, Haselow D, Fields V, Ireland M, Austin C, *et al*. Multistate epidemiology of histoplasmosis, United States, 2011-2014. Emerg Infect Dis 2018;24(3):425–431. doi:10.3201/eid2403.171258.

[9] Baker J, Setianingrum F, Wahyuningsih R, Denning DW. Mapping histoplasmosis in South East Asia - implications for diagnosis in AIDS. Emerg Microbes Infect 2019;8(1):1139–1145. doi:10.1080/22221751.2019.1644539.
[10] Lofgren SM, Kirsch EJ, Maro VP, Morrissey AB, Msuya LJ, Kinabo GD, *et al*. Histoplasmosis among hospitalized febrile patients in northern Tanzania. Trans R Soc Trop Med Hyg 2012;106(8):504–507. doi:10.1016/j.trstmh.2012.05.009.
[11] Rehman MH, Hadiuzzaman Md, Bhuiyan MKJ, Islam N, Ansari NP, Mumu SA, *et al*. Prevalence of superficial fungal infections in the rural areas of Bangladesh. Iran Journal of Dermatology 2011;14(3):86–91.
[12] Parvin R, Amin R, Mahbub MS, Hasnain M, Arif KM, Miah MT, *et al*. Deep fungal infection-an emerging problem in Bangladesh. J Medicine 2010;11(2):170–175. doi:10.3329/jom.v11i2.5466.
[13] Mahbub MS, Ahasan HN, Miah MT, Alam MB, Gupta RD, Arif KM, *et al*. Disseminated histoplasmosis. J Medicine 2010;11(1):70–73. doi:10.3329/jom.v11i1.4278.
[14] Antinori S. Histoplasma capsulatum: more widespread than previously thought. Am J Trop Med Hyg 2014;90(6):982–983. doi:10.4269/ajtmh.14-0175.
[15] Deepe GS. 265 - Histoplasma capsulatum (Histoplasmosis). In: Bennett JE, Dolin R, Blaser MJ, editors. Mandell, Douglas, and Bennett's principles and practice of infectious diseases (Eighth Edition). Philadelphia: Content Repository Only; 2015. p. 2949–2962.e1.
[16] Schlossberg D. Clinical infectious disease. Cambridge University Press; 2008.
[17] Fojtasek MF, Sherman MR, Garringer T, Blair R, Wheat LJ, Schnizlein-Bick CT. Local immunity in lung-associated lymph nodes in a murine model of pulmonary histoplasmosis. Infect Immun 1993;61(11):4607–4614. doi:10.1128/iai.61.11.4607-4614.1993.
[18] Zhou P, Sieve MC, Tewari RP, Seder RA. Interleukin-12 modulates the protective immune response in SCID mice infected with Histoplasma capsulatum. Infect Immun 1997;65(3):936–942. doi:10.1128/IAI.65.3.936-942.1997.
[19] Wheat J. Histoplasmosis. Experience during outbreaks in Indianapolis and review of the literature. Medicine (Baltimore) 1997;76(5):339–354. doi:10.1097/00005792-199709000-00002.
[20] Assi MA, Sandid MS, Baddour LM, Roberts GD, Walker RC. Systemic histoplasmosis: a 15-year retrospective institutional review of 111 patients. Medicine (Baltimore) 2007;86(3):162–169. doi:10.1097/md.0b013e3180679130.
[21] Wheat LJ, Slama TG, Norton JA, Kohler RB, Eitzen HE, French ML, *et al*. Risk factors for disseminated or fatal histoplasmosis. Analysis of a large urban outbreak. Ann Intern Med 1982;96(2):159–163. doi:10.7326/0003-4819-96-2-159.
[22] Kauffman CA. Histoplasmosis: a clinical and laboratory update. Clin Microbiol Rev 2007;20(1):115–132. doi:10.1128/CMR.00027-06.
[23] Wheat J, Sarosi G, McKinsey D, Hamill R, Bradsher R, Johnson P, *et al*. Practice guidelines for the management of patients with histoplasmosis. Infectious Diseases Society of America. Clin Infect Dis 2000;30(4):688–695. doi:10.1086/313752.
[24] Lamps LW, Molina CP, West AB, Haggitt RC, Scott MA. The pathologic spectrum of gastrointestinal and hepatic histoplasmosis. Am J Clin Pathol 2000;113(1):64–72. doi:10.1309/X0Y2-P3GY-TWE8-DM02.
[25] Goodwin RA Jr, Shapiro JL, Thurman GH, Thurman SS, Des Prez RM. Disseminated histoplasmosis: clinical and pathologic correlations. Medicine (Baltimore) 1980;59(1):1–33.
[26] Rihana NA, Kandula M, Velez A, Dahal K, O'Neill EB. Histoplasmosis presenting as granulomatous hepatitis: case report and review of the literature. Case Rep Med 2014;2014:879535. doi:10.1155/2014/879535.
[27] Wood A, Abushamma S, Esfeh JM. Extrapulmonary hepatic histoplasmosis presenting as chronic liver disease: A case report. American Journal of Gastroenterology 2018;113:S1275–S1276.
[28] Nahar L, Benzamin M, Sarkar N, Roy U, Nahar K, Rukunuzzaman M, *et al*. A 8- year Bangladeshi girl with disseminated histoplasmosis, presented as chronic liver disease with portal hypertension: a rare case report. BMC Pediatr 2020;20(1):284. doi:10.1186/s12887-020-02189-4.
[29] Wheat LJ. Laboratory diagnosis of histoplasmosis: update 2000. Semin Respir Infect 2001;16(2):131–140. doi:10.1053/srin.2001.24243.
[30] Wheat LJ, Freifeld AG, Kleiman MB, Baddley JW, McKinsey DS, Loyd JE, *et al*. Clinical practice guidelines for the management of patients with histoplasmosis: 2007 update by the Infectious Diseases Society of America. Clin Infect Dis 2007;45(7):807–825. doi:10.1086/521259.
[31] Gill D, Dean R, Virk J, Lyons M, Hess M. Unusual presentation of disseminated histoplasmosis. Am J Emerg Med 2017;35(4):668.e3–668.e4. doi:10.1016/j.ajem.2016.11.013.
[32] Hage CA, Kirsch EJ, Stump TE, Kauffman CA, Goldman M, Connolly P, *et al*. Histoplasma antigen clearance during treatment of histoplasmosis in patients with AIDS determined by a quantitative antigen enzyme immunoassay. Clin Vaccine Immunol 2011;18(4):661–666. doi:10.1128/CVI.00389-10.

*Journal of Clinical and Translational Hepatology* **2022** vol. 10(4) | 730–739
DOI: 10.14218/JCTH.2021.00494

Review Article

# Current Evidence Concerning Effects of Ketogenic Diet and Intermittent Fasting in Patients with Nonalcoholic Fatty Liver

Pimsiri Sripongpun[1], Chaitong Churuangsuk[2] and Chalermrat Bunchorntavakul[3*]

[1]*Gastroenterology and Hepatology Unit, Division of Internal Medicine, Faculty of Medicine, Prince of Songkla University, Hat Yai, Thailand;* [2]*Nutrition and Obesity Management Unit, Division of Internal Medicine, Faculty of Medicine, Prince of Songkla University, Hat Yai, Thailand;* [3]*Division of Gastroenterology and Hepatology, Department of Medicine, Rajavithi Hospital, Rangsit University, Bangkok, Thailand*

**Received:** 1 November 2021 | **Revised:** 4 February 2022 | **Accepted:** 10 April 2022 | **Published:** 6 May 2022

## Abstract

Nonalcoholic fatty liver disease (NAFLD) is emerging globally, while no therapeutic medication has been approved as an effective treatment to date, lifestyle intervention through dietary modification and physical exercise plays a critical role in NAFLD management. In terms of dietary modification, Mediterranean diet is the most studied dietary pattern and is recommended in many guidelines, however, it may not be feasible and affordable for many patients. Recently, a ketogenic diet and intermittent fasting have gained public attention and have been studied in the role of weight management. This article reviews specifically whether these trendy dietary patterns have an effect on NAFLD outcomes regarding intrahepatic fat content, fibrosis, and liver enzymes, the scientific rationales behind these particular dietary patterns, as well as the safety concerns in some certain patient groups.

**Citation of this article:** Sripongpun P, Churuangsuk C, Bunchorntavakul C. Current Evidence Concerning Effects of a Ketogenic Diet and Intermittent Fasting in Patients with Nonalcoholic Fatty Liver. J Clin Transl Hepatol 2022;10(4): 730–739. doi: 10.14218/JCTH.2021.00494.

## Introduction

Nonalcoholic fatty liver disease (NAFLD), recently named as metabolic-associated fatty liver disease, is a major noncommunicable disease pandemic, currently affecting approximately 25% of the global population.[1] The trend of NAFLD incidence has been increasing worldwide together with those of obesity and metabolic syndrome.[2] Although the efficacies of various pharmacologic treatments in NAFLD management have been studied, no effective medication has been proven and recommended as a standard treatment of NAFLD; lifestyle intervention remains the mainstay of management.

Generally, clinical practice guidelines of major international hepatology associations concordantly recommend weight reduction ≥7–10% in overweight or obese patients with NAFLD via hypocaloric diet,[3] in combination with more physical exercise.[4–6] Notably, successful weight reduction is associated with a reduction in liver enzyme levels and an improvement in histological findings related to liver steatosis, inflammation, and fibrosis.[4–6] However, a 7–10% weight loss is not easily achievable or sustainable even in the context of clinical trials. Moreover, one-fifth of patients with NAFLD were classified as lean and 40% were non-obese;[7] hypocaloric diet may not be the most appropriate treatment for such patients. Therefore, the effect of exposure to dietary patterns on weight reduction, and its benefit beyond weight loss, has been studied in patients with NAFLD.

The Mediterranean diet is the most evaluated dietary pattern in patients with NAFLD; most NAFLD guidelines have established its beneficial effects.[4–6] The Mediterranean diet is characterized by a high intake of vegetables, nuts, legumes, olive oil, fruits, whole grains, and fish, with a low intake of red meat, sugars, and refined carbohydrates.[8] Nonetheless, in other parts of the world, such as low-income countries and those with food insecurity, that dietary pattern may not be feasible for many people with NAFLD because energy-dense, high-fat, high-sugar, or processed foods are more palatable and affordable than the Mediterranean-style diet.[9,10]

In recent years, there has been a paramount interest in two dietary patterns, ketogenic diets and intermittent fasting (IF), and their benefits in the management of various health conditions have been evaluated. In this review, we focus on the role of the aforementioned dietary patterns on liver-related outcomes in patients with NAFLD. In the current review, we performed a comprehensive search regarding the effectiveness of a ketogenic diet or IF on NAFLD using the search terms ("ketogenic diet" OR "intermittent fasting") AND "fatty liver" in PubMed and Web of Science database from inception to October 10, 2021. As we focused exclusively on liver outcomes, only studies including patients with documented NAFLD, not only overweight/obese patients, and available outcomes of liver fat/intrahepatic triglycerides or liver fibrosis were reviewed and summarized in this article. The details of the literature search for the studies included in Tables 1 and

**Keywords:** Nonalcoholic fatty liver disease; Ketogenic diet, Intermittent fasting; Lifestyle modification; Weight reduction.

**Abbreviations:** ADF, alternate-day fasting; ALT, alanine transaminase; BHB, β-hydroxybutyrate; BMI, body mass index; IF, intermittent fasting; IL, interleukin; MED/LC, Mediterranean plus low-calorie diet; NAFLD, nonalcoholic fatty liver disease; RCT, randomized controlled trial; RF, Ramadan fasting; SoC, standard of care; TRF, time-restricted fasting; VLCKD, very low carbohydrate ketogenic diet.

***Correspondence to:** Chalermrat Bunchorntavakul, Division of Gastroenterology and Hepatology, Department of Medicine, Rajavithi Hospital, College of Medicine, Rangsit University, Phayathai Road, Ratchathewi District, Bangkok 10400, Thailand. ORCID: https://orcid.org/0000-0002-8842-032X. Tel.: +66-2-354-8108-9, Fax: +66-2-3548179, E-mail: dr.chalermrat@gmail.com

**Table 1. Characteristics of individual VLCKD studies and their outcomes in patients with NAFLD**

| Study | Type of study | No. of patients on VLCKD/ control | Control diet | Duration | VLCKD calories (Cal/d) | Control diet calories (Cal/d) | Weight reduction outcomes (estimated) | Liver fat or liver fibrosis outcomes | Liver enzymes outcomes |
|---|---|---|---|---|---|---|---|---|---|
| Tendler 2007[11] | Single arm | 5 | – | 6 months | Not reported | – | weight −10.9% | ↓ liver fat; ↓ fibrosis ($p$=0.07); by liver biopsy | ↔ |
| Pérez–Guisado 2011[21] | Single arm | 14 | – | 12 weeks | Not reported | – | BMI −4 kg/m$^2$ | ↓ liver fat by USG | improved |
| Yu 2014[22] | Single arm | 8 | – | 8 weeks | 800 | – | BMI −2.5 kg/m$^2$ | ↓ liver fat 67% | Not reported |
| Bian 2014[23] | Single arm | 17 | – | 6 days | 1,000 | – | weight −3 kg | ↓ liver fat 27% | ↔ |
| Mardinoglu 2018[12] | Single arm | 10 | – | 2 weeks | 3,115 | – | weight −1.8% | ↓ liver fat 43.8% | Not reported |
| Ministrini 2019[24] | Single arm | 52 | – | 25 days | 800 | – | BMI −2.7 kg/m$^2$ | ↓ liver fat by USG | ↑ AST/ ALT |
| Luukkonen 2020[25] | Single arm | 10 | – | 6 days | 1,440 | – | weight −3% | ↓ liver fat 31%; ↔ fibrosis | Not reported |
| D'Abbondanza 2020[26] | Single arm | 70 | – | 25 days | 800 | – | BMI −4 kg/m$^2$ | ↓ liver fat by USG | ↔ |
| Wolver 2020[13] (abstract only) | Single arm | 30 | – | 6 months | Not reported | – | BMI −4.4 kg/m$^2$ | ↓ liver fat by CAP 15%; ↓ fibrosis by liver stiffness measurement 12.3 to 6.8 kPa | ↓ ALT |
| Browning 2011[27] | Comparative (non–RCT) | 9/9 | Low calorie diet | 2 weeks | 1,553 | 1,325 | weight −5 kg VLCKD/−4 kg control | ↓ liver fat 31% VLCKD vs. 28% control | ↔ |
| Kirk 2009[14] | RCT | 11/11 | High carbohydrate content, equal calories | 11 weeks | 1,100 | 1,100 | weight −7.6% vs. −7.3% | ↓ liver fat 45 % VLCKD vs. 55% control | ↔ |
| Cunha 2020[28] | RCT | 20/19 | Low calorie diet | 2 months | 600–800 | 1,400–1,800 | weight −9.7 vs. −1.67 kg | ↓ liver fat 38.5% VLCKD vs. −2.7% control; ↔ fibrosis | ↔ |
| Holmer 2021[15] | RCT | 25/24 | Standard of care | 12 weeks | −184.1 from baseline | −282.9 from baseline | weight −7.7% vs. −2.6% | ↓ liver fat by CAP 61.9 vs. 20.2 dB/m; ↔ fibrosis | ↓ ALT both arms |
| Gepner 2019[16] | RCT but on VLCKD for only 2 months then up to 70 gm/d and Med/LC | 139/139 | Low fat diet | 18 months | −26% from baseline | −22% from baseline | Not reported | ↓ liver fat 4.2% (absolute unit) in Med/LC vs. 3.8% control | Not reported |

ALT, alanine aminotransferase; AST, aspartate aminotransferase; BMI, body mass index; CAP, controlled attenuation parameter; Med/LC, Mediterranean plus low-calorie diet, NAFLD, nonalcoholic fatty liver disease; RCT, randomized controlled trial; USG, ultrasonography; VLCKD, very low carbohydrate ketogenic diet.

**Table 2. Characteristics of individual IF studies and their outcomes in patients with NAFLD**

| Study | Type of study | No. of patients on IF/control | IF type | Control diet | Duration | IF calories (Cal/d) | Control diet calories (Cal/d) | Weight reduction outcomes (estimated) | Liver fat or liver fibrosis outcomes | Liver enzymes outcomes |
|---|---|---|---|---|---|---|---|---|---|---|
| Ebrahimi 2020[17] | Observational | 42/41 | Ramadan | Non–fasting | 1 month | 1,970 | 2,150 | BMI −0.8 vs. −0.02 kg/m$^2$ | ↓ liver fat by USG in IF group | Improved |
| Hodge 2014[20] (abstract only) | RCT | 17/15 | TRF 8:16 | Standard of care | 12 weeks | Not reported | Not reported | BMI −1 vs. −1 kg/m$^2$ | ↓ liver fat by CAP (IF 287 to 263 dB/m, $p$=0.012; control=NS); ↓ fibrosis by TE (IF 7.33 to 5.84 kPa, $p$=0.0088; control=NS) | Not reported |
| Johari 2019[19] | RCT | 33/10 | ADF (70% calories) | Usual habitual diet | 8 weeks | Not reported | Not reported | weight ↓ 3.06 kg more than control | ↓ liver fat by USG in IF group; ↓ fibrosis by SWE 0.74 kPa more than control | Improved |
| Cai 2019[18] | RCT | 95/79 | ADF (25% calories) | 80% calories | 12 weeks | 1,327 feed/330 fast | 1,309 | weight −6.1% IF vs. −2.54% control | No report liver on fat; But ↓ fat mass by DXA than control; ↔ fibrosis | Not reported |
| Cai 2019[18] | RCT | 97/79 | TRF 8:16 | 80% calories | 12 weeks | 1,358 | 1,309 | weight −4.8% IF vs. −2.54% control | No report on liver fat; but ↓ fat mass by DXA than control; ↔ fibrosis | Not reported |
| Holmer 2021[15] | RCT | 25/24 | 5:2 | Standard of care | 12 weeks | −587.8 from baseline | −282.9 from baseline | weight −7.4% IF vs. −2.6% control | ↓ liver fat by CAP 63.8 vs. 20.2 dB/m; ↓ fibrosis by TE 1.8 vs. 1.5 kPa control | ↓ ALT both arms |

ADF, alternate-day fasting; ALT, alanine aminotransferase; BMI, body mass index; CAP, controlled attenuation parameter; DXA, dual-energy X-ray absorptiometry; IF, intermediate fasting; Med/LC, Mediterranean plus low-calorie diet, NAFLD, nonalcoholic fatty liver disease; NS, not significant; RCT, randomized controlled trial; SWE, shear wave elastography; TE, transient elastography; TRF, time-restricted fasting; USG, ultrasonography.

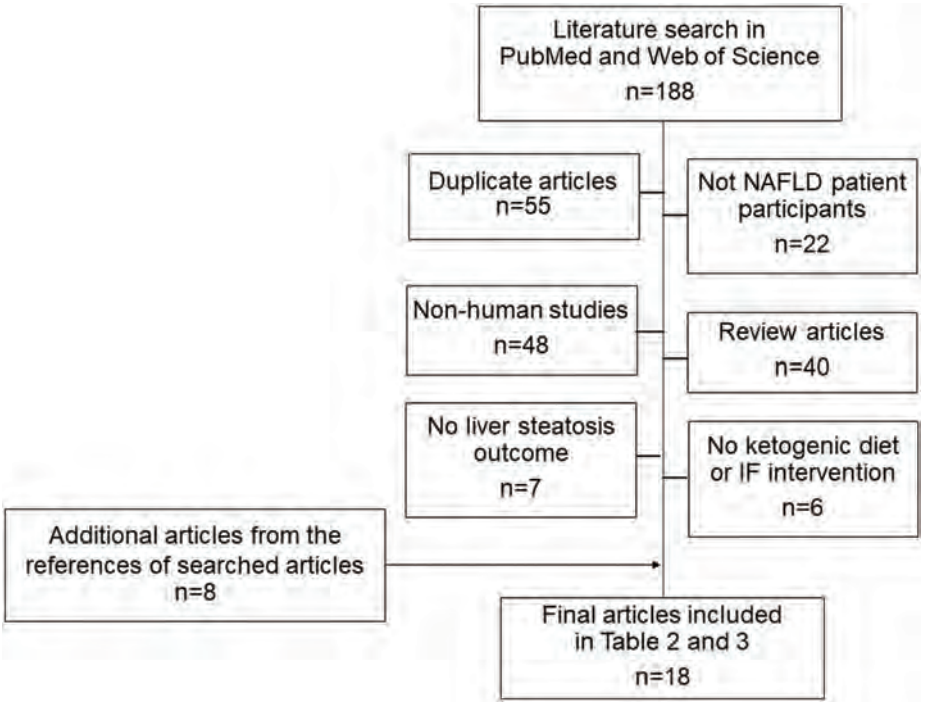


**Fig. 1. Literature search for the studies included in Tables 1 and 2.**

2 are shown in Figure 1.[11–28] Of the 18 studies included, two were available only in abstract form (see the Tables 1 and 2). PS performed the literature search and CB double checked the included studies. The outcomes beyond liver outcomes (e.g. cardiovascular, metabolic syndrome, and cancer including hepatocellular carcinoma) in patients with NAFLD were beyond the scope of this review and not included in this article.

## Ketogenic Diet

### *Rationale*

A ketogenic diet is one that induces ketosis. It can be a very low-calorie diet (<800 kcal/day) or very low carbohydrate diet that limits carbohydrate intake to <50 g/day and has an energy intake usually of >1,000 kcal/day).[29] Very low carbohydrate diets have gained much research interest in terms of health benefits and have become popular in lay public use and among some clinicians and nutrition scientists.[30,31] The current National Lipid Association Nutrition and Lifestyle Task Force classification of diets commonly confused with a ketogenic diet is shown in Table 3.[29] In this review, a very low carbohydrate ketogenic diet (VLCKD) is one that limits carbohydrate intake to <20–50 g/day or <10% of total energy intake, regardless of total daily energy intake.[32]

While emphasis is laid on carbohydrate intake, the types of fats and proteins that replace carbohydrates are less emphasized,[33] this usually results in a high intake of saturated fats and cholesterol, which is related to insulin resistance and cardiovascular risks.[29,34] The use of the ketogenic diet in patients with NAFLD stems from the notion that limiting carbohydrate intake results in relatively low blood glucose levels[34] leading to lower insulin levels, and thus in reduction of hepatic de novo lipogenesis.[35] Patients with NAFLD have high hepatic triglyceride levels resulting from three sources, de novo lipogenesis (mostly from glucose), lipolysis from adipose tissue, and dietary free fatty acids.[36] In healthy people, free fatty acids from adipose tissue contribute 60–80% of hepatic triglycerides, followed by dietary free fatty acids (15%), and de novo lipogenesis (5%).[36] On the other hand, the level of hepatic triglycerides generated from de novo lipogenesis is five times higher (26%) in patients with NAFLD than in healthy people (5%) because of insulin resistance in patients with NAFLD.[36] Given that *de novo* lipogenesis mostly results from the metabolism of

**Table 3. National Lipid Association Nutrition and Lifestyle Task Force classification of low carbohydrate, very low carbohydrate ketogenic, and very low-calorie diets[29]**

| Nomenclature | Ketogenic | Total calories per day | % Macronutrients in total calories per day | | |
|---|---|---|---|---|---|
| | | | CHO | Protein | Fat |
| VLCHF/KD | Yes | >1,000 | <10 (<20–50 g/day) | Around 10 (1.2–1.5 g/kg/day) | 70–80 |
| Low CHO | No | >1,000 | 10–25 (38–97 g/day) | 10–30 | 25–45 |
| Very low-calorie diet | Yes/No varies | <800 | Varies | Varies | Varies |
| Classic KD | Yes | Varies | 3 | 7 | 90 |

CHO, carbohydrate; KD, ketogenic diet; VLCHF, very low CHO.

circulating glucose, this physiological perspective could explain the promising role of ketogenic diet exposure in NAFLD management.

Nutritional ketosis, ketone bodies, generated in response to carbohydrate restriction could further facilitate weight loss by promoting satiety leading to reduction of total energy intake.[37] In addition, growing evidence has shown beneficial effects of ketone bodies in the inhibition of obesity-induced inflammation and oxidative stress and might play a role in modulating NAFLD pathophysiology. In particular, Youm *et al*.[38] reported that β-hydroxybutyrate (BHB) reduced NLRP3 inflammasome-mediated interleukin (IL)-1β and IL18 production in human monocytes together with an attenuation of IL1β secretion a in mouse model, a key inflammatory cytokine related to obesity and insulin resistance. Activation of NLRP3 inflammasome also had a central role in liver inflammation and fibrosis in a mouse model.[39] BHB is a ligand for hydroxycarboxylic acid receptor-2 ($HCA_2$), which is highly expressed in immune cells such as macrophages and monocytes, and has been shown to have anti-inflammatory properties in atherosclerosis, obesity, and cancer.[40] BHB is an epigenetic modifier by inhibiting histone deacetylase, resulting in histone acetylation, and expression of oxidative stress resistance gene.[41]

### *Evidence of ketogenic diet exposure effects on NAFLD outcomes*

The study that initially reported beneficial effects of VLCKD was published in 2007.[11] Tendler *et al*.[11] placed five patients with biopsy-proven NAFLD on a restricted diet of <20 g/day of carbohydrates for 6 months without total calorie restriction. At the end of the study period, the patients had an average weight reduction of 10.9%. On follow-up liver biopsy, a significant reduction in the degree of hepatic steatosis was observed, with a trend towards improvement in liver fibrosis ($p$=0.07). Table 1 summarizes the studies of VLCKD and effects on the outcomes of patients with NAFLD. The majority of studies on VLCKD had a single arm with a limited number of patients and involved caloric restriction below 1,200 kcal/day, resulting in significant weight loss and hepatic steatosis improvement. It is difficult to determine whether the reduction in hepatic fat content was caused by the VLCKD pattern or weight loss in general. Nonetheless, Mardinoglu *et al*.[12] conducted a single arm interventional study in which 10 Nordic patients with NAFLD were instructed to consume <30 g/day of carbohydrates, without total energy restriction. The average energy intake was 3,115 kcal/day). They observed a significant reduction in hepatic fat content of 43.8% despite a minimal weight loss of 1.8%. Another recent report from Wolver *et al*.[13] demonstrated interesting outcomes of VLCKD for 6-months. with significant improvement of both liver steatosis and liver fibrosis. However, this was a preliminary result of the study and presented in a conference abstract only, and no data regarding total calories per day were mentioned. The final results of that study are eagerly awaited.

A randomized controlled trial (RCT) by Kirk *et al*.,[14] observed a similar degree of weight loss in patients in VLCKD and low-calorie control diet. The intrahepatic triglyceride content decreased significantly from baseline but was not different in the two groups at the end of the study. More recently, Holmer *et al*.[15] conducted an RCT in patients with NAFLD who received a standard of care (SoC) or VLCKD for 12 weeks. Patients in the VLCKD arm experienced a significantly greater weight loss and intrahepatic fat content reduction, despite a smaller reduction in daily total energy intake. However, the benefit in terms of liver fibrosis was not demonstrated.

Previously, the largest RCT with a long-term follow-up duration was conducted by Gepner *et al*.[16] in 278 patients, with 139 on a VLCKD with 40 g/day of carbohydrates for 2 months and was gradually increased to 70 g/day for a total of 18 months with a Mediterranean-style diet (Med/LC). The control group included 139 patients on a low-fat diet for the 18 month period. The reduction in liver fat content was significantly greater in the Med/LC group than in the low-fat diet group. Unfortunately, liver fibrosis, the important surrogate marker of long-term outcomes in patients with NAFLD, was not reported. In addition, VLCKD exposure lasted only for the first 2 months of the total study period; hence, it was impossible to conclude whether the greater reduction in hepatic fat content was caused by the VLCKD or resulted from the beneficial effect of the Mediterranean-style diet.

Overall, based on the current evidence of VLCKD effects in patients with NAFLD, a significant reduction in intrahepatic fat content was observed in patients exposed to VLCKD. However, it is important to keep in mind that most data came from a combination of VLCKD with calorie restriction (hypocaloric diet). And the control arms in comparative studies, when the diets were hypo-energetic, the intrahepatic fat content was reduced as well. Without hypocaloric diet, the beneficial effect of VLCKD is yet to be defined. Furthermore, based on available data on isocaloric diet effects compared between patients exposed to low-fat, high-carbohydrate diets and in those exposed to high-fat, low-carbohydrate (above the VLCKD level) diets, intrahepatic fat content tended to be lower in patients exposed to low-fat diets than in those exposed to low-carbohydrate diets.[42]

### *Safety concerns*

Ketogenic diets require an extreme avoidance of carbohydrate foods to generate nutritional ketosis. Carbohydrates are a good source of vitamins, minerals, and bioactive compounds such as polyphenols, and thus long-term exposure to a ketogenic diet can result in micronutrient inadequacy or deficiency if the diet is not appropriately guided. Reduction in thiamine, folate, calcium, magnesium, iron, iodine, and fiber intake have been reported after ketogenic or low-carbohydrate diets.[43] Moreover, case reports have highlighted occurrences of Wernicke's encephalopathy, cardiac beriberi, and optic neuropathy in patients with low carbohydrate intake.[44,45]

As mentioned earlier, there is less emphasis on types of fat and protein consumed, which could contribute to different metabolic responses. The ketogenic diet is usually high in saturated fats, which increases LDL cholesterol levels and insulin resistance,[46,47] thereby potentially augmenting the risk of atherosclerotic cardiovascular diseases.[48,49] A longitudinal cohort study also showed that a high intake of animal fat and protein, in place of carbohydrates, is associated with high risk of mortality and type 2 diabetes.[50–52] Several recent case reports have highlighted the occurrence of ketoacidosis in people following ketogenic diets,[53–56] lactating women,[57,58] and patients with type 2 diabetes using SGLT-2 inhibitors reportedly have a higher risk of ketoacidosis.[59] Exacerbating panic and anxiety disorders in a woman on a ketogenic diet has been reported, probably resulting from diet-induced reductions brain serotonin and plasma tryptophan.[60]

Apart from possible adverse events of VLCKD in general, some had been reported in the studies of patients with NAFLD. Most of the studies did not report the adverse effects following VLCKD, however, muscle cramping had been reported in one patient in a study by Tendler *et al*.,[11] in

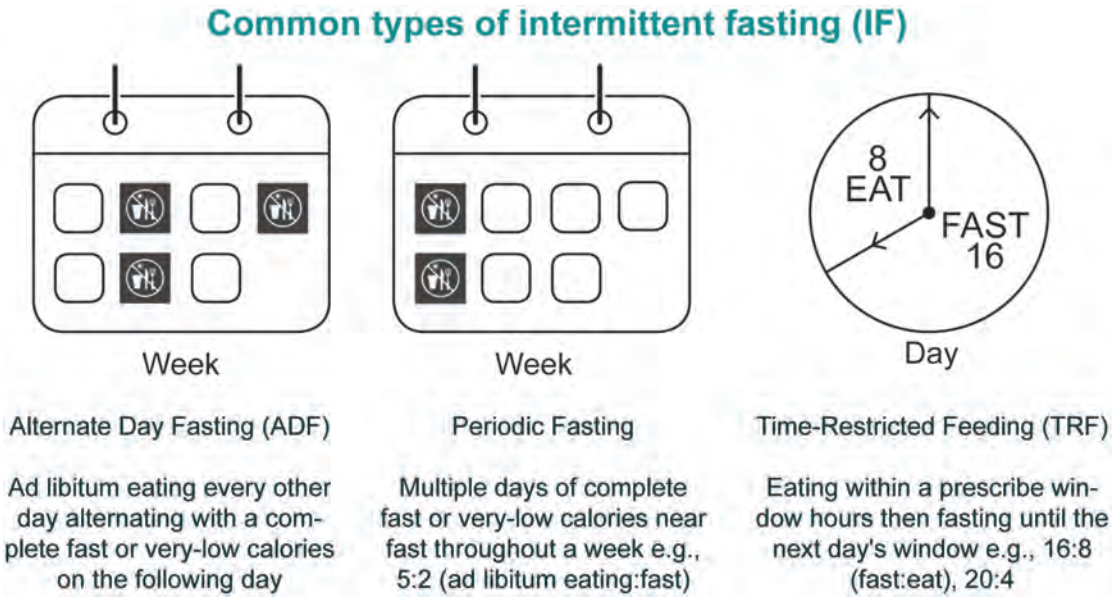


**Fig. 2. Common types of intermittent fasting (IF).**

and six of 25 patients in Holmer *et al*.[15] experienced either dyspepsia, nausea, headache, or vertigo, and felt that the diet was difficult to implement, which led to diet discontinuation in five patients. In addition, a case series reported that two cirrhotic patients tolerated VLCKD well for weight reduction for 28–30 weeks before liver transplantation without significant adverse effects.[61] Nonetheless, elevation of total bilirubin was observed at the end of the VLCKD period in both patients, and elevations in serum alanine transaminase (ALT) and creatinine were observed in one patient. In our opinion, more data are needed to confirm the safety of VLCKD in patients with cirrhosis.

## IF

### *Rationale*

IF refers to a period of voluntary abstinence from food and/or drink for caloric restriction, or no caloric intake over a specified period of time.[62] There are three types of IF, alternate-day fasting (ADF), periodic fasting, and time-restricted fasting (TRF).[63] The most well-known periodic fasting schedule is 5:2, which means having a regular diet for 5 days a week and fasting or near fasting for 2 days a week. The most well-known TRF schedule is 16:8, which means fasting for 16 h and eating for 8 h a day (Fig. 2). IF has gained attention as an effective strategy for weight loss in people with NAFLD, given that weight loss is the mainstay of NAFLD management for fat content and fibrosis extent reduction.[63] Generally, people following IF have approximately 10% or 300 kcal less energy intake than people taking normal diets or in non-fasting periods (Table 2). In addition, several health benefits of IF have been reported, including improvements in insulin resistance, inflammation, blood pressure, and blood cholesterol levels.[64] Extensive studies in rodents and non-human primates have demonstrated that the molecular mechanisms whereby dietary restriction promotes health and longevity primarily involve inhibition of mammalian target of rapamycin signaling, insulin/insulin-like growth factor signaling, growth hormone signaling, and autophagy pathways.[64]

### *Evidence of IF effects on NAFLD outcomes*

In contrast to VLCKD, IF or a time-restricted diet effects just have been recently studied in patients with NAFLD. Figure 2 depicts the common types of IF,[63,65] and Table 2 summarizes studies of the effect of IF on NAFLD outcomes. Ramadan is a holy month for Muslims and fasting is one of Islam's Five Pillars. Healthy adults are expected to practice Ramadan fasting (RF). Muslims who observe RF refrain from eating or drinking from dawn to sunset every day for 1 month.[17] Several studies have evaluated the effects of RF in NAFLD patients.[17,66–68] However, there was only one observational study evaluated the effects of RF on liver fat outcomes.[17] The study included 83 patients in Iran and demonstrated that those who fasted during Ramadan had greater weight loss and improvement in hepatic steatosis grade on ultrasound than those who did not fast. Improvements in liver enzymes and cholesterol levels were also observed in the RF group. Moreover, daily caloric intake appeared to be lower in patients who fasted.

Four RCTs investigating the effect of IF on the outcomes of patients with NAFLD who underwent different methods of fasting have been published. One was an abstract and three were published manuscripts. Two of the RCTs had conflicting results of the impact of ADF on patient outcomes. Cai *et al*.[18] randomly assigned patients to an ADF with a 25% caloric intake on fasting days or a control group for 12 weeks. Patients in ADF group had a lower daily energy intake, end-of-study weight, and total body fat mass. Nevertheless, the degree of liver fibrosis measured by transient elastography, was not improved and was comparable to that in the control group. Johari *et al*.,[19] whose study was published in the same year, reported greater weight loss, greater reduction in hepatic steatosis grade, and improved liver fibrosis measured by shear wave elastography in patients with modified ADF with 70% caloric intake during fasting days, compared with patients who consumed their usual diet for a duration of 8 weeks. Cai *et al*.[18] compared the outcomes of TRF using the 8:16 h method with SoC outcomes. Intriguingly, the TRF group had a greater weight loss than the SoC group even though the daily caloric intake appeared to be a little higher in the TRF group. The study showed no change in the extent of liver fibrosis, but the patients had a high degree

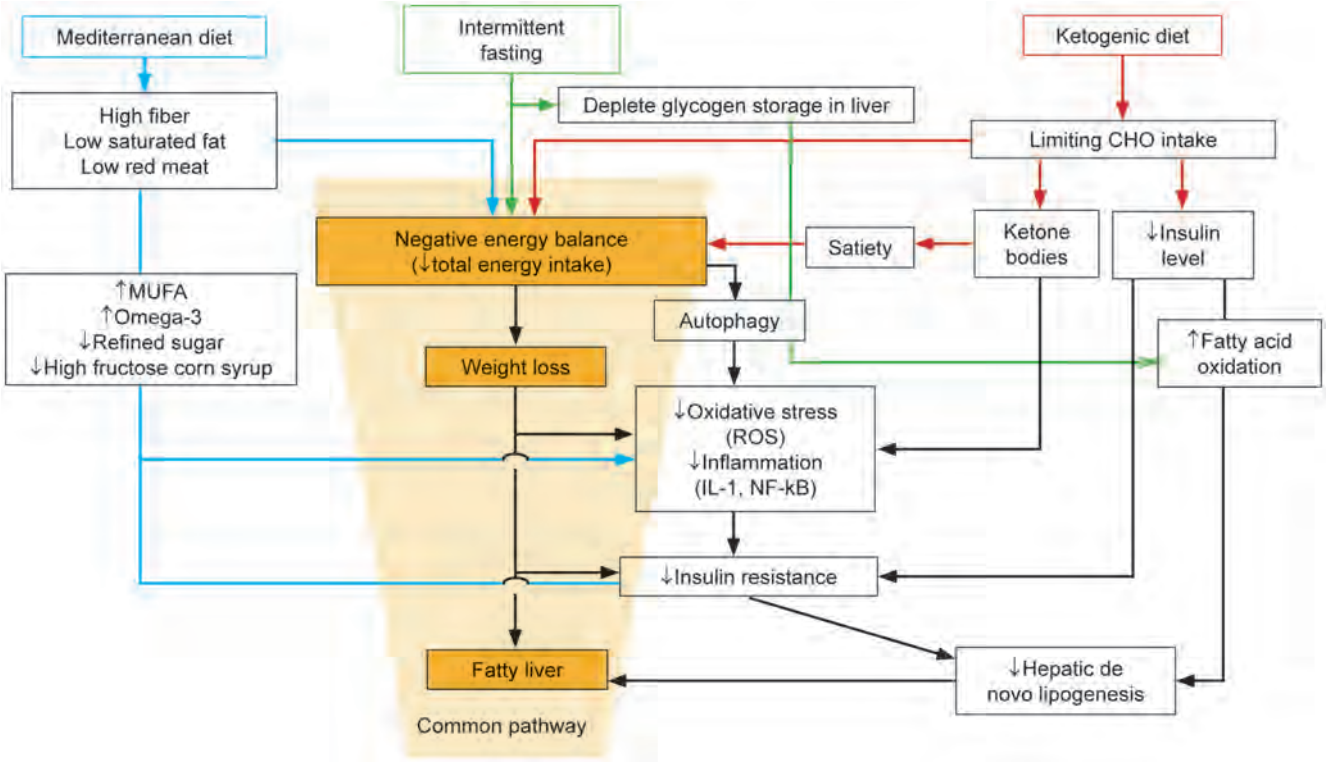


**Fig. 3. Proposed mechanistic pathways of Mediterranean diet, ketogenic diet and intermittent fasting for NAFLD.** NAFLD, nonalcoholic fatty liver disease.

of fibrosis, with a mean liver stiffness >18 kPa, which is comparable to stage 4 fibrosis or cirrhosis, in both groups. Hodge *et al*.[20] conducted an RCT using TRF as IF. Patients in IF arm had a significant reduction in both liver steatosis and liver fibrosis measured by liver stiffness. The same results were not observed in patients in the control group despite similar degrees of body mass index (BMI) reduction.[20] A recent RCT by Holmer *et al*.[15] evaluated and compared the effects of IF and SoC on patient outcome. The IF group used the 5:2 dietary approach with a caloric restriction of 500 cal/day in women and 600 kcal/day in men for two non-consecutive days per week. Patients in the IF group had a greater reduction in daily caloric intake, lost more weight, and had a greater reduction in hepatic steatosis than those in the SoC group. Moreover, an improvement in hepatic fibrosis measured by transient elastography was observed in both groups. Notably, liver stiffness improvement was numerically higher in the IF than in the SoC group (1.8 vs. 1.5 kPa). In spite of the better liver-related outcomes reported in both observational RF studies and RCTs compared with controls, it is unclear whether the improved outcomes resulted from IF or weight loss. Notwithstanding, IF may be a viable alternative for patients who are unable to maintain weight control by daily caloric restriction.

### *Safety concerns*

IF is simple and relatively safe for most people, with fewer safety concerns compared with a ketogenic diet. Possible concerns related to IF include hypoglycemia in patients with diabetes receiving insulin therapy or insulinogenic drugs and hypotension in patients taking antihypertensive medications. In addition, in patients with liver cirrhosis undergoing IF, overnight fasting can mimic 72 h starvation, resulting in malnutrition and increased complications. IF can also aggravate starvation effects, thereby causing negative outcomes. In the clinical trials of IF in patients with NAFLD, most studies reported that no significant adverse events were observed. Holmer *et al*.[15] reported only one hypoglycemic and one presyncope episode in a patient participated in the study.

There is also a concern that IF could trigger binge eating, i.e. overeating after food is made available, as IF requires a shift in regular mealtimes. Although one study showed no relationship between IF and pathologic eating patterns in people with no history of eating disorders,[65] two studies in individuals with eating disorders showed an increase in food intake following 6 h and 14 h fasts.[69,70] A longitudinal study also reported that self-reported fasting was a predictor of eating pathologies and recurrent binge eating.[71]

## Comparisons of Mediterranean Diet, Ketogenic Diet, and IF on Liver Outcomes in Patients with NAFLD

Although there was no head-to-head comparison evaluate liver fat and liver fibrosis outcomes of the three dietary patterns, there are some overlaps on proposed mechanistic pathways in the Mediterranean diet, VLKCD, and IF (Fig. 3). Briefly, all dietary patterns are associated with lower total energy intake and negative energy balance that leads to weight loss. Apart from negative energy balance, the Mediterranean diet is characterized by low saturated fat and refined sugar and high omega-3 and mono-unsaturated fatty acid intake, which has a theoretical benefit on reduction of oxidative stress and improvement of insulin resistance.[72] VLKCDs limit carbohydrate intake that results in persistently low insulin level, and fatty acid oxidation is promoted, which leads to a reduction of *de novo* hepatic lipogenesis.[34,35]

**Table 4. Key findings and concepts of Mediterranean diet, ketogenic diet, and IF on liver outcomes in patients with NAFLD**

| Dietary patterns | Mediterranean diet | Ketogenic diet | Intermittent fasting |
|---|---|---|---|
| Characteristics | High intake of plant-based food and fish, olive oil, limited consumption of refined sugar and processed food, red meat, moderate consumption of yogurt and wine[63] | Limits carbohydrate intake to <20–50 g/day or <10% of total energy intake, regardless of total daily energy | Voluntary abstinence from foods and/or drinks for caloric restriction in a specific period, or no caloric intake over a specified period of time |
| Concept | Healthy dietary pattern, low in saturated fat, high in polyunsaturated fat. High fiber and low refined sugar | Limiting carbohydrate intake results in relatively low blood glucose levels and thus reduces hepatic de novo lipogenesis | Less energy intake than people taking usual diets. And possible reduce insulin resistance, inflammation, and enhance autophagy |
| Fatty liver outcomes | Significant reduction in liver fat compared with their respective control groups in the literature. Improvement in liver fibrosis measured by liver stiffness had been observed | Significant reduction in liver fat compared with their respective control groups in the literature. Inconclusive results on liver fibrosis improvement | Significant reduction in liver fat compared with their respective control groups in the literature. Improvement in liver fibrosis measured by liver stiffness had been observed |
| Follow-up time in the literature | Longitudinal data available up to 18 months | Most are short term data no longer than 3 months except Tendler *et al*.[11] and Wolver *et al*.[13] | To date, all are short term data no longer than 3 months |
| Concerns | Availability. Palatability. Affordability | Risk of micronutrients deficiency. Might induced ketoacidosis. Might experience an adverse event of gastrointestinal disturbance. Patients might shift to consume high saturated fat and long-term cardiovascular risk is uncertain | Might not be suitable in patients with cirrhosis. Hypoglycemia in patients with diabetes should be aware |

Lastly, for IF, prolonged fasting of more than 12 h also leads to hepatic glycogen depletion and augmented hepatic lipolysis, that would reduce hepatic steatosis.[72]

The key concepts and evidence of the effects of dietary pattern on liver outcomes in patients with NAFLD are summarized in Table 4.[11,13,63] The Mediterranean diet is associated with the lowest possible adverse effects and long-term liver-related benefits.[16,73–75] Ketogenic diets and IF also have scientific rationales and clinical results of improving liver outcomes in patients with NAFLD, but some concerns and long-term results are uncertain.

## Summary

In the light of an increasing global burden of NAFLD, lifestyle intervention is the mainstay of NAFLD management, as effective therapeutic medications have not been established. Although the Mediterranean diet is recommended by many guidelines, it is not easily accessible for many patients. Ketogenic diets and IF have recently become dietary patterns of general interest. The pros and the cons of both dietary patterns are summarized in Table 4. With some plausible mechanisms underlying a reduction in intrahepatic fat content, it remains inconclusive whether the abovementioned outcomes resulted from the dietary pattern itself or from a hypocaloric intake after exposure to the dietary pattern. In our opinion, ketogenic diets and IF appear acceptable in patients without significant comorbidities. Both ketogenic diets and IF should not be routinely recommended in all patients with NAFLD, but can be considered as alternative therapeutic options in patients who do not achieve targeted weight loss by conventional lifestyle intervention recommendations. They may have some additional benefits in patients who can tolerate and adhere to the dietary patterns, such as reduction in liver fat, and to a lesser extent, reduction in liver fibrosis. Nonetheless, there are concerns of possible adverse events following exposure to the dietary patterns, which should be considered.

## Funding

None to declare.

## Conflict of interest

CB has been an editorial board member of *Journal of Clinical and Translational Hepatology* since 2013. The other authors have no conflict of interests related to this publication.

## Author contributions

Manuscript concept and design (PS, CB), drafting of the manuscript (PS, CC), and critical revision of the manuscript for important intellectual content (PS, CC, CB).

## References

[1] Younossi ZM, Koenig AB, Abdelatif D, Fazel Y, Henry L, Wymer M. Global epidemiology of nonalcoholic fatty liver disease-Meta-analytic assessment of prevalence, incidence, and outcomes. Hepatology 2016;64(1):73–84. doi:10.1002/hep.28431, PMID:26707365.

[2] Li J, Zou B, Yeo YH, Feng Y, Xie X, Lee DH, *et al*. Prevalence, incidence, and outcome of non-alcoholic fatty liver disease in Asia, 1999-2019: a systemat-

ic review and meta-analysis. Lancet Gastroenterol Hepatol 2019;4(5):389–398. doi:10.1016/S2468-1253(19)30039-1, PMID:30902670.
[3] Younossi ZM, Corey KE, Lim JK. AGA Clinical Practice Update on Lifestyle Modification Using Diet and Exercise to Achieve Weight Loss in the Management of Nonalcoholic Fatty Liver Disease: Expert Review. Gastroenterology 2021;160(3):912–918. doi:10.1053/j.gastro.2020.11.051, PMID:33307021.
[4] Chalasani N, Younossi Z, Lavine JE, Charlton M, Cusi K, Rinella M, *et al*. The diagnosis and management of nonalcoholic fatty liver disease: Practice guidance from the American Association for the Study of Liver Diseases. Hepatology 2018;67(1):328–357. doi:10.1002/hep.29367, PMID:28714183.
[5] European Association for the Study of the Liver (EASL), European Association for the Study of Diabetes (EASD), European Association for the Study of Obesity (EASO). EASL-EASD-EASO Clinical Practice Guidelines for the management of non-alcoholic fatty liver disease. J Hepatol 2016;64(6):1388–1402. doi:10.1016/j.jhep.2015.11.004, PMID:27062661.
[6] Eslam M, Sarin SK, Wong VW, Fan JG, Kawaguchi T, Ahn SH, *et al*. The Asian Pacific Association for the Study of the Liver clinical practice guidelines for the diagnosis and management of metabolic associated fatty liver disease. Hepatol Int 2020;14(6):889–919. doi:10.1007/s12072-020-10094-2, PMID:33006093.
[7] Ye Q, Zou B, Yeo YH, Li J, Huang DQ, Wu Y, *et al*. Global prevalence, incidence, and outcomes of non-obese or lean non-alcoholic fatty liver disease: a systematic review and meta-analysis. Lancet Gastroenterol Hepatol 2020;5(8):739–752. doi:10.1016/S2468-1253(20)30077-7, PMID:32413340.
[8] Zelber-Sagi S. Dietary Treatment for NAFLD: New Clinical and Epidemiological Evidence and Updated Recommendations. Semin Liver Dis 2021;41(3):248–262. doi:10.1055/s-0041-1729971, PMID:34139786.
[9] Golovaty I, Tien PC, Price JC, Sheira L, Seligman H, Weiser SD. Food Insecurity May Be an Independent Risk Factor Associated with Nonalcoholic Fatty Liver Disease among Low-Income Adults in the United States. J Nutr 2020;150(1):91–98. doi:10.1093/jn/nxz212, PMID:31504710.
[10] Tamargo JA, Sherman KE, Campa A, Martinez SS, Li T, Hernandez J, *et al*. Food insecurity is associated with magnetic resonance-determined nonalcoholic fatty liver and liver fibrosis in low-income, middle-aged adults with and without HIV. Am J Clin Nutr 2021;113(3):593–601. doi:10.1093/ajcn/nqaa362, PMID:33515016.
[11] Tendler D, Lin S, Yancy WS Jr, Mavropoulos J, Sylvestre P, Rockey DC, *et al*. The effect of a low-carbohydrate, ketogenic diet on nonalcoholic fatty liver disease: a pilot study. Dig Dis Sci 2007;52(2):589–593. doi:10.1007/s10620-006-9433-5, PMID:17219068.
[12] Mardinoglu A, Wu H, Bjornson E, Zhang C, Hakkarainen A, Räsänen SM, *et al*. An Integrated Understanding of the Rapid Metabolic Benefits of a Carbohydrate-Restricted Diet on Hepatic Steatosis in Humans. Cell Metab 2018;27(3):559–571.e5. doi:10.1016/j.cmet.2018.01.005, PMID:29456073.
[13] Wolver S, Fieger EI, Fadel K, Sanyal AJ, Puri P. Low Carbohydrate Ketogenic Diet As A Treatment For Non-Alcoholic Fatty Liver Disease: A Novel Observation Beyond Weight Loss. Hepatology 2020;72:1024.
[14] Kirk E, Reeds DN, Finck BN, Mayurranjan SM, Patterson BW, Klein S. Dietary fat and carbohydrates differentially alter insulin sensitivity during caloric restriction. Gastroenterology 2009;136(5):1552–1560. doi:10.1053/j.gastro.2009.01.048, PMID:19208352.
[15] Holmer M, Lindqvist C, Petersson S, Moshtaghi-Svensson J, Tillander V, Brismar TB, *et al*. Treatment of NAFLD with intermittent calorie restriction or low-carb high-fat diet - a randomised controlled trial. JHEP Rep 2021;3(3):100256. doi:10.1016/j.jhepr.2021.100256, PMID:33898960.
[16] Gepner Y, Shelef I, Komy O, Cohen N, Schwarzfuchs D, Bril N, *et al*. The beneficial effects of Mediterranean diet over low-fat diet may be mediated by decreasing hepatic fat content. J Hepatol 2019;71(2):379–388. doi:10.1016/j.jhep.2019.04.013, PMID:31075323.
[17] Ebrahimi S, Gargari BP, Aliasghari F, Asjodi F, Izadi A. Ramadan fasting improves liver function and total cholesterol in patients with nonalcoholic fatty liver disease. Int J Vitam Nutr Res 2020;90(1-2):95–102. doi:10.1024/0300-9831/a000442, PMID:30932777.
[18] Cai H, Qin YL, Shi ZY, Chen JH, Zeng MJ, Zhou W, *et al*. Effects of alternate-day fasting on body weight and dyslipidaemia in patients with non-alcoholic fatty liver disease: a randomised controlled trial. BMC Gastroenterol 2019;19(1):219. doi:10.1186/s12876-019-1132-8, PMID:31852444.
[19] Johari MI, Yusoff K, Haron J, Nadarajan C, Ibrahim KN, Wong MS, *et al*. A Randomised Controlled Trial on the Effectiveness and Adherence of Modified Alternate-day Calorie Restriction in Improving Activity of Non-Alcoholic Fatty Liver Disease. Sci Rep 2019;9(1):11232. doi:10.1038/s41598-019-47763-8, PMID:31375753.
[20] Hodge A, Mack A, Tuck C, Tchongue J, Holt DQ, Sievert W, *et al*. Non-alcoholic fatty liver disease intermittent fasting time intervention (NIFTI): fasting without calorie restriction improves hepatic transient elastography, visceral adiposity and insulin resistance compared to standard care. J Gastroenterol Hepatol 2014;29:68.
[21] Pérez-Guisado J, Muñoz-Serrano A. The effect of the Spanish Ketogenic Mediterranean Diet on nonalcoholic fatty liver disease: a pilot study. J Med Food 2011;14(7-8):677–680. doi:10.1089/jmf.2011.0075, PMID:21688989.
[22] Yu H, Jia W, Guo Z. Reducing Liver Fat by Low Carbohydrate Caloric Restriction Targets Hepatic Glucose Production in Non-Diabetic Obese Adults with Non-Alcoholic Fatty Liver Disease. J Clin Med 2014;3(3):1050–1063. doi:10.3390/jcm3031050, PMID:25411646.
[23] Bian H, Hakkarainen A, Lundbom N, Yki-Järvinen H. Effects of dietary interventions on liver volume in humans. Obesity (Silver Spring) 2014;22(4):989–995. doi:10.1002/oby.20623, PMID:24115747.
[24] Ministrini S, Calzini L, Nulli Migliola E, Ricci MA, Roscini AR, Siepi D, *et al*. Lysosomal Acid Lipase as a Molecular Target of the Very Low Carbohydrate Ketogenic Diet in Morbidly Obese Patients: The Potential Effects on Liver Steatosis and Cardiovascular Risk Factors. J Clin Med 2019;8(5):E621. doi:10.3390/jcm8050621, PMID:31067824.
[25] Luukkonen PK, Dufour S, Lyu K, Zhang XM, Hakkarainen A, Lehtimäki TE, *et al*. Effect of a ketogenic diet on hepatic steatosis and hepatic mitochondrial metabolism in nonalcoholic fatty liver disease. Proc Natl Acad Sci U S A 2020;117(13):7347–7354. doi:10.1073/pnas.1922344117, PMID:32179679.
[26] D'Abbondanza M, Ministrini S, Pucci G, Nulli Migliola E, Martorelli EE, Gandolfo V, *et al*. Very Low-Carbohydrate Ketogenic Diet for the Treatment of Severe Obesity and Associated Non-Alcoholic Fatty Liver Disease: The Role of Sex Differences. Nutrients 2020;12(9):E2748. doi:10.3390/nu12092748, PMID:32916989.
[27] Browning JD, Baker JA, Rogers T, Davis J, Satapati S, Burgess SC. Short-term weight loss and hepatic triglyceride reduction: evidence of a metabolic advantage with dietary carbohydrate restriction. Am J Clin Nutr 2011;93(5):1048–1052. doi:10.3945/ajcn.110.007674, PMID:21367948.
[28] Cunha GM, Guzman G, Correa De Mello LL, Trein B, Spina L, Bussade I, *et al*. Efficacy of a 2-Month Very Low-Calorie Ketogenic Diet (VLCKD) Compared to a Standard Low-Calorie Diet in Reducing Visceral and Liver Fat Accumulation in Patients With Obesity. Front Endocrinol (Lausanne) 2020;11:607. doi:10.3389/fendo.2020.00607, PMID:33042004.
[29] Kirkpatrick CF, Bolick JP, Kris-Etherton PM, Sikand G, Aspry KE, Soffer DE, *et al*. Review of current evidence and clinical recommendations on the effects of low-carbohydrate and very-low-carbohydrate (including ketogenic) diets for the management of body weight and other cardiometabolic risk factors: A scientific statement from the National Lipid Association Nutrition and Lifestyle Task Force. J Clin Lipidol 2019;13(5):689–711.e1. doi:10.1016/j.jacl.2019.08.003, PMID:31611148.
[30] Churuangsuk C, Kherouf M, Combet E, Lean M. Low-carbohydrate diets for overweight and obesity: a systematic review of the systematic reviews. Obes Rev 2018;19(12):1700–1718. doi:10.1111/obr.12744, PMID:30194696.
[31] Churuangsuk C, Lean MEJ, Combet E. Carbohydrate knowledge, dietary guideline awareness, motivations and beliefs underlying low-carbohydrate dietary behaviours. Sci Rep 2020;10(1):14423. doi:10.1038/s41598-020-70905-2, PMID:32879368.
[32] Feinman RD, Pogozelski WK, Astrup A, Bernstein RK, Fine EJ, Westman EC, *et al*. Dietary carbohydrate restriction as the first approach in diabetes management: critical review and evidence base. Nutrition 2015;31(1):1–13. doi:10.1016/j.nut.2014.06.011, PMID:25287761.
[33] Churuangsuk C, Lean MEJ, Combet E. Low and reduced carbohydrate diets: challenges and opportunities for type 2 diabetes management and prevention. Proc Nutr Soc 2020;79(4):498–513. doi:10.1017/S0029665120000105, PMID:32131904.
[34] Rosenbaum M, Hall KD, Guo J, Ravussin E, Mayer LS, Reitman ML, *et al*. Glucose and Lipid Homeostasis and Inflammation in Humans Following an Isocaloric Ketogenic Diet. Obesity (Silver Spring) 2019;27(6):971–981. doi:10.1002/oby.22468, PMID:31067015.
[35] Crosby L, Davis B, Joshi S, Jardine M, Paul J, Neola M, *et al*. Ketogenic Diets and Chronic Disease: Weighing the Benefits Against the Risks. Front Nutr 2021;8:702802. doi:10.3389/fnut.2021.702802, PMID:34336911.
[36] Marchesini G, Petta S, Dalle Grave R. Diet, weight loss, and liver health in nonalcoholic fatty liver disease: Pathophysiology, evidence, and practice. Hepatology 2016;63(6):2032–2043. doi:10.1002/hep.28392, PMID:26663351.
[37] Gibson AA, Seimon RV, Lee CM, Ayre J, Franklin J, Markovic TP, *et al*. Do ketogenic diets really suppress appetite? A systematic review and meta-analysis. Obes Rev 2015;16(1):64–76. doi:10.1111/obr.12230, PMID:25402637.
[38] Youm YH, Nguyen KY, Grant RW, Goldberg EL, Bodogai M, Kim D, *et al*. The ketone metabolite β-hydroxybutyrate blocks NLRP3 inflammasome-mediated inflammatory disease. Nat Med 2015;21(3):263–269. doi:10.1038/nm.3804, PMID:25686106.
[39] Wree A, Eguchi A, McGeough MD, Pena CA, Johnson CD, Canbay A, *et al*. NLRP3 inflammasome activation results in hepatocyte pyroptosis, liver inflammation, and fibrosis in mice. Hepatology 2014;59(3):898–910. doi:10.1002/hep.26592, PMID:23813842.
[40] Graff EC, Fang H, Wanders D, Judd RL. Anti-inflammatory effects of the hydroxycarboxylic acid receptor 2. Metabolism 2016;65(2):102–113. doi:10.1016/j.metabol.2015.10.001, PMID:26773933.
[41] Shimazu T, Hirschey MD, Newman J, He W, Shirakawa K, Le Moan N, *et al*. Suppression of oxidative stress by β-hydroxybutyrate, an endogenous histone deacetylase inhibitor. Science 2013;339(6116):211–214. doi:10.1126/science.1227166, PMID:23223453.
[42] Yki-Järvinen H, Luukkonen PK, Hodson L, Moore JB. Dietary carbohydrates and fats in nonalcoholic fatty liver disease. Nat Rev Gastroenterol Hepatol 2021;18(11):770–786. doi:10.1038/s41575-021-00472-y, PMID:34257427.
[43] Churuangsuk C, Griffiths D, Lean MEJ, Combet E. Impacts of carbohydrate-restricted diets on micronutrient intakes and status: A systematic review. Obes Rev 2019;20(8):1132–1147. doi:10.1111/obr.12857, PMID:31006978.
[44] McKenna LA, Drummond RS, Drummond S, Talwar D, Lean ME. Seeing double: the low carb diet. BMJ 2013;346:f2563. doi:10.1136/bmj.f2563, PMID:23635648.
[45] Hoyt CS, Billson FA. Optic neuropathy in ketogenic diet. Br J Ophthalmol 1979;63(3):191–194. doi:10.1136/bjo.63.3.191, PMID:435431.
[46] Chiu S, Williams PT, Krauss RM. Effects of a very high saturated fat diet on LDL particles in adults with atherogenic dyslipidemia: A randomized controlled trial. PLoS One 2017;12(2):e0170664. doi:10.1371/journal.pone.0170664, PMID:28166253.
[47] von Frankenberg AD, Marina A, Song X, Callahan HS, Kratz M, Utzschneider KM. A high-fat, high-saturated fat diet decreases insulin sensitivity with-

out changing intra-abdominal fat in weight-stable overweight and obese adults. Eur J Nutr 2017;56(1):431–443. doi:10.1007/s00394-015-1108-6, PMID:26615402.
[48] Ference BA, Ginsberg HN, Graham I, Ray KK, Packard CJ, Bruckert E, *et al*. Low-density lipoproteins cause atherosclerotic cardiovascular disease. 1. Evidence from genetic, epidemiologic, and clinical studies. A consensus statement from the European Atherosclerosis Society Consensus Panel. Eur Heart J 2017; 38(32):2459–2472. doi:10.1093/eurheartj/ehx144, PMID:28444290.
[49] Sheikh M, Chahal M, Rock-Willoughby J, Grubb BP. Carbohydrate-restricted diet and acute coronary syndrome: a case report and review of this conflicting and yet unknown association. Am J Ther 2014;21(2):e41–e44. doi:10.1097/MJT.0b013e318235f1df, PMID:23584309.
[50] Bao W, Li S, Chavarro JE, Tobias DK, Zhu Y, Hu FB, *et al*. Low Carbohydrate-Diet Scores and Long-term Risk of Type 2 Diabetes Among Women With a History of Gestational Diabetes Mellitus: A Prospective Cohort Study. Diabetes Care 2016;39(1):43–49. doi:10.2337/dc15-1642, PMID:26577416.
[51] de Koning L, Fung TT, Liao X, Chiuve SE, Rimm EB, Willett WC, *et al*. Low-carbohydrate diet scores and risk of type 2 diabetes in men. Am J Clin Nutr 2011;93(4):844–850. doi:10.3945/ajcn.110.004333, PMID:21310828.
[52] Shan Z, Guo Y, Hu FB, Liu L, Qi Q. Association of Low-Carbohydrate and Low-Fat Diets With Mortality Among US Adults. JAMA Intern Med 2020; 180(4):513–523. doi:10.1001/jamainternmed.2019.6980, PMID:31961383.
[53] Charoensri S, Sothornwit J, Trirattanapikul A, Pongchaiyakul C. Ketogenic Diet-Induced Diabetic Ketoacidosis in a Young Adult with Unrecognized Type 1 Diabetes. Case Rep Endocrinol 2021;2021:6620832. doi:10.1155/2021/6620832, PMID:33628529.
[54] Shah P, Isley WL. Ketoacidosis during a low-carbohydrate diet. N Engl J Med 2006;354(1):97–98. doi:10.1056/NEJMc052709, PMID:16394313.
[55] Shaikh S, Mohamed MM, Mujeeb A, Shaikh F, Harris B. Euglycemic Diabetic Ketoacidosis Precipitated by a Keto Diet: Importance of Dietary History in Diagnosis. Cureus 2020;12(9):e10199. doi:10.7759/cureus.10199, PMID:33033677.
[56] White-Cotsmire AJ, Healy AM. Ketogenic Diet as a Trigger for Diabetic Ketoacidosis in a Misdiagnosis of Diabetes: A Case Report. Clin Diabetes 2020;38(3):318–321. doi:10.2337/cd20-0001, PMID:32699486.
[57] Marzban S, Arbee M, Vorajee N, Richards GA. Non-diabetic ketoacidosis associated with a low carbohydrate, high fat diet in a postpartum lactating female. Oxf Med Case Reports 2020;2020(8):omz026. doi:10.1093/omcr/omz026, PMID:32793371.
[58] von Geijer L, Ekelund M. Ketoacidosis associated with low-carbohydrate diet in a non-diabetic lactating woman: a case report. J Med Case Rep 2015;9:224. doi:10.1186/s13256-015-0709-2, PMID:26428083.
[59] Tougaard NH, Faber J, Eldrup E. Very low carbohydrate diet and SGLT-2-inhibitor: double jeopardy in relation to ketoacidosis. BMJ Case Rep 2019;12(4):e227516. doi:10.1136/bcr-2018-227516, PMID:30954957.
[60] Ehrenreich MJ. A case of the re-emergence of panic and anxiety symptoms after initiation of a high-protein, very low carbohydrate diet. Psychosomatics 2006;47(2):178–179. doi:10.1176/appi.psy.47.2.178, PMID:16508034.
[61] Temmerman JC, Friedman AN. Very low calorie ketogenic weight reduction diet in patients with cirrhosis: a case series. Nutr Diabetes 2013;3:e95. doi:10.1038/nutd.2013.36, PMID:24247485.
[62] Morales-Suarez-Varela M, Collado Sánchez E, Peraita-Costa I, Llopis-Morales A, Soriano JM. Intermittent Fasting and the Possible Benefits in Obesity, Diabetes, and Multiple Sclerosis: A Systematic Review of Randomized Clinical Trials. Nutrients 2021;13(9):3179. doi:10.3390/nu13093179, PMID:34579056.
[63] Parra-Vargas M, Rodriguez-Echevarria R, Jimenez-Chillaron JC. Nutritional Approaches for the Management of Nonalcoholic Fatty Liver Disease: An Evidence-Based Review. Nutrients 2020;12(12):E3860. doi:10.3390/nu12123860, PMID:33348700.
[64] Green CL, Lamming DW, Fontana L. Molecular mechanisms of dietary restriction promoting health and longevity. Nat Rev Mol Cell Biol 2022;23(1):56–73. doi:10.1038/s41580-021-00411-4, PMID:34518687.
[65] Becker A, Gaballa D, Roslin M, Gianos E, Kane J. Novel Nutritional and Dietary Approaches to Weight Loss for the Prevention of Cardiovascular Disease: Ketogenic Diet, Intermittent Fasting, and Bariatric Surgery. Curr Cardiol Rep 2021;23(7):85. doi:10.1007/s11886-021-01515-1, PMID:34081228.
[66] Aliasghari F, Izadi A, Gargari BP, Ebrahimi S. The Effects of Ramadan Fasting on Body Composition, Blood Pressure, Glucose Metabolism, and Markers of Inflammation in NAFLD Patients: An Observational Trial. J Am Coll Nutr 2017;36(8):640–645. doi:10.1080/07315724.2017.1339644, PMID:28922096.
[67] Ebrahimi S, Gargari BP, Izadi A, Imani B, Asjodi F. The effects of Ramadan fasting on serum concentrations of vaspin and omentin-1 in patients with nonalcoholic fatty liver disease. Eur J Integr Med 2018;19:110–114. doi:10.1016/j.eujim.2018.03.002.
[68] Mari A, Khoury T, Baker M, Said Ahmad H, Abu Baker F, Mahamid M. The Impact of Ramadan Fasting on Fatty Liver Disease Severity: A Retrospective Case Control Study from Israel. Isr Med Assoc J 2021;23(2):94–98. PMID:33595214.
[69] Agras WS, Telch CF. The effects of caloric deprivation and negative affect on binge eating in obese binge-eating disordered women. Behavior Therapy 1998;29(3):491–503. doi:10.1016/S0005-7894(98)80045-2.
[70] Telch CF, Agras WS. The effects of short-term food deprivation on caloric intake in eating-disordered subjects. Appetite 1996;26(3):221–233. doi:10.1006/appe.1996.0017, PMID:8800479.
[71] Stice E, Davis K, Miller NP, Marti CN. Fasting increases risk for onset of binge eating and bulimic pathology: a 5-year prospective study. J Abnorm Psychol 2008;117(4):941–946. doi:10.1037/a0013644, PMID:19025239.
[72] Pugliese N, Plaz Torres MC, Petta S, Valenti L, Giannini EG, Aghemo A. Is there an 'ideal' diet for patients with NAFLD? Eur J Clin Invest 2022;52(3):e13659. doi:10.1111/eci.13659, PMID:34309833.
[73] Katsagoni CN, Papatheodoridis GV, Ioannidou P, Deutsch M, Alexopoulou A, Papadopoulos N, *et al*. Improvements in clinical characteristics of patients with non-alcoholic fatty liver disease, after an intervention based on the Mediterranean lifestyle: a randomised controlled clinical trial. Br J Nutr 2018; 120(2):164–175. doi:10.1017/S000711451800137X, PMID:29947322.
[74] Properzi C, O'Sullivan TA, Sherriff JL, Ching HL, Jeffrey GP, Buckley RF, *et al*. Ad Libitum Mediterranean and Low-Fat Diets Both Significantly Reduce Hepatic Steatosis: A Randomized Controlled Trial. Hepatology 2018; 68(5):1741–1754. doi:10.1002/hep.30076, PMID:29729189.
[75] Ryan MC, Itsiopoulos C, Thodis T, Ward G, Trost N, Hofferberth S, *et al*. The Mediterranean diet improves hepatic steatosis and insulin sensitivity in individuals with non-alcoholic fatty liver disease. J Hepatol 2013;59(1):138–143. doi:10.1016/j.jhep.2013.02.012, PMID:23485520.

*Journal of Clinical and Translational Hepatology* **2022** vol. 10(4) | 740–747
DOI: 10.14218/JCTH.2021.00336

Review Article

# Subsequent Treatment after Transarterial Chemoembolization Failure/Refractoriness: A Review Based on Published Evidence

Shen Zhang, Wan-Sheng Wang, Bin-Yan Zhong* and Cai-Fang Ni*

*Department of Interventional Radiology, The First Affiliated Hospital of Soochow University, Suzhou, Jiangsu, China*

**Received:** 13 August 2021 | **Revised:** 29 October 2021 | **Accepted:** 27 November 2021 | **Published:** 4 January 2022

## Abstract

Transarterial chemoembolization (TACE) is widely applied for the treatment of hepatocellular carcinoma. Repeat TACE is often required in clinical practice because a satisfactory tumor response may not be achieved with a single session. However, repeated TACE procedures can impair liver function and increase treatment-related adverse events, all of which prompted the introduction of the concept of "TACE failure/refractoriness". Mainly based on evidence from two retrospective studies conducted in Japan, sorafenib is recommended as the first choice for subsequent treatment after TACE failure/refractoriness. Several studies have investigated the outcomes of other subsequent treatments, including locoregional, other molecular targeted, anti-programmed death-1/anti-programed death ligand-1 therapies, and combination therapies after TACE failure/refractoriness. In this review, we summarize the up-to-date information about the outcomes of several subsequent treatment modalities after TACE failure/refractoriness.

**Citation of this article:** Zhang S, Wang WS, Zhong BY, Ni CF. Subsequent Treatment after Transarterial Chemoembolization Failure/Refractoriness: A Review Based on Published Evidence. J Clin Transl Hepatol 2022;10(4):740–747. doi: 10.14218/JCTH.2021.00336.

## Introduction

Transarterial chemoembolization (TACE) plays a fundamental role in the treatment of unresectable hepatocellular carcinoma (HCC), either as a palliative approach for unresectable condition, as bridging therapy prior to liver transplantation, or for tumor downstaging prior to surgical resection.[1–3] According to the global HCC BRIDGE (i.e. Bridge to Better Outcomes in HCC) study involving 18,031 patients in 14 countries, TACE is the most widely applied approach both for intermediate- and advanced-stage HCC.[4] Nevertheless, the prognosis of HCC treated with TACE varies because of high patientheterogeneity of patients and biological characteristics of HCC.[5–7] Repeat TACE is often recommended because it is sometimes difficult to achieve a satisfactory tumor response with a single session.[8] Nonetheless, high frequency and number of repeat TACE procedures can impair liver function and increase treatment-related adverse events, negating the benefits achieved from tumor necrosis. Meticulous assessment of the risks and benefits of repeat TACE is warranted to improve the long-term outcomes of TACE for HCC. The concept of TACE failure/refractoriness was subsequently introduced by several organizations including the Japan Society of Hepatology (JSH), the International Association for the Study of the Liver, and a European expert panel (Table 1).[9–11]

Appropriate subsequent treatment after TACE failure/refractoriness is another key point to improve long-term prognosis of patients with HCC. The current TACE failure/refractoriness guidelines recommend sorafenib therapy after occurrence of TACE failure/refractoriness. Notably, this recommendation was mainly based on the results of two retrospective studies with small sample sizes.[12,13] Apart from those two studies, several others have investigated the outcomes of other subsequent treatments, including locoregional therapies, other molecular targeted agents (MTAs), anti-programmed death ligand-1/anti-programmed death-1 therapies, and combination therapies after TACE failure/refractoriness. Therefore, we reviewed the available evidence about the efficacy and safety of subsequent therapies after TACE failure/refractoriness in the treatment of HCC.

## Search strategy and selection criteria

A comprehensive literature search was performed on the PubMed and Web of Science databases for relevant studies published in English language through April 2021. The search terms were: ("transarterial chemoembolization" OR "transcatheter arterial chemoembolization" OR "TACE") AND ("failure" OR "refractoriness" OR "refractory"). Only original research articles that focused on the subsequent treatments after TACE failure/refractoriness were included. Duplicate publications, reviews, case reports, conference

**Keywords:** Transarterial chemoemboization; Failure; Refractoriness; Subsequent treatment.

**Abbreviations:** DCB-TACE, DC beads TACE; DEB-TACE, drug-eluting beads TACE; HAIC, hepatic arterial infusion chemotherapy; ICI, immune checkpoint inhibitor; JSH–LCSGJ, JSH-Liver Cancer Study Group of Japan; JSH, Japan Society of Hepatology; MVI, macroscopic vascular invasion; MWA, microwave ablation; OS, overall survival; PFS, progression-free survival; TACE, transarterial chemoembolization; TARE, transarterial radioembolization; TTP, time to progression.

***Correspondence to:** Cai-Fang Ni and Bin-Yan Zhong, Department of Interventional Radiology, The First Affiliated Hospital of Soochow University, No. 188, Shizi Street, Suzhou, Jiangsu 215006, China. Tel/Fax: +86-512-67780375, E-mail: cjr.nicaifang@vip.163.com, szncf@suda.edu.cn (CFN) or Tel/Fax: +86-512-67972173, E-mail: byzhongir@sina.com (BYZ)

**Table 1. Concepts of TACE failure/refractoriness**

| Organization | Definition |
|---|---|
| JSH criteria, 2010 | (1) Intrahepatic lesion: more than two consecutive incomplete necrosis (depositions ( 50%) of lipiodol) are seen by response evaluation CT within the treated tumors at the 4 weeks after adequately performed TACE; more than two consecutive appearances of a new lesion (recurrence) are seen in the liver by response evaluation CT at the 4 weeks after adequately performed TACE. (2) Appearance of vascular invasion. (3) Appearance of extrahepatic spread continuous elevation of tumor markers even though right after TACE. (4) Tumor marker continuous elevation of tumor markers even though right after TACE |
| JSH–LCSGJ criteria, 2014 | (1) Intrahepatic lesion: two or more consecutive insufficient responses of the treated tumor (viable lesion >50%) even after changing the chemotherapeutic agents and/ or reanalysis of the feeding artery seen on response evaluation CT/MRI at 1–3 months after having adequately performed selective TACE; Two or more consecutive progressions in the liver (tumor number increases as compared with tumor number before the previous TACE procedure) even after having changed the chemotherapeutic agents and/or reanalysis of the feeding artery seen on response evaluation CT/MRI at 1–3 months after having adequately performed selective TACE. (2) Continuous elevation of tumor makers immediately after TACE even though slight transient decrease is observed. (3) Appearance of vascular invasion. (4) Appearance of extrahepatic spread |
| International Association for the Study of the Liver | No response after 3 or more TACE procedures within a 6 month period, to the same area |
| Europe | Depending on the purpose of TACE, if TACE is used as palliative therapy, stable lesions can be regarded as effective. Conversely, if TACE is used as a curative therapy, stable lesions are considered as TACE failure |

CT, computed tomography; JSH, Japan Society of Hepatology; LCSGJ, Liver Cancer Study Group of Japan; MRI, magnetic resonance imaging; TACE, transarterial chemoembolization.

abstracts, and studies published in languages other than English were excluded.

## Subsequent treatment and prognosis after TACE failure/refractoriness

After the introduction of the concept of TACE failure/refractoriness in 2010 by the JSH, several studies have investigated the outcomes of subsequent treatments after TACE failure/refractoriness. A total of 23 studies were finally included in the review (Table 2).[12–34] Among them, seven reported outcomes of subsequent treatments without comparison to other treatments. Eight compared the outcomes of sorafenib therapy as subsequent treatment with those of other treatments. Eight studies compared the outcomes of continuation of TACE in combination with systemic therapies with those of other treatments.

### *Subsequent treatments without comparison*

Iwasa *et al*.[14] administered transcatheter arterial infusion chemotherapy with a fine-powder formulation of cisplatin for advanced HCC after TACE failure/refractoriness. Notably, the criteria for TACE failure/refractoriness in their study was an increase in size or 25% reduction in the size of hypervascular lesions 1 month after TACE, which was different from the 2010 JSH criteria. The study included 84 patients, and the median overall survival (OS) was 7.1 months. The authors reported only a modest effect of transcatheter arterial infusion chemotherapy using cisplatin, a median progression-free survival (PFS) of only 1.7 months and an objective response rate (ORR) of 3.6%. Besides, adverse events (AEs) occurred frequently during the treatment, and nearly 50% patients experienced grade 3/4 elevations of liver enzymes. Recently, Hus *et al*.[15] reported the outcomes of hepatic arterial infusion chemotherapy (HAIC) with a modified FOLFOX regimen in 87 patients with advanced HCC after TACE failure/refractoriness, based on 2014 JSH–LCSGJ criteria. The majority of patients in the cohort had multinodular HCC and large tumors with a mean diameter of largest tumors of 7.1 cm. The OS, PFS, and time to tumor progression (TTP) were up to 9 months, 3.7 months, and 4.1 months, respectively. However, approximately 29% (25/87) of patients received concurrent treatment with MTAs and the related information was not reported, which may have introduced an element of bias resulting in weaker efficacy of HAIC monotherapy.

In addition, various locoregional therapies including different types of TACE or percutaneous therapies have been investigated. A small pilot study investigated the efficacy of TACE with DC beads (DCB-TACE) in 10 patients with solitary HCC nodules that were insensitive to lipiodol-TACE.[16] All tumor nodules responded to DCB-TACE at the 1 month follow-up, and the median TTP was 7.8 months. Unfortunately, the end point of DCB-TACE was not reported and eight of the 10 patients received additional treatments such as HAIC and radiation therapy. Kobayashi *et al*.[17] explored the potential of Hepasphere Microspheres for HCC refractory to conventional TACE following the 2014 JSH–LCSGJ criteria. The targeted tumors had a good response to Hepasphere-TACE, with an ORR of 19.1% and a disease control rate (DCR) of 76.4%. The median PFS and OS in the study were 2.9 and 16.3 months, respectively. Besides, grade 3/4 AEs were not documented, and liver function was preserved during TACE. Transarterial radioembolization (TARE) for HCC after drug-eluting beads TACE (DEB-TACE) failure/refractoriness was reported in 2017.[18] The majority of patients (22/30) in the cohort had multinodular HCCs, and the mean diameter of largest tumor was 4.1 cm. The median OS after first TARE was 14.8 months and the safety profile was acceptable. In addition, eleven patients (36.7%) had partial responses and three (10%) were downstaged within the Milan criteria and subsequently received liver transplants. Kim *et al*.[19] reported the outcomes of balloon-occluded TACE for multinodular HCC after conventional TACE. The study included 60 patients with Barcelona Clinic Liver Cancer A/B/C stages and a mean tumor diameter of 3 cm. The primary efficacy out-

**Table 2. Studies of treatment and prognosis subsequent to TACE failure/refractoriness**

| Study[Ref] | Patients, *n* | BCLC stage | Definition of TACE failure/refractoriness | Subsequent treatment | Median OS (95% CI), months; *p*-value |
|---|---|---|---|---|---|
| Iwasa *et al*., 2011[14] | 84 | C | An increase in size or 25% reduction in size of the hypervascular lesions 1 month after TACE | TAI with cisplatin | – |
| Song *et al*., 2013[16] | 10 | A/B | More than two consecutive incomplete necrosis (depositions <50% of lipiodol) | DEB-TACE | 22.2 (N/A) |
| Ikeda *et al*., 2014[21] | 114 | N/A | Progression or a tumor shrinkage rate of <25% of the hypervascular lesions 1–3 months after TACE | sorafenib vs. hepatic arterial infusion chemotherapy | 16.4 (N/A) vs. 8.6 (N/A); $p<0.01$ |
| Ogasawara *et al*., 2014[13] | 56 | B | 2010 JSH criteria | sorafenib vs. continued TACE | 25.4 (9.3–41.5) vs. 11.5 (8.3–14.8); $p=0.003$ |
| Arizumi *et al*., 2015[12] | 56 | B | 2014 JSH–LCSGJ criteria | sorafenib vs. continued TACE | 24.7 (17.16–54.7) vs. 13.6 (8.96–17.43); $p=0.002$ |
| Hatooka *et al*., 2016[23] | 96 | B/C | 2010 JSH criteria | HAIC vs. sorafenib | 8 (N/A) vs. 15 (N/A); $p=0.021$ |
| Huang *et al*., 2016[32] | 26 | B | Disease progression or shrinkage of <25% in hypervascular tumor lesions after 1–2 cycles of TACE | S–1 chemotherapy plus TACE vs. TACE monotherapy | 17 (15.6–18.4) vs. 15 (9.2–20.8); $p=0.549$ |
| Huang *et al*., 2016[31] | 26 | B | Disease progression or shrinkage of <25% in hypervascular tumor lesions after 1–2 cycles of TACE | S–1 chemotherapy plus TACE vs. TACE monotherapy | 18 (15.3–24.7) *vs.* 13 (9.8–16.2); $p=0.040$ |
| Wu *et al*., 2017[28] | 61 | C | No details presented | TACE plus sorafenib vs. TACE | 17.9 (N/A) vs. 7.1 (N/A); $p<0.001$ |
| Klompenhouwer *et al*., 2017[18] | 30 | B/C | Progression or stable disease after one or more sessions of DEB-TACE | TARE | 14.8 (8.33–26.5) |
| Kodama *et al*., 2018[22] | 152 | N/A | 2014 JSH–LCSGJ criteria | HAIC vs. sorafenib | 7 vs. 7 for MVI positive; $p=0.6710.5$ vs. 20 for MVI negative; $p=0.001$ |
| Qiu *et al*., 2019[33] | 58 | B/C | 2014 JSH–LCSGJ criteria | TACE plus apatinib vs. TACE | 17.0 (12.0–22.0) vs. 10.7 (6.4–15.0); $p=0.027$ |
| Lin *et al*., 2020[29] | 66 | A/B/C | Progressive disease after two consecutive of transarterial chemoembolization treatment within 6 months | TACE plus sorafenib vs. TACE | 23.1 (N/A) vs. 11.0 (N/A); $p=0.001$ |
| Chen *et al*., 2020[26] | 44 | B | No less than 2 consecutive ineffective responses of treated tumors (necrotic lesion <50%) or one ineffective response of treated tumors (necrotic lesion <25%) or tumor number increased | MWA vs. sorafenib | Not reached vs. 16.6 (13.4–19.8); $p=0.001$ |
| Kim *et al*., 2020[19] | 60 | A/B/C | No details presented | balloon-occluded TACE | Median TTP: 5.3 (4.0–6.9) |
| Yoo *et al*., 2020[24] | 94 | B/C | 2014 JSH–LCSGJ criteria | TACE plus chemotherapy vs. sorafenib | 6.4 (2.9–9.9) vs. 4.1 (2.6–5.6); $p=0.355$ |
| Shimose *et al*., 2020[27] | 171 | B | 2014 JSH–LCSGJ criteria | lenvatinib vs. sorafenib vs. TACE | Median PFS: 5.8 *vs.* 3.2 vs. 2.8; $p=0.01$, $p<0.001$ |

*(continued)*

**Table 2.** *(continued)*

| Study[Ref] | Patients, *n* | BCLC stage | Definition of TACE failure/refractoriness | Subsequent treatment | Median OS (95% CI), months; *p*-value |
|---|---|---|---|---|---|
| Villani *et al*., 2021[25] | 76 | B | Development of new intrahepatic lesions, the appearance of vascular invasion, the appearance of extrahepatic spread after 3 months from TACE session | continue TACE vs. sorafenib | 10.6 (2.3–14.0) vs. 9.5 (1.7–12.3); $p$=0.72 |
| Kobayashi *et al*., 2020[17] | 27 | B/C | 2014 JSH–LCSGJ criteria | DEB-TACE | 16.3 (8.6–24.0) |
| Zheng *et al*., 2021[34] | 51 | B/C | 2014 JSH–LCSGJ criteria | TACE+ICIs+sorafenib vs. TACE+sorafenib | 23.3 (17.56–29.07) vs. 13.8 (9.11–18.50); $p$=0.012 |
| Kaibori *et al*., 2021[30] | 70 | B | 2014 JSH–LCSGJ criteria | TACE+sorafenib vs. TACE | 20.5 vs. 15.4; $p$=0.009 |
| Hsu *et al*., 2021[15] | 87 | C | 2014 JSH–LCSGJ criteria | HAIC | 9.0 (7.6–10.4) |
| Xu *et al*., 2021[20] | 19 | A/B | 2014 JSH–LCSGJ criteria | $^{125}$I brachytherapy | Median TTP: 8.8 |

BCLC, Barcelona Clinic Liver Cancer; CI, confidence interval; DEB-TACE, drug-eluting bead transarterial chemoembolization; HAIC, hepatic arterial infusion chemotherapy; ICIs, immune checkpoint inhibitors; JSH, Japan Society of Hepatology; LCSGJ, Liver Cancer Study Group of Japan; MWA, microwave ablation; OS, overall survival; PFS, progression-free survival; TACE, transarterial chemoembolization; TAI, transcatheter arterial infusion; TARE, transarterial radioembolization; TTP, time to progression.

come of the study was TTP and not OS. The median TTP was 5.3 months and the major complication rate was only 6.7% (4/60). At the first follow-up, tumor response was achieved in all 60 patients, among whom 45 (75%) had complete responses and 15 (25%) had partial responses. Xu *et al*.[20] reported computed tomography-guided Iodine-125 ($^{125}$I) seed implantation for the treatment of HCC after TACE failure/refractoriness. All 21 patients in their cohort had solitary HCC nodules with a mean diameter of 4.3 cm. The median TTP was 8.8 months and the 6 month ORR of the targeted tumors was 90.5%. The findings suggested that aggressive locoregional therapies, including $^{125}$I brachytherapy and thermal ablation can achieve favorable outcomes in residual HCC nodules ≤5 cm, as tumors of that size tend to undergo complete necrosis with minimal postoperative liver damage. However, all were single-arm studies with small sample sizes. Larger studies are required to provide more robust evidence.

### *Switching to sorafenib and comparison with other treatments*

During the past 10 years, sorafenib has been used as the standard treatment for advanced HCC with preserved liver function. Whether it is also the ideal treatment for patients after TACE failure/refractoriness is of considerable interest to the researchers. Ikeda *et al*.[21] compared the efficacy of sorafenib therapy ($n$=48) with that of HAIC using cisplatin ($n$=66) in a study of 114 patients with HCC after TACE failure/refractoriness. They defined TACE failure/refractoriness as tumor progression or a tumor shrinkage rate of <25% for hypervascular lesions 1–3 months after TACE. The median OS in the sorafenib group was significantly longer than that in the HAIC group (16.4 vs. 8.6 months; $p$<0.01). The corresponding DCRs were 60.4% *vs.* 28.8% ($p$=0.001) and the median TTPs were 3.9 vs. 2.0 months ($p$<0.01), which were also significantly better in the sorafenib group. The study results favored sorafenib over HAIC as the subsequent treatment after TACE failure/refractoriness. A large study by Kodama *et al*.[22] compared sorafenib and HAIC as subsequent treatment after TACE failure/refractoriness based on the 2014 JSH–LCSGJ criteria. Patients were divided into two groups by their macroscopic vascular invasion (MVI) status. In the MVI-positive group, the median OS was not significantly different between patients receiving sorafenib and HAIC (7 months in both groups, $p$=0.67). In the MVI-negative group, the median OS of patients receiving sorafenib was significantly longer than that of patients receiving HAIC (20 months vs. 10.5 months, $p$=0.001). The authors concluded that sorafenib may be a better choice compared to HAIC for HCC with MVI after TACE failure/refractoriness. Notably, Hatooka *et al*.[23] found that HAIC tended to cause vascular damage and led to drug resistance compared with sorafenib, thereby resulting in a shorter time to treatment failure and shorter median OS for patients with TACE failure/refractoriness. Yoo *et al*.[24] compared the effectiveness of conventional TACE combined with systemic infusion of 5-fluorouracil and sorafenib. Of the 94 patients with unresectable HCC who were refractory to DEB-TACE, 49 received transarterial infusion of epirubicin and cisplatin in a mixture of 5 to 10 mL of iodized oil without gelatin sponge embolization, followed by systemic infusion of 5-FU (200 mg/m$^2$) for 12 h. Although patients treated with TACE combined with systemic chemotherapy had longer median OS, the between-group difference was not statistically significant (6.4 vs. 4.1 months; $p$=0.355). Notably, grade 3/4 AEs occurred more frequently in the sorafenib group than in the combination group ($p$=0.024). The authors concluded that TACE combined with HAIC may be a better alternative for patients who experience TACE failure/refractoriness along with sorafenib intolerance. However, more definitive evidence is required to support the efficacy and safety of combination therapy.

Ogasawara *et al*.[13] and Arizumi *et al*.[12] performed similar retrospective studies that compared the treatment efficacy of sorafenib monotherapy and continued TACE for intermediate HCC after TACE failure/refractoriness in 2014 and 2015, respectively. Both studies demonstrated the superiority of sorafenib monotherapy over continued TACE with respect to survival outcomes and preservation of liver function. The study by Ogasawara *et al*.[13] included 56 patients, and approximately 80% patients had ≥3 tumor nodules. Compared with patients who received continued TACE, patients in the sorafenib group (n=36) had significantly longer median OS

(25.4 vs. 11.5 months; $p$=0.003). Simultaneously, time to liver dysfunction, defined as the period from judgment as TACE-refractory until diagnosis of Child-Pugh C disease, was significantly longer in the sorafenib group (29.8 vs. 17 months; $p$=0.030). A study by Arizumi *et al*.[12] included 32 patients who switched to sorafenib and 24 patients who continued to receive TACE. The median OS in the sorafenib group was significantly longer than that in the TACE group (24.7 vs. 13.6 months; $p$=0.002). At the 6 month follow-up, the TACE group experienced more serious deterioration of liver function ($p$=0.005). Nevertheless, as information related to tumor characteristics was not reported, it is debatable whether the difference of OS was related to the between-group differences in the baseline characteristics of patients. Additionally, the median treatment time in the sorafenib group was only 4.13 months, and the survival time after tumor progression was up to 20 months. The long treatment time after tumor progression may have challenged the efficacy of sorafenib. Recently, Villani *et al*.[25] reported results that conflicted with those of the two aforementioned studies. Their study included 76 elderly patients ≥65 years of age with intermediate-stage HCC after TACE failure/refractoriness. The median OS of the two groups were comparable, with an OS of 9.5 months for sorafenib and 10.6 months for continued TACE ($p$=0.72). The corresponding 1 year survival rates were 43.6% and 32% ($p$=0.12). Interestingly, microwave ablation (MWA) had better outcomes than sorafenib for viable residual nodules that were insensitive to TACE. Chen *et al*.[26] compared the outcomes of sorafenib and MWA for intermediate HCC with tumor sizes ≤7 cm and tumor numbers ≤5 after TACE failure/refractoriness. The study included 52 patients and after one-to-one propensity score matching (PSM), 22 pairs were enrolled for further analysis. Median OS in the MWA group was significantly longer than that in the sorafenib group both before (48.8 *vs.* 16.6 months, $p$=0.001) and after (not reached vs. 16.6 months; $p$=0.001) PSM. In spite of the favorable OS, the safety of MWA as well as tumor response was not documented in the study.

The REFLECT trial demonstrated the efficacy and safety of lenvatinib for advanced HCC.[35] Subsequently, it has been applied as another first-line treatment for advanced HCC. Shimose *et al*.[27] compared sorafenib ($n$=53), lenvatinib ($n$=45), and continued TACE ($n$=73) for intermediate HCC after TACE failure/refractoriness. The definition of TACE failure/refractoriness was based on the 2014 JSH–LCSGJ criteria, and 84% of patients (144/171) were beyond the up-to-seven criteria. The median PFS was significantly longer in the lenvatinib group (5.8 months) than in the sorafenib (3.2 months), and continued TACE (2.8 months) groups ($p$<0.001). The up-to-seven criteria, albumin-bilirubin (ALBI) grade and treatment modality were prognostic factors for PFS. Building upon the positive outcomes of previous studies, molecular targeted-agent monotherapy may be a good alternative for patients who have TACE failure/refractoriness along with a heavy tumor burden.[36]

### *Continued TACE combined with systemic therapies compared with other treatments*

Although many randomized controlled trials in addition to the TACTICS trial, failed to demonstrate the efficacy of combination therapy with TACE and sorafenib for intermediate-stage HCC, additional sorafenib administration to patients with TACE refractoriness may potentially improve the prognosis.[37–39] In a study by Wu *et al*.[28] TACE-refractory patients treated with TACE plus sorafenib had significantly better median OS than TACE monotherapy, (17.9 vs. 7.1 months, $p$<0.001). Similarly, the combination treatment group had significantly better median TTP (9.3 vs. 3.4 months, $p$<0.001). The toxicity of sorafenib was effectively mitigated by lowering the drug dose; only two patients in the combination group experienced severe AEs. A study by Lin *et al*.[29] also supported the efficacy of additional sorafenib administration for patients with TACE refractoriness, with a median OS of 23.1 months with combination therapy and 11.0 months with TACE monotherapy ($p$=0.001). Furthermore, by analyzing the characteristics of the 202 TACE-refractory patients in the study, a tumor number >3, tumor size ≥5 cm, bilateral tumor extent, or baseline AFP level ≥200 mg/dL were identified as risk factors for TACE refractoriness. Early initiation of combination therapy was recommended for such high-risk patients. In a recent study that supported combination therapy with TACE and sorafenib for intermediate HCC after TACE failure/refractoriness, additional sorafenib administration increased the interval between two TACE sessions, prolonged the maintenance of liver function, prolonged the time to extrahepatic spread, and improved. the transition to post-treatments.[30]

Huang *et al*.[31,32] performed two similar studies comparing the treatment outcomes of TACE monotherapy and TACE combined with S-1 chemotherapy. Both studies included 26 patients with intermediate HCC, and TACE failure/refractoriness was defined as disease progression or shrinkage of <25% in hypervascular tumor lesions after 1–2 cycles of TACE. Combination treatment had significantly better median OS (18 vs. 13 months; $p$=0.040) in one of the two studies.[31] Interestingly, in the other study, the median OS was not significantly different between the two treatments (17 months for TACE plus S-1 and 15 months for TACE monotherapy, $p$=0.549).[32] The difference in the last day of follow-up may be responsible for the difference clinical outcomes. Qiu *et al*.[33] investigated the treatment outcomes of concurrent apatinib administration for unresectable HCC after TACE failure/refractoriness. A total of 58 patients were included and TACE failure/refractoriness was defined following the 2014 JSH–LCSGJ criteria. Patients treated with TACE combined with apatinib had significantly better median OS compared with those treated with TACE monotherapy (17.0 vs. 10.7 months; $p$=0.027). Similar results were observed with respect to median PFS (7 vs. 2 months; $p$<0.001). Three patients in the combination group experienced severe AEs and the remaining 39 experienced a series of apatinib-related AEs that were relieved by symptomatic treatment or dosage reduction. The positive outcomes of combination treatment using apatinib instead of sorafenib were consistent with previous studies that investigated the use of sorafenib as systemic therapy.

Recently, Zheng *et al*.[34] reported the efficacy and safety of TACE combined with immune checkpoint inhibitor (ICI) therapy and sorafenib for patients with TACE failure/refractoriness. A total of 51 patients with unresectable HCC who were refractory to TACE were included and were assigned to treatment with TACE combined with sorafenib ($n$=29), or TACE combined with sorafenib plus an ICI, either pembroizumab ($n$=10) or nivolumab ($n$=12). Patients in the triple combination treatment group had significantly better treatment efficacy compared with those in the TACE combined with sorafenib group, with longer median OS (23.3 vs. 13.8 months; $p$=0.012), better DCR (81.82% vs. 55.17%; $p$=0.046), and longer median PFS (16.26 vs. 7.30 months; $p$<0.001). However, there was no significant difference in median OS or PFS between patients receiving different ICIs. Four patients in the triple combination group and three patients in the TACE combined with sorafenib group required dose reduction or treatment interruption (18.18% vs. 10.34%, $p$=0.421). The incidence of AEs was comparable in both groups. The study was the first attempt to explore treatment outcomes of TACE combined with recently recommended systemic therapy with

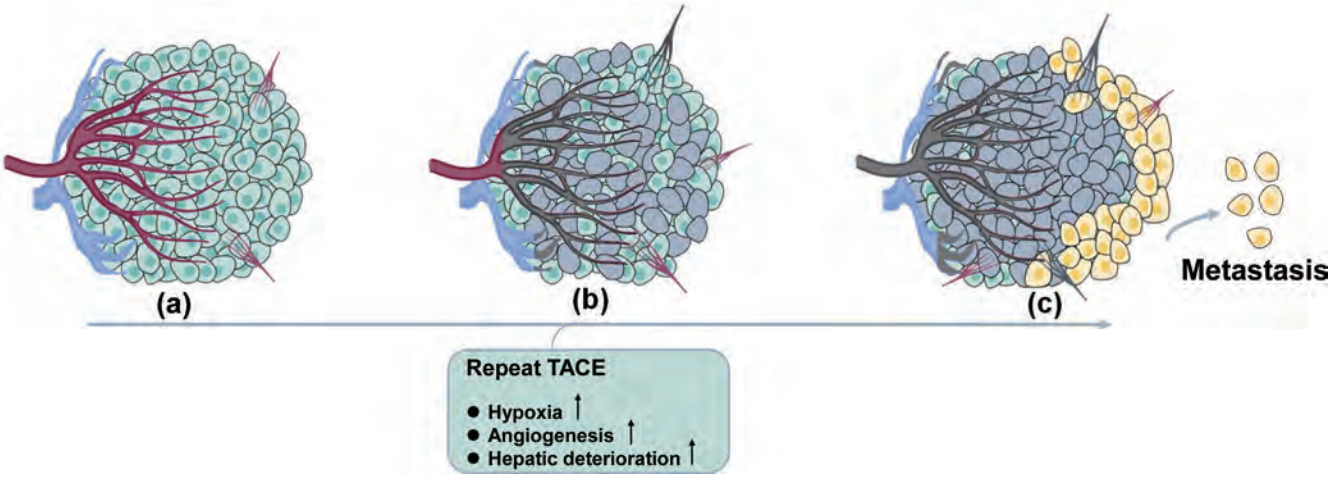


**Fig. 1. Pathological and physiological changes in HCCs with consecutive insufficient responses to TACE.** (A) HCCs can be nourished by several potential arteries other than the main feeding artery, and peritumor tissue can be supported by the portal vein as well. (B) After consecutive super selective TACE, HCCs may still be viable or even undergo progression because of a blood supply from delicate collateral arteries or the distal portal vein. Hypovascular HCCs tend to have unsatisfied iodized oil deposition. Under those circumstances, additional TACE is no longer effective, and define TACE failure/refractoriness. (C) Additional TACE sessions after TACE failure/refractoriness not only insignificantly increase tumor response rate but also damage liver function. Frequent interventional insults put pressure on the tumor microenvironment, making the residual HCCs more malignant and aggressive. TACE, transarterial chemoembolization.

ICIs combined with a molecular agent for HCC refractory to TACE. Further studies are required to draw more definitive conclusions.

## Discussion

In spite of the multitude of studies of TACE failure/refractoriness, standardized treatment recommendations for patients with TACE failure/refractoriness have not yet been developed. That is largely attributable to two main reasons. Firstly, there is no clear consensus on the definition of TACE failure/refractoriness; a widely-accepted definition is expected to guide study designs and protocols. Notably, seven of the 23 retrieved studies used local tumor response as the sole criterion for judging TACE failure/refractoriness, which may be attributable to the locoregional nature of TACE. It seems to be well-accepted that insufficient radiologic response of treated tumors after repeat TACE sessions is one of the unambiguous definitions of TACE failure/refractoriness (Fig. 1). However, whether portal vein tumor thrombosis, extrahepatic spread, and new lesion(s) are TACE endpoints is still under debate. Secondly, the definition of TACE failure/refractoriness incorporates many situations and considerable patient heterogeneity poses a challenge to the formulation of a unequivocal treatment strategy. In 2020, a nationwide online survey of 257 clinicians treating HCC in 184 hospitals in China was conducted to identify the real-world trends in the clinical application of TACE and recognition of TACE failure/refractoriness.[40] Most clinicians ($n$=229, 89.1%) agreed that TACE was a palliative treatment but can achieve curative effects under certain conditions. Despite the varied treatment outcomes of TACE, nearly all ($n$=252, 98.1%) still choose TACE as the first-line treatment of patients with intermediate-stage HCC. In addition, 90% ($n$=226) did not think the current scoring systems, including the ART and ABCR scores or the up-to-seven criteria, were effective in guiding TACE treatment or repeated TACE procedures. Nearly three-quarters ($n$=199, 74.3%) supported the rationale of the concept of TACE failure/refractoriness, but 91.4% ($n$=235) did not agree with the current definition of TACE failure/refractoriness. Most participants ($n$=221, 86%) believed that repeated TACE can be performed for HCC nodules with insufficient necrosis, especially when the tumor-feeding artery was identified by angiography. However, they reported that TACE should be performed no more than three times before assessment of treatment outcome, nearly one-third ($n$=75, 29.2%) thought that three insufficient TACE sessions was the ideal number to define TACE failure/refractoriness. Notably, only a small proportion ($n$=42, 16.3%) of participants agreed that appearance of new intrahepatic lesion(s) should be considered as a criterion for TACE failure/refractoriness. Combination therapy, including TACE, was considered as the ideal treatment for new HCC nodule(s). Similarly, as long as patients had well-preserved liver function, over 90% of respondents would choose continuing TACE or TACE-based combination therapy to interfere with intrahepatic tumor progression even in the setting of invasion of portal vein ($n$=242, 94.2%) or extrahepatic organs ($n$=253, 98.5%). Based on the evidence from previous studies as well as the survey outcomes, a potentially useful schematic illustration (Fig. 2) is presented to judge TACE failure/refractoriness and to guide subsequent treatment to overcome TACE failure/refractoriness.

## Conclusion

Overall, not only sorafenib but also other therapies such as DEB-TACE, HAIC, ablation, and TACE combined with systemic therapies are potentially useful as subsequent treatment after TACE failure/refractoriness. However, all the available evidence is based on retrospective studies. Prospective studies are warranted to identify the ideal treatment for HCC after TACE failure/refractoriness.

## Funding

This study was supported by the National Natural Science Foundation of China (No. 81901847), the Natural Science Foundation of Jiangsu Province (No. BK20190177), and the Suzhou Science and Technology Youth Plan (No. KJXW2018003).

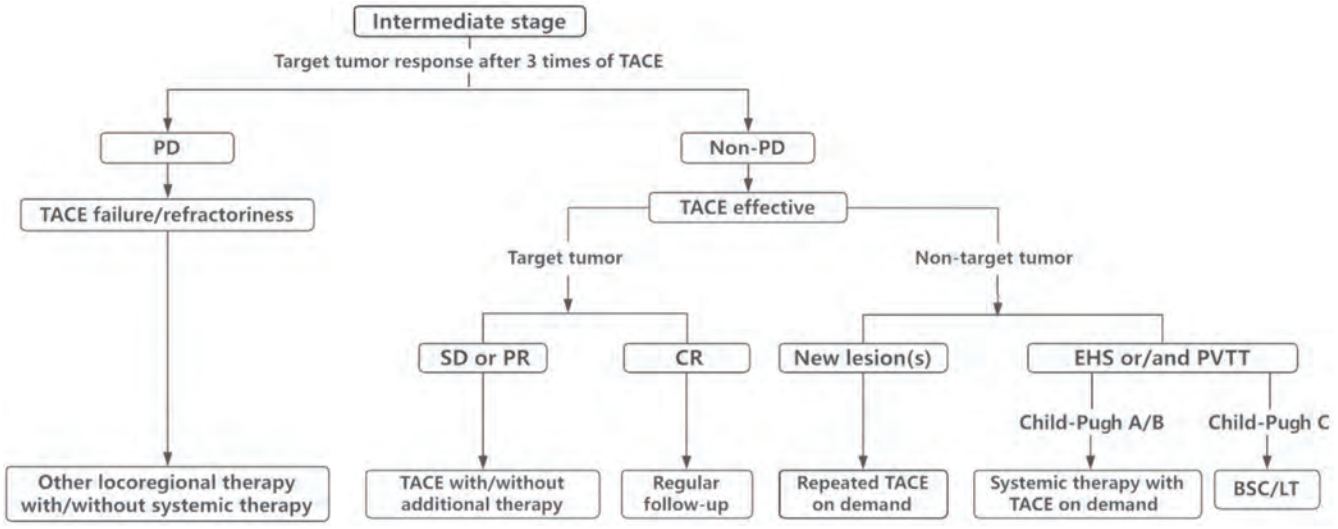


**Fig. 2. Algorithm decision tree for judging TACE failure / refractoriness and recommending subsequent treatment.** BSC, best supportive care; CR, complete response; EHS, extrahepatic spread; HCC, hepatocellular carcinoma; LT, liver transplantation; PD, progressing disease; PR, partial response; PVTT, portal vein tumor thrombosis; SD, stable disease; TACE, transarterial chemoembolization.

## Conflict of interest

The authors have no conflict of interests related to this publication.

## Author contributions

Conception and design of the review (CFN, WSW), and collection of the articles and preparation of the manuscript (BYZ, SZ).

## References


[1] Llovet JM, Kelley RK, Villanueva A, Singal AG, Pikarsky E, Roayaie S, *et al*. Hepatocellular carcinoma. Nat Rev Dis Primers 2021;7(1):6. doi:10.1038/s41572-020-00240-3.

[2] Villanueva A. Hepatocellular carcinoma. N Engl J Med 2019;380(15):1450–1462. doi:10.1056/NEJMra1713263.

[3] Forner A, Reig M, Bruix J. Hepatocellular carcinoma. Lancet 2018;391(10127):1301–1314. doi:10.1016/S0140-6736(18)30010-2.

[4] Park JW, Chen M, Colombo M, Roberts LR, Schwartz M, Chen PJ, *et al*. Global patterns of hepatocellular carcinoma management from diagnosis to death: the BRIDGE Study. Liver Int 2015;35(9):2155–2166. doi:10.1111/liv.12818.

[5] Ringelhan M, Pfister D, O'Connor T, Pikarsky E, Heikenwalder M. The immunology of hepatocellular carcinoma. Nat Immunol 2018;19(3):222–232. doi:10.1038/s41590-018-0044-z.

[6] EASL Clinical Practice Guidelines: Management of hepatocellular carcinoma. J Hepatol 2018;69(1):182–236. doi:10.1016/j.jhep.2018.03.019.

[7] Marrero JA, Kulik LM, Sirlin CB, Zhu AX, Finn RS, Abecassis MM, *et al*. Diagnosis, staging, and management of hepatocellular carcinoma: 2018 practice guidance by the American Association for the Study of Liver Diseases. Hepatology 2018;68(2):723–750. doi:10.1002/hep.29913.

[8] Terzi E, Golfieri R, Piscaglia F, Galassi M, Dazzi A, Leoni S, *et al*. Response rate and clinical outcome of HCC after first and repeated cTACE performed "on demand". J Hepatol 2012;57(6):1258–1267. doi:10.1016/j.jhep.2012.07.025.

[9] Kudo M, Matsui O, Izumi N, Kadoya M, Okusaka T, Miyayama S, *et al*. Transarterial chemoembolization failure/refractoriness: JSH-LCSGJ criteria 2014 update. Oncology 2014;87(Suppl 1):22–31. doi:10.1159/000368142.

[10] Park JW, Amarapurkar D, Chao Y, Chen PJ, Geschwind JF, Goh KL, *et al*. Consensus recommendations and review by an International Expert Panel on Interventions in Hepatocellular Carcinoma (EPOIHCC). Liver Int 2013;33(3):327–337. doi:10.1111/liv.12083.

[11] Raoul JL, Gilabert M, Piana G. How to define transarterial chemoembolization failure or refractoriness: a European perspective. Liver Cancer 2014;3(2):119–124. doi:10.1159/000343867.

[12] Arizumi T, Ueshima K, Minami T, Kono M, Chishina H, Takita M, *et al*. Effectiveness of sorafenib in patients with transcatheter arterial chemoembolization (TACE) refractory and intermediate-stage hepatocellular carcinoma. Liver Cancer 2015;4(4):253–262. doi:10.1159/000367743.

[13] Ogasawara S, Chiba T, Ooka Y, Kanogawa N, Motoyama T, Suzuki E, *et al*. Efficacy of sorafenib in intermediate-stage hepatocellular carcinoma patients refractory to transarterial chemoembolization. Oncology 2014;87(6):330–341. doi:10.1159/000365993.

[14] Iwasa S, Ikeda M, Okusaka T, Ueno H, Morizane C, Nakachi K, *et al*. Transcatheter arterial infusion chemotherapy with a fine-powder formulation of cisplatin for advanced hepatocellular carcinoma refractory to transcatheter arterial chemoembolization. Jpn J Clin Oncol 2011;41(6):770–775. doi:10.1093/jjco/hyr037.

[15] Hsu SJ, Xu X, Chen MP, Zhao ZY, Wang Y, Yin X, *et al*. Hepatic arterial infusion chemotherapy with modified FOLFOX as an alternative treatment option in advanced hepatocellular carcinoma patients with failed or unsuitability for transarterial chemoembolization. Acad Radiol 2021;28(Suppl 1):S157–S166. doi:10.1016/j.acra.2021.01.024.

[16] Song DS, Choi JY, Yoo SH, Kim HY, Song MJ, Bae SH, *et al*. DC bead transarterial chemoembolization is effective in hepatocellular carcinoma refractory to conventional transarteral chemoembolization: A pilot study. Gut Liver 2013;7(1):89–95. doi:10.5009/gnl.2013.7.1.89.

[17] Kobayashi S, Tajiri K, Murayama A, Entani T, Futsukaichi Y, Nagata K, *et al*. Drug-eluting bead-transcatheter arterial chemoembolization for advanced hepatocellular carcinoma refractory to conventional lipiodol-based transcatheter arterial chemoembolization. J Hepatocell Carcinoma 2020;7:181–189. doi:10.2147/JHC.S273929.

[18] Klompenhouwer EG, Dresen RC, Verslype C, Laenen A, De Hertogh G, Deroose CM, *et al*. Safety and efficacy of transarterial radioembolisation in patients with intermediate or advanced stage hepatocellular carcinoma refractory to chemoembolisation. Cardiovasc Intervent Radiol 2017;40(12):1882–1890. doi:10.1007/s00270-017-1739-5.

[19] Kim PH, Gwon DI, Kim JW, Chu HH, Kim JH. The safety and efficacy of balloon-occluded transcatheter arterial chemoembolization for hepatocellular carcinoma refractory to conventional transcatheter arterial chemoembolization. Eur Radiol 2020;30(10):5650–5662. doi:10.1007/s00330-020-06911-9.

[20] Xu X, Ding Y, Pan T, Gao F, Huang X, Sun Q. CT-guided $^{125}$I brachytherapy in the treatment of hepatocellular carcinoma refractory to conventional transarterial chemoembolization: A pilot study. Cancer Manag Res 2021;13:3317–3326. doi:10.2147/CMAR.S305422.

[21] Ikeda M, Mitsunaga S, Shimizu S, Ohno I, Takahashi H, Okuyama H, *et al*. Efficacy of sorafenib in patients with hepatocellular carcinoma refractory to transcatheter arterial chemoembolization. J Gastroenterol 2014;49(5):932–940. doi:10.1007/s00535-013-0853-7.

[22] Kodama K, Kawaoka T, Aikata H, Uchikawa S, Inagaki Y, Hatooka M, *et al*. Comparison of clinical outcome of hepatic arterial infusion chemotherapy and sorafenib for advanced hepatocellular carcinoma according to macrovascular invasion and transcatheter arterial chemoembolization refractory status. J Gastroenterol Hepatol 2018;33(10):1780–1786. doi:10.1111/jgh.14152.

[23] Hatooka M, Kawaoka T, Aikata H, Morio K, Kobayashi T, Hiramatsu A, *et al*. Comparison of outcome of hepatic arterial infusion chemotherapy and sorafenib in patients with hepatocellular carcinoma refractory to transcatheter arterial chemoembolization. Anticancer Res 2016;36(7):3523–3529.

[24] Yoo SH, Kwon JH, Nam SW, Lee JY, Kim YW, Shim DJ, *et al*. Transarterial infusion of epirubicin and cisplatin combined with systemic infusion of

5-flurouracil versus sorafenib for hepatocellular carcinoma with refractoriness of transarterial chemoembolization using doxorubicin. Cancer Control 2020;27(2):1073274820935843. doi:10.1177/1073274820935843.
[25] Villani R, Cavallone F, Sangineto M, Fioravanti G, Romano AD, Serviddio G. Management of intermediate-stage hepatocellular carcinoma in the elderly with transcatheter arterial chemoembolization failure: Retreatment or switching to systemic therapy? Int J Clin Pract 2021;75(4):e13733. doi:10.1111/ijcp.13733.
[26] Chen S, Shi M, Shen L, Qi H, Wan W, Cao F, *et al*. Microwave ablation versus sorafenib for intermediate-Stage Hepatocellular carcinoma with transcatheter arterial chemoembolization refractoriness: a propensity score matching analysis. Int J Hyperthermia 2020;37(1):384–391. doi:10.1080/02656736.2020.1752400.
[27] Shimose S, Kawaguchi T, Tanaka M, Iwamoto H, Miyazaki K, Moriyama E, *et al*. Lenvatinib prolongs the progression-free survival time of patients with intermediate-stage hepatocellular carcinoma refractory to transarterial chemoembolization: A multicenter cohort study using data mining analysis. Oncol Lett 2020;20(3):2257–2265. doi:10.3892/ol.2020.11758.
[28] Wu J, Li A, Yang J, Lu Y, Li J. Efficacy and safety of TACE in combination with sorafenib for the treatment of TACE-refractory advanced hepatocellular carcinoma in Chinese patients: a retrospective study. Onco Targets Ther 2017;10:2761–2768. doi:10.2147/OTT.S131022.
[29] Lin PT, Teng W, Jeng WJ, Hsieh YC, Hung CF, Huang CH, *et al*. Add-on sorafenib is beneficial for hepatocellular carcinoma patients with transarterial chemoembolization refractoriness: a real-world experience. Eur J Gastroenterol Hepatol 2020;32(9):1192–1199. doi:10.1097/MEG.0000000000001637.
[30] Kaibori M, Matsushima H, Ishizaki M, Kosaka H, Matsui K, Kariya S, *et al*. The impact of sorafenib in combination with transarterial chemoembolization on the outcomes of intermediate-stage hepatocellular carcinoma. Asian Pac J Cancer Prev 2021;22(4):1217–1224. doi:10.31557/APJCP.2021.22.4.1217.
[31] Huang WK, Yang SF, You LN, Liu M, Liu DY, Gu P, *et al*. Transcatheter arterial chemoembolisation (TACE) plus S-1 for the treatment of BCLC stage B hepatocellular carcinoma refractory to TACE. Contemp Oncol (Pozn) 2016;20(6):468–474. doi:10.5114/wo.2016.65607.
[32] Huang W, You L, Yang S, Liu D, Liu M, Wang H, *et al*. Metronomic S-1 chemotherapy plus transcatheter arterial chemoembolization (TACE): a promising treatment of hepatocellular carcinoma refractory to TACE. J BUON 2016;21(4):909–916.
[33] Qiu Z, Shen L, Chen S, Qi H, Cao F, Xie L, *et al*. Efficacy of apatinib in transcatheter arterial chemoembolization (TACE) refractory intermediate and advanced-stage hepatocellular carcinoma:A propensity score matching analysis. Cancer Manag Res 2019;11:9321–9330. doi:10.2147/CMAR.S223271.
[34] Zheng L, Fang S, Wu F, Chen W, Chen M, Weng Q, *et al*. Efficacy and safety of TACE combined with sorafenib plus immune checkpoint inhibitors for the treatment of intermediate and advanced TACE-refractory hepatocellular carcinoma: A retrospective study. Front Mol Biosci 2021;7:609322. doi:10.3389/fmolb.2020.609322.
[35] Kudo M, Finn RS, Qin S, Han KH, Ikeda K, Piscaglia F, *et al*. Lenvatinib versus sorafenib in first-line treatment of patients with unresectable hepatocellular carcinoma: a randomised phase 3 non-inferiority trial. Lancet 2018;391(10126):1163–1173. doi:10.1016/S0140-6736(18)30207-1.
[36] Kudo M, Ueshima K, Chan S, Minami T, Chishina H, Aoki T, *et al*. Lenvatinib as an initial treatment in patients with intermediate-stage hepatocellular carcinoma beyond up-to-seven criteria and child-pugh A liver function: A proof-of-concept study. Cancers (Basel) 2019;11(8):1084. doi:10.3390/cancers11081084.
[37] Kudo M, Ueshima K, Ikeda M, Torimura T, Tanabe N, Aikata H, *et al*. Randomised, multicentre prospective trial of transarterial chemoembolisation (TACE) plus sorafenib as compared with TACE alone in patients with hepatocellular carcinoma: TACTICS trial. Gut 2020;69(8):1492–1501. doi:10.1136/gutjnl-2019-318934.
[38] Lencioni R, Llovet JM, Han G, Tak WY, Yang J, Guglielmi A, *et al*. Sorafenib or placebo plus TACE with doxorubicin-eluting beads for intermediate stage HCC: The SPACE trial. J Hepatol 2016;64(5):1090–1098. doi:10.1016/j.jhep.2016.01.012.
[39] Meyer T, Fox R, Ma YT, Ross PJ, James MW, Sturgess R, *et al*. Sorafenib in combination with transarterial chemoembolisation in patients with unresectable hepatocellular carcinoma (TACE 2): a randomised placebo-controlled, double-blind, phase 3 trial. Lancet Gastroenterol Hepatol 2017;2(8):565–575. doi:10.1016/S2468-1253(17)30156-5.
[40] Zhong BY, Wang WS, Zhang S, Zhu HD, Zhang L, Shen J, *et al*. Re-evaluating transarterial chemoembolization failure/refractoriness: A survey by Chinese college of interventionalists. J Clin Transl Hepatol 2021;9(4):521–527. doi:10.14218/JCTH.2021.00049.

*Journal of Clinical and Translational Hepatology* **2022** vol. 10(4) | 748–756
DOI: 10.14218/JCTH.2021.00368

Review Article

# Impact of Liver Functions by Repurposed Drugs for COVID-19 Treatment

Rongzhi Zhang[1], Qiang Wang[2] and Jianshe Yang[1,2,3*]

*[1]The Second Clinical Medical College of Lanzhou University, Lanzhou, Gansu, China; [2]Gansu Medical College, Pingliang, Gansu, China; [3]Shanghai Tenth People's Hospital, Tongji University School of Medicine, Shanghai, China*

**Received:** 26 August 2021 | **Revised:** 17 September 2021 | **Accepted:** 10 October 2021 | **Published:** 4 January 2022

## Abstract

Liver injury is an important complication that may arise in patients suffering from coronavirus disease 2019 (COVID-19) and is accompanied by a transient increase of transaminases and/or other liver enzymes. Liver function test (LFT) abnormalities generally disappear when the COVID-19 resolves or hepatotoxic drugs are discontinued. The LFT abnormalities are associated with drug-induced liver injury (DILI), due to the overuse of antimalarials, antivirals, and antimicrobials. Studies have reported varying levels of these liver injuries in COVID-19 patients; however, most involve elevated serum aminotransferases. Hepatic dysfunction is significantly high in patients with severe illness and has poor outcome. Normally, the liver is involved in the metabolism of many drugs, including nucleoside analogs and protease inhibitors, which are currently repurposed to treat COVID-19. In addition to the manifestation of COVID-19, drugs implemented in its treatment may aggravate liver injuries. Thus, DILI should be considered especially in those COVID-19 patients with underlying liver disease. It was unclear whether the elevated liver enzymes have originated from the underlying disease or DILI in this population. Furthermore, it is difficult to establish a direct relationship between a specific drug and liver injury. Another possible effect of liver damage may due to inflammatory cytokine storm in severe COVID-19. Liver injury can change metabolism, excretion, dosing, and expected concentrations of the drugs, which may make it difficult to achieve a therapeutic dose of the drug or increase the risk of adverse effects. These repurposed drugs have shown limited efficacy against the virus and the disease itself; however, they still pose risk of adverse effects. Careful and close monitoring of LFTs in COVID-19 patients can provide early diagnosis of liver injury, and the risk of DILI could be reduced. Also, drug interactions in liver-transplanted patients should always be kept in mind for certain immunosuppressive therapies and their known signs of DILI. Altogether, abnormal LFTs should not be regarded as a contraindication to use COVID-19 experimental therapies if needed under emergent status.

**Citation of this article:** Zhang R, Wang Q, Yang J. Impact of Liver Functions by Repurposed Drugs for COVID-19 Treatment. J Clin Transl Hepatol 2022;10(4):748–756. doi: 10.14218/JCTH.2021.00368.

## Introduction

Coronavirus disease 2019 (COVID-19) continues to affect our lives, yet there are still no specific antiviral therapies for it. Global efforts have been put forth to develop a vaccine against the causative pathogen, severe acute respiratory syndrome-coronavirus-2 (SARS-CoV-2), due to the knowledge that vaccines are the most efficient method against viruses. The routine strategy for creating such a vaccine includes exploration of mRNA, inactivated viruses, DNA and/or recombinant protein, and viral vectors. However, the time consumption requirement of around 18 months or more makes it even harder to develop an efficacious vaccine in a timely manner, although massive-scale efforts are underway. In the meantime, a number of drugs used for other diseases have been repurposed to tackle the COVID-19 pandemic, since this approach may be one of the quickest ways to discover an efficacious treatment for this new viral infection.

Since the SARS-CoV-2 shares extensive homology with SARS-CoV and the Middle East respiratory syndrome coronavirus (MERS-CoV), effective therapies for these two viruses may also have therapeutic potential for the current SARS-CoV-2 outbreak.

Besides mainly targeting the respiratory system, SARS-CoV-2 attacks nearly all the other organs and systems, causing myocardial damage, acute coronary syndromes, acute kidney injury, gastrointestinal symptoms, and liver injury.[1] Liver injury is an important complication observed in COVID-19 patients. A ephemeral increase of transaminases and/or other liver enzymes may occur in COVID-19 patients within the range of 10.5–53.1%.[2,3] These abnormalities are generally self-limiting, mild to moderate increases, and mainly seen among symptomatic and severe COVID-19 patients.[3,4] Liver function test (LFT) abnormalities generally disappear when the COVID-19 infection resolves or hepatotoxic drugs are discontinued.[5]

**Keywords:** Liver injury; Hepatotoxicity; COVID-19; Antivirals; Aminotransferases; DILI.

**Abbreviations:** ADEs, adverse drug events; ALP, alkaline phosphatase; ALT, alanine aminotransferase; AST, aspartate transaminase; COVID-19, coronavirus disease 2019; CPT, Child Pugh Turcotte; CYP, cytochrome P450 enzymes; DILI, drug-induced liver injury; GGT, gamma-glutamyl transferase; LFT, liver function test; LPV/r, lopinavir/ritonavir; OATP, organic anion transporting polypeptide; SARS-CoV-2, severe acute respiratory syndrome-coronavirus-2; ULN, upper limit of normal.

***Correspondence to:** Jianshe Yang, Shanghai Tenth People's Hospital, Tongji University School of Medicine, Shanghai 200072, China. ORCID: https://orcid.org/0000-0001-7069-6072. Tel/Fax: +86-21-66302721, E-mail: yangjs@impcas.ac.cn

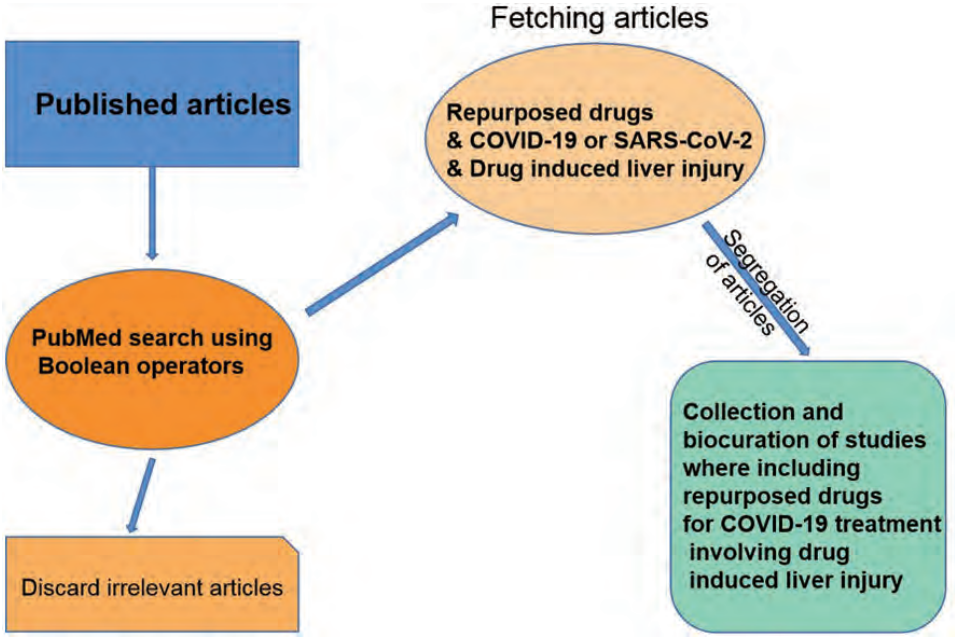


**Fig. 1. Schema of literature fetching and filtering for repurposed drugs in treatment to COVID-19 with DILI. DILI, drug-induced liver injury.**

Although the underlying mechanisms remain unknown, virus-induced inflammation, liver hypoxia and drug-induced liver injury (DILI) are three primary factors associated with hepatic injury.[6] LFT abnormalities associated with DILI due to the overuse of antimalarials, antivirals, and antimicrobials during COVID-19 necessitate special attention of the attending physicians.[7]

Rising levels of alanine aminotransferase (ALT) and aspartate transaminase (AST) are frequently indicative of hepatocellular damage, while this trend for alkaline phosphatase (ALP) and gamma-glutamyl transferase (GGT) is associated with bile duct damage or cholestasis. Serum bilirubin levels indicate liver secretion capacity, while serum albumin level and prothrombin time indicate liver synthesis capacity. ALT and AST enzymes have wide tissue distributions. The AST enzyme is found in the liver, heart, kidney, brain, pancreas, and leucocytes; thus, isolated AST elevations usually indicate organ injury. ALT is also found in skeletal muscle, myocardium, lungs, and kidneys. Hence, minor AST and ALT elevations remain nonspecific, especially in severe illness with multiorgan injury, as in severe COVID-19. As expected, there is heterogeneity in the reported literature regarding the incidence and impact of liver injury in COVID-19.

We used "Boolean Operators" such as AND, OR and NOT to search relevant research articles/reviews from the PubMed for repurposed drugs applied as COVID-19 treatment. The repurposed drugs of chloroquine and hydroxychloroquine, remdesivir, ribavirin, umifenovir, and favipiravir are already being used in clinical trials to treat the COVID-19 patients. These drugs have been approved for a different indication and belong to diverse categories, such as antimalarial/antiparasitic, antiretroviral/anti-viral, or protective against rheumatoid arthritis. As described above, though a vaccine would be an ideal option for providing active immunity against the SARS-CoV-2, it is time-consuming. The repurposed drugs are the most viable option against SARS-CoV-2 currently. Hence, we searched, obtained and filtered the relevant articles in the literature, with the schema as shown in Figure 1.

We have searched the literature and screened published research articles to further investigation to determine which molecule the repurposed drug targets and their route of administration. Based on the literature survey, we divided the repurposed drugs that can be used for the trials to treat COVID-19 into four categories: (I) antimalarial/antiparasitic drugs; (II) drugs used for rheumatoid arthritis; (III) antiretroviral/antiviral drugs; (IV) others. Liver injuries were involved in each of these five categories. Altogether, a total of 106 articles/reviews (all in English language) containing "COVID-19 & drug-induced liver injury" were screened and selected for analysis, among which there were 44 reviews, 5 books and documents, 1 meta-analysis and 1 systematic review, and 55 other type articles, including clinical trials.

## Liver and COVID-19

Studies have reported varying levels of liver injury in COVID-19 patients but mostly elevated serum aminotransferases.[8] Two to eleven percent of patients have existing chronic liver disease and 14–53% develop hepatic dysfunction, particularly in severe COVID-19. Hepatic dysfunction is significantly high in severe patients and associated with poor outcomes.[3]

In a study by Zhang *et al*.,[9] the mean level of ALT (37.9 vs. 21.2 IU/L), AST (38.9 vs. 24.4 IU/L), GGT (56.9 vs. 28.5 IU/L), and total bilirubin (14.1 vs. 10.3 mg/dL) was higher in severe COVID-19 patients than that in mild COVID-19 patients. Most of the LFTs in COVID-19 patients were found to be correlated with C-reactive protein (CRP) and neutrophil-to-lymphocyte ratio (NLR) levels. Histological examination of the needle biopsy specimens reveals mild sinusoidal dilatation and minimal lymphocytic infiltration, while other specific damages are absent. In another study with 417 COVID-19 patients, 21.8% developed severe disease, 318 had abnormal LFTs and 90 had signs of liver injury during hospitalization.[10]

Goel *et al*.[7] showed that baseline and ≥3×upper limit of normal (ULN) transaminase elevations was present in 61.2% and 9.4% of patients at admission, respectively.

Furthermore, 72.1% and 22.4% of patients developed in baseline and ≥3×ULN elevated transaminases during the course of COVID-19, respectively. However, bilirubin and ALP elevations were less likely to be apparent at admission (11.4% and 12.6%, respectively) and through the course of the disease (17.7% and 22%). All LFT changes were correlated with inflammatory markers, while hyperbilirubinemia was correlated with elevated mortality. On the other hand, the effect of AST and ALT levels on mortality are different, with elevated AST being associated with mortality but ALT with survival.

A study reported that the hospitalized patients have a 76.3% abnormal LFTs and 21.5% have liver injury. Patients with severe pneumonia tended to have abnormal LFTs. The emergence of abnormal LFTs (3×ULN) was more common in the first 2 weeks of hospitalization. Lopinavir/ritonavir (LPV/r) treatment was found to be related to increased risk for liver injury.[10] In another study, it was reported that liver injury occurred in 14.8% of COVID-19 patients, mostly in severe cases. They also stated that liver injury occurred after administrating multiple drugs, such as LPV/r (18.6%), which are tightly associated with liver morbidity.[11] Huang *et al*.,[12] have reported that 30.7% of COVID-19 patients were diagnosed with nonalcoholic fatty liver disease (NAFLD) and 35.7% had abnormal LFTs, according to the clinical features of COVID-19 patients with NAFLD. The median ALT levels (35 IU/L vs. 23 U/L) and the elevated ALT (>40 U/L) (40.7% vs. 10.8%) were significantly higher in patients with NAFLD compared to those without, respectively. Multivariate analysis showed that age >50 years and concurrent NAFLD were independent risk factors of ALT elevation; however, the usage of interferon α-2b inhalation reduced the risk of ALT elevation.

## Liver and Proposed Drugs of COVID-19

### *Effects of drugs on liver function*

The liver is a principal site for the metabolization and elimination of chemical substances. Besides, it is involved in the metabolism of various drugs, including nucleoside analogs and protease inhibitors, which are currently repurposed for COVID-19 treatment. In addition to the manifestation of COVID-19, drugs implemented in its treatment may aggravate liver injury. Thus, DILI should be further evaluated especially for those patients with underlying liver disease.[13] It has remained unclear where the elevated liver enzymes originate from (either the disease or DILI) in this population. It has also been difficult to confirm the direct relationship between a specific drug and liver injury, due to the common combined use of antimalarials, antivirals, antimicrobials, and anticoagulants during COVID-19.[14] Finally, inflammatory cytokine storms in severe COVID-19 can result in liver damage.[13]

Some medications previously used to treat a variety of other diseases, i.e. antivirals (such as LPV/r, remdesivir, ribavirin, favipiravir, umifenovir), antimalarials (chloroquine and hydroxychloroquine), antimicrobials (azithromycin, interferons), and immunomodulators (corticosteroids, tocilizumab) have been the widely repurposed in the fight against COVID-19.[15] These drugs have a comparable risk for liver injury (Table 1).[10,11,16–37]

Cai *et al*.[10] demonstrated that patients under LPV/r had higher total bilirubin and GGT levels during hospitalization. In a study by Sun *et al*.,[16] evaluating adverse drug events (ADEs) in 217 COVID-19 patients, ADEs were associated with LPV/r and umifenovir, at rates of 63.8% and 18.1%, respectively; in addition, liver system disorders were the most frequently observed ADEs, after gastrointestinal disorders. In a meta-analysis,[17] the pooled incidence of DILI among COVID-19 patients was 25.4%; DILI occurred in 37.2% and 15.2% of COVID19 patients receiving LPV/r and remdesivir, respectively.

Interferon-β is produced by recombinant technology and is a cytokine with antiviral, immunomodulatory and antiproliferative properties. Interferon-β is available in three subtypes – 1a, 1b and pegylated β-1a – and all are approved for use in multiple sclerosis by either subcutaneous or intramuscular administration.[38] All forms of interferon-β may also induce liver injury, though most of such cases are mild and even asymptomatic. Interferon-related DILI is transient, with mild elevations in serum aminotransferases (ALT and AST), and with normal or mildly elevated ALP levels.[18] Whereas, LPV/r treatment had a higher rate of enzymes elevation (56% vs. 25%).[19]

LPV/r administration will induce moderate to severe elevations in serum aminotransferase levels (>5×ULN). Low-dose ritonavir has less impact on the frequency or severity of LFT elevations. Additionally, ritonavir has some properties similar to an enzymatic inhibitor and it can increase the serum level of co-administered drugs, resulting in a higher risk of hepatotoxicity.[18]

Hydroxychloroquine and chloroquine are antiviral/immune modulators that are used for the treatment and prophylaxis of malaria, rheumatoid arthritis, lupus erythematosus, photodermatosis, and liver amoebiasis. Hydroxychloroquine is metabolized by several CYP enzymes in the liver, with desethylhydroxychloroquine being an active metabolite. The USA's Food and Drug Administration's prescribing information cautions use in patients with existing liver disease and/or concomitant use with hepatotoxic drugs.[39,40] Hydroxychloroquine is known to accumulate in the liver.[41] and animal studies have shown that accumulation occurs rapidly, in the first 2 weeks of treatment.[42] However, hydroxychloroquine was found to have a low hepatic extraction ratio, indicating that a reduction in liver blood flow in cirrhosis may not directly result in increased exposure to the drug.[43] Hydroxychloroquine is also known to be hydrophilic,[44] and this should be a consideration in patients with ascites and decompensated cirrhosis. Based on these lines of evidence, hydroxychloroquine is regarded as a possible but rare cause of DILI.[18] Falcao *et al*.[20] reported a severe COVID-19 patient who showed a 10-fold increase of transaminases after using hydroxychloroquine, which returned to normal levels after withdrawal of the drug.

Remdesivir is a nucleotide analog for treatment of hepatitis C virus, used formerly.[45,46] Currently, data regarding hepatotoxicity of remdesivir is inadequate to draw firm conclusions. There was no liver injury in LiverTox,[18] and liver toxicity data were not reported in Ebola trials; however, abnormal liver enzyme profiles are common during Ebola infection, making it difficult to rule-out accompanying drug-induced liver toxicity.[47–49] The specificity of the cyano group in the remdesivir molecule allows for it to avoid inhibition by the host mitochondrial DNA polymerase and consequently limits the potential risk for lactic acidosis or mitochondrial toxicity. LFT elevations have varied widely among trials of remdesivir, accounting for 1% to 32% of participants.[21–23] LFT elevation rate was 23% among 53 patients, which led to remdesivir discontinuation in two patients, while bilirubin elevation was not detected in that trial.[24] Wang *et al*.[25] showed that hypoalbuminemia, hyperbilirubinemia, and AST elevation were present in 13%, 10%, and 5% of patients treated with remdesivir, respectively; also, in the remdesivir group, three patients discontinued treatment due to ALT elevation. Sabers *et al*.[50] reported that a patient presented with high liver enzymes (≥20×ULN) and had received remdesivir; eventually, the patient's liver enzymes improved through the course of the disease and they were discharged on day 10 of hospitalization.

**Table 1. Changes in liver functions and liver enzymes in COVID-19 trials**

| Drugs | Toxicity | Type of toxicity | | Reference |
|---|---|---|---|---|
| LPV/r | 8.8% | ALT elevation (>3 ULN) | | 10 |
| | 4.8% | AST elevation (>3 ULN) | | |
| | 10.3% | GGT elevation (>3 ULN) | | |
| | 2.6% | Total bilirubin elevation (>3 ULN) | | |
| | 18.6% | Liver injury | | 11 |
| | 37.2% | Liver injury | | 17 |
| | 63.8% | Any adverse drug effect | | 16 |
| | 57.8% | Elevation is more than the ULN value (ALT, AST, ALP, GGT, and total bilirubin) | | 19 |
| Umifenovir | 18.1% | Any adverse drug effect | | 16 |
| Remdesivir | 15.2% | Liver injury | | 17 |
| | 3.4% | AST elevation | | 21 |
| | 2.3% | ALT elevation | | |
| | 7% | ALT elevation | | 22 |
| | 5.8% | AST elevation | | |
| | 32% | AST-ALT elevation | | 23 |
| | 23% | Increased LFTs | | 24 |
| | 10% | Hyperbilirubinemia | | 25 |
| | 5% | AST elevation | | |
| | 2% | ALT elevation leading to discontinuation of remdesivir | | |
| Ribavirin Favipiravir | No data | Elevation in serum aminotransferases | | 18 |
| | 2.1-fold | ALT and AST elevation | CPT A | 26–28 |
| | 2.0-fold | | CPT B | |
| | 3.7-fold | | CPT C | |
| Hydroxychloroquine | 10-fold | Elevation in transaminases | | 18,20 |
| Azithromycin | 1–2% | Elevation in serum aminotransferases | | 18 |
| Interferons | 25% | ALT and AST elevation, and mildly elevated ALP | | 18,19 |
| Corticosteroids | N/A | No ADEs for short duration | | 18,32,33 |
| Convalescent plasma (antibody) | N/A | No detailed information | | 28,34 |
| Tocilizumab | Mild | Liver enzyme elevation | | 18,29–31 |
| Acetaminophen | $48\%_{max}$ | Dose-related hepatotoxicity | | 35–37 |

COVID-19, coronavirus disease 2019; ALP, alkaline phosphatase; ALT, alanine aminotransferase; AST, aspartate transaminase; GGT, gamma-glutamyl transferase; LFT, liver function test; LPV/r, lopinavir/ritonavir; ULN, upper limit of normal; CPT, Child Pugh Turcotte; ADEs, adverse drug events.

There is a theoretical risk of P-glycoprotein interaction with remdesivir. Inhibition of P-glycoprotein with comedications reduces efflux of remdesivir from hepatocytes, raising cellular remdesivir concentration to supratherapeutic levels. However, the occurrence of this interaction is very low, because of remdesivir being the minor substrate of P-glycoprotein, as well as its short half-life.[51] In the recent case report by Carothers *et al*.,[52] the benefit of acetylcysteine continuous infusion was investigated in acute liver injury related to remdesivir. Both of the two patients investigated showed significant increases in transaminase levels with coagulopathy and encephalopathy in response to remdesivir therapy; the continuous infusion of acetylcysteine rapidly resolved the high transaminase levels in these patients.

Favipiravir is a type of RNA-dependent RNA polymerase (RdRp) inhibitor. It presumably acts as a nucleotide analog that selectively inhibits the viral RdRp or causes lethal mutagenesis upon embedding into the virus RNA.[53–57] Favipiravir, when used for the treatment of influenza, is administered at a dose of 1600 mg twice daily on day 1, followed by 600 mg twice daily on days 2–5. Besides being a treatment for influenza virus,[58] favipiravir has shown potent antiviral activity against other segmented negative-strand RNA viruses in both *in vitro* and *in vivo* studies.[59,60] Furthermore, some positive-strand RNA viruses can also be inactivated by favipiravir,[61,62] and the virus replication process can be interfered with by the drug's competition with purine nucleosides, as has been shown to consequently inhibit the viral RdRp of SARS-CoV-2.[26] Studies have also shown that

favipiravir administration provides better prognosis in COVID-19 patients in terms of disease progression and viral clearance.[27] ALT and AST elevation is just a possible adverse effect of favipiravir, however no data are available in cirrhosis patients.[28]

Tocilizumab is a monoclonal antibody against the interleukin-6 (IL-6) receptor, which is usually used to treat the cytokine storm that occurs in the advanced stages of the disease.[63] Though small series and case reports suggest its beneficial effects, it was not proven in randomized controlled trials.[29,64,65] Tocilizumab administration can lead to liver enzyme elevation but rarely to severe liver injury.[18] Recently, a patient with COVID-19 was reported on due to their transaminase levels increasing 40-fold after 24 h of initiation of tocilizumab administration.[66] Tocilizumab may pose a risk of hepatitis B virus (HBV) reactivation, thereby causing risk of indirect liver damage.[67] A study predicted that patients with severe COVID-19 and resolved HBV under immune modulator treatment had a low risk for HBV reactivation, and recommended that patients without antibodies to hepatitis B surface antigen (anti-HBs) be followed-up after discharge, if possible, and suggested that a short course of antiviral prophylaxis may be preferred. No hepatitis B surface antigen seroreversion was detected in their cohort and only two (3%) patients had detectable serum HBV-DNA.[30] In another study, liver injury was observed in COVID-19 patients with or without chronic HBV. Also, three patients experienced hepatitis B reactivation. Thus, monitoring of LFTs and HBV-DNA levels was recommended in COVID-19 patients treated with tocilizumab.[31]

Furthermore, membrane transporters localized on the cell membrane, especially those on tissues in the central organ for drug metabolism, such as the liver, can effectively influence pharmacokinetic characteristics and ADEs. Canalicular ABC transporters in hepatocytes, such as ABCC2/MRP2, ABCG2/BCRP, ABCB1/MDR1/P-gp and ABCB11/BSEP, mediate the extrusion of endo- and xenobiotics into the bile. P-gp, MRP2 and ABCG2 are multispecific transporters mediating the efflux of hydrophobic or partially detoxified amphiphilic compounds. MRP2 is the key transporter for bilirubin conjugates. The SLC-type transporter MATE1 in the hepatocyte canalicular membrane mainly transports cationic drugs, but also some zwitterionic and anionic molecules,[68,69] and mediates their biliary excretion. Inhibition of these drug exporters may cause elevated liver toxicity, such as cholestasis or DILI. All of the above repurposed drugs have various effects in inducing DILI through the special inhibition to transporters. A recent study showed that lopinavir and ritonavir, given in low micromolar concentrations, inhibited BSEP and MATE1 exporters as well as OATP1B1/1B3 uptake transporters. Ritonavir had a similar inhibitory pattern but also inhibiting OCT1. Specifically, remdesivir strongly inhibited MRP4, OATP1B1/1B3, MATE1 and OCT1. Favipiravir had no significant effect on any of these transporters.[70]

Corticosteroid is used in the treatment of a variety of inflammatory and autoimmune conditions. It is used at a wide range of doses, ranging from 0.5 to 80 mg daily.[71] Other glucocorticoids, including prednisolone, are used regularly for patients with significant liver disease in the treatment of autoimmune and alcoholic hepatitis, including for patients with cirrhosis, acute liver failure, ALT/AST >10×ULN and post-liver transplant.[72,73] Dexamethasone is metabolized in the liver via CYP3A4,[74] and has very limited influence in hepatic impairment, though its half-life is prolonged in severe liver disease.[71] Corticosteroid treatments are associated with hepatic steatosis, hepatic glycogenosis, and hepatic enlargement.[18] Corticosteroids can also promote hepatic gluconeogenesis, reduce peripheral use of glucose, and increase insulin levels consequently. Glucocorticoids have a pro-adipogenic function of increasing deposition of abdominal fat, and leading to glucose intolerance and hypertriglyceridemia. In addition, these drugs play a role in controlling liver metabolism and can lead to the development of hepatic steatosis.[32] But, in COVID-19 patients, this effect is unlikely to be significant given the very low dose (6 mg daily) and short duration.[33] Although toxicities that may arise in long-term use are not a problem for COVID-19 patients, it should be considered that there are short-term risks, such as HBV reactivation.[30]

Convalescent plasma has shown a potential therapeutic effect, with low risk for the treatment of severe COVID-19 patients.[34] At the same, there are still few experiences of convalescent plasma therapy in COVID-19 patients with chronic liver disease.[28]

Azithromycin is a macrolide antibiotic used in treatment of various infections, such as community-acquired pneumonia, bronchitis, soft tissue infections and uncomplicated genital infections due to *Chlamydia trachomatis* and *Neisseria gonorrhoeae*. The liver is the main site for metabolism of azithromycin and 50% is excreted unchanged in the bile, although some inactive metabolites are also found.[35] A previous study demonstrated that azithromycin has an association with a low rate of acute, transient, and asymptomatic elevations in serum aminotransferases, occurring in 1% to 2% of patients treated for short periods.[18] This drug can, thus, be exempted for further evaluation when used in COVID-19 patients, especially with low dose and short duration.

Ribavirin is a guanosine nucleoside analogue, approved for use in combination with direct acting antivirals or pegylated-interferon 2a or 2b for treatment of hepatitis C. In the treatment of hepatitis C, ribavirin is given orally and is dosed dependent on weight, ranging from 800 mg to 1200 mg daily. However, it has not been associated with serum aminotransferase elevations. Ribavirin treatment is usually used in COVID-19 patients with underlying liver disease; however, it is difficult to interpret increases in serum aminotransferase levels during therapy.[18]

Because of the fever and pain experienced by COVID-19 patients, several medicines agencies have warned physicians against the excessive use of non-steroidal anti-inflammatory drugs (NSAIDs), while the acetaminophen (paracetamol) was strongly recommended.[35] However, this recommendation could possibly result in the misuse of acetaminophen and consequently increase liver injury. Acetaminophen use is associated with generally mild ADEs, such as hepatitis, cholestasis, or other nonspecific liver enzyme elevation, but acetaminophen-induced hepatotoxicity is mostly estimated to account for 48% of acute liver injury diagnoses, providing caution for acetaminophen-caused dose-related hepatotoxicity.[36,37]

Another important point is the potential drug-drug interactions (DDIs) between the drugs used in patients with transplantation (such as tacrolimus and steroids) and COVID-19. These DDIs may also indirectly increase the risk of hepatotoxicity if the effect of the immunosuppressive or the COVID-19 drug were to become altered pharmacodynamically or pharmacokinetically.[75]

### *Clarify the liver injury by DILI vs. systemic inflammation from COVID-19*

As described above, drugs implemented in the treatment may aggravate liver injury, which can occur besides the manifestation of COVID-19 or other underlying liver disease.[13] However, it was difficult to confirm the direct relationship between a specific drug and liver injury due to the combined use of all of above repurposed drugs during COVID-19.[14] According to the existing literature, we tried to conclude this complexity in order to caution the physicians

**Table 2. Potential ADEs of repurposed drugs on liver in COVID-19 patients and non-COVID-19 patients**

| Drugs | COVID-19 | Non-COVID-19 | Reference |
|---|---|---|---|
| LPV/r | + | +++ | 10,16,17,18,19 |
| | – | / | |
| Remdesivir | + | + | 17,18,21–25,50,51,52 |
| | – | / | |
| Ribavirin | + | +/– | 18 |
| | – | – | |
| Favipiravir | + | –/+ | 27,28 |
| | – | – | |
| Umifenovir | + | + | 16 |
| | – | / | |
| Hydroxychloroquine | + | –/+ | 18,20 |
| | – | N/A | |
| Azithromycin | + | –/+ | 18 |
| | – | – | |
| Interferons | + | +/– | 18 |
| | – | / | |
| Convalescent plasma (antibody) | + | –/+ | 28,34 |
| | – | N/A | |
| Corticosteroids | + | +/– | 30,32,33 |
| | – | – | |
| Tocilizumab | + | +/– | 18,63,29,64,65,66,67,30,31 |
| | – | – | |
| Acetaminophen | + | +++ | 35–37 |
| | – | +/– | |

Note: In COVID-19 column: with COVID-19(+), without COVID-19(–); in ADEs column: severe (+++), mild to Moderate (+), no ADEs (–), possible ADEs (+/–), possible no ADEs (–/+), with no report (N/A). COVID-19, coronavirus disease 2019; ADEs, adverse drug events.

and guide the drug use, and our findings are shown in Table 2.[10,16–25,50–52,27–37,63–67]

### *Recommendation on drug use in liver injury*

Liver injury can change metabolism, excretion, dosing, and expected concentrations of drugs, which may make it difficult to achieve an effective therapeutic dose or can increase the risk of ADEs.[76]

Acute liver injury has been commonly defined by the ULN of serum ALT, ALP, and serum concentration of total bilirubin based on the biological criteria, that is, elevation of ALT ≥5×ULN or ALP ≥2×ULN, or combination of ALT ≥3×ULN with a simultaneous total bilirubin concentration exceeding 2 ×ULN.[77,78]

Till now, the pharmacokinetics of remdesivir have not been evaluated in patients with hepatic injury. Hence, the hepatic function should be monitored in all patients before initiating and during daily treatment with remdesivir. Currently, remdesivir is not recommended in patients with ALT ≥5×ULN at baseline. It should be discontinued if ALT rises to higher than 5×ULN during treatment or if ALT elevation is accompanied by signs or symptoms of liver inflammation or increasing conjugated bilirubin, ALP, or INR, however, this therapy can be restarted if ALT is less than 5×ULN[79,80]

Since hydroxychloroquine commonly accumulates in the liver, it is recommended to monitor LFTs continuously and administrate it cautiously with concurrent hepatotoxic drugs.[81] It is also recommended that LFTs should be closely monitored for each patient while initiating tocilizumab; if ALT or AST are higher than 1.5×ULN, the treatment needs to be discontinued immediately.[82]

Since LPV/r is primarily metabolized by the liver, it is recommended to evaluate patient response and use with caution in case of liver injury. Although there is no need to reduce the dose for mild to moderate hepatic injury, frequent monitoring of LFTs is strongly recommended.[33] LPV/r administration has not been studied in patients with severe hepatic injury and its use is contraindicated.[83]

Azithromycin is eliminated predominantly in liver, and as such it should be used with caution due to its potential risk of hepatotoxicity and it should be avoided in patients with severe liver disease. A study has demonstrated that azithromycin pharmacokinetics do not differ consistently in patients with Child-Pugh A or B cirrhosis, in comparison with healthy volunteer; therefore, dosage modification is not required in these patient groups.[84] No difference in single-dose pharmacokinetics of ribavirin was noted in pa-

**Table 3. Four categories of repurposed drugs for COVID-19 treatment and their detailed information**

| Drug category | Drug | Dose recommendation | Metabolism | Reference |
|---|---|---|---|---|
| I. Anti-malarial/ anti-parasitic drugs | Hydroxychloroquine | Maximum dosage based on minimal data and risk of hepatotoxicity | Major: CYP3A4/5, Minor: CYP2D6, CYP2C8 | 18,20 |
| II. Drugs used for rheumatoid arthritis | Hydroxychloroquine | | | |
| | Tocilizumab | In patients with baseline ALT or AST >5×ULN, treatment is not recommended | Catabolic pathway | 18,63,29,64,65,66,67,30,31 |
| | corticosteroids | / | Hydroxylation via CYP3A4, followed by glucuronidation or sulfation | 30,32,33 |
| | Interferon-β | Caution if ALT >2.5×ULN, Dose reduction advised if ALT >5×ULN | Metabolized and excreted by liver and kidneys | 18 |
| | Azithromycin | Discontinue if signs of hepatic dysfunction | Liver: 35% to inactive metabolites | 18 |
| III. Anti-retroviral/anti-viral drugs | LPV/r | Use with caution in mild to moderate hepatic impairment and monitor for toxicities | CYP3A4/5, auto-induction own metabolism; stabilization after 10–16 days | 10,16,17,18,19 |
| | Remdesivir | Discontinuation: ALT >5×ULN or ALT elevation | *In vitro*: CYP2C8 CYP2D6, CYP3A4, OATP1B1, P-gp substrate | 17,18,21–25,50,51,52 |
| | Favipiravir | Dose adjustment should be considered | Extensive metabolism by hydroxylation (aldehyde oxidase and xanthine oxidase) to M1 and M2 | 27,28 |
| | Ribavirin | Discontinue if progressive and clinically significant ALT rises, despite dose reduction, or accompanied by increased bilirubin | Intracellular phosphorylation by adenosine kinase to ribavirin mono-, di-, and triphosphate metabolites | 18 |
| IV. Others | Acetaminophen | / | / | 35–37 |
| | Convalescent plasma (antibody) | / | / | 28,34 |

COVID-19, coronavirus disease 2019; ALT, alanine aminotransferase; AST, aspartate transaminase; LPV/r, lopinavir/ritonavir; ULN, upper limit of normal; CYP, cytochrome P450 enzymes; OATP, organic anion transporting polypeptide.

tients with mild, moderate, or severe hepatic dysfunction (Child-Pugh score A, B, or C).[85] Full-dose ribavirin can be used in severe hepatic dysfunction with caution; mild and moderate hepatic dysfunction associated renal impairment are suggested to make a proper dose reduction based on estimated glomerular filtration rate (eGFR).[33] Alteration of favipiravir dose is not recommended in mild and moderate hepatic impairment (Child-Pugh A and B), while it should be considered in severe hepatic injury (Child-Pugh C).[33]

Altogether, the detailed information of these repurposed drugs for COVID-19 treatment, including the family of the drug, the mode of action, and the possible mechanism by which it induces liver injury, are presented in the Table 3.[10,16–25,50–52,27–37,63–67]

## Conclusion

Through the last year, COVID-19 devastated our health care systems and invoked an unprecedented need for new treatment options to heal its notorious manifestations. The scientific community is still far from finding a 'silver bullet' to overcome its detrimental effects; thus, some medications with limited *in vitro* activity against the eliciting virus are

being repurposed for its treatment. Those repurposed drugs have had limited efficacy against the virus and the disease itself; however, they still pose risk of adverse effects. Close monitoring of liver functions in COVID-19 patients can provide early diagnosis of liver injury, and reduce the risk of DILI as much as possible. A special caution should be given to those patients who are liver-transplanted, for drug-drug interactions occurring under certain immunosuppressive therapies. Abnormal liver tests should not be a contraindication against use of COVID-19 experimental therapies, if needed.

## Limitations

Many measures have been applied against this virus during the pandemic, which have included officially approved Emergency Use Authorization (EUA) candidates and even some unofficial treatment methods. Among them, the repurposed old drugs have accounted for the majority in clinic, and most had been used before as anti-malarial/anti-parasitic, anti-retroviral/anti-viral, anti-cancer, or against rheumatoid arthritis drugs. Yet, there was no standard and systematic evaluation for their ADEs in COVID-19 patients, especially for their DILI aspects. As such, this review was limited by the ability to collect information on all of the repurposed drugs used worldwide. In-depth systematic exploration and discovery should be further improved for this topic.

## Acknowledgments

The authors would like to acknowledge Professor Xigang Jing at the Medical College of Wisconsin, USA, for his expert opinions on pathology and virology in support of this review.

## Funding

This work was supported by the Cuiying Scientific and Technological Innovation Program of Lanzhou University Second Hospital (Grant No. CY2019-BJ07) and the Gansu Natural Science Foundation (Grant No. 20JR10RA745).

## Conflict of interest

The authors have no conflict of interests related to this publication.

## Author contributions

Design of the work (JY) and writing of the manuscript (RZ, QW, JY). All authors have read and approved the final manuscript.

## References

[1] Gupta A, Madhavan MV, Sehgal K, Nair N, Mahajan S, Sehrawat TS, *et al*. Extrapulmonary manifestations of COVID-19. Nature Med 2020;26(7):1017–1032. doi:10.1038/s41591-020-0968-3.
[2] Guan WJ, Ni ZY, Hu Y, Liang WH, Ou CQ, He JX, *et al*. Clinical characteristics of coronavirus disease 2019 in China. N Engl J Med 2020;382(18):1708–1720. doi:10.1056/NEJMoa2002032.
[3] Zhang C, Shi L, Wang FS. Liver injury in COVID-19: management and challenges. Lancet Gastroenterol Hepatol 2020;5(5):428–430. doi:10.1016/S2468-1253(20)30057-1.
[4] Xu L, Liu J, Lu M, Yang D, Zheng X. Liver injury during highly pathogenic human coronavirus infections. Liver Int 2020;40(5):998–1004. doi:10.1111/liv.14435.
[5] Pawlotsky JM. COVID-19 and the liver-related deaths to come. Nature Rev Gastroenterol Hepatol 2020;17(9):523–525. doi:10.1038/s41575-020-0328-2.
[6] Olry A, Meunier L, Délire B, Larrey D, Horsmans Y, Le Louët H. Drug-induced liver injury and COVID-19 infection: The rules remain the same. Drug Saf 2020;43(7):615–617. doi:10.1007/s40264-020-00954-z.
[7] Goel H, Harmouch F, Garg K, Saraiya P, Daly T, Kumar A, *et al*. The liver in COVID-19: prevalence, patterns, predictors, and impact on outcomes of liver test abnormalities. Eur J Gastroenterol Hepatol 2020. doi:10.1097/meg.0000000000002021.
[8] Boettler T, Marjot T, Newsome PN, Mondelli MU, Maticic M, Cordero E, *et al*. Impact of COVID-19 on the care of patients with liver disease: EASL-ESCMID position paper after 6 months of the pandemic. JHEP Rep 2020;2(5):100169. doi:10.1016/j.jhepr.2020.100169.
[9] Zhang Y, Zheng L, Liu L, Zhao M, Xiao J, Zhao Q. Liver impairment in COVID-19 patients: A retrospective analysis of 115 cases from a single centre in Wuhan city, China. Liver Int 2020;40(9):2095–2103. doi:10.1111/liv.14455.
[10] Cai Q, Huang D, Yu H, Zhu Z, Xia Z, Su Y, *et al*. COVID-19: Abnormal liver function tests. J Hepatol 2020;73(3):566–574. doi:10.1016/j.jhep.2020.04.006.
[11] Cai Q, Huang D, Ou P, Yu H, Zhu Z, Xia Z, *et al*. COVID-19 in a designated infectious diseases hospital outside Hubei Province, China. Allergy 2020;75(7):1742–1752. doi:10.1111/all.14309.
[12] Huang R, Zhu L, Wang J, Xue L, Liu L, Yan X, *et al*. Clinical features of patients with COVID-19 with nonalcoholic fatty liver disease. Hepatol Commun 2020;4(12):1758–1768. doi:10.1002/hep4.1592.
[13] Alqahtani SA, Schattenberg JM. Liver injury in COVID-19: The current evidence. United European Gastroenterol J 2020;8(5):509–519. doi:10.1177/2050640620924157.
[14] Brito CA, Barros FM, Lopes EP. Mechanisms and consequences of COVID-19 associated liver injury: What can we affirm? World J Hepatol 2020;12(8):413–422. doi:10.4254/wjh.v12.i8.413.
[15] Sanders JM, Monogue ML, Jodlowski TZ, Cutrell JB. Pharmacologic treatments for coronavirus disease 2019 (COVID-19): A review. JAMA 2020;323(18):1824–1836. doi:10.1001/jama.2020.6019.
[16] Sun J, Deng X, Chen X, Huang J, Huang S, Li Y, *et al*. Incidence of adverse drug reactions in COVID-19 patients in China: An active monitoring study by hospital pharmacovigilance system. Clin Pharmacol Ther 2020;108(4):791–797. doi:10.1002/cpt.1866.
[17] Kulkarni AV, Kumar P, Tevethia HV, Premkumar M, Arab JP, Candia R, *et al*. Systematic review with meta-analysis: liver manifestations and outcomes in COVID-19. Aliment Pharmacol Ther 2020;52(4):584–599. doi:10.1111/apt.15916.
[18] Her M, Lee Y, Jung E, Kim T, Kim D. Liver enzyme abnormalities in systemic lupus erythematosus: a focus on toxic hepatitis. Rheumatol Int 2011;31(1):79–84. doi:10.1007/s00296-009-1237-4.
[19] Fan Z, Chen L, Li J, Cheng X, Yang J, Tian C, *et al*. Clinical features of COVID-19-related liver functional abnormality. Clin Gastroenterol Hepatol 2020;18(7):1561–1566. doi:10.1016/j.cgh.2020.04.002.
[20] Falcão MB, Pamplona de Góes Cavalcanti L, Filgueiras Filho NM, Antunes de Brito CA. Case report: Hepatotoxicity associated with the use of hydroxychloroquine in a patient with COVID-19. Am J Trop Med Hyg 2020;102(6):1214–1216. doi:10.4269/ajtmh.20-0276.
[21] Beigel JH, Tomashek KM, Dodd LE, Mehta AK, Zingman BS, Kalil AC, *et al*. Remdesivir for the treatment of Covid-19-Final report. N Engl J Med 2020;383(19):1813–1826. doi:10.1056/NEJMoa2007764.
[22] Goldman JD, Lye DCB, Hui DS, Marks KM, Bruno R, Montejano R, *et al*. Remdesivir for 5 or 10 days in patients with severe Covid-19. N Engl J Med 2020;383(19):1827–1837. doi:10.1056/NEJMoa2015301.
[23] Spinner CD, Gottlieb RL, Criner GJ, Arribas López JR, Cattelan AM, Soriano Viladomiu A, *et al*. Effect of Remdesivir vs. standard care on clinical status at 11 days in patients with moderate COVID-19: A randomized clinical trial. JAMA 2020;324(11):1048–1057. doi:10.1001/jama.2020.16349.
[24] Grein J, Ohmagari N, Shin D, Diaz G, Asperges E, Castagna A, *et al*. Compassionate use of Remdesivir for patients with severe Covid-19. N Engl J Med 2020;382(24):2327–2336. doi:10.1056/NEJMoa2007016.
[25] Wang Y, Zhang D, Du G, Du R, Zhao J, Jin Y, *et al*. Remdesivir in adults with severe COVID-19: A randomised, double-blind, placebo-controlled, multicentre trial. Lancet 2020;395(10236):1569–1578. doi:10.1016/S0140-6736(20)31022-9.
[26] Fujifilm Pharmaceuticals U.S.A., Inc. Study of the use of Favipiravir in hospitalized subjects with COVID-19. 2020. Available from: https://clinicaltrials.gov/ct2/show/NCT04358549.
[27] Cai Q, Yang M, Liu D, Chen J, Shu D, Xia J, *et al*. Experimental treatment with Favipiravir for COVID-19: An open-label control study. Engineering (Beijing) 2020;6(10):1192–1198. doi:10.1016/j.eng.2020.03.007.
[28] Boettler T, Newsome PN, Mondelli MU, Maticic M, Cordero E, Cornberg M, *et al*. Care of patients with liver disease during the COVID-19 pandemic: EASL-ESCMID position paper. JHEP Rep 2020;2(3):100113. doi:10.1016/j.jhepr.2020.100113.
[29] Michot JM, Albiges L, Chaput N, Saada V, Pommeret F, Griscelli F, *et al*. Tocilizumab, an anti-IL-6 receptor antibody, to treat COVID-19-related respiratory failure: a case report. Ann Oncol 2020;31(7):961–964. doi:10.1016/j.annonc.2020.03.300.
[30] Rodríguez-Tajes S, Miralpeix A, Costa J, López-Suñé E, Laguno M, Pocurull A, *et al*. Low risk of hepatitis B reactivation in patients with severe COVID-19 who receive immunosuppressive therapy. J Viral Hepat 2021;28(1):89–94. doi:10.1111/jvh.13410.

[31] Liu J, Wang T, Cai Q, Sun L, Huang D, Zhou G, *et al*. Longitudinal changes of liver function and hepatitis B reactivation in COVID-19 patients with pre-existing chronic hepatitis B virus infection. Hepatol Res 2020;50(11):1211–1221. doi:10.1111/hepr.13553.
[32] Alessi J, de Oliveira GB, Schaan BD, Telo GH. Dexamethasone in the era of COVID-19: friend or foe? An essay on the effects of dexamethasone and the potential risks of its inadvertent use in patients with diabetes. Diabetol Metab Syndr 2020;12(1):80. doi:10.1186/s13098-020-00583-7.
[33] Marra F, Smolders EJ, El-Sherif O, Boyle A, Davidson K, Sommerville AJ, *et al*. Recommendations for dosing of repurposed COVID-19 medications in patients with renal and hepatic impairment. Drugs R D 2021;21(1):9–27. doi:10.1007/s40268-020-00333-0.
[34] Duan K, Liu B, Li C, Zhang H, Yu T, Qu J, *et al*. Effectiveness of convalescent plasma therapy in severe COVID-19 patients. Proc Natl Acad Sci U S A 2020;117(17):9490–9496. doi:10.1073/pnas.2004168117.
[35] Moore N, Bosco-Levy P, Thurin N, Blin P, Droz-Perroteau C. NSAIDs and COVID-19: A systematic review and meta-analysis. Drug Saf 2021;44:929–938. doi:10.1007/s40264-021-01089-5.
[36] Yoon E, Babar A, Choudhary M, Kutner M, Pyrsopoulos N. Acetaminophen-induced hepatotoxicity: a comprehensive update. J Clin Transl Hepatol 2016;4(2):131–142. doi:10.14218/jcth.2015.00052.
[37] Bunchorntavakul C, Reddy KR. Acetaminophen-related hepatotoxicity. Clin Liver Dis 2013;17(4):587–607. doi:10.1016/j.cld.2013.07.005.
[38] Truven Health Analytics Inc. and Micromedex Inc., Micromedex gateway 2011, Truven Health Analytics.
[39] Plaquenil Hydroxychloroquine Sulfate Tablets US Prescribing Information 2017.
[40] Plaquenil-Hydroxychloroquine sulfate 200mg Film-coated Tablets, Summary of Product Characteristics. Zentiva; 2020.
[41] Dollery C. Therapeutic drugs. 2nd ed. Churchill Livingstone, London; 1998.
[42] McChesney EW. Animal toxicity and pharmacokinetics of hydroxychloroquine sulfate. Am J Med 1983;75(1A):11–18. doi:10.1016/0002-9343(83)91265-2.
[43] Tett SE, Cutler DJ, Day RO, Brown KF. Bioavailability of hydroxychloroquine tablets in healthy volunteers. Br J Clin Pharmacol 1989;27(6):771–779. doi:10.1111/j.1365-2125.1989.tb03439.x.
[44] Warhurst DC, Steele JC, Adagu IS, Craig JC, Cullander C. Hydroxychloroquine is much less active than chloroquine against chloroquine-resistant plasmodium falciparum, in agreement with its physicochemical properties. J Antimicrob Chemother 2003;52(2):188–193. doi:10.1093/jac/dkg319.
[45] Cho A, Saunders OL, Butler T, Zhang L, Xu J, Vela JE, *et al*. Synthesis and antiviral activity of a series of 1′-substituted 4-aza-7,9-dideazaadenosine C-nucleosides. Bioorg Med Chem Lett 2012;22(8):2705–2707. doi:10.1016/j.bmcl.2012.02.105.
[46] Siegel D, Hui HC, Doerffler E, Clarke MO, Chun K, Zhang L, *et al*. Discovery and synthesis of a phosphoramidate prodrug of a pyrrolo[2,1- ftriazin-4-amino] adenine C-nucleoside (GS-5734) for the treatment of Ebola and emerging viruses. J Med Chem 2017;60(5):1648–1661. doi:10.1021/acs.jmedchem.6b01594.
[47] Sheahan TP, Sims AC, Graham RL, Menachery VD, Gralinski LE, Case JB, *et al*. Broad-spectrum antiviral GS-5734 inhibits both epidemic and zoonotic coronaviruses. Sci Transl Med 2017;9(396):eaal3653. doi:10.1126/scitranslmed.aal3653.
[48] de Wit E, Feldmann F, Cronin J, Jordan R, Okumura A, Thomas T, *et al*. Prophylactic and therapeutic remdesivir (GS-5734) treatment in the rhesus macaque model of MERS-CoV infection. Proc Natl Acad Sci U S A 2020;117(12):6771–6776. doi:10.1073/pnas.1922083117.
[49] Wang M, Cao R, Zhang L, Yang X, Liu J, Xu M, *et al*. Remdesivir and chloroquine effectively inhibit the recently emerged novel coronavirus (2019-nCoV) in vitro. Cell Res 2020;30(3):269–271. doi:10.1038/s41422-020-0282-0.
[50] Sabers AJ, Williams AL, Farley TM. Use of Remdesivir in the presence of elevated LFTs for the treatment of severe COVID-19 infection. BMJ Case Rep 2020;13(10):e239210. doi:10.1136/bcr-2020-239210.
[51] Leegwater E, Strik A, Wilms EB, Bosma LBE, Burger DM, Ottens TH, *et al*. Drug-induced liver injury in a patient with coronavirus disease 2019: Potential interaction of Remdesivir with p-Glycoprotein inhibitors. Clin Infect Dis 2021;72(7):1256–1258. doi:10.1093/cid/ciaa883.
[52] Carothers C, Birrer K, Vo M. Acetylcysteine for the treatment of suspected Remdesivir-associated acute liver failure in COVID-19: A case series. Pharmacotherapy 2020;40(11):1166–1171. doi:10.1002/phar.2464.
[53] Baranovich T, Wong SS, Armstrong J, Marjuki H, Webby RJ, Webster RG, *et al*. T-705 (favipiravir) induces lethal mutagenesis in influenza A H1N1 viruses in vitro. J Virol 2013;87(7):3741–3751. doi:10.1128/JVI.02346-12.
[54] Furuta Y, Takahashi K, Kuno-Maekawa M, Sangawa H, Uehara S, Kozaki K, *et al*. Mechanism of action of T-705 against influenza virus. Antimicrob Agents Chemother 2005;49(3):981–986. doi:10.1128/AAC.49.3.981-986.2005.
[55] Jin Z, Smith LK, Rajwanshi VK, Kim B, Deval J. The ambiguous base-pairing and high substrate efficiency of T-705 (Favipiravir) Ribofuranosyl 5′-triphosphate towards influenza A virus polymerase. PLoS One 2013;8(7):e68347. doi:10.1371/journal.pone.0068347.
[56] Smee DF, Hurst BL, Egawa H, Takahashi K, Kadota T, Furuta Y. Intracellular metabolism of favipiravir (T-705) in uninfected and influenza A (H5N1) virus-infected cells. J Antimicrob Chemother 2009;64(4):741–746. doi:10.1093/jac/dkp274.
[57] Vanderlinden E, Vrancken B, Van Houdt J, Rajwanshi VK, Gillemot S, Andrei G, *et al*. Distinct effects of T-705 (Favipiravir) and Ribavirin on influenza virus replication and viral RNA synthesis. Antimicrob Agents Chemother 2016;60(11):6679–6691. doi:10.1128/AAC.01156-16.
[58] Furuta Y, Komeno T, Nakamura T. Favipiravir (T-705), a broad spectrum inhibitor of viral RNA polymerase. Proc Jpn Acad Ser B Phys Biol Sci 2017;93(7):449–463. doi:10.2183/pjab.93.027.
[59] Gowen BB, Wong MH, Jung KH, Sanders AB, Mendenhall M, Bailey KW, *et al*. In vitro and in vivo activities of T-705 against arenavirus and bunyavirus infections. Antimicrob Agents Chemother 2007;51(9):3168–3176. doi:10.1128/AAC.00356-07.
[60] Safronetz D, Rosenke K, Westover JB, Martellaro C, Okumura A, Furuta Y, *et al*. The broad-spectrum antiviral favipiravir protects guinea pigs from lethal Lassa virus infection post-disease onset. Sci Rep 2015;5:14775. doi:10.1038/srep14775.
[61] Rocha-Pereira J, Jochmans D, Dallmeier K, Leyssen P, Nascimento MS, Neyts J. Favipiravir (T-705) inhibits in vitro norovirus replication. Biochem Biophys Res Commun 2012;424(4):777–780. doi:10.1016/j.bbrc.2012.07.034.
[62] Sidwell RW, Barnard DL, Day CW, Smee DF, Bailey KW, Wong MH, *et al*. Efficacy of orally administered T-705 on lethal avian influenza A (H5N1) virus infections in mice. Antimicrob Agents Chemother 2007;51(3):845–851. doi:10.1128/AAC.01051-06.
[63] Mehta P, McAuley DF, Brown M, Sanchez E, Tattersall RS, Manson JJ. COVID-19: consider cytokine storm syndromes and immunosuppression. Lancet 2020;395(10229):1033–1034. doi:10.1016/S0140-6736(20)30628-0.
[64] Luo P, Liu Y, Qiu L, Liu X, Liu D, Li J. Tocilizumab treatment in COVID-19: A single center experience. J Med Virol 2020;92(7):814–818. doi:10.1002/jmv.25801.
[65] Stone JH, Frigault MJ, Serling-Boyd NJ, Fernandes AD, Harvey L, Foulkes AS, *et al*. Efficacy of Tocilizumab in patients hospitalized with Covid-19. N Engl J Med 2020;383(24):2333–2344. doi:10.1056/NEJMoa2028836.
[66] Muhović D, Bojović J, Bulatović A, Vukčević B, Ratković M, Lazović R, *et al*. First case of drug-induced liver injury associated with the use of Tocilizumab in a patient with COVID-19. Liver Int 2020;40(8):1901–1905. doi:10.1111/liv.14516.
[67] Chen LF, Mo YQ, Jing J, Ma JD, Zheng DH, Dai L. Short-course Tocilizumab increases risk of hepatitis B virus reactivation in patients with rheumatoid arthritis: a prospective clinical observation. Int J Rheum Dis 2017;20(7):859–869. doi:10.1111/1756-185X.13010.
[68] Koepsell H. Organic cation transporters in health and disease. Pharmacol Rev 2020;72(1):253–319. doi:10.1124/pr.118.015578.
[69] Yonezawa A, Inui K. Importance of the multidrug and toxin extrusion MATE/SLC47A family to pharmacokinetics, pharmacodynamics/toxicodynamics and pharmacogenomics. Br J Pharmacol 2011;164:1817–1825. doi:10.1111/j.1476-5381.2011.01394.x.
[70] Ambrus C, Bakos É, Sarkadi B, Özvegy-Laczka C, Telbisz Á. Interactions of anti-COVID-19 drug candidates with hepatic transporters may cause liver toxicity and affect pharmacokinetics. Sci Rep 2021;11(1):17810. doi:10.1038/s41598-021-97160-3.
[71] Aspen. Dexamethasone 2mg tablets, Summary of Product Characteristics; Accessed 10 Nov 2020. Available from: https://www.medicines.org.uk/emc/product/5411/smpc.
[72] Zhao B, Zhang HY, Xie GJ, Liu HM, Chen Q, Li RF, *et al*. Evaluation of the efficacy of steroid therapy on acute liver failure. Exp Ther Med 2016;12(5):3121–3129. doi:10.3892/etm.2016.3720.
[73] Heneghan MA, Yeoman AD, Verma S, Smith AD, Longhi MS. Autoimmune hepatitis. Lancet 2013;382(9902):1433–1444. doi:10.1016/S0140-6736(12)62163-1.
[74] Tomlinson ES, Maggs JL, Park BK, Back DJ. Dexamethasone metabolism in vitro: species differences. J Steroid Biochem Mol Biol 1997;62(4):345–52. doi:10.1016/s0960-0760(97)00038-1.
[75] El Kassas M, Alboraie M, Al Balakosy A, Abdeen N, Afify S, Abdalgaber M, *et al*. Liver transplantation in the era of COVID-19. Arab J Gastroenterol 2020;21(2):69–75. doi:10.1016/j.ajg.2020.04.019.
[76] Rismanbaf A, Zarei S. Liver and kidney injuries in COVID-19 and their effects on drug therapy; a letter to editor. Arch Acad Emerg Med 2020;8(1):e17.
[77] Fontana RJ, Seeff LB, Andrade RJ, Björnsson ES, Day CP, Serrano J, *et al*. Standardization of nomenclature and causality assessment in drug-induced liver injury: summary of a clinical research workshop. Hepatol 2010;52(2):730–742. doi:10.1002/hep.23696.
[78] Andrade RJ, Aithal GP, Björnsson ES, Kaplowitz N, Kullak-Ublick GA, Larrey D, *et al*. EASL clinical practice guidelines: drug-induced liver injury. J Hepatol 2019;70(6):1222–1261. doi:10.1016/j.jhep.2019.02.014.
[79] Malin JJ, Suárez I, Priesner V, Fätkenheuer G, Rybniker J. Remdesivir against COVID-19 and other viral diseases. Clin Microbiol Rev 2020;34(1):e00162–20. doi:10.1128/CMR.00162-20.
[80] Lamb YN. Remdesivir: first approval. Drugs 2020;80(13):1355–1363. doi:10.1007/s40265-020-01378-w.
[81] Piszczatoski CR, Powell J. Emergency authorization of chloroquine and hydroxychloroquine for treatment of COVID-19. Ann Pharmacother 2020;54(8):827–831. doi:10.1177/1060028020925558.
[82] Zhao M, Lu J, Tang Y, Dai Y, Zhou J, Wu Y. Tocilizumab for treating COVID-19: a systemic review and meta-analysis of retrospective studies. Eur J Clin Pharmacol 2021;77(3):311–319. doi:10.1007/s00228-020-03017-5.
[83] Stower H. Lopinavir-ritonavir in severe COVID-19. Nat Med 2020;26(4):465. doi:10.1038/s41591-020-0849-9.
[84] Mazzei T, Surrenti C, Novelli A, Crispo A, Fallani S, Carlà V, *et al*. Pharmacokinetics of azithromycin in patients with impaired hepatic function. J Antimicrob Chemother 1993;31(Suppl E):57–63. doi:10.1093/jac/31.suppl_e.57.
[85] Falade-Nwulia O, Suarez-Cuervo C, Nelson DR, Fried MW, Segal JB, Sulkowski MS. Oral direct-acting agent therapy for hepatitis C virus infection: A systematic review. Ann Intern Med 2017;166(9):637–648. doi:10.7326/M16-2575.

*Journal of Clinical and Translational Hepatology* **2022** vol. 10(4) | 757–769
DOI: 10.14218/JCTH.2022.00147

Guideline

# Guidelines for the Management of Cholestatic Liver Diseases (2021)

Lungen Lu* and Chinese Society of Hepatology and Chinese Medical Association

*Department of Gastroenterology, Shanghai General Hospital, Shanghai Jiaotong University School of Medicine, Shanghai, China*

**Received:** 25 March 2022 | **Revised:** 17 April 2022 | **Accepted:** 18 April 2022 | **Published:** 29 April 2022

## Abstract

In 2015, the Chinese Society of Hepatology and the Chinese Society of Gastroenterology issued a consensus statement on the diagnosis and management of cholestatic liver diseases. More clinical data on this topic have appeared during recent years. The Autoimmune Liver Disease Group of the Chinese Society of Hepatology organized an expert group to review recent evidence and provide an update to these previous guidelines. Herein, we provide 22 recommendations as a working reference for the management of cholestatic liver diseases by clinical practitioners.

**Citation of this article:** Lu L, Chinese Society of Hepatology and Chinese Medical Association. Guidelines for the Management of Cholestatic Liver Diseases (2021). J Clin Transl Hepatol 2022;10(4):757–769. doi: 10.14218/JCTH.2022.00147.

## Introduction

Cholestasis is a pathological condition in which various intrahepatic or extrahepatic factors impede bile formation, secretion, or excretion, leading to increased flow of bile into the duodenum and blood. The clinical characteristics of affected patients include pruritus, fatigue, darkened urine, and jaundice. During early-stage cholestasis, patients are usually asymptomatic and may only present with elevations of serum alkaline phosphatase (ALP) and gamma- glutamyl transferase (GGT). Hyperbilirubinemia may occur as disease progresses, and may lead to liver cirrhosis, liver failure, or even death.[1,2] Hepatobiliary diseases with cholestasis from various causes are called cholestatic liver diseases, and cholestasis itself further aggravates liver damage in these patients.

To help clinicians standardize the diagnosis and treatment of cholestatic liver diseases, the Chinese Society of Hepatology, Chinese Society of Gastroenterology, and Chinese Society of Infectious Diseases formulated the "Consensus on Diagnosis and Treatment of Cholestatic Liver Diseases" in 2015.[3] Because of the publication of additional clinical data regarding cholestatic liver diseases in China since then, we updated this guideline and revised the original consensus. The present guideline describes the etiology, classification, clinical manifestations, diagnostic criteria, treatment principles, diagnosis, and treatment of cholestatic liver diseases. The cholestasis induce by drugs, alcohol, hepatitis B virus, hepatitis C virus, primary biliary cholangitis (PBC), primary sclerosing cholangitis (PSC), autoimmune hepatitis, metabolic-related fatty liver disease and other liver diseases can be diagnosed and treated according to the corresponding guideline. We rated the evidence and recommendations in this guideline using the GRADE system for the evaluation of clinical guidelines (Table 1).

## Etiology and classification

Hepatocytes and cholangiocytes produce bile, and the daily total flow of bile in a healthy adult is about 600 mL. Hepatocytes produce bile salt-dependent bile (about 225 mL/day) and bile salt-independent bile (about 225 mL/day), and cholangiocytes produce additional bile (about 150 mL/day). Cholestasis is a disorder caused by the reduced flow or formation of bile,[4] and the cause can be intrahepatic or extrahepatic. Intrahepatic cholestasis[4–7] is characterized by dysfunction of hepatocytes, bile canaliculus, canals of Hering, bile ductule (<15 μm,), or cholangiocytes of the interlobular bile duct (15 to 100 μm), without obvious manifestations of bile duct obstruction based on imaging examination. The main causes are use of drugs or alcohol, viral or bacterial infection, and immune system disorders, etc. (Fig. 1). Extrahepatic cholestasis is characterized by obstruction or injuries of the septal bile duct (>100 μm), regional bile duct (300 to 400 μm), segmental bile duct (400 to 800 μm), left or right hepatic ducts, or the common bile duct to the ampulla.[2,7] Although the main causes are outside the liver, biliary cancer growing into the intrahepatic bile duct and hilar bile duct is also a cause. Bile duct stones, a malignancy from the pancreas or bile duct

**Keywords:** Cholestatic liver disease; Diagnosis; Therapeutics; Practice guidelines.

**Abbreviations:** ALP, alkaline phosphatase; BRIC, benign recurrent intrahepatic cholestasis; CFLD, cystic fibrosis-associated liver disease; CFTR, cystic fibrosis transmembrane conductance regulator gene; CT, computed tomography; DEXA, dual energy X-ray absorptiometry; ERCP, endoscopic retrograde cholangiopancreatography; FIC, familial intrahepatic cholestasis; FXR, farnesoid X receptor; GGT, gamma glutamyl transferase; HELLP, hemolysis, elevated liver enzymes, and low platelet count syndrome; 5-HT, 5-hydroxytryptamine; IBAT, ileal bile acid transporter; ICP, intrahepatic cholestasis of pregnancy; MDR3, multidrug resistance protein 3; MRCP, magnetic resonance cholangiopancreatography; PBC, primary biliary cholangitis; PFIC, progressive familial intrahepatic cholestasis; PSC, primary sclerosing cholangitis; PT, prothrombin time; SAMe, S-adenosyl-L-methionine; TJP2, tight junction protein 2; UDCA, ursodeoxycholic acid; ULN, upper limit of normal.

***Correspondence to:** Lungen Lu, Department of Gastroenterology, Shanghai General Hospital, Shanghai Jiaotong University School of Medicine, Shanghai 200080, China. ORCID: https://orcid.org/0000-0002-1533-4068. Tel: +86-13381616206, E-mail: lungenlu1965@163.com

**Table 1. GRADE system used to evaluate all recommendations**

| Grading of evidence | Notes | Symbol |
|---|---|---|
| High quality | Further research is very unlikely to change confidence in the estimated effect. | A |
| Moderate quality | Further research is likely to have an important impact on confidence in the estimated effect and may change the estimated effect. | B |
| Low or very low quality | Further research is very likely to have an important impact on confidence in the estimated effect and may change the estimated effect. Any estimated effect is uncertain. | C |

| Grading of recommendations | Notes | Symbol |
|---|---|---|
| Strong recommendation warranted | Factors influencing the strength of the recommendation included quality of evidence, presumed patient-important outcomes, and cost. | 1 |
| Weaker recommendation | Variability in preferences and values, or more uncertainty; more likely a weak recommendation is warranted. Recommendation has less certainty; higher cost or resource consumption. | 2 |

and ampulla, or a benign biliary stricture are the main causes of extrahepatic cholestasis, and these conditions usually cause acute cholestasis.[8] Cholestasis that persists more than 6 months is defined as chronic cholestasis.[5] It is important for clinicians to distinguish extrahepatic and intrahepatic cholestasis, but this could be difficult when only considering symptoms, signs, and biochemical parameters. Instead, a detailed diagnostic procedure is needed to distinguish these different conditions. PSC is a pathology that affects small and large intrahepatic bile ducts and/or extrahepatic bile ducts, and some patients with this condition can have intrahepatic or extrahepatic lesions (Fig. 1). According to the location of cytological damages, Cholestasis may be classified as hepatocellular or cholangiocytotic,[5] and injuries of both hepatocytes and cholangiocytes are known as mixed cholestasis.

## Epidemiology

At present, there are no reliable data on the incidence of cholestatic liver diseases. Bortolini *et al*.[9] reported that cholestasis was present in 882 (35%) of 2,520 patients who were diagnosed with chronic liver diseases for the first time, and that cholestasis was more common in patients with PBC and PSC. A study of 1,000 patients with chronic viral hepatitis showed that 56% of them had elevated ALP or GGT at discharge, and that elevation of these enzymes

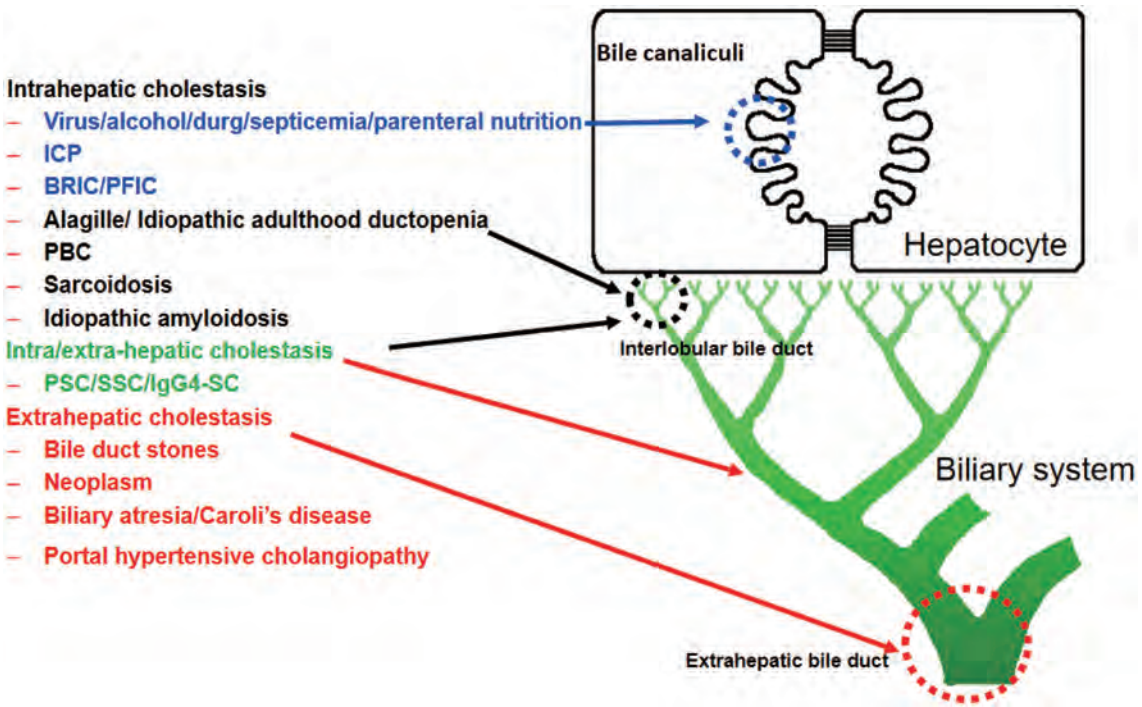


**Fig. 1. Location of injuries that lead to cholestatic liver disease.** BRIC, benign recurrent intra-hepatic cholestasis; ICP, intrahepatic cholestasis of pregnancy; IgG4-SC, IgG4-related sclerosing cholangitis; PBC, primary biliary cholangitis; PFIC, progressive familial intrahepatic cholestasis; PSC, primary sclerosing cholangitis; SSC, secondary sclerosing cholangitis.

was associated with increased risk for and severity of liver fibrosis and cirrhosis.[10] Cao *et al*.[11] performed a survey of 4,660 patients who were hospitalized with chronic liver diseases in Shanghai and reported that the total incidence of cholestasis was 10.26%, and that the incidence increased with patient age.

## Clinical manifestations

In addition to the clinical symptoms caused by the original disease, cholestasis itself can cause clinical symptoms, as well as secondary changes due to alterations in bile. Patients with early-stage disease may have no symptoms or nonspecific symptoms, such as fatigue, anorexia, nausea, and epigastric discomfort. The main clinical manifestations of cholestasis are jaundice, pruritus, fatigue, steatorrhea, xanthoma, and hepatic osteodystrophy.

## Biomarkers

The most common biomarkers for cholestasis are ALP, GGT, bile acid, bilirubin, and several molecular markers.

### *ALP and GGT*

Elevation of ALP and GGT are the most common manifestations of early cholestasis. It is generally thought that the retention of bile salts in cholestasis leads to the proliferating of small bile ductules with increase in ALP and GGT production. The mechanism by which ALP and GGT enters the blood and increases during cholestasis is still unclear. The internal pressure of the bile canaliculus and ductules leads to abnormally increased bile excretion and this increases ALP production. In addition, bile acid, because of its surface activity, dissolves ALP from lipid membranes, and this may also serum increased ALP.[12] Moreover, elevation of ALP can also occur during pregnancy, child growth, and in patients with bone diseases and certain tumors. Compared with other serum enzymes in these patients, GGT increases earlier and the increase remains longer. Among liver enzymes, GGT has the highest diagnostic sensitivity for cholestasis, but its specificity is low. The sensitivity and specificity of GGT in the diagnosis of cholestasis are noninferior or even better than those of ALP. If ALP and GGT are both elevated and other causes of liver injury are excluded (alcoholism, infection, etc.), this indicates damage of hepatocytes and cholangiocytes. If GGT is elevated but ALP is not, this indicates damage of bile canaliculus and cholangiocytes. If ALP is elevated but GGT is not, this indicates that liver injuries can often be excluded. However, in some specific cholestatic liver diseases, such as familial intrahepatic cholestasis (FIC type 1, 2, 4, 5, and 6), and USP53 deficiency disease, the levels of combined bilirubin or bile acid are increased, but GGT is normal or often reduced.[13,14]

### *Bile acids*

Bile acid is more sensitive than bilirubin for the diagnosis of bile secretion disorder, but it is not as sensitive as ALP. Patients with many liver diseases, such as cirrhosis and acute and chronic hepatitis, have elevated serum bile acid. The normal range of fasting serum bile acid is 1.0 to 6.0 μmol/L, and the normal postprandial range (2 h after eating) is 6.0 to 9.0 μmol/L. This level of bile acid can be more than 10 μmol/L in patients with cholestasis, and there are standard ranges for defining mild elevation (10 to 20 μmol/L), moderate elevation (20 to 40 μmol/L), and severe elevation (>40 μmol/L).[1,4] Although bile acid and cholic acid are sensitive markers for cholestasis, these measurements have limited use in China and elsewhere due to the lack of reliable detection methodologies and standardization, the presence of various interfering factors, and poor diagnostic specificity. The elevation of bile acid is specific to hepatobiliary diseases, the sensitivity is low and cannot be increased by the additional measurement of bile acid at 2 h after a meal.[4]

### *Bilirubin*

Cholestasis can cause elevated serum bilirubin, especially direct bilirubin. Hepatocellular damage can increase direct and indirect bilirubin due to abnormalities in bilirubin synthesis, conjugation, and excretion, but the increase of direct bilirubin is generally more obvious than that of indirect bilirubin. An increase of bilirubin without an increase of liver enzymes generally indicates hereditary diseases such as Gilbert's disease, or hemolysis diseases.

### *Molecular markers*

Mutations of specific genes can cause hereditary cholestatic liver diseases. Traditional sequencing can directly detect mutations in specific genes whose alteration may be suggested by patient phenotype. Second-generation sequencing has also been applied in the clinic and has made it easier to identify certain hereditary cholestatic liver diseases, such as FIC. Table 2 summarizes specific hereditary cholestatic liver diseases and the genes with causative mutations.[15] However, mutations in individual genes account for only a small portion of liver diseases, and most hereditary liver diseases are caused by mutations of multiple genes or a combination of gene mutations and environmental factors.

## Pathology

Patients with cholestasis have gross liver specimens that are yellow-green and liver biopsy specimens with scattered green or dark green spots. The basic pathological changes of intrahepatic cholestasis begin from zone 3 in the bile canaliculus and canals of Hering, and are characterized by feather degeneration of hepatocytes and plugs in the dilated bile ducts.[6,7,16] In severe cases, the hepatocytes are arranged in an acinar shape around the dilated bile canaliculus, and there are characteristic pathological changes indicative of intrahepatic cholestasis. There may also be hypertrophic Kupffer cells in the sinusoid bile and cholestasis of the interlobular bile duct in the portal area, with bile plug formation. Electron microscopy typically shows edematous and shortened microvilli of the capillary bile duct, and histopathology of extrahepatic obstructive cholestasis shows bile lakes in the liver around the portal area, with bile granulomas. Long-term extrahepatic obstruction can cause secondary intrahepatic cholestasis, and late-stage cholestasis can progress to portal fibrosis or even cirrhosis.

## Diagnosis

### *Diagnostic criteria*

There are currently no unified diagnostic criteria or specific

**Table 2. Genes related to cholestatic diseases[15]**

| Cholestatic disease | Gene(s) affected |
|---|---|
| Alagille syndrome | *JAG1, NOTCH2* |
| 1-antitrypsin deficiency | *SERPINA1* |
| α-methylacyl-CoA racemase deficiency | *AMACR* |
| Arthrogryposis-renal dysfunction-cholestasis syndrome | *VIPAS39, VPS33B* |
| Autosomal recessive polycystic kidney disease | *PKHD1* |
| BA conjugation disorder | *SLC27A5* |
| BA reabsorption disorder | *SLC10A1, SLC10A2* |
| BA receptor defect | *GPBAR1* |
| BA synthesis disorders | *CYP7A1* |
| Biliary atresia | *SLC51B* |
| BRIC | *ABCB11, ATP8B1, SLC51A* |
| Cerebrotendinous xanthomatosis | *CYP27A1* |
| Cholesteryl ester storage disease | *LIPA* |
| Citrullinemia | *SLC25A13* |
| Congenital bile acid synthesis defect | *ACOX2, AKR1D1, AMACR, CYP7B1, HSD3B7* |
| Cystic fibrosis | *CFTR* |
| D-bifunctional protein deficiency | *HSD17B4* |
| Dubin–Johnson syndrome | *ABCC2* |
| Extrahepatic cholestasis | *SLC51B* |
| Familial hypercholanemia | *BAAT, TJP2* |
| Lucey–Driscoll syndrome | *UGT1A1* |
| Crigler–Najjar syndrome | *UGT1A1* |
| Fanconi renotubular syndrome 3 | *EHHADH* |
| Gallbladder disease | *ABCB4, ABCG8* |
| Hereditary fructose intolerance | *ALDOB* |
| Ichthyosis, leukocyte vacuoles, alopecia and sclerosing cholangitis | *CLDN1* |
| ICP | *ABCB4, ATP8B1* |
| Joubert syndrome | *CC2D2A, MKS1, TMEM216, NPHP1* |
| Lipid storage disorder | *SCP2* |
| Transient infantile liver failure | *TRMU* |
| Meckel syndrome | *CC2D2A, MKS1, NPHP3, TMEM216* |
| Mitochondrial DNA depletion syndrome | *DGUOK, POLG, MPV17* |
| Neonatal sclerosing cholangitis | *DCDC2* |
| Nephronophthisis | *INVS, NPHP1, NPHP3, NPHP4* |
| Niemann–Pick disease | *NPC1, NPC2, SMPD1* |
| North American Indian childhood cirrhosis | *UTP4* |
| Peroxisomal disorders | *PEX1, PEX10, PEX11B, PEX12, PEX13, PEX14, PEX16, PEX19, PEX2, PEX26, PEX3, PEX5, PEX6, PEX7* |
| PFIC | *ABCB11, ABCB4, SLC51A, TJP2, ATP8B1, NR1H4, MYO5B* |
| Renal cysts and diabetes syndrome | *HNF1B* |
| Renal-hepatic-pancreatic dysplasia 1 | *NPHP3* |
| Sitosterolemia | *ABCG5, ABCG8* |
| Smith–Lemli–Opitz syndrome | *DHCR7* |
| Transaldolase deficiency | *TALDO1* |
| Tyrosinemia type I | *FAH* |

indicators of cholestatic liver diseases, and the diagnostic value of ALP and GGT are uncertain. The European Association for the Study of the Liver, which presented guidelines for the management of cholestatic liver diseases in 2009, recommended diagnosis of cholestatic liver diseases using upper limit of normal (ULN) thresholds; in particular they considered an ALP exceeding 1.5×ULN and a GGT exceeding 3×ULN as pathological indicators.[5] In 2015, the Chinese Association of Hepatology supported the same recommendation.[3] However, it should be noted that GGT is not elevated in some specific cholestatic liver diseases, such as some progressive familial intrahepatic cholestasis (PFIC) and benign recurrent intrahepatic cholestasis (BRIC). Thus, in view recent progress and current understanding, the present guideline recommends a diagnosis of cholestasis when the ALP exceeds 1.5×ULN and the GGT exceeds 3×ULN, but that some specific cholestatic liver diseases (FIC 1, 2, 4, 5, and 6, and USP53 deficiency) are characterized by increased conjugated bilirubin or bile acid, but normal or nearly normal GGT. GGT may be elevated in FIC type 3, Alagille syndrome, Citrin deficiency, biliary duct plate dysplasia (Caroli disease, congenital and cystic fibrosis), and Niemann-ck disease (C1/C2 type).

### *Diagnostic steps*

First, the presence of cholestasis should be determined by serological measurements. Second, imaging and endoscopy should be used to distinguish intrahepatic from extrahepatic cholestasis. Finally, the diagnosis should be obtained using a comprehensive analysis of medical history, symptoms, and signs, blood biochemistry, imaging, endoscopy, liver biopsy, and gene detection (Fig. 2).

### *Difference and connection with jaundice*

Cholestasis has some similarities to jaundice, a condition due to the accumulation of all bile components, including bilirubin.[1] However, jaundice is characterized by increased serum bilirubin with yellow skin and sclera. Patients with early-stage cholestasis typically have only elevated ALP and GGT, but no signs of jaundice, which appears only when the serum bilirubin exceeds 34.2 μmol/L. Some diseases, such as hereditary hyperbilirubinemia (Gilbert syndrome, Crigler-Najjar syndrome, Dubin-Johnson syndrome, and Rotor syndrome) are characterized by disruption of bilirubin metabolism, and affected patients have increased serum bilirubin; however, patients with these diseases have normal levels of the other components of bile, and normal levels of ALP and GGT, and are not considered cholestatic disorders. Jaundice may also occur in some hemolytic diseases, such as hereditary spherocytosis, thalassemia, paroxysmal nocturnal hemoglobinuria, acquired hemolytic anemia, and newborn hemolytic disease, but these patients usually have normal levels of liver enzymes. Therefore, genetic factors and hemolytic diseases should first be excluded when a patient presents with jaundice.

## Recommendations

1. We recommend a diagnosis of cholestatic liver diseases when ALP exceeds 1.5×ULN and GGT exceeds 3×ULN (B1), although some familial intrahepatic cholestastic diseases are characterized by elevated conjugated bilirubin and/or bile acids, but normal or nearly normal GGT (B2).
2. We recommend computed tomography (CT), magnetic resonance cholangiopancreatography (MRCP), and/or ultrasound imaging as the main approach to distinguish intrahepatic and extrahepatic cholestasis (C1).
3. We recommend endoscopic retrograde cholangiopancreatography (ERCP) or endoscopic ultrasonography when a routine imaging examination cannot provide a definite diagnosis, and when extrahepatic biliary obstruction or cholangitis is highly suspected (B1).
4. When the tests are negative for AMA, AMA2, anti-SP100, and anti-GP210, we recommend additional autoantibody tests to exclude systemic or autoimmune diseases for unexplained intrahepatic cholestasis. We recommend a liver biopsy when the cause of cholestasis remains uncertain (C1). We recommend detection of gene variants for patients with suspected hereditary cholestasis (B1).
5. We recommend exclusion of hemolytic disease in patients who present with jaundice, although jaundice may be absent in patients with early-stage cholestatic liver diseases or hereditary hyperbilirubinemia (B1).

## Treatment

### *Treatment principle*

The main treatment principle is to etiological treatment and management of symptoms. Etiological treatment, such as removal of stones or surgical resection of tumors to relieve obstruction, is often the most effective treatment. Ursodeoxycholic acid (UDCA) can also be used for PBC and PSC. Cessation in the use of drugs or alcohol is the most important intervention for patients with drug- or alcohol-induced liver diseases. Patients with hepatitis B or C should receive antiviral treatment, those with autoimmune hepatitis should be considered for glucocorticoid and/or immunosuppressant treatment, and those with metabolic-related fatty liver diseases should be encouraged to change their lifestyles, especially diet and exercise.

### *Drug treatment*

The purpose of treatment is to reduce the clinical symptoms and liver damage caused by cholestasis. The main drugs are UDCA, S-adenosyl-L-methionine (SAMe), cholestyramine, obeticholic acid, and fibrates.[17–19]

### *UDCA*

UDCA is used to treat cholestasis because of its hydrophilic, cytoprotective, and non-cytotoxic properties. UDCA functions as a replacement for lipophilic, detergent-like toxic bile acids, and it promotes of secretion of bile and immune regulation. It can successfully manage symptoms in patients with PBC, PSC, intrahepatic cholestasis of pregnancy (ICP), cystic fibrosis, cholestasis after liver transplantation, drug-induced cholestasis, FIC, and Alagille syndrome. The typical dose is 10 to 15 mg/kg/day, but it can be increased 20 to 25 mg/kg/day for cystic fibrosis and 45 mg/kg/ day for Byler's disease and Alagille syndrome.

### *SAMe*

SAMe functions as an *in vivo* as a methyl donor in transmethylation and a precursor of sulfhydryl compounds (cysteine, taurine, glutathione, and coenzyme A). SAMe can be used to treat hepatocellular cholestasis, ICP, and drug-induced

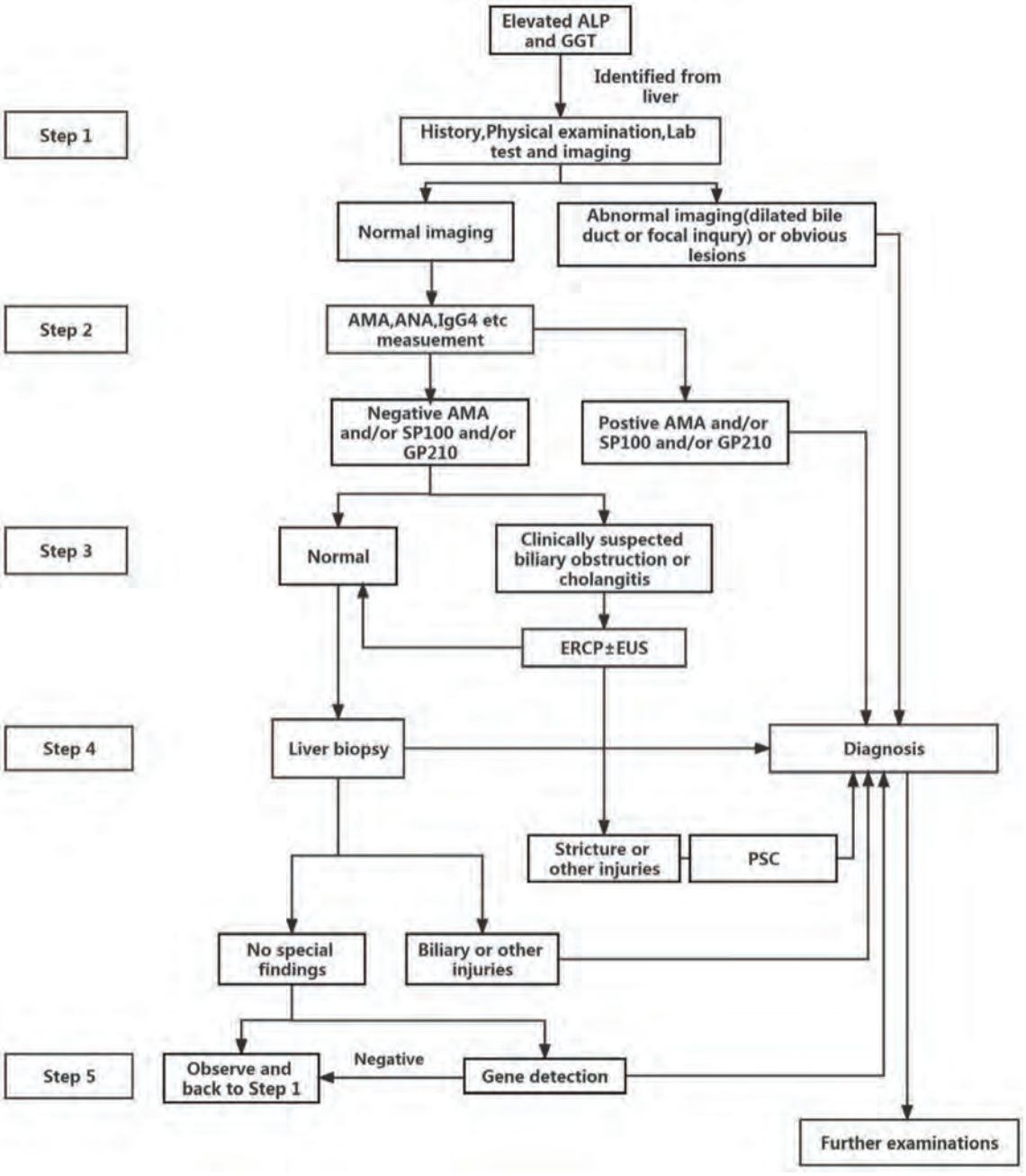


**Fig. 2. Recommended procedures for diagnosis of cholestatic liver diseases.** ALP, alkaline phosphatase; AMA, anti-mitochondrial antibodies; ANA, antinuclear antibodies; ERCP, endoscopic retrograde cholangiopancreatography; EUS, endoscopic ultrasound; GGT, gamma-glutamyl transferase; IgG4, immunoglobulin G4; PSC, primary sclerosing cholangitis.

cholestasis. Intravenous SAMe (0.5 to 1.0 g/day) is recommended for initial treatment, and oral SAMe tablets (1.0 to 2.0 g/day) is recommended for maintenance treatment.

### *Cholestyramine*

Cholestyramine is an anion exchange resin that combines with bile acids in the intestine, and then increases the excretion of bile acids by 3 to 4-fold above the normal level. Oral cholestyramine (12 to 16 g/day, *t.i.d.*) can be taken with water or another drink ~20 minutes before meals and before bed. There should be an interval of at least 4 h between taking cholestyramine, UDCA, or other drugs.

### *Obeticholic acid*

Obeticholic acid is a farnesoid X receptor (FXR) agonist that indirectly inhibits the expression of cytochrome 7A1 (CYP7A1) and the synthesis of bile acid. It is mainly used to treat patients with PBC who had poor responses to UDCA,

and the recommended oral dose is 5 to 10 mg/day. Obeticolic acid should be avoided in advanced and decompensated liver disease.

### *Fibrates*

Fibrates are peroxisome proliferator-activated receptor agonists that reduce bile acid synthesis by inhibiting the expression of a bile acid synthase (CYP7A1). Fibrates can also increase bile excretion by up-regulating the expression of a bile acid transporter and multidrug resistance protein 3 (MDR3). The recommended dose for oral fenofibrate is 160 to 200 mg/day and for oral bezafibrate is 400 mg/day.

### *Other treatments*

After fully weighing the risks and benefits, patients with immune-mediated cholestasis may be considered for glucocorticoid or immunosuppressant treatment. Other treatments, such as ultraviolet irradiation, albumin dialysis, and nasobiliary drainage may also be considered. Patients with cholestatic liver diseases who have poor responses to active treatment and have a risk of death within 6 to 12 months or a MELD score of more than 15 should be evaluated for liver transplantation. Traditional Chinese medicines, such as Yinzhihuang and Kuhuang, may provide some benefit for cholestatic liver diseases, but further investigations are needed. There are many new drugs under development, including FGF19 analogues, nor-UDCA, simtuzumab, infliximab, and fecal transplantation, that may provide new alternatives in the future.

### Recommendations

6. We recommend etiological treatment and management of cholestasis as the treatment principle for cholestatic liver diseases. We recommend UDCA (A1), SAMe (B1), cholestyramine (B1), fibrates (B1), and obeticholic acid (B1), alone or in combination, as the main therapeutic drugs.
7. We recommend a glucocorticoid and/or immunosuppressant, ultraviolet irradiation, albumin dialysis, and nasobiliary drainage (as appropriate) for patients who fail to respond to the above treatments (C2).
8. We recommend evaluation of patients for liver transplantation if the active medical treatments for cholestatic liver disease were unsuccessful, or if death within 6 to 12 months seems likely, or if the MELD score is 15 or more (B1).

## Hereditary cholestatic liver diseases

### *Cystic fibrosis-associated liver disease (CFLD)*

CFLD is an autosomal recessive disease caused by a mutation of a cystic fibrosis transmembrane conductance regulator gene (*CFTR*) on the long arm of chromosome 7, and it affects 27% of patients with cystic fibrosis. It is characterized by hepatomegaly, abnormal liver biochemistry and ultrasound results, and may be accompanied by congenital cholestasis, hepatic steatosis, and focal or multilobular cirrhosis.[20,21] There is no clear diagnostic standard for CFLD. About one-third of these patients have hepatomegaly, and this can be caused by the CFLD itself or by liver congestion or *cor pulmonale*. If the levels of ALP, ALT, AST, bilirubin, and GGT are more than 1.5×ULN, further examinations should assess liver injury (prothrombin time and albumin) and exclude other causes. Ultrasonography can find signs of CFLD, such as hepatomegaly, abnormal bile duct, or echoless lesions in the liver. An abdominal CT can show the size of a cyst and the amount of remaining normal liver tissue. Because many patients have focal or multilobular fibrosis and cirrhosis, a liver biopsy provides little benefit. No therapy of proven benefit for the long-term prognosis of CFLD exists. There are only limited drugs used for management of CFLD. UDCA (20 to 30 mg/kg/day) can improve liver biochemical indexes, stimulate bile secretion from a damaged bile duct, improve histology (after more than 2 years), and improve nutritional status. Patients generally live long lives, and prognosis depends on the severity of CFLD, and cancerization is seldom. This disease rarely needs surgical treatment, but puncture and aspiration with ultrasound guidance can be used when there are acute symptoms, while fluids regenerate. Liver transplantation[20–22] should be considered when a patient's daily life is severely restricted or the patient has progressed to the terminal stage.

### Recommendations

9. We recommend a diagnosis of CFLD based on the presence of cystic fibrosis, hepatomegaly, abnormal biochemical indexes, and the numbers and sizes of cystic lesions from imaging (C2). We recommend UDCA (20 to 30 mg/kg/day) to improve liver biochemical and histological indexes (C1). We recommend liver transplantation when a patient's daily life is severely restricted or when a patient has progressed to the terminal stage (B1).

### *FIC*

FIC is a family of autosomal recessive diseases caused by mutations of the *ATP8B1*, *ABCB11*, *ABCB4*, *TJP2*, *NR1H4*, *MYO5b*, or *USO53* genes. These mutations directly or indirectly lead to abnormal function of bile canaliculus transporters in hepatocytes. The incidence is similar in males and females.[8,13,14] The most common manifestation is intrahepatic cholestatic jaundice with severe pruritus, conditions that can seriously affect quality-of-life. A physical examination shows obvious skin scratches, and cholangiography indicates normal intrahepatic or extrahepatic bile ducts. The disease exists on a spectrum that ranges from benign BRIC to severe PFIC. Bile duct hyperplasia is not common, but liver fibrosis can eventually develop and progress into cirrhosis or liver failure. Some patients may experience recurrent and self-limited severe pruritus and cholestasis, in which an attack lasting weeks or months is followed by no symptoms for months or years, leading to the name BRIC. At the onset of BRIC, the liver histology shows cholestasis in the hepatocytes or cholangiocytes, with no obvious fibrosis; the liver histology and function are normal during the interictal period. It was initially thought that although each individual BRIC attack was serious, progressive liver injury and cirrhosis would not occur. However, there was also evidence that some so-called BRIC cases were recurrent and progressed to end-stage liver disease, and that the word "benign" should not be used.[4] There is also evidence that some patients only had cholestasis during infancy without recurrence, a condition called "transient infantile cholestasis".[23] FIC 1,2,4,5,6 are characterized by low GGT, and usually begins during the neonatal period. The serum bilirubin and bile acid levels are significantly increased, but there is no significant increase of GGT, and the level is often less than 100 U/L.[13,14] ATP8B1

deficiency includes PFIC1, but the pathogenetic mechanism is still unclear. Patients with PFIC1 (also known as Byler's disease) present with cholestasis, and may also have diarrhea, pancreatitis, developmental disorders, hearing loss, hypothyroidism, and other extrahepatic manifestations. Electron microscopy can be used to identify coarse particles of bile in the bile canaliculus (Byler bile). The phenotype of ATP8B1 deficiency appears unrelated to the genotype.[24] ABCB11 defect includes PFIC2 (formerly Byler's syndrome) and BRIC2. The *ABCB11* gene encodes a bile salt export pump (BSEP), the only transporter of bile salt in the bile canaliculus. A defective gene causes bile acid accumulation in hepatocytes, leading to portal inflammation and giant cell hepatitis. Patients with PFIC2 have an increased risk of liver cancer and gallstones.[25,26], and there is a close relationship between the genotype and phenotype. The tight junction protein 2 (TJP2) occurs in the junctions between epithelial cells and endothelial cells and interacts with several other proteins. Patients with TJP2 deficiency, also known as FIC4, have loss of TJP2 protein expression in severe cases (based on immunohistochemistry), often leading to death or the need for liver transplantation. Recent studies found a significant relationship between genotype and phenotype, with a continuous spectrum of clinical severity.[27] The synthesis, secretion, and metabolism of bile acids are finely regulated by nuclear receptor proteins. FXR (encoded by *NR1H4*, also called *FIC5*) is activated by bile acid, functions in feedback regulation, and is the most important protein in bile acid homeostasis. Patients with FIC5 can experience severe neonatal cholestasis, early onset of non-vitamin K-dependent coagulation disorders, rapid development to end-stage liver disease, and often need early liver transplantation for survival. MYO5b functions in intracellular transport and has an important role in the formation of microvilli on the surfaces of intestinal epithelial cells and hepatocytes in the bile canaliculus. There is a close relationship between genotype and phenotype in patients with defective *MYO5b* genes. In particular, complete loss of the gene causes microvilli inclusion body disease; a partial loss of this gene causes wrong location of BSEP through a special toxic negative effect, and is also called FIC 6.[28] *USP53* encodes ubiquitin specific peptidase 53, a protein that interacts with TJP2. USP53 deficiency leads to cholestasis, and may be accompanied by hearing impairment or hearing loss in severe cases. Electron microscopy shows an elongation of the tight junction structure between hepatocytes.[29] FIC 3 is caused by a mutation of the *ABCB4* gene, which encodes MDR3, a phosphatidylcholine translocation enzyme in the canaliculi bile that transfers phosphatidylcholine from hepatocytes to the canaliculi bile. In contrast to other FICs, patients with FIC 3 usually have significantly elevated GGT. Histopathology shows diffuse bile duct hyperplasia with portal inflammation and fibrosis or cirrhosis. FIC3 may be associated with intrahepatic cholelithiasis. A recent study reported that a novel type of PFIC could be induced by a homozygous R148W mutation of the *SEMA7A* gene.[30] At present, there no curative drugs for FIC, but UDCA and bile acid blocking agents are generally recommended. A dietary supplement of medium-chain triglycerides and fat-soluble vitamins are also generally recommended. UDCA may improve biochemical indexes and prolong survival of some patients with mild FIC3. Rifampicin can be used to relieve itching. Liver transplantation is recommended for patients with advanced FIC.

### Recommendation

10. We recommend a diagnosis of FIC (a group of autosomal recessive hereditary diseases) when the main symptoms are pruritus and jaundice, manifesting in varying degrees (B1). We recommend genetic analysis for detection as the gold standard for diagnosis of FIC (B1). We recommend a diagnosis of FIC 1, 2, 4, 5, or 6 when the GGT is normal or nearly normal, and there is severe pruritus and different extrahepatic manifestations; we recommend a diagnosis of FIC3 when the GGT is elevated. Although there are no curative treatments for FIC (C2), we recommend UDCA to improve liver function in some patients with FIC3 (C2). We recommend a bile shunt to improve some liver biochemical indexes for suitable patients with FIC (C2). We recommend assessment of the suitability for liver transplantation in patients with advanced disease (B1).

#### *Alagille syndrome*

Alagille syndrome has an autosomal dominant inheritance and is caused by mutations of the *JAG1* gene (94%) or *NOTCH2* gene (2.5%), both of which function in the Notch signaling pathway. The incidence of this disease is higher in children and adolescents. The disease is characterized by elevated GGT and involvement of various extrahepatic organs, including the cardiovascular system, bones, kidneys, eyes, and face. The estimated incidence is 1/30,000 to 1/70,000. There is no significant relationship between genotype and phenotype in this disease.[31,32] The most important feature of Alagille disease is a decrease or total lack of the interlobular bile ducts as indicated by liver biopsy, but some patients lack this manifestation or have bile ductule or interlobular hyperplasia in the early stage. The diagnostic criteria are: (1) reduced or absent interlobular bile ducts based on histology, with at least three characteristic clinical features (chronic cholestasis, heart murmur, butterfly vertebrae, eye abnormalities, kidney abnormalities, and characteristic facial features); (2) at least four of the above clinical features in the absence of hepatic histologic interlobular bile duct decrease or lack of evidence; (3) at least two of the above clinical features with clear family history of the disease, or identification of the gene mutation. There are no satisfactory treatments for Alagille syndrome, but symptoms can be managed using UDCA, drugs blocking bile acid enterohepatic circulation, and a dietary supplement of fat-soluble vitamins. The US Federal Drug Administration recently approved oral miracidia chloride (Livmarli) for treatment of cholestatic pruritus in patients with Alagille syndrome who are aged 1 year and older.[33] Ileal bile acid transporter (IBAT) inhibitors have also been approved for PFIC1 and 2 in Europe. The drug inhibits IBAT and blocks the intestinal hepatic circulation of bile acids.

### Recommendation

11. We recommend considering Alagille syndrome when children or adolescents present with cholestasis. We recommend confirmation of mutations in *JAG1* or *NOTCH2*, which lead to a decrease of interlobular bile ducts, cholestasis with pruritus, and multiple system damage (especially disorders of the cardiovascular system, eyes, and bones, and facial abnormalities) to confirm the diagnosis. We recommend symptomatic and supportive management as the main treatments (C2).

#### *ICP*

Genetic, hormonal, and environmental factors can contribute to the pathogenesis of ICP. Affected patients experience increased flow of bile acid from the mother to the fetus,

and increased bile acid in the amniotic fluid, umbilical cord blood, and meconium.[34,35] The incidence of ICP is higher in twin pregnancies. Use of high-dose contraceptives and progesterone might induce ICP, suggesting that hormones function in the pathogenesis. An increased incidence among family members and differences among races suggest a role of genetic factors. Recent genetic studies identified mutations of canaliculi bile transporter genes (*ABCB4*, *ABCB11*, *ABCC2*, and *ATP8B1*) and *NR1H4* in some ICP patients. During pregnancy, when hormones and other substrates exceed the transport capacity of the bile canaliculi transporter, a mild dysfunction of bile transportation can apparently induce cholestasis. Therefore, if cholestasis with elevated GGT level persists after delivery, an *ABCB4* mutation should be considered.

**Diagnosis:** These patients experience cholestasis during late pregnancy, with rapid and spontaneous recovery after delivery. The three main characteristics in pregnant women are: (1) severe pruritus, typically during the second or third trimester; (2) increased levels of ALT, fasting bile acid, and glycocholic acid; (3) spontaneous remission of symptoms and signs after delivery, typically within 4 to 6 weeks.[34–36] Pruritus can cause significant discomfort and distress in pregnant women, and ICP increases the risk of premature delivery and sudden fetal death. Patients usually have good prognoses, but if the jaundice is persistent then massive hemorrhage may occur during labor due to a deficiency of vitamin K-dependent coagulation factors II, VII, and X. The risks of fetal distress, premature delivery, and stillbirth are relatively high. ICP can be diagnosed according to clinical manifestations of elevated serum glycocholic acid (≥10.75 μmol/L) and total bile acid (≥10 μmol/L). A diagnosis can be confirmed when these liver biochemical indexes return to normal after delivery. ICP patients who have the *ABCB4* mutation have an elevated GGT, but are otherwise normal. About 10 to 15% of these patients have only a moderate increase of serum conjugated bilirubin and mild jaundice. ICP diagnosis requires the exclusion of other diseases, and the final diagnosis is made by postpartum recovery. A liver biopsy is usually not necessary.

In addition to ICP, preeclampsia, Hemolysis, Elevated Liver enzymes, and Low Platelet count (HELLP) syndrome, and acute fatty liver of pregnancy.[4] should be considered when abnormal biochemical parameters occur during pregnancy. Preeclampsia, the rapid elevation of blood pressure during pregnancy, can lead to organ damage. Organ damage is multifaceted and kidney damage during preeclampsia manifests as increased urine protein. Preeclampsia can also cause abnormal liver biochemical parameters, thrombocytopenia, and hemolysis.

HELLP syndrome is characterized by hemolysis, elevated liver enzymes, and thrombocytopenia ($<50\times10^9$ platelets/L), and is a serious complication from hypertension disorders during pregnancy. HELLP mostly occurs during the prenatal period, and these patients have bilirubin below 85 μmol/L, liver necrosis, hemangioma, and evidence of hepatic rupture based on imaging. Acute fatty liver of pregnancy is a kind of acute hepatic steatosis that can occur during late pregnancy, mostly in young primiparas. It usually occurs during the last three months of pregnancy or early postpartum. The onset is sudden and the prognosis is poor without aggressive and rapid treatment. The clinical manifestations are similar to those of acute severe hepatitis, and it is characterized by acute liver failure, often accompanied by renal failure. Liver steatosis can be identified by imaging.

**Treatment:** UDCA can be used as a first-line drug for treatment of ICP. This treatment can reduce pruritus and improve liver biochemical parameters in 67% to 80% of patients.[34–36] The effect of SAMe is inferior to UDCA, but it may provide additional benefit. If pruritus does not decrease after several days of standard UDCA treatment, SAMe or rifampicin should be considered. There is also a need for increased fetal monitoring during treatment, and birth induction should be considered to reduce perinatal mortality. In particular, birth induction should be considered after 35 weeks of pregnancy if there is evidence of disease progression, no inhibition of uterine contraction, abnormal fetal movement, fetal heart rate variability or no response to a stress test, or contamination of the amniotic fluid with meconium.[4]

### Recommendations

12. We recommend the following diagnostic criteria for IPC: (1) pruritus during pregnancy; (2) increased levels of serum ALT, fasting bile acid, and glycocholic acid; and (3) exclusion of other causes of liver dysfunction or pruritus. Diagnosis is confirmed if the liver biochemical parameters return to normal after delivery (B2).
13. We recommend UDCA and SAMe for symptomatic patients who have cholestasis during the second or third trimesters of pregnancy to relieve pruritus and improve liver biochemistry (B1). Other than supportive care, we are unable to recommend a treatment to protect the fetus and reduce fetal complications (C2).

### Extrahepatic manifestations and management

#### *Pruritus*

Pruritus is the sensation of skin irritation in the absence of primary skin damage that leads to excessive scratching. It differs from the senses of touch and pain in nature, persistence, and location. The existence of pruritus itself has no prognostic value and does not reflect disease severity. The pathogenesis of pruritus is not clear, but it may be related to increased activity of an autocrine movement factor (autotaxin) and the formation of lysophosphatidic acid.[37,38] In addition, bile acid salt, endogenous opioid peptide, 5-hydroxytryptamine (5-HT), hyperactivity of sensory neurons, estrogen and progesterone, hepato-intestinal pruritus changes, and genetic factors may contribute to pruritis. The relationship between pruritus and cholestasis suggests that the substances causing pruritus are normally excreted in bile. The resolution of pruritus during hepatocyte failure indicates that these substances are produced by hepatocytes, but serum bile acid remains very high in this situation.[4] Pruritus can be divided into three categories based on severity.[38,39] First, a visual analog scale classifies the severity of pruritus as scratch, plaque, nodule, and/or scar according to the characteristics of skin scratches, and the degrade is 0–3 according to the light, moderate, and severe degree, and the total score ranges from 0 to 10. Second, an Itch Severity Scale considers the frequency of itching, sleep, mood, sexual desire, sexual function, and uses a Likert scale to assess the intensity of pruritus and the total surface area of the body that is affected; the total score ranges from 0 to 21, with 21 indicating the most severe itching. Third, a semiquantitative evaluation of pruritus can be performed by recording the frequency of pruritus, with division into four stages: occasional, daily intermittent without clinical symptoms, daily intermittent with clinical symptoms, and persistent.

Several drugs can be used alone or in combination to reduce pruritus, including cholestyramine, antihistamines, pregnane X receptor agonists, opioid receptor antagonists, and 5-HT receptor antagonists. Oral cholestyramine is a first-line treatment for cholestatic pruritus.[5,40], with a recommended dose of 4 g/day and a maximum dose of 16

g/day. When administered with other drugs (especially UDCA), cholestyramine should be taken at intervals of 4 to 6 h to prevent interactions. Rifampicin, a pregnane X receptor agonist, is a second-line treatment for pruritus. Rifampicin down-regulates ATX and reduces the formation of lysophosphatidic acid, especially in patients who are intolerant or nonresponsive to cholestyramine.[41] The recommended oral dose is 150 mg/day initially, and this dose can be maintained if it is effective. If necessary, the dose can be increased to 600 mg/day every other week. When rifampicin is used to treat methadone addicts, it can cause opioid withdrawal reactions. Therefore, rifampicin might relieve cholestatic pruritus due to its opioid antagonistic effects. Red urine, toxic kidney damage, liver toxicity, and hemolysis (rarely) may occur after use of rifampicin. Due to the potential of rifampicin to cause liver damage, it is necessary to closely monitor biochemical parameters during treatment. Oral naltrexone, an opioid receptor antagonist, can be given at a dose of 25 to 50 mg/day as a third-line treatment for pruritus. Some patients have nausea, vomiting, mild pain, and other side effects due to this treatment. The metabolites of naltrexone can accumulate in patients with decompensated liver disease, so caution should be used when treating these patients. Treatment should begin with a low dose, and the dose can then be gradually increased to avoid withdrawal effects, similar to the recommendations for anesthetics.[40]

If the above drugs are ineffective, sertraline (a selective 5-HT reuptake inhibitor) can be used as a fourth-line treatment. The initial dose of 50 mg/day can be increased to 100 mg/day after a few weeks. In recent years, ultraviolet radiation, albumin dialysis, and nasobiliary drainage have been used to manage cholestatic pruritus, and favorable curative effects were reported. Liver transplantation should be considered for patients with intractable pruritus who have poor responses to drugs or other approaches.

### Recommendations

14. We recommend cholestyramine as a first-line drug for treatment of pruritis, with an initial dose of 4 g/day and a maximum dose of 16 g/day. We recommend doses taken at intervals of 4 to 6 h when using other drugs (especially UDCA) so as not to affect their absorption (B2).
15. We recommend oral rifampicin as a second-line drug for treatment of pruritus, with an initial dose of 150 mg/day, and continuation at this dose if effective. If necessary, the dose can be increased to 300 mg/day every other week. We recommend close monitoring of liver biochemical parameters should during treatment (C2).
16. We recommend oral naltrexone, an opioid receptor antagonist, as a third-line drug for treatment of pruritus, beginning with a dose of 25 mg/day, and gradually increasing the dose to 50 mg/day to prevent withdrawal effects, similar to anesthetics (C1).
17. We recommend sertraline, a selective 5-HT reuptake inhibitor, as a fourth-line drug for treatment of pruritus, with an initial dose of 50 mg/day, and increasing the dose to 100 mg/day after a few weeks if necessary (C2).
18. We recommend ultraviolet irradiation, albumin dialysis, or nasobiliary drainage if the other treatments for pruritus are ineffective (C2). We recommend consideration of liver transplantation in patients with severe pruritus who have poor responses to drugs and other approaches (C2).

#### *Fatigue*

Patients with cholestasis, especially those with PBC, often experience fatigue, and fatigue occurs in 70 to 80% of patients with chronic cholestasis.[4] Fatigue is a complex symptom that includes persistent feelings of exhaustion, loss of normal working ability, and decline of psychological and physiological functions. Because it is a non-specific symptom, the Fatigue Impact Score or the Primary Biliary Cirrhosis 40 scale (PBC-40) may be used to assess symptoms and severity.[42,43] The pathogenesis of fatigue is still not clear, and there is no effective treatment. Anemia, diabetes, hypothyroidism, renal and adrenal insufficiency, and depression should be excluded before treatment. At present, the possible therapeutic methods and drugs are selective 5-HT3 receptor antagonists such as ondansetron, opioid receptor antagonists, and the central nervous stimulant modafinil. The initial dose of modafinil is 100 mg/day, and it may be gradually increased to 200 mg/day according to tolerance and responsiveness, but further studies of its efficacy are needed. Although UDCA is an effective treatment for PBC, it apparently has no significant effect on the accompanying symptoms of fatigue. Even 1 year after liver transplantation, fatigue may remain a persistent symptom for these patients, although the degree of fatigue may be less. A healthy lifestyle, including adequate sleep, regular exercise, abstinence from alcohol, and avoidance of coffee at night are beneficial. Antidepressants may partly reduce the fatigue of patients with depression.

#### *Xanthoma*

Xanthomas are common in patients with chronic cholestasis. This condition is characterized by flat or slightly raised fat deposits on the skin surface that are yellow and soft and often occur around the eyes. They may also occur in the palmar fold, breast, neck, chest, and back. Their occurrence is related to an elevated level of blood lipids, with serum cholesterol usually more than 4.5 g/L. When jaundice subsides or liver failure occurs, the level of cholesterol drops and these manifestations might disappear. Xanthomas require no special treatment.

#### *Dyslipidemia*

Cholestasis inhibits the metabolism of cholesterol due to the increase of bile acid, and this often leads to lipid metabolic disorder. Thus, patients with cholestasis often have elevated levels of cholesterol and triglycerides, although there is no evidence that this increases their risk of atherosclerosis. Statins and fibrates are safe treatments for patients who have cholestatic liver disease with lipid metabolic disorders.[44] Cholestyramine can also reduce the level of blood lipids.

#### *Steatorrhea*

Steatorrhea is characterized by large stools that are soft, excessively oily, gray, and with a peculiar smell. This may occur in patients with cholestasis because the intestinal tract lacks sufficient bile salt, leading to impaired digestion and absorption of fats and fat-soluble vitamins (A, D, E, and K). Thus, steatorrhea is positively correlated to the degree of jaundice.

### Recommendations

19. We recommend exclusion of anemia, diabetes melli-

tus, hypothyroidism, renal and adrenal insufficiency, and depression when a patient presents with cholestatic fatigue. We recommend adequate sleep, regular exercise, and abstaining from alcohol and coffee for management of fatigue (C2). We recommend selective 5-HT3 receptor antagonists, such as ondansetron, an opioid receptor antagonist, or the central nervous stimulant modafinil as drug treatments (C2). We recommend antidepressants to assist in reducing fatigue in patients with depression. We do not recommend liver transplantation for management of fatigue (C2).

20. We recommend no special treatment for xanthoma (B2). We recommend statins and fibrates for patients with dyslipidemia, and cholestyramine to help resolve dyslipidemia (B2).

### *Hepatic osteodystrophy*

Bone complications may occur in patients with chronic liver disease due to osteoporosis and osteomalacia, and these can manifest as bone pain and fracture. Osteoporosis is characterized by bone matrix or mineral loss and osteomalacia as osteoid mineralization defects. Dual energy X-ray absorptiometry (DEXA) is used to diagnose osteoporosis based on bone mineral density (BMD).[4,5,45] According to the diagnostic criteria of the World Health Organization, BMD measured by DEXA is defined by T-score, which indicates the number of standard deviations above or below the mean (normal: T-score ≥ −1.0; osteopenia: −2.5 < T-score < −1.0; osteoporosis: T-score ≤ −2.5). The treatments for osteoporosis include following a healthy diet and lifestyle with exercise, use of calcium and vitamin D supplements, and drug interventions. The Chinese Nutrition Association recommends 800 mg calcium per day for adults and a 1,000 mg calcium per day for postmenopausal women and the elderly. The recommended dose of vitamin D for adults is 200 IU/day, and the dose for the elderly is 400 to 800 IU/day, especially when there is a lack of exposure to sunshine and/or impaired intake or absorption. The dose of vitamin D should be 800 to 1,200 IU/day for treatment of osteoporosis. Epidemiological data support the use of calcium supplements (1,000 to 1,200 mg/day) and vitamin D (400 to 800 IU/day) for reducing or reversing the rate of bone loss. Hormone replacement therapy is effective in postmenopausal women. To decrease the risk of hepatocellular carcinoma, males should avoid testosterone. Research supports the use of diphosphonates (alendronate at 70 mg/week, ibandronate at 150 mg/month, or other similar drugs) to treat and prevent osteoporosis. Annual BMD measurements should be performed during follow-up to assess treatment efficacy.

### *Deficiency of fat-soluble vitamins*

Cholestasis leads to disruption in the secretion of bile from the liver to the small intestine, and this decreases bile salt in the intestine and can cause a deficiency of fat-soluble vitamins and steatorrhea. Therefore, fat-soluble vitamins should be administered as dietary supplements.[45] If the prothrombin time(PT) is prolonged, intramuscular vitamin K1 (10 mg/day) can be given until it returns to normal. Oral vitamin A at a dose of 25,000 to 50,000 IU/day can be used to treat night blindness. Vitamin E deficiency is rare, but children with cerebellar ataxia, posterior funicular dysfunction, peripheral neuropathy and retinal degeneration, might benefit from oral supplements. Measuring the blood levels of fat-soluble vitamins can help guide their administration, but these measurements are not common.

## Recommendations

21. We recommend calcium and vitamin D supplements for prevention of osteoporosis. For calcium, adults should take 800 mg/day and postmenopausal women and the elderly should take 1,000 mg/day. For vitamin D, adults should take 200 IU/day, and the elderly should take 400 to 800 IU/day (C1). We recommend diphosphonates (alendronate, 70 mg/week; ibandronate, 150 mg/month; and others) for treatment and prevention of osteoporosis (C2). We recommend annual BMD measurements during the treatment and follow-up of patients with osteoporosis (C2).
22. We recommend monitoring and supplementation of fat-soluble vitamins. We recommend intramuscular vitamin K1 (10 mg/day) for patients with prolonged PT (B1) and oral vitamin A (25,000 to 50,000 IU/day) for night blindness due to vitamin A deficiency (C1). Although vitamin E deficiency is rare, if present we recommend an oral dose of 10 to 100 mg/day (C2).

## Problems to be Solved

Although there has been significant progress in the diagnosis and treatment of cholestatic liver diseases during recent years, many problems and challenges remain. In terms of basic research, there is a need for more studies that examine the mechanisms of these diseases (especially at the molecular level), the effect of heritable risk factors and alterations of different bile acid transporters on the occurrence and development of disease, and the influence of bile acid composition on the liver and the whole body. PBC and PSC are the major cholestatic liver diseases, and their etiologies are not yet fully clear. UDCA is the main treatment for PBC, but some patients have poor responses to this drug. In addition, there is no effective drug for PSC. The epidemiology, diagnostic markers, and diagnostic criteria for cholestatic liver diseases require further studies for verification. There is also an urgent need to identify additional drugs and treatments for the different cholestatic liver diseases.

## Acknowledgments

The following experts participated in the discussion on the formulation of this guideline and put forward constructive opinions and suggestions (sorted by Pinyin surname): Jihong An (Department of Infection, People's Hospital of Inner Mongolia Autonomous Region); Guohong Deng (Department of Infectious Diseases, The First Affiliated Hospital of Military Medical University of the Army); Yan Huang (Department of Infection, Xiangya Hospital, Central South University); Yuan Huang (Department of Hepatobiliary Medicine, Changgeng Hospital, Tsinghua University, Beijing); Rongkuan Li (Department of Infection, The Second Affiliated Hospital, Dalian Medical University); Shuchen Li (Department of Infection; Second Affiliated Hospital, Harbin Medical University); Haiying Lu (Department of Infection, The First Hospital, Peking University, Beijing); Li Shi (Department of Infection, People's Hospital of Tibet Autonomous Region); Minghua Su (Department of Infection, The First Affiliated Hospital, Guangxi Medical University); Lizhi Wen (Department of Gastroenterology, Second Affiliated Hospital, Nanchang University); Biao Wu (Department of Infection, Hainan Provincial People's Hospital); Jinghang Xu (Department of Hepatology, The First Hospital, Peking University, Beijing); Yang Li (Department of Gastroenterology, West China Hospital, Sichuan University); Jiming Yang

(Department of Infection, Tianjin Second People's Hospital); Jinhui Yang (Department of Gastroenterology, Second Affiliated Hospital, Kunming Medical University); Yaoyun Zhang (Department of Infection, The First Hospital, Shanxi Medical University); Lu Zhou (Department of Gastroenterology, General Hospital of Tianjin Medical University); Yongjian Zhou (Department of Gastroenterology, The First People's Hospital of Guangzhou); Hongmei Zu (Department of Infection, The Fourth People's Hospital of Qinghai Province).

## Conflict of interest

LL has been an associate editor of *Journal of Clinical and Translational Hepatology* since 2013. HY has been an editorial board member of *Journal of Clinical and Translational Hepatology* since 2021. YH has been an editorial board member of *Journal of Clinical and Translational Hepatology* since 2013. LW and JJ have been an executive associate editor of *Journal of Clinical and Translational Hepatology* since 2021. The other authors have no conflict of interests related to this publication.

## Authors

Lungen Lu, Xiaobo Cai, Jianshe Wang, Ying Qu, Hong You, Xiong Ma, Ying Han, Yuemin Nan, Xiaoyuan Xu, Zhongping Duan, Lai Wei, Jidong Jia, Hui Zhuang.

## Experts in formulating the guidelines (sorted by Pinyin surname)

Xiaobo Cai (Department of Gastroenterology, Shanghai General Hospital, Shanghai Jiaotong University School of Medicine, Shanghai); Sha Chen (Center for Liver Diseases, Beijing Friendship Hospital, Capital Medical University, Beijing); Yu Chen (Center for Liver Diseases, Beijing You'an Hospital, Capital Medical University, Beijing), Hongsong Chen (Institute of Hepatology, People's Hospital, Peking University, Beijing); Lina Cui (Department of Gastroenterology, The First Affiliated Hospital of Air Force Military Medical University, Xi'an); Jianqiang Dong (Department of Gastroenterology, The First Affiliated Hospital of Air Force Military Medical University, Xi'an); Xiaoguang Dou (Department of Infection, Shengjing Hospital, Chinese Medical University, Shenyang); Weijia Duan (Center for Liver Diseases, Beijing Friendship Hospital, Capital Medical University, Beijing); Zhongping Duan (Center for Liver Diseases, You'an Hospital, Capital Medical University, Beijing); Jiangao Fan (Department of Gastroenterology, Xinhua Hospital, Shanghai Jiaotong University School of Medicine, Shanghai); Changcun Guo (Department of Gastroenterology, The First Affiliated Hospital of Air Force Military Medical University, Xi'an); Guanya Guo (Department of Gastroenterology, The First Affiliated Hospital of Air Force Military Medical University, Xi'an); Tao Han (Department of Hepatology, Third Central Hospital, Tianjin); Ying Han (Department of Gastroenterology, The First Affiliated Hospital of Air Force Military Medical University, Xi'an); Jinlin Hou (Department of Infection, Nanfang Hospital, Southern Medical University, Guangzhou); Peng Hu (Department of Infection, The Second Affiliated Hospital, Chongqing Medical University, Chongqing); Yi Huan (Department of Radiology, The First Affiliated Hospital of Air Force Military Medical University, Xi'an); Jidong Jia (Center for Liver Disease, Beijing Friendship Hospital, Capital Medical University, Beijing); Yuanyuan Kong (Methodology Platform of National Clinical Research Center of Digestive System Diseases, Beijing Friendship Hospital, Capital Medical University, Beijing); Jie Li (Department of Pathogenic Biology, School of Basic Medicine, Peking University); Jun Li (Department of Infectious Diseases, Jiangsu Provincial People's Hospital, Nanjing); Shuxiang Li (Liver Disease Center, Beijing Friendship Hospital, Capital Medical University, Beijing); Zengshan Li (Department of Pathology, First Affiliated Hospital of Air Force Military Medical University, Xi'an); Enqiang Lihu (Department of Gastroenterology, First Medical Center, General Hospital of Chinese PLA); Jiayun Liu (Department of Laboratory Medicine, The First Affiliated Hospital of Air Force Military Medical University, Xi'an); Jingfeng Liu (Department of Hepatobiliary Surgery, Mengchao Hepatobiliary Hospital, Fujian Medical University); Yanmin Liu (Department of Hepatology, Beijing You'an Hospital, Capital Medical University, Beijing); Yingdi Liu (Department of Gastroenterology, First Medical Center, General Hospital of Chinese PLA); Lungen Lu (Department of Gastroenterology, Shanghai General Hospital, Shanghai Jiaotong University School of Medicine, Shanghai); Xinhua Luo (Department of Infection, People's Hospital of Guizhou Province); Tingting Lu (Center for Liver Diseases, Beijing Friendship Hospital, Capital Medical University, Beijing); Xiong Ma (Department of Gastroenterology, Renji Hospital, Shanghai Jiaotong University School of Medicine, Shanghai); Yimin Mao (Department of Gastroenterology, Renji Hospital, Shanghai Jiaotong University School of Medicine, Shanghai); Qi Miao (Department of Gastroenterology, Renji Hospital, Shanghai Jiaotong University School of Medicine, Shanghai); Yuemin Nan (Department of Hepatology, The Third Hospital of Hebei Medical University); Ying Qu (Department of Gastroenterology, Shanghai General Hospital, Shanghai Jiaotong University School of Medicine, Shanghai); Hong Ren (Department of Infectious Diseases, Second Hospital of Chongqing Medical University); Wanhua Ren(Department of infectious diseases, Shandong Provincial Hospital); Jia Shang (Department of Infectious Diseases, Henan Provincial People's Hospital); Yulong Shang (Department of Gastroenterology, The First Affiliated Hospital of Air Force Military Medical University); Yongquan Shi (Department of Gastroenterology, The First Affiliated Hospital of Air Force Military Medical University); Chengwei Tang (Department of Gastroenterology, West China Hospital, Sichuan University); Jianshe Wang (Department of Infection, Pediatric Hospital, Fudan University, Shanghai); Jingwen Wang (Department of Pharmacy, First Affiliated Hospital of Air Force Military Medical University); Qixia Wang (Department of Gastroenterology, Renji Hospital, Shanghai Jiaotong University School of Medicine, Shanghai); Lai Wei (Department of Hepatobiliary Medicine, Changgeng Hospital, Tsinghua University, Beijing); Hao Wu (Department of Gastroenterology, West China Hospital, Sichuan University); Xiaoyuan Xu (Department of Infectious Diseases, The First Hospital, Peking University, Beijing); Ming Yan (Department of Gastroenterology, Qilu Hospital, Shandong University, Jinan); Dongliang Yang (Department of Infection, Union Hospital, Tongji Medical College, Huazhong University of Science and Technology, Wuhan); Yongfeng Yang (Department of Hepatology, Second Hospital of Nanjing); Zhaoxu Yang (Department of Hepatobiliary Surgery, The First Affiliated Hospital of Air Force Military Medical University); Hong You (Center for Liver Diseases, Beijing Friendship Hospital, Capital Medical University, Beijing); Xinxin Zhang (Department of Infection, Ruijin Hospital, Shanghai Jiaotong University School of Medicine, Shanghai); Yuexin Zhang (Department of Infection, The First Affiliated Hospital, Xinjiang Medical University); Jingmin Zhao (Department of Pathology, Fifth Medical Center, General Hospital of Chinese PLA); Shousong Zhao (Department of Infectious Diseases, The First Affiliated Hospital of Bengbu Medical College); Xinyan Zhao (Liver Disease Center, Beijing Friendship Hospital, Capital Medical University, Beijing); Linhua Zheng (Department of Gastroenterology,

First Affiliated Hospital of Air Force Military Medical University); Xinmin Zhou (Department of Gastroenterology, The First Affiliated Hospital of Air Force Military Medical University); Hui Zhuang (Department of Pathogenic Biology, School of Basic Medicine, Peking University).

## References


[1] Kuntz K, Kuntz HD. Hepatology: Principles and Practice. 2nd ed. Heidelberg, Germany: Springer Medizin Verlag Heidelberg. 2006:227–242.

[2] Wu H, Chen C, Ziani S, Nelson LJ, Ávila MA, Nevzorova YA, *et al*. Fibrotic Events in the Progression of Cholestatic Liver Disease. Cells 2021;10(5):1107. doi:10.3390/cells10051107, PMID:34062960.

[3] Chinese Medical Association of Hepatology, Gastroenterology, Chinese Medical Association. Consensus on diagnosis and treatment of cholestatic liver disease (2015). Chinese Zhonghua Gan Zang Bing Za Zhi 2015;23(12):924–933. doi:10.3760/cma.j.issn.1007-3418.2015.12.004.

[4] Sherlock S, Dooley J. Disease of the liver and biliary system. 11th ed. Oxford, England: Blackwell Publishing. 2002:219–240.

[5] European Association for the Study of the Liver. EASL Clinical Practice Guidelines: management of cholestatic liver diseases. J Hepatol 2009;51(2):237–267. doi:10.1016/j.jhep.2009.04.009, PMID:19501929.

[6] Burt A, Portmann B, Ferrell L. MacSween's pathology of the liver. 6th ed. London, England: Churchill Livingstone Elsevier. 2012:503–562.

[7] Lefkowitch JH. Scheuer's liver biopsy interpretation. 9th ed. New York, USA: Elsevier. 2016:53.

[8] Hilscher MB, Kamath PS, Eaton JE. Cholestatic Liver Diseases: A Primer for Generalists and Subspecialists. Mayo Clin Proc 2020;95(10):2263–2279. doi:10.1016/j.mayocp.2020.01.015, PMID:33012354.

[9] Bortolini M, Almasio P, Bray G, Budillon G, Coltorti M, Frezza M, *et al*. Multicentre survey of the prevalence of intrahepatic cholestasis in 2520 consecutive patients with newly diagnosed chronic liver disease. Drug Invest 1992;4(Suppl 4):83–89. doi:10.1007/BF03258368.

[10] Xie W, Cao Y, Xu M, Wang J, Zhou C, Yang X, *et al*. Prognostic Significance of Elevated Cholestatic Enzymes for Fibrosis and Hepatocellular Carcinoma in Hospital Discharged Chronic Viral Hepatitis Patients. Sci Rep 2017;7(1):10289. doi:10.1038/s41598-017-11111-5, PMID:28860489.

[11] Cao X, Gao Y, Zhang W, Xu P, Fu Q, Chen C, *et al*. Based on the prevalence of cholestasis in hospitalized patients with chronic liver disease in Shanghai. Zhonghua Gan Zang Bing Za Zhi 2015;23(8):569–573. doi:10.3760/cma.j.issn.1007-3418.2015.08.003.

[12] Siddique A, Kowdley KV. Approach to a patient with elevated serum alkaline phosphatase. Clin Liver Dis 2012;16(2):199–229. doi:10.1016/j.cld.2012.03.012, PMID:22541695.

[13] Reichert MC, Hall RA, Krawczyk M, Lammert F. Genetic determinants of cholangiopathies: Molecular and systems genetics. Biochim Biophys Acta Mol Basis Dis 2018;1864(4 Pt B):1484–1490. doi:10.1016/j.bbadis.2017.07.029, PMID:28757171.

[14] Vitale G, Gitto S, Vukotic R, Raimondi F, Andreone P. Familial intrahepatic cholestasis: New and wide perspectives. Dig Liver Dis 2019;51(7):922–933. doi:10.1016/j.dld.2019.04.013, PMID:31105019.

[15] Pieters A, Gijbels E, Cogliati B, Annaert P, Devisscher L, Vinken M. Biomarkers of cholestasis. Biomark Med 2021;15(6):437–454. doi:10.2217/bmm-2020-0691, PMID:33709780.

[16] Geller S, Petovic LM. Biopsy interpretation of the liver. 2nd ed. Philadelphia, USA: Lippincott Williams & Wilkins. 2009:404–416.

[17] Paumgartner G, Beuers U. Ursodeoxycholic acid in cholestatic liver disease: mechanisms of action and therapeutic use revisited. Hepatology 2002;36(3):525–531. doi:10.1053/jhep.2002.36088, PMID:12198643.

[18] Appanna G, Kallis Y. An update on the management of cholestatic liver diseases. Clin Med (Lond) 2020;20(5):513–516. doi:10.7861/clinmed.2020-0697, PMID:32934048.

[19] Wagner M, Fickert P. Drug Therapies for Chronic Cholestatic Liver Diseases. Annu Rev Pharmacol Toxicol 2020;60:503–527. doi:10.1146/annurev-pharmtox-010818-021059, PMID:31506007.

[20] Fabris L, Fiorotto R, Spirli C, Cadamuro M, Mariotti V, Perugorria MJ, *et al*. Pathobiology of inherited biliary diseases: a roadmap to understand acquired liver diseases. Nat Rev Gastroenterol Hepatol 2019;16(8):497–511. doi:10.1038/s41575-019-0156-4, PMID:31165788.

[21] Staufer K. Current Treatment Options for Cystic Fibrosis-Related Liver Disease. Int J Mol Sci 2020;21(22):E8586. doi:10.3390/ijms21228586, PMID:33202578.

[22] Boëlle PY, Debray D, Guillot L, Clement A, Corvol H, French CF Modifier Gene Study Investigators. Cystic Fibrosis Liver Disease: Outcomes and Risk Factors in a Large Cohort of French Patients. Hepatology 2019;69(4):1648–1656. doi:10.1002/hep.30148, PMID:30058245.

[23] Li LT, Li ZD, Yang Y, Lu Y, Xie XB, Chen L, *et al*. ABCB11 deficiency presenting as transient neonatal cholestasis: Correlation with genotypes and BSEP expression. Liver Int 2020;40(11):2788–2796. doi:10.1111/liv.14642, PMID:32808743.

[24] Li L, Deheragoda M, Lu Y, Gong J, Wang J. Hypothyroidism Associated with ATP8B1 Deficiency. J Pediatr 2015;167(6):1334–9.e1. doi:10.1016/j.jpeds.2015.08.037, PMID:26382629.

[25] Li LT, Li ZD, Yang Y, Lu Y, Xie XB, Chen L, *et al*. ABCB11 deficiency presenting as transient neonatal cholestasis: Correlation with genotypes and BSEP expression. Liver Int 2020;40(11):2788–2796. doi:10.1111/liv.14642, PMID:32808743.

[26] van Wessel DBE, Thompson RJ, Gonzales E, Jankowska I, Sokal E, Grammatikopoulos T, *et al*. Genotype correlates with the natural history of severe bile salt export pump deficiency. J Hepatol 2020;73(1):84–93. doi:10.1016/j.jhep.2020.02.007, PMID:32087350.

[27] Zhang J, Liu LL, Gong JY, Hao CZ, Qiu YL, Lu Y, *et al*. TJP2 hepatobiliary disorders: Novel variants and clinical diversity. Hum Mutat 2020;41(2):502–511. doi:10.1002/humu.23947, PMID:31696999.

[28] Qiu YL, Gong JY, Feng JY, Wang RX, Han J, Liu T, *et al*. Defects in myosin VB are associated with a spectrum of previously undiagnosed low γ-glutamyltransferase cholestasis. Hepatology 2017;65(5):1655–1669. doi:10.1002/hep.29020, PMID:28027573.

[29] Zhang J, Yang Y, Gong JY, Li LT, Li JQ, Zhang MH, *et al*. Low-GGT intrahepatic cholestasis associated with biallelic USP53 variants: Clinical, histological and ultrastructural characterization. Liver Int 2020;40(5):1142–1150. doi:10.1111/liv.14422, PMID:32124521.

[30] Pan Q, Luo G, Qu J, Chen S, Zhang X, Zhao N, *et al*. A homozygous R148W mutation in Semaphorin 7A causes progressive familial intrahepatic cholestasis. EMBO Mol Med 2021;13(11):e14563. doi:10.15252/emmm.202114563, PMID:34585848.

[31] Gonzales E, Hardikar W, Stormon M, Baker A, Hierro L, Gliwicz D, *et al*. Efficacy and safety of maralixibat treatment in patients with Alagille syndrome and cholestatic pruritus (ICONIC): a randomised phase 2 study. Lancet 2021;398(10311):1581–1592. doi:10.1016/S0140-6736(21)01256-3, PMID:34755627.

[32] Emerick KM, Rand EB, Goldmuntz E, Krantz ID, Spinner NB, Piccoli DA. Features of Alagille syndrome in 92 patients: frequency and relation to prognosis. Hepatology 1999;29(3):822–829. doi:10.1002/hep.510290331, PMID:10051485.

[33] Shneider BL, Spino C, Kamath BM, Magee JC, Bass LM, Setchell KD, *et al*. Placebo-Controlled Randomized Trial of an Intestinal Bile Salt Transport Inhibitor for Pruritus in Alagille Syndrome. Hepatol Commun 2018;2(10):1184–1198. doi:10.1002/hep4.1244, PMID:30288474.

[34] Floreani A, Gervasi MT. New Insights on Intrahepatic Cholestasis of Pregnancy. Clin Liver Dis 2016;20(1):177–189. doi:10.1016/j.cld.2015.08.010, PMID:26593298.

[35] Wood AM, Livingston EG, Hughes BL, Kuller JA. Intrahepatic Cholestasis of Pregnancy: A Review of Diagnosis and Management. Obstet Gynecol Surv 2018;73(2):103–109. doi:10.1097/OGX.0000000000000524, PMID:29480924.

[36] Smith DD, Rood KM. Intrahepatic Cholestasis of Pregnancy. Clin Obstet Gynecol 2020;63(1):134–151. doi:10.1097/GRF.0000000000000495, PMID:31764000.

[37] Langedijk JAGM, Beuers UH, Oude Elferink RPJ. Cholestasis-Associated Pruritus and Its Pruritogens. Front Med (Lausanne) 2021;8:639674. doi:10.3389/fmed.2021.639674, PMID:33791327.

[38] Patel SP, Vasavda C, Ho B, Meixiong J, Dong X, Kwatra SG. Cholestatic pruritus: Emerging mechanisms and therapeutics. J Am Acad Dermatol 2019;81(6):1371–1378. doi:10.1016/j.jaad.2019.04.035, PMID:31009666.

[39] Bergasa NV, Jones EA. Assessment of the Visual Analogue Score in the Evaluation of the Pruritus of Cholestasis. J Clin Transl Hepatol 2017;5(3):203–207. doi:10.14218/JCTH.2017.00001, PMID:28936401.

[40] Thébaut A, Habes D, Gottrand F, Rivet C, Cohen J, Debray D, *et al*. Sertraline as an Additional Treatment for Cholestatic Pruritus in Children. J Pediatr Gastroenterol Nutr 2017;64(3):431–435. doi:10.1097/MPG.0000000000001385, PMID:27557426.

[41] Webb GJ, Rahman SR, Levy C, Hirschfield GM. Low risk of hepatotoxicity from rifampicin when used for cholestatic pruritus: a cross-disease cohort study. Aliment Pharmacol Ther 2018;47(8):1213–1219. doi:10.1111/apt.14579, PMID:29468705.

[42] Phaw NA, Leighton J, Dyson JK, Jones DE. Managing cognitive symptoms and fatigue in cholestatic liver disease. Expert Rev Gastroenterol Hepatol 2021;15(3):235–241. doi:10.1080/17474124.2021.1844565, PMID:33131347.

[43] Swain MG, Jones DEJ. Fatigue in chronic liver disease: New insights and therapeutic approaches. Liver Int 2019;39(1):6–19. doi:10.1111/liv.13919, PMID:29935104.

[44] Dubrovsky AMK, Bowlus CL. Statins, Fibrates, and Other Peroxisome Proliferator-Activated Receptor Agonists for the Treatment of Cholestatic Liver Diseases. Gastroenterol Hepatol (N Y) 2020;16(1):31–38. PMID:33867886.

[45] European Association for the Study of the Liver. EASL Clinical Practice Guidelines on nutrition in chronic liver disease. J Hepatol 2019;70(1):172–193. doi:10.1016/j.jhep.2018.06.024, PMID:30144956.

*Journal of Clinical and Translational Hepatology* **2022** vol. 10(4) | 770–777
DOI: 10.14218/JCTH.2021.00303

Short Communication

# Impact of Living Donor Liver Transplantation on COVID-19 Clinical Outcomes from a Quaternary Care Centre in Delhi

Imtiakum Jamir[1*], Niteen Kumar[1], Gaurav Sood[1], Ashish George[1], Pankaj Lohia[2], Samba Siva Rao Pasupuleti[3], Amrish Sahney[4], Manav Wadhawan[4], Ajay Kumar[4] and Abhideep Chaudhary[1*]

*[1]Department of HPB Surgery and Liver Transplantation, BLK Super Speciality Hospital, New Delhi, India; [2]Department of Critical Care, BLK Super Speciality Hospital, New Delhi, India; [3]Department of Statistics, Mizoram University (A Central University), Pachhunga University College Campus, Aizawl, Mizoram, India; [4]Institute of Digestive and Liver Diseases, BLK Super Speciality Hospital, New Delhi, India*

**Received:** 23 July 2021 | **Revised:** 1 September 2021 | **Accepted:** 9 September 2021 | **Published:** 12 October 2021

## Abstract

***Background and Aims:*** The anticipated fear of serious outcomes in coronavirus infected liver transplant recipients led to disruption of transplant services globally. The aim of our study was to analyze COVID-19 severity in transplant recipients and to compare the difference of COVID-19 clinical outcomes in early (<1 year) vs. late (>1 year) post-transplant period. ***Methods:*** 41 post-living donor liver transplant recipients with COVID-19 infection were studied retrospectively from 1st April 2020 to 28th February 2021. ***Results:*** The median age was 49.00 years with a male preponderance (80.49%). Fifteen patients had infection within 1 year of transplant and 26 were infected after 1 year of transplant. The overall median interval between transplantation and COVID-19 diagnosis was 816.00 days. Fever and malaise were the common presenting symptoms. The most common associated comorbidities were diabetes mellitus (65.85%) and hypertension (46.34%). The severity of illness was mild in 28 (68.29%), moderate in 4 (9.76%), severe in 6 (14.63%) and critical in 3 (7.32%). To identify associated risk factors, we divided our patients into less severe and more severe groups. Except for lymphopenia, there was no worsening of total bilirubin, transaminases, alkaline phosphatase, and gamma-glutamyl transferase in the more severe group. Eight (19.51%) patients required intensive care unit admission and three (7.32%) died, while none suffered graft rejection. In recipients with early vs. late post-transplant COVID-19 infection, there were similar outcomes in terms of severity of COVID-19 illness, intensive care unit care need, requirement of respiratory support, and death. ***Conclusion:*** Living donor liver transplantation can be performed during the COVID-19 pandemic without the fear of poor recipient outcome in cases of unfortunate contraction of severe acute respiratory syndrome coronavirus-2.

**Citation of this article:** Jamir I, Kumar N, Sood G, George A, Lohia P, Pasupuleti SSR, *et al*. Impact of Living Donor Liver Transplantation on COVID-19 Clinical Outcomes from a Quaternary Care Centre in Delhi. J Clin Transl Hepatol 2022;10(4):770–777. doi: 10.14218/JCTH.2021.00303.

## Introduction

The current coronavirus disease-19 (COVID-19) pandemic caused by severe acute respiratory syndrome coronavirus-2 (SARS-CoV-2) has witnessed a disruption in transplant activities worldwide. The anticipated fear of potential serious outcome in solid organ liver transplantation, particularly in the perioperative and early postoperative periods, when there is maximal immune suppression, led to this disruption. There is also a possibility of eligible liver donors being infected with SARS-CoV-2 and transmitting the same to their recipients. Furthermore, the added risk of nosocomial infections during hospital stays and follow-up visits put the transplantation program on the back foot. Last year, transplant services were restarted in most centers across the world after an initial suspension and subsequent revamp.[1,2] The emerging reports of increased morbidity and mortality due to COVID-19 infection in patients with chronic liver disease and cirrhosis, as compared to the general population, vs. denial of a timely life-saving transplant procedure in already sick patients poses an ethical dilemma. At the same time, by subjecting these patients to a major liver transplantation procedure followed by iatrogenic immunosuppression, which can lead to the worsening of perioperative and short-term outcomes in case of unfortunate contraction of SARS-CoV-2, needs to be investigated.

Our transplant center is located at Delhi, which is a major hotspot for the COVID-19 pandemic. We restarted our transplant services after an initial period of precaution, with restructuring of COVID safe clinical protocols.[1] While India is currently reeling under the tsunami of the pandemic's 2nd

**Keywords:** COVID-19; SARS-CoV-2; Living donor liver transplantation, LDLT; Mortality; Perioperative.

**Abbreviations:** ALT, alanine transaminase; AST, aspartate transaminase; BMI, body mass index; COVID-19, coronavirus disease-19; GGT, gamma-glutamyl transferase; LOR, low oxygen requirement; HOR, high oxygen requirement; ICU, intensive care unit; IQR, interquartile range; LDLT, living donor liver transplantation; LOR, low oxygen requirement; LT, liver transplantation; MV, mechanical ventilation; SARS-CoV-2, severe acute respiratory syndrome coronavirus-2; WHO, World Health Organization.

***Correspondence to:** Imtiakum Jamir and Abhideep Chaudhary, Department of HPB Surgery and Liver Transplantation, BLK Super Speciality Hospital, Pusa Road, Rajendra Place, New Delhi 110005, India. ORCID: https://orcid.org/0000-0003-2217-1372 (IJ), https://orcid.org/0000-0003-4817-4336 (AC). Tel: +91-11-3040-3040, Fax: +91-11-2575-2885, E-mail: dr.imtiakumjamir@gmail.com (IJ), drabhideep@yahoo.com (AC)

wave caused by new variants of the SARS-CoV, the data presented here is from the 1st wave, which was kinder to the Indian sub-continent compared to the west.[3,4]

The data on outcome of COVID-19 infection in living donor liver transplantation (LDLT) recipients is sparse, with most reports being from the west and involving primarily deceased donor programs. The aim of this study was to investigate the severity of COVID-19 infection in our transplant recipients and to compare the impact of liver transplantation on COVID-19 clinical outcomes in the early (<1 year) vs. late (>1 year) post-transplant period.

## Methods

This was a retrospective observational study of 41 post-LDLT recipients who contracted SARS-CoV-2 infection during the 1st wave of the COVID-19 pandemic (1st April 2020 to 28th February 2021). During this period, a total of 54 LDLT and 3 simultaneous live liver-kidney transplants were conducted at our center, out of which 12 recipients contracted SARS-CoV-2 infection. The remaining 29 were recipients who had been transplanted prior to 1st April 2020 and were infected during this time interval.

### *Inclusion criteria*

All LDLT recipients (age at COVID-19 diagnosis >18 years) being followed up at the BLK-MAX hospital with positive nasopharyngeal swab real time-polymerase chain reaction between 1st April 2020 to 28th February 2021.

### *Exclusion criteria*

Recipients with negative real time-polymerase chain reaction test.

### *Definitions*

The need for respiratory support was categorized as no oxygen, low oxygen requirement (LOR), high oxygen requirement (HOR), and mechanical ventilation (MV). LOR used a nasal cannula hooked up to Venturi mask, with $FiO_2$ of 0.5. HOR used a Venturi mask, with $FiO_2$ of 0.6, a reservoir mask with oxygen at 15 L/min, and high-flow nasal ventilation as well as non-invasive ventilation.

Recipients with SARS-CoV-2 infection were further classified into categories of severity per World Health Organization guidelines, as detailed here:[5]

**Mild illness:** Clinical symptoms (e.g., fever, cough, sore throat, malaise, headache, nausea, vomiting, diarrhea, loss of taste and smell) and no radiological evidence of pneumonia.

**Moderate illness:** Fever, respiratory symptoms, and imaging findings of pneumonia.

**Severe illness:** Any of the following: respiratory rate of >30 times per minute, $SpO_2$ of <94% on room air, a ratio of arterial partial pressure of oxygen to fraction of inspired oxygen of <300 mmHg, or lung infiltrates of >50%.

**Critical illness:** Any one of the following: respiratory failure, requirement of mechanical assistance, shock, or "extrapulmonary" organ failure.

### *Clinical outcome measures*

For the purpose of identifying risk factors and evaluating their clinical profile, patients were divided into two broad groups, namely less severe and more severe. The less severe group was comprised of those with mild illness and the more severe group was comprised of moderate, severe, and critical illnesses.

To compare COVID-19 clinical outcomes in the early vs. late post-transplant periods, the cohort was divided into two groups. The early period represented when COVID-19 infection was contracted within 1 year of undergoing transplant. The late period was represented when recipients were infected after 1 year past the transplant. The impact of time duration from transplant surgery to SARS-CoV-2 infection was evaluated with respect to degree of requirement of respiratory support, hospital admissions, intensive care unit (ICU) need, COVID-19 illness severity, and mortality.

The institutional review board of Dr. B.L. Kapur Memorial Hospital approved this study protocol (IRB committee/AARCE/July/2021/34), which waived the requirement for informed consent due to the retrospective nature of the study design.

### *Statistical analysis*

Descriptive statistics are presented in the form of mean ± standard deviation for continuous variables and as frequencies and percentages for categorical variables. For comparing means of two groups, independent samples *t*-test was used for normally distributed data and Mann-Whitney *U*-test was used for non-normally distributed data. Fisher's exact test was used to test the association between two categorical variables. All statistical analyses were performed using SPSS version 20 (IBM Corp., Armonk, NY, USA).

## Results

The baseline demographic and clinical characteristics are described as median (range) or frequency (percentage) (Table 1). The majority of the patients were male. The median patient age was 49.00 years (interquartile range [IQR]: 44.00, 60.00) and BMI was 29 kg/m$^2$ (IQR: 26.00, 31.00). Ethanol was the primary etiology for liver cirrhosis. The median time from liver transplantation to COVID-19 infection was 816.00 days (IQR: 223.00, 2,081.00). All patients presented with fever, with a median temperature of 100.60 °F (IQR: 99.50, 101.00). The next most common presenting symptom was malaise (in 68.29%), and 65.85% had diabetes mellitus while 46.34% had hypertension as comorbidities (Table 1).

The majority of our patients ($n$=27, 65.85%) did not require any oxygen support, while 7 (17.07%) required LOR, 4 (9.76%) required HOR, and 3 (7.3.2%) required MW.

### *Observed immunosuppressant strategies and clinical management*

Of the 41 recipients, 39 (95.12%) were on tacrolimus and 24 (58.54%) were on oral mycophenolate sodium (Myfortic, Novartis, Wehr, Germany). Tacrolimus was continued without dose alteration in non-hospitalized patients (i.e. those with mild and moderate illness). Those hospitalized underwent minimization of tacrolimus to 1/3rd dose (target level: 4–6 ng/dL). Tacrolimus was withheld in cases of severe illness with underlying or suspected sepsis and in cases of critical illness. The antimetabolite Myfortic was withheld temporarily in all patients with active infection, for a minimum of 2 weeks or until resolution of symptoms.

Eighteen (43.90%) recipients were on baseline mainte-

**Table 1. Clinical and laboratory characteristics of COVID-19 in LDLT recipients**

| Factor | Value, *n*=41 |
|---|---|
| Male sex, *n* (%) | 33 (80.49) |
| Female sex, *n* (%) | 8 (19.51) |
| BMI in kg/m$^2$, median (IQR) | 29.00 (26.00, 31.00) |
| Age in years at diagnosis of COVID-19, median (IQR) | 49.00 (44.00, 60.00) |
| Days from LT to COVID-19, median (IQR) | 816.00 (223.00, 2,081.00) |
| Perioperative SAR-CoV-2 diagnosis within 30 days | 3 (7.3) |
| Primary etiology, *n* (%) | |
| Ethanol | 17 (41.46) |
| Hepatitis B | 9 (21.95) |
| Nonalcoholic fatty liver disease | 8 (19.51) |
| Hepatitis C | 4 (9.76) |
| Others | 3 (7.32) |
| Hepatocellular carcinoma, *n* (%) | 7 (17.50) |
| Hospital-acquired SARS-CoV-2, *n* (%) | 3 (7.32) |
| Severity of COVID-19, *n* (%) | |
| Mild | 28 (68.29) |
| Moderate | 4 (9.76) |
| Severe | 5 (14.63) |
| Critical | 3 (7.32) |
| $SpO_2$ lowest %, median (IQR) | 96.00 (94.00, 98.00) |
| COVID symptoms | |
| Fever (maximum temperature in °F), median (IQR) | 100.60 (99.50, 101.00) |
| Malaise, *n* (%) | 28 (68.29) |
| Cough, *n* (%) | 14 (34.15) |
| Difficulty in breathing, *n* (%) | 12 (29.27) |
| Sore throat, *n* (%) | 11 (26.83) |
| GI symptoms, *n* (%) | 6 (14.63) |
| Loss of smell, *n* (%) | 4 (9.76) |
| Loss of taste, *n* (%) | 2 (4.88) |
| Comorbidities, *n* (%) | |
| Diabetes mellitus | 27 (65.85) |
| Hypertension | 19 (46.34) |
| Chronic kidney disease | 1 (2.44) |
| Malignancy | 1 (2.44) |
| Total admissions, *n* (%) | 14 (34.15) |
| ICU, *n* (%) | 8 (19.51) |
| Oxygenation, *n* (%) | |
| Room air, *n* (%) | 27 (65.85) |
| LOR, *n* (%) | 7 (17.07) |
| HOR, *n* (%) | 4 (9.76) |
| MV, *n* (%) | 3 (7.32) |
| Laboratory assessment at time of diagnosis, median (IQR) | |
| Lowest ALC recorded as ×10$^3$ cells/μL | 1.20 (0.80, 1.60) |

*(continued)*

**Table 1.** *(continued)*

| Factor | Value, *n*=41 |
|---|---|
| Total bilirubin as upper limit of normal 1.3 mg/dL | 0.80 (0.50, 1.20) |
| Peak AST as upper limit of normal 40 U/L | 44.00 (31.00, 55.00) |
| Peak ALT as upper limit of normal 50 U/L | 47.00 (29.00, 83.00) |
| ALP as upper limit of normal 130 U/L | 120.00 (94.93, 198.00) |
| GGT as upper limit of normal 60 U/L | 76.00 (45.00, 158.00) |
| Peak creatinine in mg/dL | 0.98 (0.83, 1.21) |
| Immunosuppression, *n* (%) | |
| Pre-COVID-19 infection tacrolimus | 39 (95.12) |
| During COVID-19 tacrolimus continued | 31 (79.49) |
| Mycophenolic acid | 24 (58.54) |
| Oral steroids | 18 (43.90) |
| Bolus steroids | 11 (26.83) |
| Everolimus | 6 (14.63) |
| Everolimus continued | 4 (9.75) |
| Class of antibiotics, *n* (%) | |
| Azithromycin | 10 (24.39) |
| Meropenem | 8 (19.51) |
| Cefuroxime | 6 (14.63) |
| Piperacillin/tazobactam | 2 (4.88) |
| Levofloxacin | 1 (2.44) |
| Other medications, *n* (%) | |
| Ecosprin at 75 mg | 29 (70.73) |
| Rivaroxaban | 17 (41.46) |
| Enoxaparin | 14 (34.15) |
| CPT | 5 (12.20) |
| Remdesivir | 5 (12.20) |

LDLT, living donor liver transplantation; COVID-19, coronavirus disease-19; BMI, body mass index; IQR, interquartile range; ICU, intensive care unit; LT, liver transplantation; SAR-CoV-2, severe acute respiratory syndrome coronavirus-2; SpO2, oxygen saturation; LOR, low oxygen requirement; HOR, high oxygen requirement; MV, mechanical ventilation; ALT, alanine transaminase; AST, aspartate transaminase; GGT, gamma-glutamyl transferase; ALP, alkaline phosphatase; ALC, absolute lymphocyte count; CPT, convalescent plasma therapy.

nance oral prednisolone pre-COVID-19. Our strategy was to double the oral steroid on a case-to-case basis, with a maximum ceiling dose of 20 mg/day. Of the 14 (34.15%) patients who needed admission, injectable steroids were administered in 11 (26.83%) patients.

None of the patients developed acute cellular rejection during the COVID-19 illness with our immunosuppressant strategies. One recipient underwent percutaneous liver biopsy for suspected acute rejection, which was subsequently diagnosed as severe steatosis.

In total, 65.85% patients received antibiotic prophylaxis. Five (12.20%) patients received convalescent plasma therapy (CPT), and remdesivir was given to five (12.20%) patients, out of which three received both CPT and remdesivir. Four patients in severe illness category and one patient with critical illness received CPT and /or remdesivir, with complete recovery of four of the severely ill patients. In total, 29 (70.73%) and 17 (41.46%) patients were on ecosprin and rivaroxaban, respectively, and 11 received both; injected enoxaparin was started in all admitted patients. None of our patients received ritonavir, hydroxychloroquine, ivermectin or tocilizumab.

The potential risk factors impacting the severity of COVID-19 illness were analyzed. In total, 28 (68.29%) patients were classified into the less severe group and 13 (31.7%) patients were classified into the more severe group. The two groups were similar in age, BMI, sex, primary etiologies, and comorbidities (Table 2). Control for comorbidities like diabetes mellitus and hypertension was not carried out in this study, as they were not found to be associated with severity of COVID-19 infection in our bivariate analysis (Table 2). In both groups, total bilirubin levels (0.71 mg/dL vs. 0.80 mg/dL, $p$=0.70), aspartate aminotransferase (AST) (47.00 IU/L vs. 40.00 IU/L, $p$=0.50), alanine aminotransferase (ALT) (48.50 IU/L vs. 40.00 IU/L, $p$=0.39), alkaline phosphatase (ALP) (130.50 U/L vs. 108.00 U/L $p$=0.64), gamma-glutamyl transferase (GGT) (76.50 U/L vs. 61.00 U/L, $p$=0.79), and creatinine (0.98 mg/dl vs. 0.90 mg/dl, $p$=0.99) at admissions were comparable, and thus were not affected by severity. Only the absolute lymphocyte count ($1.40\times10^3$/μL vs. $0.65\times10^3$/μL, $p$<0.001) was significantly lower in the more severe group (Table 2). In the patients who required ICU admission, the absolute lymphocyte count was significantly lower than in the group who did not require ICU care

**Table 2. Risk factors and clinical profile in the less severe (mild) and the more severe (moderate, severe, and critical) group**

| Factors | Less severe group, *n*=28 | More severe group, *n*=13 | *p* |
|---|---|---|---|
| Age in years at diagnosis of COVID-19, median (IQR) | 49.50 (41.00, 59.00) | 49.00 (45.00, 61.00) | 0.60 |
| Sex, *n* (%) | | | 0.69 |
| Male | 23 (82.14) | 10 (76.92) | |
| Female | 5 (17.86) | 3 (23.08) | |
| BMI, median (IQR) | 28.00 (25.50, 31.50) | 29.80 (27.00, 30.70) | 0.80 |
| Primary etiology, *n* (%) | | | 0.89 |
| Ethanol | 12 (42.86) | 5 (38.46) | |
| Hepatitis B | 7 (25.00) | 2 (15.38) | |
| Non alcoholic fatty liver disease | 5 (17.86) | 3 (23.08) | |
| Hepatitis C | 2 (7.14) | 2 (15.38) | |
| Others | 2 (7.14) | 1 (7.69) | |
| Comorbidities, *n* (%) | | | |
| Diabetes mellitus | 16 (57.14) | 11 (84.62) | 0.16 |
| Hypertension | 12 (42.86) | 7 (53.85) | 0.74 |
| Laboratory assessment at time of diagnosis, median (IQR) | | | |
| ALC recorded as $\times 10^3$ cells/μL | *1.40 (1.00, 1.77)* | *0.65 (0.30, 0.90)* | *<0.001* |
| Peak creatinine in mg/dL | 0.98 (0.84, 1.06) | 0.90 (0.76, 1.36) | 0.99 |
| Total bilirubin upper limit of normal 1.3 mg/dL | 0.71 (0.48, 1.27) | 0.80 (0.50, 1.00) | 0.70 |
| Peak AST upper limit of normal 40 U/L | 47.00 (32.00, 53.50) | 40.00 (22.00, 72.00) | 0.50 |
| Peak ALT upper limit of normal 50 U/L | 48.50 (39.50, 78.50) | 40.00 (21.00, 84.90) | 0.39 |
| ALP upper limit for normal 130 U/L | 130.50 (96.47, 192.00) | 108.00 (78.30, 248.00) | 0.64 |
| GGT upper limit of normal 60 U/L | 76.50 (45.00, 140.00) | 61.00 (43.00, 158.00) | 0.79 |
| Medicines, *n* (%) | | | |
| Oral steroid | 12 (42.86) | 6 (46.15) | 1.00 |
| Pre-COVID-19 tacrolimus | 27 (96.43) | 12 (92.31) | 0.54 |

Mann-Whitney *U*-test and Fisher's test were used to compare samples and proportions, as appropriate. Italicized values indicate *p*-values less than 0.05 (for visual purposes). COVID-19, coronavirus disease-19; BMI, body mass index; IQR, interquartile range; ALC, absolute lymphocyte count; ALT, alanine transaminase; AST, aspartate transaminase; ALP, alkaline phosphatase; GGT, gamma-glutamyl transferase.

($0.47\pm0.31\times10^3$/μL vs. $1.39\pm0.57\times10^3$/μL, $p=0.001$).

In total, 15 (36.58%) and 26 (63.42%) post-transplant recipients were infected during the early period (<1 year) and the late period (>1 year) respectively (Fig. 1). The need for oxygen was similar in both the groups; the early group involved LOR in 19.23%, HOR in 7.69%, and MV in 7.69%, and the late group involved LOR in 13.33%, HOR in 13.33%, and MV in 6.67%. Hospital admission was 46.67% and 26.92%, respectively, in the early and late groups, and 4 recipients in each group required ICU admission. The overall mortality involved 3 (7.32%) patients, out of which 1 (6.67%) death occurred in the early period and 2 (7.69%) deaths occurred in the late post-transplant period (Table 3).

Transplant patients who were not admitted were instructed to self-isolate, monitor temperature daily, and scheduled for weekly electronic follow-up and WhatsApp video calls to avoid face-to-face consultations.

## Discussion

In our study, we included transplant recipients who contracted SARS-CoV-2 during the 1st wave of the pandemic (1st April 2020 till 28 Feb 2021). The SARS-CoV-2 delta variant (lineage B.1.617.2), which was first detected in India in October 2020 and named as the Delta variant on 31 May 2021 by the WHO, was identified as the primary cause of the 2nd wave (beginning from mid-March 2021 and ongoing).[6] As genome sequences of our patients were not done to determine the causative variant, we retrospectively infer that most of our recipients could have been infected with the alpha variant, which was responsible for the 1st wave.

The impact and outcomes of SARS-CoV-2 infection in LDLT recipients is still evolving. Herein, we discuss a single-center experience of 41 post LDLT recipients who contracted SARS-CoV-2 infection. Our study predominately consisted of nonelderly (<60 years old) male LDLT recipients.[7–9] The comorbidities in our group were similar to other registries which were primarily comprised of deceased donor recipients. Two-thirds of our patients were successfully managed with home quarantine. Only 19.51% of our patients required ICU admission and 7.32% required MV.

Hepatocellular injury was not more frequent in our more severe group, in consonance with most center reports.[10] None of our patients had new onset of acute kidney injury during their course of COVID-19 illness.

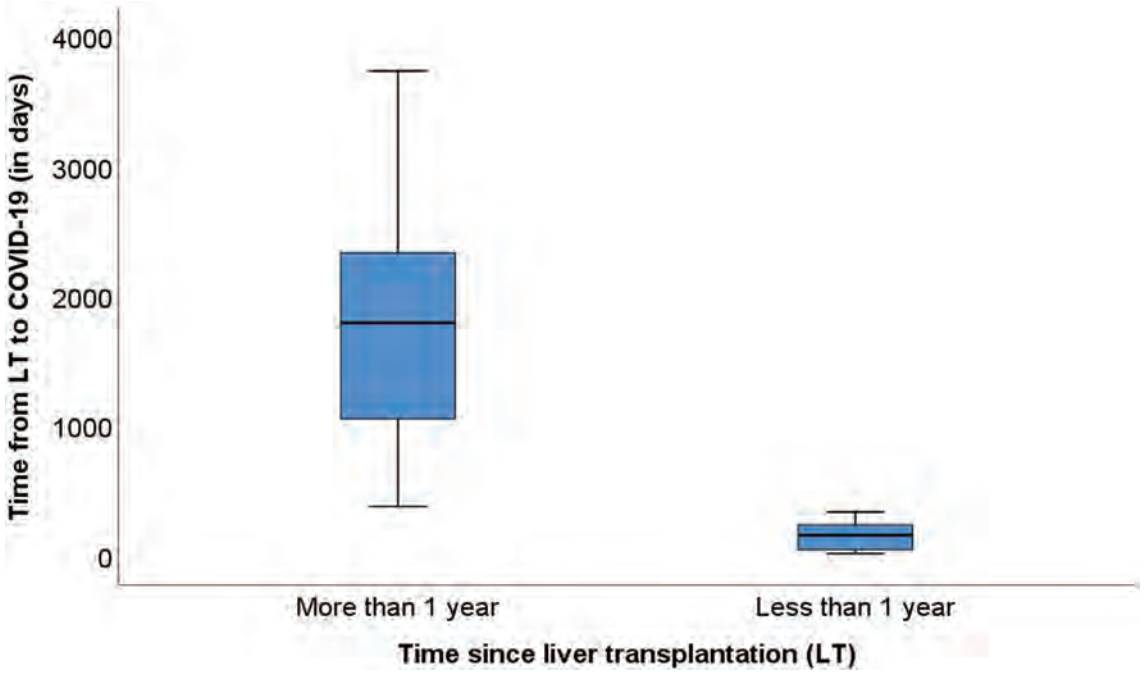


**Fig. 1. Time from liver transplantation to COVID-19 infection.** COVID-19, coronavirus disease-19.

The overall mortality was 7.32%, which was less than the reported mortality of 18% to 20% in two large cohort registries.[7,9] In the study group reported by Bhoori *et al*.,[11] which was predominantly comprised of long-term liver transplant recipients (>10 years), the authors noted a mortality of 30%, which could be attributed to older age and presence of coexisting multiple comorbidities. The median age in our study was more than a decade younger than these large cohort registries, which could be the possible reason for the lower rate of ICU admission and lower mortality rate, despite half of our patients having associated comorbidities.

The other reasons for overall favorable outcome in our patients could be the immunosuppressant protocol. Calcineurin inhibitors (CNIs) were not discontinued, except in critical COVID-19 cases and in recipients with suspected nonviral sepsis, as such was reported to be associated with better

**Table 3. Association of time from liver transplantation and COVID-19 clinical outcome**

| Factors | Time of liver transplantation to COVID-19 infection | | *p* |
|---|---|---|---|
| | Less than 1 year, *n*=15 | More than 1 year, *n*=26 | |
| Severity of COVID-19 illness, *n* (%) | | | 0.43 |
| Mild | 9 (60.00) | 19 (73.08) | |
| Moderate | 3 (20.00) | 1 (3.85) | |
| Severe | 2 (13.33) | 4 (15.38) | |
| Critical | 1 (6.67) | 2 (7.69) | |
| Outcome, *n* (%) | | | |
| Recovered | 14 (93.33) | 24 (92.31) | 1.00 |
| Died | 1 (6.67) | 2 (7.69) | |
| Total admissions, *n* (%) | 7 (46.67) | 7 (26.92) | 0.31 |
| ICU, *n* (%) | 4 (26.67) | 4 (15.38) | 0.43 |
| Oxygenation, *n* (%) | | | 0.89 |
| Room air | 10 (66.67) | 17 (65.38) | |
| LOR | 2 (13.33) | 5 (19.23) | |
| HOR | 2 (13.33) | 2 (7.69) | |
| MV | 1 (6.67) | 2 (7.69) | |

Mann-Whitney *U*-test and Fisher's exact test were used to compare samples and proportions, as appropriate. COVID-19, coronavirus disease-19; ICU, intensive care unit; LOR, low oxygen requirement; HOR, high oxygen requirement; MV, mechanical ventilation.

outcomes; moreover, CNIs have been found to inhibit SARS-CoV in a dose-dependent manner in *in vitro* studies.[12,13]

The antimetabolite Myfortic was temporarily withdrawn in all patients, as continuation of mycophenolate mofetil was associated with poor outcomes in various studies; furthermore, it could worsen COVID-associated lymphopenia.[7,14] Early temporary withdrawal of Myfortic could be the reason for the low incidence of diarrhea in our cohort (14.63%). Up to 43.9% of our recipients were on oral minimal maintenance steroids pre-COVID. In liver transplant recipients on oral steroids, their dosage was doubled to cover the potential risk of rejection when antimetabolites were on hold; this strategy became more prevalent during the 2nd half of 2020, as emerging reports suggested benefit of glucocorticoid to attenuate the effect of cytokine storm.[15] The use of steroids in mild to moderate COVID-19 (not requiring any respiratory support) is not recommended; nevertheless, we continued such in recipients who were already on oral corticosteroids, with a dose equivalent to half the recommended dose of dexamethasone (6 mg) in COVID pneumonia.[15] Whether the use of steroids resulted in halting the disease progression and the need for oxygen supplements needs to be further evaluated in patients on persistent immunosuppressants.

The transplant activity decreased in most of the centers last year during the pandemic. Since the current wave continues to wax and wane, denying a timely life-saving procedure for these sick decompensated cirrhotics awaiting transplant, particularly in those with a potential live donor, may not be justified. International registries have consistently reported increased COVID-19-related mortality in cirrhotics compared to non-cirrhotics and the trajectory of COVID-19 adverse events increased with higher Child-Pugh score.[16,17] Paradoxically, various studies did not show an increased risk of mortality in immunosuppressed liver transplant recipients compared to matched general population following SARS-CoV-2 infection.[7,9] Most of these reports are from recipients transplanted before the pandemic and, hence, they cannot be extrapolated to recipient outcomes for those transplanted during the pandemic.

Most published reports predominately deal with deceased donor recipients who contracted SARS-CoV-2 infection years after LT. In an early Spanish liver transplantation registry report 13.5% (15 of total 111) liver recipients had early posttransplant (<1 year) COVID-19 infection while we had 36.58% (15 of total 41) in the early post-transplant group.[7] Our study demonstrated that COVID-19 clinical outcomes in early (<1 year) post-transplant were not inferior to late (>1 year) post-transplant recipients. The proportion of hospital admissions and ICU care was more in the early post-transplant group, although it was not statistically significant. There was no difference in terms of mortality, oxygen supplementation and MV. This is in contrast to the recent findings of the COVIDSOT working team, which identified the early post-transplant infection (<6 months) as a novel risk factor for increased mortality and need for ICU admission in all solid organ transplant (SOT) recipients. However, separate organ specific subgroup analysis of outcomes was not mentioned in which the liver transplant subgroup constituted 50 (23.8 %) of the total 210 SOT recipients.[18]

In the early post-transplant period, the 1st perioperative week is the crucial phase during which liver transplant recipients recover from cirrhosis-associated immune dysfunction, effects of prolonged anesthesia, multiple blood and product transfusion, and surgical trauma.[19,20] Since there is no clear consensus on the definition of perioperative period in LT, any COVID-19 infection occurring up to postoperative day 30, was considered as critical time zone of COVID-19 infection. A cautious approach and COVID-safe protocols need to be followed, since the failure to detect SARS-CoV-2 infection during this perioperative incubation period or asymptomatic state can lead to rapid progression of COVID-19 illness.[21] There is a paucity of data regarding the outcome of living donor recipients with COVID-19 infection during the perioperative period. There are conflicting sporadic reports of successful recovery of recipients who contracted early COVID-19 after LT. Massoumi *et al*.[22] described good outcome in five patients with early COVID-19 (range 11–68 days) after LT; in addition, three had mild cases, while two had moderate diseases. Contrary to this report, Waisberg *et al*.[23] described their experience of seven patients with early COVID-19 (range of 9–39 days) after LT in which three recipients had severe disease and two died. Notably, their outcome was adversely impacted by their patients' older age, obesity, and associated comorbidities. However, important to note is that most infections reported were after the 1st week post-LT. Similarly, in our study three recipients contracted COVID-19 during the 3rd and 4th postoperative week (1 severe,1 moderate and 1 mild case), none expired due to COVID-19 pneumonia; possibly, the impact of early 1st week perioperative stress was crossed. The highly cited 1st grim report from Wuhan of a fatal outcome of a liver transplant recipient due to failure-to-be-detected during the perioperative work-up should not be ignored.[24] Following the point from all major guidelines, the stringent preoperative testing for SARS-CoV-2 with at least two negative reports and the 2nd negative report less than 48 h before the surgery was followed by our center.[1,25] We infer that crossing this perioperative bridge without SARS-CoV-2 infection will be the most important milestone in prevention of poor outcome of COVID-19 infection.

The limitations of our study were small sample size and data from a single center. However, our study certainly makes an important contribution to the evolving data on COVID-19 in LDLT recipients reported in the literature. Also, our study may have suffered from underreporting for asymptomatic positives or milder symptoms not being reported. The time is ripe for a large multicentric study from centers with primarily LDLT programs, which will help in addressing and possibly resolving the pertinent issues related to LDLT recipients with COVID-19 illness.

## Conclusions

In our study of LDLT recipients with COVID-19 infection, most of our recipients had only mild illness and did not require hospital admission. Notably, based on our observations, we infer that COVID-19 clinical outcomes in the early vs. late post-transplant period are similar, with the early group not having a severe course, as expected. In case of unfortunate perioperative contraction of SARS-CoV-2 infection, recipients can be successfully navigated towards recovery. Hence, postponing life-saving liver transplantation is not justified in these patients with debilitating illness. Further data will throw light on the COVID-19 clinical outcome in the 1st perioperative week. The continuation of steroids and tacrolimus with dose modification during the active phase of infection may attenuate COVID-19 severity.

## Acknowledgments

We thank Dr. Angelynn Singh for proofreading the manuscript.

## Funding

None to declare.

## Conflict of interest

The authors have no conflict of interests related to this publication.

## Author contributions

Conceptualization (AC, IJ, AK), data curation (IJ, PL, GS, AG, NK), formal analysis (IJ, SS, AC), writing of the original draft (IJ, AC, AS), critical revision of the manuscript for important intellectual content (AC, MW, AJ), and administrative and study supervision (AC, MW).

## Data sharing statement

The data that support the findings of this study are available from the corresponding author upon reasonable request.

## References


[1] Jha SK, Jamir I, Sisodia K, Kumar N, Sood G, Shanker N, *et al*. Restarting LDLT During COVID-19: Early Results After Restructuring. Transplant Proc 2021;53(4):1118–1125. doi:10.1016/j.transproceed.2020.10.049.

[2] Lembach H, Hann A, McKay SC, Hartog H, Vasanth S, El-Dalil P, *et al*. Resuming liver transplantation amid the COVID-19 pandemic. Lancet Gastroenterol Hepatol 2020;5(8):725–726. doi:10.1016/S2468-1253(20)30187-4.

[3] WHO Coronavirus (COVID-19) Dashboard | WHO Coronavirus (COVID-19) Dashboard with Vaccination Data. Available from: https://covid19.who.int/table.

[4] Cherian S, Potdar V, Jadhav S, Yadav P, Gupta N, Das M, *et al*. Convergent evolution of SARS-CoV-2 spike mutations, L452R, E484Q and P681R, in the second wave of COVID-19 in Maharashtra, India. bioRxiv Published online May 3, 2021:2021.04.22.440932. doi:10.1101/2021.04.22.440932.

[5] Clinical Spectrum | COVID-19 Treatment Guidelines. Available from: https://www.covid19treatmentguidelines.nih.gov/overview/clinical-spectrum/.

[6] Kar SK, Ransing R, Arafat SMY, Menon V. Second wave of COVID-19 pandemic in India: Barriers to effective governmental response. EClinicalMedicine 2021;36:100915. doi:10.1016/j.eclinm.2021.100915.

[7] Colmenero J, Rodríguez-Perálvarez M, Salcedo M, Arias-Milla A, Muñoz-Serrano A, Graus J, *et al*. Epidemiological pattern, incidence, and outcomes of COVID-19 in liver transplant patients. J Hepatol 2021;74(1):148–155. doi:10.1016/j.jhep.2020.07.040.

[8] Becchetti C, Zambelli MF, Pasulo L, Donato MF, Invernizzi F, Detry O, *et al*. COVID-LT group. COVID-19 in an international European liver transplant recipient cohort. Gut 2020;69(10):1832–1840. doi:10.1136/gutjnl-2020-321923.

[9] Webb GJ, Marjot T, Cook JA, Aloman C, Armstrong MJ, Brenner EJ, *et al*. Outcomes following SARS-CoV-2 infection in liver transplant recipients: an international registry study. Lancet Gastroenterol Hepatol 2020;5(11):1008–1016. doi:10.1016/S2468-1253(20)30271-5.

[10] Lee BT, Perumalswami PV, Im GY, Florman S, Schiano TD, COBE Study Group. COVID-19 in Liver Transplant Recipients: An Initial Experience From the US Epicenter. Gastroenterology 2020;159(3):1176–1178.e2. doi:10.1053/j.gastro.2020.05.050.

[11] Bhoori S, Rossi RE, Citterio D, Mazzaferro V. COVID-19 in long-term liver transplant patients: preliminary experience from an Italian transplant centre in Lombardy. Lancet Gastroenterol Hepatol 2020;5(6):532–533. doi:10.1016/S2468-1253(20)30116-3.

[12] Belli LS, Fondevila C, Cortesi PA, Conti S, Karam V, Adam R, *et al*. Protective Role of Tacrolimus, Deleterious Role of Age and Comorbidities in Liver Transplant Recipients With Covid-19: Results From the ELITA/ELTR Multicenter European Study. Gastroenterology 2021;160(4):1151–1163.e3. doi:10.1053/j.gastro.2020.11.045.

[13] Tanaka Y, Sato Y, Sasaki T. Suppression of coronavirus replication by cyclophilin inhibitors. Viruses 2013;5(5):1250–1260. doi:10.3390/v5051250.

[14] Rodriguez-Peralvarez M, Salcedo M, Colmenero J, Pons JA. Modulating immunosuppression in liver transplant patients with COVID-19. Gut 2021;70(7):1412–1414. doi:10.1136/gutjnl-2020-322620.

[15] RECOVERY Collaborative Group, Horby P, Lim WS, Emberson JR, Mafham M, Bell JL, *et al*. Dexamethasone in Hospitalized Patients with Covid-19. N Engl J Med 2021;384(8):693–704. doi:10.1056/NEJMoa2021436.

[16] Sarin SK, Choudhury A, Lau GK, Zheng MH, Ji D, Abd-Elsalam S, *et al*. Pre-existing liver disease is associated with poor outcome in patients with SARS CoV2 infection; The APCOLIS Study (APASL COVID-19 Liver Injury Spectrum Study). Hepatol Int 2020;14(5):690–700. doi:10.1007/s12072-020-10072-8.

[17] Bajaj JS, Garcia-Tsao G, Biggins SW, Kamath PS, Wong F, McGeorge S, *et al*. Comparison of mortality risk in patients with cirrhosis and COVID-19 compared with patients with cirrhosis alone and COVID-19 alone: multicentre matched cohort. Gut 2021;70(3):531–536. doi:10.1136/gutjnl-2020-322118.

[18] Salto-Alejandre S, Jiménez-Jorge S, Sabé N, Ramos-Martínez A, Linares L, Valerio M, *et al*. Risk factors for unfavorable outcome and impact of early post-transplant infection in solid organ recipients with COVID-19: A prospective multicenter cohort study. PLoS One 2021;16(4):e0250796. doi:10.1371/journal.pone.0250796.

[19] Albillos A, Lario M, Álvarez-Mon M. Cirrhosis-associated immune dysfunction: distinctive features and clinical relevance. J Hepatol 2014;61(6):1385–1396. doi:10.1016/j.jhep.2014.08.010.

[20] Almaadany FS, Samadov E, Namazov I, *et al*. Mortality and pulmonary complications in patients undergoing surgery with perioperative sars-cov-2 infection: An international cohort study. Lancet 2020;396(10243):27–38. doi:10.1016/S0140-6736(20)31182-X.

[21] Lei S, Jiang F, Su W, Chen C, Chen J, Mei W, *et al*. Clinical characteristics and outcomes of patients undergoing surgeries during the incubation period of COVID-19 infection. EClinicalMedicine 2020;21:100331. doi:10.1016/j.eclinm.2020.100331.

[22] Massoumi H, Rocca J, Frager S, Kinkhabwala M. Changes in Liver Transplant Center Practice in Response to Coronavirus Disease 2019: Unmasking Dramatic Center-Level Variability. Liver Transpl 2020;26(9):1198–1199. doi:10.1002/lt.25811.

[23] Waisberg DR, Abdala E, Nacif LS, Haddad LB, Ducatti L, Santos VR, *et al*. Liver transplant recipients infected with SARS-CoV-2 in the early postoperative period: Lessons from a single center in the epicenter of the pandemic. Transpl Infect Dis 2021;23(1):e13418. doi:10.1111/tid.13418.

[24] Qin J, Wang H, Qin X, Zhang P, Zhu L, Cai J, Yuan Y, Li H. Perioperative Presentation of COVID-19 Disease in a Liver Transplant Recipient. Hepatology 2020;72(4):1491–1493. doi:10.1002/hep.31257.

[25] Saigal S, Gupta S, Sudhindran S, Goyal N, Rastogi A, Jacob M, *et al*. Liver transplantation and COVID-19 (Coronavirus) infection: guidelines of the liver transplant Society of India (LTSI). Hepatol Int 2020;14(4):429–431. doi:10.1007/s12072-020-10041-1.

*Journal of Clinical and Translational Hepatology* **2022** vol. 10(4) | 778–782
DOI: 10.14218/JCTH.2021.00266

Case Report

# Giant Hepatic Regenerative Nodule in a Patient With Hepatitis B Virus-related Cirrhosis

Long Li[1*] and Jie Feng[2]

[1]*Division of Diagnostic Radiology, Department of Medical Imaging, Guangdong Provincial Corps Hospital of Chinese People's Armed Police Forces, Guangzhou Medical University, Guangzhou, Guangdong, China;* [2]*Department of Medical Imaging Center, Nanfang Hospital, Southern Medical University, Guangzhou, Guangdong, China*

**Received:** 4 July 2021 | **Revised:** 18 September 2021 | **Accepted:** 22 October 2021 | **Published:** 4 January 2022

## Abstract

Hepatic regenerative nodules are reactive hepatocellular proliferations that develop in response to liver injury. Giant hepatic regenerative nodules of 10 cm or more are extremely rare and have only been reported in patients with biliary atresia or Alagille syndrome. A 50-year-old man presented with a pathologically confirmed giant 11.3×9.4×11.2 cm hepatic regenerative nodule and hepatitis B virus-related cirrhosis. Imaging of intrahepatic nodule included mild hyperenhancement in the portal phase of contrast-enhanced CT and the hepatobiliary phase in the gadoxetic acid-enhanced MRI scan, as well as the portal vein crossing through sign in the setting of liver cirrhosis. This case highlights the imaging characteristics of giant hepatic regenerative nodules in hepatitis cirrhosis.

**Citation of this article:** Li L, Feng J. Giant Hepatic Regenerative Nodule in a Patient With Hepatitis B Virus-related Cirrhosis. J Clin Transl Hepatol 2022;10(4):778–782. doi: 10.14218/JCTH.2021.00266.

## Introduction

Histopathological, regenerative nodules are hyperplastic proliferations of hepatocytes in response to necrosis, altered circulations, or other stimuli.[1] They usually occur in patients with hepatitis or alcoholic cirrhosis, vascular liver diseases such as Budd-Chiari syndrome,[2] or cholangiopathic disorders such as biliary atresia[3] or Alagille syndrome.[4,5] Regenerative nodules are classified by size as micronodules (<3 mm) or macronodules (≥3 mm).[1,6] Large regenerative nodules are usually 5 to 15 mm in diameter, but they can be 5 cm or larger.[1,6] Giant nodules as larger as 5 cm have been reported in patients with liver cirrhosis,[7] Budd-Chiari syndrome,[8] biliary atresia,[3] or Alagille syndrome.[4,5] Giant nodules of 10 cm in diameter or more have only been reported in patients with biliary atresia[3] or Alagille syndrome.[4,5] We report a rare and unique case who presented with a giant hepatic regenerative nodule more than 10 cm in size and associated with hepatitis B virus (HBV)-related cirrhosis.

## Case report

A 50 year-old man was found to have a hepatic mass suspected to be liver cancer by ultrasonography. He denied any clinical symptoms. Physical examination revealed an enlarged non-tender liver with a firm and uneven surface. The lower edge of the liver extended to the right iliac crest. The spleen was not palpable. A routine blood workup found a white blood cell count of $5.3\times10^9$/L, a red blood cell count of $4.5\times10^{12}$/L, a hemoglobin level of 141 g/L, and a platelet count of $80\times10^9$/L. Liver function tests showed increased levels of alanine aminotransferase (ALT) 107.8 IU/L (reference range, 0–40 IU/L), aspartate aminotransferase (AST) 69.4 IU/L (reference range, 0–38 IU/L), alkaline phosphatase 171.3 IU/L (reference range, 30–150 IU/L), and gamma-glutamyl transferase 452.4 IU/L (reference range, 0–47 IU/L), normal serum total bilirubin, albumin, plasma prothrombin time, international normalized ratio, and ammonia. Hepatitis virus tests were positive for hepatitis B surface antigen (HBsAg), HB e antigen, HB e antibody, and HB core antibody, and negative for HB surface antibody, hepatitis C virus antibody, and hepatitis C antigen. Alpha-fetoprotein and carcinoembryonic antigen assays were negative.

A CT scan showed pronounced nodular irregularity of the liver surface, enlargement of the interlobar fissure, hypertrophy of the left lobe, and dilatation of the portal vein, with a diameter of 21.0 mm (Fig. 1). Diffuse multiple nodules of <1 cm diameter in the liver parenchyma showed slight hyperdensity on precontrast CT images and became isodense in post-contrast phases (Fig. 1). Precontrast CT showed a well-circumscribed 11.3×9.4×11.2 cm oval hypodense mass in segment VI of the liver, including a focal hypodense area extending downward to the right iliac fossa (Fig. 2A, A′). Contrast-enhanced CT showed isoenhancement in the arterial phase (Fig. 2B, B′) with slight hyperenhancement, a portal vein branch crossing through the lesion in the portal phase (Fig. 2C, C′), and slight hypoenhancement in the de-

**Keywords:** Regenerative nodules; Cirrhosis; Hepatitis B virus; Computed tomography; Magnetic resonance imaging.

**Abbreviations:** ALT, alanine aminotransferase; APRI, aspartate aminotransferase-to-platelet ratio index; AST, aspartate aminotransferase; CT, computed tomography; FIB-4, fibrosis-4 score; HBsAg, hepatitis B surface antigen; HBV, hepatitis B virus; HCC, hepatocellular carcinoma; HU, Hounsfield units; IU, international unit; MRI, magnetic resonance imaging.

***Correspondence to:** Long Li, Division of Diagnostic Radiology, Department of Medical Imaging, Guangdong Provincial Corps Hospital of Chinese People's Armed Police Forces, Guangzhou Medical University, 268 Yanling Road, Guangzhou, Guangdong 510507, China. ORCID: https://orcid.org/0000-0002-1342-860X. Tel/Fax: +86-20-61627576, E-mail: radiolilong@hotmail.com

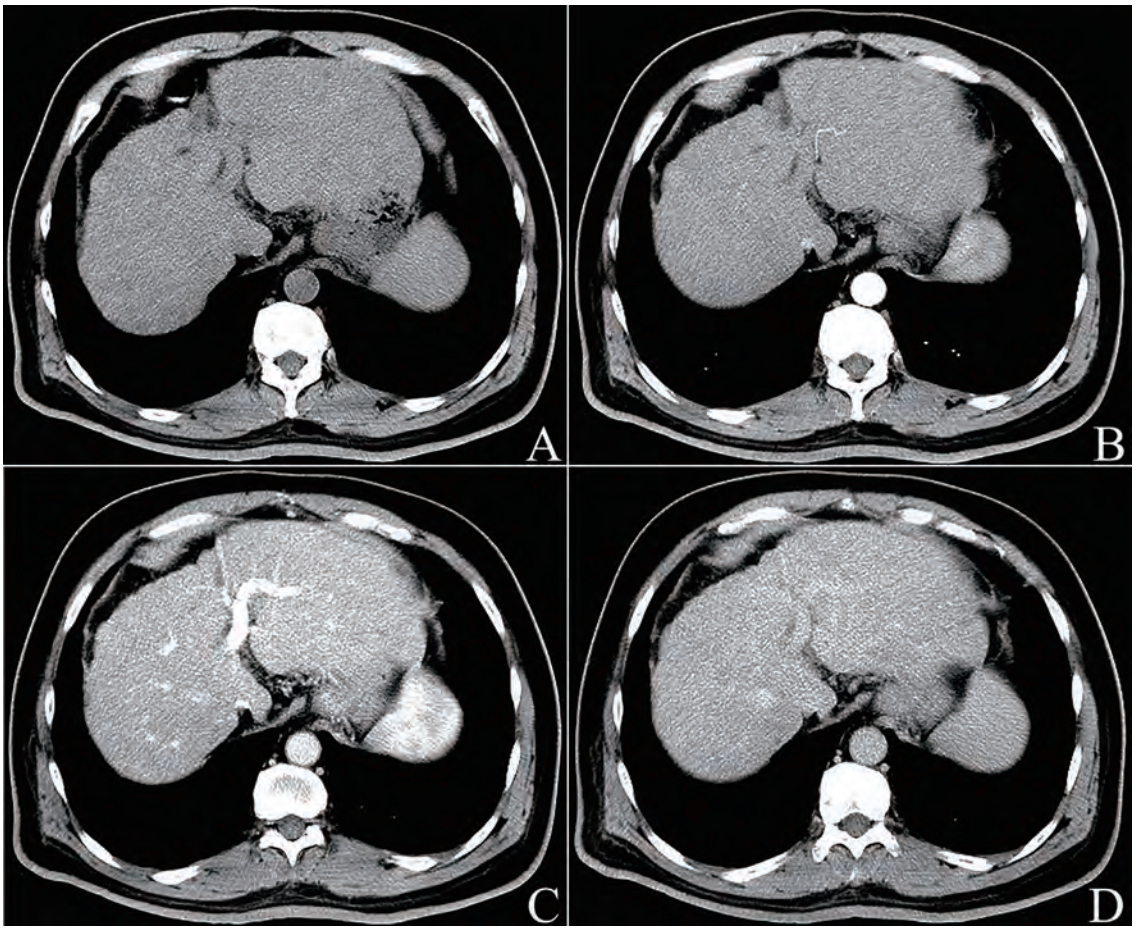


**Fig. 1. CT images of liver cirrhosis.** Axial CT images show dysmorphia of the liver, including pronounced nodular irregularity of the liver surface, enlargement of the interlobar fissure, and hypertrophy of the left lobe (A–D). A precontrast CT image shows diffuse multiple nodules of <1 cm diameter and slight hyperdensity in the liver parenchyma (A), and contrast-enhanced isodense CT images in liver during the arterial (B), portal (C), and delayed phases (D). CT, computed tomography.

layed phase (Fig. 2D, D′). The focal hypodense area within the lesion was not enhanced from the arterial phase to the delayed phase.

A follow-up contrast-enhanced MRI with gadoxetic acid at 6 months found no significant differences in the size, shape, margin, internal characteristics, and three-phase contrast-enhancement patterns compared with the original CT images, except for slight hyperenhancement in the delayed 20 and 30 m hepatobiliary phases (Fig. 3). At 10.5 months after the first hospital admission, a CT-guided percutaneous biopsy resulted in pathological confirmation of a hepatic regenerative nodule (Fig. 4).

## Discussion

When assessing a patient with a liver mass, noninvasive diagnosis of HBV-related cirrhosis and the imaging characteristics of hepatic regenerative nodules are important. Non-invasive diagnosis of HBV-related cirrhosis depends on calculation of the AST-to-platelet ratio index (APRI) and the fibrosis-4 score (FIB-4) using indirect markers of fibrosis such as ALT, AST and platelet count.[9] APRI = [(AST/$AST_{ULN}$)/platelet count] × 100 and the Fib-4 score = (age in years × AST)/(platelet count × √ALT). In clinical practice, liver biopsy has been replaced by noninvasive methods as APRI and FIB-4 scores and imaging.[9] An APRI score >2 is recommended as the preferred noninvasive threshold to determine the presence of cirrhosis in resource-limited settings by the World Health Organization HBV guidelines. A FIB-4 >3.25 has a 97% specificity and a 65% positive predictive value for advanced fibrosis.[9] Conventional ultrasound, CT, and MRI can detect morphologic changes in the liver related to advanced fibrosis, but the methods have a limited ability to identify early-stage fibrosis.[10,11] Our patient was positive for HBV, with an APRI of 2.283 and a FIB-4 of 4.18. CT scan showed morphological changes in the liver and the dilation of portal veins. We diagnosed HBV-related cirrhosis based on the findings.

During imaging evaluation, predominant portal perfusion was visible in dynamic contrast-enhanced imaging, including CT, MRI, and ultrasound. The vascular supply of regenerative nodules is similar to the surrounding hepatic parenchyma,[3-5,7,12] unlike hepatocellular carcinoma (HCC), which usually shows arterial wash-in and late washout, regenerative nodules are usually isointense during the arterial and portal venous phases and become more isointense or hypointense during the equilibrium and delayed phases.[7,12] In the hepatobiliary phase of gadoxetic acid-enhanced MRI, regenerative nodules commonly appear as isointense or mildly hyperintense signals, and not hypointense, relative to the surrounding liver parenchyma because of the preserved hepatocellular function.[13] In addition to the contrast-enhancement pattern, the image of the portal vein crossing through the mass is re-

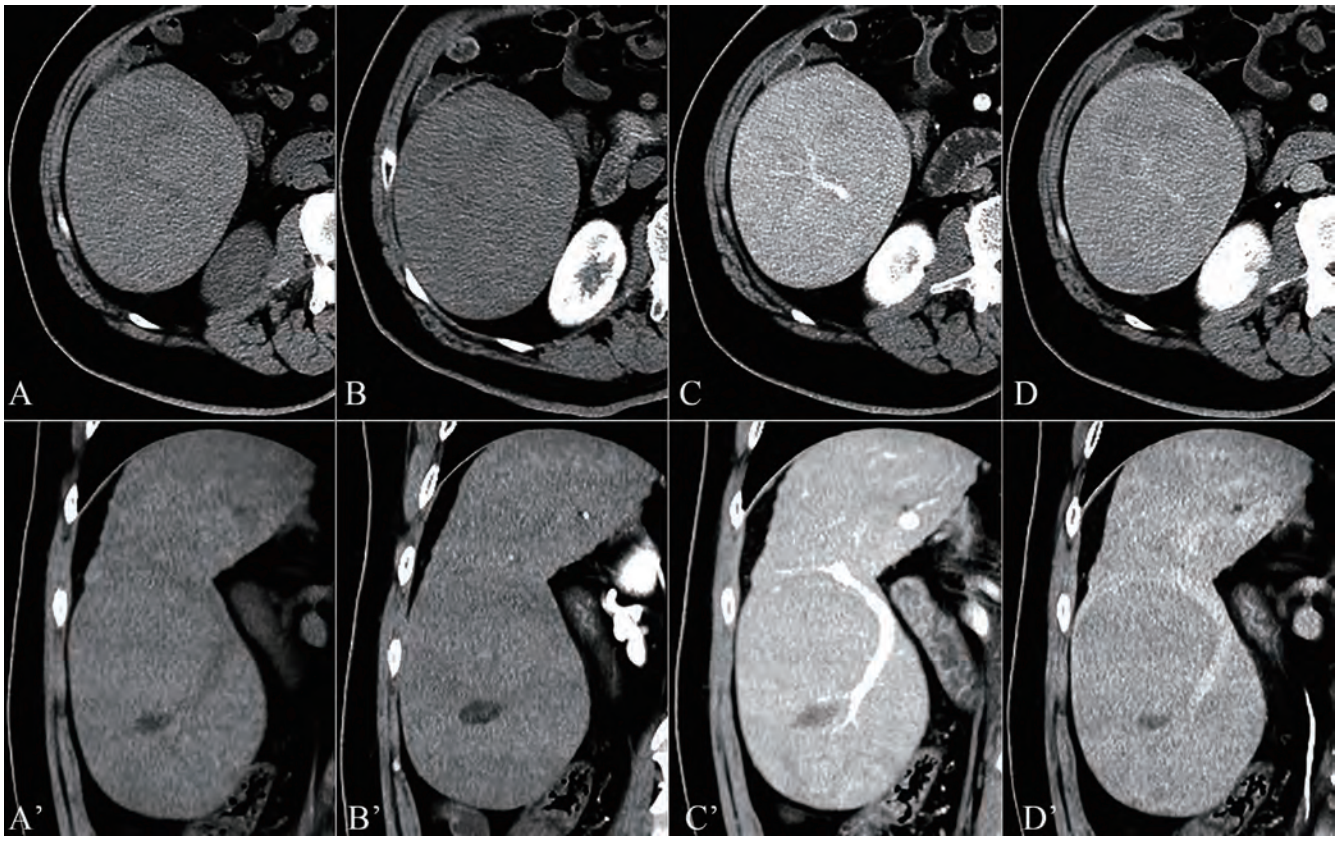


**Fig. 2. CT images of a giant hepatic mass.** (A and A′) Precontrast CT scan shows a well-circumscribed oval hypodense mass with an average attenuation of 50.5 HU in segment VI of the liver, including a focal hypodense area (18.5 HU) and extending downward to the right iliac fossa. (B and B′) Contrast-enhanced CT scan in the arterial phase showing a nodule (53.5 HU) with a density similar to that of the surrounding liver cirrhosis (52.0 HU). (C and C′) The portal phase shows that the mass density (91.3 HU) was slightly greater than that of the surrounding liver cirrhosis (83.0 HU), with a portal vein branch crossing through the lesion. (D and D′) The delayed phase shows a mass density (77.3 HU) that is slightly lower than that of the surrounding liver cirrhosis (81.0 HU). The focal hypodense area within the lesion was not enhanced from the arterial phase to the delayed phase. A–D, axial images; A′–D′, coronal reformation images. CT, computed tomography; HU, Hounsfield units.

ported to be characteristic of giant hepatic regenerative nodules in the portal phase images[3–5] because the nodules have normal portal tracts at the center.[1–5,7,12] Therefore, hepatic regenerative nodules of various sizes should be categorized as Liver Imaging and Reporting Data System category 2, as they did not have the major and ancillary imaging features of HCC and other malignancies.[14,15]

Current international guidelines recommend that all HBsAg-positive patients with cirrhosis should be routinely monitoring for disease activity and progression to HCC.[9] Recent clinical practice guidelines include gadoxetic acid-enhanced liver MRI as the first-line diagnostic and monitoring tool for hepatic nodules instead of biopsy. A single dynamic CT or MRI study rather than two dynamic imaging modalities is recommended for the diagnosis of HCC lesions of < 2 cm.[13] Huge lesions should be considered as focal malignant transformations if major and/or ancillary imaging features of Liver Imaging and Reporting Data System category to assess HCC or other malignancies have developed.[16] Percutaneous needle biopsies may be difficult to obtain in cases of focal malignant transformation. During the initial stage of tumor initiation, HCC may retain hepatocellular function and isointense or mildly hyperintense signals similar to regenerative nodules.[17] For early HCC in cirrhotic livers, patients should be evaluated with multiparametric imaging, including $T_1$ hypointensity, $T_2$ hyperintensity, diffusion-weighted imaging hyperintensity, arterial enhancement, late washout, and hepatobiliary hypointensity at a size threshold of ≥1.5 cm on gadoxetic acid-enhanced MRI. The findings should be interpreted with care.[18–20] Finally, if imaging features and laboratory results still cannot support a definitive diagnosis, a multidisciplinary team may discuss the atypical features to help to develop an appropriate approach for the patient.[19] In conclusion, giant hepatic regenerative nodules in the background of liver cirrhosis have characteristic imaging features that can help guide clinical management and avoid unnecessary medical interventions.

## Funding

None to declare.

## Conflict of interest

The authors have no conflict of interests related to this publication.

## Author contributions

Both authors, LL and FJ, contributed to the design and implementation of the study and to the analysis of the results and to the writing of the manuscript.

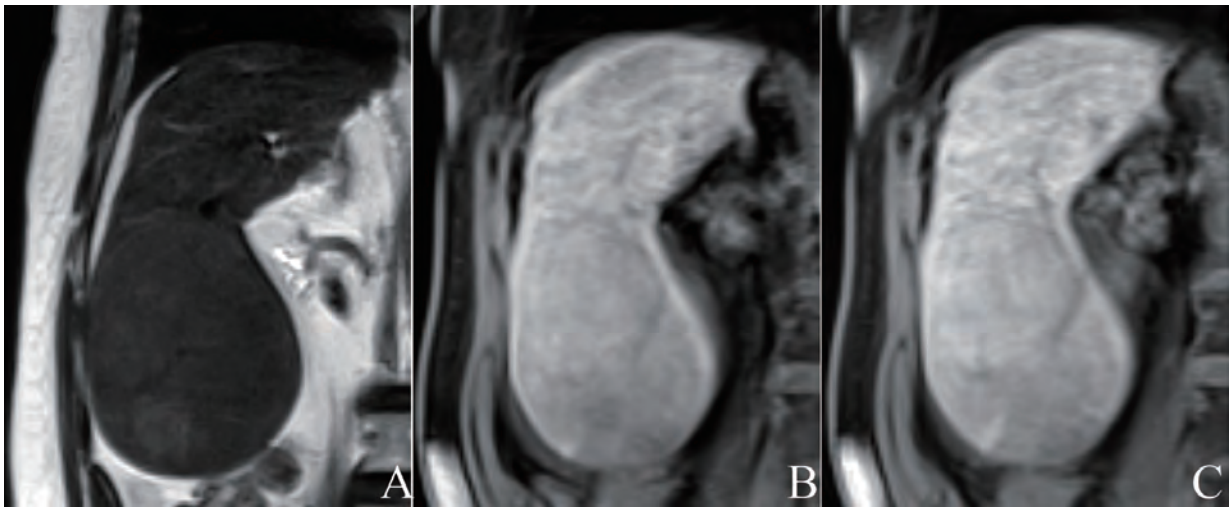


**Fig. 3. Follow-up contrast-enhanced MRI with gadoxetic acid.** (A) Precontrast coronal T2-weighted image shows an oval, well-circumscribed iso-signal mass in segment VI of the liver. (B) Delayed 20 m hepatobiliary phase in the gadoxetic acid-enhanced MRI shows a slightly hyperenhanced mass and surrounding liver cirrhosis with heterogeneous. (C) Delayed 30 m hepatobiliary phase in the gadoxetic acid-enhanced MRI shows a persistent slightly hyperenhanced mass. MRI, magnetic resonance imaging.

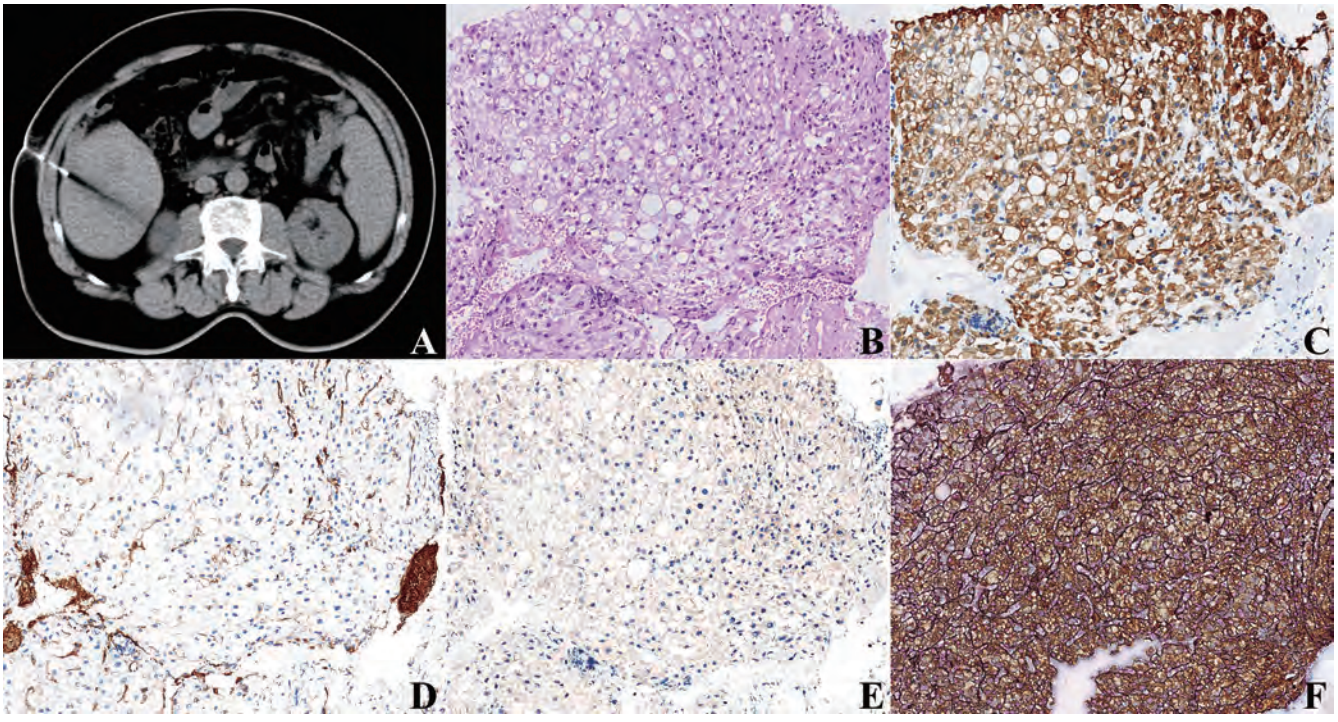


**Fig. 4. CT-guided percutaneous biopsy and pathological findings of a giant mass in segment VI of the liver** (A) CT image showing a biopsy needle inserted into the margin of the mass in segment VI of the liver. (B) Hematoxylin and eosin staining indicates vacuolar degeneration in the cytoplasm of most hepatocytes, bilirubin deposition in cytoplasm of some hepatocytes, and interstitial fibrous proliferation with focal lymphocytic infiltration of portal areas. 100× magnification. (C) Anti-cytokeratin 8 immunostaining is strongly positive in hepatocytes, indicating normal and mature differentiation. 100× magnification. (D) Anti-cluster of differentiation 34 immunostaining is positive in vascular endothelial cells in portal areas and hepatic sinusoid endotheliocytes. 100× magnification. (E) Anti- alpha-fetoprotein immunostaining is negative in hepatocytes. 100× magnification. (F) Gordon and Sweet silver staining (black) shows a reticular fiber network in the subendothelial spaces of the hepatic sinusoids. 200× magnification. CT, computed tomography.

## Patient consent

The patient provided written informed consent and gave permission for publication of this case report and any accompanying images.

## References

[1] International working party. Terminology of nodular hepatocellular lesions. Hepatology 1995;22(3):983–993. doi:10.1016/0270-9139(95)90324-0, PMID:7657307.
[2] Sempoux C, Balabaud C, Paradis V, Bioulac-Sage P. Hepatocellular nodules

in vascular liver diseases. Virchows Arch 2018;473(1):33–44. doi:10.1007/s00428-018-2373-6, PMID:29804132.
[3] Yoon HJ, Jeon TY, Yoo SY, Kim JH, Eo H, Lee SK, *et al*. Hepatic tumours in children with biliary atresia: single-centre experience in 13 cases and review of the literature. Clin Radiol 2014;69(3):e113–e119. doi:10.1016/j.crad.2013.10.017, PMID:24332171.
[4] Rapp JB, Bellah RD, Maya C, Pawel BR, Anupindi SA. Giant hepatic regenerative nodules in Alagille syndrome. Pediatr Radiol 2017;47(2):197–204. doi:10.1007/s00247-016-3728-2, PMID:27796468.
[5] Andrews AR, Putra J. Central Hepatic Regenerative Nodules in Alagille Syndrome: A Clinicopathological Review. Fetal Pediatr Pathol 2021;40(1):69–79. doi:10.1080/15513815.2019.1675834, PMID:31608763.
[6] Hanna RF, Aguirre DA, Kased N, Emery SC, Peterson MR, Sirlin CB. Cirrhosis-associated hepatocellular nodules: correlation of histopathologic and MR imaging features. Radiographics 2008;28(3):747–769. doi:10.1148/rg.283055108, PMID:18480482.
[7] Elsayes KM, Chernyak V, Morshid AI, Tang A, Kielar AZ, Bashir MR, *et al*. Spectrum of Pitfalls, Pseudolesions, and Potential Misdiagnoses in Cirrhosis. AJR Am J Roentgenol 2018;211(1):87–96. doi:10.2214/AJR.18.19781, PMID:29932761.
[8] Mamone G, Carollo V, Di Piazza A, Cortis K, Degiorgio S, Miraglia R. Budd-Chiari Syndrome and hepatic regenerative nodules: Magnetic resonance findings with emphasis of hepatobiliary phase. Eur J Radiol 2019;117:15–25. doi:10.1016/j.ejrad.2019.05.015, PMID:31307641.
[9] World Health Organization. Guidelines for the Prevention, Care and Treatment of Persons with Chronic Hepatitis B Infection. Geneva: World Health Organization; 2015. Available from: https://www.who.int/hiv/pub/hepatitis/hepatitis-b-guidelines/en/.
[10] Aubé C, Bazeries P, Lebigot J, Cartier V, Boursier J. Liver fibrosis, cirrhosis, and cirrhosis-related nodules: Imaging diagnosis and surveillance. Diagn Interv Imaging 2017;98(6):455–468. doi:10.1016/j.diii.2017.03.003, PMID:28461073.
[11] Jiang H, Zheng T, Duan T, Chen J, Song B. Non-invasive in vivo Imaging Grading of Liver Fibrosis. J Clin Transl Hepatol 2018;6(2):198–207. doi:10.14218/JCTH.2017.00038, PMID:29951365.
[12] Borzio M, Paladino F, Francica G. Liver carcinogenesis: diagnostic and clinical aspects of preneoplastic nodules. Hepatoma Res 2019;5:15. doi:10.20517/2394-5079.2019.11.
[13] Zech CJ, Ba-Ssalamah A, Berg T, Chandarana H, Chau GY, Grazioli L, *et al*. Consensus report from the 8th International Forum for Liver Magnetic Resonance Imaging. Eur Radiol 2020;30(1):370–382. doi:10.1007/s00330-019-06369-4, PMID:31385048.
[14] Shah A, Tang A, Santillan C, Sirlin C. Cirrhotic liver: What's that nodule? The LI-RADS approach. J Magn Reson Imaging 2016;43(2):281–294. doi:10.1002/jmri.24937, PMID:25996905.
[15] Abdel Razek AAK, El-Serougy LG, Saleh GA, Shabana W, Abd El-Wahab R. Liver Imaging Reporting and Data System Version 2018: What Radiologists Need to Know. J Comput Assist Tomogr 2020;44(2):168–177. doi:10.1097/RCT.0000000000000995, PMID:32195795.
[16] Sato T, Kondo F, Ebara M, Sugiura N, Okabe S, Sunaga M, *et al*. Natural history of large regenerative nodules and dysplastic nodules in liver cirrhosis: 28-year follow-up study. Hepatol Int 2015;9(2):330–336. doi:10.1007/s12072-015-9620-6, PMID:25788204.
[17] Chen N, Motosugi U, Sano K, Ichikawa T, Nakano M, Morisaka H, *et al*. Early hepatocellular carcinomas showing isointensity or hyperintensity in gadoxetic acid-enhanced, hepatocyte-phase magnetic resonance images. J Comput Assist Tomogr 2013;37(3):466–469. doi:10.1097/RCT.0b013e3182873799, PMID:23674023.
[18] Rhee H, Kim MJ, Park MS, Kim KA. Differentiation of early hepatocellular carcinoma from benign hepatocellular nodules on gadoxetic acid-enhanced MRI. Br J Radiol 2012;85(1018):e837–844. doi:10.1259/bjr/13212920, PMID:22553295.
[19] Kim JH, Joo I, Lee JM. Atypical Appearance of Hepatocellular Carcinoma and Its Mimickers: How to Solve Challenging Cases Using Gadoxetic Acid-Enhanced Liver Magnetic Resonance Imaging. Korean J Radiol 2019;20(7):1019–1041. doi:10.3348/kjr.2018.0636, PMID:31270973.
[20] Xiong J, Luo J, Bian J, Wu J. Overall diagnostic accuracy of different MR imaging sequences for detection of dysplastic nodules: a systematic review and meta-analysis. Eur Radiol 2021. doi:10.1007/s00330-021-08022-5, PMID:34357448.

JCTH

Journal of Clinical and Translational Hepatology [Print ISSN: 2225-0719; Online ISSN: 2310-8819] is owned by the Second Affiliated Hospital of Chongqing Medical University and published by XIA & HE Publishing Inc.

# Biographies of the Editors-in-Chief

### Prof. Hong Ren (General Editor-in-Chief)

Prof. Ren, is the President, Director [Key Laboratory of Molecular Biology of Infectious Diseases (Ministry of Education of China), Medical Imaging Department, Liver and Viral Hepatitis Research Institute], Leader and Distinguished Super Specialist Consultant [Division of Infectious Diseases (one of the national key discipline in China), Department of Internal Medicine] of the Second Affiliated Hospital of Chongqing Medical University. In addition, he is also the Vice-Chairman and Group Head of the Chinese Society of Hepatology, Chinese Medical Association.

### Prof. George Y. Wu (Comprehensive Editor-in-Chief)

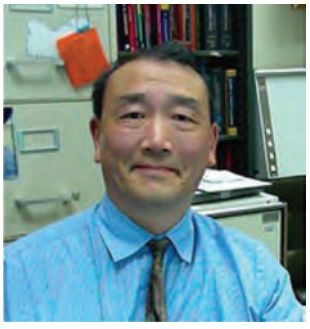

Prof. Wu obtained his MD and PhD degree at Albert Einstein College of Medicine in 1976. He was a resident at Harlem Hospital Center from 1976 to 1979. He worked as a postdoctoral fellow at Albert Einstein College of Medicine from 1979 to 1982. From 1983, he worked as Assistant Professor and then Professor at University of Connecticut School of Medicine. He is now the Director of Hepatology Section, Division of Gastroenterology-Hepatology. Dr. Wu's awards include the following: Research Prize awarded by the American Liver Foundation in 1982; Industry Research Scholar Award from the American Gastroenterological Association for 1985 to 1988; Gastroenterology Research Group Young Scientist Award from the American Gastroenterological Association in 1990; Herman Lopata Chair in Hepatitis Research from 1992 to date; Scientific Award from the Chinese American Medical Society in 1992; He was elected to membership in exclusive societies: American Society for Clinical Investigation in 1989; Association of American Physicians in 1995; and Top Doctor in the U.S. awarded by U.S. News and World Report in 2011. He has published about 180 peer-reviewed academic articles, 11 books, and is series editor for Clinical Gastroenterology book series by Springer-Nature, and is Senior Associate editor of J. Digestive Diseases.

### Prof. Harry Hua-Xiang Xia (Editor-in-Chief)

Prof. Xia obtained his PhD in 1994 and worked as a postdoctoral fellow at Trinity College, Dublin University, Ireland. He spent 5 years as a senior Research Officer at Nepean Hospital, University of Sydney, Australia, and 6 years as an Assistant Professor at Queen Mary Hospital, University of Hong Kong to continue his research on Helicobacter pylori and associated diseases. He has achieved an academic reputation worldwide in the field. He was elected as a fellow of the American College of Gastroenterology in 2008. He joined Novartis Pharmaceuticals Corporation, USA, in 2006 for clinical development of new investigational drugs in different therapeutic areas. He is currently an Adjunct Professor of Beijing Friendship Hospital, Capital Medical University, Beijing; Municipal Hospital, Qingdao University, Qingdao; and First Affiliated Hospital, Guangdong Pharmaceutical University, Guangdong, China. He has published about 180 peer-reviewed academic articles. He has published two books, namely, "Helicobacter pylori infection: Basic Principles and Clinical Practice" (1997), and A Comprehensive Guide to English Medical Manuscript Writing and Publication (2017).

Updated on August 28, 2022

Published by Xia & He Publishing Inc.
14090 Southwest Freeway, Suite 300, Sugar Land, Texas, 77478, USA
Telephone: +1 281-980-0553
E-mail: service@xiahepublishing.com
Website: www.xiahepublishing.com